

# **Sustainable Ruthenium- and Rhodium- Catalyzed C–H Activations with Photochemistry and Electrochemistry**

Dissertation

for the award of the degree

“Doctor rerum naturalium” (Dr. rer. nat.)

of the Georg-August-Universität Göttingen



UNIVERSITÄT  
GÖTTINGEN

within the doctoral program of chemistry

of the Georg-August-Universität School of Science (GAUSS)

Submitted by

**Agnese Zangarelli**

From Città di Castello, Italy

Göttingen, 2024



## **Thesis Committee**

*Prof. Dr. Lutz Ackermann*

Institute of Organic and Biomolecular Chemistry

*Prof. Dr. Konrad Koszinowski*

Institute of Organic and Biomolecular Chemistry

*Prof. Dr. Franc Meyer*

Institute of Inorganic Chemistry

## **Members of the Examination Board**

1<sup>st</sup> Reviewer: *Prof. Dr. Lutz Ackermann*

Institute of Organic and Biomolecular Chemistry, Göttingen

2<sup>nd</sup> Reviewer: *Prof. Dr. Konrad Koszinowski*

Institute of Organic and Biomolecular Chemistry, Göttingen

3<sup>d</sup> Reviewer: *Prof. Dr. Franc Meyer*

Institute of Inorganic Chemistry, Göttingen

## **Further Members of the Examination Board**

Prof. Dr. Dr. h. c. mult. Lutz F. Tietze, Institute of Organic and Biomolecular Chemistry, Göttingen

Dr. Daniel Janßen-Müller, Institute of Organic and Biomolecular Chemistry, Göttingen

Dr. Holm Frauendorf, Institute of Organic and Biomolecular Chemistry, Göttingen

**Date of the Oral Examination:** 29.02.2024





## Table of Contents

1 Introduction .....	1
1.1 Transition Metal-Catalyzed Coupling Reactions.....	1
1.1.1 Cross-Coupling .....	1
1.2 C–H Activation .....	3
1.3 Ruthenium-Catalyzed C–H Activation .....	8
1.3.1 Ruthenium-Catalyzed C–H Arylation.....	10
1.3.2 Ruthenium-Catalyzed C–H Allylations.....	15
1.4 Rhodium-Catalyzed C–H Olefination of Arenes .....	17
1.5 Sustainable Methods in C–H Activation .....	22
1.5.1 Photoredox Catalysis.....	22
1.5.2 Metalla-Electrocatalysis .....	27
1.5.3 Aryl Sulfonium Salts and Late-Stage Diversification.....	33
2 Objectives .....	38
3 Results and Discussion .....	41
3.1 Ruthenium-Catalyzed C–H Arylation of <i>N</i> -Aryl Triazoles and Aryl Tetrazoles with Aryl Sulfonium Salts .....	41
3.1.1 Optimization Studies.....	42
3.1.2 Substrate Scope .....	44
3.1.3 Late-Stage Incorporation of <i>N</i> -Aryl Triazoles and Tetrazoles.....	46
3.1.4 Mechanistic Investigation.....	50
3.1.5 Proposed Catalytic Cycle.....	53
3.2 Photo-Induced Ruthenium-Catalyzed C–H Allylation at Ambient Temperature .....	54
3.2.1 Optimization Studies.....	54
3.2.2 Substrate Scope .....	57
3.2.3 Mechanistic Investigation.....	59
3.2.4 Proposed Catalytic Cycle.....	60

3.3 Electrooxidative C7-Indole Alkenylation <i>via</i> Rhodium Catalysis .....	62
3.3.1 Optimization Studies .....	63
3.3.2 Substrate Scope .....	65
3.3.3 Investigations of Practical Utility .....	67
3.3.4 Mechanistic Investigation .....	68
3.3.5 Proposed Catalytic Cycle .....	70
4 Summary .....	72
5 Experiment Section .....	74
5.1 General Remarks .....	74
5.2 General Procedures .....	78
5.3 Experimental Procedures and Analytical Data .....	80
5.3.1 Ruthenium-Catalyzed C–H Arylation with Sulfonium Salts .....	80
Characterization Data .....	80
Competition Experiments .....	122
Radical Scavenger Experiment .....	122
Deuterium Exchange Experiment I .....	123
Deuterium Exchange Experiment II .....	123
Detection of Free <i>p</i> -Cymene .....	124
Poisoning Experiment .....	124
5.3.2 Photo-Induced Ruthenium-Catalyzed C–H Allylation at Ambient Temperature .....	125
Characterization Data .....	125
Photo-Induced C–H Benzylolation by Ruthenacycle <b>221</b> as Catalyst ...	129
Radical Scavenger Experiments .....	129
5.3.3 Electrochemical C7-Indole Alkenylation <i>via</i> Rhodium Catalysis .....	131
Characterization Data .....	131
Diversification of Product <b>242</b> .....	147
Procedure for the Traceless Removal of Pivaloyl Group .....	147
Synthesis of 5,6-dihydro-4 <i>H</i> -pyrrolo[3,2,1- <i>ij</i> ]quinolin-4-one .....	147
Deuterium Exchange Experiment .....	149

---

KIE Studies .....	152
Current Dependence of the Reaction Rate.....	153
6 References.....	154
7 NMR Spectra.....	172
7.1 Ruthenium-Catalyzed C–H Arylation with Sulfonium Salts.....	172
7.2 Photo-Induced Ruthenium-Catalyzed C–H Allylation .....	231
7.3 Electrochemical C7-Indole Alkenylation <i>via</i> Rhodium Catalysis .....	238
Acknowledgement.....	262
Curriculum Vitae.....	264

## List of Abbreviations

A	Ampere
Ac	acetyl
acac	acetyl acetate
Ad	1-adamantane
Alk	alkyl
AMLA	ambiphilic metal-ligand activation
API	active pharmaceutical ingredient
aq.	aqueous
Ar	aryl
atm	atmospheric pressure
BDE	bond dissociation energy
BHT	butylated hydroxytoluene
BIES	base-assisted internal electrophilic substitution
Bn	benzyl
Boc	<i>tert</i> -butyloxycarbonyl
Bpy	2,2'-bipyridyl
BQ	1,4-benzoquinone
Bu	butyl
calc.	calculated
<i>cat.</i>	catalytic
CCE	constant current electrolysis
CFL	compact fluorescent lamp
CMD	concerted-metalation-deprotonation
Cod	1,5-cyclooctadiene
conv.	conversion
Cp*	1,2,3,4,5-pentamethylcyclopenta-1,3-diene
CPE	constant potential electrolysis
Cy	cyclohexyl
$\delta$	chemical shift
d	doublet
DBT	dibenzothiophene
DCE	1,2-dichloroethane
DG	directing group
DME	dimethoxyethane
DMA	<i>N,N</i> -dimethylacetamide
DMF	<i>N,N</i> -dimethylformamide
DMSO	dimethyl sulfoxide
dt	doublet of triplet
e	fundamental charge
e <sup>-</sup>	electron
EI	electron ionization
equiv.	equivalent
ES	electrophilic substitution

---

ESI	electrospray ionization
Et	ethyl
FG	functional group
g	gram
GC	gas chromatography
GF	graphite felt
h	hour
Hal	halogen
Het	heteroatom
Hex	hexyl
HFIP	1,1,1,3,3,3-hexafluoro-2-propanol
HIV	human immunodeficiency virus
HPLC	high performance liquid chromatography
HR-MS	high resolution mass spectrometry
Hz	Hertz
<i>i</i>	<i>iso</i>
IES	internal electrophilic substitution
IR	infrared spectroscopy
ISC	intersystem crossing
<i>J</i>	coupling constant
KIE	kinetic isotope effect
L	ligand
LED	light-emitting diode
LMCT	ligand-to-metal charge-transfer
LSF	late-stage functionalization
<i>m</i>	<i>meta</i>
m	multiplet
M	molar
[M] <sup>+</sup>	molecular ion peak
Me	methyl
Mes	mesityl
mg	milligram
MHz	megahertz
min	minute
mL	milliliter
mmol	millimole
M.p.	melting point
MPAA	monoprotected amino acid
MS	mass spectrometry
<i>m/z</i>	mass-to-charge ratio
NHC	<i>N</i> -heterocyclic carbene
NMP	<i>N</i> -methylpyrrolidinone
NMR	nuclear magnetic resonance
n.r.	no reaction
<i>o</i>	<i>ortho</i>

## List of Abbreviations

---

OPV	oil pump vacuum
<i>p</i>	<i>para</i>
Ph	phenyl
Phen	1,10-phenanthroline
Piv	pivaloyl
PMP	4-methoxyphenyl
ppm	parts per million
Pr	propyl
PTH	10-phenylphenothiazine
Py	pyridyl
Pym	pyrimidine
q	quartet
R	organic rest / substituent
rt	room temperature (23 °C)
RVC	reticulous vitreous carbon
s	singlet
SCE	saturated calomel electrode
SET	single electron transfer
SPO	secondary phosphine oxide
SPS	solvent purification system
<i>t</i>	<i>tert</i>
t	triplet
T	temperature
tDG	transient directing group
TEMPO	2,2,6,6-tetramethylpiperidine-1-oxyl
Tf	triflate
TFAA	trifluoroacetic anhydride
TFE	2,2,2-trifluoroethanol
THF	tetrahydrofuran
TIPS	triisopropylsilyl
TLC	thin layer chromatography
TM	transition metal
TOF	time-of-flight
TS	transition state
UV	ultraviolet
V	Volt
Vis	visible
W	Watt
X	(pseudo)halide

# 1 Introduction

During the past decades, environmental and geopolitical<sup>[1]</sup> concerns have raised the need for advancing environmentally-friendly and sustainable industrial production techniques. In the global effort to achieve sustainable development, scientists from all fields have promoted a shift towards renewable energies and raw materials together with the reduction of potential hazard. Indeed, this has greatly affected the extension of work done to revolutionize synthetic organic chemistry. Many chemists have been studying to create novel practical procedures employing catalysis<sup>[2]</sup> to improve, among other things, synthetic utility<sup>[3]</sup> and decrease chemical waste. Thus, Paul T. Anastas and John C. Warner summarized *12 Principles of Green Chemistry*<sup>[4]</sup> as the core guidelines for any chemist attempting to lessen the harmful effects of chemical manufacturing on the environment and human health.

## 1.1 Transition Metal-Catalyzed Coupling Reactions

### 1.1.1 Cross-Coupling

One of the most effective and efficient tools for molecular synthesis is transition metal catalysis, which considerably facilitates the assembly of previously difficult to prepare arene motifs, frequently found in natural products, physiologically active chemicals, and pharmaceuticals.<sup>[5]</sup> In this context, cross-coupling<sup>[6]</sup> reactions have become a cornerstone technology in a wide range of research sectors, thanks to their simplicity and versatility.

Groundbreaking studies were conducted in the 1900s by Ullman, Goldberg, and Hurlley on copper-mediated and copper-catalyzed protocols.<sup>[7]</sup> Since then, several reactions were developed for the selective construction of C–C and C–Het bonds under mild reaction conditions, making use of the precious transition metal palladium. These were named, Mizoroki–Heck,<sup>[8]</sup> Kumada–Corriu,<sup>[9]</sup> Sonogashira–Hagihara,<sup>[10]</sup> Negishi,<sup>[11]</sup> Migita–Stille,<sup>[12]</sup> Suzuki–Miyaura<sup>[13]</sup>, Hiyama<sup>[14]</sup>, Buchwald–Hartwig,<sup>[15]</sup> and Chan–Evans–Lam<sup>[16]</sup> cross-coupling reactions ([Figure 1-1](#)).

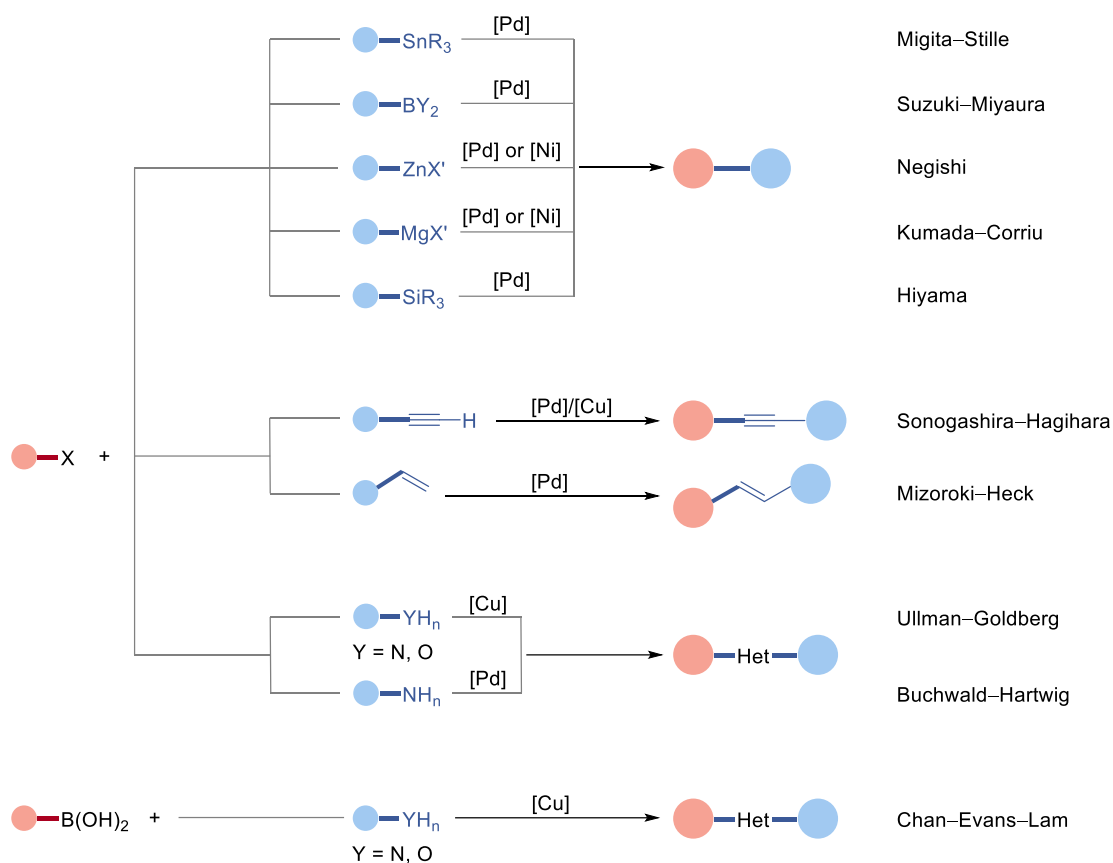


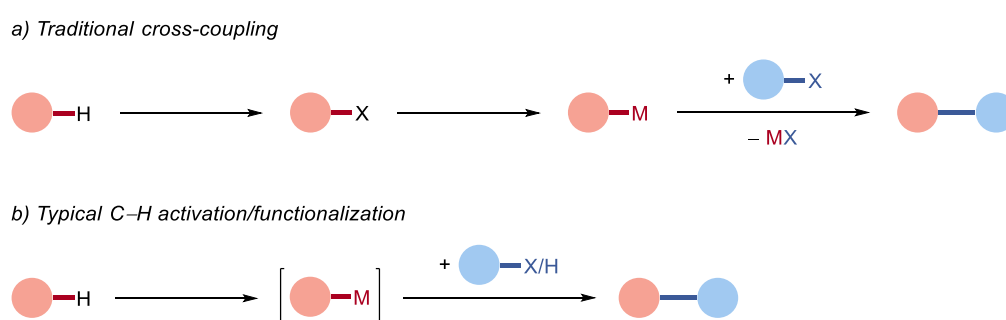
**Figure 1-1** Transition metal-catalyzed cross coupling reactions.

The great impact and advancement brought by this type of chemistry were reflected by the award of Nobel Prize in Chemistry in 2010 to Richard F. Heck, Ei-ichi Negishi and Akira Suzuki.<sup>[17]</sup> Although tremendous strides have been made by classical cross-coupling reactions, their use still bears significant inherent disadvantages. Pre-functionalization of the starting materials is one of them, along with the use of organometallic coupling partners, such Grignard reagents, organostannanes, and organozinc compounds.<sup>[18]</sup>



## 1.2 C–H Activation

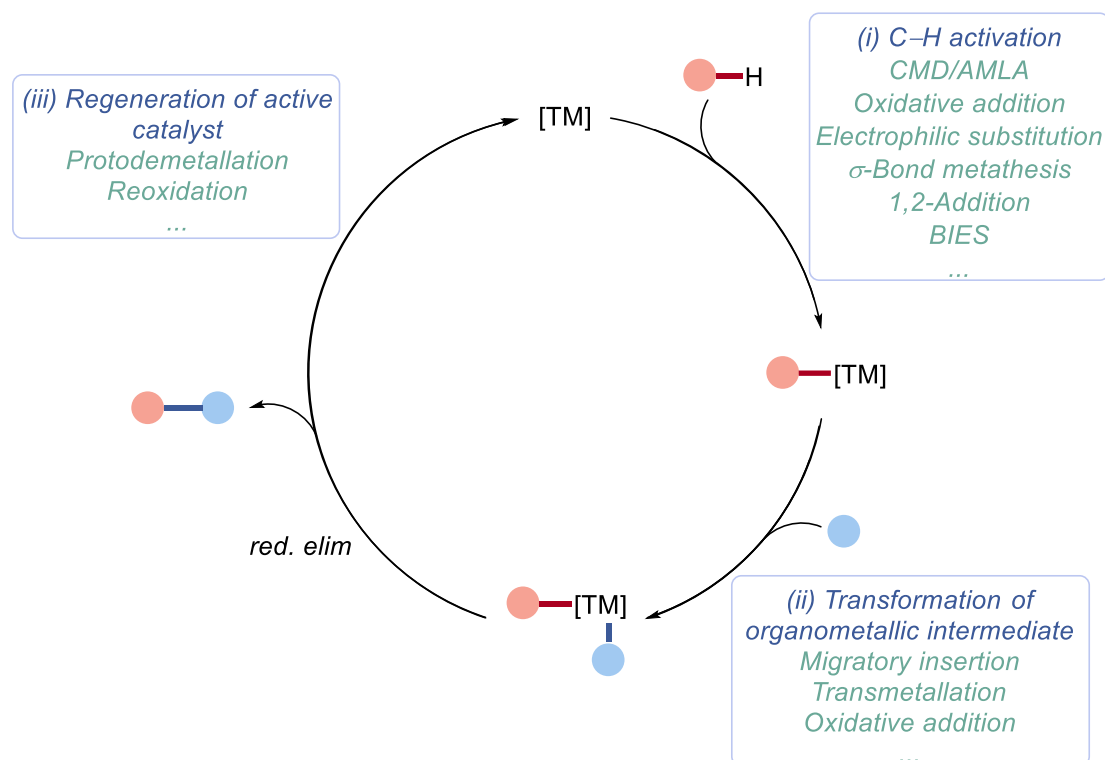
Due to numerous issues of the atom- and step-economy of traditional cross-couplings (Figure 1-2, a), research has moved towards procedures that would reduce pre-functionalization and unwanted byproduct formation.<sup>[19]</sup> In this regard, transition metal-catalyzed site-selective C–H functionalizations<sup>[20]</sup> are able to overcome many of the aforementioned limitations, promising to decrease step-count and hence mass intensity of chemical processes.<sup>[21]</sup>



**Figure 1-2.** Different methods of C–C bond formation.

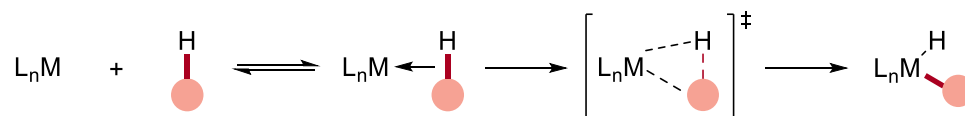
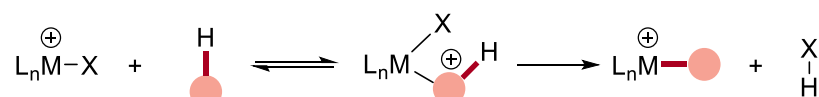
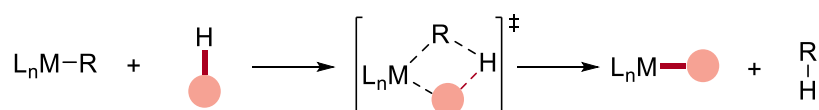
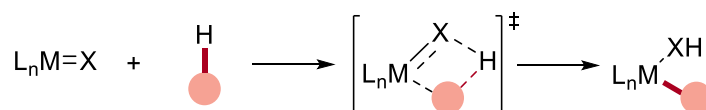
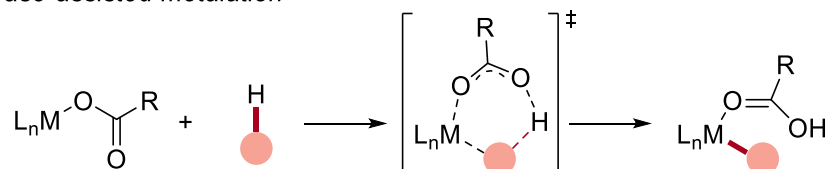
The most generally used approach of C–H activation reactions calls for a single pre-functionalized substrate as the electrophile, typically containing halogen as organic halides or phenol derivatives, which are widely accessible. (Figure 1-2, b).<sup>[22]</sup> An effective way to achieve C–C bond formation is through dual oxidative C–H/C–H activation reactions, which produces molecular hydrogen as the sole byproduct, despite the fact that costly silver and copper salts are usually needed to facilitate product formation.<sup>[23]</sup>

Clarifying the reaction mechanism is crucial for the widespread expansion of C–H activation. The catalytic cycle (Figure 1-3) can be summarized into three simple steps, including (i) C–H activation of the substrate, (ii) transformation of organometallic intermediate and (iii) reductive elimination delivering the desired product and regeneration of the active catalytic species.



**Figure 1-3.** General catalytic cycle for transition metal-catalyzed C-H activation reactions.

Contingent on the nature of the metal catalyst, ligands and oxidation state, the C-H bond cleavage can occur *via* five main modes of action.<sup>[22c]</sup> These disregard outer-sphere/radical-type mechanism.<sup>[24]</sup> Oxidative addition of the C-H bond to the metal center is usually expected for electron-rich late transition metals with low oxidation states (Figure 1-4, a).<sup>[25]</sup> Late transition metals with higher oxidation states are more prone for electrophilic substitution *via* electrophilic attack of the transition metal center to the carbon (Figure 1-4, b).<sup>[26]</sup> C-H cleavage through  $\sigma$ -bond metathesis is preferentially observed in high-valent early transition metals, but also in metal-hydrides and metal alkyl complexes (Figure 1-4, c).<sup>[27]</sup> 1,2-Addition is considered the main mechanistic pathway for complexes with unsaturated M=X bonds, such as group IV and V metal imido complexes (Figure 1-4, d).<sup>[28]</sup> When the cleavage of the C-H bond as well as the formation of the C-M bond occur almost simultaneously, it is termed base-assisted metalation step (Figure 1-4, e).<sup>[29]</sup> This event is observed for complexes bearing a coordinated base, e.g. ruthenium(II)-carboxylate complexes,<sup>[30, 22c]</sup> and proceeds through an electrophilic attack of the metal and deprotonation by carboxylate

ligands.<sup>[31]</sup>a) *Oxidative addition*b) *Electrophilic substitution*c) *σ-Bond metathesis*d) *1,2-Addition*e) *Base-assisted metalation*

**Figure 1-4.** Mechanistic pathways for C–H cleavage step.

The base-assisted metalation route can be further subdivided based on the precise transition state structure and the associated accumulation of partial charges. This has led to the main description of two unique types of transition states. (Figure 1-5). A notable one features a bifunctional carboxylate group and is named concerted metalation-deprotonation (CMD)<sup>[32]</sup> or ambiphilic metal-ligand activation (AMLA).<sup>[33]</sup> This mechanism occurs through a six-membered cyclic transition state, and usually involves electron-deficient substrates with significant kinetic C–H acidity. The second type, base-assisted internal electrophilic substitution (BIES) mechanism, is the most common and utilized for the activation of electron-rich and electron-neutral substrates

and proceeds *via* an electrophilic substitution-like pathway.<sup>[34]</sup>

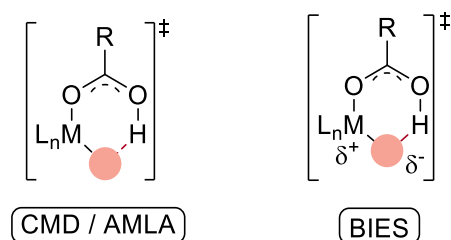


**Figure 1-5.** Diverse transition state models for the base-assisted C–H activation.

C–H activation has gained notable momentum in the synthesis of natural products<sup>[35]</sup> and complex organic scaffolds, being a powerful tool to construct molecular complexity. Nevertheless, the number of ubiquitous and ambiguous C–H bonds, with similar bond dissociation energies (BDEs),<sup>[36]</sup> found in every organic molecule has made it difficult to achieve high position-selectivity. Thus, a few methodologies can be adopted to get past the selectivity issue (Figure 1-6). Position-selectivity can be obtained by inherent properties of the targeted molecule, for example electronic and steric features. In electronically-activated substrates, e.g. azoles, it is possible in fact to pinpoint a specific C–H bond based on its lower  $pK_a$  (Figure 1-6, a).<sup>[37]</sup> The utilization of sterically demanding groups is another way to shield certain bonds and promote the functionalization at more accessible positions (Figure 1-6, b).<sup>[38]</sup> It is important to keep in mind that both strategies have a limited number of applications, because they need a particular substrate to produce certain outcomes. Another well-established approach implies an heteroatom-containing, Lewis-basic directing group (DG) that coordinates the Lewis-acidic metal center, bringing it in close proximity to a specific C–H bond (Figure 1-6, c).<sup>[39]</sup> This method significantly improves the possibility of an effective interaction between the metal center and the desired C–H bond, at the same time limiting byproduct formation.

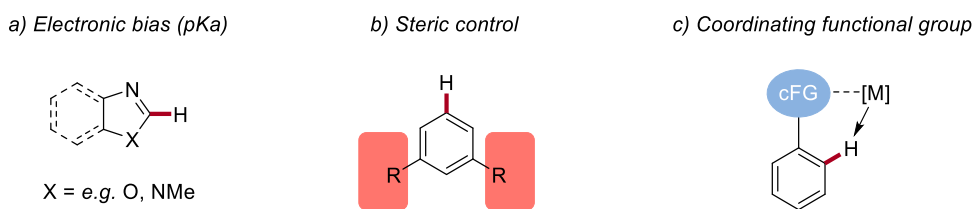


**Figure 1-6.** Diverse strategies for site selective C–H activation.

Different types of directing groups may favor completely diverse functionalizations (Figure 1-7). Some substituents have inherent *ortho*-directing effect (Figure 1-7, a) and others can act as anchors for a directing template or a transient directing group (Figure 1-7, b and c). The latter are particularly interesting, since they bond upon catalytic reaction with an external ligand *in situ*, coordinate to the metal center and are released after the C–H activation. Spacers or auxiliary templates can also be featured to enable remote functionalization (Figure 1-7, d).

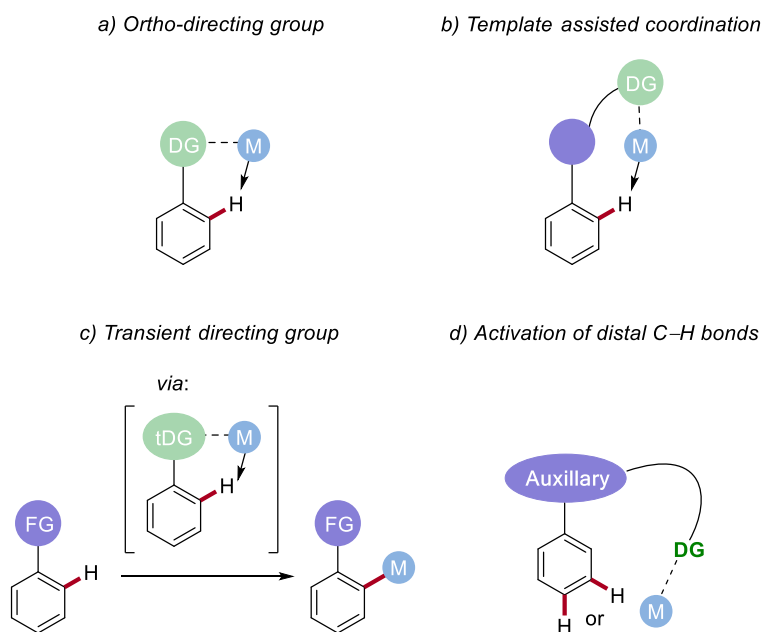


**Figure 1-7.** Different directing groups.

### 1.3 Ruthenium-Catalyzed C–H Activation

In the past few decades, outstanding advancements have been made in C–H functionalization through organometallic C–H bond cleavage. Thus, the strongest and most effective homogeneous catalysts available for the functionalization of  $sp^2$  and  $sp^3$  C–H bonds are based on precious metals, like palladium,<sup>[40]</sup> rhodium,<sup>[41]</sup> ruthenium,<sup>[42]</sup> and iridium.<sup>[43]</sup> Ruthenium, in particular, stands out between the 4d-transition metals as cost-effective and versatile, offering a wide range of catalytic applications. Inspired by earlier stoichiometric studies on sodium naphthalene by Chatt and Davidson,<sup>[44]</sup> in 1986 Lewis and Smith reported one of the first instances of ruthenium-catalyzed C–H activation.<sup>[45]</sup> A variety of mono- and dialkylated compounds were produced by hydroarylation of ethylene gas **2** with phenol **1**, employing the first transient directing group methodology (Figure 1-8).<sup>[46]</sup> Despite the harsh reaction conditions, this report set the stage for other uses of ruthenium-catalyzed C–H activation.

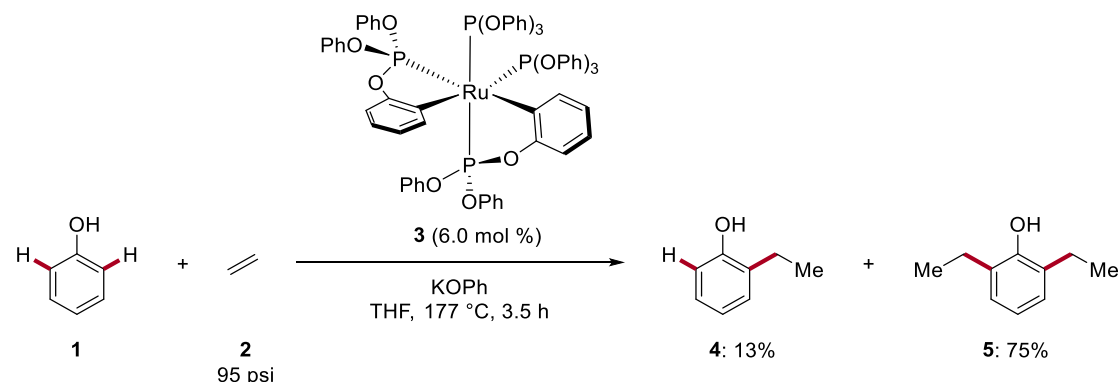
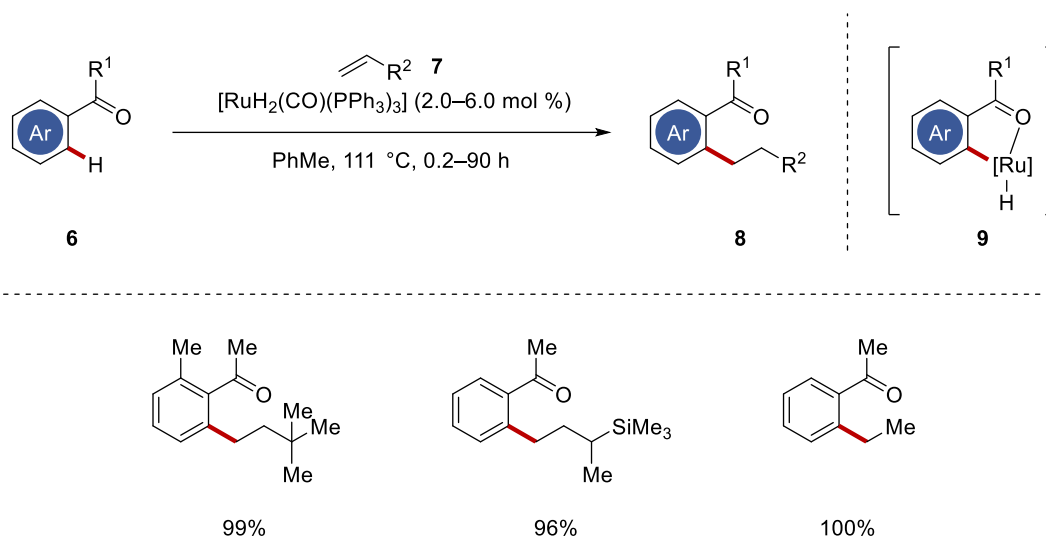


Figure 1-8. First ruthenium-catalyzed C–H activation.

Nearly a decade later, Murai, Kakiuchi and Chatani reported on the *ortho* C–H hydroarylation of unisomerizable alkenes **7**, *via* ruthenium(0) catalysis (Figure 1-9).<sup>[47]</sup> Upon heating, the ruthenium precatalyst  $[RuH_2(CO)(PPh_3)_3]$  produced a ruthenium(0) species, that enabled the crucial C–H cleavage leading to a five-membered ruthenacycle **9** with the help of weak O-coordination. As a result, the olefin inserted into a ruthenium hydride species, and subsequent reductive elimination generated

linear *anti*-Markovnikov addition products. This accomplishment showcased an ample scope and, for the first time, the wide applicability of ruthenium-catalyzed C–H activation.



**Figure 1-9.** Ruthenium-catalyzed hydroarylation.

Later, less expensive and more effective catalytic systems, employing more stable and simpler ruthenium(II) precatalysts were developed, based on the groundbreaking work done by Inoue and Oi,<sup>[48]</sup> as well as Ackermann,<sup>[49]</sup> and Dixneuf.<sup>[50]</sup> In the mechanism of the ruthenium(0) catalyst, the C–H activation step occurs *via* oxidative addition. On the contrary, for a ruthenium(II) catalyst, the C–H bond-activation process happens *via in situ* coordinated carboxylate to the ruthenium(II) site, through a six-membered transition state **11** (Figure 1-10).<sup>[51]</sup> The ease with which ruthenium(II) catalysts can be converted into cyclometalated species through C–H cleavage, their compatibility with commonly employed oxidants, and the stability of certain of them to functional groups, air and water are all likely contributing factors to their unique effectiveness.

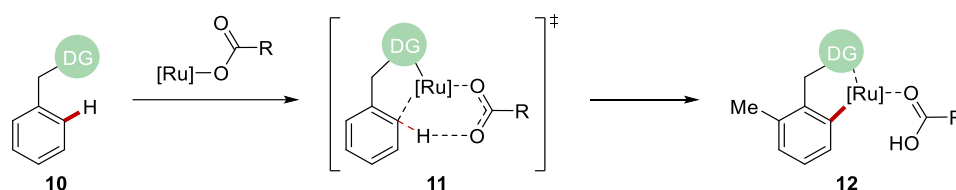


**Figure 1-10.** Base-assisted ruthenium-catalyzed C–H activation.

### 1.3.1 Ruthenium-Catalyzed C–H Arylation

An early example of direct C–H arylation of pyridine derivatives with aryl bromides under ruthenium catalysis was reported by Oi and Inoue in 2001.<sup>[48b]</sup> This simple catalytic system, composed of a ruthenium(II)-arene complex as precatalyst and catalytic quantities of  $\text{PPh}_3$  in NMP as solvent, could be employed for the functionalization of ketimines,<sup>[48a]</sup> oxazolines,<sup>[52]</sup> as well as imidazolines<sup>[53]</sup> (Figure 1-11). Notably, the reaction only occurred in the sterically less hindered *ortho*-position when the optimized conditions were applied to *meta*-substituted arenes.

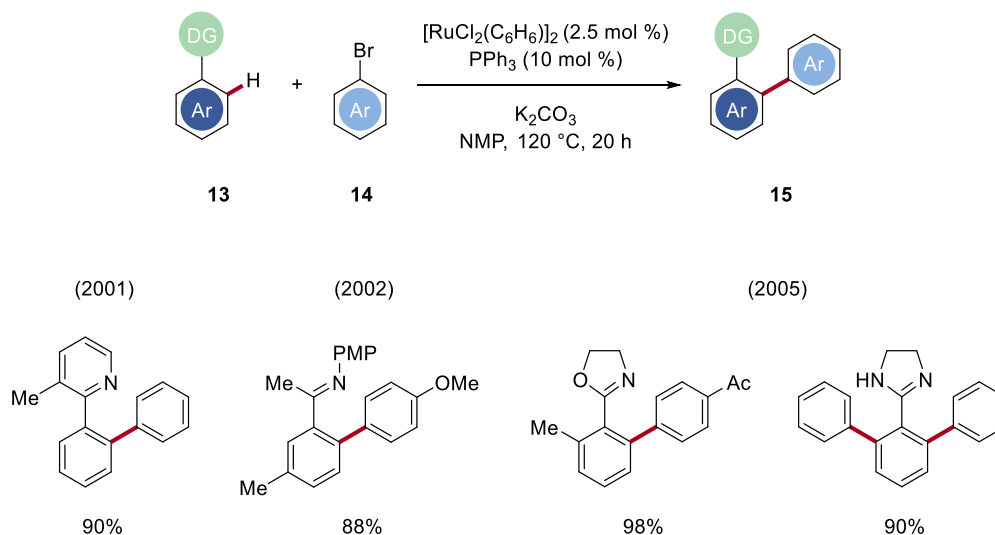


**Figure 1-11.** Ruthenium-catalyzed C–H arylation with aryl bromides.

Their catalytic cycle was proposed to involve an initial oxidative addition of the aryl bromide to the ruthenium(II) complex. Thus, through C–H ruthenation a zwitterionic intermediate was obtained. Subsequently, *via* reductive elimination the desired product was delivered, and the active catalytic species regenerated. It is important to note that



the catalytic efficacy of this ruthenium catalysis was not reproducible and was due to impurities in the NMP solvent, which resulted in a lack of robustness.<sup>[54]</sup>

An unprecedented procedure for the ruthenium-catalyzed arylation of phenylpyridines and imines by means of aryl chlorides was first developed by Ackermann. The use of air-stable, electron-rich phosphine oxides (SPO) as preligands allowed for high efficiency and functional group tolerance (Figure 1-12). The dual nature of the ligand favored an effective deprotonation assistance in a five-membered transition state. This idea set the base for the subsequent establishment of carboxylate-assisted C–H activations.

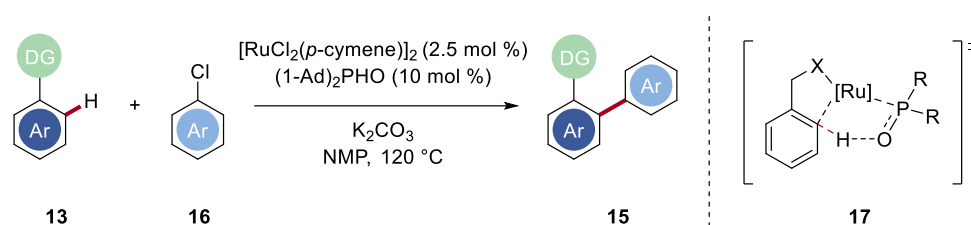


Figure 1-12. Ruthenium-catalyzed arylations with phosphine-oxide *via* transition state 17.

In 2007, Ackermann revealed the use of simple  $\text{RuCl}_3 \cdot n\text{H}_2\text{O}$  as a precatalyst in the chelation-assisted C–H arylation of alkenes and arenes with aryl halides, under phosphine-free conditions (Figure 1-13).<sup>[55]</sup>

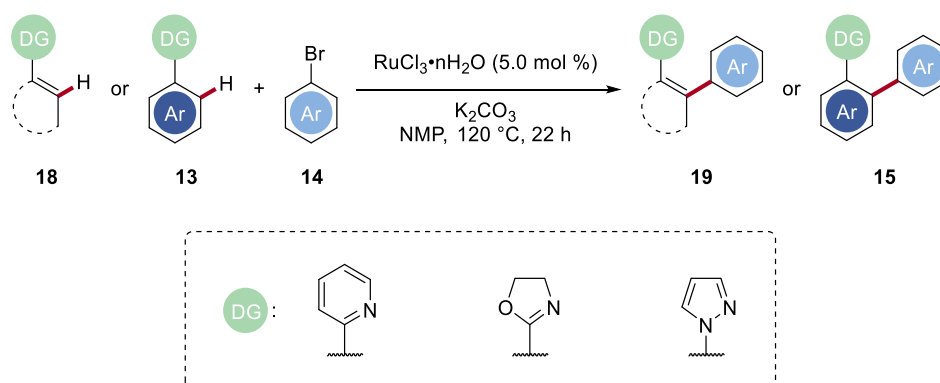
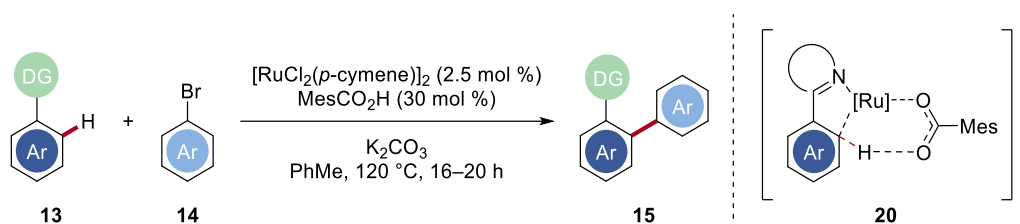


Figure 1-13. Ruthenium-catalyzed C–H arylations.

One year later, the same group made significant progress by employing carboxylate as auxiliary ligands in ruthenium-catalyzed C–H arylations.<sup>[56]</sup> Sterically hindered MesCO<sub>2</sub>H along with base performed with high catalytic efficacy in nonpolar solvents, overcoming frequently employed NHC and phosphine ligands. Many aromatic substrates proved to be viable for the aforementioned transformation. The authors proposed the involvement of a carboxylate ligand in the C–H bond cleavage event, which occurred *via* a six-membered transition state (Figure 1-14).



**Figure 1-14.** Ruthenium-catalyzed C–H arylations with carboxylic acid additives *via* transition state **20**.

Subsequent studies conducted by the Ackermann group disclosed the synthesis and mode of action of the [Ru(O<sub>2</sub>CMes)<sub>2</sub>(*p*-cymene)] complex, which displayed a unique performance in direct C–H arylations.<sup>[57]</sup> Extensive mechanistic investigations revealed the reversible nature of the chelation-assisted C–H ruthenation step, as shown in Figure 1-15. Consequently, oxidative addition of Ar–X to **24** produced ruthenium(IV) intermediate **25**, which generated the desired arylated product **26** by undergoing reductive elimination.

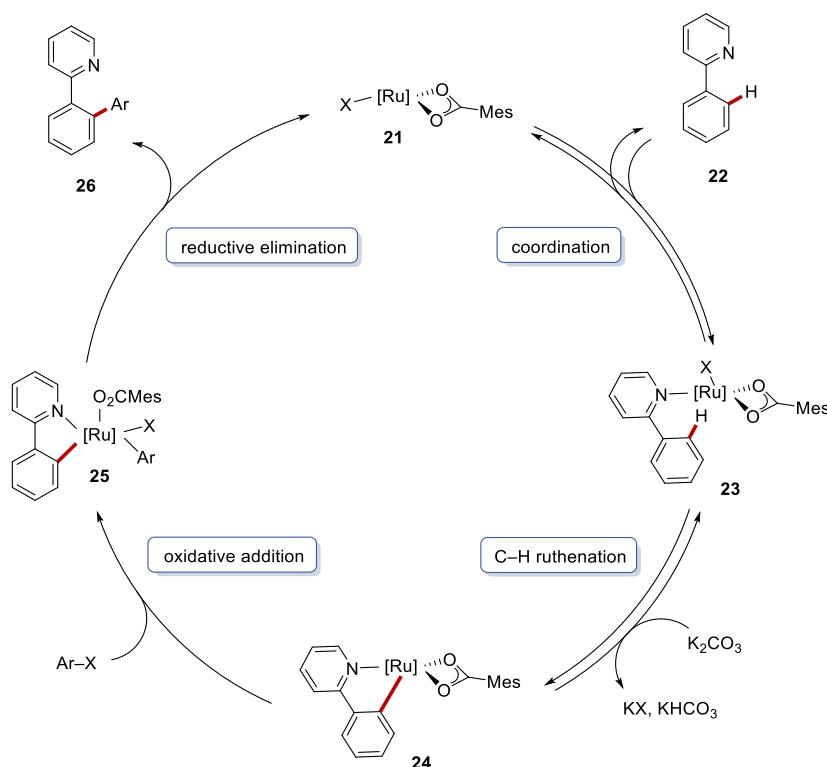


**Figure 1-15.** Proposed catalytic cycle for direct arylation *via* ruthenium-carboxylate catalysis.

In 2011, Davis reported a preparative scale synthesis of the biaryl core of Anacetrapib *via* a ruthenium-catalyzed direct arylation reaction (Figure 1-16).<sup>[58]</sup> The catalytic process between oxazolines **27** and aryl bromide **28** was achieved using [RuCl<sub>2</sub>(μ<sup>6</sup>-C<sub>6</sub>H<sub>6</sub>)]<sub>2</sub> and PPh<sub>3</sub> in the presence of K<sub>3</sub>PO<sub>4</sub> in NMP. Careful examination of the reaction parameters revealed the high impact of a low-level impurity in the solvent. The reproducibility was strictly dependent on the presence of this impurity, identified as being γ-butyrolactone **30**. The carboxylate resulting from the hydrolysis of γ-butyrolactone acted as the cocatalyst, enhancing the reactivity. This discovery enabled the creation of a reliable and high yield arylation technique that was shown on a multikilogram scale.

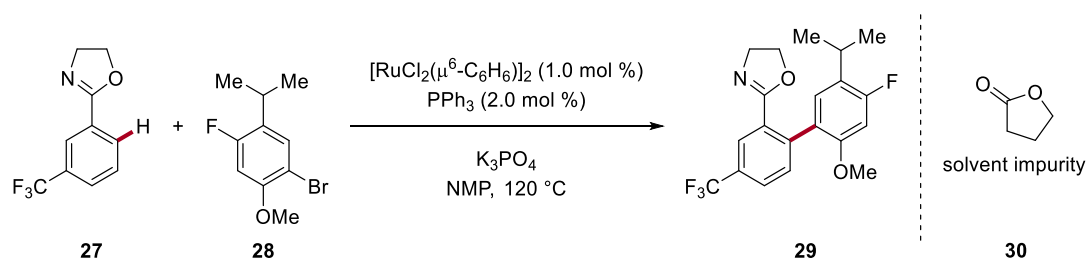


**Figure 1-16.** Carboxylate-assisted ruthenium-catalyzed C–H arylation on multikilogram scale.

In 2016, Larrosa reported a directing group-free C–H arylation of polyfluorinated arenes **31** with aryl bromides **14**, employing a cationic ruthenium complex  $[\text{Ru}(\text{NCtBu})_6][\text{BF}_4]_2$  (Figure 1-17).<sup>[59]</sup> Catalytic amounts of benzoate and pivalate as ligands were required to facilitate the C–H activation step, and, therefore, achieve high conversions.

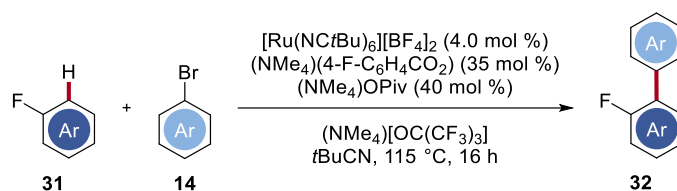


**Figure 1-17.** Undirected C–H arylation of fluoroarenes **31**.

The same group is also author of the chelation-assisted C–H arylation with aryl (pseudo-)halides under mild reaction conditions (Figure 1-18).<sup>[60]</sup> The cyclometalated ruthenium complex and the reaction temperatures of 35–50 °C allowed for the late-stage C–H functionalization of pharmaceuticals.

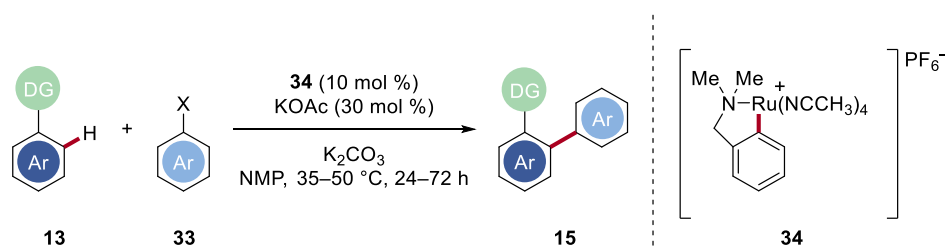


**Figure 1-18.** C–H arylation with cyclometalated complex **34** under mild reaction conditions.

### 1.3.2 Ruthenium-Catalyzed C–H Allylations

In 2006, the Inoue group went on to show the effectiveness of a ruthenium(II)-phosphine complex in the *ortho*-selective C–H allylation of 2-pyridylarenes (Figure 1-19).<sup>[61]</sup>

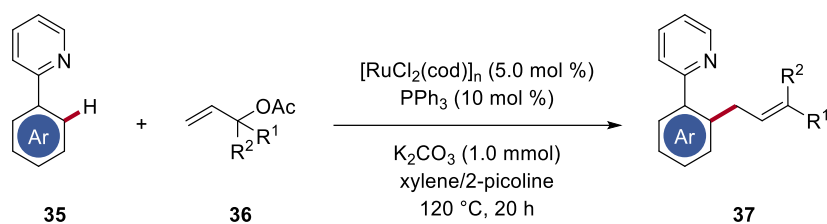


**Figure 1-19.** Ruthenium-catalyzed C–H allylation of 2-pyridylarenes **35**.

The reaction was shown to proceed *via* the formation of a stable five-membered ruthenacycle intermediate. The presence of substitutions at the *ortho*-position to the pyridyl group resulted in a reduced efficacy of the protocol, due to steric interactions with the pyridyl ring preventing the production of the ruthenacycle.

In 2015, Jeganmohan demonstrated the versatility of allyl acetate in the ruthenium-catalyzed functionalization of ketoximes (Figure 1-20).<sup>[62]</sup> The acetate source was employed as allylating agent, but also to accelerate the C–H activation step.

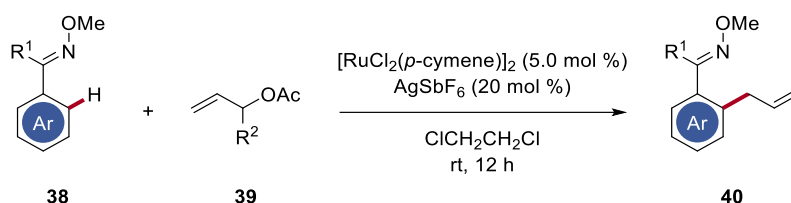


**Figure 1-20.** C–H allylation of ketoximes **38** under ruthenium catalysis.

The carboxylate-directed C–H allylation with allyl alcohols under ruthenium catalysis was achieved by Gooßen (Figure 1-21).<sup>[63]</sup> The reaction system's acidity was controlled by the use of 2,2,2-trichloroethanol. The role of the C–H activation as the rate-determining step was further supported by kinetic investigations.

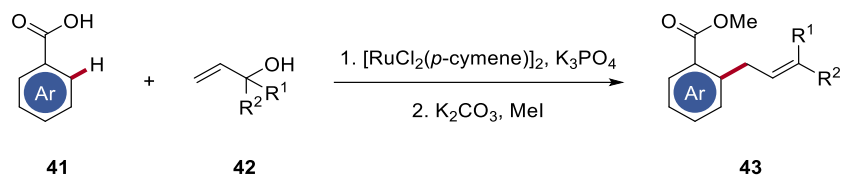


**Figure 1-21.** Carboxylate-directed ruthenium-catalyzed C–H allylation with allyl alcohols **42**.

One year later, Kapur disclosed the potential of allyl alcohols in the C–H allylation of aryl oxazolines *via* ruthenium(II) catalysis (**Figure 1-22**).<sup>[64]</sup> This transformation unraveled the unusual reactivity of the allyl species in the generation of the allylated products **46** and syntheses of 4-methyleneisochroman-1-ones **47**.

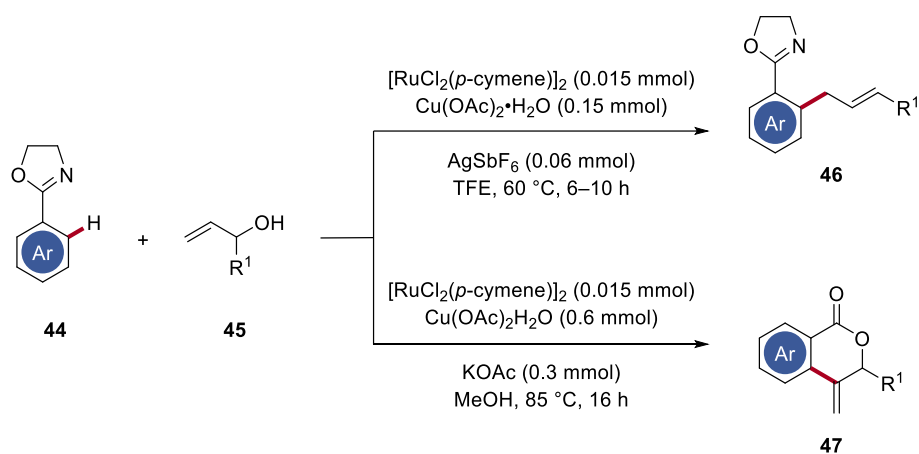


**Figure 1-22.** Ruthenium(II)-catalyzed C–H allylation of aryl oxazolines **44** with allyl alcohols **45**.

## 1.4 Rhodium-Catalyzed C–H Olefination of Arenes

Rhodium catalysts appeared in organic synthesis first in hydroformylation reactions and then in 1960's with the development of the Wilkinson catalyst used in the hydrogenation reaction of alkenes and alkynes.<sup>[65]</sup> In contrast to the overwhelming majority of findings on palladium-catalyzed reactions, rhodium-catalyzed processes remain much less examined.<sup>[66]</sup> Regardless of the generally higher cost of rhodium compounds, their use in organic synthesis is fundamental for reaction systems that are inaccessible under palladium catalysis or where a different selectivity can be achieved by changing the transition metal employed. Rhodium(III)/(I) cycles are readily present in catalysis due to their similarity with palladium(II)/(0) processes.<sup>[67]</sup> An example is the thoroughly investigated Monsanto acetic acid process.<sup>[68]</sup> Moreover, early studies on directed rhodium-catalyzed C–H activation of 2-phenylpyridine **22** were conducted by Kang in 1994 (Figure 1-23).<sup>[69]</sup> The Wilkinson catalyst was efficiently employed in the *ortho*-alkylation of arenes with neohexene **48** under chelation-assistance.

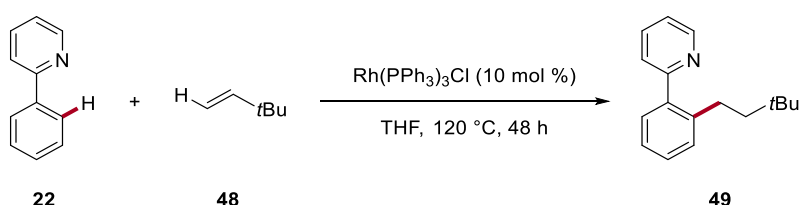
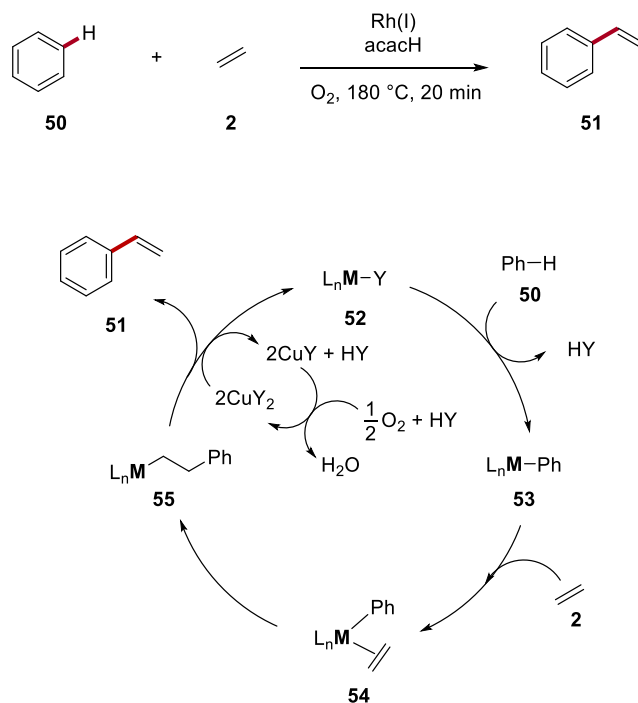


Figure 1-23. Chelation-assisted rhodium-catalyzed *ortho*-alkylation of **22**.

These findings have led to the development of a number of redox-neutral procedures, including arylations and alkenylations that involve oxidative addition to a rhodium(I) catalyst. The first discoveries on the oxidative olefination of arenes with rhodium(I) complexes were accomplished by Matsumoto in the early 2000s.<sup>[70]</sup> The synthesis of styrene was achieved combining benzene and ethylene in the presence of a rhodium(I) catalyst and acetylacetone (Figure 1-24). No oxidizing agents were required for the efficacy of the reaction. The mechanism, still not fully understood, was proposed to proceed *via in situ* oxidation of the rhodium(I) catalyst to generate a rhodium(III) species **52**. Aromatic C–H activation afforded a Rh–aryl intermediate **53**, followed by

olefin insertion to produce a Rh-alkyl species **55**.  $\beta$ -Hydride elimination would lead to the final product **51** and the reoxidation of the reduced metal center **52**.

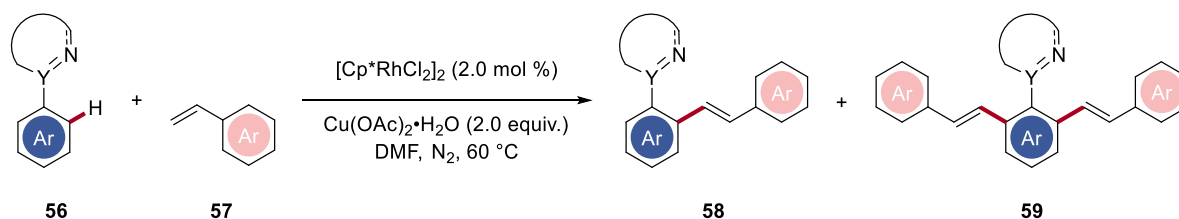


**Figure 1-24.** Rh(I)-catalyzed oxidative olefination of benzene **50** with ethylene **2**.

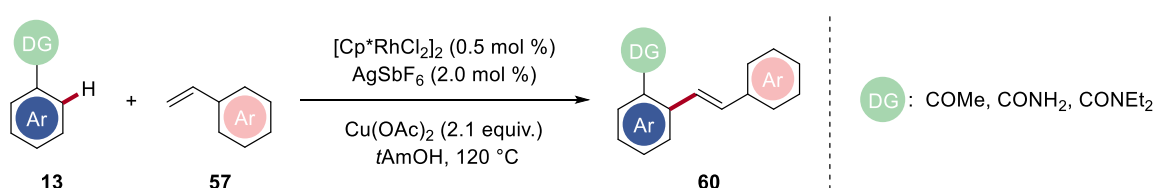
As a result of their higher efficiency, selectivity and functional group tolerance compared to rhodium(I) catalysts, rhodium(III) catalysts, in particular [Cp\*RhCl<sub>2</sub>]<sub>2</sub> and [Cp\*Rh(MeCN)<sub>3</sub>]<sup>2+</sup>, emerged as the primary choice for the functionalization of C–H bonds *via* a C–H activation pathway. Miura,<sup>[71]</sup> Glorius<sup>[72]</sup> and others<sup>[73]</sup> have documented a series of rhodium-catalyzed oxidative *ortho*-olefination reactions for a variety of functional/directing groups (Figure 1-25).



a) Rh-catalyzed mono- and divinylolation of phenylpyrazole and phenylpyridine, Miura (2009)



b) Rh-catalyzed olefination of arenes containing electron-withdrawing FG, Glorius (2010)



c) Rh-catalyzed regioselective olefination directed by a carboxylic group, Miura (2011)

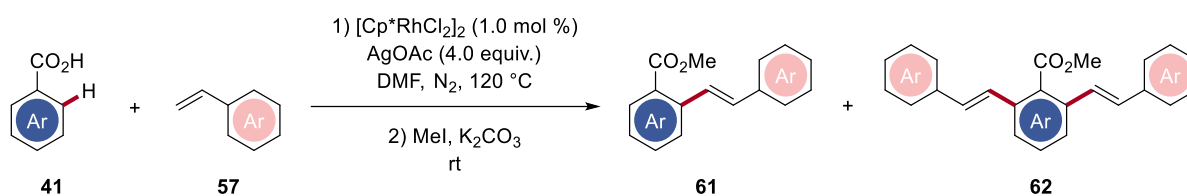


**Figure 1-25.** Rh-catalyzed *ortho*-olefination of arenes displaying diverse directing groups.

In 2011, Glorius and coworkers reported a rare example of olefination of arenes without chelation assistance. A  $[\text{Cp}^*\text{RhCl}_2]_2/\text{AgSbF}_6$  system was able to catalyze the reaction between bromobenzenes **14** and styrenes **57** in the presence of a  $\text{Cu}(\text{OAc})_2$  oxidant and PivOH additive (Figure 1-26).<sup>[74]</sup> This protocol showed selectivity issues with the formation of both *meta*- and *para*-olefination products, together with the *homo*-oxidative dimerization product of the styrene. Given that the ratio of *meta*- to *para*-olefination is close to 2:1, the authors hypothesized that the C–H activation was the result of random collisions between primarily accessible C–H bonds and the rhodium catalyst.

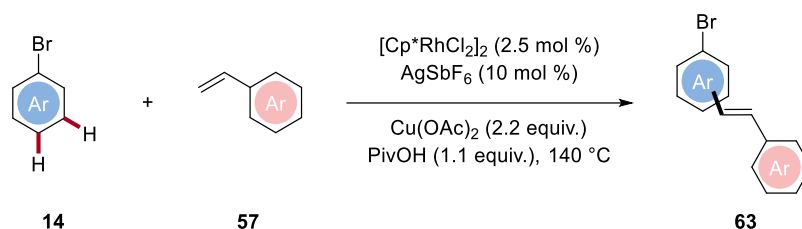


**Figure 1-26.** Olefination of arenes without chelation assistance.

Rhodium(III) catalysts have also been employed in the direct functionalization of indoles. One of the first examples of rhodium(III)-catalyzed selective oxidative coupling of indoles with alkenes was disclosed by Li and coworkers in 2013 (Figure 1-27).<sup>[75]</sup> Their catalytic strategy was able to give access exclusively to the C2-substituted product, thereby showing high position-selectivity. The potential synthetic utility of this procedure was particularly highlighted by the use of an accessible and simple to remove *N,N*-dimethylcarbamoyl as a directing group.

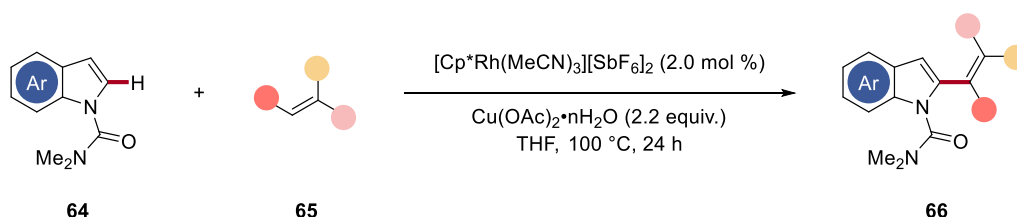


**Figure 1-27.** Rhodium-catalyzed C2-olefination of indoles **64**.

Indole has six unique C–H functionalization sites, however because of the inherent reactivity of the pyrrole ring, methods to access the C2 and C3 have been developed most frequently.<sup>[76]</sup> Therefore, establishing syntheses with complementary site selectivity is of tremendous scientific interest.<sup>[77]</sup> Two techniques have been employed for direct functionalization at the C7-position. The use of indoline derivatives as the substrates is one strategy, while the other is to protect or block the indole C2-position. The first regioselective C7-olefination of indoles with the aid of a rhodium catalyst was described by Ma in 2015.<sup>[78]</sup> This novel observation could be explained by the propensity of the bulky pivaloyl directing group of the indole species for the formation of a six-membered intermediate **70** rather than a five-membered one **71** (Figure 1-28).

This methodology featured low catalyst loading, mild reaction conditions as well as high compatibility with diverse functional groups.

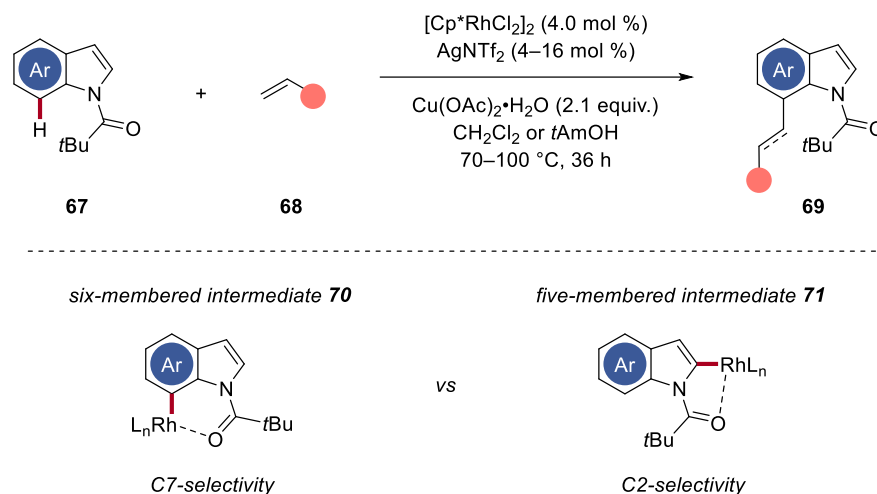


**Figure 1-28.** Rhodium-catalyzed C7-functionalization of indoles **67** via six-membered intermediate **70**.

Following these discoveries, a series of methodologies based on different directing groups capable of interacting with the rhodium metal center to exclusively furnish the C7 products, were established (Figure 1-29). For instance, in 2017, Ma showed that *N*-imino indoles were able to react with acrylates to deliver highly selective alkenylated products.<sup>[79]</sup> Subsequently, Shi and coworkers demonstrated the efficacy of *N*-PtBu<sub>2</sub> indoles in C7-selective reactions with carboxylic acid derivatives.<sup>[80]</sup> In 2021, Miura introduced a robust *N*-SCy directing group that was simply installed in one step and removed under mild reaction conditions.<sup>[81]</sup> In all cases, the selectivity control was strictly dependent on the ring size of the metallacycle intermediates.

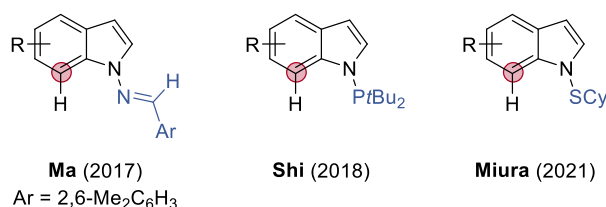


**Figure 1-29.** Rhodium-catalyzed olefinations of indoles displaying diverse directing groups.

## 1.5 Sustainable Methods in C–H Activation

The need for more environmentally-friendly industrial chemical processes has gained international consensus. The scientific community has responded to this critical requirement over the past ten years by creating revolutionary sustainable approaches focused on molecular transformations that employ cleaner and renewable energy sources, while also producing fewer wastes. Additionally, C–H functionalizations have been regarded as viable alternatives to conventional organic conversions for the access to complicated scaffolds and their late-stage diversification.<sup>[82]</sup> Protocols fusing the benefits of C–H activation technique and greener technologies stand out as particularly appealing alternatives than traditional organic transformations.<sup>[83]</sup> Recent advances in environmentally-friendly C–H activation methodologies include the use of harmless reagents and solvents, recyclable catalytic systems, efficient directing groups, mild reaction conditions and finally green oxidants. The possibility to employ substrates that would shorten reaction routes, making a procedure highly atom- and step-economical is a feature of central key importance in C–H activation.

### 1.5.1 Photoredox Catalysis

Conventionally, thermal conditions are predominant in the field of molecular synthesis and catalysis. Specifically, temperatures over 100 °C are often required for the cleavage of strong C–H bonds (110 kcal mol<sup>-1</sup> for C(aryl)–H bonds), which then limit substrate scope and functional group tolerance. Therefore, throughout the past few decades, a large number of more environmentally-friendly advancements in synthetic organic chemistry has been focused on alternative energy sources. Interesting yet cutting-edge platforms like photochemistry<sup>[84]</sup> and electrochemistry,<sup>[85]</sup> among others,<sup>[86]</sup> have enabled impressive improvements in organic synthesis. Photoredox catalysis, in particular, has recently experienced a rapid development in many fields. This methodology responds to the need for greener and sustainable synthetic strategies by favoring mild reaction conditions at ambient temperature. The use of light as an inexpensive, abundant, renewable, and non-polluting reagent for chemical synthesis

was first combined with C–H activation in 2011 by Sanford (Figure 1-30).<sup>[87]</sup> The process concerned the direct arylation of diverse aromatic compounds containing various directing groups in combination with aryldiazonium salts. In a previous publication, the authors reported a similar study on palladium-catalyzed C–H arylation with diazonium salts. However, elevated reaction temperatures and the use of acetic acid were necessary.<sup>[88]</sup> The substantial improvement came by speculating that if an aryl radical could be created *in situ* and used as a highly reactive coupling partner, a similar product might have been obtained. The reaction was performed at ambient temperature and was irradiated with visible light.

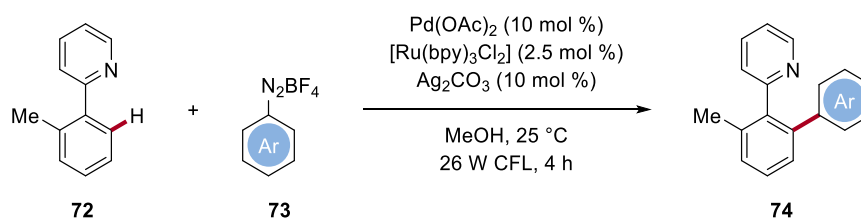
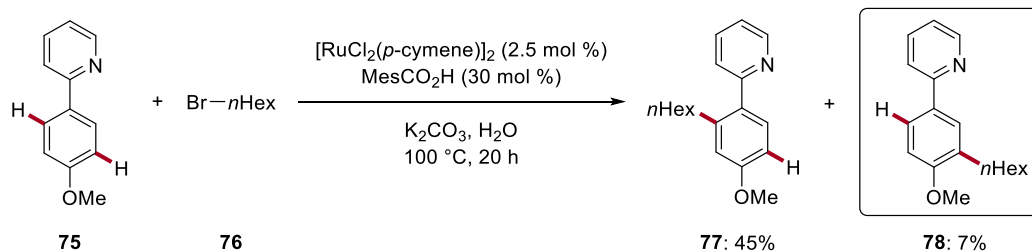


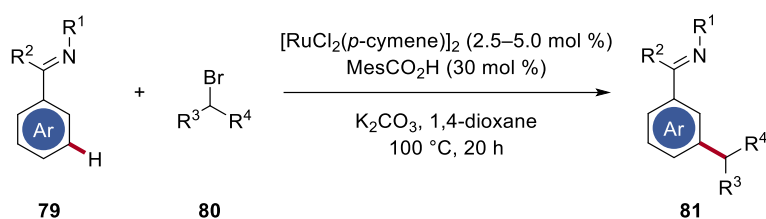
**Figure 1-30.** Visible light-induced C–H arylation of **72** with diazonium salt **73**.

The need for two metal catalysts, one capable of activating a weakly reactive C–H bond and the second employed in the light absorption process, was not ideal. Pioneering work in designing a catalyst able to play a double role was achieved for the development of ruthenium-catalyzed *meta*-selective C–H alkylations. This type of functionalization was known in literature, though limited to harsh reaction conditions. Already in 2011, Ackermann conducted a series of studies which brought to the discovery of the first catalytic remote C–H functionalization, albeit delivering rather low yields (Figure 1-31, a).<sup>[51e]</sup> Subsequently, inspired by these first findings, the same group disclosed a remote *meta*-C–H alkylation reaction using secondary alkyl bromides **80** via an *ortho*-ruthenation strategy (Figure 1-31, b).<sup>[89]</sup> In 2015, concurrently Ackermann<sup>[90]</sup> and Frost<sup>[91]</sup> reported carboxylate-assisted ruthenium-catalyzed tertiary *meta*-C–H alkylations (Figure 1-31, c and d). Ackermann's protocol highlighted the use of monoprotected amino acids **83** (MPAA) as the carboxylate ligand, unprecedented in ruthenium-catalyzed C–H activation.

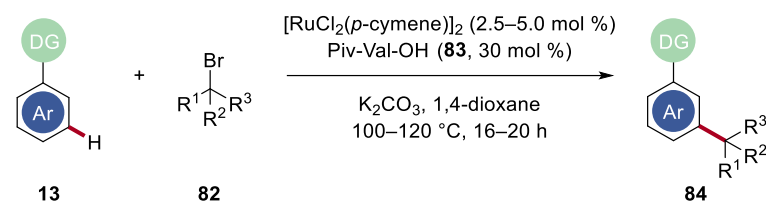
a) Ackermann (2011)



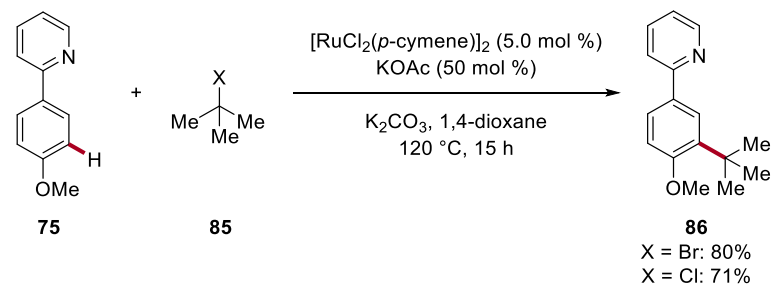
b) Ackermann (2013)



c) Ackermann (2015)



d) Frost (2015)

Figure 1-31. Ruthenium-catalyzed *meta*-C–H alkylations.

These pioneering studies served as inspiration for the publication of alternative protocols, which combined remote C–H activation and photoredox catalysis. The groups of Ackermann<sup>[92]</sup> and later Greaney<sup>[93]</sup> established a unique ruthenium-catalyzed *meta*-selective C–H alkylation of arenes with secondary and tertiary alkyl halides. The new method involved the formation of a ruthenacyclic intermediate, produced by directed *ortho*-metalation, capable of visible-light absorption. Thus, the C–H functionalization of arylazines was achieved utilizing a  $[\text{RuCl}_2(p\text{-cymene})]_2$

catalyst and blue LED irradiation at ambient temperature, with slightly different optimized parameters (Figure 1-32).

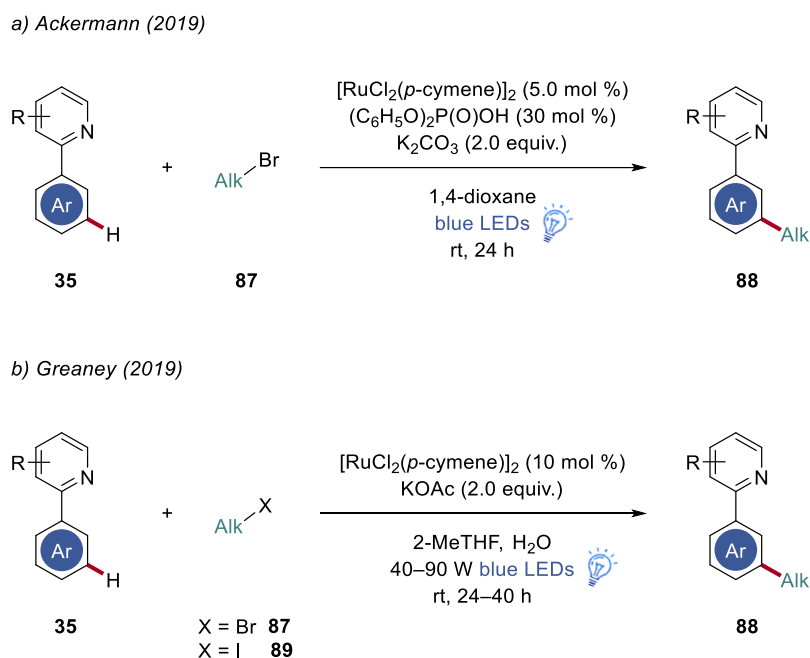
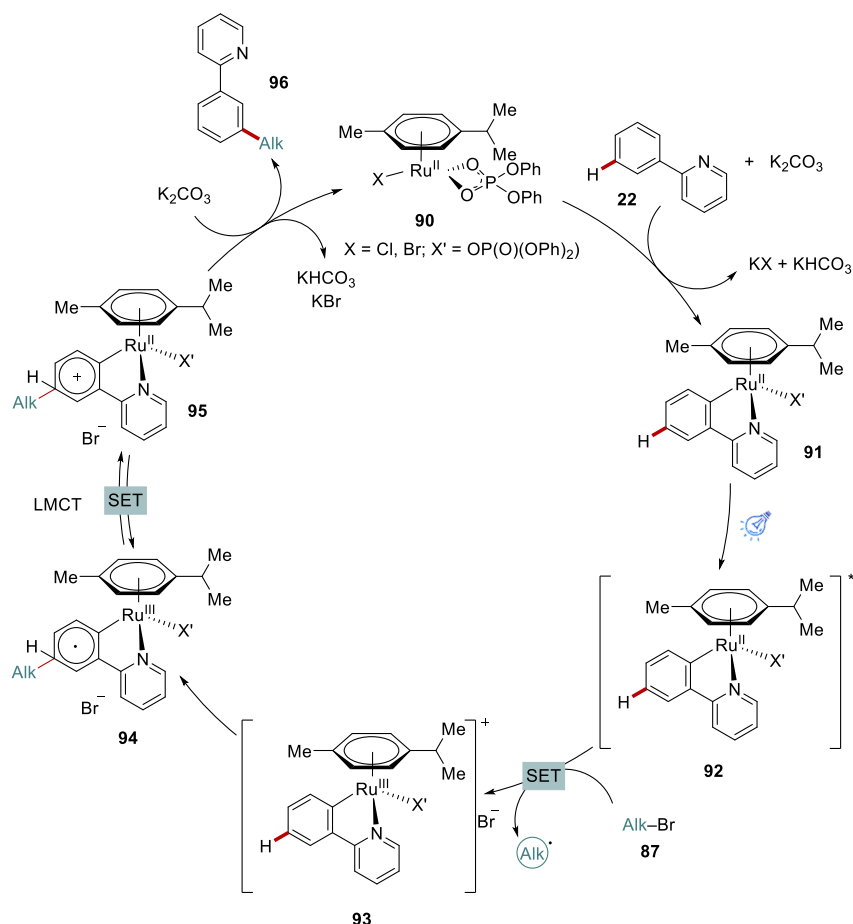


Figure 1-32. Metalla-photocatalysis enabled *meta*-C–H alkylation of arenes.

The Ackermann group conducted detailed mechanistic studies, which confirmed the light absorption in the blue region by the metallacyclic intermediate deriving from the C–H cleavage step. Furthermore, light on-off experiments showed no product formation in the dark. Their catalytic proposal (Figure 1-33) started with the formation of the photoactive intermediate by pyridine-directed *ortho*-C–H activation, followed by photoexcitation to generate intermediate **92**. Subsequently, SET from the excited **92** to the haloalkane delivered a stabilized alkyl radical, which attacked in *para* to the ruthenium center. Finally, SET and rearomatization released the *meta*-alkylated product **96** and regenerated the active ruthenium(II) species **90**.



**Figure 1-33.** Proposed catalytic cycle for *meta*-C–H alkylation via visible light metalla-photocatalysis.

Later on, the dual-function catalyst system was used for other C–H functionalizations. In 2020, Greaney proved a visible light-induced ruthenium-catalyzed *ortho*-arylation of 2-arylpyridines **35** with a range of aryl bromides and iodides **33** (Figure 1-34).<sup>[94]</sup> In their initial mechanistic studies, they proposed a photodecomplexation of the cymene ligand from the pre-catalyst, however the role of light was further delineated in subsequent publications.



**Figure 1-34.** *ortho*-C–H Arylation of arenes **35** at ambient temperature.



## 1.5.2 Metalla-Electrocatalysis

Electrosynthesis has evolved since its first steps with Volta,<sup>[95]</sup> Faraday,<sup>[96]</sup> and Kolbe<sup>[97]</sup> into a green and environmentally friendly process. The supplied electrons along with protons act as redox equivalents, which eliminate the requirement for superstoichiometric amounts of redox chemicals and, as a result, decrease the generation of undesired byproducts. The widespread development of user-friendly electrochemical cells and commercialized equipment is also a relevant incentive to relate to this alternative technology.<sup>[98]</sup> Furthermore, electrosynthesis offers milder conditions that could improve the chemoselectivity and therefore the overall synthetic usefulness, when compared to traditional chemical redox reagents, because of its ability to fine-tune the required reaction potential.<sup>[99]</sup> Moreover, the simplicity of the procedure, together with its affordable nature, attracted over the years the interest in developing industrial protocols, e.g. Simons fluorination process,<sup>[100]</sup> Monsanto adiponitrile processes<sup>[101]</sup> and BASF Lysmeral<sup>®</sup> Lilial synthesis for the fragrance industry.<sup>[102]</sup> It has been, however, only in the late 20<sup>th</sup> century that significant steps forward in the field of electroorganic synthesis were made, thanks to the pioneering works of Schäfer,<sup>[103]</sup> Amatore,<sup>[104]</sup> Jutand,<sup>[105]</sup> Little,<sup>[106]</sup> Yoshida,<sup>[107]</sup> Lund<sup>[108]</sup> and Moeller.<sup>[109, 65b]</sup> Simultaneously, C–H activation evolved as a viable alternative to traditional cross-couplings, although still being limited by the need of (super-)stoichiometric amounts of toxic chemical oxidants. Thus, the combination of electrochemistry as an unlimited source of renewable energy with step- and atom-economical C–H activation led to the creation of innovative ecofriendly methods (Figure 1-35).

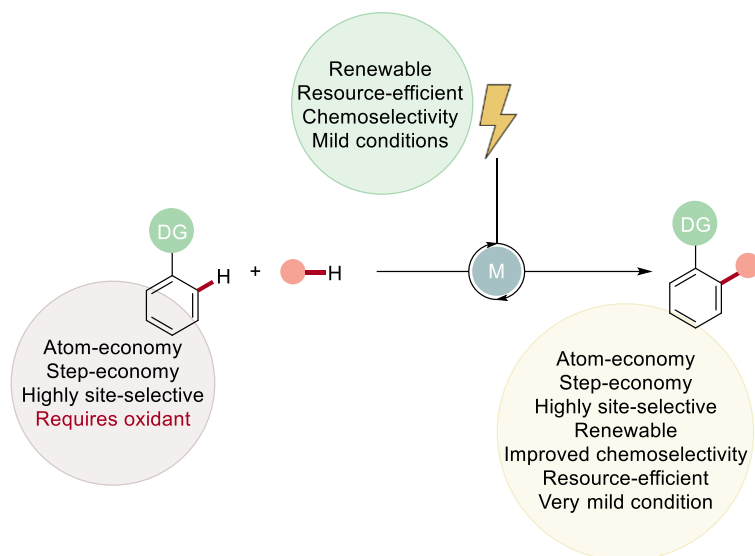


**Figure 1-35.** The merger of electrocatalysis and directed oxidative C–H activation.

The majority of the early studies on electrochemical C–H activation were conducted with palladium catalysts.<sup>[110]</sup> An example of merging palladium-catalyzed C–H activation and electrocatalysis was reported by Amatore and Jutand in 2007 (Figure 1-36).<sup>[111]</sup> This electro-enabled Fujiwara–Moritani alkenylation<sup>[112]</sup> made use of catalytic amounts of benzoquinone as indirect mediates of the palladium(II/0) catalysis. The catalytic cycle could be completed by the benzoquinone reoxidation at the carbon cloth anode.

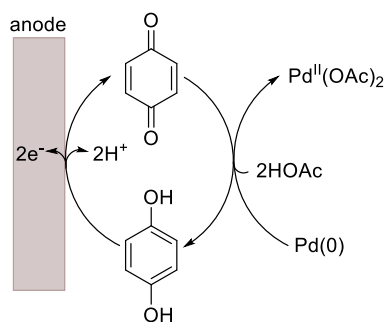
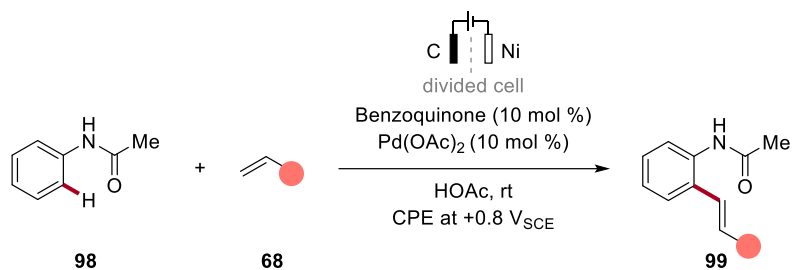


**Figure 1-36.** Electrochemical palladium-catalyzed alkenylation.

Few years later, Kakiuchi established an electrochemical chlorination and bromination of 2-phenylpyridine **35** catalyzed by palladium (**Figure 1-37**).<sup>[113]</sup> This study avoided expensive halogenation reagents by generating the reactive halonium ion from mineral acids using electricity. The palladacycle then attacked the cation to obtain the desired product **100**. The same group expanded the strategy to iodinations using potassium iodide or elemental iodine,<sup>[114]</sup> while Mei demonstrated that palladium-catalyzed electrochemical bromination is also possible with less corrosive ammonium bromides.<sup>[115]</sup> Nonetheless, the functionality of these methods was strictly bound to the use of strongly coordinating pyridyl directing groups.

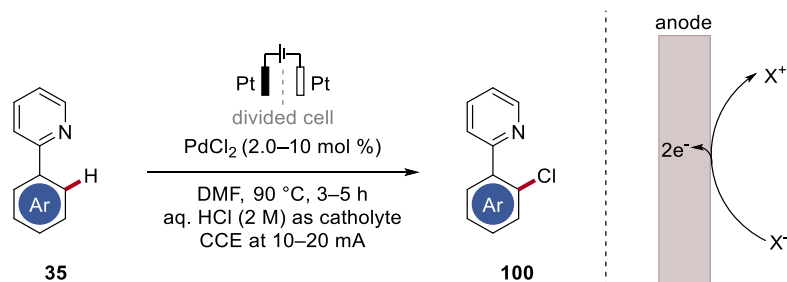


**Figure 1-37.** Electrochemical palladium-catalyzed halogenation of 2-phenylpyridine **35**.

The use of electrochemistry for the direct oxidation of the metal catalyst was first shown by Budnikova for the C–H perfluorocarboxylation of phenylpyridines.<sup>[116]</sup> Later, Mei established a novel electrochemical procedure in which palladium was used for the C(sp<sup>3</sup>)–H oxygenation of oximes (**Figure 1-38**).<sup>[117]</sup> Their proposed catalytic cycle included an initial coordination of the palladium catalyst with the oxime **101** and subsequent C–H activation, which resulted in palladacycle **104**. Direct oxidation of the resultant complex **104** at the anode produced a palladium(III) or palladium(IV) species **105**. After reductive elimination, the product **102** was released and the active catalytic palladium(II) species regenerated.

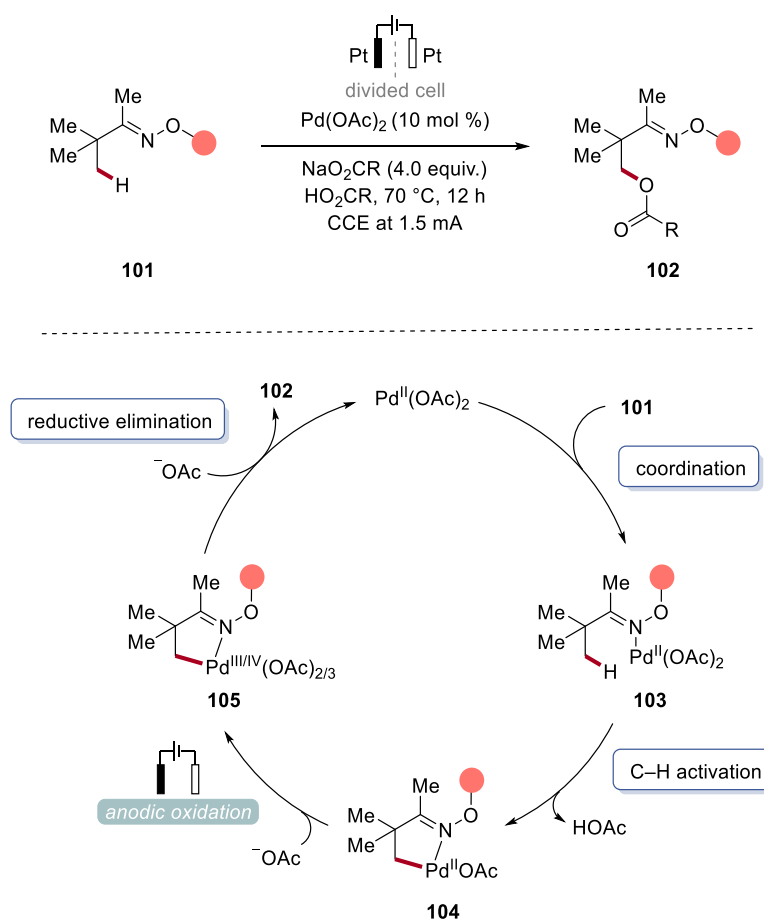


**Figure 1-38.** Palladium-catalyzed C(sp<sup>3</sup>)–H oxygenation *via* electrocatalysis.

The continuous developments in electrocatalysis led to the formulation of new methods involving the use of other transition metals. Ackermann was the first to combine

rhodium-catalyzed C–H activation and electricity. In 2018, the group reported a cross-dehydrogenative alkene annulation on weakly O-coordinating benzoic acids **41** in the presence of  $[\text{Cp}^*\text{RhCl}_2]_2$  as catalyst (Figure 1-39).<sup>[118]</sup> The reaction was performed in an undivided cell setup at 4.0 mA constant current electrolysis. The catalytic cycle was said to commence with a carboxylate-assisted C–H activation step, followed by alkene migratory insertion to generate complex **112**.  $\beta$ -Hydride elimination and reductive elimination led to rhodium(I) intermediate **113**, which *via* anodic oxidation was converted into the active rhodium(III) catalytic species **108** with concomitant product **114** formation.

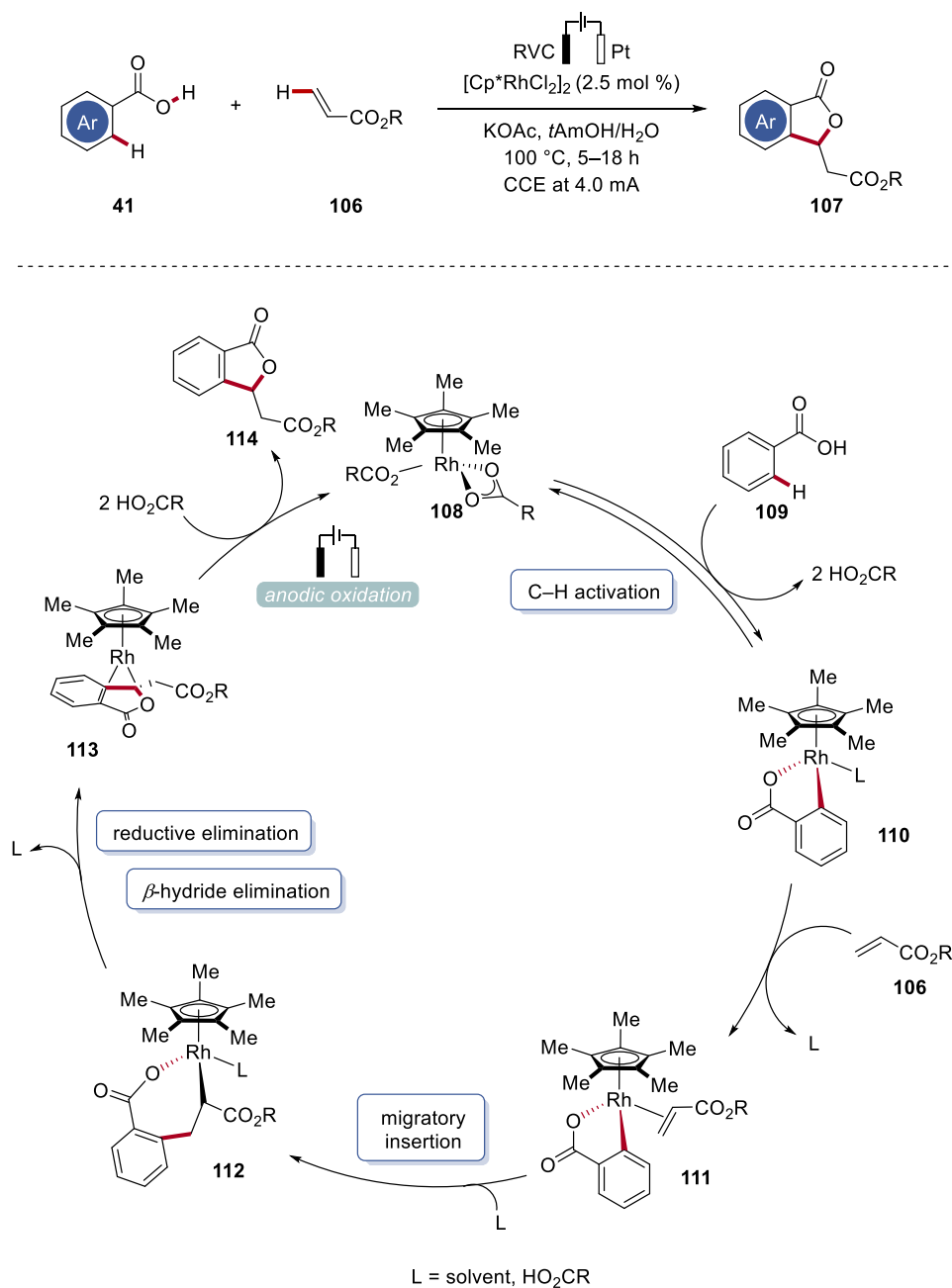


**Figure 1-39.** First example of rhodium-catalyzed electrooxidative C–H activation.

Site-selective C–H activation with electrocatalysis has continued to flourish in combination with Earth-abundant transition metals, opening up new avenue for developments of novel and innovative protocols with many contributions from Ackermann,<sup>[119]</sup> Lei,<sup>[120]</sup> Xu,<sup>[121]</sup> and Mei,<sup>[122]</sup> among others.<sup>[123]</sup>

### 1.5.3 Aryl Sulfonium Salts and Late-Stage Diversification

Late-stage diversification represents a chemoselective strategy able to furnish molecular complexity, without the need for the installation of a functional group that solely serves this goal.<sup>[124]</sup> LSF facilitates synthetic efforts and allows access to derivatives of potential value that would be far more difficult or time consuming to obtain, starting from simple molecular building components. Shorter reactions routes, cost-efficiency, functional group tolerance, and limited or absent side-product formation are all features that makes LSF a sustainable process (Figure 1-40). C–H activation strategies are naturally best suited for LSF due to the ubiquity of carbon-hydrogen bonds, the absence of preinstalled functional groups and the exceptional site- and chemoselectivity. Since its advent, late-stage C–H functionalization has shown a great impact in the diversification of drug candidates and bioactive natural products, rendering *de novo* approaches more and more obsolete.<sup>[125]</sup>

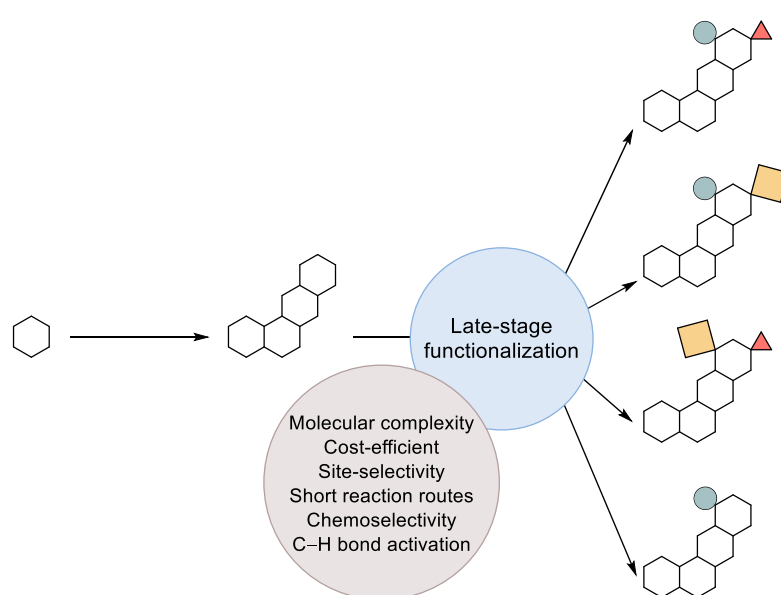


**Figure 1-40.** Late-stage functionalization as a sustainable process.

The field of C–H LSF has recently been enhanced by the revived use of sulfonium salts as highly versatile electrophilic arylating agents. These substrates made their first appearances in the early 70's with reports by Silber and Shine. In their report,

thianthrenium perchlorate **116** was employed as electrophile in a  $S_EAr$ -type reaction, which led to the production of *para*-selective sulfonium salts **117** deriving from mono substituted benzenes **115** (Figure 1-41).<sup>[126]</sup>

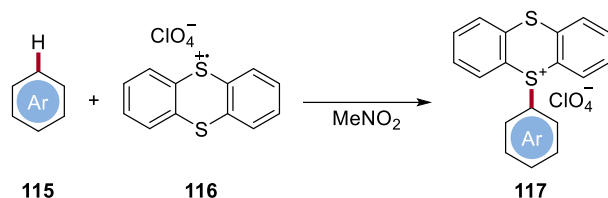


**Figure 1-41.** C–H thianthration of benzene derivatives **115**.

After these early studies, no significant reports on sulfonium salts are present in literature, probably due to the potentially explosive nature of thianthrenium perchlorate **116**. It was only in 1988 that Gerber addressed this problem by generating reactive sulfur species *in situ* starting from stable dialkyl or diaryl S-oxide (Figure 1-42).<sup>[127]</sup>

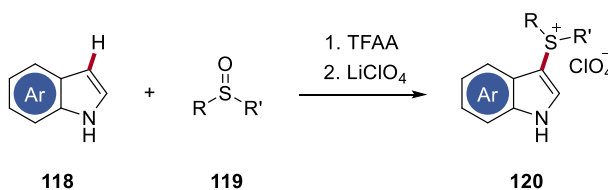


**Figure 1-42.** Activation of dialkyl or diaryl S-oxides **119** for the synthesis of sulfonium salts **120**.

This methodology, *per contra*, was limited to electron-rich indoles and pyrrole moieties. In 2019, Ritter outlined a milder synthetic route to access differently substituted thianthrenium salts (Figure 1-43).<sup>[124c]</sup> The highly site- and chemo-selective approach allowed for the incorporation of versatile sulfonium scaffolds into valuable natural products and drug molecules.

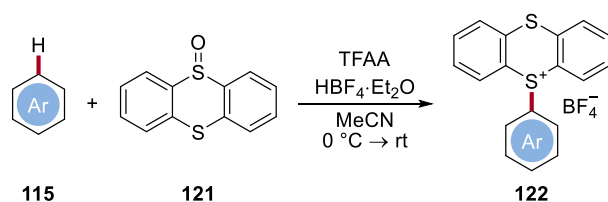


**Figure 1-43.** C–H thianthration *via* activation of thianthrene S-oxide **121** *in situ*.



One year later, Alcarazo was able to obtain several substituted aryl dibenzothiophenium salts **124**, through selective metal-free C–H sulfenylation of arenes **115** (Figure 1-44).<sup>[128]</sup>

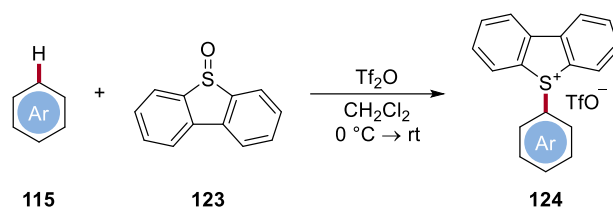


**Figure 1-44.** Synthesis of dibenzothiophenium salts **124**.

Together with their syntheses, a few possible catalytic applications of sulfonium salts were also investigated. Among the various contributing authors, Ritter's group explored the field of C–C and C–Het bond formation, achieving late-stage diversification of complex organic molecules and relevant pharmaceutical scaffolds by employing aryl sulfonium salts.<sup>[124c]</sup> They were able to introduce a persistent sulfur-based radical capable of highly selective arene functionalizations to achieve thianthrenium salts used efficiently in a plethora of transformations (Figure 1-45).

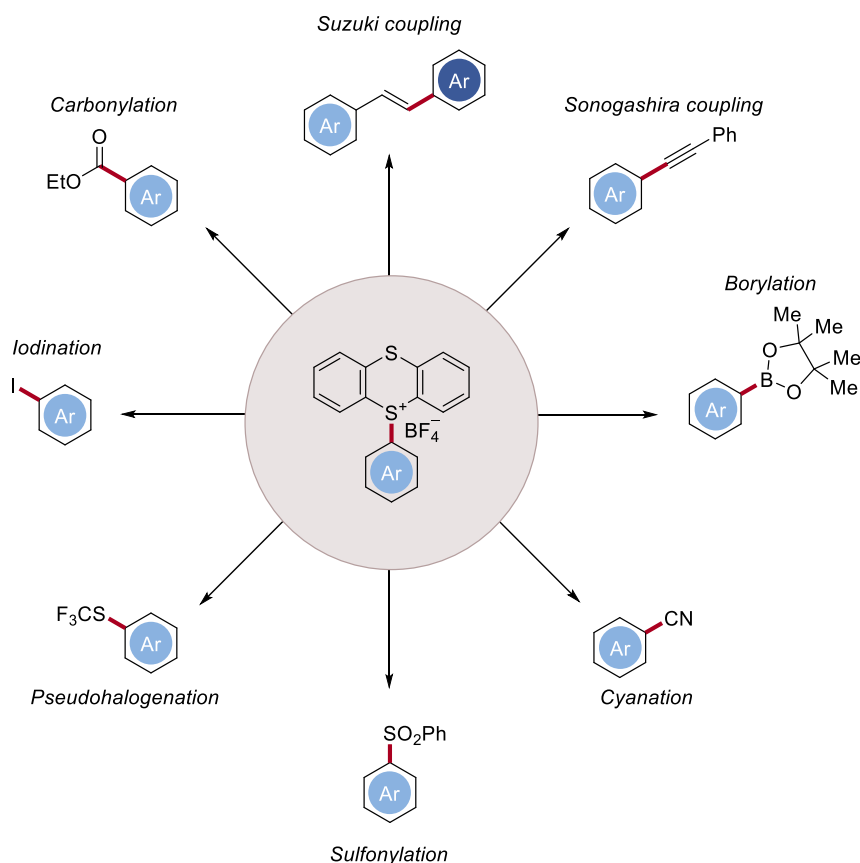


**Figure 1-45.** Transformations enabled by aryl thianthrenium salts.

In 2020, Procter used the ability of dibenzothiophenium salts **124** to serve as carbon-centered radicals for the metal-free photoredox C–H/C–H coupling of heteroarenes **125** (Figure 1-46).<sup>[129]</sup> This strategy featured an excellent selectivity and broad substrate scope and was also employed in the modification of complex molecules.

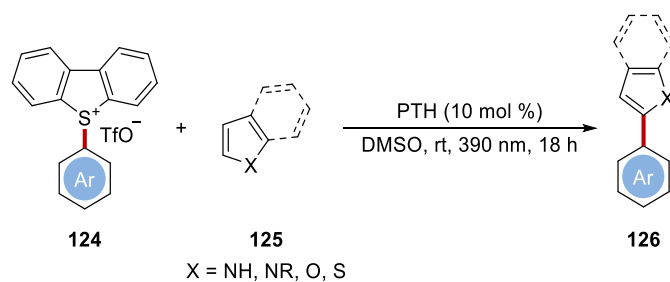


**Figure 1-46.** C–C/C–C coupling of heteroarenes **125** with DBT salts **124**.

So far, the reported examples in C–H functionalization relied on the potential of the sulfonium salts to serve as aryl radical precursors to perform Minisci-type reactions.

However, the Ackerman group established sulfonium salts for the palladium catalyzed

C–H arylation of tryptophan derivatives, by changing their innate reactivity from radical precursors to electrophilic coupling partners under catalyst control (Figure 1-47).<sup>[130]</sup> This reaction manifold did not require time-consuming and expensive prefunctionalization, and the tunable nature of arylthianthrenium salts **122** made it possible to efficiently assemble peptide/drug conjugates and ligated peptides containing unconventional biaryl motifs.

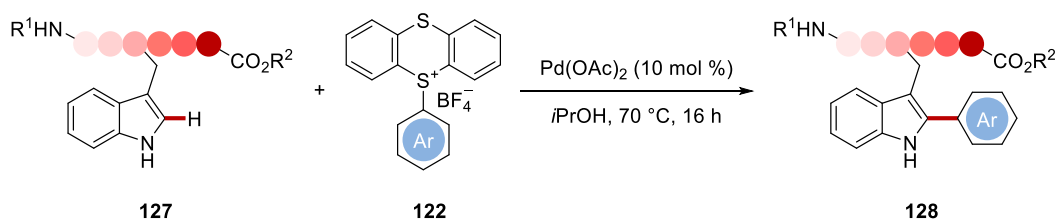


**Figure 1-47.** Late-stage C–H arylation of tryptophan containing peptides **127** with thianthrenium salts **122**.

## 2 Objectives

Huge strides have been achieved with transition metal-catalyzed C–H activation, which has proven to be an incredibly powerful tool for the functionalization of inert C–H bonds found in all organic molecules.<sup>[20]</sup> Furthermore, this outstanding atom- and step-economical strategy, in combination with renewable energy sources, has been particularly effective for creating C–C and C–Het bonds in a sustainable fashion. Flourishing metalla-electrocatalysis<sup>[131]</sup> and photoredox chemistry<sup>[84]</sup> have surpassed synthetic procedures limited by the use of stoichiometric amounts of toxic chemical oxidants and harsh reaction conditions, respectively. Also, the late-stage C–H functionalization of natural products and drugs candidates has greatly improved the value of organic catalysis. In this context, over the past two decades, the Ackermann group has extensively contributed with novel catalytic C–H activation strategies featuring a wide range of transition metals.<sup>[36e, 132]</sup> Thus, the objective of this thesis was to address long-standing problems, e.g. harsh reactions conditions, expensive and often toxic chemical oxidants, selectivity issues, as well as to avoid side-product formation.

Aryl sulfonium salts represent an attractive alternative to commonly used electrophilic arylating agents. In fact bromide and iodide are often difficult to be selectively introduced into complex molecular architectures.<sup>[128, 124c]</sup> So far, the majority of the reports featuring sulfonium salts involved cross-couplings<sup>[133]</sup> or photoredox catalysis.<sup>[129]</sup> Nonetheless, their facile synthesis and tunable nature make them suitable substrates in synthetically useful C–H activation reactions. *N*-Aryl triazole and aryl tetrazole act as stable bioisosters of amides and carboxylic acids, respectively, which render them relevant structural motifs in a variety of pharmaceuticals.<sup>[134]</sup> In the first project, we intended to study the distinct reactivity of dibenzothiophenium salts, employed to enrich the aforementioned aromatic architectures with a multitude of drug derivatives (Figure 2-1).

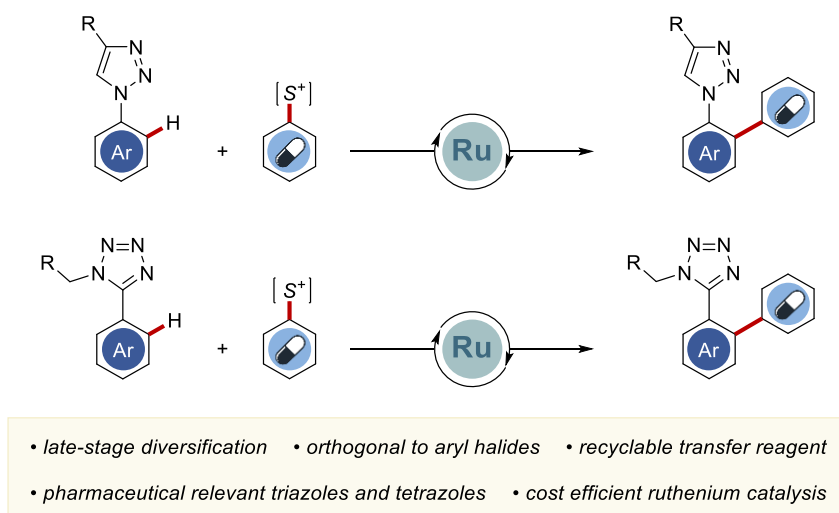


**Figure 2-1.** Ruthenium-catalyzed C–H arylation of *N*-aryl triazoles and aryl tetrazoles with API-derived sulfonium salts.

Among all transition metals, ruthenium stands out as a highly reactive, economical catalyst in a wide range of viable transformations. Thanks to the distinctive character of the cyclometalated complexes, ruthenium can be employed in the *ortho*-selective functionalization of heteroarenes.<sup>[135]</sup> Typically, these protocols require harsh temperatures above 100 °C.<sup>[136]</sup> Therefore, photochemistry<sup>[84]</sup> has brought a significant advancement, characterized by sustainable synthetic strategies and milder reaction parameters. Herein, we study a photocatalysts free ruthenium-catalyzed allylation reaction at ambient temperature (Figure 2-2).

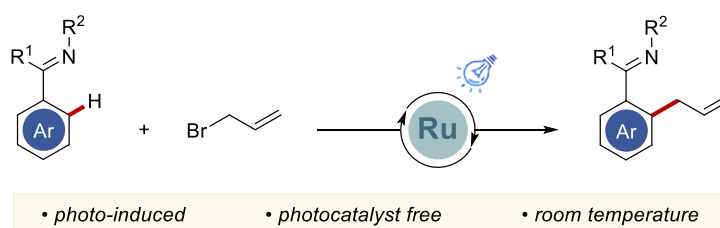


**Figure 2-2.** Photo-induced ruthenium-catalyzed C–H allylation of phenyl pyridines and phenyl pyrazoles at room temperature.

Any mediator would not be necessary if a transition metal was effectively directly oxidized at the anode. As a result, a method that is even more atom-economical could be possible.<sup>[85]</sup> Electrochemistry, as a versatile and sustainable methodology, was used

in combination with rhodium catalysis for the site-selective C7-functionalization of indoles (Figure 2-3). These challenging substrates, important structural units in many bioactive compounds,<sup>[137]</sup> offer inherent reactivity at the C2- and C3-position. Therefore, the identification of novel strategies for accessing the benzenoid positions is of utmost relevance.

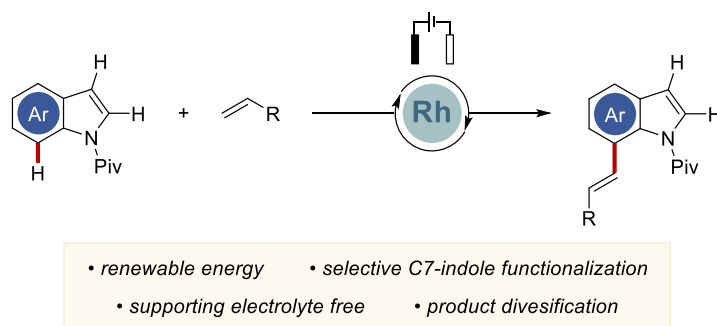


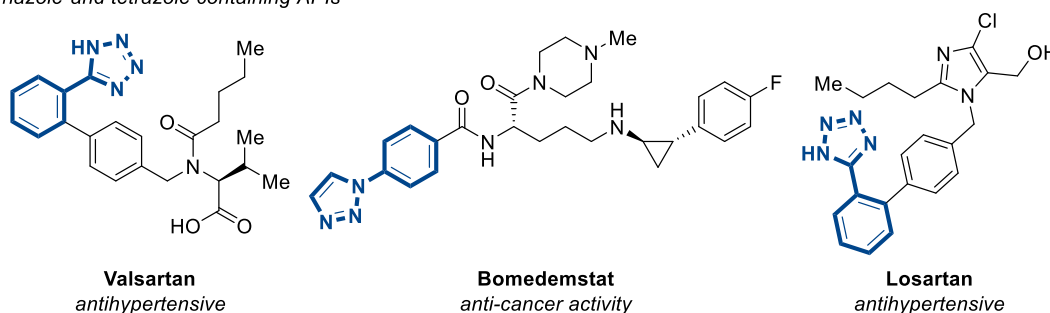
**Figure 2-3.** Electrochemical C7-indole alkenylation *via* rhodium catalysis.

### 3 Results and Discussion

#### 3.1 Ruthenium-Catalyzed C–H Arylation of *N*-Aryl Triazoles and Aryl Tetrazoles with Aryl Sulfonium Salts

Heteroaromatic rings are ubiquitous in medicinal chemistry.<sup>[138]</sup> Among them, *N*-aryl triazoles and aryl tetrazoles are fundamental components in a range of active pharmaceutical compounds. Specifically, the Angiotensin II receptor blockers, which include well-known medications, like Valsartan and Losartan, are a prominent class of APIs that contain tetrazole moieties (Figure 3-1).<sup>[139]</sup> Due to the similar size, polarity, planarity and ability to engage in hydrogen bonding, these five-membered *N*-heterocycles have been employed to replace amides and carboxylic acids in order to improve pharmacological characteristics of biologically active ingredients.<sup>[134]</sup> Tetrazoles and carboxylic acids have comparable  $pK_a$ -values and tautomeric behaviour, while 1,2,3-triazoles and cis-amides share close hydrogen bond donor and acceptor site orientations.

a) Triazole and tetrazole containing APIs



b) Medicinal relevance of triazoles and tetrazoles

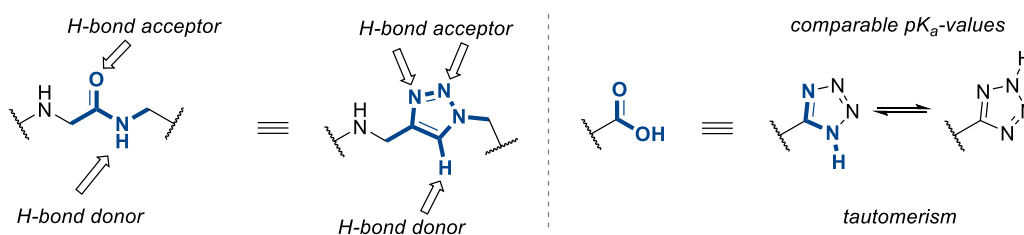


**Figure 3-1.** a) Representative examples of *N*-aryl triazoles and tetrazoles containing pharmaceuticals. b)

Triazoles and tetrazoles as cis-amide and carboxylic acid bonds mimics.

Given that the derivatization of the benzoid moiety is less explored, we envisioned to design a method capable of late-stage diversification including these relevant scaffolds, without the need for *de novo* syntheses known to be time and resources consuming. We were able to introduce triazoles and tetrazoles fragments into a variety of bioactive compounds *via* ruthenium(II)-catalyzed C–H arylation, using easily accessible dibenzothiophenium salts.

### 3.1.1 Optimization Studies

This work was carried out in collaboration with M.Sc. H. Simon in the Ackermann group. *N*-aryl triazole **131a** and L-phenyl alanine derived sulfonium salt **130** were selected as model substrates in the envisioned transformation. The salt **130** was easily accessed from the protected amino acid **129** by dibenzothiophenation and obtained in a 7:1 mixture of the *para* **130'** and *ortho* **130''** regioisomers (Figure 3-2).

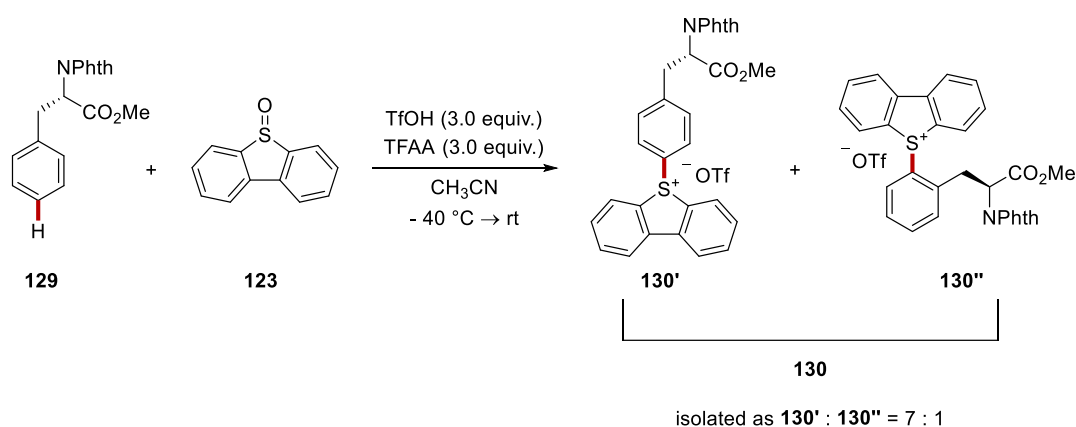
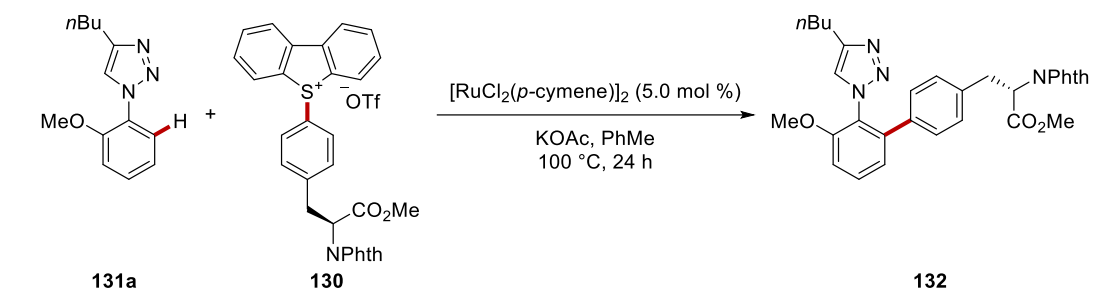


**Figure 3-2.** Synthesis of L-phenyl alanine derived sulfonium salt **130** as a regioisomeric mixture.

Several reaction conditions were tested, starting with  $[\text{RuCl}_2(p\text{-cymene})]_2$  as the catalyst (Table 3-1). We were pleased to see that a combination of toluene as reaction medium and simple KOAc as base afforded the desired arylated product **132** in 91% isolated yield (entry 1). The product was obtained with almost full retention of the chiral information of the amino acid (*e.r.* 94:6). Only the *para*-regioisomer **121'** reacted.

**Table 3-1.** Optimization studies for the ruthenium-catalyzed arylation of *N*-aryl triazole **131** with aryl sulfonium salt **130**.<sup>[a]</sup>





Entry	Deviation from standard conditions	Isolated yield of <b>132</b>
1	none	91% <sup>[b]</sup>
2*	<i>t</i> AmOH instead of PhMe	85%
3*	1,4-dioxane instead of PhMe	90%
4*	DCE instead of PhMe	43%
5	RuCl <sub>3</sub> instead of [RuCl <sub>2</sub> ( <i>p</i> -cymene)] <sub>2</sub>	--
6	[Cp*RhCl <sub>2</sub> ] <sub>2</sub> instead of [RuCl <sub>2</sub> ( <i>p</i> -cymene)] <sub>2</sub>	--
7	[Cp*IrCl <sub>2</sub> ] <sub>2</sub> instead of [RuCl <sub>2</sub> ( <i>p</i> -cymene)] <sub>2</sub>	--
8	no [RuCl <sub>2</sub> ( <i>p</i> -cymene)] <sub>2</sub>	--
9	80 °C instead of 100 °C	65%
10	60 °C instead of 100 °C	--
11*	blue LED irradiation at 450 nm at room temperature	5%

[a] Reaction conditions: **131a** (0.2 mmol), **130** (0.3 mmol), KOAc (0.4 mmol), [RuCl<sub>2</sub>(*p*-cymene)]<sub>2</sub> (5.0 mol %), toluene (2.0 mL), 100 °C, 24 h. \*Performed by H. Simon. [b] Enantiomeric ratios was determined by chiral HPLC to be *e.r.* 94:6.

Other solvents proved also viable for the envisioned transformation, namely *t*AmOH and 1,4-dioxane (entries 2 and 3), while in DCE a major drop in yield was observed (entry 4). Various transition-metal catalysts did not show any reactivity (entries 5–7). A control experiment demonstrated the fundamental role of the ruthenium catalyst (entry 8). A reaction temperature of 100 °C was found to be optimal, given that at 80 °C a significant loss in yield was registered (entry 9) and at 60 °C no product was observed

(entry 10). Subjecting the reaction to blue LED irradiation at 450 nm at ambient temperature did not give the product **132** (entry 11).

### 3.1.2 Substrate Scope

With the optimized reactions conditions in hand, we were keen to elucidate the robustness of and versatility of our methodology (Figure 3-3). We, first, explored the reactivity of different substituted *N*-aryl triazoles **131a–131k**. Alkyl, alkoxy, and halo substituents at the *ortho*-position of the aryl triazole **131a–131g** were well tolerated delivering the desired arylated products **132**, **134–139** in good to excellent yields. Moreover, triazole **131h** containing the *para*-methoxy phenyl substituent at the C5-position generated exclusively the monosubstituted product **140** in 88% yield, while small amounts of the diarylated product **141'** were obtained with bulkier groups at the C4-position. Interestingly, also 1-naphthyl triazole **131j** and 2-naphthyl derivative **131k** were within the scope of the reaction, although giving lower yields.

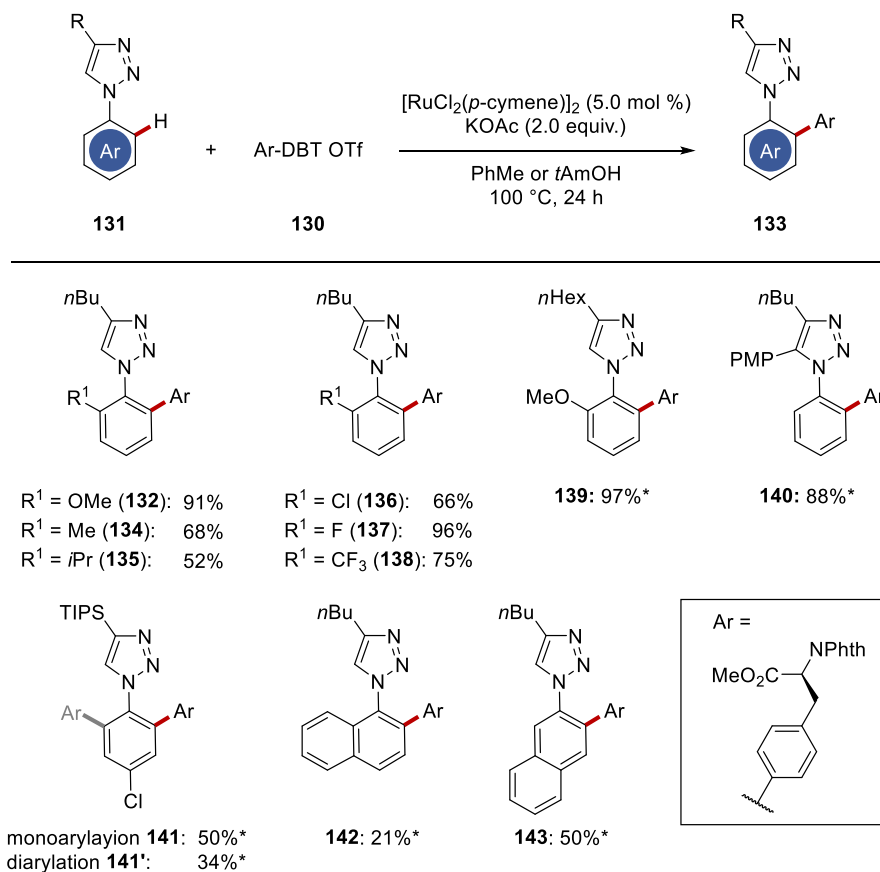


Figure 3-3. C–H Arylation of substituted *N*-aryl triazoles **131** with DBT salt **130**. \*Performed by H. Simon.

Our ruthenium-catalyzed arylation strategy tolerated a variety of substituted dibenzothiophenium salts **124** (Figure 3-4). Mildly or strongly electron-donating substituents in *para*-position on the arene moiety of the DBT salt were permitted (**145**–**149**). Also, aryl halides were amenable (**150**–**154**). Aryl sulfonium salts containing ester (**155**) or aldehyde (**156**) proved also compatible. Excellent yields were obtained employing protected catechol (**157**), cyclic (**158**), and N–H-free amide (**159**) substituted DBT salts. Additionally, heterocyclic pyrrole (**160**) and thiophene (**161**) derivatives were successfully incorporated.

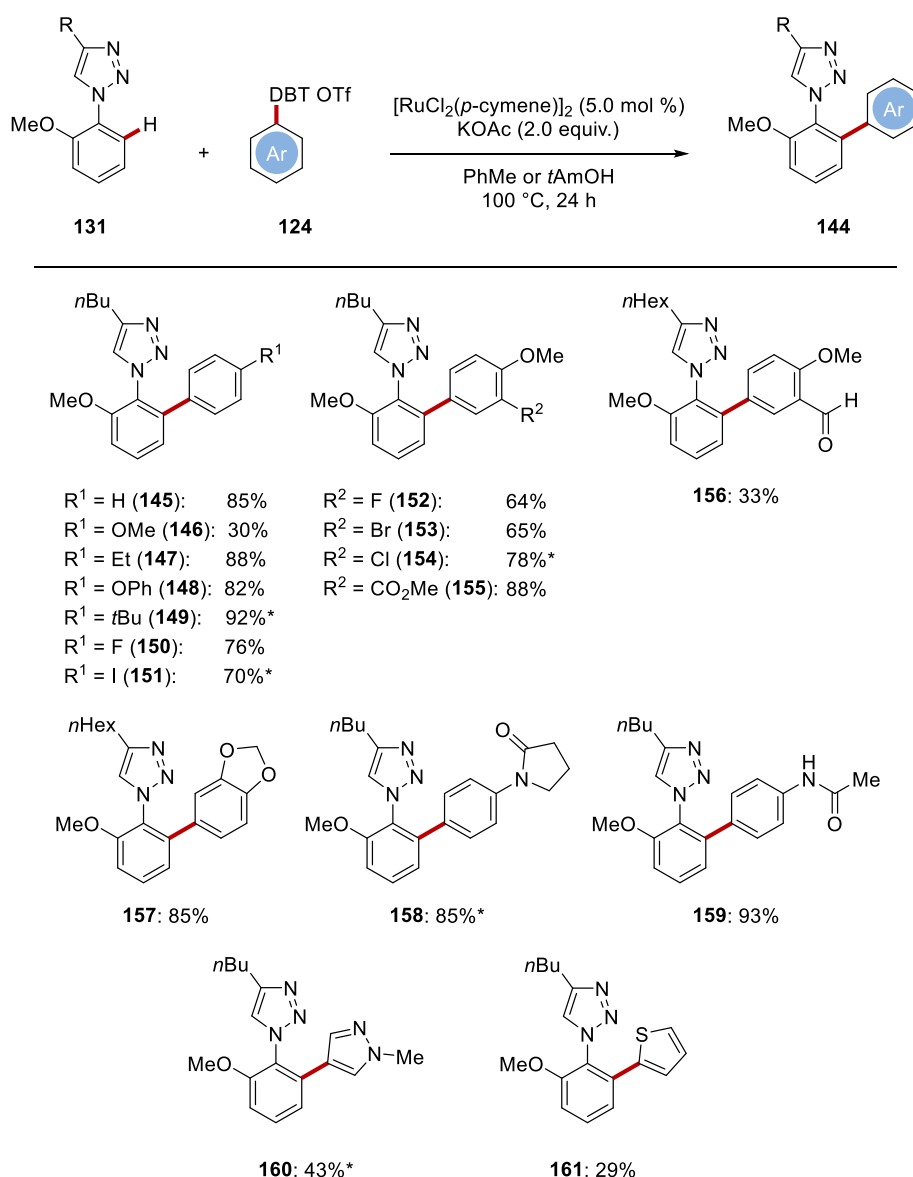
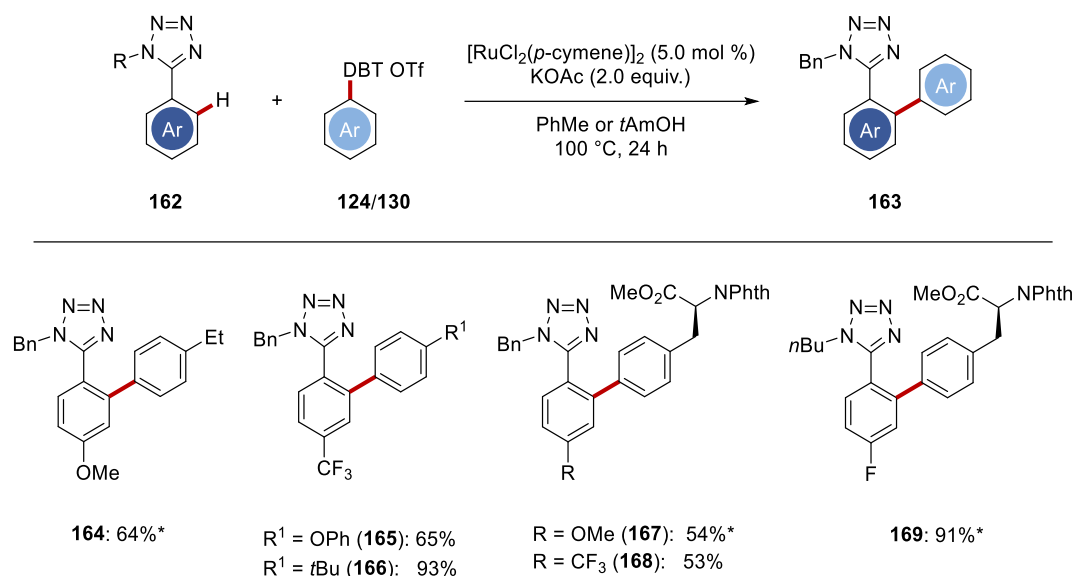


Figure 3-4. C–H Arylation of *N*-aryl triazoles **131** with substituted DBT salts **124**. \*Performed by H. Simon.

To further prove the versatility of our strategy, we turned the attention to substrates containing a tetrazole directing group **162** (Figure 3-5). Importantly, only mono arylated products **163** were formed here. Electron-rich substituted aryl sulfonium salts were suitable coupling partners (**164–166**). Moreover, high reactivity was observed with the amino acids derived reagent **130**. Aryl tetrazoles containing electron-donating ether **162a** as well as electron-withdrawing trifluoromethyl **162b** and fluoro **162c** groups gave good yields.



**Figure 3-5.** C–H Arylation of aryl tetrazoles **162** with substituted DBT salts **124** and **130**. \*Performed by H. Simon.

### 3.1.3 Late-Stage Incorporation of *N*-Aryl Triazoles and Tetrazoles

Eventually, we wondered whether our approach could be used to incorporate useful triazole and tetrazole derivatives (see above) into highly functionalized, medically relevant compounds. It was encouraging to observe that our strategy gave satisfactory reactivity even with complex dibenzothiophenium salts **170** (Figure 3-6). Several sulfonium salts **170** derived from active pharmaceutical ingredients or natural products were successfully modified and purified by simply being poured into diethylether, without the need for column chromatography. Many functionalities were thereby tolerated, such as the pentaacyl-Salicin derivative, displaying glucose, which was

efficiently utilized leading to the desired sugar containing product **172** in high yield. Likewise, challenging *ortho*-substituted sulfonium salts **170b** and **170e–170g** efficiently delivered the arylated products **173** and **176–178**, specifically derivatives of the anti-inflammatory drug Indomethacin, Gemfibrozil, Clofibrate or Aniracetam. Sulfonamides present in Tianeptine precursor (**174**) or Nimesulide derivative (**175**) were well tolerated. Despite with slightly lower yield of the desired product **179**, Boscalid, featuring a highly reactive 2-chloro pyridine, proved to be suitable. Finally, Ticlopidine (**180**), a heteroaromatic sulfonium salt, underwent arylation with excellent outcome.

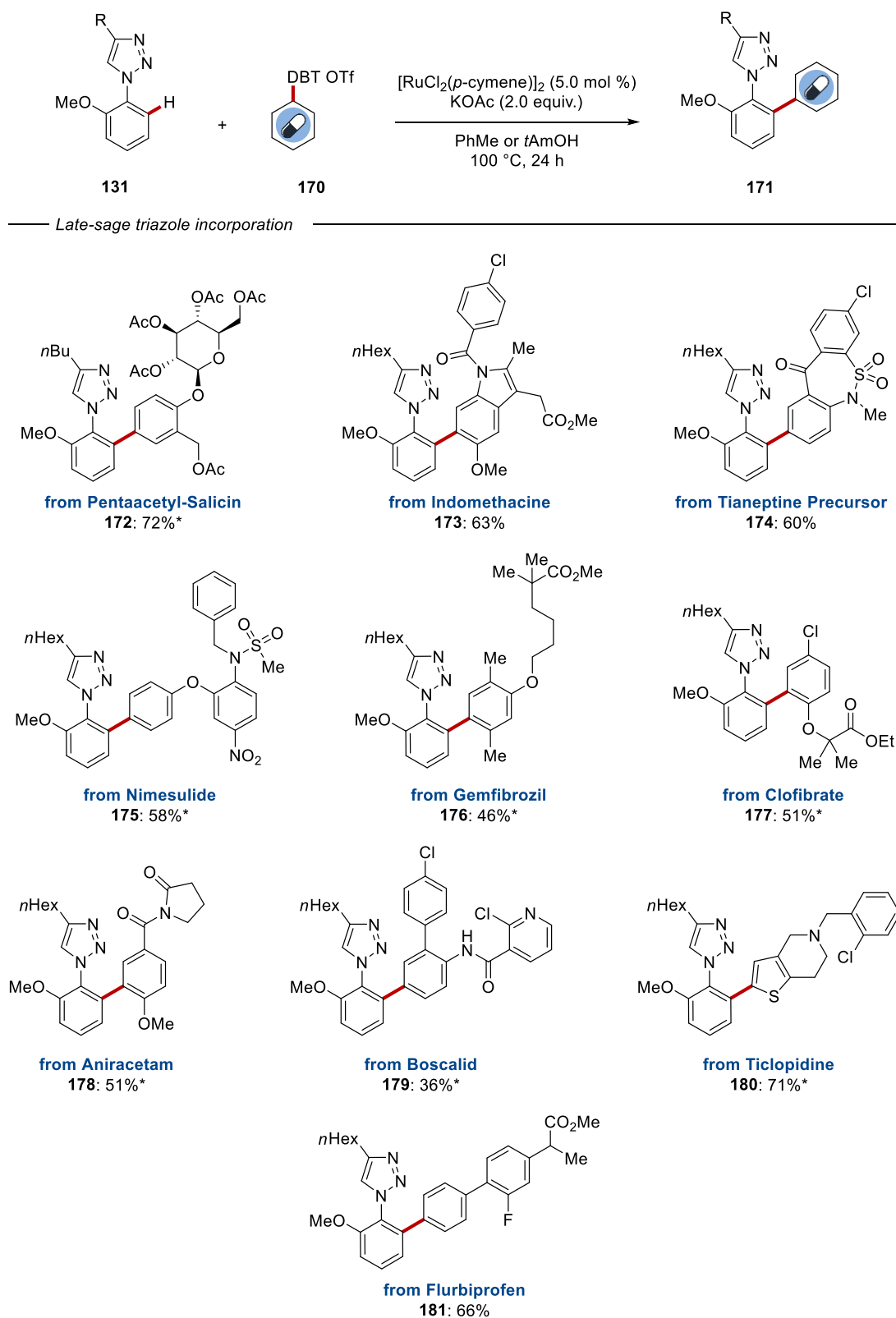


**Figure 3-6.** C–H Arylation of *N*-aryl triazoles **131** with APIs derived DBT salts **170**. \*Performed by H. Simon.

To our delight, the late-stage incorporation of highly decorated scaffolds could be applied to challenging aryl tetrazoles **162** (Figure 3-7). Good yields of the desired products **183** and **184** were achieved in case of the pentaacetyl-Salicin and Tianeptine derived dibenzothiophenium salts. Biaryl containing Flurbiprofen was incorporated with higher efficacy into the electron-poor aryl tetrazole **162b** compared to the electron-rich **162a**; the corresponding products **186** and **185** were afforded in 82% and 45% yield, respectively. *ortho*-Substituted arylating agent, Aniracetam (**187**), and Boscalid (**188**) were also suitable coupling partners in the late-stage incorporation of aryl tetrazoles **162**.

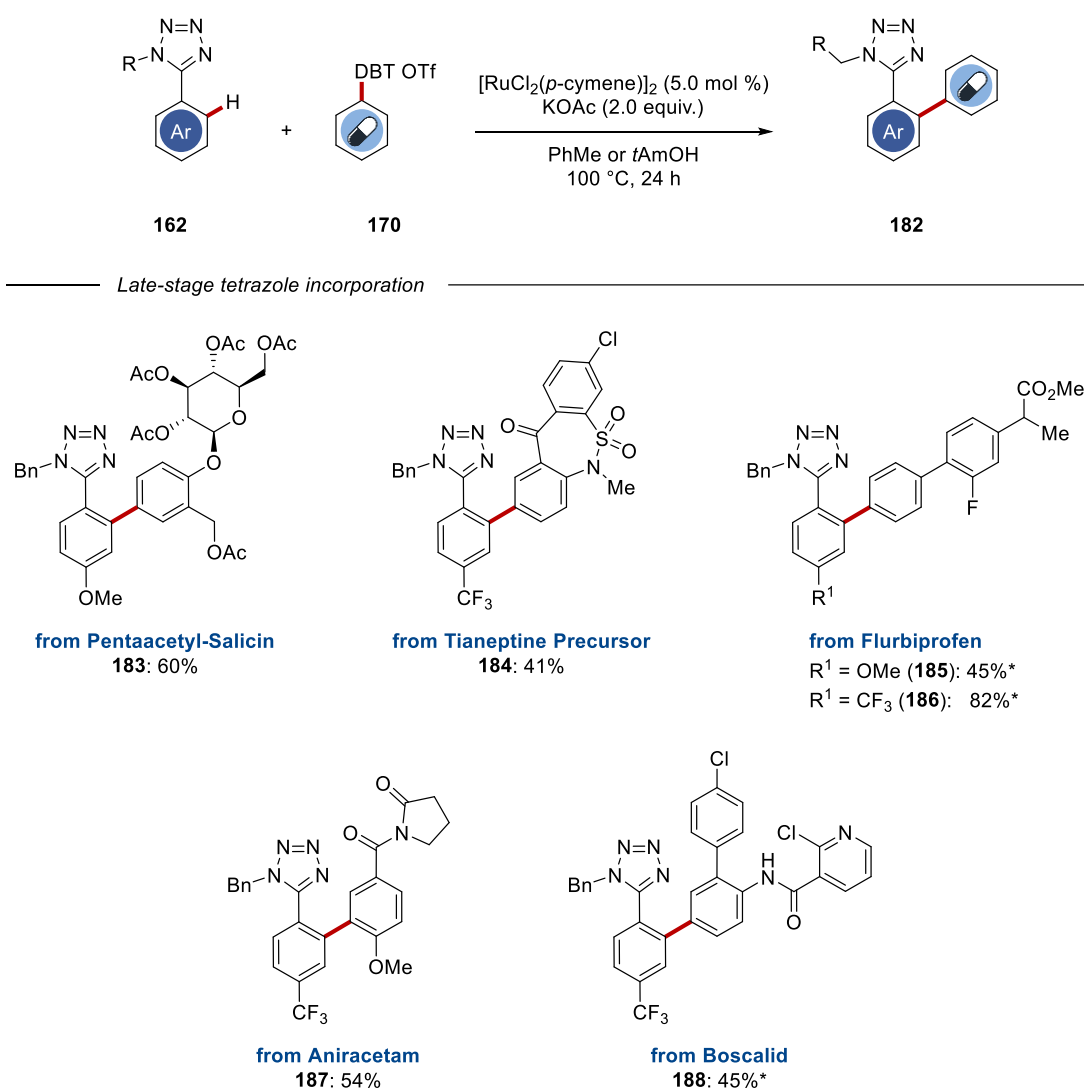


**Figure 3-7.** C–H Arylation of aryl tetrazoles **162** with APIs derived DBT salts **170**. \*Performed by H. Simon.

### 3.1.4 Mechanistic Investigation

After assessing the versatility of our methodology, we started investigating its mode of action. As shown in the substrate scope, our reaction manifold tolerates the presence of several aryl halides. Thus, we studied competition experiments between the aryl sulfonium salt **124e** and the aryl halides **189–191** (Figure 3-8).

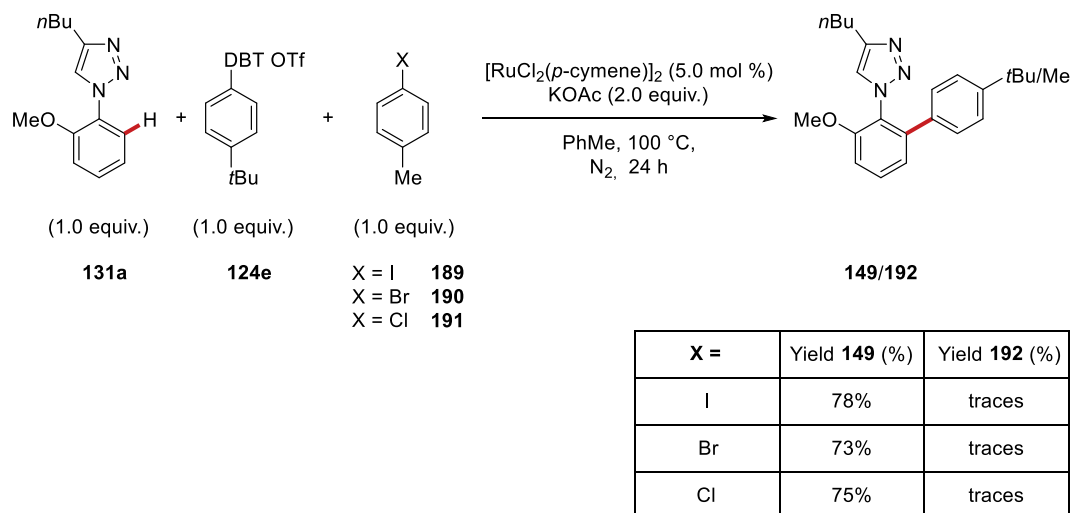


**Figure 3-8.** Competition experiment between aryl sulfonium salt **124e** and aryl halides **189–191**.

Performed by H. Simon.

In all three cases, the product formation derived from the aryl sulfonium salt **124e** and only traces of products from the aryl halides. This result highlights the higher reactivity of the aryl sulfonium salt in comparison to the corresponding halides, and demonstrates the orthogonal selectivity for the electrophilic coupling partner, which allows future modification of the unreacted aryl halide. Next, we became interested in the way the aryl sulfonium salt is activated. A C–S bond activation by single electron reduction followed by homolytic bond cleavage would lead to the formation of open shell aryl species. As a consequence, radical scavengers should prevent the product formation if this mode of action is operative. In order to validate the hypothesis, we performed the standard reaction in the presence of stoichiometric amounts of TEMPO, diphenylethylene, or BHT (Figure 3-9). No major influence on the yield could be identified, with the exception of the reaction including TEMPO. Therefore, it is



improbable that a mechanism involving the single-electron reduction of the aryl sulfonium salt and a subsequent radical generation would be active.

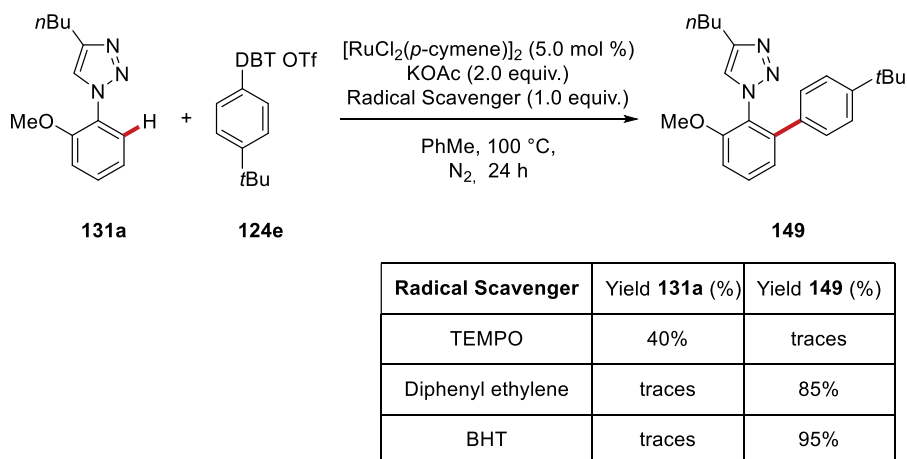
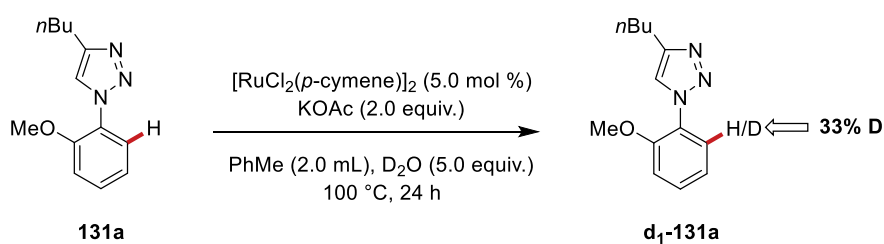


**Figure 3-9.** Radical scavenger experiments.

Another important point was to prove a potential reversibility of the C–H activation. Hence, we performed a first experiment under the standard reaction conditions in the presence  $D_2O$  as deuterium source (**Figure 3-10b**) and repeated the same setup without the sulfonium salt **124e** (**Figure 3-10a**). Significant deuterium incorporation in the starting material **131a** was observed *via* NMR-spectroscopic analysis.

a) Deuterium exchange without coupling partner



b) Standard reaction in the presence of  $D_2O$

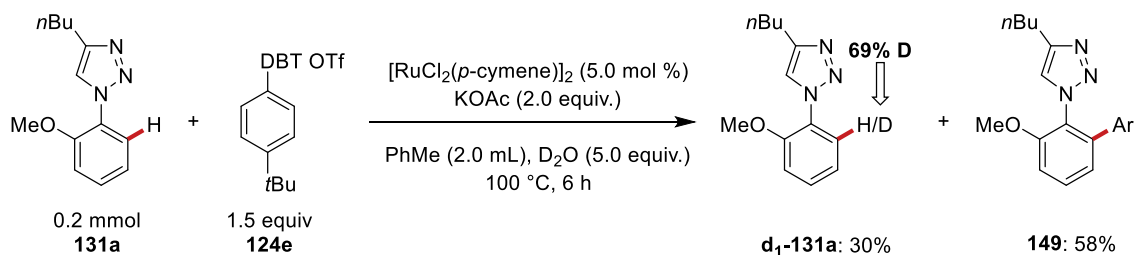


**Figure 3-10.** Deuterium exchange experiments.

We were then able to gain deeper insights into the nature of the active catalytic species by monitoring the reaction by GC (Figure 3-11). It turned out that with the progressing product formation significant amount of the *p*-cymene (**193**) dissociated from the ruthenium, suggesting that a *p*-cymene free catalytically active complex could be operating.<sup>[140]</sup>

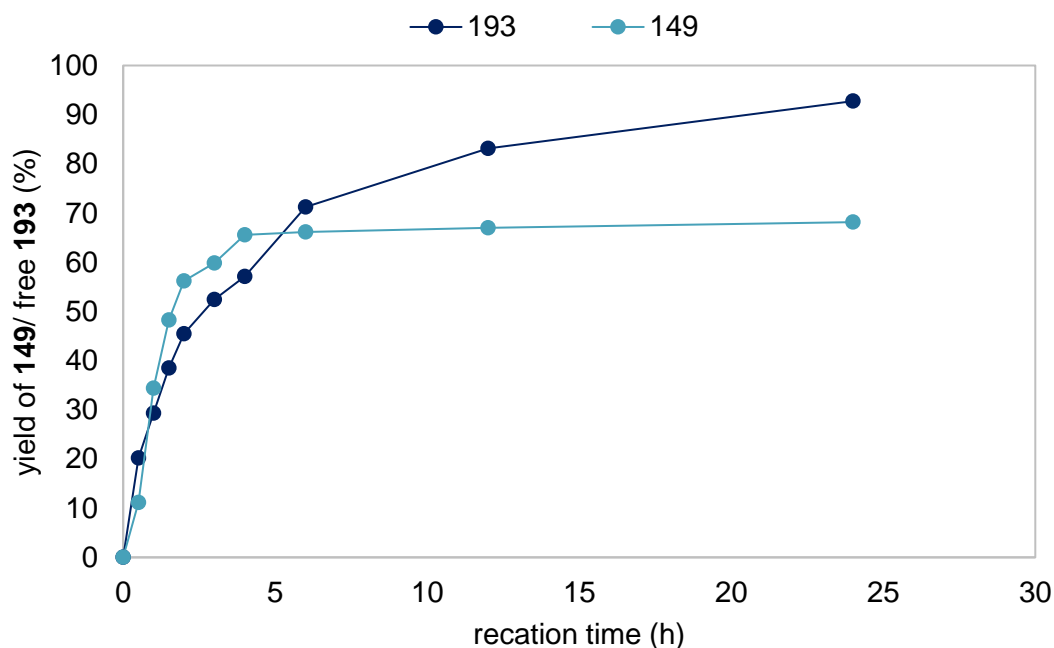


Figure 3-11. Reaction profile monitoring free *p*-cymene **193** and product **149** formation.

To further support this hypothesis, a catalyst poisoning experiment was conducted (Figure 3-12). The reaction performance was indeed drastically reduced by the addition of *p*-cymene **193**.

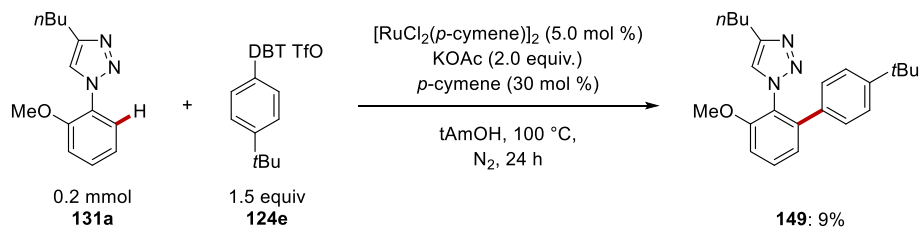
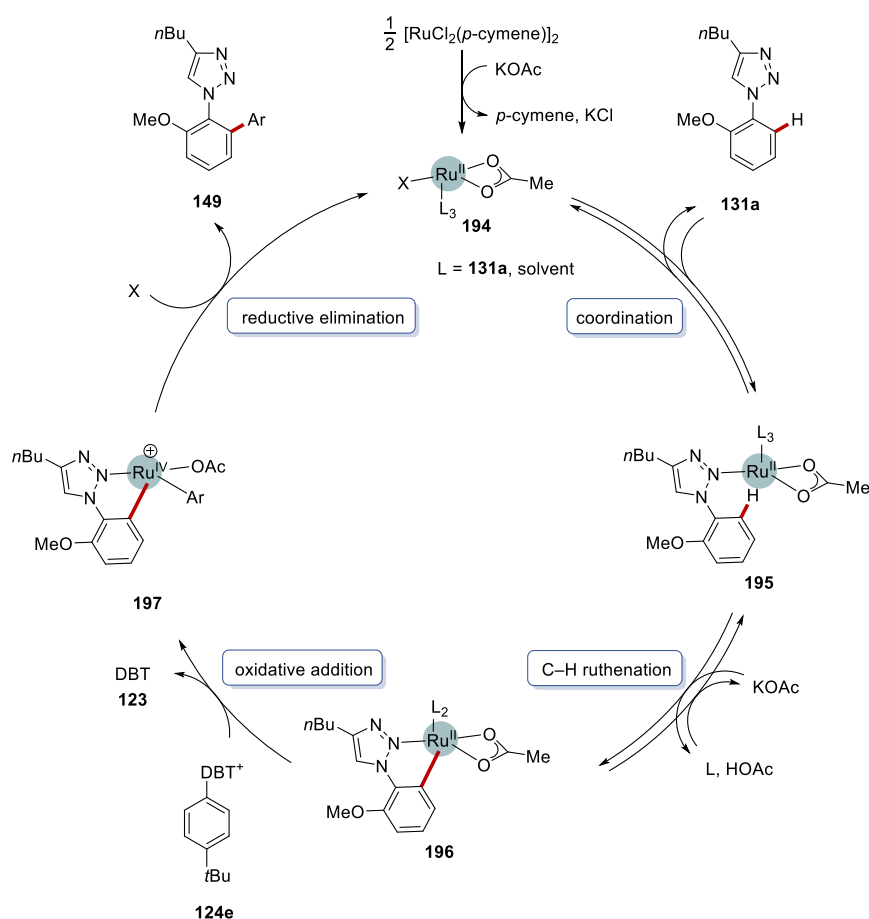


Figure 3-12. Poisoning experiment.

### 3.1.5 Proposed Catalytic Cycle

Based on our mechanistic investigations and the literature precedents,<sup>[57]</sup> we propose the following catalytic cycle (Figure 3-13). First, the active catalytic species **194** is generated by dissociation of *p*-cymene. Subsequent coordination by the Lewis-basic triazole **131a** gives ruthenium(II) complex **195**, which then *via* a reversible C–H ruthenation converts into the ruthenium(II) intermediate **196**. Oxidative addition of the aryl sulfonium salt **124e** produces complex **197**. Finally, reductive elimination furnishes the desired product **149** and regenerates the active catalytic species **194**.



**Figure 3-13.** Proposed catalytic cycle for the ruthenium-catalyzed C–H arylation.

## 3.2 Photo-Induced Ruthenium-Catalyzed C–H Alkylation at Ambient Temperature

Alkylation reactions are among the most useful C–C bond-forming transformations, because the allyl group can enhance synthetic utility and serve as a handy grip for subsequent manipulation.<sup>[141]</sup> In addition, their abundance in bioactive species makes them essential in flavor and fragrance industries as well as medical and pharmaceutical companies. While there are many synthetic routes to incorporate an allyl moiety,<sup>[142]</sup> C–H activation is highly desirable, since it assures selective product formation by precluding extra steps and reducing byproduct formation. Known reports often require harsh reaction conditions.<sup>[143]</sup> Direct C–H functionalizations are also possible at room temperature through photoredox catalysis,<sup>[144]</sup> however additional iridium<sup>[145]</sup> or ruthenium<sup>[146a, 87, 146b]</sup> photocatalysts are frequently needed for these catalytic reactions. To avoid this problem, the groups of Ackermann<sup>[92]</sup> and later Greaney<sup>[93]</sup> revealed visible light-induced remote C–H alkylations, using ruthenium as the sole catalyst. These techniques demonstrated that an *in situ* generated cyclometalated ruthenium complex served both as the photocatalyst and for the C–H activation. Inspired by these results, we have developed a photo-induced ruthenium-catalyzed C–H alkylation, which does not require any additional photocatalyst.

### 3.2.1 Optimization Studies

We commenced our studies by probing various reaction media to enable the formation of the desired alkylation product using the arene **22** and the allyl bromide **198**, in the presence of [Ru(OAc)<sub>2</sub>(*p*-cymene)] and K<sub>2</sub>CO<sub>3</sub> (Table 3-2).

**Table 3-2.** Optimization studies for the photo-induced ruthenium-catalyzed C–H allylation of arene **22** with allyl bromide **201**.<sup>[a]</sup>



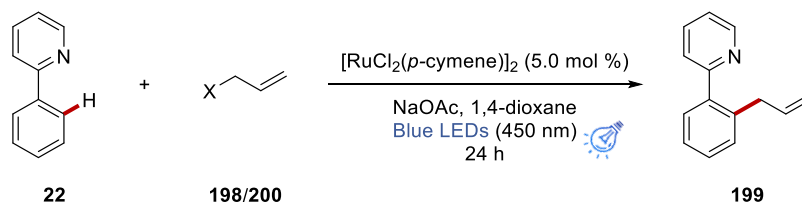
Entry	Deviation from standard conditions	Isolated yield of <b>199</b>
1	none	61%
2	DCE instead of 1,4-dioxane	traces
3	DMA instead of 1,4-dioxane	11%
4	TFE instead of 1,4-dioxane	52%
5	PhMe instead of 1,4-dioxane	15%
6	THF instead of 1,4-dioxane	37%
7	DMF instead of 1,4-dioxane	31%
8	HFIP instead of 1,4-dioxane	33%
9	$\text{Na}_2\text{CO}_3$ instead of $\text{K}_2\text{CO}_3$	49%
10	$\text{K}_3\text{PO}_4$ instead of $\text{K}_2\text{CO}_3$	60%
11	KOAc instead of $\text{K}_2\text{CO}_3$	traces
12	$\text{PPh}_3$	25%
13	$(\text{PhO})_2\text{P}(\text{O})\text{OH}$	27%
14	$\text{P}(\text{4-CF}_3\text{C}_6\text{H}_4)_3$	--
15	$[\text{RuCl}_2(p\text{-cymene})]_2$	63% <sup>[b]</sup>
16	$\text{Ru}_3(\text{CO})_{12}$	--

[a] Reaction conditions: **22** (0.5 mmol), **198** (0.75 mmol),  $\text{K}_2\text{CO}_3$  (1.0 mmol),  $[\text{Ru}(\text{OAc})_2(p\text{-cymene})]$  (10 mol %), 1,4-dioxane (2.0 mL), under  $\text{N}_2$ , 30–33 °C, 24 h, blue LEDs (450 nm). [b] NaOAc instead of  $\text{K}_2\text{CO}_3$ .

Among the various solvents tested (entries 1–8), 1,4-dioxane proved to be the most suitable, delivering the product **199** in 61% isolated yield (entry 1). Other commonly used reaction media, such as DCE or DMA were inefficient (entries 2, 3). TFE gave moderate results, however, also the diallylated product was observed here (entry 4). We continued our studies with bases (entries 9–11), which led to lower efficacy. Different additives did not improve the yield of the product **199** (entries 12–14). Thus, we examined other ruthenium sources. A combination of  $[\text{RuCl}_2(p\text{-cymene})]_2$  and the carboxylate base NaOAc led to slightly improved results (entry 15) and were ultimately chosen as the optimal conditions.

Notably, allyl bromide **198** proved to be the most effective substrate in the photo-induced allylation (Table 3-3). The reaction of allyl chloride **200a** failed to deliver the desired product **199** in high yield (entry 2). Other allyl species **200b–200e** were completely ineffective.

**Table 3-3.** Screening of allyl species for the photo-induced ruthenium-catalyzed allylation.<sup>[a]</sup>



Entry	X	Isolated yield of <b>199</b>
1	Br	63%
2	Cl	10%
3	OAc	--
4	OCO <sub>2</sub> Me	--
5	OP(O)(OC <sub>2</sub> H <sub>5</sub> ) <sub>2</sub>	--
6	OH	--

[a] Reaction conditions: **22** (0.5 mmol), **198** and **200a–200e** (0.75 mmol), NaOAc (1.0 mmol),  $[\text{RuCl}_2(p\text{-cymene})]_2$  (5.0 mol %), 1,4-dioxane (2.0 mL), under N<sub>2</sub>, 30–33 °C, 24 h, blue LEDs (450 nm).

Control experiments (Table 3-4) demonstrated the crucial role of the ruthenium catalyst and of the light (entries 1, 2). Furthermore, when the reaction was performed under air atmosphere, no desired product was formed (entry 3). Carrying out the reaction in thermal conditions at 100 °C led to only traces of several isomers (entry 4).

**Table 3-4.** Control experiments for the photo-induced ruthenium-catalyzed allylation.<sup>[a]</sup>

Entry	Deviation from standard conditions	Isolated yield of <b>199</b>
1	no [Ru]	--
2	no light	--
3	under air	--
4	at 100 °C	traces <sup>[b]</sup>

[a] Reaction conditions: **22** (0.5 mmol), **198** (0.75 mmol), NaOAc (1.0 mmol), [RuCl<sub>2</sub>(*p*-cymene)]<sub>2</sub> (5.0 mol %), 1,4-dioxane (2.0 mL), under N<sub>2</sub>, 30–33 °C, 24 h, blue LEDs (450 nm). [b] Without blue light irradiation.

### 3.2.2 Substrate Scope

Having the optimized reaction conditions in hand, the versatility of the photo-induced ruthenium-catalyzed allylation reaction was investigated (Figure 3-14). This protocol tolerated both pyridine **22** and **201a**, pyrazole **201b–201d** and oxazoline **201c** directing groups. Electron-donating methyl (**204**) and methoxy (**203**, **205**) substituents were within the scope of the reaction. Also, phenyl pyrazole **201d** bearing an electron-withdrawing trifluoromethyl substituent at the *ortho*-position could be converted into the desired product **206** in high yield.

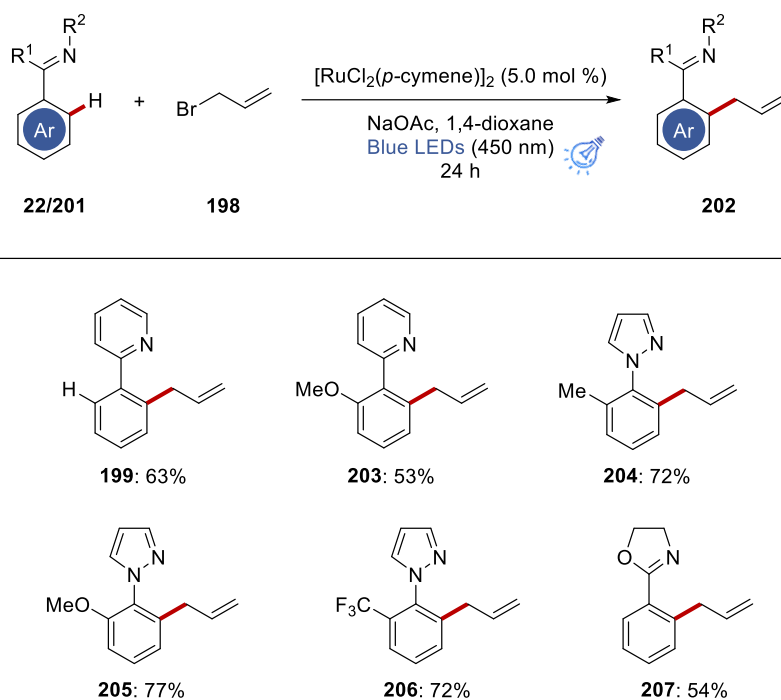


**Figure 3-14.** Allylation of arenes **22** and **201** and allyl bromide **198**.

Despite the variety of substrates tested, many of them failed to deliver the desired allylated product (**Figure 3-15**). Specifically, *para* (**208–210**, **213**) and *meta* (**211**, **212**, **214**, **215**) substituents on the arenes did not give mono- and diallylated products. Moreover, the photo-induced ruthenium allylation reaction did not tolerate pyrimidine (**216**, **217**) and triazole (**218**) directing groups, as well as sterically hindered pyrazole directing group (**219**).



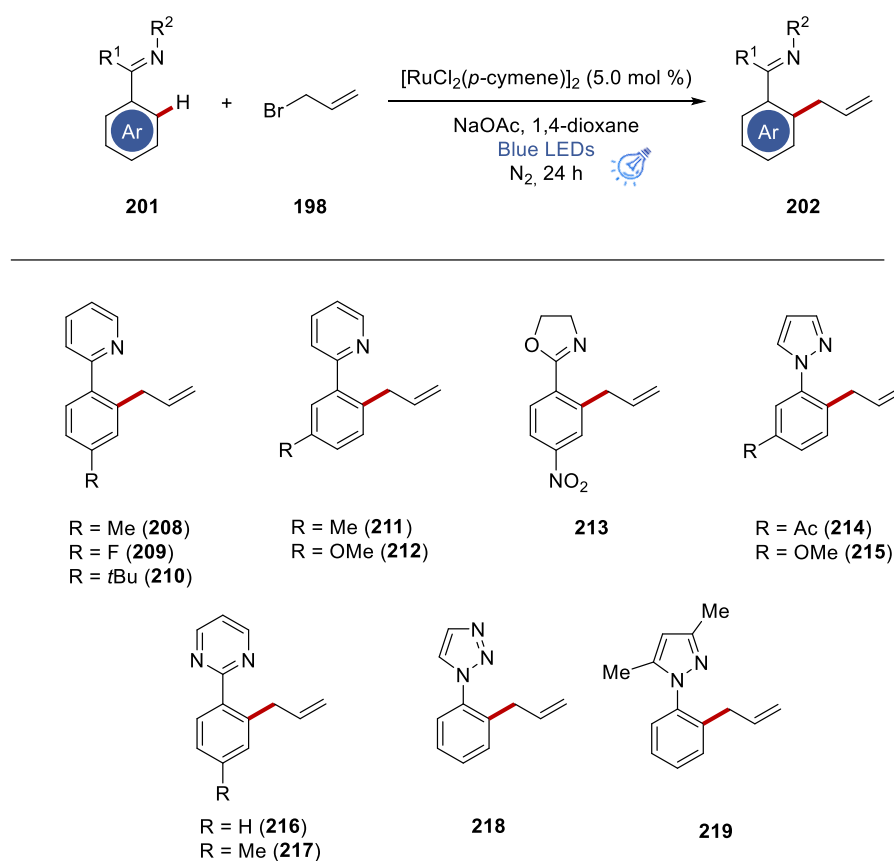
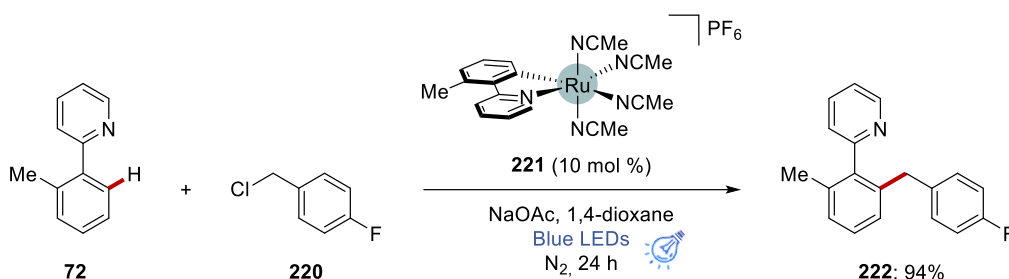


**Figure 3-15.** Failed substrates in the allylation of arenes **201** and allyl bromide **198**.

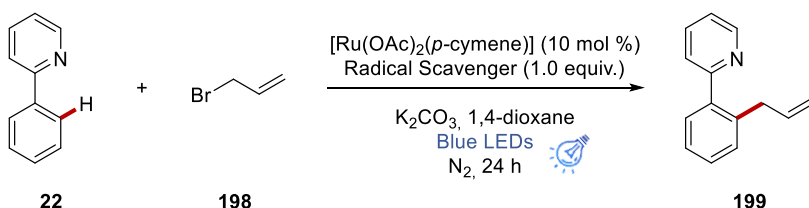
### 3.2.3 Mechanistic Investigation

Next, we became interested in defining the mode of action of the photo-induced ruthenium-catalyzed functionalization of arenes. As part of a bigger project on benzylic and allylic transformations,<sup>[147]</sup> the mechanistic studies were carried out together with Dr. K. Korvorapun and Dr. J. Struwe. To this end, a cationic monocyclometalated complex was tested and proved to be highly effective in the presence of NaOAc (**Figure 3-16a**). These findings were suggestive of a carboxylate-ligated, arene-ligand-free ruthenacycle being a key intermediate in the C–H benzylation/allylation.<sup>[140]</sup> Furthermore, a light on/off experiment performed by Dr. J. Struwe was indicative of the photoredox arylation not involving a radical chain process.<sup>[147]</sup> Consequently, radical scavengers were added to the standard conditions; as a result, the formation of the corresponding product was significantly reduced (**Figure 3-16b**).

## a) Cyclometalated complex as catalyst



## b) Radical scavenger experiments



Radical Scavenger	Yield <b>22</b> (%)	Yield <b>199</b> (%)
TEMPO	52%	40%
Diphenyl ethylene	55%	34%

**Figure 3-16.** a) Light-driven benzylation catalyzed by cyclometalated ruthenium **221**. Performed by Dr. J Struwe. b) Radical scavenger experiments.

## 3.2.4 Proposed Catalytic Cycle

Based on our mechanistic investigations and our earlier findings,<sup>[148, 92]</sup> a reasonable catalytic cycle is depicted in **Figure 3-17**. The mechanism begins with the dissociation of the *p*-cymene ligand and twofold carboxylate-assisted C–H ruthenation, which results in the generation of species **223**. Subsequent coordination with allyl bromide **198** affords ruthenium complex **224**. Then, blue light absorption leads to the singlet excited species **224\***. A long-lived triplet ruthenacycle **224\*\*** is produced as a result of relaxation through intersystem crossing. Subsequently, an inner-sphere electron transfer to allyl bromide delivers ruthenium(III) intermediate **225** and allyl radical **226**. Then, a stable ruthenium(IV) complex **227** is formed by fast radical recombination. This complex then undergoes ligand exchange and reductive elimination to provide the

allylated product **199** and the monocyclometalated species **228**, which is converted into the active catalytic species **223** via C–H activation.

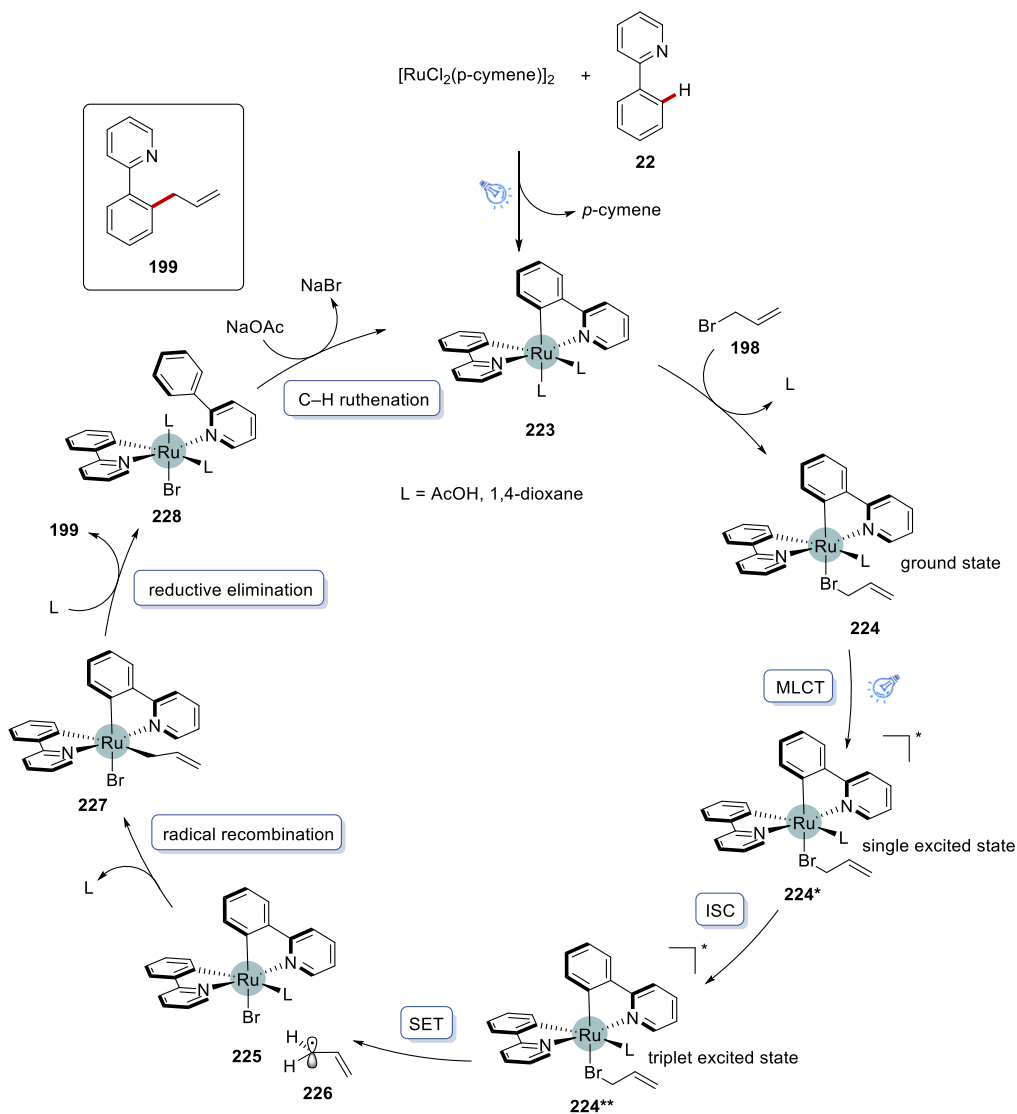


**Figure 3-17.** Proposed catalytic cycle for the photo-induced ruthenium-catalyzed allylation of arenes.

### 3.3 Electrooxidative C7-Indole Alkenylation *via* Rhodium Catalysis

Indoles and their substituted derivatives have emerged as one of the most investigated groups of organic molecules, given their application as functional building blocks in numerous marketed pharmaceuticals and molecular materials (Figure 3-18).<sup>[149]</sup> As a precursor, indole features one N–H and six distinctive C–H functionalization sites, yet given the intrinsic reactivity of the pyrrole ring, methodologies to access the C2- and C3-positions rather than the less reactive benzenoid positions have mainly been examined. Therefore, the design of syntheses with complementary site-selectivity is of great scientific interest.<sup>[77c, 150]</sup> Transition-metal catalysis has been shown to favor the functionalization of indoles,<sup>[151]</sup> nonetheless, protocols directing the selectivity to the C7-position remained scarce.<sup>[152]</sup> Recently C7-alkenylation and arylation of indoles were developed, which however displayed the restraints given by the use of superstoichiometric amounts of silver and copper as chemical oxidants.<sup>[78, 153]</sup> Our protocol merges organic electrochemistry with C–H activation to provide a novel platform for site-selective<sup>[154]</sup> C7-functionalization of indoles, which addresses the aforementioned limitation. To this end, we reported the first electrochemical C7-alkenylation of indole using a weakly coordinating<sup>[155]</sup> pivaloyl directing group to access biorelevant molecules and enable their diversification.<sup>[156]</sup>

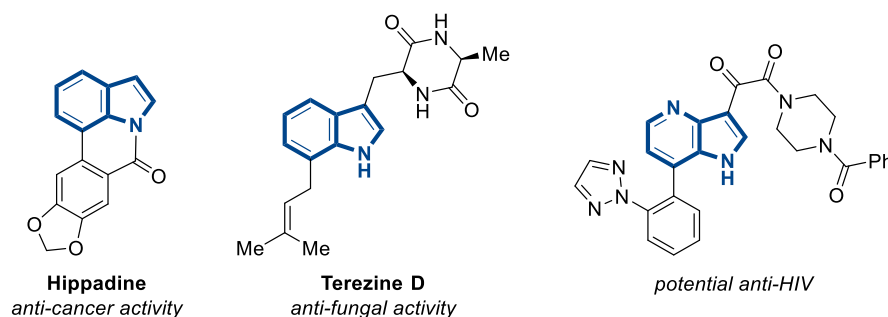


Figure 3-18. APIs and natural products displaying the indole moiety.



## Results and Discussion

Entry	Deviation from standard conditions	Isolated yield of <b>230</b>
1	none	61%
2	Pd(OAc) <sub>2</sub> instead of [Cp*RhCl <sub>2</sub> ] <sub>2</sub>	--
3	[Cp*IrCl <sub>2</sub> ] <sub>2</sub> instead of [Cp*RhCl <sub>2</sub> ] <sub>2</sub>	14%
4	without electricity	--
5	without [Cp*RhCl <sub>2</sub> ] <sub>2</sub>	--
6	At 80 °C instead of 90 °C	54%
7	At 50 °C instead of 90 °C	traces
8	under air	48%
9	1.0 mA instead of 4.0 mA	10%
10	3.0 mA instead of 4.0 mA	48%
11	5.0 mA instead of 4.0 mA	23%
12	6.0 mA instead of 4.0 mA	--
13	CPE = 0.7 V (vs Ag/Ag <sup>+</sup> )	28%
14	divided cell	5%
15	HFIP instead of TFE	9%
16	<i>t</i> AmOH/H <sub>2</sub> O (3:1) instead of TFE	traces
17	NaOPiv instead of NaOAc	10%
18	<i>n</i> Bu <sub>4</sub> NPF <sub>6</sub> (0.25 mmol)	27%
19	glassy carbon instead of graphite felt	--
20	with IKA ElectraSyn 2.0	52% <sup>[b]</sup>

[a] Reaction conditions: undivided cell, graphite felt (GF) anode, Pt cathode, constant current electrolysis (CCE = 4.0 mA), **67a** (0.5 mmol), **229** (1.5 mmol), NaOAc (0.5 mmol), [Cp\*RhCl<sub>2</sub>]<sub>2</sub> (5.0 mol %), TFE (2.0 mL), under N<sub>2</sub>, 90 °C, 24 h. [b] **67a** (0.75 mmol), **229** (2.25 mmol), TFE (3.0 mL).

The choice of the directing group was essential to achieve the desired C7-site-selectivity. Thus, numerous *N*-substituted directing groups in substrate **231** were tested (Figure 3-19). Despite the variety of ketones, amides, esters, phosphine oxides, sulfones, and pyridines used, only *N*-pivaloylindole **67a** led to the desired alkenylated product.

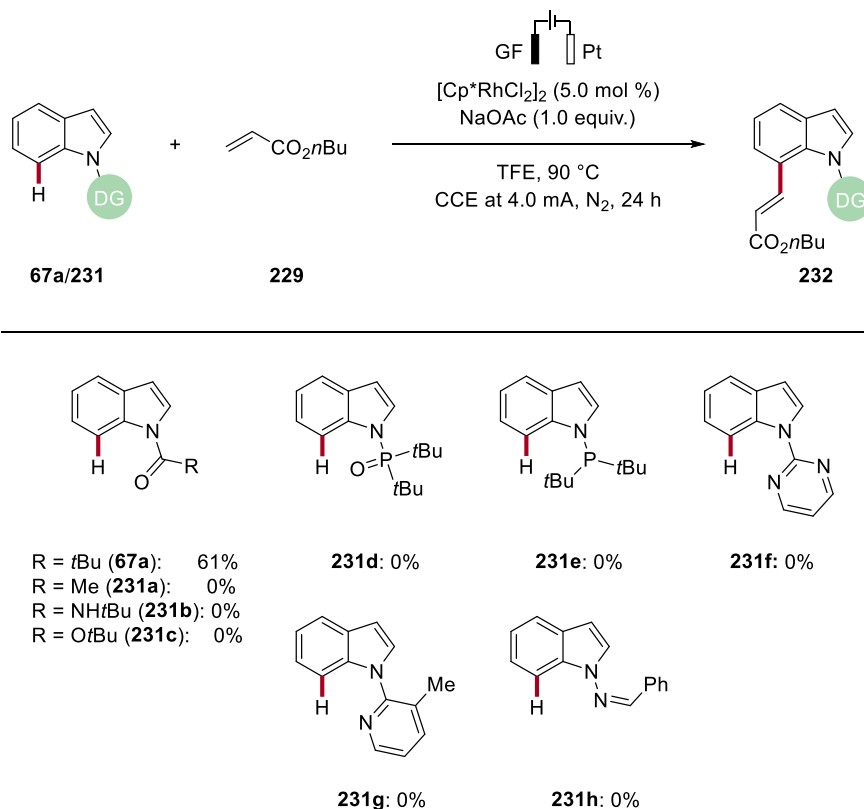


**Figure 3-19.** Electrooxidative C7-alkenylation of indoles **231** displaying different *N*-substituents.

### 3.3.2 Substrate Scope

With the optimized reaction conditions in hand, we were keen to elucidate the robustness of our methodology. First, indoles **67** bearing different substituents at the C3-, C4-, and C5-positions were investigated (Figure 3-20). Electron-rich indoles **67b–67e** and **67g** were transformed into the alkenylated products **233–236**, and **238**, maintaining good efficacy. In addition, indole **67f** bearing a fluoro substituent at the C5-position was compatible. Moreover, aryl substituted indole **67h** was also viable. We were delighted to observe that amino acid-containing indole **67i** was also successfully

alkenylated at the C7-position in moderate yield, showcasing the versatility of the transformation.

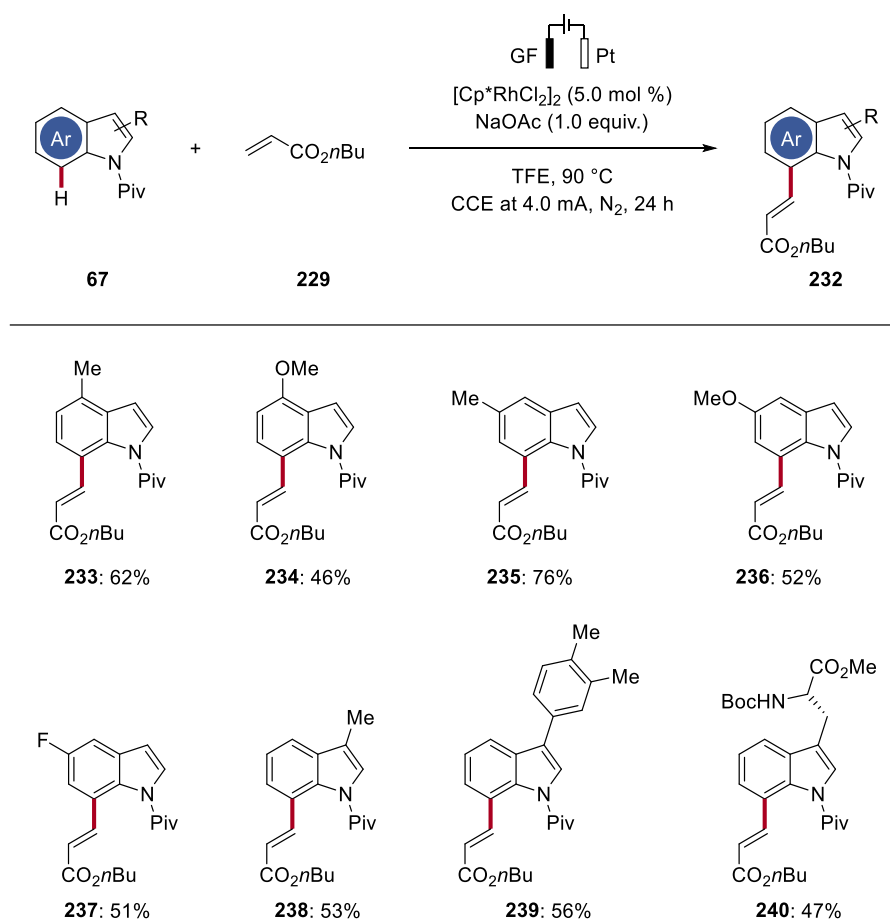


**Figure 3-20.** Electrooxidative C7-alkenylation of substituted indoles **67** with acrylate **229**.

Additionally, a number of acrylates **106** with various electronic substituents were effectively used, demonstrating the efficacy of this technique (Figure 3-21). Commercially accessible alkyl and benzyl acrylates gave moderate to high yields of the target products **242–246**. Thus, octyl acrylate provided the corresponding C7-functionalized indole **247** in 58% isolated yield. Remarkably, fluoro-substituted acrylates were successfully transformed into the envisioned indole-C7-alkenyl derivatives **248–250** with excellent site selectivity. Acrylates derived from natural products, such as menthol (**251**) and galactose (**252**), proved viable in the C7-electro functionalization. Likewise, sterically demanding acrylates (**253**) were suitable coupling partners.



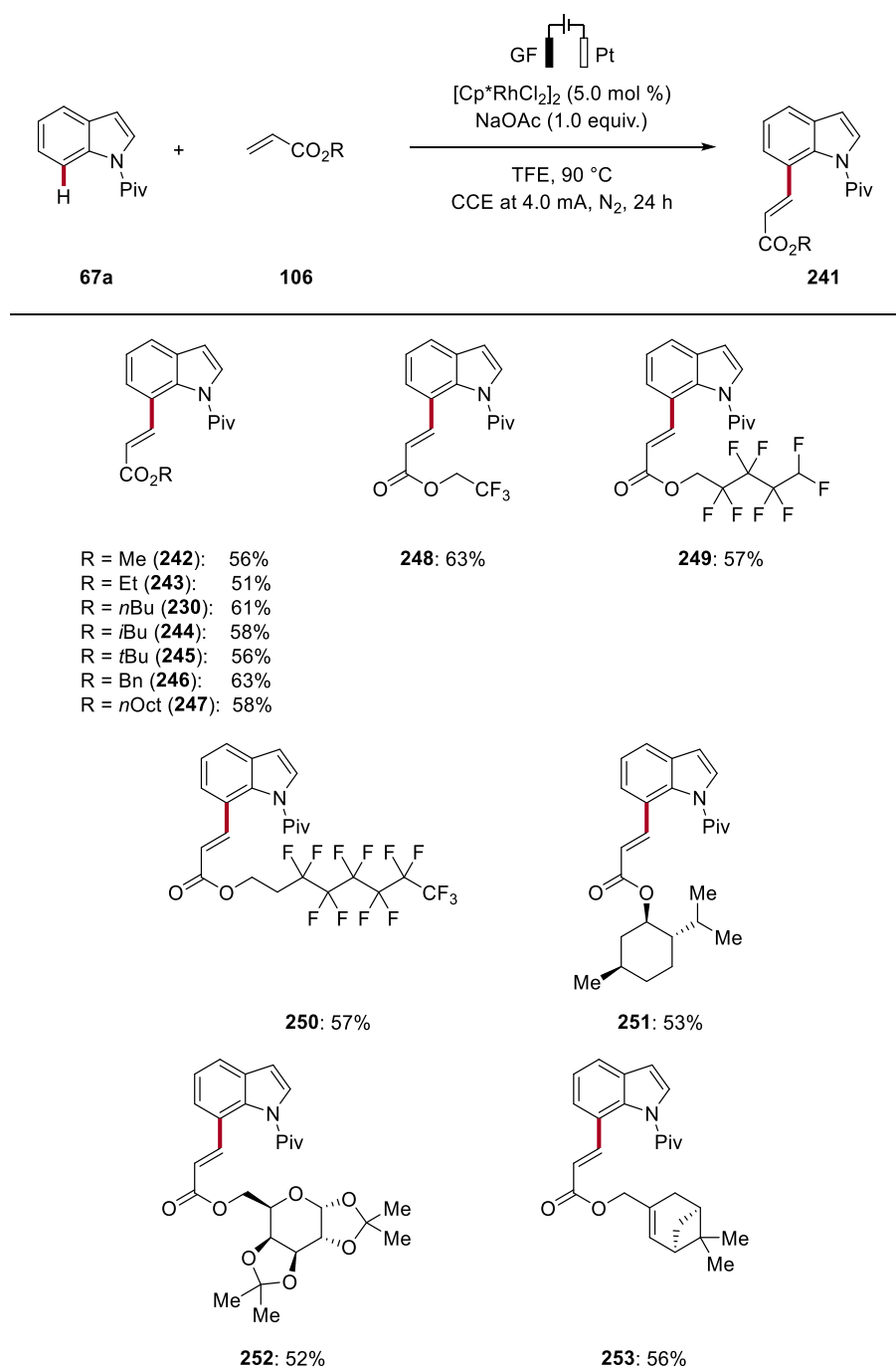
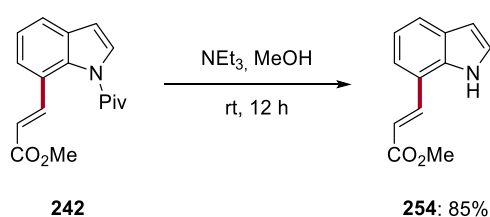


**Figure 3-21.** Electrooxidative C7-alkenylation of indole **67a** with acrylates **106**.

### 3.3.3 Investigations of Practical Utility

The practical utility of the established electro-catalyzed C7–H activation was proven through product **242** diversification to obtain the desired dihydro-pyrrolo-quinolinone **256** in an overall yield of 71% (Figure 3-22b).<sup>[157]</sup> Notably, the first step of the synthesis included the successful traceless removal of the pivaloyl directing group (Figure 3-22a).

a) Traceless removal of the pivaloyl directing group



b) Synthesis of dihydro-pyrroloquinolinone **256**

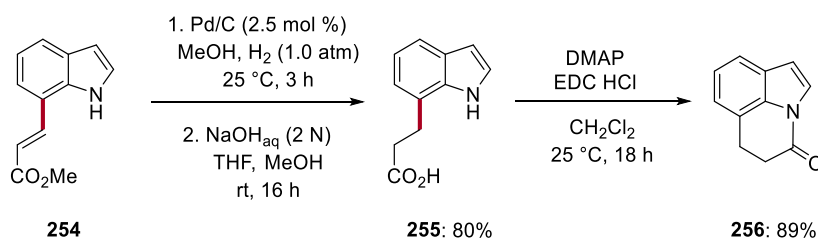


**Figure 3-22.** a) Traceless removal of the pivaloyl directing group. b) Diversification of product **242**.

Furthermore, the rhodium(III)-catalyzed alkenylation could be easily carried out on a gram-scale, without significant loss of catalytic efficacy, thereby manifesting the robustness of this transformation (**Figure 3-23**).

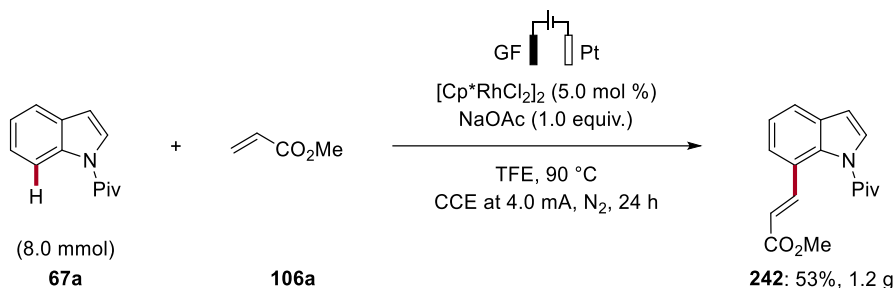


**Figure 3-23.** Gram-scale C7-H indole alkenylation.

### 3.3.4 Mechanistic Investigation

A series of mechanistic investigations were conducted in order to understand the catalyst's mode of action in the rhodaelectro-catalyzed C7-alkenylation. Initially, deuterium exchange studies were attempted in the presence of isotopically labeled TFE solvent (**Figure 3-24**). Significant H/D scrambling was observed at the C7-position, being a clear indication for a fast, reversible C-H activation step.

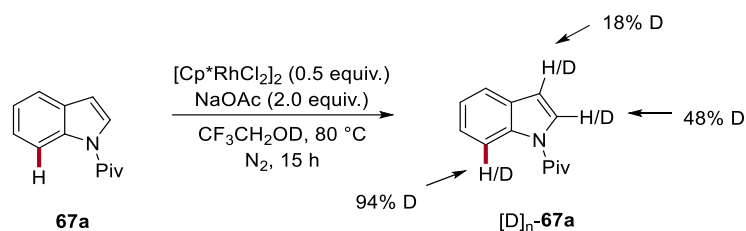


Figure 3-24. H/D exchange study.

Subsequently, the reaction was performed in the presence of isotopically labeled compound  $[\text{D}]_2\text{-67a}$ , and a kinetic isotope effect of  $k_H/k_D \approx 1.1$  was observed, being in support of a fast C(7)–H scission (Figure 3-25).

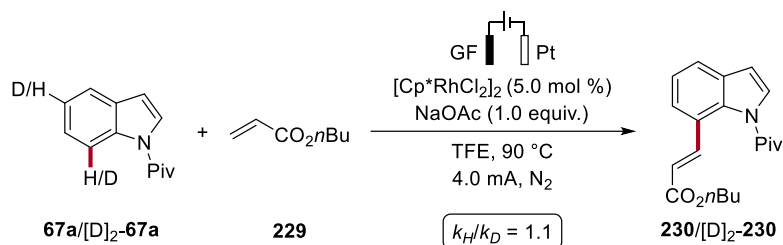


Figure 3-25. KIE study.

Considerable dependence of the catalytic efficacy on the current was observed for the electrooxidative C7-alkenylation upon altering the applied current during the galvanostatic electrolysis, thus providing support for a turnover-limiting redox event (Figure 3-26).

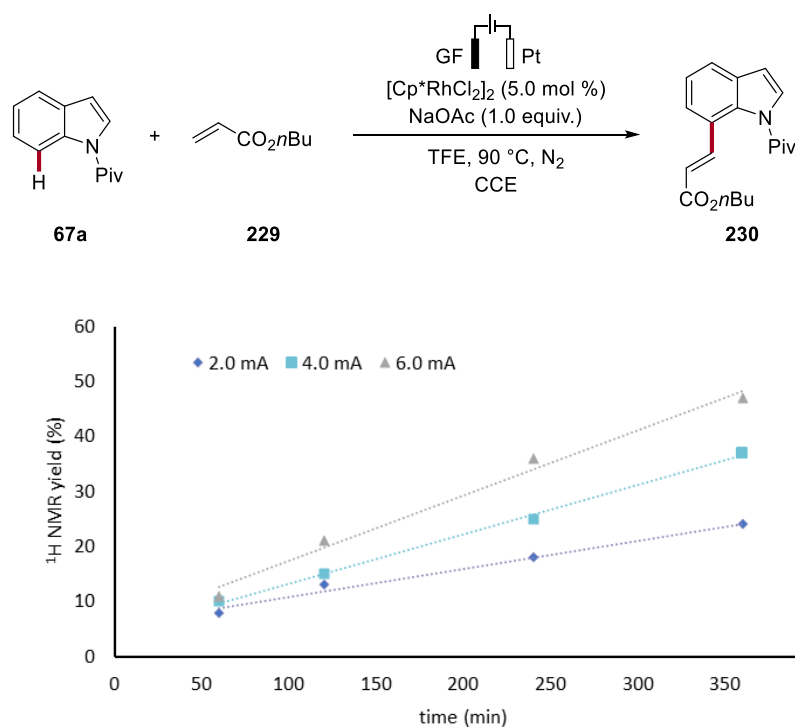


Figure 3-26. Dependence on current.

### 3.3.5 Proposed Catalytic Cycle

On the basis of our experimental mechanistic studies, a plausible catalytic cycle for the rhodaelectro-catalyzed C7–H indole alkenylation was proposed in Figure 3-27. The mechanism rationale commences with the coordination of the indole **67a** to the active catalytic species **257** followed by fast C–H activation to generate the rhodacycle **258**. Then, ligand exchange and subsequent coordination of the acrylate species **229** at the rhodium center deliver intermediate **259**, followed by regioselective migratory insertion of the alkene into the Rh–C bond, producing intermediate **260**. Afterwards,  $\beta$ -hydride elimination takes place leading to the desired product **230** and the formation of rhodium(III) hydride complex **261**. Subsequent anodic oxidation furnishes rhodium(IV) complex **262**. Reductive elimination to rhodium(II) intermediate **263** and subsequent anodic oxidation complement the catalytic cycle.



## 4 Summary

The negative consequences of climate change are a major driver of the ongoing need for improvements in sustainable synthetic organic chemistry. Indeed, transition metal catalyzed C–H activation has contributed especially in recent years with a plethora of transformations spurred by key concepts, such as atom-, step- and resource-economy. In this context, late-stage C–H functionalization has the potential to combine the benefit of shortening reaction routes and favoring product diversification, two fundamental aspects of drug discovery and medicinal chemistry. Novel mechanistic pathways require renewable energy sources. Electrocatalysis and photocatalysis can be implemented to solve the long-lasting problems associated with the use of toxic and expensive chemical oxidants and harsh reaction conditions, respectively. These are the main topics that have been explored within this thesis.

In the first part, the incorporation of medicinally-relevant *N*-aryl triazoles and aryl tetrazoles into complex pharmaceutical scaffolds have been devised. The functionalization of these heterocycles was achieved *via* ruthenium-catalyzed C–H arylation, employing aryl dibenzothiophenium salts as electrophilic arylating agents (Figure 4-1). This mild and cost-effective approach was characterized by a broad functional group tolerance, including aryl halides, which allow for further functionalization with orthogonal selectivity.

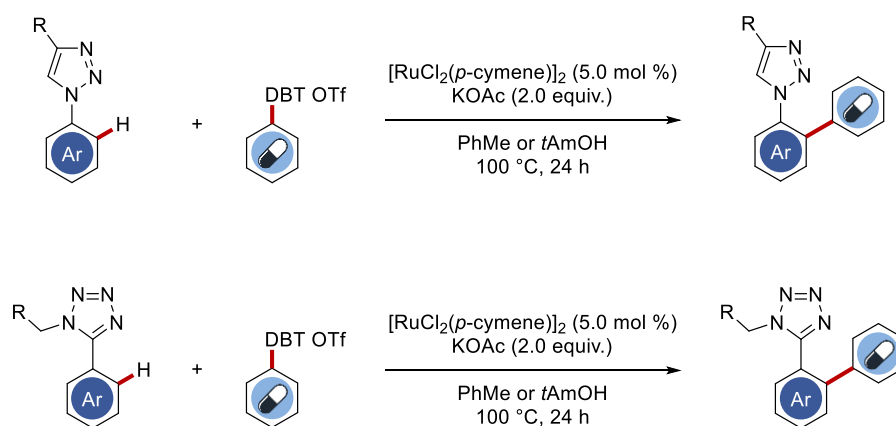


**Figure 4-1.** Ruthenium-catalyzed late-stage incorporation of valuable *N*-aryl triazoles and aryl tetrazoles into medicinally relevant scaffolds.

In the second part, the synergistic cooperation between C–H activation and photoredox catalysis have been employed for the direct allylation of arenes under exceedingly mild reaction conditions (Figure 4-2). Visible light-induced ruthenium-catalyzed C–H allylations at room temperature were developed, notably without the need of exogenous photocatalysts.<sup>[147]</sup> The catalytic protocol was tolerant of various functional groups. The introduction of a highly versatile allyl moiety improves utility and acts as a valuable intermediate for further manipulation.

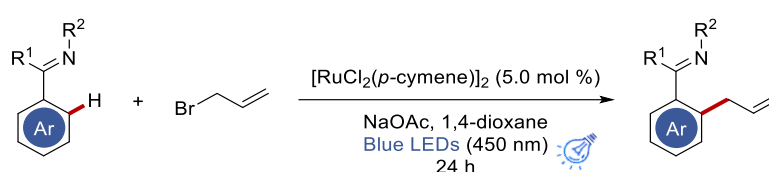


**Figure 4-2.** Ruthenium-catalyzed direct allylation of arenes under blue light irradiation at room temperature.

In the third part, the challenging indole functionalization at the C7-position has been addressed through an unprecedented electrochemical approach. Thus, the rhodaelectro-catalyzed alkenylation of indoles was described (Figure 4-3).<sup>[156]</sup> Within this powerful protocol, harsh chemical oxidants as well as additional supporting electrolytes were not required, and yet a broad substrate scope, including natural products, was presented. Detailed mechanistic studies gave evidence for a plausible catalytic cycle with rate-limiting catalyst oxidation.

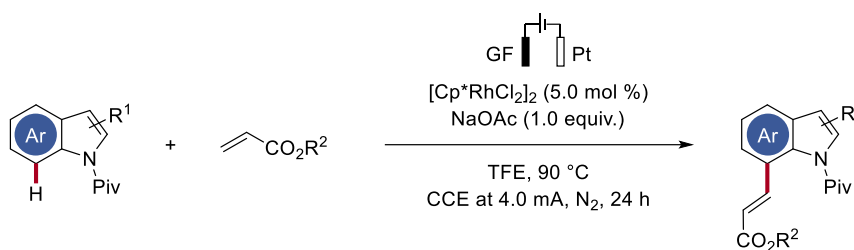


**Figure 4-3.** Rhodium-catalyzed electrochemical C7-indole alkenylation.

## 5 Experiment Section

### 5.1 General Remarks

Catalysis reactions were performed under N<sub>2</sub> atmosphere using pre-dried glassware and standard Schlenk techniques. Reactions under an atmosphere of air were conducted in the sealed tubes or Schlenk tubes.

If not mentioned otherwise, yields refer to isolated compounds, estimated to be >95% pure as determined by <sup>1</sup>H NMR.

#### Vacuum

A Vacuumbrand® RD4 rotary vane vacuum pump was employed. The following pressure was measured on the used vacuum pump and was not corrected: 0.1 mbar.

#### Melting Points (m.p.)

A *Stuart*® Melting Point Apparatus *SMP3* from BARLOWORLD SCIENTIFIC was used to measure melting points. The recorded values are uncorrected.

#### Chromatography

Analytical thin layer chromatography (TLC) was carried out on 0.25 mm silica gel 60F-plates (MACHEREY-NAGEL) with 254 nm fluorescent indicator from MERCK. Plates were visualized under UV-light. Chromatographic purification of products was achieved by flash column chromatography on MERCK silica gel, grade 60 (0.040–0.063 mm and 0.063–0.200 mm).

#### Gas Chromatography (GC)

Monitoring of reactions' conversion was accomplished by applying coupled gas chromatography/mass spectrometry using G1760C GCDplus with mass detector *HP 5971*, *5890 Series II* with mass detector *HP 5972* from HEWLETT-PACKARD and 7890A GC-System with mass detector *5975C (Triplex-Axis-Detector)* from AGILENT TECHNOLOGIES equipped with *HP-5MS* columns (30 m × 0.25 mm × 0.25 m).



### **Gel Permeation Chromatography (GPC)**

GPC purifications were executed on a JAI system (JAI-LC-9260 II NEXT) equipped with two sequential columns *JAIGEL-2HR*, gradient rate: 5.000; *JAIGEL-2.5HR*, gradient rate: 20.000; internal diameter = 20 mm; length = 600 mm; flush rate = 10.0 mL/min and chloroform (HPLC-quality with 0.6% ethanol as stabilizer) was the eluent of choice.

### **Infrared Spectroscopy**

Infrared spectra were obtained through a BRUKER *Alpha-P ATR FT-IR* spectrometer. Liquid samples were recorded as a film, solid samples neat. The software from BRUKER *OPUS 6* was used for the analysis of the spectra. The absorption was given in wave numbers ( $\text{cm}^{-1}$ ) and the spectra were measured in the range of 4000–400  $\text{cm}^{-1}$ .

### **Mass Spectrometry**

EI-HRMS or GC-EI-HRMS measurements were performed on the Exactive GC Orbitrap MS (ThermoFisher) or alternatively by GC-MS in the low-resolution mode on the DSQ quadrupol instrument (Thermo). Electrospray-ionization (ESI) mass spectra were recorded on Bruker micrOTOF and maXis instruments. All systems were supplied with time-of-flight (TOF) analyzers. The ratios of mass to charge ( $m/z$ ) and the intensity relative to the base peak ( $I = 100$ ) were given.

### **Nuclear Magnetic Resonance Spectroscopy (NMR)**

Nuclear magnetic resonance (NMR) spectra were measured via VARIAN *Inova 500*, *600*, VARIAN *Mercury 300*, *VX 300*, VARIAN *Avance 300*, VARIAN *VNMRS 300* and BRUKER *Avance III 300*, *400* and *HD 500* spectrometers. Chemical shifts were reported as  $\delta$ -values in ppm relative to the residual proton peak of the deuterated solvent or its carbon atom, respectively.  $^1\text{H}$  NMR spectra were referenced through the residual proton, while  $^{13}\text{C}$  NMR spectra using the solvent carbon peak (see table below).  $^{13}\text{C}$  and  $^{19}\text{F}$  NMR were recorded as proton-decoupled spectra.

	<sup>1</sup> H NMR	<sup>13</sup> C NMR
CDCl <sub>3</sub>	7.26	77.16
d <sub>6</sub> -DMSO	2.50	39.52

The following abbreviations described the observed resonance-multiplicities: s (singlet), d (doublet), t (triplet), q (quartet), hept (heptet), m (multiplet) or analogous representations. The coupling constants *J* were given in Hertz (Hz). *MestReNova 10* software was used to analyze the recorded spectra.

### Photochemistry

Photochemical reactions were conducted under visible light irradiation employing two Kessil A360N lamps. The temperature was maintained between 30 °C and 33 °C, using a fan.

### Electrochemistry

Electrolyses were carried out in undivided electrochemical cells. Platinum (Pt) electrodes (15 mm × 10 mm × 0.25 mm, 99.9%; obtained from CHEMPUR Karlsruhe, Germany) and graphite felt (GF) or reticulous vitreous carbon (RVC) electrodes (10 mm × 15 mm × 6 mm, SIGRACELL®GFA 6 EA, obtained from SGL Carbon, Wiesbaden, Germany) were attached using stainless steel adapters. Electrolysis was conducted using ROHDE&SCHWARZ (HMP4040) or AXIOMET (AX-3003P) potentiostats in constant current mode.

### Solvents

All solvents for reactions involving moisture-sensitive reagents were dried, distilled and stored under inert atmosphere (N<sub>2</sub>) according to the following standard procedures.

Purified by solvent purification system (SPS-800, M. Braun): **CH<sub>2</sub>Cl<sub>2</sub>**, **toluene**, **tetrahydrofuran**, **dimethylformamide**, **diethylether**. **1,2-dichloroethane**, ***N,N*-dimethylacetamide (DMA)**, and **dimethylsulfoxide (DMSO)** were dried over CaH<sub>2</sub> for 8 h, degassed and distilled under reduced pressure. **1,2-dimethoxyethane (DME)** was dried over sodium and freshly distilled under N<sub>2</sub>. **1,1,1,3,3,3-hexafluoropropan-2-ol (HFIP)** was distilled from 3 Å molecular sieves. **2,2,2-trifluoroethanol (TFE)** was

stirred over CaSO<sub>4</sub> and distilled under reduced pressure. **Water** was degassed by repeated *Freeze-Pump-Thaw* degassing procedure. **1,4-dioxane** was distilled from sodium benzophenone ketyl.

### Reagents

Chemicals obtained from commercial sources with purity above 95% were used without further purification. The following compounds were known therefore synthesized according to previously described methodologies.

*N*-aryl triazoles **131**,<sup>[158]</sup> aryl tetrazoles **162**,<sup>[159]</sup> aryl sulfonium salts **124** and **170**,<sup>[160]</sup> 2-arylpiperidines **22** and **201**,<sup>[161]</sup> and indoles **67**.<sup>[162]</sup>

## 5.2 General Procedures

### General Procedure A: Ruthenium-Catalyzed Arylation with Sulfonium Salts

Aryl azoles **131** or **162** (0.2 mmol), aryl dibenzothiophenium triflate **124** or **170** (1.5 equiv.),  $[\text{RuCl}_2(p\text{-cymene})]_2$  (6.0 mg, 0.01 mmol, 5.0 mol %) and KOAc (39.3 mg, 2.0 equiv.) were suspended in toluene or *t*AmOH (2.0 mL). The mixture was stirred for 24 h at 100 °C under nitrogen atmosphere. Purification by column chromatography on silica gel yielded the desired products **133**, **144**, **163**, **171** or **182**.

### General Procedure B: Ruthenium-Catalyzed Arylation with Sulfonium Salts

Aryl dibenzothiophenium triflate **124** or **170** (0.2 mmol), arenes **131** or **162** (2.0 equiv.),  $[\text{RuCl}_2(p\text{-cymene})]_2$  (6.0 mg, 0.01 mmol, 5.0 mol %) and KOAc (39.3 mg, 2.0 equiv.) were suspended in toluene or *t*AmOH (2.0 mL). The mixture was stirred for 24 h at 100 °C under nitrogen atmosphere. Purification by column chromatography on silica gel yielded the desired products **133**, **144**, **163**, **171** or **182**.

### General Procedure C: Light-Induced Ruthenium-Catalyzed *ortho*-C–H Allylation

Heteroarene **22** or **201** (0.5 mmol),  $[\text{RuCl}_2(p\text{-cymene})]_2$  (15.3 mg, 0.025 mmol, 5.0 mol %) and dry NaOAc (82.0 mg, 1.0 mmol) from the glovebox were placed in a 10 mL vial. The vial was capped with a septum and wrapped with parafilm, then evacuated and purged with N<sub>2</sub> three times. Allyl bromide **198** (0.75 mmol) and 1,4-dioxane (2.0 mL) were then added and the mixture was stirred under visible light irradiation. After 24 h, the resulting mixture was filtered through a pad of silica gel and washed with EtOAc. The filtrate was concentrated in vacuo. Purification by column chromatography afforded *ortho*-allylated products **202**.

### General Procedure D: Electrochemical Rhodium-Catalyzed C7-Alkenylation of Indole

Under an atmosphere of N<sub>2</sub>, the oven-dried undivided electrochemical cell with GF anode (10.0 mm x 15.0 mm x 6.0 mm) and Pt cathode (15.0 mm x 10.0 mm x 0.25

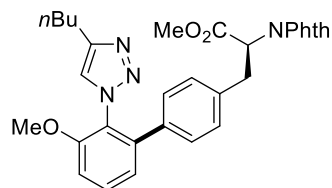
mm) was charged with *N*-pivaloyl indoles **67** (0.5 mmol, 1.0 equiv.), acrylates **106** or **229** (1.50 mmol, 3.0 equiv.), [Cp\*RhCl<sub>2</sub>]<sub>2</sub> (15.5 mg, 0.025 mmol, 5.0 mol %), NaOAc (41.0 mg, 1.0 equiv.) and TFE (2.0 mL). Electrocatalysis was then performed at 90 °C with a constant current of 4.0 mA maintained for 24 h with a stirring rate of 250 rpm. After completion, the reaction mixture was diluted with CH<sub>2</sub>Cl<sub>2</sub> (30 mL). Both electrodes were washed and sonicated thoroughly with CH<sub>2</sub>Cl<sub>2</sub> (3 x 5.0 mL). The washings were added to the reaction mixture and filtered through silica gel. Evaporation of the solvents and subsequent column chromatography on silica gel afforded the corresponding products **232** or **241**.

## 5.3 Experimental Procedures and Analytical Data

### 5.3.1 Ruthenium-Catalyzed C–H Arylation with Sulfonium Salts

#### Characterization Data

#### Methyl-(S)-3-(2'-(4-butyl-1*H*-1,2,3-triazol-1-yl)-3'-methoxy-[1,1'-biphenyl]-4-yl)-2-(1,3-dioxoisoindolin-2-yl)propanoate (**132**)



The general procedure A was followed using 4-butyl-1-(2-methoxyphenyl)-1*H*-1,2,3-triazole **131a** (46.3 mg, 0.20 mmol), dibenzothiophene salt **130** (192 mg, 0.30 mmol), [RuCl<sub>2</sub>(*p*-cymene)]<sub>2</sub> (6.0 mg, 0.01 mmol, 5.0 mol %), and KOAc (39.3 mg, 2.0 equiv.) in toluene (2.0 mL). Purification by column chromatography on silica gel (*n*hexane/EtOAc: 10/1) yielded **132** (98.0 mg, 91%) as a transparent oil.

**<sup>1</sup>H NMR** (400 MHz, CDCl<sub>3</sub>): δ 7.78 – 7.71 (m, 2H), 7.69 – 7.62 (m, 2H), 7.44 – 7.36 (m, 1H), 7.02 – 6.93 (m, 5H), 6.87 (dd, *J* = 8.2, 1.8 Hz, 2H), 5.06 (ddd, *J* = 10.8, 5.5, 1.5 Hz, 1H), 3.73 (dd, *J* = 5.1, 3.1 Hz, 6H), 3.57 – 3.35 (m, 2H), 2.58 (td, *J* = 7.6, 1.9 Hz, 2H), 1.58 – 1.46 (m, 2H), 1.26 – 1.16 (m, 2H), 0.85 (td, *J* = 7.4, 2.2 Hz, 3H).

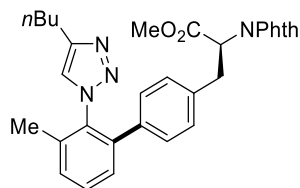
**<sup>13</sup>C NMR** (101 MHz, CDCl<sub>3</sub>): δ 169.3 (C<sub>q</sub>), 167.4 (C<sub>q</sub>), 155.2 (C<sub>q</sub>), 147.4 (C<sub>q</sub>), 140.4 (C<sub>q</sub>), 136.4 (C<sub>q</sub>), 135.9 (C<sub>q</sub>), 134.2 (CH), 131.6 (C<sub>q</sub>), 130.8 (CH), 128.7 (CH), 128.4 (CH), 124.4 (C<sub>q</sub>), 123.7 (CH), 123.5 (CH), 122.2 (CH), 111.0 (CH), 56.2 (CH<sub>3</sub>), 53.1 (CH), 52.9 (CH<sub>3</sub>), 34.3 (CH<sub>2</sub>), 31.4 (CH<sub>2</sub>), 25.1 (CH<sub>2</sub>), 22.0 (CH<sub>2</sub>), 13.9 (CH<sub>3</sub>).

**IR** (ATR): 2955, 1746, 1715, 1472, 1387, 1243, 1016, 908, 719 cm<sup>-1</sup>.

**MS** (ESI) *m/z* (relative intensity): 561.2 [M+Na]<sup>+</sup> (100), 539.2 [M+H]<sup>+</sup> (40).

**HR-MS** (ESI): *m/z* calcd for C<sub>31</sub>H<sub>31</sub>N<sub>4</sub>O<sub>5</sub><sup>+</sup> [M+H]<sup>+</sup> 539.2289, found 539.2285.

**Methyl-(S)-3-(2'-(4-butyl-1*H*-1,2,3-triazol-1-yl)-3'-methyl-[1,1'-biphenyl]-4-yl)-2-(1,3-dioxisoindolin-2-yl)propanoate (134)**



The general procedure A was followed using 4-butyl-1-(2-methylphenyl)-1*H*-1,2,3-triazole **131b** (43.1 mg, 0.20 mmol), dibenzothiophene salt **130** (192 mg, 0.30 mmol), [RuCl<sub>2</sub>(*p*-cymene)]<sub>2</sub> (6.0 mg, 0.01 mmol, 5.0 mol %), and KOAc (39.3 mg, 2.0 equiv.) in toluene (2.0 mL). Purification by column chromatography on silica gel (*n*hexane/EtOAc: 10/1) yielded **134** (71.0 mg, 68%) as a transparent oil.

**<sup>1</sup>H NMR** (400 MHz, CDCl<sub>3</sub>): δ 7.77 (dd, *J* = 5.6, 3.0 Hz, 2H), 7.69 (dd, *J* = 5.6, 3.0 Hz, 2H), 7.42 – 7.35 (m, 1H), 7.29 (d, *J* = 7.8 Hz, 1H), 7.21 (d, *J* = 7.6 Hz, 1H), 6.99 (d, *J* = 7.8 Hz, 2H), 6.87 (d, *J* = 5.9 Hz, 3H), 5.06 (dd, *J* = 10.8, 5.4 Hz, 1H), 3.75 (s, 3H), 3.60 – 3.36 (m, 2H), 2.57 (t, *J* = 7.5 Hz, 2H), 2.07 (s, 3H), 1.58 – 1.43 (m, 2H), 1.25 – 1.17 (m, 2H), 0.85 (t, *J* = 7.3 Hz, 3H).

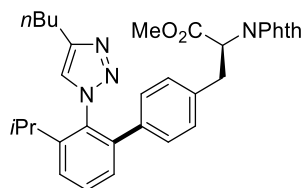
**<sup>13</sup>C NMR** (101 MHz, CDCl<sub>3</sub>): δ 169.3 (C<sub>q</sub>), 167.5 (C<sub>q</sub>), 148.0 (C<sub>q</sub>), 139.1 (C<sub>q</sub>), 136.4 (C<sub>q</sub>), 136.3 (C<sub>q</sub>), 136.3 (C<sub>q</sub>), 134.6 (C<sub>q</sub>), 134.3 (CH), 131.7 (C<sub>q</sub>), 130.1 (CH), 129.9 (CH), 128.8 (CH), 128.5 (CH), 128.3 (CH), 123.6 (CH), 123.1 (CH), 53.2 (CH), 53.0 (CH<sub>3</sub>), 34.4 (CH<sub>2</sub>), 31.5 (CH<sub>2</sub>), 25.0 (CH<sub>2</sub>), 22.0 (CH<sub>2</sub>), 17.8 (CH<sub>3</sub>), 13.9 (CH<sub>3</sub>).

**IR** (ATR): 2955, 1747, 1715, 1468, 1387, 1242, 1021, 788, 720 cm<sup>-1</sup>.

**MS** (ESI) *m/z* (relative intensity): 545.2 [M+Na]<sup>+</sup> (100), 523.2 [M+H]<sup>+</sup> (50).

**HR-MS** (ESI): *m/z* calcd for C<sub>31</sub>H<sub>31</sub>N<sub>4</sub>O<sub>4</sub><sup>+</sup> [M+H]<sup>+</sup> 523.2340, found 523.2342.

**Methyl-(S)-3-(2'-(4-butyl-1*H*-1,2,3-triazol-1-yl)-3'-isopropyl-[1,1'-biphenyl]-4-yl)-2-(1,3-dioxisoindolin-2-yl)propanoate (135)**



The general procedure A was followed using 4-butyl-1-(2-iso-propylphenyl)-1*H*-1,2,3-

triazole **131c** (48.7 mg, 0.20 mmol), dibenzothiophene salt **130** (192 mg, 0.30 mmol), [RuCl<sub>2</sub>(*p*-cymene)]<sub>2</sub> (6.0 mg, 0.01 mmol, 5.0 mol %), and KOAc (39.3 mg, 2.0 equiv.) in toluene (2.0 mL). Purification by column chromatography on silica gel (*n*hexane/EtOAc: 10/1) yielded **135** (57.0 mg, 52%) as a transparent oil.

**<sup>1</sup>H NMR** (400 MHz, CDCl<sub>3</sub>): δ 7.82 – 7.67 (m, 5H), 7.51 – 7.44 (m, 1H), 7.42 (d, *J* = 7.9 Hz, 1H), 7.21 (d, *J* = 7.5 Hz, 1H), 6.99 (d, *J* = 7.9 Hz, 2H), 6.87 (d, *J* = 7.3 Hz, 2H), 5.07 (dd, *J* = 10.9, 5.5 Hz, 1H), 3.76 (s, 3H), 3.55 – 3.41 (m, 2H), 2.58 (t, *J* = 7.5 Hz, 2H), 2.49 (q, *J* = 6.9 Hz, 1H), 1.50 (p, *J* = 7.5 Hz, 2H), 1.27 – 1.08 (m, 8H), 0.86 (t, *J* = 7.3 Hz, 3H).

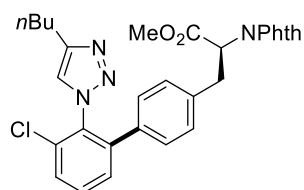
**<sup>13</sup>C NMR** (101 MHz, CDCl<sub>3</sub>): δ 169.3 (C<sub>q</sub>), 167.4 (C<sub>q</sub>), 147.8 (C<sub>q</sub>), 146.7 (C<sub>q</sub>), 139.2 (C<sub>q</sub>), 136.6 (C<sub>q</sub>), 136.2 (C<sub>q</sub>), 134.2 (CH), 133.3 (C<sub>q</sub>), 131.6 (C<sub>q</sub>), 130.2 (CH), 128.7 (CH), 128.5 (CH), 128.0 (CH), 125.7 (CH), 123.8 (CH), 123.5 (CH), 53.2 (CH), 52.9 (CH), 34.3 (CH<sub>2</sub>), 31.4 (CH<sub>2</sub>), 28.2 (CH<sub>3</sub>), 25.0 (CH<sub>2</sub>), 24.1 (CH<sub>3</sub>), 21.9 (CH<sub>2</sub>), 13.8 (CH<sub>3</sub>).

**IR** (ATR): 2955, 1746, 1716, 1468, 1387, 1243, 1020, 884, 719 cm<sup>-1</sup>.

**MS** (ESI) *m/z* (relative intensity): 573.2 [M+Na]<sup>+</sup> (100), 551.2 [M+H]<sup>+</sup> (45).

**HR-MS** (ESI): *m/z* calcd for C<sub>33</sub>H<sub>35</sub>N<sub>4</sub>O<sub>4</sub><sup>+</sup> [M+H]<sup>+</sup> 551.2653, found 551.2649.

**Methyl-(S)-3-(2'-(4-butyl-1*H*-1,2,3-triazol-1-yl)-3'-chloro-[1,1'-biphenyl]-4-yl)-2-(1,3-dioxisoindolin-2-yl)propanoate (**136**)**



The general procedure A was followed using 4-butyl-1-(2-chlorophenyl)-1*H*-1,2,3-triazole **131d** (47.1 mg, 0.20 mmol), dibenzothiophene salt **130** (192 mg, 0.30 mmol), [RuCl<sub>2</sub>(*p*-cymene)]<sub>2</sub> (6.0 mg, 0.01 mmol, 5.0 mol %), and KOAc (39.3 mg, 2.0 equiv.) in toluene (2.0 mL). Purification by column chromatography on silica gel (*n*hexane/EtOAc: 10/1) yielded **136** (72.0 mg, 66%) as a transparent oil.

**<sup>1</sup>H NMR** (400 MHz, CDCl<sub>3</sub>): δ 7.81 – 7.75 (m, 2H), 7.72 – 7.67 (m, 2H), 7.49 (d, *J* = 7.9 Hz, 1H), 7.46 – 7.40 (m, 1H), 7.30 (d, *J* = 7.7 Hz, 1H), 7.01 (d, *J* = 7.1 Hz, 3H), 6.89



(d,  $J = 7.9$  Hz, 2H), 5.06 (dd,  $J = 10.8, 5.4$  Hz, 1H), 3.74 (s, 3H), 3.57 – 3.40 (m, 2H), 2.61 (t,  $J = 7.5$  Hz, 2H), 1.54 (p,  $J = 7.5$  Hz, 2H), 1.27 – 1.18 (m, 2H), 0.86 (t,  $J = 7.3$  Hz, 3H).

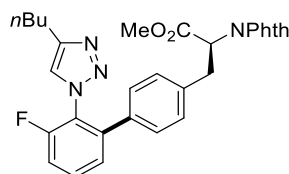
$^{13}\text{C}$  NMR (101 MHz,  $\text{CDCl}_3$ ):  $\delta$  169.2 ( $\text{C}_q$ ), 167.4 ( $\text{C}_q$ ), 148.0 ( $\text{C}_q$ ), 141.4 ( $\text{C}_q$ ), 137.0 ( $\text{C}_q$ ), 135.2 ( $\text{C}_q$ ), 134.3 (CH), 133.2 ( $\text{C}_q$ ), 132.8 ( $\text{C}_q$ ), 131.6 ( $\text{C}_q$ ), 130.9 (CH), 129.3 (CH), 129.2 (CH), 129.0 (CH), 128.4 (CH), 123.6 (CH), 123.3 (CH), 53.1 (CH), 53.0 ( $\text{CH}_3$ ), 34.4 ( $\text{CH}_2$ ), 31.4 ( $\text{CH}_2$ ), 25.0 ( $\text{CH}_2$ ), 22.0 ( $\text{CH}_2$ ), 13.9 ( $\text{CH}_3$ ).

IR (ATR): 2955, 1776, 1715, 1455, 1386, 1244, 1020, 908, 719  $\text{cm}^{-1}$ .

MS (ESI)  $m/z$  (relative intensity): 565.2  $[\text{M}+\text{Na}]^+$  (100), 543.2  $[\text{M}+\text{H}]^+$  (80).

HR-MS (ESI):  $m/z$  calcd for  $\text{C}_{30}\text{H}_{28}^{35}\text{ClN}_4\text{O}_4^+$   $[\text{M}+\text{H}]^+$  543.1794, found 543.1795.

**Methyl-(S)-3-(2'-(4-butyl-1H-1,2,3-triazol-1-yl)-3'-fluoro-[1,1'-biphenyl]-4-yl)-2-(1,3-dioxoisoindolin-2-yl)propanoate (137)**



The general procedure A was followed using 4-butyl-1-(2-fluorophenyl)-1H-1,2,3-triazole **131e** (43.8 mg, 0.20 mmol), dibenzothiophene salt **130** (192 mg, 0.30 mmol),  $[\text{RuCl}_2(p\text{-cymene})]_2$  (6.0 mg, 0.01 mmol, 5.0 mol %), and KOAc (39.3 mg, 2.0 equiv.) in toluene (2.0 mL). Purification by column chromatography on silica gel (*n*hexane/EtOAc: 10/1) yielded **137** (102 mg, 96%) as a transparent oil.

$^1\text{H}$  NMR (400 MHz,  $\text{CDCl}_3$ ):  $\delta$  7.84 (dd,  $J = 5.5, 3.0$  Hz, 2H), 7.75 (dd,  $J = 5.5, 3.1$  Hz, 2H), 7.58 – 7.42 (m, 1H), 7.33 – 7.11 (m, 2H), 7.04 (d,  $J = 8.1$  Hz, 3H), 6.94 (d,  $J = 8.3$  Hz, 2H), 5.13 (dd,  $J = 10.8, 5.4$  Hz, 1H), 3.71 (s, 2H), 3.63 – 3.33 (m, 2H), 2.64 (t,  $J = 7.6$  Hz, 2H), 1.78 – 1.45 (m, 2H), 1.40 – 1.01 (m, 2H), 0.97 (t,  $J = 7.3$  Hz, 3H).

$^{13}\text{C}$  NMR (101 MHz,  $\text{CDCl}_3$ ):  $\delta$  169.2 ( $\text{C}_q$ ), 167.4 ( $\text{C}_q$ ), 157.5 (d,  $^1J_{\text{C-F}} = 254.0$  Hz,  $\text{C}_q$ ), 148.1 ( $\text{C}_q$ ), 140.8 ( $\text{C}_q$ ), 137.1 ( $\text{C}_q$ ), 134.9 (d,  $^3J_{\text{C-F}} = 2.5$  Hz,  $\text{C}_q$ ), 134.3 (CH), 131.6 ( $\text{C}_q$ ), 131.1 (d,  $^3J_{\text{C-F}} = 8.6$  Hz, CH), 129.1 (CH), 128.5 (CH), 126.0 (d,  $^4J_{\text{C-F}} = 3.4$  Hz, CH), 123.8 (d,  $^2J_{\text{C-F}} = 13.0$  Hz,  $\text{C}_q$ ), 123.6 (CH), 123.5 (CH), 115.5 (d,  $^2J_{\text{C-F}} = 20.1$  Hz, CH),

53.1 (CH<sub>3</sub>), 53.0 (CH<sub>3</sub>), 34.4 (CH<sub>2</sub>), 31.4 (CH<sub>2</sub>), 25.0 (CH<sub>2</sub>), 22.1 (CH<sub>2</sub>), 13.9 (CH<sub>3</sub>).

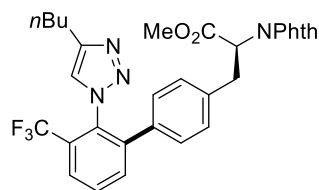
<sup>19</sup>F NMR (377 MHz, CDCl<sub>3</sub>): δ -121.3 – -121.4 (m).

IR (ATR): 2956, 1712, 1469, 1385, 1248, 1098, 1038, 895, 717 cm<sup>-1</sup>.

MS (ESI) *m/z* (relative intensity): 549.2 [M+Na]<sup>+</sup> (100), 527.2 [M+H]<sup>+</sup> (15).

HR-MS (ESI): *m/z* calcd for C<sub>30</sub>H<sub>27</sub>FN<sub>4</sub>O<sub>4</sub><sup>+</sup> [M+H]<sup>+</sup> 527.2089, found 527.2088.

**Methyl-(S)-3-(2'-(4-butyl-1*H*-1,2,3-triazol-1-yl)-3'-(trifluoromethyl)-[1,1'-biphenyl]-4-yl)-2-(1,3-dioxoisindolin-2-yl)propanoate (**138**)**



The general procedure A was followed using 4-butyl-1-(2-trifluoromethylphenyl)-1*H*-1,2,3-triazole **131f** (53.8 mg, 0.20 mmol), dibenzothiophene salt **130** (192 mg, 0.30 mmol), [RuCl<sub>2</sub>(*p*-cymene)]<sub>2</sub> (6.0 mg, 0.01 mmol, 5.0 mol %), and KOAc (39.3 mg, 2.0 equiv.) in toluene (2.0 mL). Purification by column chromatography on silica gel (*n*hexane/EtOAc: 10/1) yielded **138** (86.8 mg, 75%) as a pale-yellow oil.

<sup>1</sup>H NMR (400 MHz, CDCl<sub>3</sub>): δ 7.81 – 7.75 (m, 3H), 7.69 (dd, *J* = 5.7, 3.2 Hz, 2H), 7.66 – 7.57 (m, 2H), 7.07 – 6.98 (m, 3H), 6.87 (d, *J* = 7.8 Hz, 2H), 5.06 (dd, *J* = 10.8, 5.3 Hz, 1H), 3.74 (s, 3H), 3.56 – 3.43 (m, 2H), 2.57 (t, *J* = 7.5 Hz, 2H), 1.50 (p, *J* = 7.5 Hz, 2H), 1.25 – 1.15 (m, 2H), 0.85 (t, *J* = 7.3 Hz, 3H).

<sup>13</sup>C NMR (101 MHz, CDCl<sub>3</sub>): δ 169.2 (C<sub>q</sub>), 167.4 (C<sub>q</sub>), 147.8 (C<sub>q</sub>), 141.8 (C<sub>q</sub>), 137.1 (C<sub>q</sub>), 134.7 (C<sub>q</sub>), 134.5 (CH), 134.2 (CH), 132.9 (C<sub>q</sub>), 131.5 (C<sub>q</sub>), 130.3 (CH), 128.9 (CH), 128.4 (CH), 128.2 (q, <sup>2</sup>*J*<sub>C-F</sub> = 31.3 Hz, C<sub>q</sub>), 126.2 (q, <sup>3</sup>*J*<sub>C-F</sub> = 5.1 Hz, CH), 124.2 (CH), 123.5 (CH), 122.7 (q, <sup>1</sup>*J*<sub>C-F</sub> = 274.7 Hz, C<sub>q</sub>), 53.0 (CH), 53.0 (CH<sub>3</sub>), 34.3 (CH<sub>2</sub>), 31.3 (CH<sub>2</sub>), 24.8 (CH<sub>2</sub>), 21.8 (CH<sub>2</sub>), 13.8 (CH<sub>3</sub>).

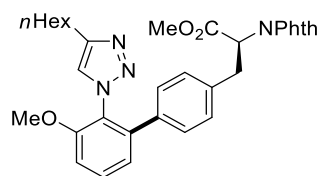
<sup>19</sup>F NMR (377 MHz, CDCl<sub>3</sub>): δ -59.5 (s).

IR (ATR): 2957, 1716, 1469, 1388, 1329, 1141, 1047, 805, 721 cm<sup>-1</sup>.

MS (ESI) *m/z* (relative intensity): 599.2 [M+Na]<sup>+</sup> (100), 577.2 [M+H]<sup>+</sup> (50).

HR-MS (ESI): *m/z* calcd for C<sub>31</sub>H<sub>28</sub>F<sub>3</sub>N<sub>4</sub>O<sub>4</sub><sup>+</sup> [M+H]<sup>+</sup> 577.2057, found 577.2051.

**Methyl-(S)-2-(1,3-dioxisoindolin-2-yl)-3-(2'-(4-hexyl-1*H*-1,2,3-triazol-1-yl)-3'-methoxy-[1,1'-biphenyl]-4-yl)propanoate (139)**



The general procedure A was followed using 4-hexyl-1-(2-methoxyphenyl)-1*H*-1,2,3-triazole **131g** (54.6 mg, 0.20 mmol), dibenzothiophene salt **130** (192.3 mg, 0.30 mmol), [RuCl<sub>2</sub>(*p*-cymene)]<sub>2</sub> (6.0 mg, 0.01 mmol, 5.0 mol %), and KOAc (39.3 mg, 2.0 equiv.) in toluene (2.0 mL). Purification by column chromatography on silica gel (*n*hexane/EtOAc: 10/1) yielded **139** (110 mg, 97%) as a transparent oil.

**<sup>1</sup>H NMR** (400 MHz, CDCl<sub>3</sub>): δ 7.78 (dd, *J* = 5.5, 3.1 Hz, 2H), 7.69 (dd, *J* = 5.5, 3.0 Hz, 2H), 7.48 – 7.38 (m, 1H), 7.05 – 6.92 (m, 5H), 6.92 – 6.83 (m, 2H), 5.07 (dd, *J* = 10.8, 5.4 Hz, 1H), 3.77 (s, 3H), 3.75 (s, 3H), 3.56 – 3.42 (m, 2H), 2.60 (t, *J* = 7.6 Hz, 2H), 1.61 – 1.49(m, 2H), 1.26 (td, *J* = 9.6, 5.2 Hz, 6H), 0.90 – 0.84 (m, 3H).

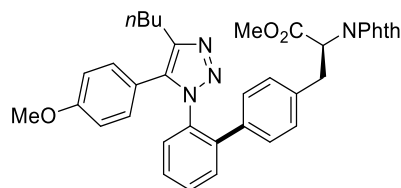
**<sup>13</sup>C NMR** (101 MHz, CDCl<sub>3</sub>): δ 169.4 (C<sub>q</sub>), 167.5 (C<sub>q</sub>), 155.3 (C<sub>q</sub>), 147.6 (C<sub>q</sub>), 140.6 (C<sub>q</sub>), 136.5 (C<sub>q</sub>), 136.0 (C<sub>q</sub>), 134.3 (CH), 131.7 (C<sub>q</sub>), 130.8 (CH), 128.8 (CH), 128.5 (CH), 124.6 (C<sub>q</sub>), 123.8 (CH), 123.6 (CH), 122.4 (CH), 111.0 (CH), 56.3 (CH<sub>3</sub>), 53.2 (CH<sub>3</sub>), 53.0 (CH), 34.4 (CH<sub>2</sub>), 31.7 (CH<sub>2</sub>), 29.4 (CH<sub>2</sub>), 28.8 (CH<sub>2</sub>), 25.5 (CH<sub>2</sub>), 22.7 (CH<sub>2</sub>), 14.2 (CH<sub>3</sub>).

**IR** (ATR): 2855, 1775, 1745, 1713, 1584, 1471, 1385, 1262, 1031 cm<sup>-1</sup>.

**MS** (ESI) *m/z* (relative intensity): 589.2 [M+Na]<sup>+</sup> (100), 567.2 [M+H]<sup>+</sup> (5).

**HR-MS** (ESI): *m/z* calcd for C<sub>33</sub>H<sub>35</sub>N<sub>4</sub>O<sub>5</sub><sup>+</sup> [M+H]<sup>+</sup> 567.2602, found 567.2602.

**Methyl-(S)-3-(2'-(4-butyl-5-(4-methoxyphenyl)-1*H*-1,2,3-triazol-1-yl)-[1,1'-biphenyl]-4-yl)-2-(1,3-dioxisoindolin-2-yl)propanoate (140)**



The general procedure A was followed using 4-butyl-5-(4-methoxyphenyl)-1-phenyl-1*H*-

1,2,3-triazole **131h** (61.4 mg, 0.20 mmol), dibenzothiophene salt **130** (192 mg, 0.30 mmol),  $[\text{RuCl}_2(p\text{-cymene})]_2$  (6.0 mg, 0.01 mmol, 5.0 mol %), and KOAc (39.3 mg, 2.0 equiv.) in *t*AmOH (2.0 mL). Purification by column chromatography on silica gel (*n*hexane/EtOAc: 3/1) yielded **140** (108 mg, 88%) as a white solid.

**m.p.:** 139–141 °C.

**<sup>1</sup>H NMR** (400 MHz, CDCl<sub>3</sub>): δ 7.86 – 7.77 (m, 2H), 7.76 – 7.68 (m, 2H), 7.67 – 7.57 (m, 2H), 7.51 – 7.36 (m, 2H), 7.17 (d, *J* = 7.1 Hz, 1H), 6.89 (d, *J* = 7.7 Hz, 2H), 6.62 – 6.40 (m, 3H), 6.28 – 6.12 (m, 2H), 5.12 (t, *J* = 8.1 Hz, 1H), 3.87 – 3.72 (m, 3H), 3.68 (s, 3H), 3.53 (d, *J* = 8.2 Hz, 2H), 2.57 – 2.23 (m, 2H), 1.64 – 1.44 (m, 2H), 1.32 – 1.17 (m, 2H), 0.84 (t, *J* = 7.3 Hz, 3H).

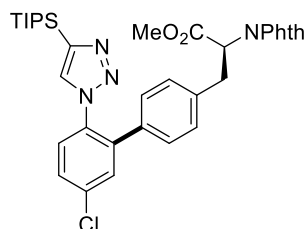
**<sup>13</sup>C NMR** (101 MHz, CDCl<sub>3</sub>): δ 169.3 (C<sub>q</sub>), 167.6 (C<sub>q</sub>), 159.4 (C<sub>q</sub>), 145.0 (C<sub>q</sub>), 138.1 (C<sub>q</sub>), 136.2 (C<sub>q</sub>), 136.1 (C<sub>q</sub>), 135.1 (C<sub>q</sub>), 134.6 (C<sub>q</sub>), 134.4 (CH), 131.7 (C<sub>q</sub>), 130.7 (CH), 130.0 (CH), 129.9 (CH), 128.7 (CH), 128.4 (CH), 128.4 (CH), 128.3 (CH), 123.7 (CH), 119.1 (C<sub>q</sub>), 113.5 (CH), 55.3 (CH), 53.4 (CH<sub>3</sub>), 53.1 (CH<sub>3</sub>), 34.2 (CH<sub>2</sub>), 31.5 (CH<sub>2</sub>), 24.6 (CH<sub>2</sub>), 22.5 (CH<sub>2</sub>), 13.9 (CH<sub>3</sub>).

**IR** (ATR): 2955, 1746, 1506, 1489, 1387, 1250, 1178, 1021, 835 cm<sup>-1</sup>.

**MS** (ESI) *m/z* (relative intensity): 637.3 [M+Na]<sup>+</sup> (100), 615.3 [M+H]<sup>+</sup> (30).

**HR-MS** (ESI): *m/z* calcd for C<sub>31</sub>H<sub>35</sub>N<sub>3</sub>O<sub>4</sub><sup>+</sup> [M+H]<sup>+</sup> 615.2602, found 615.2606.

**Methyl-(S)-3-(5'-chloro-2'-(4-(triisopropylsilyl)-1*H*-1,2,3-triazol-1-yl)-[1,1'-biphenyl]-4-yl)-2-(1,3-dioxoisindolin-2-yl)propanoate (**141**)**



The general procedure A was followed using 1-(4-chlorophenyl)-4-(tri-*iso*-propylsilyl)-1*H*-1,2,3-triazole **131i** (61.4 mg, 0.20 mmol), dibenzothiophene salt **130** (192 mg, 0.30 mmol),  $[\text{RuCl}_2(p\text{-cymene})]_2$  (6.0 mg, 0.01 mmol, 5.0 mol %), and KOAc (39.3 mg, 2.0 equiv.) in *t*AmOH (2.0 mL). Purification by column chromatography on silica gel (*n*hexane/EtOAc: 3/1) yielded **141** (64 mg, 50%) as a transparent oil.

**<sup>1</sup>H NMR** (400 MHz, CDCl<sub>3</sub>): δ 7.88 – 7.76 (m, 2H), 7.74 – 7.67 (m, 2H), 7.59 (d, *J* = 8.3 Hz, 1H), 7.48 – 7.41 (m, 1H), 7.39 (d, *J* = 1.8 Hz, 1H), 7.13 – 7.02 (m, 3H), 6.87 (d, *J* = 7.7 Hz, 2H), 5.11 (dd, *J* = 10.6, 5.7 Hz, 1H), 3.77 (s, 3H), 3.65 – 3.22 (m, 2H), 1.22 (hept, *J* = 8.0 Hz, 3H), 0.96 (d, *J* = 7.5 Hz, 18H).

**<sup>13</sup>C NMR** (101 MHz, CDCl<sub>3</sub>): δ 169.3 (C<sub>q</sub>), 167.6 (C<sub>q</sub>), 141.9 (C<sub>q</sub>), 138.3 (C<sub>q</sub>), 137.3 (C<sub>q</sub>), 135.3 (C<sub>q</sub>), 135.0 (C<sub>q</sub>), 134.4 (CH), 133.9 (C<sub>q</sub>), 132.3 (CH), 131.7 (C<sub>q</sub>), 130.8 (CH), 129.5 (CH), 128.6 (CH), 128.6 (CH), 127.9 (CH), 123.7 (CH), 53.1 (CH<sub>3</sub>), 53.0 (CH<sub>3</sub>), 34.4 (CH<sub>2</sub>), 18.5 (CH<sub>3</sub>), 11.1 (CH).

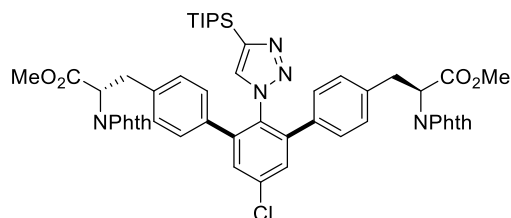
**<sup>29</sup>Si NMR** (80 MHz, CDCl<sub>3</sub>): δ -1.22.

**IR** (ATR): 2942, 1714, 1495, 1384, 1197, 1033, 1017, 882, 720 cm<sup>-1</sup>.

**MS** (ESI) *m/z* (relative intensity): 665.2 [M+Na]<sup>+</sup> (100), 643.2 [M+H]<sup>+</sup> (20).

**HR-MS** (ESI): *m/z* calcd for C<sub>35</sub>H<sub>40</sub>N<sub>4</sub>O<sub>4</sub>Si<sup>35</sup>Cl<sup>+</sup> [M+H]<sup>+</sup> 643.2502, found 643.2498.

**Dimethyl-3,3'-(5'-chloro-2'-(4-(triisopropylsilyl)-1*H*-1,2,3-triazol-1-yl)-[1,1':3',1''-terphenyl]-4,4''-diyl)(2*S*,2'*S*)-bis(2-(1,3-dioxisoindolin-2-yl)propanoate) (141')**



The general procedure A was followed using 1-(4-chlorophenyl)-4-(triisopropylsilyl)-1*H*-1,2,3-triazole **131i** (61.4 mg, 0.20 mmol), dibenzothiophene salt **130** (192 mg, 0.30 mmol), [RuCl<sub>2</sub>(*p*-cymene)]<sub>2</sub> (6.0 mg, 0.01 mmol, 5.0 mol %), and KOAc (39.3 mg, 2.0 equiv.) in *t*AmOH (2.0 mL). Purification by column chromatography on silica gel (*n*hexane/EtOAc: 3/1) yielded **141'** (65 mg, 34%) as a transparent oil.

**<sup>1</sup>H NMR** (400 MHz, CDCl<sub>3</sub>): δ 7.83 – 7.74 (m, 4H), 7.69 (dd, *J* = 5.6, 2.4 Hz, 4H), 7.35 (s, 2H), 7.04 (s, 1H), 6.97 (d, *J* = 7.7 Hz, 4H), 6.83 (d, *J* = 7.6 Hz, 4H), 5.13 (dd, *J* = 10.9, 5.5 Hz, 2H), 3.74 (s, 6H), 3.57 – 3.33 (m, 4H), 1.14 (hept, *J* = 7.2 Hz, 3H), 0.87 (d, *J* = 7.5 Hz, 18H).

**<sup>13</sup>C NMR** (101 MHz, CDCl<sub>3</sub>): δ 169.3 (C<sub>q</sub>), 167.5 (C<sub>q</sub>), 141.3 (C<sub>q</sub>), 141.1 (C<sub>q</sub>), 136.9 (C<sub>q</sub>), 135.5 (C<sub>q</sub>), 135.1 (C<sub>q</sub>), 134.3 (CH), 133.5 (CH), 131.7 (C<sub>q</sub>), 129.5 (CH), 128.9

(CH), 128.4 (CH), 123.6 (CH), 53.0 (CH<sub>3</sub>), 53.0 (CH), 34.3 (CH<sub>2</sub>), 18.4 (C<sub>q</sub>), 14.3 (CH<sub>3</sub>), 10.9 (CH<sub>3</sub>).

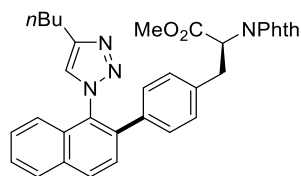
**<sup>29</sup>Si NMR** (80 MHz, CDCl<sub>3</sub>): δ -1.25.

**IR** (ATR): 2941, 2863, 1713, 1384, 1240, 1196, 1005, 881, 718 cm<sup>-1</sup>.

**MS** (ESI) *m/z* (relative intensity): 972.3 [M+Na]<sup>+</sup> (100), 950.3 [M+H]<sup>+</sup> (10).

**HR-MS** (ESI): *m/z* calcd for C<sub>53</sub>H<sub>53</sub>N<sub>5</sub>O<sub>8</sub>Si<sup>35</sup>Cl<sup>+</sup> [M+H]<sup>+</sup> 950.3346, found 950.3343.

**Methyl-(S)-3-(4-(3-(4-butyl-1*H*-1,2,3-triazol-1-yl)naphthalen-2-yl)phenyl)-2-(1,3-dioxoisindolin-2-yl)propanoate (142)**



The general procedure A was followed using 4-butyl-1-(1-naphthyl)-1*H*-1,2,3-triazole **131j** (50.2 mg, 0.20 mmol), dibenzothiophene salt **130** (192 mg, 0.30 mmol), [RuCl<sub>2</sub>(*p*-cymene)]<sub>2</sub> (6.0 mg, 0.01 mmol, 5.0 mol %), and KOAc (39.3 mg, 2.0 equiv.) in toluene (2.0 mL). Purification by column chromatography on silica gel (*n*hexane/EtOAc: 3/1) yielded **142** (24 mg, 21%) as a transparent oil.

**<sup>1</sup>H NMR** (400 MHz, CDCl<sub>3</sub>): δ 8.00 (d, *J* = 8.6 Hz, 1H), 7.91 (d, *J* = 7.9 Hz, 1H), 7.84 – 7.76 (m, 2H), 7.71 (q, *J* = 3.9 Hz, 2H), 7.59 – 7.44 (m, 3H), 7.12 – 6.96 (m, 5H), 5.10 (dd, *J* = 10.8, 5.5 Hz, 1H), 3.78 (s, 3H), 3.61 – 3.45 (m, 2H), 2.66 (t, *J* = 7.6 Hz, 2H), 1.64 – 1.52 (m, 2H), 1.39 – 1.17 (m, 3H), 0.91 (t, *J* = 7.8 Hz, 3H).

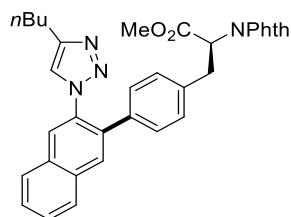
**<sup>13</sup>C NMR** (101 MHz, CDCl<sub>3</sub>): δ 169.3 (C<sub>q</sub>), 167.5 (C<sub>q</sub>), 148.2 (C<sub>q</sub>), 136.7 (C<sub>q</sub>), 136.3 (C<sub>q</sub>), 136.2 (C<sub>q</sub>), 134.3 (CH), 133.3 (C<sub>q</sub>), 131.7 (C<sub>q</sub>), 131.0 (C<sub>q</sub>), 130.6 (C<sub>q</sub>), 130.3 (CH), 129.0 (CH), 128.9 (CH), 128.2 (CH), 127.9 (CH), 127.6 (CH), 124.4 (CH), 123.7 (CH), 123.1 (CH), 53.3 (CH<sub>3</sub>), 53.1 (CH<sub>3</sub>), 34.4 (CH<sub>2</sub>), 31.6 (CH<sub>2</sub>), 25.2 (CH<sub>2</sub>), 22.1 (CH<sub>2</sub>), 14.0 (CH<sub>3</sub>).

**IR** (ATR): 2952, 1789, 1732, 1514, 1491, 1245, 813, 743, 623 cm<sup>-1</sup>.

**MS** (ESI) *m/z* (relative intensity): 581.2 [M+Na]<sup>+</sup> (100), 559.2 [M+H]<sup>+</sup> (10).

**HR-MS** (ESI): *m/z* calcd for C<sub>34</sub>H<sub>31</sub>N<sub>4</sub>O<sub>4</sub><sup>+</sup> [M+H]<sup>+</sup> 559.2340, found 559.2339.

**Methyl-(S)-3-(4-(3-(4-butyl-1*H*-1,2,3-triazol-1-yl)naphthalen-2-yl)phenyl)-2-(1,3-dioxisoindolin-2-yl)propanoate (143)**



The general procedure A was followed using 4-butyl-1-(2-naphthyl)-1*H*-1,2,3-triazole **131k** (50.2 mg, 0.20 mmol), dibenzothiophene salt **130** (192 mg, 0.30 mmol), [RuCl<sub>2</sub>(*p*-cymene)]<sub>2</sub> (6.0 mg, 0.01 mmol, 5.0 mol %), and KOAc (39.3 mg, 2.0 equiv.) in toluene (2.0 mL). Purification by column chromatography on silica gel (*n*hexane/EtOAc: 3/1) yielded **143** (56 mg, 50%) as a transparent oil.

**<sup>1</sup>H NMR** (400 MHz, CDCl<sub>3</sub>): δ 8.13 (s, 1H), 7.97 – 7.87 (m, 3H), 7.88 – 7.78 (m, 2H), 7.74 – 7.68 (m, 2H), 7.60 (q, *J* = 5.6 Hz, 2H), 7.15 (d, *J* = 7.7 Hz, 2H), 7.03 (d, *J* = 7.8 Hz, 2H), 6.92 (s, 1H), 5.16 (dd, *J* = 11.0, 5.2 Hz, 1H), 3.82 (d, *J* = 1.4 Hz, 3H), 3.61 (qd, *J* = 14.3, 7.9 Hz, 2H), 2.64 (t, *J* = 7.6 Hz, 2H), 1.55 (dp, *J* = 17.1, 7.5 Hz, 2H), 1.32 – 1.17 (m, 2H), 0.93 (t, *J* = 7.4 Hz, 3H).

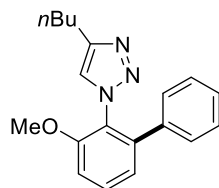
**<sup>13</sup>C NMR** (101 MHz, CDCl<sub>3</sub>): δ 169.3 (C<sub>q</sub>), 167.5 (C<sub>q</sub>), 148.2 (C<sub>q</sub>), 136.7 (C<sub>q</sub>), 136.2 (C<sub>q</sub>), 134.3 (CH), 133.5 (C<sub>q</sub>), 133.3 (C<sub>q</sub>), 132.4 (C<sub>q</sub>), 131.7 (C<sub>q</sub>), 130.3 (CH), 129.2 (CH), 129.0 (CH), 128.1 (CH), 127.9 (CH), 127.7 (CH), 127.3 (CH), 125.6 (CH), 123.6 (CH), 123.3 (CH), 53.3 (CH), 53.1 (CH<sub>3</sub>), 34.5 (CH<sub>2</sub>), 31.6 (CH<sub>2</sub>), 25.1 (CH<sub>2</sub>), 22.1 (CH<sub>2</sub>), 13.9 (CH<sub>3</sub>). *Missing C<sub>q</sub>.*

**IR** (ATR): 2954, 1746, 1714, 1498, 1387, 1220, 884, 722, 530 cm<sup>-1</sup>.

**MS** (ESI) *m/z* (relative intensity): 581.2 [M+Na]<sup>+</sup> (100), 559.2 [M+H]<sup>+</sup> (10).

**HR-MS** (ESI): *m/z* calcd for C<sub>34</sub>H<sub>31</sub>N<sub>4</sub>O<sub>4</sub><sup>+</sup> [M+H]<sup>+</sup> 559.2340, found 559.2332.

**4-Butyl-1-(3-methoxy-[1,1'-biphenyl]-2-yl)-1*H*-1,2,3-triazole (145)**



The general procedure A was followed using 4-butyl-1-(2-methoxyphenyl)-1*H*-1,2,3-triazole **131a** (46.3 mg, 0.20 mmol), 5-phenyl-5*H*-dibenzo[*b,d*]thiophen-5-ium triflate **124a** (123 mg, 0.30 mmol), [RuCl<sub>2</sub>(*p*-cymene)]<sub>2</sub> (6.0 mg, 0.01 mmol, 5.0 mol %), and KOAc (39.3 mg, 2.0 equiv.) in toluene (2.0 mL). Purification by column chromatography on silica gel (*n*hexane/EtOAc: 3/1) yielded **145** (52.0 mg, 85%) as a transparent oil.

**<sup>1</sup>H NMR** (400 MHz, CDCl<sub>3</sub>): δ 7.49 (dd, *J* = 8.1, 8.1 Hz, 1H), 7.19 (dd, *J* = 5.1, 2.1 Hz, 3H), 7.10 – 7.01 (m, 5H), 3.80 (s, 3H), 2.64 (t, *J* = 7.5 Hz, 2H), 1.59 – 1.44 (m, 2H), 1.29 – 1.12 (m, 2H), 0.85 (t, *J* = 7.3 Hz, 3H).

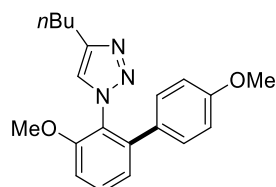
**<sup>13</sup>C NMR** (101 MHz, CDCl<sub>3</sub>): δ 155.2 (C<sub>q</sub>), 147.4 (C<sub>q</sub>), 141.0 (C<sub>q</sub>), 137.4 (C<sub>q</sub>), 130.9 (CH), 128.2 (CH), 128.2 (CH), 127.6 (CH), 124.6 (C<sub>q</sub>), 123.8 (CH), 122.3 (CH), 111.0 (CH), 56.2 (CH<sub>3</sub>), 31.4 (CH<sub>2</sub>), 25.1 (CH<sub>2</sub>), 21.9 (CH<sub>2</sub>), 13.8 (CH<sub>3</sub>).

**IR** (ATR): 2920, 1586, 1470, 1262, 1122, 1039, 1018, 759, 700 cm<sup>-1</sup>.

**MS** (ESI) *m/z* (relative intensity): 330.2 [M+Na]<sup>+</sup> (100), 308.2 [M+H]<sup>+</sup> (60).

**HR-MS** (ESI): *m/z* calcd for C<sub>19</sub>H<sub>22</sub>N<sub>3</sub>O<sup>+</sup> [M+H]<sup>+</sup> 308.1757, found 308.1763.

#### 4-Butyl-1-(3,4'-dimethoxy-[1,1'-biphenyl]-2-yl)-1*H*-1,2,3-triazole (**146**)



The general procedure A was followed using 4-butyl-1-(2-methoxyphenyl)-1*H*-1,2,3-triazole **131a** (46.3 mg, 0.20 mmol), 5-(4-methoxyphenyl)-5*H*-dibenzo[*b,d*]thiophen-5-ium triflate **124b** (132 mg, 0.30 mmol), [RuCl<sub>2</sub>(*p*-cymene)]<sub>2</sub> (6.0 mg, 0.01 mmol, 5.0 mol %), and KOAc (39.3 mg, 2.0 equiv.) in toluene (2.0 mL). Purification by column chromatography on silica gel (*n*hexane/EtOAc: 3/1) yielded **146** (20 mg, 30%) as a white solid.

**m.p.**: 60–62 °C.

**<sup>1</sup>H NMR** (400 MHz, CDCl<sub>3</sub>): δ 7.48 (dd, *J* = 8.3, 7.8 Hz, 1H), 7.09 – 6.97 (m, 5H), 6.73 (d, *J* = 8.8 Hz, 2H), 3.80 (s, 3H), 3.75 (s, 3H), 2.67 (t, *J* = 7.5 Hz, 2H), 1.62 – 1.51 (m, 2H), 1.32 – 1.18 (m, 2H), 0.86 (t, *J* = 7.3 Hz, 3H).



**<sup>13</sup>C NMR** (101 MHz, CDCl<sub>3</sub>): δ 159.3 (C<sub>q</sub>), 155.4 (C<sub>q</sub>), 147.6 (C<sub>q</sub>), 140.8 (C<sub>q</sub>), 130.9 (CH), 129.8 (C<sub>q</sub>), 129.5 (CH), 124.7 (C<sub>q</sub>), 123.9 (CH), 122.3 (CH), 113.8 (CH), 110.7 (CH), 56.3 (CH<sub>3</sub>), 55.3 (CH<sub>3</sub>), 31.5 (CH<sub>2</sub>), 25.3 (CH<sub>2</sub>), 22.1 (CH<sub>2</sub>), 13.9 (CH<sub>3</sub>).

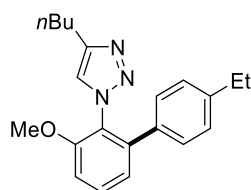
**IR** (ATR): 2932, 1611, 1472, 1439, 1246, 1123, 1022, 833, 791 cm<sup>-1</sup>.

**MS** (ESI) *m/z* (relative intensity): 360.2 [M+Na]<sup>+</sup> (100), 338.2 [M+H]<sup>+</sup> (35).

**HR-MS** (ESI): *m/z* calcd for C<sub>20</sub>H<sub>24</sub>N<sub>3</sub>O<sub>2</sub><sup>+</sup> [M+H]<sup>+</sup> 338.1863, found 338.1866.

The spectral data were in accordance with those reported in the literature.<sup>[163]</sup>

#### 4-Butyl-1-(4'-ethyl-3-methoxy-[1,1'-biphenyl]-2-yl)-1*H*-1,2,3-triazole (**147**)



The general procedure A was followed using 4-butyl-1-(2-methoxyphenyl)-1*H*-1,2,3-triazole **131a** (46.3 mg, 0.20 mmol), 5-(4-ethylphenyl)-5*H*-dibenzo[*b,d*]thiophen-5-ium triflate **124c** (132 mg, 0.30 mmol), [RuCl<sub>2</sub>(*p*-cymene)]<sub>2</sub> (6.0 mg, 0.01 mmol, 5.0 mol %), and KOAc (39.3 mg, 2.0 equiv.) in toluene (2.0 mL). Purification by column chromatography on silica gel (*n*hexane/EtOAc: 10/1) yielded **147** (59.0 mg, 88%) as a white solid.

**m.p.:** 110–114 °C

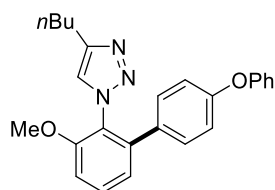
**<sup>1</sup>H NMR** (400 MHz, CDCl<sub>3</sub>): δ 7.47 (dd, *J* = 8.1, 8.1 Hz, 1H), 7.07 (d, *J* = 8.0 Hz, 2H), 7.04 – 7.00 (m, 3H), 6.97 (d, *J* = 8.0 Hz, 2H), 3.78 (s, 3H), 2.65 (t, *J* = 7.5 Hz, 2H), 2.61 – 2.53 (m, 2H), 1.58 – 1.48 (m, 2H), 1.26 – 1.15 (m, 5H), 0.85 (t, *J* = 7.3 Hz, 3H).

**<sup>13</sup>C NMR** (101 MHz, CDCl<sub>3</sub>): δ 155.2 (C<sub>q</sub>), 147.4 (C<sub>q</sub>), 143.7 (C<sub>q</sub>), 141.0 (C<sub>q</sub>), 134.7 (C<sub>q</sub>), 130.8 (CH), 128.2 (CH), 127.7 (CH), 124.6 (C<sub>q</sub>), 123.9 (CH), 122.3 (CH), 110.8 (CH), 56.2 (CH<sub>3</sub>), 31.5 (CH<sub>2</sub>), 28.5 (CH<sub>2</sub>), 25.1 (CH<sub>2</sub>), 21.9 (CH<sub>2</sub>), 15.4 (CH<sub>3</sub>), 13.8 (CH<sub>3</sub>).

**IR** (ATR): 2931, 1584, 1472, 1312, 1262, 1122, 1031, 833, 793 cm<sup>-1</sup>.

**MS** (ESI) *m/z* (relative intensity): 358.2 [M+Na]<sup>+</sup> (100), 336.2 [M+H]<sup>+</sup> (45).

**HR-MS** (ESI): *m/z* calcd for C<sub>21</sub>H<sub>26</sub>N<sub>3</sub>O<sup>+</sup> [M+H]<sup>+</sup> 336.2070, found 336.2071.

**4-Butyl-1-(3-methoxy-4'-phenoxy-[1,1'-biphenyl]-2-yl)-1H-1,2,3-triazole (148)**

The general procedure A was followed using 4-butyl-1-(2-methoxyphenyl)-1H-1,2,3-triazole **131a** (46.3 mg, 0.20 mmol), 5-(4-phenoxyphenyl)-5H-dibenzo[*b,d*]thiophen-5-ium triflate **124d** (151 mg, 0.30 mmol), [RuCl<sub>2</sub>(*p*-cymene)]<sub>2</sub> (6.0 mg, 0.01 mmol, 5.0 mol %), and KOAc (39.3 mg, 2.0 equiv.) in toluene (2.0 mL). Purification by column chromatography on silica gel (*n*hexane/EtOAc: 10/1) yielded **148** (65.2 mg, 82%) as a white solid.

**m.p.:** 126–128 °C.

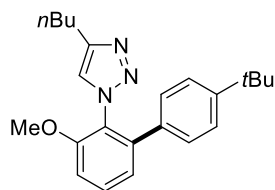
**<sup>1</sup>H NMR** (400 MHz, CDCl<sub>3</sub>): δ 7.54 – 7.46 (m, 1H), 7.32 (ddd, *J* = 9.9, 5.9, 2.2 Hz, 2H), 7.15 – 7.07 (m, 3H), 7.07 – 7.00 (m, 3H), 6.99 – 6.94 (m, 2H), 6.82 – 6.79 (m, 2H), 3.81 (s, 3H), 2.69 (t, *J* = 7.5 Hz, 2H), 1.63 – 1.55 (m, 2H), 1.32 – 1.23 (m, 2H), 0.89 (t, *J* = 7.4 Hz, 3H).

**<sup>13</sup>C NMR** (101 MHz, CDCl<sub>3</sub>): δ 157.2 (C<sub>q</sub>), 156.8 (C<sub>q</sub>), 155.4 (C<sub>q</sub>), 147.7 (C<sub>q</sub>), 140.6 (C<sub>q</sub>), 132.3 (C<sub>q</sub>), 131.0 (CH), 129.9 (CH), 129.8 (CH), 124.7 (C<sub>q</sub>), 123.9 (CH), 123.7 (CH), 122.3 (CH), 119.3 (CH), 118.3 (CH), 111.0 (CH), 56.3 (CH<sub>3</sub>), 31.6 (CH<sub>2</sub>), 25.3 (CH<sub>2</sub>), 22.1 (CH<sub>2</sub>), 13.9 (CH<sub>3</sub>).

**IR** (ATR): 2930, 1587, 1471, 1439, 1233, 1169, 1122, 793, 693 cm<sup>-1</sup>.

**MS** (ESI) *m/z* (relative intensity): 422.2 [M+Na]<sup>+</sup> (95), 400.2 [M+H]<sup>+</sup> (100).

**HR-MS** (ESI): *m/z* calcd for C<sub>25</sub>H<sub>26</sub>N<sub>3</sub>O<sub>2</sub><sup>+</sup> [M+H]<sup>+</sup> 400.2020, found 400.2016.

**4-Butyl-1-(4'-(*tert*-butyl)-3-methoxy-[1,1'-biphenyl]-2-yl)-1H-1,2,3-triazole (149)**

The general procedure A was followed using 4-butyl-1-(2-methoxyphenyl)-1H-1,2,3-triazole **131a** (46.3 mg, 0.20 mmol), 5-(4-*tert*-butylphenyl)-5H-dibenzo[*b,d*]thiophen-5-

ium triflate **124e** (140 mg, 0.30 mmol), [RuCl<sub>2</sub>(*p*-cymene)]<sub>2</sub> (6.0 mg, 0.01 mmol, 5.0 mol %), and KOAc (39.3 mg, 2.0 equiv.) in toluene (2.0 mL). Purification by column chromatography on silica gel (*n*hexane/EtOAc: 10/1) yielded **149** (67.0 mg, 92%) as a white solid.

**m.p.:** 124–126 °C.

**<sup>1</sup>H NMR** (400 MHz, CDCl<sub>3</sub>): δ 7.53 – 7.43 (m, 1H), 7.24 – 7.17 (m, 2H), 7.09 (dd, *J* = 7.8, 1.2 Hz, 1H), 7.04 – 6.96 (m, 4H), 3.80 (s, 3H), 2.65 (t, *J* = 7.5 Hz, 2H), 1.52 (p, *J* = 7.5 Hz, 2H), 1.25 (s, 9H), 1.19 (d, *J* = 7.0 Hz, 2H), 0.85 (t, *J* = 7.4 Hz, 3H).

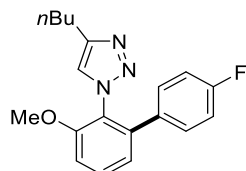
**<sup>13</sup>C NMR** (101 MHz, CDCl<sub>3</sub>): δ 155.2 (C<sub>q</sub>), 150.6 (C<sub>q</sub>), 147.4 (C<sub>q</sub>), 141.0 (C<sub>q</sub>), 134.4 (C<sub>q</sub>), 130.8 (CH), 127.9 (CH), 125.1 (CH), 124.6 (C<sub>q</sub>), 123.8 (CH), 122.3 (CH), 110.8 (CH), 56.2 (CH<sub>3</sub>), 34.5 (C<sub>q</sub>), 31.6 (CH<sub>2</sub>), 31.2 (CH<sub>3</sub>), 25.1 (CH<sub>2</sub>), 21.9 (CH<sub>2</sub>), 13.8 (CH<sub>3</sub>).

**IR** (ATR): 2956, 1600, 1583, 1473, 1313, 1263, 1130, 1012, 730 cm<sup>-1</sup>.

**MS** (ESI) *m/z* (relative intensity): 386.2 [M+Na]<sup>+</sup> (100), 364.2 [M+H]<sup>+</sup> (20).

**HR-MS** (ESI): *m/z* calcd for C<sub>23</sub>H<sub>30</sub>N<sub>3</sub>O<sup>+</sup> [M+H]<sup>+</sup> 364.2383, found 364.2374.

#### 4-Butyl-1-(4'-fluoro-3-methoxy-[1,1'-biphenyl]-2-yl)-1*H*-1,2,3-triazole (**150**)



The general procedure A was followed using 4-butyl-1-(2-methoxyphenyl)-1*H*-1,2,3-triazole **131a** (46.3 mg, 0.20 mmol), 5-(4-fluorophenyl)-5*H*-dibenzo[*b,d*]thiophen-5-ium triflate **124f** (129 mg, 0.30 mmol), [RuCl<sub>2</sub>(*p*-cymene)]<sub>2</sub> (6.0 mg, 0.01 mmol, 5.0 mol %), and KOAc (39.3 mg, 2.0 equiv.) in toluene (2.0 mL). Purification by column chromatography on silica gel (*n*hexane/EtOAc: 10/1) yielded **150** (49.4 mg, 76%) as a white solid.

**m.p.:** 86–88 °C.

**<sup>1</sup>H NMR** (400 MHz, CDCl<sub>3</sub>): δ 7.52 – 7.46 (m, 1H), 7.10 – 6.99 (m, 5H), 6.88 (dd, *J* = 8.7, 8.7 Hz, 2H), 3.80 (s, 3H), 2.66 (t, *J* = 7.5 Hz, 2H), 1.55 (p, *J* = 7.5 Hz, 2H), 1.26 – 1.16 (m, 2H), 0.86 (t, *J* = 7.3 Hz, 3H).

**<sup>13</sup>C NMR** (101 MHz, CDCl<sub>3</sub>): δ 162.5 (d, <sup>1</sup>J<sub>C-F</sub> = 248 Hz, C<sub>q</sub>), 155.3 (C<sub>q</sub>), 147.7 (C<sub>q</sub>), 140.1 (C<sub>q</sub>) 133.5 (d, <sup>4</sup>J<sub>C-F</sub> = 3 Hz, C<sub>q</sub>), 131.0 (CH), 130.0 (d, <sup>3</sup>J<sub>C-F</sub> = 8 Hz, CH), 124.7 (C<sub>q</sub>), 123.8 (CH), 122.2 (CH), 115.3 (d, <sup>2</sup>J<sub>C-F</sub> = 22 Hz, CH), 111.2 (CH), 56.3 (CH<sub>3</sub>), 31.5 (CH<sub>2</sub>), 25.2 (CH<sub>2</sub>), 22.0 (CH<sub>2</sub>), 13.8 (CH<sub>3</sub>).

**<sup>19</sup>F NMR** (282 MHz, CDCl<sub>3</sub>): δ -113.5 – -115.8 (m).

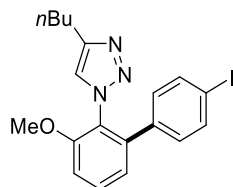
**IR** (ATR): 2933, 1607, 1472, 1313, 1222, 1121, 1026, 838, 791 cm<sup>-1</sup>.

**MS** (ESI) *m/z* (relative intensity): 348.2 [M+Na]<sup>+</sup> (100), 326.2 [M+H]<sup>+</sup> (10).

**HR-MS** (ESI): *m/z* calcd for C<sub>19</sub>H<sub>21</sub>FN<sub>3</sub>O<sup>+</sup> [M+H]<sup>+</sup> 326.1663, found 326.1665.

The spectral data were in accordance with those reported in the literature.<sup>[148]</sup>

#### 4-Butyl-1-(4'-iodo-3-methoxy-[1,1'-biphenyl]-2-yl)-1*H*-1,2,3-triazole (**151**)



The general procedure A was followed using 4-butyl-1-(2-methoxyphenyl)-1*H*-1,2,3-triazole **131a** (43.8 mg, 0.20 mmol), 5-(4-iodophenyl)-5*H*-dibenzo[*b,d*]thiophen-5-ium triflate **124g** (160.8 mg, 0.30 mmol), [RuCl<sub>2</sub>(*p*-cymene)]<sub>2</sub> (6.0 mg, 0.01 mmol, 5.0 mol %), and KOAc (39.3 mg, 2.0 equiv.) in toluene (2.0 mL). Purification by column chromatography on silica gel (*n*hexane/EtOAc: 10/1) yielded **151** (61 mg, 70%) as a transparent oil.

**m.p.**: 110–112 °C.

**<sup>1</sup>H NMR** (400 MHz, CDCl<sub>3</sub>): δ 7.57 (d, *J* = 8.3 Hz, 2H), 7.58 (d, *J* = 8.1 Hz, 1H), 7.25 – 6.99 (m, 3H), 6.84 (d, *J* = 8.4 Hz, 2H), 3.85 (s, 3H), 2.7 (t, *J* = 7.5 Hz, 2H), 1.77 – 1.49 (m, 2H), 1.54 – 1.13 (m, 2H), 0.99 (t, *J* = 7.4 Hz, 3H).

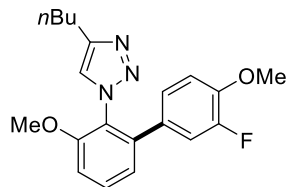
**<sup>13</sup>C NMR** (101 MHz, CDCl<sub>3</sub>): δ 155.3 (C<sub>q</sub>), 147.7 (C<sub>q</sub>), 139.9 (C<sub>q</sub>), 137.4 (CH), 137.0 (C<sub>q</sub>), 131.1 (CH), 130.1 (CH), 124.4 (C<sub>q</sub>), 123.9 (CH), 122.0 (CH), 111.4 (CH), 93.9 (C<sub>q</sub>), 56.3 (CH), 31.5 (CH<sub>2</sub>), 25.2 (CH<sub>2</sub>), 22.0 (CH<sub>2</sub>), 14.0 (CH<sub>3</sub>).

**IR** (ATR): 2928, 2867, 1582, 1552, 1441, 1268, 1209, 1001, 792 cm<sup>-1</sup>.

**MS** (ESI) *m/z* (relative intensity): 456.1 [M+Na]<sup>+</sup> (100), 434.1 [M+H]<sup>+</sup> (30).

**HR-MS** (ESI):  $m/z$  calcd for  $C_{19}H_{21}N_3O_1^+$   $[M+H]^+$  434.0724, found 434.0720.

**4-Butyl-1-(3'-fluoro-3,4'-dimethoxy-[1,1'-biphenyl]-2-yl)-1H-1,2,3-triazole (152)**



The general procedure A was followed using 4-butyl-1-(2-methoxyphenyl)-1H-1,2,3-triazole **131a** (46.3 mg, 0.20 mmol), 5-(3-fluoro-4-methoxyphenyl)-5H-dibenzo[*b,d*]thiophen-5-ium triflate **124h** (138 mg, 0.30 mmol),  $[RuCl_2(p\text{-cymene})]_2$  (6.0 mg, 0.01 mmol, 5.0 mol %), and KOAc (39.3 mg, 2.0 equiv.) in toluene (2.0 mL). Purification by column chromatography on silica gel (*n*hexane/EtOAc: 5/1) yielded **152** (45.7 mg, 64%) as a transparent oil.

**$^1H$  NMR** (400 MHz,  $CDCl_3$ ):  $\delta$  7.50 – 7.45 (m, 1H), 7.10 (d,  $J = 1.0$  Hz, 1H), 7.07 – 7.00 (m, 2H), 6.81 (d,  $J = 11.9$  Hz, 1H), 6.76 (dt,  $J = 2.7, 1.2$  Hz, 2H), 3.81 (s, 3H), 3.79 (s, 3H), 2.68 (t,  $J = 7.5$  Hz, 2H), 1.62 – 1.53 (m, 2H), 1.29 – 1.21 (m, 2H), 0.87 (t,  $J = 7.5$  Hz, 3H).

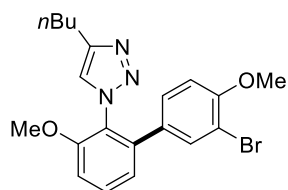
**$^{13}C$  NMR** (101 MHz,  $CDCl_3$ ):  $\delta$  155.2 ( $C_q$ ), 151.9 (d,  $^1J_{C-F} = 246.4$  Hz,  $C_q$ ), 147.6 ( $C_q$ ), 147.3 (d,  $^3J_{C-F} = 10.2$  Hz,  $C_q$ ), 139.6 ( $C_q$ ), 130.9 (CH), 130.3 (d,  $^2J_{C-F} = 6.7$  Hz,  $C_q$ ), 124.5 ( $C_q$ ), 124.3 (d,  $^4J_{C-F} = 3.6$  Hz, CH), 123.8 (CH), 122.1 (CH), 116.0 (d,  $^2J_{C-F} = 19.2$  Hz, CH), 113.0 (CH), 111.0 (CH), 56.2 ( $CH_3$ ), 56.1 ( $CH_3$ ), 31.5 ( $CH_2$ ), 25.2 ( $CH_2$ ), 22.0 ( $CH_2$ ), 13.8 ( $CH_3$ ).

**$^{19}F$  NMR** (377 MHz,  $CDCl_3$ ):  $\delta$  -130.8 – -136.8 (m).

**IR** (ATR): 2934, 1573, 1521, 1440, 1268, 1204, 1108, 1022, 761  $cm^{-1}$ .

**MS** (ESI)  $m/z$  (relative intensity): 378.2  $[M+Na]^+$  (100), 356.2  $[M+H]^+$  (65).

**HR-MS** (ESI):  $m/z$  calcd for  $C_{20}H_{23}FN_3O_2^+$   $[M+H]^+$  356.1769, found 356.1770.

**1-(3'-Bromo-3,4'-dimethoxy-[1,1'-biphenyl]-2-yl)-4-butyl-1H-1,2,3-triazole (153)**

The general procedure A was followed using 4-butyl-1-(2-methoxyphenyl)-1H-1,2,3-triazole **131a** (46.3 mg, 0.20 mmol), 5-(3-bromo-4-methoxyphenyl)-5H-dibenzo[*b,d*]thiophen-5-ium triflate **124i** (156 mg, 0.30 mmol), [RuCl<sub>2</sub>(*p*-cymene)]<sub>2</sub> (6.0 mg, 0.01 mmol, 5.0 mol %), and KOAc (39.3 mg, 2.0 equiv.) in toluene (2.0 mL). Purification by column chromatography on silica gel (*n*hexane/EtOAc: 10/1) yielded **153** (54.1 mg, 65%) as a transparent oil.

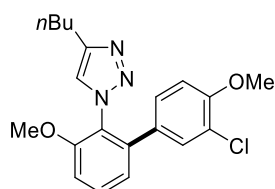
**<sup>1</sup>H NMR** (400 MHz, CDCl<sub>3</sub>): δ 7.50 – 7.44 (m, 1H), 7.30 (t, *J* = 2.2 Hz, 1H), 7.11 (s, 1H), 7.06 – 7.01 (m, 2H), 6.92 (dt, *J* = 8.5, 1.7 Hz, 1H), 6.68 (dd, *J* = 8.5, 1.2 Hz, 1H), 3.80 (dd, *J* = 10.3, 1.9 Hz, 6H), 2.68 (t, *J* = 7.5 Hz, 2H), 1.63 – 1.53 (m, 2H), 1.31 – 1.18 (m, 2H), 0.87 (t, *J* = 7.3 Hz, 3H).

**<sup>13</sup>C NMR** (101 MHz, CDCl<sub>3</sub>): δ 155.4 (C<sub>q</sub>), 155.2 (C<sub>q</sub>), 147.6 (C<sub>q</sub>), 139.3 (C<sub>q</sub>), 133.0 (CH), 131.1 (C<sub>q</sub>), 130.9 (CH), 128.4 (CH), 124.5 (C<sub>q</sub>), 123.9 (CH), 122.1 (CH), 111.5 (CH), 111.4 (C<sub>q</sub>), 111.1 (CH), 56.2 (CH<sub>3</sub>), 56.2 (CH<sub>3</sub>), 31.5 (CH<sub>2</sub>), 25.2 (CH<sub>2</sub>), 22.0 (CH<sub>2</sub>), 13.9 (CH<sub>3</sub>).

**IR** (ATR): 2930, 1583, 1471, 1288, 1265, 1123, 1017, 790, 731 cm<sup>-1</sup>.

**MS** (ESI) *m/z* (relative intensity): 438.1 (<sup>79</sup>Br) [M+Na]<sup>+</sup> (100), 416.1 (<sup>79</sup>Br) [M+H]<sup>+</sup> (50).

**HR-MS** (ESI): *m/z* calcd for C<sub>20</sub>H<sub>23</sub><sup>79</sup>BrN<sub>3</sub>O<sub>2</sub><sup>+</sup> [M+H]<sup>+</sup> 416.0968, found 416.0970.

**4-Butyl-1-(3'-chloro-3,4'-dimethoxy-[1,1'-biphenyl]-2-yl)-1H-1,2,3-triazole (154)**

The general procedure A was followed using 4-butyl-1-(2-methoxyphenyl)-1H-1,2,3-triazole **131a** (46.3 mg, 0.20 mmol), 5-(3-chloro-4-methoxyphenyl)-5H-dibenzo[*b,d*]thiophen-5-ium triflate **124j** (142.2 mg, 0.30 mmol), [RuCl<sub>2</sub>(*p*-cymene)]<sub>2</sub>

(6.0 mg, 0.01 mmol, 5.0 mol %), and KOAc (39.3 mg, 2.0 equiv.) in toluene (2.0 mL). Purification by column chromatography on silica gel (*n*hexane/EtOAc: 10/1) yielded **154** (66 mg, 85%) as a transparent oil.

**<sup>1</sup>H NMR** (400 MHz, CDCl<sub>3</sub>): δ 7.47 (dd, *J* = 8.1, 8.1 Hz, 1H), 7.12 (d, *J* = 2.3 Hz, 1H), 7.11 (s, 1H), 7.06 – 7.03 (m, 1H), 7.03 – 7.00 (m, 1H), 6.88 (dd, *J* = 8.5, 2.2 Hz, 1H), 6.71 (d, *J* = 8.6 Hz, 1H), 3.82 (s, 3H), 3.79 (s, 3H), 2.68 (t, *J* = 7.5 Hz, 2H), 1.74 – 1.47 (m, 2H), 1.38 – 1.12 (m, 2H), 0.87 (t, *J* = 7.3 Hz, 3H).

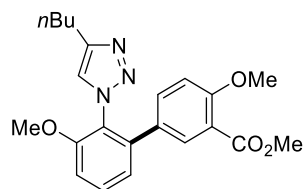
**<sup>13</sup>C NMR** (101 MHz, CDCl<sub>3</sub>): δ 155.3 (C<sub>q</sub>), 154.6 (C<sub>q</sub>), 147.7 (C<sub>q</sub>), 139.5 (C<sub>q</sub>), 131.0 (CH), 130.7 (C<sub>q</sub>), 130.0 (CH), 127.7 (CH), 124.6 (C<sub>q</sub>), 123.9 (CH), 122.3 (C<sub>q</sub>), 122.2 (CH), 111.7 (CH), 111.1 (CH), 56.3 (CH<sub>3</sub>), 56.1 (CH<sub>3</sub>), 31.5 (CH<sub>2</sub>), 25.2 (CH<sub>2</sub>), 22.1 (CH<sub>2</sub>), 13.9 (CH<sub>3</sub>).

**IR** (ATR): 2955, 2842, 1602, 1583, 1490, 1261, 789, 743, 701 cm<sup>-1</sup>.

**MS** (ESI) *m/z* (relative intensity): 394.1 (<sup>35</sup>Cl) [M+Na]<sup>+</sup> (100), 372.1 (<sup>35</sup>Cl) [M+H]<sup>+</sup> (50).

**HR-MS** (ESI): *m/z* calcd for C<sub>20</sub>H<sub>23</sub>IN<sub>3</sub>O<sub>2</sub><sup>35</sup>Cl<sup>+</sup> [M+H]<sup>+</sup> 372.1473, found 372.1473.

### Methyl-2'-(4-butyl-1*H*-1,2,3-triazol-1-yl)-3',4-dimethoxy-[1,1'-biphenyl]-3-carboxylate (**155**)



The general procedure A was followed using 4-butyl-1-(2-methoxyphenyl)-1*H*-1,2,3-triazole **131a** (46.3 mg, 0.20 mmol), 5-(4-methoxy-3-(methoxycarbonyl)phenyl)-5*H*-dibenzo[*b,d*]thiophen-5-ium triflate **124k** (150 mg, 0.30 mmol), [RuCl<sub>2</sub>(*p*-cymene)]<sub>2</sub> (6.0 mg, 0.01 mmol, 5.0 mol %), and KOAc (39.3 mg, 2.0 equiv.) in toluene (2.0 mL). Purification by column chromatography on silica gel (*n*hexane/EtOAc: 10/1) yielded **155** (69.5 mg, 88%) as a transparent oil.

**<sup>1</sup>H NMR** (400 MHz, CDCl<sub>3</sub>): δ 7.60 (d, *J* = 2.4 Hz, 1H), 7.46 (dd, *J* = 8.1, 8.1 Hz, 1H), 7.11 – 6.97 (m, 4H), 6.74 (d, *J* = 8.7 Hz, 1H), 3.81 (d, *J* = 4.8 Hz, 6H), 3.77 (s, 3H), 2.63 (t, *J* = 7.6 Hz, 2H), 1.54 (p, *J* = 7.6 Hz, 2H), 1.30 – 1.14 (m, 2H), 0.84 (t, *J* = 7.4

Hz, 3H).

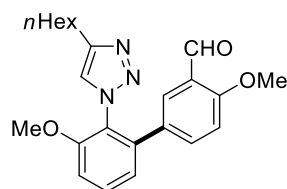
**<sup>13</sup>C NMR** (101 MHz, CDCl<sub>3</sub>): δ 166.2 (C<sub>q</sub>), 158.7 (C<sub>q</sub>), 155.3 (C<sub>q</sub>), 147.61 (C<sub>q</sub>), 139.6 (C<sub>q</sub>), 133.2 (CH), 131.7 (CH), 131.0 (CH), 129.3 (C<sub>q</sub>), 124.5 (C<sub>q</sub>), 123.8 (CH), 122.1 (CH), 119.7 (C<sub>q</sub>), 111.8 (CH), 111.0 (CH), 56.2 (CH<sub>3</sub>), 56.0 (CH<sub>3</sub>), 52.0 (CH<sub>3</sub>), 31.4 (CH<sub>2</sub>), 25.1 (CH<sub>2</sub>), 22.0 (CH<sub>2</sub>), 13.8 (CH<sub>3</sub>).

**IR** (ATR): 2932, 1730, 1473, 1434, 1266, 1083, 1021, 793, 727 cm<sup>-1</sup>.

**MS** (ESI) *m/z* (relative intensity): 418.2 [M+Na]<sup>+</sup> (100), 396.2 [M+H]<sup>+</sup> (20).

**HR-MS** (ESI): *m/z* calcd for C<sub>22</sub>H<sub>26</sub>N<sub>3</sub>O<sub>4</sub><sup>+</sup> [M+H]<sup>+</sup> 396.1918, found 396.1918.

**2'-(4-Hexyl-1*H*-1,2,3-triazol-1-yl)-3',4-dimethoxy-[1,1'-biphenyl]-3-carbaldehyde (156)**



The general procedure A was followed using 4-hexyl-1-(2-methoxyphenyl)-1*H*-1,2,3-triazole **131g** (51.9 mg, 0.20 mmol), 5-(3-formyl-4-methoxyphenyl)-5*H*-dibenzo[*b,d*]thiophen-5-ium triflate **124i** (145 mg, 0.30 mmol), [RuCl<sub>2</sub>(*p*-cymene)]<sub>2</sub> (6.0 mg, 0.01 mmol, 5.0 mol %), and KOAc (39.3 mg, 2.0 equiv.) in *t*AmOH (2.0 mL). Purification by column chromatography on silica gel (*n*hexane/EtOAc: 10/1) yielded **156** (26.0 mg, 33%) as a pale-yellow oil.

**<sup>1</sup>H NMR** (400 MHz, CDCl<sub>3</sub>): δ 10.38 (s, 1H), 7.65 (s, 1H), 7.49 (t, *J* = 8.1 Hz, 1H), 7.22 – 7.13 (m, 2H), 7.11 – 7.01 (m, 2H), 6.76 (d, *J* = 8.7 Hz, 1H), 3.86 (s, 3H), 3.79 (s, 3H), 2.66 (t, *J* = 7.5 Hz, 2H), 1.61 – 1.54 (m, 2H), 1.24 (s, 6H), 0.85 (s, 3H).

**<sup>13</sup>C NMR** (101 MHz, CDCl<sub>3</sub>): δ 189.7 (CH), 161.7 (C<sub>q</sub>), 155.6 (C<sub>q</sub>), 148.1 (C<sub>q</sub>), 139.9 (C<sub>q</sub>), 136.0 (CH), 131.4 (CH), 130.5 (C<sub>q</sub>), 128.8 (CH), 124.9 (C<sub>q</sub>), 124.9 (C<sub>q</sub>), 124.4 (CH), 122.6 (CH), 112.0 (CH), 111.5 (CH), 56.6 (CH<sub>3</sub>), 56.1 (CH<sub>3</sub>), 32.0 (CH<sub>2</sub>), 29.7 (CH<sub>2</sub>), 29.1 (CH<sub>2</sub>), 25.9 (CH<sub>2</sub>), 23.0 (CH<sub>2</sub>), 14.5 (CH<sub>3</sub>).

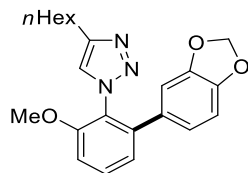
**IR** (ATR): 2927, 1681, 1472, 1391, 1262, 1181, 1105, 1020, 794 cm<sup>-1</sup>.

**MS** (ESI) *m/z* (relative intensity): 416.2 [M+Na]<sup>+</sup> (100), 394.2 [M+H]<sup>+</sup> (30).



**HR-MS** (ESI):  $m/z$  calcd for  $C_{23}H_{28}N_3O_3^+$   $[M+H]^+$  394.2125, found 394.2125.

**1-(2-(Benzo[d][1,3]dioxol-5-yl)-6-methoxyphenyl)-4-hexyl-1H-1,2,3-triazole (157)**



The general procedure A was followed using 4-hexyl-1-(2-methoxyphenyl)-1H-1,2,3-triazole **131g** (51.9 mg, 0.20 mmol), 5-(benzo[d][1,3]dioxol-5-yl)-5H-dibenzo[b,d]thiophen-5-ium triflate **124m** (136 mg, 0.30 mmol),  $[RuCl_2(p\text{-cymene})]_2$  (6.0 mg, 0.01 mmol, 5.0 mol %), and KOAc (39.3 mg, 2.0 equiv.) in *t*AmOH (2.0 mL). Purification by column chromatography on silica gel (*n*hexane/EtOAc: 10/1) yielded **157** (64.5 mg, 85%) as a transparent oil.

**$^1H$  NMR** (400 MHz,  $CDCl_3$ ):  $\delta$  7.45 (t,  $J$  = 8.1 Hz, 1H), 7.10 (s, 1H), 7.02 (t,  $J$  = 8.8 Hz, 2H), 6.62 (d,  $J$  = 7.9 Hz, 1H), 6.58 – 6.49 (m, 2H), 5.87 (s, 2H), 3.78 (s, 3H), 2.67 (t,  $J$  = 7.5 Hz, 2H), 1.65 – 1.53 (m, 2H), 1.25 (s, 6H), 0.86 (s, 3H).

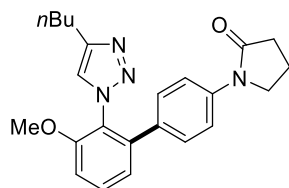
**$^{13}C$  NMR** (101 MHz,  $CDCl_3$ ):  $\delta$  155.2 ( $C_q$ ), 147.6 ( $C_q$ ), 147.2 ( $C_q$ ), 140.7 ( $C_q$ ), 131.3 ( $C_q$ ), 130.8 (CH), 124.6 ( $C_q$ ), 123.9 (CH), 122.3 (CH), 122.1 (CH), 110.8 (CH), 108.8 (CH), 108.2 (CH), 101.1 ( $CH_2$ ), 56.3 ( $CH_3$ ), 31.6 ( $CH_2$ ), 29.4 ( $CH_2$ ), 28.6 ( $CH_2$ ), 25.5 ( $CH_2$ ), 22.6 ( $CH_2$ ), 14.2 ( $CH_3$ ).

**IR** (ATR): 2928, 1580, 1470, 1431, 1267, 1227, 1094, 1039, 788  $cm^{-1}$ .

**MS** (ESI)  $m/z$  (relative intensity): 402.2  $[M+Na]^+$  (100), 380.2  $[M+H]^+$  (90).

**HR-MS** (ESI):  $m/z$  calcd for  $C_{22}H_{26}N_3O_3^+$   $[M+H]^+$  380.1969, found 380.1970.

**1-(2'-(4-Butyl-1H-1,2,3-triazol-1-yl)-3'-methoxy-[1,1'-biphenyl]-4-yl)pyrrolidin-2-one (158)**



The general procedure A was followed using 4-butyl-1-(2-methoxyphenyl)-1H-1,2,3-

triazole **131a** (46.3 mg, 0.20 mmol), 5-(4-(2-oxopyrrolidin-1-yl)phenyl)-5H-dibenzo[b,d]thiophen-5-ium triflate **124n** (148 mg, 0.30 mmol), [RuCl<sub>2</sub>(*p*-cymene)]<sub>2</sub> (6.0 mg, 0.01 mmol, 5.0 mol %), and KOAc (39.3 mg, 2.0 equiv.) in toluene (2.0 mL). Purification by column chromatography on silica gel (*n*hexane/EtOAc: 10/1) yielded **158** (66 mg, 85%) as a transparent oil.

**<sup>1</sup>H NMR** (400 MHz, CDCl<sub>3</sub>): δ 7.66 – 7.45 (m, 3H), 7.11 – 7.08 (m, 4H), 7.08 (d, *J* = 1.2 Hz, 1H), 3.87 (s, 3H), 3.81 (d, *J* = 7.1 Hz, 2H), 2.74 (t, *J* = 7.5 Hz, 2H), 2.66 (t, *J* = 8.1 Hz, 2H), 2.20 – 2.14 (m, 2H), 1.61 – 1.54 (m, 2H), 1.31 – 1.27 (m, 2H), 0.99 (t, *J* = 7.4 Hz, 3H).

**<sup>13</sup>C NMR** (101 MHz, CDCl<sub>3</sub>): δ 174.3 (C<sub>q</sub>), 155.3 (C<sub>q</sub>), 147.6 (C<sub>q</sub>), 140.5 (C<sub>q</sub>), 139.0 (C<sub>q</sub>), 133.4 (C<sub>q</sub>), 131.0 (CH), 128.8 (CH), 124.6 (C<sub>q</sub>), 123.9 (CH), 122.4 (CH), 119.4 (CH), 111.0 (CH), 56.3 (CH), 48.6 (CH<sub>2</sub>), 32.9 (CH<sub>2</sub>), 31.5 (CH<sub>2</sub>), 25.3 (CH<sub>2</sub>), 22.1 (CH<sub>2</sub>), 18.0 (CH<sub>2</sub>), 13.9 (CH<sub>3</sub>).

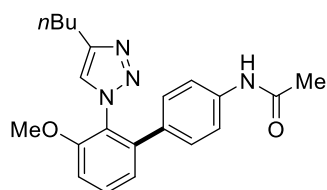
**IR** (ATR): 3137, 2953, 2929, 2869, 1692, 1608, 1583, 1388, 1122 cm<sup>-1</sup>.

**MS** (ESI) *m/z* (relative intensity): 413.2 [M+Na]<sup>+</sup> (100), 391.2 [M+H]<sup>+</sup> (25).

**HR-MS** (ESI): *m/z* calcd for C<sub>23</sub>H<sub>27</sub>N<sub>4</sub>O<sub>2</sub><sup>+</sup> [M+H]<sup>+</sup> 391.2129, found 391.2126.

### ***N*-(2'-(4-Butyl-1*H*-1,2,3-triazol-1-yl)-3'-methoxy-[1,1'-biphenyl]-4-yl)acetamide**

**(159)**



The general procedure A was followed using 4-butyl-1-(2-methoxyphenyl)-1*H*-1,2,3-triazole **131a** (46.3 mg, 0.20 mmol), 5-(4-acetamidophenyl)-5*H*-dibenzo[b,d]thiophen-5-ium triflate **124o** (140 mg, 0.30 mmol), [RuCl<sub>2</sub>(*p*-cymene)]<sub>2</sub> (6.0 mg, 0.01 mmol, 5.0 mol %), and KOAc (39.3 mg, 2.0 equiv.) in toluene (2.0 mL). Purification by column chromatography on silica gel (*n*hexane/EtOAc: 1/1) yielded **159** (68.7 mg, 93%) as a transparent oil.

**<sup>1</sup>H NMR** (400 MHz, CDCl<sub>3</sub>): δ 9.44 (s, 1H), 7.49 – 7.44 (m, 1H), 7.36 (d, *J* = 8.6 Hz,

2H), 7.17 (s, 1H), 7.02 (ddd,  $J = 14.9, 8.1, 1.2$  Hz, 2H), 6.92 (d,  $J = 8.6$  Hz, 2H), 3.77 (s, 3H), 2.64 (t,  $J = 7.5$  Hz, 2H), 2.05 (s, 3H), 1.58 – 1.49 (m, 2H), 1.28 – 1.14 (m, 2H), 0.82 (t,  $J = 7.3$  Hz, 3H).

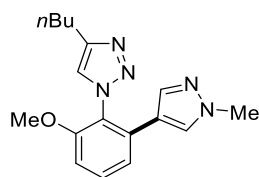
**$^{13}\text{C}$  NMR** (101 MHz,  $\text{CDCl}_3$ ):  $\delta$  169.3 ( $\text{C}_q$ ), 155.0 ( $\text{C}_q$ ), 147.6 ( $\text{C}_q$ ), 140.9 ( $\text{C}_q$ ), 138.8 ( $\text{C}_q$ ), 132.2 ( $\text{C}_q$ ), 131.1 (CH), 128.5 (CH), 124.5 (CH), 124.1 ( $\text{C}_q$ ), 122.5 (CH), 119.2 (CH), 110.6 (CH), 56.2 ( $\text{CH}_3$ ), 31.3 ( $\text{CH}_2$ ), 25.1 ( $\text{CH}_2$ ), 24.2 ( $\text{CH}_3$ ), 22.0 ( $\text{CH}_2$ ), 13.7 ( $\text{CH}_3$ ).

**IR** (ATR): 2931, 1671, 1598, 1416, 1267, 1124, 1013, 791, 727  $\text{cm}^{-1}$ .

**MS** (ESI)  $m/z$  (relative intensity): 387.2  $[\text{M}+\text{Na}]^+$  (100), 365.2  $[\text{M}+\text{H}]^+$  (40).

**HR-MS** (ESI):  $m/z$  calcd for  $\text{C}_{21}\text{H}_{25}\text{N}_4\text{O}_2^+$   $[\text{M}+\text{H}]^+$  365.1972, found 365.1975.

#### 4-Butyl-1-(2-methoxy-6-(1-methyl-1H-pyrazol-4-yl)phenyl)-1H-1,2,3-triazole (160)



The general procedure A was followed using 4-butyl-1-(2-methoxyphenyl)-1H-1,2,3-triazole **131a** (46.2 mg, 0.20 mmol), 5-(1-methyl-1H-pyrazol-4-yl)-5H-dibenzo[*b,d*]thiophen-5-ium triflate **124p** (79.5 mg, 0.30 mmol),  $[\text{RuCl}_2(\textit{p}\text{-cymene})]_2$  (6.0 mg, 0.01 mmol, 5.0 mol %), and KOAc (39.3 mg, 2.0 equiv.) in toluene (2.0 mL). Purification by column chromatography on silica gel (*n*hexane/EtOAc: 3/1) yielded **160** (27 mg, 43%) as a transparent oil.

**$^1\text{H}$  NMR** (400 MHz,  $\text{CDCl}_3$ ):  $\delta$  7.45 (dd,  $J = 8.1, 8.1$  Hz, 1H), 7.33 (s, 1H), 7.23 (s, 1H), 7.19 (d,  $J = 8.0$  Hz, 1H), 6.91 (d,  $J = 8.3$  Hz, 1H), 6.51 (s, 1H), 3.75 (s, 3H), 3.72 (s, 3H), 2.80 (t,  $J = 7.6$  Hz, 2H), 1.70 (p,  $J = 7.7$  Hz, 2H), 1.38 (h,  $J = 7.4$  Hz, 2H), 0.94 (t,  $J = 7.4$  Hz, 3H).

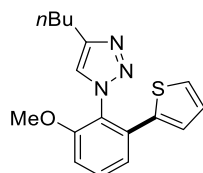
**$^{13}\text{C}$  NMR** (101 MHz,  $\text{CDCl}_3$ ):  $\delta$  155.8 ( $\text{C}_q$ ), 148.3 ( $\text{C}_q$ ), 138.1 (CH), 132.6 ( $\text{C}_q$ ), 131.3 (CH), 128.2 (CH), 123.6 (CH), 123.2 ( $\text{C}_q$ ), 120.1 (CH), 117.7 ( $\text{C}_q$ ), 109.7 (CH), 56.1 ( $\text{CH}_3$ ), 38.9 ( $\text{CH}_3$ ), 31.7 ( $\text{CH}_2$ ), 25.3 ( $\text{CH}_2$ ), 22.2 ( $\text{CH}_2$ ), 13.9 ( $\text{CH}_3$ ).

**IR** (ATR): 2930, 1711, 1604, 1477, 1370, 1269, 1052, 979, 787  $\text{cm}^{-1}$ .

**MS** (ESI)  $m/z$  (relative intensity): 334.2  $[M+Na]^+$  (100), 312.2  $[M+H]^+$  (25).

**HR-MS** (ESI):  $m/z$  calcd for  $C_{17}H_{22}N_5O^+$   $[M+H]^+$  312.1819, found 312.1820.

#### 4-Butyl-1-(2-methoxy-6-(thiophen-2-yl)phenyl)-1H-1,2,3-triazole (161)



The general procedure A was followed using 4-butyl-1-(2-methoxyphenyl)-1H-1,2,3-triazole **131a** (43.1 mg, 0.20 mmol), 5-(thiophen-2-yl)-5H-dibenzo[*b,d*]thiophen-5-ium triflate **124q** (80.2 mg, 0.30 mmol),  $[RuCl_2(p\text{-cymene})]_2$  (6.0 mg, 0.01 mmol, 5.0 mol %), and KOAc (39.3 mg, 2.0 equiv.) in toluene (2.0 mL). Purification by column chromatography on silica gel (*n*hexane/EtOAc: 10/1) yielded **161** (18.1 mg, 29%) as a transparent oil.

**<sup>1</sup>H NMR** (400 MHz,  $CDCl_3$ ):  $\delta$  7.52 (dd,  $J = 8.2, 8.2$  Hz, 1H), 7.34 – 7.26 (m, 3H), 7.05 (d,  $J = 8.4$  Hz, 1H), 6.91 (t,  $J = 4.5$  Hz, 1H), 6.63 (d,  $J = 3.6$  Hz, 1H), 3.83 (s, 3H), 2.81 (t,  $J = 7.7$  Hz, 2H), 1.74 – 1.68 (m, 2H), 1.42 – 1.34 (m, 2H), 0.96 (t,  $J = 7.3$  Hz, 3H).

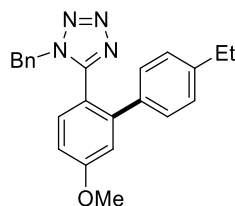
**<sup>13</sup>C NMR** (101 MHz,  $CDCl_3$ ):  $\delta$  156.0 ( $C_q$ ), 148.3 ( $C_q$ ), 138.2 ( $C_q$ ), 134.1 ( $C_q$ ), 131.2 (CH), 129.9 (CH), 127.6 (CH), 126.8 (CH), 126.7 (CH), 123.9 ( $C_q$ ), 121.9 (CH), 111.1 (CH), 56.4 ( $CH_3$ ), 31.6 ( $CH_2$ ), 25.4 ( $CH_2$ ), 22.3 ( $CH_2$ ), 14.0 ( $CH_3$ ).

**IR** (ATR): 2931, 1580, 1473, 1277, 1259, 1112, 1039, 788, 698  $cm^{-1}$ .

**MS** (ESI)  $m/z$  (relative intensity): 336.1  $[M+Na]^+$  (60), 314.1  $[M+H]^+$  (100).

**HR-MS** (ESI):  $m/z$  calcd for  $C_{17}H_{20}N_3SO^+$   $[M+H]^+$  314.1322, found 314.1324.

#### 1-Benzyl-5-(4'-ethyl-5-methoxy-[1,1'-biphenyl]-2-yl)-1H-tetrazole (164)



The general procedure A was followed using 1-benzyl-5-(4-methoxyphenyl)-1H-tetrazole **162a** (53.2 mg, 0.20 mmol), 5-(4-ethylphenyl)-5H-dibenzo[*b,d*]thiophen-5-

ium triflate **124c** (131 mg, 0.30 mmol), [RuCl<sub>2</sub>(*p*-cymene)]<sub>2</sub> (6.0 mg, 0.01 mmol, 5.0 mol %), and KOAc (39.3 mg, 2.0 equiv.) in *t*AmOH (2.0 mL). Purification by column chromatography on silica gel (*n*hexane/EtOAc: 3/1) yielded **164** (48 mg, 64%) as a white solid.

**m.p.:** 120–123 °C.

**<sup>1</sup>H NMR** (400 MHz, CDCl<sub>3</sub>): δ 7.51 – 7.42 (m, 1H), 7.43 – 7.28 (m, 5H), 7.25 (dd, *J* = 8.1, 1.7 Hz, 3H), 7.12 (d, *J* = 2.1 Hz, 1H), 6.96 (d, *J* = 7.3 Hz, 2H), 4.93 (s, 2H), 4.09 (d, *J* = 1.5 Hz, 3H), 2.83 (q, *J* = 7.6 Hz, 2H), 1.42 (t, *J* = 7.6 Hz, 3H).

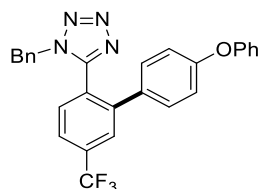
**<sup>13</sup>C NMR** (101 MHz, CDCl<sub>3</sub>): δ 162.0 (C<sub>q</sub>), 154.9 (C<sub>q</sub>), 144.6 (C<sub>q</sub>), 143.4 (C<sub>q</sub>), 136.3 (C<sub>q</sub>), 133.4 (C<sub>q</sub>), 132.9 (CH), 128.8 (CH), 128.6 (CH), 128.6 (CH), 128.0 (CH), 115.8 (CH), 114.7 (C<sub>q</sub>), 113.3 (CH), 55.7 (CH<sub>3</sub>), 50.8 (CH<sub>2</sub>), 28.6 (CH<sub>2</sub>), 15.5 (CH<sub>3</sub>).

**IR** (ATR): 2934, 2841, 1607, 1559, 1467, 1404, 1214, 989, 724 cm<sup>-1</sup>.

**MS** (ESI) *m/z* (relative intensity): 393.2 [M+Na]<sup>+</sup> (100), 371.2 [M+H]<sup>+</sup> (10).

**HR-MS** (ESI): *m/z* calcd for C<sub>23</sub>H<sub>23</sub>N<sub>4</sub>O<sup>+</sup> [M+H]<sup>+</sup> 371.1866, found 371.1868.

### 1-Benzyl-5-(4'-phenoxy-5-(trifluoromethyl)-[1,1'-biphenyl]-2-yl)-1*H*-tetrazole (**165**)



The general procedure A was followed using 1-benzyl-5-(4-trifluoromethylphenyl)-1*H*-tetrazole **162b** (60.9 mg, 0.20 mmol), 5-(4-phenoxyphenyl)-5*H*-dibenzo[*b,d*]thiophen-5-ium triflate **124d** (151 mg, 0.30 mmol), [RuCl<sub>2</sub>(*p*-cymene)]<sub>2</sub> (6.0 mg, 0.01 mmol, 5.0 mol %), and KOAc (39.3 mg, 2.0 equiv.) in toluene (2.0 mL). Purification by column chromatography on silica gel (*n*hexane/EtOAc: 10/1) yielded **165** (67.5 mg, 65%) as a transparent oil.

**<sup>1</sup>H NMR** (400 MHz, CDCl<sub>3</sub>): δ 7.81 (s, 1H), 7.64 (d, *J* = 8.1 Hz, 1H), 7.56 – 7.31 (m, 4H), 7.29 – 6.99 (m, 8H), 6.85 (dd, *J* = 53.4, 7.9 Hz, 3H), 4.89 (s, 2H).

**<sup>13</sup>C NMR** (101 MHz, CDCl<sub>3</sub>): δ 158.4 (C<sub>q</sub>), 155.9 (C<sub>q</sub>), 153.6 (C<sub>q</sub>), 142.1 (C<sub>q</sub>), 133.7 (q, <sup>2</sup>*J*<sub>C-F</sub> = 32.9 Hz, C<sub>q</sub>), 132.8 (C<sub>q</sub>), 132.0 (CH), 131.7 (C<sub>q</sub>), 130.1 (q, <sup>3</sup>*J*<sub>C-F</sub> = 8.1 Hz, CH),

128.9 (q,  $^4J_{C-F} = 3.3$  Hz, CH), 127.8 (CH), 127.0 (q,  $^3J_{C-F} = 3.8$  Hz, CH), 126.4 (C<sub>q</sub>), 124.3 (CH), 124.3 (CH), 124.2 (CH), 123.5 (q,  $^1J_{C-F} = 273.4$  Hz, C<sub>q</sub>), 119.7 (CH), 118.6 (CH), 51.2 (CH<sub>2</sub>).

$^{19}\text{F}$  NMR (377 MHz, CDCl<sub>3</sub>):  $\delta$  -63.0 (s).

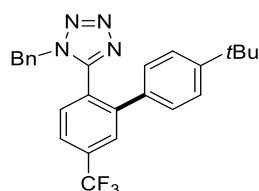
IR (ATR): 1587, 1489, 1424, 1336, 1243, 1127, 1038, 841, 693 cm<sup>-1</sup>.

MS (ESI) *m/z* (relative intensity): 495.1 [M+Na]<sup>+</sup> (100), 473.1 [M+H]<sup>+</sup> (30).

HR-MS (ESI): *m/z* calcd for C<sub>27</sub>H<sub>20</sub>F<sub>3</sub>N<sub>4</sub>O<sup>+</sup> [M+H]<sup>+</sup> 473.1584, found 473.1580.

### 1-Benzyl-5-(4'-(*tert*-butyl)-5-(trifluoromethyl)-[1,1'-biphenyl]-2-yl)-1*H*-tetrazole

(166)



The general procedure A was followed using 1-benzyl-5-(4-trifluoromethylphenyl)-1*H*-tetrazole **162b** (60.9 mg, 0.20 mmol), 5-(4-*tert*-butylphenyl)-5*H*-dibenzo[*b,d*]thiophen-5-ium triflate **124e** (140 mg, 0.30 mmol), [RuCl<sub>2</sub>(*p*-cymene)]<sub>2</sub> (6.0 mg, 0.01 mmol, 5.0 mol %), and KOAc (39.3 mg, 2.0 equiv.) in *t*AmOH (2.0 mL). Purification by column chromatography on silica gel (*n*hexane/EtOAc: 20/1) yielded **166** (79.0 mg, 93%) as a transparent oil.

$^1\text{H}$  NMR (400 MHz, CDCl<sub>3</sub>):  $\delta$  7.83 (s, 1H), 7.63 (d,  $J = 8.0$  Hz, 1H), 7.44 (d,  $J = 8.0$  Hz, 1H), 7.36 (d,  $J = 6.7$  Hz, 2H), 7.24 – 7.18 (m, 1H), 7.18 – 7.07 (m, 4H), 6.74 (d,  $J = 7.5$  Hz, 2H), 4.77 (s, 2H), 1.32 (s, 9H).

$^{13}\text{C}$  NMR (101 MHz, CDCl<sub>3</sub>):  $\delta$  153.8 (C<sub>q</sub>), 152.3 (C<sub>q</sub>), 142.5 (C<sub>q</sub>), 134.5 (C<sub>q</sub>), 133.6 (q,  $^2J_{C-F} = 32.9$  Hz, C<sub>q</sub>), 132.7 (C<sub>q</sub>), 132.1 (CH), 128.8 (CH), 128.8 (CH), 128.3 (CH), 127.9 (CH), 127.1 (q,  $^3J_{C-F} = 3.8$  Hz, CH), 126.4 (C<sub>q</sub>), 126.3 (CH), 124.2 (q,  $^3J_{C-F} = 3.6$  Hz, CH), 123.5 (q,  $^1J_{C-F} = 272.9$  Hz, C<sub>q</sub>), 51.1 (C<sub>q</sub>), 34.7 (CH<sub>2</sub>), 31.2 (CH<sub>3</sub>).

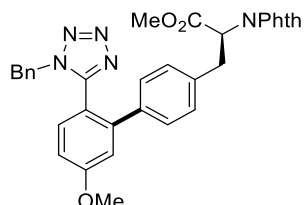
$^{19}\text{F}$  NMR (377 MHz, CDCl<sub>3</sub>):  $\delta$  -63.0 (s).

IR (ATR): 2966, 1335, 1288, 1171, 1129, 1102, 907, 839, 719 cm<sup>-1</sup>.

MS (ESI) *m/z* (relative intensity): 459.2 [M+Na]<sup>+</sup> (100).

**HR-MS** (ESI):  $m/z$  calcd for  $C_{25}H_{24}F_3N_4^+$   $[M+H]^+$  437.1948, found 437.1941.

**Methyl-(S)-3-(2'-(1-benzyl-1H-tetrazol-5-yl)-5'-methoxy-[1,1'-biphenyl]-4-yl)-2-(1,3-dioxoisoindolin-2-yl)propanoate (167)**



The general procedure A was followed using 1-benzyl-5-(4-methoxyphenyl)-1H-tetrazole **162a** (53.2 mg, 0.20 mmol), dibenzothiophene salt **130** (192 mg, 0.30 mmol),  $[RuCl_2(p\text{-cymene})]_2$  (6.0 mg, 0.01 mmol, 5.0 mol %), and KOAc (39.3 mg, 2.0 equiv.) in *t*AmOH (2.0 mL). Purification by column chromatography on silica gel (*n*hexane/EtOAc: 3/1) yielded **167** (62 mg, 54%) as a transparent oil.

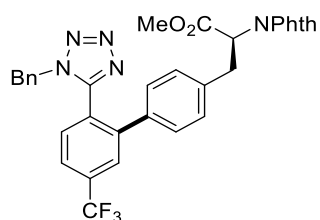
**$^1H$  NMR** (400 MHz,  $CDCl_3$ ):  $\delta$  8.14 – 8.07 (m, 2H), 8.00 (dd,  $J$  = 5.6, 2.8 Hz, 2H), 7.61 – 7.50 (m, 2H), 7.47 – 7.39 (m, 3H), 7.38 – 7.31 (m, 2H), 7.24 (d,  $J$  = 1.5 Hz, 2H), 7.18 (dt,  $J$  = 8.7, 2.0 Hz, 1H), 7.07 – 6.99 (m, 2H), 5.33 (dd,  $J$  = 11.4, 4.6 Hz, 1H), 5.00 – 4.54 (m, 2H), 4.14 (d,  $J$  = 1.5 Hz, 3H), 4.06 (d,  $J$  = 1.5 Hz, 3H), 3.85 (dd,  $J$  = 14.2, 4.6 Hz, 1H), 3.80 – 3.69 (m, 1H).

**$^{13}C$  NMR** (101 MHz,  $CDCl_3$ ):  $\delta$  169.2 ( $C_q$ ), 167.5 ( $C_q$ ), 161.9 ( $C_q$ ), 154.5 ( $C_q$ ), 142.7 ( $C_q$ ), 137.7 ( $C_q$ ), 137.4 ( $C_q$ ), 134.5 (CH), 133.7 ( $C_q$ ), 133.0 (CH), 131.4 ( $C_q$ ), 129.7 (CH), 128.9 (CH), 128.8 (CH), 128.5 (CH), 127.8 (CH), 123.9 (CH), 115.7 (CH), 114.8 ( $C_q$ ), 113.5 (CH), 55.7 (CH), 53.3 ( $CH_3$ ), 53.1 ( $CH_3$ ), 50.5 ( $CH_2$ ), 34.6 ( $CH_2$ ).

**IR** (ATR): 1744, 1605, 1467, 1386, 1221, 1101, 835, 719, 530  $cm^{-1}$ .

**MS** (ESI)  $m/z$  (relative intensity): 596.2  $[M+Na]^+$  (100), 574.2  $[M+H]^+$  (5).

**HR-MS** (ESI):  $m/z$  calcd for  $C_{33}H_{28}N_5O_5F^+$   $[M+H]^+$  574.2085, found 574.2084.

**Methyl-(S)-3-(2'-(1-benzyl-1H-tetrazol-5-yl)-5'-(trifluoromethyl)-[1,1'-biphenyl]-4-yl)-2-(1,3-dioxisoindolin-2-yl)propanoate (168)**

The general procedure A was followed using 1-benzyl-5-(4-trifluoromethylphenyl)-1H-tetrazole **162b** (60.9 mg, 0.20 mmol), dibenzothiophene salt **130** (192 mg, 0.30 mmol), [RuCl<sub>2</sub>(*p*-cymene)]<sub>2</sub> (6.0 mg, 0.01 mmol, 5.0 mol %), and KOAc (39.3 mg, 2.0 equiv.) in toluene (2.0 mL). Purification by column chromatography on silica gel (*n*hexane/EtOAc: 10/1) yielded **168** (65.0 mg, 53%) as a transparent oil.

**<sup>1</sup>H NMR** (400 MHz, CDCl<sub>3</sub>): δ 7.83 (s, 2H), 7.74 (s, 3H), 7.60 (d, *J* = 8.1 Hz, 1H), 7.41 (d, *J* = 8.1 Hz, 1H), 7.22 – 7.09 (m, 5H), 6.99 (d, *J* = 7.8 Hz, 2H), 6.73 (d, *J* = 7.5 Hz, 2H), 5.05 (dd, *J* = 11.5, 4.5 Hz, 1H), 4.71 – 4.49 (m, 2H), 3.78 (s, 3H), 3.59 (dd, *J* = 14.2, 4.7 Hz, 1H), 3.48 (t, *J* = 12.8 Hz, 1H).

**<sup>13</sup>C NMR** (101 MHz, CDCl<sub>3</sub>): δ 171.1 (C<sub>q</sub>), 169.0 (C<sub>q</sub>), 167.4 (C<sub>q</sub>), 153.4 (C<sub>q</sub>), 142.0 (C<sub>q</sub>), 138.1 (C<sub>q</sub>), 136.1 (C<sub>q</sub>), 134.5 (CH), 133.6 (q, <sup>2</sup>*J*<sub>C-F</sub> = 33.0 Hz, C<sub>q</sub>), 133.0 (C<sub>q</sub>), 132.1 (CH), 131.3 (C<sub>q</sub>), 129.9 (CH), 128.8 (CH), 128.8 (CH), 128.7 (CH), 127.6 (CH), 126.9 (q, <sup>3</sup>*J*<sub>C-F</sub> = 3.7 Hz, CH), 124.5 (q, <sup>3</sup>*J*<sub>C-F</sub> = 5.0 Hz, CH), 123.8 (CH), 123.4 (q, <sup>1</sup>*J*<sub>C-F</sub> = 273.0 Hz, C<sub>q</sub>), 53.2 (CH), 53.0 (CH<sub>3</sub>), 50.8 (CH<sub>2</sub>), 34.5 (CH<sub>2</sub>).

**<sup>19</sup>F NMR** (377 MHz, CDCl<sub>3</sub>): δ -63.0 (s).

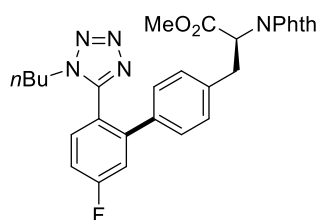
**IR** (ATR): 1746, 1714, 1387, 1336, 1243, 1136, 906, 840, 718 cm<sup>-1</sup>.

**MS** (ESI) *m/z* (relative intensity): 634.2 [M+Na]<sup>+</sup> (100), 612.2 [M+H]<sup>+</sup> (30).

**HR-MS** (ESI): *m/z* calcd for C<sub>33</sub>H<sub>25</sub>F<sub>3</sub>N<sub>5</sub>O<sub>4</sub><sup>+</sup> [M+H]<sup>+</sup> 612.1853, found 612.1852.



**Methyl-(S)-3-(2'-(1-butyl-1*H*-tetrazol-5-yl)-5'-fluoro-[1,1'-biphenyl]-4-yl)-2-(1,3-dioxisoindolin-2-yl)propanoate (**169**)**



The general procedure A was followed using 1-butyl-5-(4-fluorophenyl)-1*H*-tetrazole **162c** (44.0 mg, 0.20 mmol), dibenzothiophene salt **130** (192 mg, 0.30 mmol), [RuCl<sub>2</sub>(*p*-cymene)]<sub>2</sub> (6.0 mg, 0.01 mmol, 5.0 mol %), and KOAc (39.3 mg, 2.0 equiv.) in *t*AmOH (2.0 mL). Purification by column chromatography on silica gel (*n*hexane/EtOAc: 3/1) yielded **169** (69 mg, 91%) as a white solid.

**m.p.:** 72–74 °C.

**<sup>1</sup>H NMR** (400 MHz, CDCl<sub>3</sub>): δ 7.90 – 7.79 (m, 2H), 7.78 – 7.71 (m, 2H), 7.54 – 7.45 (m, 1H), 7.23 – 7.12 (m, 2H), 7.08 (d, *J* = 7.7 Hz, 2H), 6.96 – 6.88 (m, 2H), 5.04 (dd, *J* = 11.4, 5.0 Hz, 1H), 3.76 (d, *J* = 1.5 Hz, 3H), 3.63 – 3.40 (m, 2H), 3.38 – 3.04 (m, 2H), 1.40 – 1.23 (m, 2H), 0.94 (h, *J* = 7.4 Hz, 2H), 0.67 (t, *J* = 7.3 Hz, 3H).

**<sup>13</sup>C NMR** (101 MHz, CDCl<sub>3</sub>): δ 169.1 (C<sub>q</sub>), 167.4 (C<sub>q</sub>), 164.5 (d, <sup>1</sup>*J*<sub>C-F</sub> = 252.6 Hz, C<sub>q</sub>), 153.8 (C<sub>q</sub>), 143.8 (d, <sup>3</sup>*J*<sub>C-F</sub> = 8.6 Hz, C<sub>q</sub>), 137.8 (C<sub>q</sub>), 136.6 (d, <sup>4</sup>*J*<sub>C-F</sub> = 1.7 Hz, C<sub>q</sub>), 134.5 (CH), 133.7 (d, <sup>3</sup>*J*<sub>C-F</sub> = 9.1 Hz, CH), 131.4 (C<sub>q</sub>), 129.7 (CH), 128.7 (CH), 123.8 (CH), 119.0 (d, <sup>4</sup>*J*<sub>C-F</sub> = 3.2 Hz, C<sub>q</sub>), 117.3 (d, <sup>2</sup>*J*<sub>C-F</sub> = 22.5 Hz, CH), 115.3 (d, <sup>2</sup>*J*<sub>C-F</sub> = 21.8 Hz, CH), 53.1 (CH<sub>3</sub>), 53.1 (CH), 46.8 (CH<sub>2</sub>), 34.5 (CH<sub>2</sub>), 30.7 (CH<sub>2</sub>), 19.4 (CH<sub>2</sub>), 13.2 (CH<sub>3</sub>).

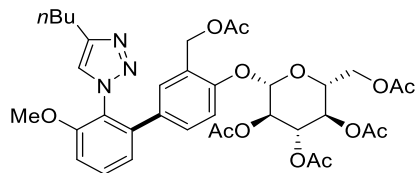
**<sup>19</sup>F NMR** (377 MHz, CDCl<sub>3</sub>): δ -108.0 – -108.3 (m).

**IR** (ATR): 2957, 2874, 1746, 1610, 1361, 1221, 1184, 722, 530 cm<sup>-1</sup>.

**MS** (ESI) *m/z* (relative intensity): 550.2 [M+Na]<sup>+</sup> (100), 528.2 [M+H]<sup>+</sup> (20).

**HR-MS** (ESI): *m/z* calcd for C<sub>29</sub>H<sub>27</sub>N<sub>5</sub>O<sub>4</sub>F<sup>+</sup> [M+H]<sup>+</sup> 528.2042, found 528.2034.

**(2*R*,3*R*,4*S*,5*R*,6*S*)-2-(acetoxymethyl)-6-((3-(acetoxymethyl)-2'-(4-butyl-1*H*-1,2,3-triazol-1-yl)-3'-methoxy-[1,1'-biphenyl]-4-yl)oxy)tetrahydro-2*H*-pyran-3,4,5-triyl triacetate (**172**)**



The general procedure A was followed using 4-butyl-1-(2-methoxyphenyl)-1*H*-1,2,3-triazole **131a** (46.3 mg, 0.20 mmol), the pentaacyl-Salicin derived dibenzothiophenium salt **170a** (248 mg, 0.30 mmol), [RuCl<sub>2</sub>(*p*-cymene)]<sub>2</sub> (6.0 mg, 0.01 mmol, 5.0 mol %), and KOAc (39.3 mg, 2.0 equiv.) in *t*AmOH (2.0 mL). Purification by column chromatography on silica gel (*n*hexane/EtOAc: 3/1) yielded **172** (105 mg, 72%) as a transparent oil.

**<sup>1</sup>H NMR** (400 MHz, CDCl<sub>3</sub>): δ 7.54 – 7.38 (m, 1H), 7.09 (d, *J* = 1.7 Hz, 2H), 7.05 – 6.99 (m, 2H), 6.99 (dd, *J* = 8.6, 2.0 Hz, 1H), 6.92 – 6.81 (m, 1H), 5.32 – 5.21 (m, 1H), 5.19 – 5.07 (m, 1H), 5.05 – 4.96 (m, 2H), 4.96 – 4.86 (m, 1H), 4.35 – 4.21 (m, 1H), 4.20 – 4.00 (m, 2H), 3.85 – 3.79 (m, 4H), 2.67 (t, *J* = 7.5 Hz, 2H), 2.22 – 1.80 (m, 15H), 1.63 – 1.51 (m, 2H), 1.31 – 1.17 (m, 2H), 0.86 (t, *J* = 1.8 Hz, 3H).

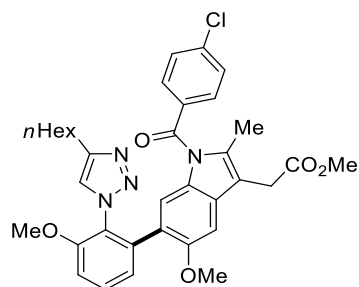
**<sup>13</sup>C NMR** (101 MHz, CDCl<sub>3</sub>): δ 170.7 (C<sub>q</sub>), 170.6 (C<sub>q</sub>), 170.3 (C<sub>q</sub>), 169.5 (C<sub>q</sub>), 169.3 (C<sub>q</sub>), 155.4 (C<sub>q</sub>), 154.1 (C<sub>q</sub>), 147.6 (C<sub>q</sub>), 140.0 (C<sub>q</sub>), 132.8 (C<sub>q</sub>), 131.0 (CH), 129.3 (CH), 129.3 (C<sub>q</sub>), 126.1 (C<sub>q</sub>), 124.6 (CH), 123.9 (CH), 122.3 (CH), 115.2 (CH), 111.1 (CH), 99.1 (CH), 72.7 (CH), 72.2 (CH), 71.0 (CH), 68.3 (CH), 61.9 (CH<sub>2</sub>), 60.7 (CH<sub>2</sub>), 60.5 (CH<sub>3</sub>), 56.3 (CH<sub>3</sub>), 31.4 (CH<sub>2</sub>), 25.2 (CH<sub>2</sub>), 22.1 (CH<sub>2</sub>), 21.0 (CH<sub>3</sub>), 20.8 (CH<sub>3</sub>), 20.7 (CH<sub>3</sub>), 20.7 (CH<sub>3</sub>), 13.9 (CH<sub>3</sub>).

**IR** (ATR): 2956, 1743, 1710, 1473, 1363, 1116, 1038, 906, 792 cm<sup>-1</sup>.

**MS** (ESI) *m/z* (relative intensity): 748.3 [M+Na]<sup>+</sup> (100), 726.3 [M+H]<sup>+</sup> (5).

**HR-MS** (ESI): *m/z* calcd for C<sub>36</sub>H<sub>44</sub>N<sub>3</sub>O<sub>13</sub><sup>+</sup> [M+H]<sup>+</sup> 726.2869, found 726.2868.

**Methyl-2-(1-(4-chlorobenzoyl)-6-(2-(4-hexyl-1*H*-1,2,3-triazol-1-yl)-3-methoxyphenyl)-5-methoxy-2-methyl-1*H*-indol-3-yl)acetate (**173**)**



The general procedure A was followed using 4-hexyl-1-(2-methoxyphenyl)-1*H*-1,2,3-triazole **131g** (51.9 mg, 0.20 mmol), the Indomethacine-derived dibenzothiophenium salt **170b** (211 mg, 0.30 mmol), [RuCl<sub>2</sub>(*p*-cymene)]<sub>2</sub> (6.0 mg, 0.01 mmol, 5.0 mol %), and KOAc (39.3 mg, 2.0 equiv.) in *t*AmOH (2.0 mL). Purification by column chromatography on silica gel (*n*hexane/EtOAc: 10/1) yielded **173** (79.5 mg, 63%) as yellow solid.

**m.p.:** 150–152 °C.

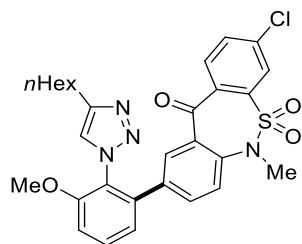
**<sup>1</sup>H NMR** (400 MHz, CDCl<sub>3</sub>): δ 7.63 (d, *J* = 8.1 Hz, 2H), 7.46 (d, *J* = 8.2 Hz, 2H), 7.40 (t, *J* = 8.1 Hz, 1H), 7.18 (s, 1H), 7.00 (d, *J* = 8.4 Hz, 1H), 6.89 (s, 1H), 6.85 (d, *J* = 7.7 Hz, 1H), 6.74 (s, 1H), 3.76 (s, 3H), 3.68 (s, 3H), 3.59 (d, *J* = 13.6 Hz, 5H), 2.61 (t, *J* = 7.7 Hz, 2H), 2.31 (s, 3H), 1.58 – 1.47 (m, 2H), 1.22 (s, 6H), 0.86 (s, 3H).

**<sup>13</sup>C NMR** (101 MHz, CDCl<sub>3</sub>): δ 171.3 (C<sub>q</sub>), 168.1 (C<sub>q</sub>), 154.2 (C<sub>q</sub>), 152.8 (C<sub>q</sub>), 146.1 (C<sub>q</sub>), 139.3 (C<sub>q</sub>), 138.1 (C<sub>q</sub>), 135.8 (C<sub>q</sub>), 133.6 (C<sub>q</sub>), 131.4 (CH), 130.2 (C<sub>q</sub>), 130.2 (CH), 129.1 (CH), 125.9 (C<sub>q</sub>), 123.6 (CH), 123.3 (CH), 123.2 (C<sub>q</sub>), 116.6 (CH), 112.3 (C<sub>q</sub>), 111.1 (CH), 98.8 (CH), 60.4 (C<sub>q</sub>), 56.1 (CH<sub>3</sub>), 55.5 (CH<sub>3</sub>), 52.1 (CH<sub>3</sub>), 31.6 (CH<sub>2</sub>), 30.2 (CH<sub>2</sub>), 29.4 (CH<sub>2</sub>), 28.8 (CH<sub>2</sub>), 25.5 (CH<sub>2</sub>), 22.6 (CH<sub>2</sub>), 14.1 (CH<sub>3</sub>), 13.4 (CH<sub>3</sub>).

**IR** (ATR): 2928, 1736, 1583, 1466, 1348, 1222, 1145, 1041, 728 cm<sup>-1</sup>.

**MS** (ESI) *m/z* (relative intensity): 651.3 [M+Na]<sup>+</sup> (100), 629.3 [M+H]<sup>+</sup> (25).

**HR-MS** (ESI): *m/z* calcd for C<sub>35</sub>H<sub>38</sub><sup>35</sup>ClN<sub>4</sub>O<sub>5</sub><sup>+</sup> [M+H]<sup>+</sup> 629.2525, found 629.2521.

**3-Chloro-9-(2-(4-hexyl-1*H*-1,2,3-triazol-1-yl)-3-methoxyphenyl)-6-methyldibenzo[*c,f*][1,2] thiazepin-11(6*H*)-one 5,5-dioxide (174)**

The general procedure A was followed using 4-hexyl-1-(2-methoxyphenyl)-1*H*-1,2,3-triazole **131g** (51.9 mg, 0.20 mmol), the Tianeptine-precursor derived dibenzothiophenium salt **170c** (191 mg, 0.30 mmol), [RuCl<sub>2</sub>(*p*-cymene)]<sub>2</sub> (6.0 mg, 0.01 mmol, 5.0 mol %), and KOAc (39.3 mg, 2.0 equiv.) in *t*AmOH (2.0 mL). Purification by column chromatography on silica gel (*n*hexane/EtOAc: 10/1) yielded **174** (68.0 mg, 60%) as a transparent oil.

**<sup>1</sup>H NMR** (400 MHz, CDCl<sub>3</sub>): δ 8.10 (s, 1H), 7.88 (s, 1H), 7.80 (d, *J* = 8.3 Hz, 1H), 7.63 (d, *J* = 8.3 Hz, 1H), 7.52 (t, *J* = 8.1 Hz, 1H), 7.22 (d, *J* = 10.2 Hz, 1H), 7.13 (d, *J* = 7.9 Hz, 1H), 7.07 (d, *J* = 8.7 Hz, 2H), 3.79 (s, 3H), 3.28 (s, 3H), 2.64 (t, *J* = 7.7 Hz, 2H), 1.57 (t, *J* = 7.3 Hz, 2H), 1.22 (s, 7H), 0.81 (s, 3H).

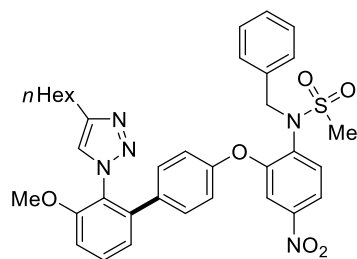
**<sup>13</sup>C NMR** (101 MHz, CDCl<sub>3</sub>): δ 189.5 (C<sub>q</sub>), 155.1 (C<sub>q</sub>), 147.9 (C<sub>q</sub>), 140.8 (C<sub>q</sub>), 138.8 (C<sub>q</sub>), 138.7 (C<sub>q</sub>), 138.3 (C<sub>q</sub>), 135.5 (C<sub>q</sub>), 134.5 (C<sub>q</sub>), 134.5 (CH), 133.4 (CH), 133.2 (CH), 132.0 (CH), 131.3 (CH), 130.2 (C<sub>q</sub>), 125.2 (CH), 124.5 (C<sub>q</sub>), 124.3 (CH), 123.9 (CH), 122.5 (CH), 111.8 (CH), 56.4 (CH<sub>3</sub>), 38.8 (CH<sub>3</sub>), 31.6 (CH<sub>2</sub>), 29.5 (CH<sub>2</sub>), 28.9 (CH<sub>2</sub>), 25.6 (CH<sub>2</sub>), 22.7 (CH<sub>2</sub>), 14.2 (CH<sub>3</sub>).

**IR** (ATR): 2928, 1657, 1583, 1471, 1361, 1170, 1104, 1037, 728 cm<sup>-1</sup>.

**MS** (ESI) *m/z* (relative intensity): 587.2 [M+Na]<sup>+</sup> (100), 565.2 [M+H]<sup>+</sup> (20).

**HR-MS** (ESI): *m/z* calcd for C<sub>29</sub>H<sub>30</sub><sup>35</sup>ClN<sub>4</sub>O<sub>4</sub>S<sup>+</sup> [M+H]<sup>+</sup> 565.1671, found 565.1666.

***N*-Benzyl-*N*-(2-((2'-(4-hexyl-1*H*-1,2,3-triazol-1-yl)-3'-methoxy-[1,1'-biphenyl]-4-yl)oxy)-4-nitrophenyl)methanesulfonamide (175)**



The general procedure B was followed using 4-hexyl-1-(2-methoxyphenyl)-1*H*-1,2,3-triazole **131g** (104 mg, 0.40 mmol), the Nimesulide-derived dibenzothiophenium salt **170d** (146 mg, 0.20 mmol),  $[\text{RuCl}_2(p\text{-cymene})]_2$  (6.0 mg, 0.01 mmol, 5.0 mol %), and KOAc (39.3 mg, 2.0 equiv.) in *t*AmOH (2.0 mL). Purification by column chromatography on silica gel (*n*hexane/EtOAc: 3/1) yielded **175** (66 mg, 58%) as a transparent oil.

**<sup>1</sup>H NMR** (400 MHz, CDCl<sub>3</sub>): δ 7.81 (dd, *J* = 8.8, 2.5 Hz, 1H), 7.63 – 7.55 (m, 2H), 7.36 (d, *J* = 8.7 Hz, 1H), 7.34 – 7.21 (m, 8H), 7.18 (d, *J* = 7.8 Hz, 1H), 7.13 (d, *J* = 8.4 Hz, 1H), 6.94 (d, *J* = 8.2 Hz, 2H), 4.91 (s, 2H), 3.87 (s, 3H), 3.08 (s, 3H), 2.74 (t, *J* = 7.7 Hz, 2H), 1.71 – 1.63 (m, 2H), 1.36 – 1.27 (m, 6H), 0.92 – 0.85 (m, 3H).

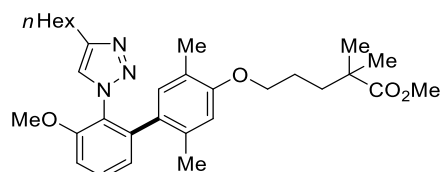
**<sup>13</sup>C NMR** (101 MHz, CDCl<sub>3</sub>): δ 155.3 (C<sub>q</sub>), 155.2 (C<sub>q</sub>), 153.9 (C<sub>q</sub>), 148.0 (C<sub>q</sub>), 147.9 (C<sub>q</sub>), 139.7 (C<sub>q</sub>), 135.4 (C<sub>q</sub>), 135.3 (C<sub>q</sub>), 134.6 (CH), 134.4 (C<sub>q</sub>), 131.2 (CH), 130.8 (CH), 128.8 (CH), 128.4 (CH), 124.6 (C<sub>q</sub>), 123.9 (CH), 122.4 (CH), 119.7 (CH), 118.0 (CH), 112.4 (CH), 111.5 (CH), 56.4 (CH<sub>3</sub>), 54.0 (CH<sub>2</sub>), 40.6 (CH<sub>3</sub>), 31.6 (CH<sub>2</sub>), 29.4 (CH<sub>2</sub>), 28.8 (CH<sub>2</sub>), 25.6 (CH<sub>2</sub>), 22.7 (CH<sub>2</sub>), 14.2 (CH<sub>3</sub>). *Missing CH*

**IR** (ATR): 2928, 2855, 1713, 1526, 1472, 1344, 1215, 1154, 1122 cm<sup>-1</sup>.

**MS** (ESI) *m/z* (relative intensity): 678.3 [M+Na]<sup>+</sup> (60), 656.3 [M+H]<sup>+</sup> (100).

**HR-MS** (ESI): *m/z* calcd for C<sub>35</sub>H<sub>38</sub>N<sub>5</sub>O<sub>6</sub>S<sup>+</sup> [M+H]<sup>+</sup> 656.2537, found 656.2530.

**Methyl-5-((2'-(4-hexyl-1*H*-1,2,3-triazol-1-yl)-3'-methoxy-2,5-dimethyl-[1,1'-biphenyl]-4-yl)oxy)-2,2-dimethylpentanoate (176)**



The general procedure B was followed using 4-hexyl-1-(2-methoxyphenyl)-1*H*-1,2,3-triazole **131g** (104 mg, 0.40 mmol), the Gemfibrozil-derived dibenzothiophenium salt **170e** (119 mg, 0.20 mmol), [RuCl<sub>2</sub>(*p*-cymene)]<sub>2</sub> (6.0 mg, 0.01 mmol, 5.0 mol %), and KOAc (39.3 mg, 2.0 equiv.) in *t*AmOH (2.0 mL). Purification by column chromatography on silica gel (*n*hexane/EtOAc: 3/1) yielded **176** (58 mg, 36%) as a white solid.

**m.p.:** 55–57 °C.

**<sup>1</sup>H NMR** (400 MHz, CDCl<sub>3</sub>): δ 7.44 (dd, *J* = 8.0, 8.0 Hz, 1H), 7.02 (d, *J* = 8.9 Hz, 2H), 6.92 (d, *J* = 7.7 Hz, 1H), 6.71 (s, 1H), 6.47 (s, 1H), 3.86 – 3.80 (m, 2H), 3.81 (s, 3H), 3.65 (s, 3H), 2.60 (t, *J* = 7.4 Hz, 2H), 2.05 (s, 3H), 2.02 (s, 3H), 1.81 – 1.60 (m, 4H), 1.50 (p, *J* = 7.5 Hz, 2H), 1.31 – 1.06 (m, 12H), 0.86 (t, *J* = 6.6 Hz, 3H).

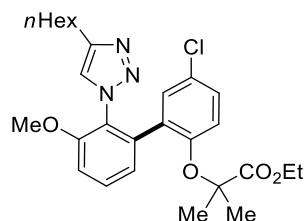
**<sup>13</sup>C NMR** (101 MHz, CDCl<sub>3</sub>): δ 178.4 (C<sub>q</sub>), 156.6 (C<sub>q</sub>), 155.0 (C<sub>q</sub>), 147.0 (C<sub>q</sub>), 141.1 (C<sub>q</sub>), 134.3 (C<sub>q</sub>), 131.3 (CH), 130.2 (CH), 128.6 (C<sub>q</sub>), 125.8 (C<sub>q</sub>), 123.5 (CH), 123.4 (C<sub>q</sub>), 123.2 (CH), 112.2 (CH), 110.8 (CH), 67.9 (C<sub>q</sub>), 56.2 (CH<sub>3</sub>), 51.8 (CH<sub>3</sub>), 42.2 (CH<sub>2</sub>), 37.2 (CH<sub>2</sub>), 31.6 (CH<sub>2</sub>), 29.4 (CH<sub>2</sub>), 28.5 (CH<sub>2</sub>), 25.5 (CH<sub>2</sub>), 25.3 (CH<sub>2</sub>), 25.3 (CH<sub>3</sub>), 22.6 (CH<sub>2</sub>), 20.2 (CH<sub>3</sub>), 15.6 (CH<sub>3</sub>), 14.2 (CH<sub>3</sub>).

**IR** (ATR): 2952, 1729, 1473, 1266, 1092, 1040, 984, 788, 747 cm<sup>-1</sup>.

**MS** (ESI) *m/z* (relative intensity): 544.3 [M+Na]<sup>+</sup> (80), 522.3 [M+H]<sup>+</sup> (100).

**HR-MS** (ESI): *m/z* calcd for C<sub>31</sub>H<sub>44</sub>N<sub>3</sub>O<sub>4</sub><sup>+</sup> [M+H]<sup>+</sup> 522.3326, found 522.3320.

#### Ethyl-2-((5-chloro-2'-(4-hexyl-1*H*-1,2,3-triazol-1-yl)-3'-methoxy-[1,1'-biphenyl]-2-yl)oxy)-2-methylpropanoate (**177**)



The general procedure B was followed using 4-hexyl-1-(2-methoxyphenyl)-1*H*-1,2,3-triazole **131g** (104 mg, 0.40 mmol), the Clofibrate-derived dibenzothiophenium salt **170f** (85.2 mg, 0.20 mmol), [RuCl<sub>2</sub>(*p*-cymene)]<sub>2</sub> (6.0 mg, 0.01 mmol, 5.0 mol %), and KOAc (39.3 mg, 2.0 equiv.) in *t*AmOH (2.0 mL). Purification by column chromatography on silica gel (*n*hexane/EtOAc: 10/1) yielded **177** (51.0 mg, 51%) as a transparent oil.

**<sup>1</sup>H NMR** (400 MHz, CDCl<sub>3</sub>): δ 7.44 (dd, *J* = 8.0, 8.0 Hz, 1H), 7.31 (s, 1H), 7.03 (dd, *J* = 9.0, 9.0 Hz, 3H), 6.96 (s, 1H), 6.54 (d, *J* = 9.0 Hz, 1H), 4.16 (q, *J* = 7.1 Hz, 2H), 3.80 (s, 3H), 2.65 (t, *J* = 7.5 Hz, 2H), 1.58 (q, *J* = 7.3 Hz, 2H), 1.38 (s, 6H), 1.32 – 1.15 (m, 9H), 0.86 (t, *J* = 6.4 Hz, 3H).

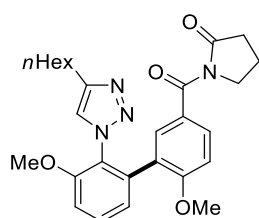
**<sup>13</sup>C NMR** (101 MHz, CDCl<sub>3</sub>): δ 173.8 (C<sub>q</sub>), 154.5 (C<sub>q</sub>), 151.2 (C<sub>q</sub>), 146.8 (C<sub>q</sub>), 136.7 (C<sub>q</sub>), 130.9 (C<sub>q</sub>), 130.4 (CH), 129.9 (CH), 128.3 (CH), 126.3 (C<sub>q</sub>), 125.6 (C<sub>q</sub>), 123.9 (CH), 123.3 (CH), 117.8 (CH), 111.3 (CH), 79.7 (C<sub>q</sub>), 61.4 (CH<sub>2</sub>), 56.2 (CH<sub>3</sub>), 31.6 (CH<sub>2</sub>), 29.4 (CH<sub>2</sub>), 28.6 (CH<sub>2</sub>), 25.5 (CH<sub>2</sub>), 25.2 (CH<sub>3</sub>), 22.6 (CH<sub>2</sub>), 14.1 (CH<sub>3</sub>), 14.1 (CH<sub>3</sub>).

**IR** (ATR): 2931, 2858, 1731, 1468, 1268, 1134, 1027, 794, 746 cm<sup>-1</sup>.

**MS** (ESI) *m/z* (relative intensity): 522.2 [M+Na]<sup>+</sup> (100), 500.2 [M+H]<sup>+</sup> (50).

**HR-MS** (ESI): *m/z* calcd for C<sub>27</sub>H<sub>35</sub><sup>35</sup>CIN<sub>3</sub>O<sub>4</sub><sup>+</sup> [M+H]<sup>+</sup> 500.2311, found 500.2307.

**1-(2'-(4-Hexyl-1*H*-1,2,3-triazol-1-yl)-3',6-dimethoxy-[1,1'-biphenyl]-3-carbonyl)pyrrolidin-2-one (178)**



The general procedure A was followed using 4-hexyl-1-(2-methoxyphenyl)-1*H*-1,2,3-triazole **131g** (51.8 mg, 0.20 mmol), the Aniracetam-derived dibenzothiophenium salt **170g** (165 mg, 0.30 mmol), [RuCl<sub>2</sub>(*p*-cymene)]<sub>2</sub> (6.0 mg, 0.01 mmol, 5.0 mol %), and KOAc (39.3 mg, 2.0 equiv.) in *t*AmOH (2.0 mL). Purification by column chromatography on silica gel (*n*hexane/EtOAc: 3/1) yielded **178** (50 mg, 51%) as a transparent oil.

**<sup>1</sup>H NMR** (400 MHz, CDCl<sub>3</sub>): δ 7.62 (dd, *J* = 8.6, 2.1 Hz, 1H), 7.52 – 7.43 (m, 2H), 7.15 (s, 1H), 7.08 (d, *J* = 8.4 Hz, 1H), 7.04 (d, *J* = 7.6 Hz, 1H), 6.69 (d, *J* = 8.7 Hz, 1H), 3.89 (t, *J* = 7.1 Hz, 2H), 3.81 (s, 3H), 3.56 (s, 3H), 2.58 (dt, *J* = 14.2, 7.8 Hz, 4H), 2.10 (p, *J* = 7.7 Hz, 2H), 1.52 (d, *J* = 7.4 Hz, 2H), 1.23 (s, 6H), 0.86 (t, *J* = 6.2 Hz, 3H).

**<sup>13</sup>C NMR** (101 MHz, CDCl<sub>3</sub>): δ 174.6 (C<sub>q</sub>), 169.6 (C<sub>q</sub>), 159.5 (C<sub>q</sub>), 154.5 (C<sub>q</sub>), 146.6 (C<sub>q</sub>), 136.8 (C<sub>q</sub>), 133.3 (CH), 131.8 (CH), 130.5 (CH), 125.9 (C<sub>q</sub>), 125.8 (C<sub>q</sub>), 125.8 (C<sub>q</sub>), 123.6 (CH), 123.1 (CH), 111.7 (CH), 109.5 (CH), 56.3 (CH<sub>3</sub>), 55.5 (CH<sub>3</sub>), 47.0 (CH<sub>2</sub>),

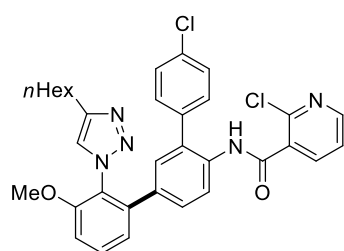
33.5 (CH<sub>2</sub>), 31.7 (CH<sub>2</sub>), 29.5 (CH<sub>2</sub>), 28.8 (CH<sub>2</sub>), 25.5 (CH<sub>2</sub>), 22.7 (CH<sub>2</sub>), 17.8 (CH<sub>2</sub>), 14.2 (CH<sub>3</sub>).

**IR** (ATR): 2926, 1737, 1710, 1666, 1320, 1263, 1223, 1031, 769 cm<sup>-1</sup>.

**MS** (ESI) *m/z* (relative intensity): 499.2 [M+Na]<sup>+</sup> (100), 477.2 [M+H]<sup>+</sup> (10).

**HR-MS** (ESI): *m/z* calcd for C<sub>27</sub>H<sub>33</sub>N<sub>4</sub>O<sub>4</sub><sup>+</sup> [M+H]<sup>+</sup> 477.2496, found 477.2489.

**2-Chloro-*N*-(4''-chloro-2-(4-hexyl-1*H*-1,2,3-triazol-1-yl)-3-methoxy-[1,1':3',1''-terphenyl]-4'-yl)nicotinamide (179)**



The general procedure B was followed using 4-hexyl-1-(2-methoxyphenyl)-1*H*-1,2,3-triazole **131g** (104 mg, 0.40 mmol), the Boscalid-derived dibenzothiophenium salt **170h** (135 mg, 0.20 mmol), [RuCl<sub>2</sub>(*p*-cymene)]<sub>2</sub> (6.0 mg, 0.01 mmol, 5.0 mol %), and KOAc (39.3 mg, 2.0 equiv.) in *t*AmOH (2.0 mL). Purification by column chromatography on silica gel (*n*hexane/EtOAc: 3/1) yielded **179** (58 mg, 36%) as a transparent oil.

**<sup>1</sup>H NMR** (400 MHz, CDCl<sub>3</sub>): δ 8.45 (dd, *J* = 4.5, 2.1 Hz, 1H), 8.39 (d, *J* = 8.5 Hz, 1H), 8.13 (dd, *J* = 5.4, 2.6 Hz, 2H), 7.53 (dd, *J* = 8.1, 8.1 Hz, 1H), 7.45 – 7.36 (m, 2H), 7.39 – 7.32 (m, 1H), 7.32 – 7.21 (m, 2H), 7.22 – 7.11 (m, 3H), 7.07 (d, *J* = 8.4 Hz, 1H), 6.89 (t, *J* = 1.8 Hz, 1H), 3.83 (d, *J* = 1.5 Hz, 3H), 2.72 (t, *J* = 7.7 Hz, 2H), 1.88 – 1.54 (m, 2H), 1.43 – 1.14 (m, 6H), 0.90 – 0.82 (m, 3H).

**<sup>13</sup>C NMR** (101 MHz, CDCl<sub>3</sub>): δ 162.5 (C<sub>q</sub>), 155.2 (C<sub>q</sub>), 151.5 (CH), 147.8 (C<sub>q</sub>), 146.8 (C<sub>q</sub>), 140.3 (CH), 139.9 (C<sub>q</sub>), 135.7 (C<sub>q</sub>), 134.7 (C<sub>q</sub>), 134.5 (C<sub>q</sub>), 134.1 (C<sub>q</sub>), 131.8 (C<sub>q</sub>), 131.1 (CH), 131.1 (C<sub>q</sub>), 130.9 (CH), 129.9 (CH), 129.5 (CH), 128.9 (CH), 124.6 (C<sub>q</sub>), 124.2 (CH), 123.1 (CH), 122.4 (CH), 121.8 (CH), 111.3 (CH), 56.4 (CH<sub>3</sub>), 31.7 (CH<sub>2</sub>), 29.5 (CH<sub>2</sub>), 29.0 (CH<sub>2</sub>), 25.7 (CH<sub>2</sub>), 22.7 (CH<sub>2</sub>), 14.2 (CH<sub>3</sub>).

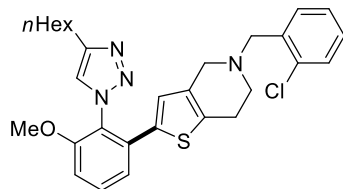
**IR** (ATR): 2926, 2855, 1677, 1580, 1518, 1398, 1276, 1118, 777 cm<sup>-1</sup>.

**MS** (ESI) *m/z* (relative intensity): 622.2 [M+Na]<sup>+</sup> (100), 600.2 [M+H]<sup>+</sup> (90).



**HR-MS** (ESI):  $m/z$  calcd for  $C_{33}H_{32}^{35}Cl_2N_5O_2^+$   $[M+H]^+$  600.1928, found 600.1930.

**5-(2-chlorobenzyl)-2-(2-(4-hexyl-1*H*-1,2,3-triazol-1-yl)-3-methoxyphenyl)-4,5,6,7-tetrahydrothieno[3,2-*c*]pyridine (180)**



The general procedure A was followed using 4-hexyl-1-(2-methoxyphenyl)-1*H*-1,2,3-triazole **131g** (51.8 mg, 0.20 mmol), Ticlopidine-derived dibenzothiophenium salt **170i** (179 mg, 0.30 mmol),  $[RuCl_2(p\text{-cymene})]_2$  (6.0 mg, 0.01 mmol, 5.0 mol %), and KOAc (39.3 mg, 2.0 equiv.) in *t*AmOH (2.0 mL). Purification by column chromatography on silica gel (*n*hexane/EtOAc: 3/1) yielded **180** (75 mg, 71%) as a transparent oil.

**<sup>1</sup>H NMR** (400 MHz,  $CDCl_3$ ):  $\delta$  7.73 (d,  $J$  = 6.8 Hz, 1H), 7.56 – 7.33 (m, 5H), 7.18 (d,  $J$  = 7.8 Hz, 1H), 7.05 (d,  $J$  = 8.4 Hz, 1H), 6.32 (s, 1H), 4.57 (s, 2H), 4.46 – 3.94 (m, 2H), 3.91 – 3.66 (m, 4H), 3.59 – 2.95 (m, 3H), 2.81 (t,  $J$  = 7.7 Hz, 2H), 1.77 – 1.52 (m, 2H), 1.41 – 1.08 (m, 6H), 0.89 (t,  $J$  = 5.7 Hz, 3H).

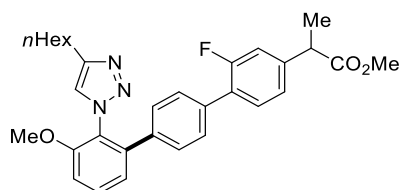
**<sup>13</sup>C NMR** (101 MHz,  $CDCl_3$ ):  $\delta$  155.4 ( $C_q$ ), 147.5 ( $C_q$ ), 138.2 ( $C_q$ ), 135.6 ( $C_q$ ), 133.5 (CH), 133.0 ( $C_q$ ), 132.7 ( $C_q$ ), 132.3 (CH), 132.1 (CH), 130.5 (CH), 128.5 (CH), 127.0 ( $C_q$ ), 126.2 ( $C_q$ ), 125.5 (CH), 124.2 (CH), 123.0 ( $C_q$ ), 122.0 (CH), 111.8 (CH), 56.4 (CH<sub>3</sub>), 55.6 (CH<sub>2</sub>), 50.4 (CH<sub>2</sub>), 49.9 (CH<sub>2</sub>), 31.5 (CH<sub>2</sub>), 29.1 (CH<sub>2</sub>), 28.8 (CH<sub>2</sub>), 24.8 (CH<sub>2</sub>), 22.7 (CH<sub>2</sub>), 21.8 (CH<sub>2</sub>), 14.1 (CH<sub>3</sub>).

**IR** (ATR): 2931, 1711, 1467, 1440, 1295, 1222, 1156, 1028, 758  $cm^{-1}$ .

**MS** (ESI)  $m/z$  (relative intensity): 543.2  $[M+Na]^+$  (1), 521.2  $[M+H]^+$  (100).

**HR-MS** (ESI):  $m/z$  calcd for  $C_{29}H_{34}ClN_4OS^+$   $[M+H]^+$  521.2136, found 521.2135.

**Methyl-2-(2-fluoro-2''-(4-hexyl-1*H*-1,2,3-triazol-1-yl)-3''-methoxy-[1,1':4',1''-terphenyl]-4-yl)propanoate (181)**



The general procedure A was followed using 4-hexyl-1-(2-methoxyphenyl)-1*H*-1,2,3-triazole **131g** (51.9 mg, 0.20 mmol), the Flurbiprofen-derived dibenzothiophenium salt **170j** (177 mg, 0.30 mmol), [RuCl<sub>2</sub>(*p*-cymene)]<sub>2</sub> (6.0 mg, 0.01 mmol, 5.0 mol %), and KOAc (39.3 mg, 2.0 equiv.) in *t*AmOH (2.0 mL). Purification by column chromatography on silica gel (*n*hexane/EtOAc: 5/1) yielded **181** (68.0 mg, 66%) as a transparent oil.

**<sup>1</sup>H NMR** (400 MHz, CDCl<sub>3</sub>): δ 7.51 (dd, *J* = 8.0, 8.0 Hz, 1H), 7.38 (d, *J* = 8.0 Hz, 2H), 7.32 (dd, *J* = 8.0, 8.0 Hz, 1H), 7.17 – 7.11 (m, 4H), 7.10 (s, 2H), 7.06 (d, *J* = 8.5 Hz, 1H), 3.80 (s, 3H), 3.73 (q, *J* = 7.4 Hz, 1H), 3.67 (s, 3H), 2.65 (t, *J* = 7.5 Hz, 2H), 1.59 – 1.53 (m, 2H), 1.51 (d, *J* = 7.4 Hz, 3H), 1.19 (s, 6H), 0.77 (s, 3H).

**<sup>13</sup>C NMR** (101 MHz, CDCl<sub>3</sub>): δ 174.4 (C<sub>q</sub>), 159.7 (d, <sup>1</sup>*J*<sub>C-F</sub> = 248.8 Hz, C<sub>q</sub>), 155.3 (C<sub>q</sub>), 147.6 (C<sub>q</sub>), 142.0 (d, <sup>3</sup>*J*<sub>C-F</sub> = 7.7 Hz, C<sub>q</sub>), 140.5 (C<sub>q</sub>), 136.7 (C<sub>q</sub>), 134.8 (d, <sup>3</sup>*J*<sub>C-F</sub> = 1.5 Hz, C<sub>q</sub>), 131.0 (CH), 130.7 (d, <sup>3</sup>*J*<sub>C-F</sub> = 3.9 Hz, CH), 128.7 (d, <sup>4</sup>*J*<sub>C-F</sub> = 3.3 Hz, CH), 128.3 (CH), 127.1 (d, <sup>2</sup>*J*<sub>C-F</sub> = 13.4 Hz, C<sub>q</sub>), 124.6 (C<sub>q</sub>), 123.9 (CH), 123.6 (d, <sup>4</sup>*J*<sub>C-F</sub> = 3.3 Hz, CH), 122.3 (CH), 115.3 (d, <sup>2</sup>*J*<sub>C-F</sub> = 23.6 Hz, CH), 111.2 (CH), 56.2 (CH<sub>3</sub>), 52.2 (CH<sub>3</sub>), 44.9 (d, <sup>4</sup>*J*<sub>C-F</sub> = 1.4 Hz, CH), 31.5 (CH<sub>2</sub>), 29.4 (CH<sub>2</sub>), 28.6 (CH<sub>2</sub>), 25.5 (CH<sub>2</sub>), 22.5 (CH<sub>2</sub>), 18.4 (CH<sub>3</sub>), 14.1 (CH<sub>3</sub>).

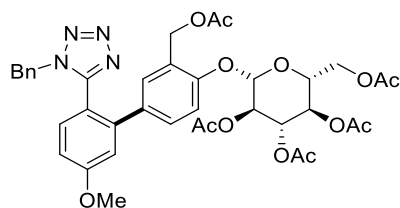
**<sup>19</sup>F NMR** (377 MHz, CDCl<sub>3</sub>): δ -116.9 – -117.6 (m).

**IR** (ATR): 2931, 1736, 1584, 1472, 1313, 1269, 1172, 1039, 792 cm<sup>-1</sup>.

**MS** (ESI) *m/z* (relative intensity): 538.3 [M+Na]<sup>+</sup> (100), 516.3 [M+H]<sup>+</sup> (90).

**HR-MS** (ESI): *m/z* calcd for C<sub>31</sub>H<sub>35</sub>FN<sub>3</sub>O<sub>3</sub><sup>+</sup> [M+H]<sup>+</sup> 516.2657, found 516.2654.

**(2*R*,3*R*,4*S*,5*R*,6*S*)-2-(acetoxymethyl)-6-((3-(acetoxymethyl)-2'-(1-benzyl-1*H*-tetrazol-5-yl)-5'-methoxy-[1,1'-biphenyl]-4-yl)oxy)tetrahydro-2*H*-pyran-3,4,5-triyl triacetate (**183**)**



The general procedure A was followed using 1-benzyl-5-(4-methoxyphenyl)-1*H*-tetrazole **162a** (53.3 mg, 0.20 mmol), the pentaacyl-Salicin-derived

dibenzothiophenium salt **170a** (249 mg, 0.30 mmol), [RuCl<sub>2</sub>(*p*-cymene)]<sub>2</sub> (6.0 mg, 0.01 mmol, 5.0 mol %), and KOAc (39.3 mg, 2.0 equiv.) in *t*AmOH (2.0 mL). Purification by column chromatography on silica gel (*n*hexane/EtOAc: 10/1) yielded **183** (91.0 mg, 60%) as a white solid.

**m.p.:** 81–83 °C.

**<sup>1</sup>H NMR** (400 MHz, CDCl<sub>3</sub>): δ 7.22 – 7.11 (m, 3H), 7.10 – 6.89 (m, 6H), 6.80 – 6.73 (m, 2H), 5.33 – 5.27 (m, 2H), 5.23 – 5.11 (m, 2H), 5.10 – 5.01 (m, 2H), 4.95 (d, *J* = 14.0 Hz, 1H), 4.89 – 4.79 (m, 2H), 4.26 (ddd, *J* = 12.6, 5.3, 2.6 Hz, 1H), 4.16 (dq, *J* = 11.7, 3.2, 2.6 Hz, 1H), 3.89 (s, 3H), 2.11 – 2.06 (m, 5H), 2.06 – 2.01 (m, 10H).

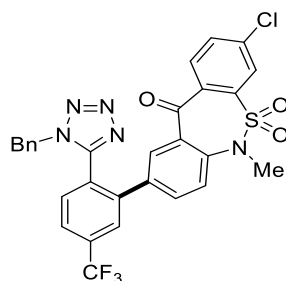
**<sup>13</sup>C NMR** (101 MHz, CDCl<sub>3</sub>): δ 170.7 (C<sub>q</sub>), 170.6 (C<sub>q</sub>), 170.2 (C<sub>q</sub>), 169.5 (C<sub>q</sub>), 169.3 (C<sub>q</sub>), 161.9 (C<sub>q</sub>), 154.6 (C<sub>q</sub>), 154.2 (C<sub>q</sub>), 142.4 (C<sub>q</sub>), 134.0 (C<sub>q</sub>), 133.3 (C<sub>q</sub>), 132.8 (CH), 129.6 (CH), 128.8 (CH), 128.6 (CH), 127.8 (CH), 126.8 (CH), 116.1 (CH), 115.6 (CH), 114.6 (C<sub>q</sub>), 113.2 (CH), 99.0 (CH), 72.6 (CH), 72.2 (CH), 70.9 (CH), 68.3 (CH<sub>3</sub>), 61.9 (CH<sub>2</sub>), 60.5 (CH<sub>2</sub>), 55.7 (CH<sub>3</sub>), 50.9 (CH<sub>2</sub>), 21.0 (CH<sub>3</sub>), 20.8 (CH<sub>3</sub>), 20.7 (CH<sub>3</sub>), 20.6 (CH<sub>3</sub>). *Missing C<sub>q</sub>, CH*

**IR** (ATR): 1737, 1607, 1470, 1364, 1226, 1032, 907, 726, 648 cm<sup>-1</sup>.

**MS** (ESI) *m/z* (relative intensity): 783.3 [M+Na]<sup>+</sup> (100), 761.3 [M+H]<sup>+</sup> (20).

**HR-MS** (ESI): *m/z* calcd for C<sub>38</sub>H<sub>41</sub>N<sub>4</sub>O<sub>13</sub><sup>+</sup> [M+H]<sup>+</sup> 761.2665, found 761.2649.

**9-(2-(1-Benzyl-1*H*-tetrazol-5-yl)-5-(trifluoromethyl)phenyl)-3-chloro-6-methyldibenzo [*c*,*f*][1,2]thiazepin-11(6*H*)-one 5,5-dioxide (**184**)**



The general procedure A was followed using 1-benzyl-5-(4-trifluoromethylphenyl)-1*H*-tetrazole **162b** (59.9 mg, 0.20 mmol), the Tianeptine-precursor-derived dibenzothiophenium salt **170c** (191 mg, 0.30 mmol), [RuCl<sub>2</sub>(*p*-cymene)]<sub>2</sub> (6.0 mg, 0.01 mmol, 5.0 mol %), and KOAc (39.3 mg, 2.0 equiv.) in *t*AmOH (2.0 mL). Purification by

column chromatography on silica gel (*n*hexane/EtOAc: 10/1) yielded **184** (50.0 mg, 41%) as a transparent oil.

**<sup>1</sup>H NMR** (400 MHz, CDCl<sub>3</sub>): δ 8.19 (s, 1H), 7.94 (s, 1H), 7.92 – 7.83 (m, 2H), 7.77 – 7.66 (m, 2H), 7.45 (d, *J* = 8.0 Hz, 1H), 7.23 – 7.12 (m, 5H), 6.82 (d, *J* = 7.5 Hz, 2H), 5.07 (s, 2H), 3.36 (s, 3H).

**<sup>13</sup>C NMR** (101 MHz, CDCl<sub>3</sub>): δ 189.0 (C<sub>q</sub>), 153.2 (C<sub>q</sub>), 141.6 (C<sub>q</sub>), 141.2 (C<sub>q</sub>), 141.0 (C<sub>q</sub>), 139.1 (C<sub>q</sub>), 138.4 (C<sub>q</sub>), 134.9 (CH), 134.8 (C<sub>q</sub>), 134.1 (C<sub>q</sub>), 134.1 (q, <sup>2</sup>*J*<sub>C-F</sub> = 33.2 Hz, C<sub>q</sub>), 133.7 (CH), 133.4 (CH), 132.6 (C<sub>q</sub>), 132.2 (CH), 131.9 (CH), 130.6 (C<sub>q</sub>), 129.3 (q, <sup>3</sup>*J*<sub>C-F</sub> = 3.1 Hz, CH), 129.1 (q, <sup>4</sup>*J*<sub>C-F</sub> = 2.9 Hz, CH), 127.8 (CH), 127.5 (q, <sup>3</sup>*J*<sub>C-F</sub> = 3.9 Hz, CH), 125.2 (CH), 124.3 (CH), 123.4 (q, <sup>1</sup>*J*<sub>C-F</sub> = 273.2 Hz, C<sub>q</sub>), 122.1 (CH), 51.6 (CH<sub>2</sub>), 38.6 (CH<sub>3</sub>).

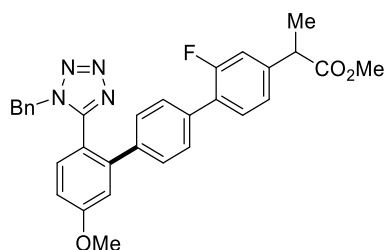
**<sup>19</sup>F NMR** (377 MHz, CDCl<sub>3</sub>): δ -63.0 (s).

**IR** (ATR): 1657, 1496, 1363, 1297, 1138, 1104, 1044, 842, 729 cm<sup>-1</sup>.

**MS** (ESI) *m/z* (relative intensity): 632.1 [M+Na]<sup>+</sup> (100), 610.1 [M+H]<sup>+</sup> (10).

**HR-MS** (ESI): *m/z* calcd for C<sub>29</sub>H<sub>20</sub><sup>35</sup>ClF<sub>3</sub>N<sub>5</sub>O<sub>3</sub>S<sup>+</sup> [M+H]<sup>+</sup> 610.0922, found 610.0906.

**Methyl-2-(2''-(1-benzyl-1*H*-tetrazol-5-yl)-2-fluoro-5''-methoxy-[1,1':4',1''-terphenyl]-4-yl)propanoate (**185**)**



The general procedure A was followed using 1-benzyl-5-(4-methoxyphenyl)-1*H*-tetrazole **162a** (53.2 mg, 0.20 mmol), the Flurbiprofen-derived dibenzothiophene salt **170j** (177 mg, 0.30 mmol), [RuCl<sub>2</sub>(*p*-cymene)]<sub>2</sub> (6.0 mg, 0.01 mmol, 5.0 mol %), and KOAc (39.3 mg, 2.0 equiv.) in *t*AmOH (2.0 mL). Purification by column chromatography on silica gel (*n*hexane/EtOAc: 3/1) yielded **185** (47 mg, 45%) as a transparent oil.

**<sup>1</sup>H NMR** (400 MHz, CDCl<sub>3</sub>): δ 7.46 (d, *J* = 7.9 Hz, 2H), 7.37 (dd, *J* = 8.0, 8.0 Hz, 1H), 7.32 (dd, *J* = 8.6, 1.4 Hz, 1H), 7.25 – 7.07 (m, 8H), 6.98 (dt, *J* = 8.9, 1.8 Hz, 1H), 6.79

(d,  $J = 7.3$  Hz, 2H), 4.83 (s, 2H), 3.92 (d,  $J = 1.4$  Hz, 3H), 3.77 (q,  $J = 7.2$  Hz, 1H), 3.71 (d,  $J = 1.4$  Hz, 3H), 1.54 (d,  $J = 7.1$  Hz, 3H).

**$^{13}\text{C}$  NMR** (101 MHz,  $\text{CDCl}_3$ ):  $\delta$  174.5 ( $\text{C}_q$ ), 162.1 ( $\text{C}_q$ ), 159.8 (d,  $^1J_{\text{C-F}} = 248.9$  Hz,  $\text{C}_q$ ), 154.7 ( $\text{C}_q$ ), 143.0 ( $\text{C}_q$ ), 142.5 (d,  $^3J_{\text{C-F}} = 7.7$  Hz,  $\text{C}_q$ ), 138.3 ( $\text{C}_q$ ), 135.6 ( $\text{C}_q$ ), 133.1 (d,  $^2J_{\text{C-F}} = 35.2$  Hz,  $\text{C}_q$ ), 130.8 (d,  $^4J_{\text{C-F}} = 3.8$  Hz, CH), 129.6 (d,  $^4J_{\text{C-F}} = 3.2$  Hz, CH), 128.9 (CH), 128.8 (CH), 128.7 (CH), 128.0 (CH), 126.8 (d,  $^3J_{\text{C-F}} = 13.2$  Hz,  $\text{C}_q$ ), 115.9 (CH), 115.5 (d,  $^2J_{\text{C-F}} = 23.6$  Hz, CH), 114.8 ( $\text{C}_q$ ), 113.7 (CH), 55.7 ( $\text{CH}_3$ ), 52.4 ( $\text{CH}_3$ ), 51.0 ( $\text{CH}_2$ ), 45.1 (CH), 18.5 ( $\text{CH}_3$ ). *Missing CH CH.*

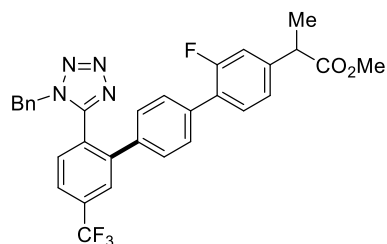
**$^{19}\text{F}$  NMR** (377 MHz,  $\text{CDCl}_3$ ):  $\delta$  -117.1 – -117.3 (m).

**IR** (ATR): 2954, 1671, 1579, 1477, 1198, 1162, 1029, 637, 518  $\text{cm}^{-1}$ .

**MS** (ESI)  $m/z$  (relative intensity): 545.2  $[\text{M}+\text{Na}]^+$  (100), 523.2  $[\text{M}+\text{H}]^+$  (25).

**HR-MS** (ESI):  $m/z$  calcd for  $\text{C}_{31}\text{H}_{28}\text{N}_4\text{O}_3\text{F}^+$   $[\text{M}+\text{H}]^+$  523.2140, found 523.2145.

### 1-Benzyl-5-(4'-ethyl-5-methoxy-[1,1'-biphenyl]-2-yl)-1H-tetrazole (186)



The general procedure A was followed using 1-benzyl-5-(4-trifluoromethylphenyl)-1H-tetrazole **162b** (60.0 mg, 0.20 mmol), the Flurbiprofen-derived dibenzothiophenium salt **170j** (177 mg, 0.30 mmol),  $[\text{RuCl}_2(p\text{-cymene})]_2$  (6.0 mg, 0.01 mmol, 5.0 mol %), and KOAc (39.3 mg, 2.0 equiv.) in *t*AmOH (2.0 mL). Purification by column chromatography on silica gel (*n*hexane/EtOAc: 3/1) yielded **186** (92 mg, 82%) as a transparent oil.

**$^1\text{H}$  NMR** (400 MHz,  $\text{CDCl}_3$ ):  $\delta$  7.87 (s, 1H), 7.68 (d,  $J = 8.1$  Hz, 1H), 7.49 (dd,  $J = 13.3$ , 8.0 Hz, 3H), 7.38 (dd,  $J = 8.0$ , 8.0 Hz, 1H), 7.28 – 7.05 (m, 7H), 6.76 (d,  $J = 7.4$  Hz, 2H), 4.87 (s, 2H), 3.77 (q,  $J = 7.2$  Hz, 1H), 3.70 (s, 3H), 1.54 (d,  $J = 7.1$  Hz, 3H).

**$^{13}\text{C}$  NMR** (101 MHz,  $\text{CDCl}_3$ ):  $\delta$  174.4 ( $\text{C}_q$ ), 159.8 (d,  $^1J_{\text{C-F}} = 249.2$  Hz,  $\text{C}_q$ ), 153.7 ( $\text{C}_q$ ), 142.7 (d,  $^3J_{\text{C-F}} = 7.7$  Hz,  $\text{C}_q$ ), 142.3 ( $\text{C}_q$ ), 136.7 ( $\text{C}_q$ ), 136.3 (q,  $^4J_{\text{C-F}} = 1.4$  Hz,  $\text{C}_q$ ), 133.9 (d,  $^2J_{\text{C-F}} = 33.0$  Hz,  $\text{C}_q$ ), 132.8 ( $\text{C}_q$ ), 132.2 (CH), 130.7 (q,  $^3J_{\text{C-F}} = 3.7$  Hz, CH), 129.8 (q,

$^3J_{C-F} = 3.3$  Hz, CH), 129.0 (CH), 128.9 (CH), 128.8 (CH), 127.9 (CH), 127.2 (q,  $^3J_{C-F} = 3.7$  Hz, CH), 126.6 (C<sub>q</sub>), 126.5 (C<sub>q</sub>), 124.7 (q,  $^4J_{C-F} = 3.7$  Hz, CH), 123.9 (d,  $^4J_{C-F} = 3.3$  Hz, CH), 115.6 (d,  $^2J_{C-F} = 23.4$  Hz, CH), 52.4 (CH<sub>3</sub>), 51.3 (CH<sub>2</sub>), 45.1 (CH), 18.5 (CH<sub>3</sub>).

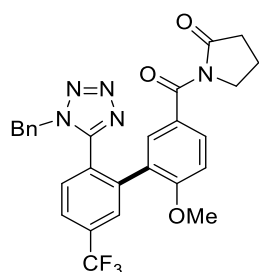
$^{19}\text{F}$  NMR (377 MHz, CDCl<sub>3</sub>):  $\delta$  -63.0, -117.1 – -117.2 (m).

IR (ATR): 2999, 2954, 1734, 1623, 1419, 1335, 1171, 1104, 722 cm<sup>-1</sup>.

MS (ESI)  $m/z$  (relative intensity): 583.2 [M+Na]<sup>+</sup> (100), 561.2 [M+H]<sup>+</sup> (5).

HR-MS (ESI):  $m/z$  calcd for C<sub>31</sub>H<sub>25</sub>F<sub>4</sub>N<sub>4</sub>O<sub>2</sub><sup>+</sup> [M+H]<sup>+</sup> 561.1908, found 561.1897.

### 1-(2'-(1-Benzyl-1*H*-tetrazol-5-yl)-6-methoxy-5'-(trifluoromethyl)-[1,1'-biphenyl]-3-carbonyl)pyrrolidin-2-one (187)



The general procedure A was followed using 1-benzyl-5-(4-trifluoromethylphenyl)-1*H*-tetrazole **162b** (60.9 mg, 0.20 mmol), the Aniracetam-derived dibenzothiophenium salt **170g** (166 mg, 0.30 mmol), [RuCl<sub>2</sub>(*p*-cymene)]<sub>2</sub> (6.0 mg, 0.01 mmol, 5.0 mol %), and KOAc (39.3 mg, 2.0 equiv.) in *t*AmOH (2.0 mL). Purification by column chromatography on silica gel (*n*hexane/EtOAc: 10/1) yielded **187** (56.0 mg, 54%) as a transparent oil.

$^1\text{H}$  NMR (400 MHz, CDCl<sub>3</sub>):  $\delta$  7.80 (s, 1H), 7.73 – 7.63 (m, 2H), 7.50 (s, 1H), 7.45 (d,  $J = 8.1$  Hz, 1H), 7.25 – 7.15 (m, 3H), 6.91 – 6.81 (m, 3H), 5.02 (s, 2H), 3.92 (t,  $J = 7.0$  Hz, 2H), 3.59 (s, 3H), 2.58 (t,  $J = 7.9$  Hz, 2H), 2.20 – 2.09 (m, 2H).

$^{13}\text{C}$  NMR (101 MHz, CDCl<sub>3</sub>):  $\delta$  174.6 (C<sub>q</sub>), 169.2 (C<sub>q</sub>), 158.6 (C<sub>q</sub>), 154.0 (C<sub>q</sub>), 138.7 (C<sub>q</sub>), 133.7 (C<sub>q</sub>), 133.2 (q,  $^2J_{C-F} = 32.8$  Hz, C<sub>q</sub>), 132.9 (CH), 132.5 (CH), 131.5 (CH), 128.8 (CH), 128.6 (q,  $^3J_{C-F} = 2.8$  Hz, CH), 128.0 (q,  $^4J_{C-F} = 1.6$  Hz, C<sub>q</sub>), 127.6 (CH), 127.3 (C<sub>q</sub>), 125.5 (C<sub>q</sub>), 124.7 (q,  $^3J_{C-F} = 3.9$  Hz, CH), 123.5 (q,  $^1J_{C-F} = 273.2$ , C<sub>q</sub>), 110.5 (CH), 55.5 (CH<sub>3</sub>), 51.1 (CH<sub>2</sub>), 46.7 (CH<sub>2</sub>), 33.3 (CH<sub>2</sub>), 17.6 (CH<sub>2</sub>). *Missing CH.*

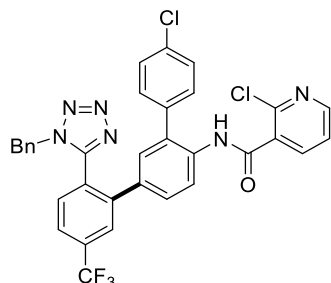
$^{19}\text{F}$  NMR (377 MHz, CDCl<sub>3</sub>):  $\delta$  -62.9 (s).

IR (ATR): 1738, 1668, 1501, 1336, 1260, 1172, 1018, 905, 726 cm<sup>-1</sup>.

**MS** (ESI)  $m/z$  (relative intensity): 544.2 [M+Na]<sup>+</sup> (100), 522.2 [M+H]<sup>+</sup> (35).

**HR-MS** (ESI):  $m/z$  calcd for C<sub>27</sub>H<sub>23</sub>F<sub>3</sub>N<sub>5</sub>O<sub>3</sub><sup>+</sup> [M+H]<sup>+</sup> 522.1748, found 522.1748.

***N*-(2-(1-Benzyl-1*H*-tetrazol-5-yl)-4''-chloro-5-(trifluoromethyl)-[1,1':3',1''-terphenyl]-4'-yl)-2-chloronicotinamide (188)**



The general procedure A was followed using 1-benzyl-5-(4-trifluoromethylphenyl)-1*H*-tetrazole **162b** (61.0 mg, 0.20 mmol), the Boscalid-derived dibenzothiophenium salt **170h** (203 mg, 0.30 mmol), [RuCl<sub>2</sub>(*p*-cymene)]<sub>2</sub> (6.0 mg, 0.01 mmol, 5.0 mol %), and KOAc (39.3 mg, 2.0 equiv.) in *t*AmOH (2.0 mL). Purification by column chromatography on silica gel (*n*hexane/EtOAc: 3/1) yielded **188** (58 mg, 45%) as a transparent oil.

**<sup>1</sup>H NMR** (400 MHz, CDCl<sub>3</sub>): δ 8.54 (d, *J* = 8.5 Hz, 1H), 8.47 (d, *J* = 4.6 Hz, 1H), 8.26 (s, 1H), 8.18 (d, *J* = 7.7 Hz, 1H), 7.86 (s, 1H), 7.69 (d, *J* = 8.1 Hz, 1H), 7.46 – 7.41 (m, 3H), 7.39 – 7.36 (m, 1H), 7.32 (d, *J* = 8.7 Hz, 1H), 7.23 – 7.18 (m, 1H), 7.14 (dd, *J* = 7.7, 7.7 Hz, 2H), 7.11 – 7.06 (m, 2H), 6.85 – 6.78 (m, 3H), 5.03 (s, 2H).

**<sup>13</sup>C NMR** (101 MHz, CDCl<sub>3</sub>): δ 162.6 (C<sub>q</sub>), 153.6 (C<sub>q</sub>), 151.8 (CH), 146.7 (C<sub>q</sub>), 142.0 (C<sub>q</sub>), 140.6 (CH), 135.3 (C<sub>q</sub>), 135.2 (C<sub>q</sub>), 134.8 (C<sub>q</sub>), 134.1 (C<sub>q</sub>), 133.8 (C<sub>q</sub>), 133.8 (C<sub>q</sub>), 132.7 (C<sub>q</sub>), 132.4 (C<sub>q</sub>), 131.9 (CH), 130.8 (CH), 130.7 (C<sub>q</sub>), 130.5 (CH), 129.8 (CH), 129.1 (CH), 129.1 (CH), 129.1 (CH), 127.9 (CH), 126.8 – 127.2 (m, CH), 126.6 (C<sub>q</sub>), 124.9 (C<sub>q</sub>), 124.2 – 124.9 (m, CH), 123.2 (CH), 122.1 (CH), 51.5 (CH<sub>2</sub>).

**<sup>19</sup>F NMR** (377 MHz, CDCl<sub>3</sub>): δ -63.0 (s).

**IR** (ATR): 1650, 1579, 1474, 1398, 1325, 1086, 1064, 758, 726 cm<sup>-1</sup>.

**MS** (ESI)  $m/z$  (relative intensity): 667.1 [M+Na]<sup>+</sup> (100), 645.1 [M+H]<sup>+</sup> (2).

**HR-MS** (ESI):  $m/z$  calcd for C<sub>33</sub>H<sub>22</sub><sup>35</sup>Cl<sub>2</sub>F<sub>3</sub>N<sub>6</sub>O<sup>+</sup> [M+H]<sup>+</sup> 645.1179, found 645.1182.





mmol), the respective radical scavenger (0.20 mmol),  $[\text{RuCl}_2(p\text{-cymene})]_2$  (6.0 mg, 0.01 mmol, 5.0 mol %), and KOAc (39.3 mg, 2.0 equiv.) were suspended in toluene (2.0 mL) and stirred at 100 °C for 24 h. The reaction was filtered over silica gel and the ratios of the starting material **131a** and product **149** were determined *via* GC-MS using docosane as the internal standard.

### Deuterium Exchange Experiment I

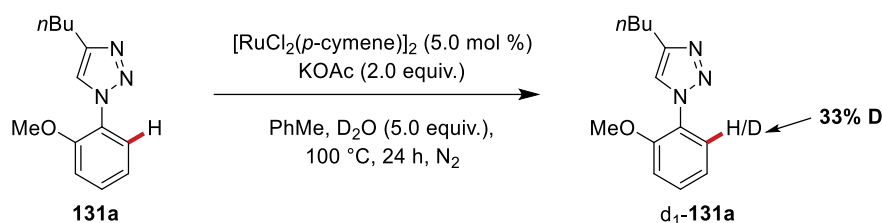


Figure 5-3. H/D exchange experiment I.

Phenyl triazole **131a** (46.2 mg, 0.20 mmol),  $[\text{RuCl}_2(p\text{-cymene})]_2$  (6.0 mg, 0.01 mmol, 5.0 mol %), KOAc (39.3 mg, 2.0 equiv.), and  $\text{D}_2\text{O}$  (18  $\mu\text{L}$ , 5.0 equiv.) were suspended in toluene (2.0 mL) and stirred at 100 °C for 24 h. The reaction mixture was filtered over silica gel and analyzed *via*  $^1\text{H}$  NMR using 1,3,5-trimethoxybenzene as the internal standard.

### Deuterium Exchange Experiment II

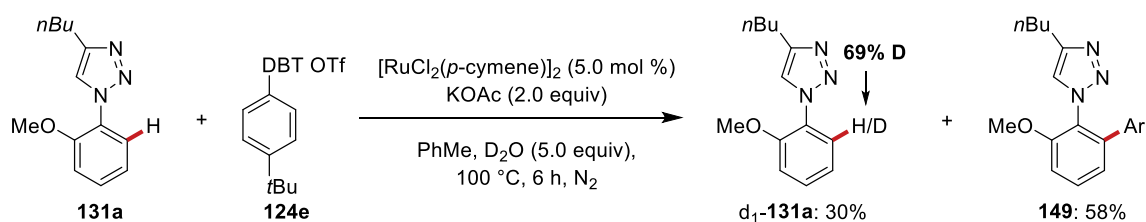
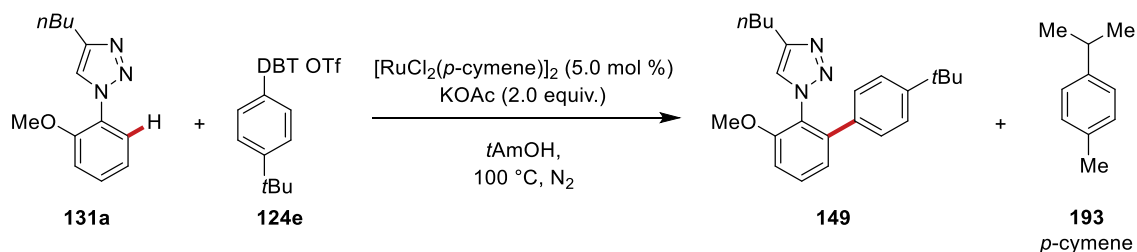


Figure 5-4. H/D exchange experiment II.

Phenyl triazole **131a** (46.2 mg, 0.20 mmol), dibenzothiophene salt **124e** (140 mg, 1.5 equiv.),  $[\text{RuCl}_2(p\text{-cymene})]_2$  (6.0 mg, 0.01 mmol, 5.0 mol %), KOAc (39.3 mg, 2.0 equiv.), and  $\text{D}_2\text{O}$  (18  $\mu\text{L}$ , 5.0 equiv.) were suspended in toluene (2.0 mL) and stirred at 100 °C for 6 h. The starting material  $\text{d}_1\text{-131a}$  and product **149** were isolated by column

chromatography on silica gel (*n*hexane/EtOAc: 10/1) and analyzed *via*  $^1\text{H}$  NMR.

### Detection of Free *p*-Cymene



**Figure 5-5.** Detection of free *p*-cymene **193**.

Phenyl triazole **131a** (46.2 mg, 0.20 mmol), dibenzothiophene salt **124e** (140 mg, 1.5 equiv.),  $[\text{RuCl}_2(\textit{p}\text{-cymene})]_2$  (6.0 mg, 0.01 mmol, 5.0 mol %), and KOAc (39.3 mg, 2.0 equiv.) were suspended in *t*AmOH (2.0 mL) and stirred at 100 °C under  $\text{N}_2$ . During the reaction, aliquots of 20  $\mu\text{L}$  were removed *via* syringe after 30 min, 60 min, 90 min, 2h, 3 h, 4 h, 6 h, 12 h and 24 h. The sample was diluted with EtOAc, filtered through a short plug of silica gel and analyzed by gas chromatography.

### Poisoning Experiment

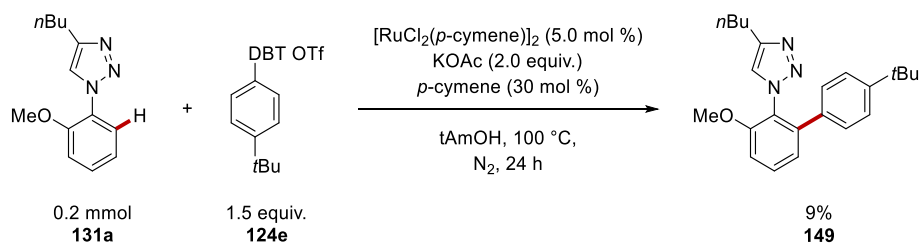


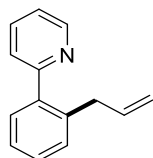
**Figure 5-6.** Poisoning experiment.

Phenyl triazole **131a** (46.2 mg, 0.20 mmol), dibenzothiophene salt **124e** (140 mg, 1.5 equiv.), *p*-cymene (9.5  $\mu\text{L}$ , 0.06 mmol, 30 mol %),  $[\text{RuCl}_2(\textit{p}\text{-cymene})]_2$  (6.0 mg, 0.01 mmol, 5.0 mol %), and KOAc (39.3 mg, 2.0 equiv.) were suspended in *t*AmOH (2.0 mL) and stirred at 100 °C under  $\text{N}_2$ . The sample was diluted with EtOAc, filtered through a short plug of silica gel and analyzed by gas chromatography.

### 5.3.2 Photo-Induced Ruthenium-Catalyzed C–H Allylation at Ambient Temperature

#### Characterization Data

##### 2-(2-Allylphenyl)pyridine (**199**)



The general procedure C was followed using 2-phenylpyridine **22** (72  $\mu$ L, 0.50 mmol), allyl bromide **198** (87  $\mu$ L, 1.00 mmol),  $[\text{RuCl}_2(p\text{-cymene})]_2$  (15.3 mg, 0.025 mmol, 5.0 mol %) and NaOAc (82 mg, 1.00 mmol) in 1,4-dioxane. After 24 h, purification by column chromatography (*n*hexane/EtOAc: 10/1) yielded **199** (62 mg, 63%) as a pale-yellow oil.

**$^1\text{H NMR}$**  (400 MHz,  $\text{CDCl}_3$ ):  $\delta$  8.69 (d,  $J = 4.4$  Hz, 1H), 7.74 (dd,  $J = 7.5$  Hz, 7.5 Hz, 1H), 7.45 – 7.38 (m, 2H), 7.37 – 7.30 (m, 3H), 7.26 (dd,  $J = 4.0, 3.9$  Hz, 1H), 5.88 (ddt,  $J = 16.6, 9.8, 6.4$  Hz, 1H), 4.96 (d,  $J = 10.1$  Hz, 1H), 4.89 (d,  $J = 17.0$  Hz, 1H), 3.50 (d,  $J = 6.4$  Hz, 2H).

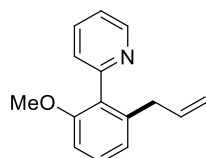
**$^{13}\text{C NMR}$**  (100 MHz,  $\text{CDCl}_3$ ):  $\delta$  159.9 ( $\text{C}_q$ ), 149.2 (CH), 140.4 ( $\text{C}_q$ ), 137.7 ( $\text{C}_q$ ), 137.6 (CH), 136.3 (CH), 130.2 (CH), 130.0 (CH), 128.6 (CH), 126.4 (CH), 124.3 (CH), 121.9 (CH), 115.6 ( $\text{CH}_2$ ), 37.5 ( $\text{CH}_2$ ).

**IR** (ATR): 2926, 1731, 1465, 1375, 1248, 1046, 905, 729, 650  $\text{cm}^{-1}$ .

**MS** (ESI)  $m/z$  (relative intensity): 196.1  $[\text{M}+\text{H}]^+$  (100).

**HR-MS** (ESI):  $m/z$  calcd for  $\text{C}_{14}\text{H}_{13}\text{N}^+$   $[\text{M}+\text{H}]^+$  196.1121, found 196.1124.

##### 2-(2-Allyl-6-methoxyphenyl)pyridine (**203**)



The general procedure C was followed using 2-(2-methoxyphenyl)pyridine **201a** (86  $\mu$ L, 0.50 mmol) and allyl bromide **198** (87  $\mu$ L, 1.00 mmol),  $[\text{RuCl}_2(p\text{-cymene})]_2$  (15.3 mg, 0.025 mmol, 5.0 mol %) and NaOAc (82 mg, 1.00 mmol) in 1,4-dioxane. After 24

h, purification by column chromatography (*n*pentane/diethyl ether: 10/1) yielded **203** (72.1 mg, 57%) as a yellow oil.

**<sup>1</sup>H NMR** (400 MHz, CDCl<sub>3</sub>): δ 8.73 (d, *J* = 4.8 Hz, 1H), 7.74 (ddd, *J* = 7.7, 7.7, 1.6 Hz, 1H), 7.38–7.30 (m, 2H), 7.29 – 7.22 (m, 1H), 6.95 (d, *J* = 7.8 Hz, 1H), 6.88 (d, *J* = 8.3 Hz, 1H), 5.81 (ddt, *J* = 16.7, 9.6, 6.7 Hz, 1H), 4.96 – 4.89 (m, 1H), 4.84 (d, *J* = 17.0 Hz, 1H), 3.74 (s, 3H), 3.20 (d, *J* = 6.7 Hz, 2H).

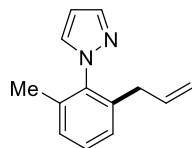
**<sup>13</sup>C NMR** (100 MHz, CDCl<sub>3</sub>): δ 157.2 (C<sub>q</sub>), 156.9 (C<sub>q</sub>), 149.4 (CH), 139.9 (C<sub>q</sub>), 137.3 (CH), 135.8 (CH), 129.9 (C<sub>q</sub>), 129.2 (CH), 126.0 (CH), 122.0 (CH), 121.9 (CH), 115.5 (CH<sub>2</sub>), 109.0 (CH), 55.9 (CH<sub>3</sub>), 37.6 (CH<sub>2</sub>).

**IR** (ATR): 1600, 1578, 1468, 1437, 1254, 1067, 989, 910, 775 cm<sup>-1</sup>.

**MS** (ESI) *m/z* (relative intensity): 226.1 [M+H]<sup>+</sup> (100).

**HR-MS** (ESI): *m/z* calcd for C<sub>15</sub>H<sub>16</sub>NO<sup>+</sup> [M+H]<sup>+</sup> 226.1226, found 226.1234.

#### 1-(2-Allyl-6-methylphenyl)-1*H*-pyrazole (**204**)



The general procedure C was followed using 1-(*o*-tolyl)-1*H*-pyrazole **201b** (76 μL, 0.50 mmol) and allyl bromide **198** (11, 87 μL, 1.00 mmol), [RuCl<sub>2</sub>(*p*-cymene)]<sub>2</sub> (15.3 mg, 0.025 mmol, 5.0 mol %) and NaOAc (82 mg, 1.00 mmol) in 1,4-dioxane. After 24 h, purification by column chromatography (*n*pentane/diethyl ether: 10/1) yielded **204** (71.2 mg, 72%) as a pale-yellow oil.

**<sup>1</sup>H NMR** (400 MHz, CDCl<sub>3</sub>): δ 7.70 (d, *J* = 1.9 Hz, 1H), 7.41 (dd, *J* = 2.2, 2.1 Hz, 1H), 7.25 (dd, *J* = 6.9, 6.1 Hz, 1H), 7.13 (d, *J* = 7.7 Hz, 2H), 6.40 (d, *J* = 2.2 Hz, 1H), 5.77 (ddt, *J* = 16.8, 9.9, 6.6 Hz, 1H), 4.95 (dt, *J* = 10.1, 1.4 Hz, 1H), 4.86 (dd, *J* = 17.0, 1.6 Hz, 1H), 3.00 (d, *J* = 6.6 Hz, 2H), 1.97 (s, 3H).

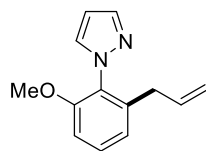
**<sup>13</sup>C NMR** (100 MHz, CDCl<sub>3</sub>): δ 140.2 (CH), 139.0 (C<sub>q</sub>), 138.2 (C<sub>q</sub>), 136.8 (CH), 136.6 (C<sub>q</sub>), 131.3 (CH), 129.2 (CH), 128.7 (CH), 127.6 (CH), 116.1 (CH<sub>2</sub>), 105.9 (CH), 35.5 (CH<sub>2</sub>), 17.4 (CH<sub>3</sub>).

**IR** (ATR): 2231, 1639, 1474, 1393, 1168, 1045, 905, 726, 626 cm<sup>-1</sup>.

**MS** (ESI)  $m/z$  (relative intensity): 199.1 [M+H]<sup>+</sup> (100).

**HR-MS** (ESI):  $m/z$  calcd for C<sub>13</sub>H<sub>15</sub>N<sub>2</sub><sup>+</sup> [M+H]<sup>+</sup> 199.1230, found 199.1233.

### 1-[2-Allyl-6-methoxyphenyl]-1*H*-pyrazole (**205**)



The general procedure C was followed using 1-(2-methoxyphenyl)-1*H*-pyrazole **201c** (79  $\mu$ L, 0.50 mmol) and allyl bromide **198** (87  $\mu$ L, 1.00 mmol), [RuCl<sub>2</sub>(*p*-cymene)]<sub>2</sub> (15.3 mg, 0.025 mmol, 5.0 mol %) and NaOAc (82 mg, 1.00 mmol) in 1,4-dioxane. After 24 h, purification by column chromatography (*n*pentane/diethyl ether: 20/1) yielded **205** (82.2 mg, 77%) as a pale-yellow oil.

**<sup>1</sup>H NMR** (400 MHz, CDCl<sub>3</sub>):  $\delta$  7.75 (d,  $J$  = 1.8 Hz, 1H), 7.49 (dd,  $J$  = 2.3 Hz, 1H), 7.34 (dd,  $J$  = 8.0, 8.0 Hz, 1H), 6.93 (d,  $J$  = 7.8 Hz, 1H), 6.88 (d,  $J$  = 8.3 Hz, 1H), 6.43 (d,  $J$  = 2.2 Hz, 1H), 5.79 (ddt,  $J$  = 16.8, 9.9, 6.7 Hz, 1H), 5.01 – 4.77 (m, 2H), 3.74 (d,  $J$  = 2.0 Hz, 3H), 3.11 (d,  $J$  = 6.7 Hz, 2H).

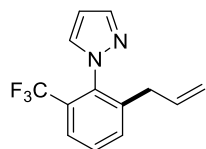
**<sup>13</sup>C NMR** (100 MHz, CDCl<sub>3</sub>):  $\delta$  155.5 (C<sub>q</sub>), 140.1 (CH), 139.8 (C<sub>q</sub>), 136.5 (CH), 132.3 (CH), 129.9 (CH), 128.7 (C<sub>q</sub>), 121.8 (CH), 116.2 (CH<sub>2</sub>), 109.8 (CH), 105.6 (CH), 56.1 (CH<sub>3</sub>), 35.4 (CH<sub>2</sub>).

**IR** (ATR): 2929, 1588, 1475, 1394, 1274, 1067, 912, 733, 615 cm<sup>-1</sup>.

**MS** (ESI)  $m/z$  (relative intensity): 215.1 [M+H]<sup>+</sup> (100).

**HR-MS** (ESI):  $m/z$  calcd for C<sub>13</sub>H<sub>15</sub>N<sub>2</sub>O<sup>+</sup> [M+H]<sup>+</sup> 215.1179, found 215.1188.

### 1-[2-Allyl-6-(trifluoromethyl)phenyl]-1*H*-pyrazole (**206**)



The general procedure C was followed using 1-(2-(trifluoromethyl)phenyl)-1*H*-pyrazole **201d** (84  $\mu$ L, 0.50 mmol) and allyl bromide **198** (87  $\mu$ L, 1.00 mmol), [RuCl<sub>2</sub>(*p*-cymene)]<sub>2</sub> (15.3 mg, 0.025 mmol, 5.0 mol %) and NaOAc (82 mg, 1.00 mmol) in 1,4-dioxane.

After 24 h, purification by column chromatography (*n*pentane/diethyl ether: 20/1) yielded **206** (91.1 mg, 72%) as a colorless oil.

**<sup>1</sup>H NMR** (400 MHz, CDCl<sub>3</sub>): δ 7.76 (d, *J* = 1.8 Hz, 1H), 7.66 (dd, *J* = 6.8, 2.4 Hz, 1H), 7.58 – 7.50 (m, 3H), 6.45 (s, 1H), 5.78 (ddt, *J* = 16.8, 10.0, 6.7 Hz, 1H), 5.03 (dd, *J* = 10.2, 1.4 Hz, 1H), 4.93 (dd, *J* = 17.2, 1.5 Hz, 1H), 3.11 – 2.83 (m, 2H).

**<sup>13</sup>C NMR** (100 MHz, CDCl<sub>3</sub>): δ 141.5 (C<sub>q</sub>), 140.8 (CH), 137.3 (C<sub>q</sub>), 135.8 (CH), 134.0 (CH), 132.8 (d, <sup>4</sup>*J*<sub>C-F</sub> = 2 Hz, CH), 129.6 (CH), 128.5 (q, <sup>2</sup>*J*<sub>C-F</sub> = 31 Hz, C<sub>q</sub>), 125.0 (q, <sup>3</sup>*J*<sub>C-F</sub> = 5 Hz, CH), 123.1 (q, <sup>1</sup>*J*<sub>C-F</sub> = 274 Hz, C<sub>q</sub>), 117.2 (CH<sub>2</sub>), 106.3 (CH), 34.9 (CH<sub>2</sub>).

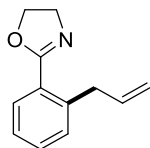
**<sup>19</sup>F NMR** (376 MHz, CDCl<sub>3</sub>): δ -59.9 (s).

**IR** (ATR): 1481, 1319, 1125, 1081, 1021, 916, 748, 679, 626 cm<sup>-1</sup>.

**MS** (ESI) *m/z* (relative intensity): 253.1 [M+H]<sup>+</sup> (100).

**HR-MS** (ESI): *m/z* calcd for C<sub>13</sub>H<sub>12</sub>F<sub>3</sub>N<sub>2</sub><sup>+</sup> [M+H]<sup>+</sup> 253.0947, found 253.0949.

## 2-(2-Allylphenyl)-4,5-dihydrooxazole (207)



The general procedure C was followed using 2-phenyl-4,5-dihydrooxazole **201e** (66 μL, 0.50 mmol), allyl bromide **198** (87 μL, 1.00 mmol), [RuCl<sub>2</sub>(*p*-cymene)]<sub>2</sub> (15.3 mg, 0.025 mmol, 5.0 mol %) and NaOAc (82 mg, 1.00 mmol) in 1,4-dioxane. After 24 h, purification by column chromatography (*n*pentane/diethyl ether: 10/1) yielded **207** (51 mg, 54%) as a brown oil.

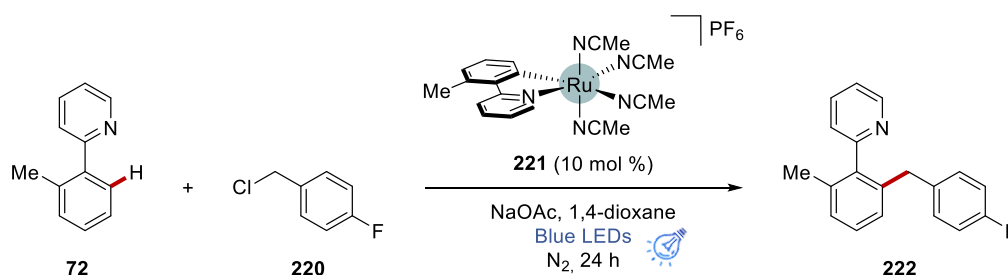
**<sup>1</sup>H NMR** (600 MHz, CDCl<sub>3</sub>): δ 7.38 (m, 4H), 5.80 (d, *J* = 93.3 Hz, 1H), 5.40 – 5.05 (m, 2H), 4.50 – 4.00 (m, 2H), 4.00 – 3.64 (m, 2H), 2.20 – 1.95 (m, 2H).

**<sup>13</sup>C NMR** (151 MHz, CDCl<sub>3</sub>): δ 172.5 (C<sub>q</sub>), 136.4 (C<sub>q</sub>), 133.5 (CH), 129.9 (CH), 128.7 (CH), 126.8 (CH), 118.1 (CH<sub>2</sub>), 62.1 (C<sub>q</sub>), 61.8 (CH<sub>2</sub>), 53.0 (CH<sub>2</sub>), 44.2 (CH<sub>2</sub>), 21.2 (CH).

**IR** (ATR): 1737, 1631, 1413, 1369, 1228, 1046, 924, 701, 605 cm<sup>-1</sup>.

**MS** (ESI) *m/z* (relative intensity): 188.1 [M+H]<sup>+</sup> (100).

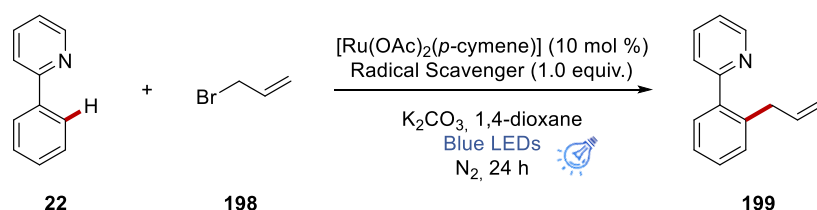
**HR-MS** (ESI): *m/z* calcd for C<sub>12</sub>H<sub>14</sub>NO<sup>+</sup> [M+H]<sup>+</sup> 188.1070, found 188.1072.

Photo-Induced C–H Benzyltion by Ruthenacycle **221** as Catalyst

**Figure 5-7.** Light-driven benzyltion catalyzed by cyclometalated ruthenium **221**.

Pyridine **72** (84.6 mg, 0.50 mmol), ruthenacycle **221** (28.9 mg, 0.05 mmol, 10 mol %) and NaOAc (82 mg, 1.00 mmol) were placed in a 10 mL vial. The vial was capped with a septum and wrapped with parafilm, then evacuated and purged with N<sub>2</sub> three times. Benzyl chloride **220** (108 mg, 0.75 mmol) and 1,4-dioxane (2.0 mL) were added and the mixture was stirred under visible light irradiation. After 24 h, the resulting mixture was filtered through a pad of silica gel and washed with EtOAc. Afterwards, the filtrate was concentrated *in vacuo* and purification of the residue by column chromatography (SiO<sub>2</sub>, *n*hexane/EtOAc: 10/1) yielded *ortho*-benzylated product **222** (130 mg, 94%) as a viscous colorless oil.

## Radical Scavenger Experiments



Radical Scavenger	Yield <b>22</b> (%)	Yield <b>199</b> (%)
TEMPO	52%	40%
Diphenyl ethylene	55%	34%

**Figure 5-8.** Radical scavenger experiments.

2-Phenylpyridine **22** (77.6 mg, 0.5 mmol), [RuCl<sub>2</sub>(*p*-cymene)]<sub>2</sub> (15.3 mg, 0.025 mmol, 5.0 mol %), the respective radical scavenger (0.5 mmol), and dry NaOAc (82.0 mg, 1.0

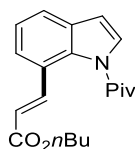
mmol) from the glovebox were placed in a 10 mL vial. The vial was capped with a septum and wrapped with parafilm, then evacuated and purged with N<sub>2</sub> three times. Allyl bromide **198** (0.75 mmol) and 1,4-dioxane (2.0 mL) were then added and the mixture was stirred under visible light irradiation. After 24 h, the resulting mixture was analyzed *via* <sup>1</sup>H NMR using 1,3,5-trimethoxybenzene as internal standard.



### 5.3.3 Electrochemical C7-Indole Alkenylation *via* Rhodium Catalysis

#### Characterization Data

#### Butyl-3-(1-pivaloyl-1*H*-indol-7-yl)acrylate (**230**)



The general procedure D was followed using 1-(1*H*-indol-1-yl)-2,2-dimethylpropan-1-one **67a** (100.6 mg, 0.50 mmol), *n*butyl acrylate **229** (192 mg, 1.50 mmol), [Cp\**Rh*Cl<sub>2</sub>]<sub>2</sub> (15.4 mg, 0.025 mmol, 5.0 mol %), and Na(OAc)<sub>2</sub> (41.0 mg, 1.0 equiv.) in TFE (2.0 mL). Purification by column chromatography on silica gel (*n*hexane/EtOAc: 99/1) yielded **230** (100 mg, 61%) as a colorless liquid.

**<sup>1</sup>H NMR** (400 MHz, CDCl<sub>3</sub>): δ 7.81 (d, *J* = 15.7 Hz, 1H), 7.59 (d, *J* = 2.7 Hz, 2H), 7.47 (d, *J* = 7.5 Hz, 1H), 7.32 – 7.25 (m, 1H), 6.64 (d, *J* = 3.7 Hz, 1H), 6.30 (d, *J* = 15.7 Hz, 1H), 4.21 (t, *J* = 6.7 Hz, 2H), 1.78 – 1.63 (m, 2H), 1.56 (s, 9H), 1.49 – 1.37 (m, 2H), 0.97 (t, *J* = 7.5 Hz, 3H).

**<sup>13</sup>C NMR** (101 MHz, CDCl<sub>3</sub>): δ 179.5 (C<sub>q</sub>), 167.2 (C<sub>q</sub>), 143.1 (CH), 135.0 (C<sub>q</sub>), 131.4 (C<sub>q</sub>), 126.7 (CH), 124.2 (CH), 123.7 (CH), 123.5 (C<sub>q</sub>), 122.5 (CH), 117.9 (CH), 107.6 (CH), 64.5 (CH<sub>2</sub>), 42.2 (C<sub>q</sub>), 31.0 (CH<sub>2</sub>), 29.1 (CH<sub>3</sub>), 19.4 (CH<sub>2</sub>), 13.9 (CH<sub>3</sub>).

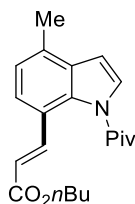
**IR** (ATR): 2959, 1710, 1638, 1414, 1286, 1166, 1077, 906, 755 cm<sup>-1</sup>.

**MS** (ESI) *m/z* (relative intensity): 350.2 [M+Na]<sup>+</sup> (100), 328.2 [M+H]<sup>+</sup> (30).

**HR-MS** (ESI): *m/z* calcd for C<sub>20</sub>H<sub>26</sub>NO<sub>3</sub><sup>+</sup> [M+H]<sup>+</sup> 328.1907, found 328.1909.

The spectral data were in accordance with those reported in the literature.<sup>[162b]</sup>

#### Butyl (*E*)-3-(4-methyl-1-pivaloyl-1*H*-indol-7-yl)acrylate (**233**)



The general procedure D was followed using 2,2-dimethyl-1-(4-methyl-1*H*-indol-1-yl)propan-1-one **67b** (107.7 mg, 0.50 mmol), *n*butyl acrylate **229** (192 mg, 1.50 mmol),

[Cp\*RhCl<sub>2</sub>]<sub>2</sub> (15.4 mg, 0.025 mmol, 5.0 mol %), and Na(OAc)<sub>2</sub> (41.0 mg, 1.0 equiv.) in TFE (2.0 mL). Purification by column chromatography on silica gel (*n*hexane/EtOAc: 98/2) yielded **233** (106 mg, 62%) as a colorless liquid.

**<sup>1</sup>H NMR** (400 MHz, CDCl<sub>3</sub>): δ 7.78 (d, *J* = 15.8 Hz, 1H), 7.58 (d, *J* = 3.8 Hz, 1H), 7.39 (d, *J* = 7.6 Hz, 1H), 7.08 (dt, *J* = 7.6, 0.8 Hz, 1H), 6.66 (d, *J* = 3.8 Hz, 1H), 6.27 (d, *J* = 15.8 Hz, 1H), 4.20 (t, *J* = 6.6 Hz, 2H), 2.54 (s, 3H), 1.77 – 1.64 (m, 2H), 1.56 (s, 9H), 1.50 – 1.39 (m, 2H), 0.96 (t, *J* = 7.4 Hz, 3H).

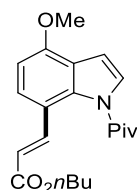
**<sup>13</sup>C NMR** (101 MHz, CDCl<sub>3</sub>): δ 179.4 (C<sub>q</sub>), 167.1 (C<sub>q</sub>), 142.7 (CH), 134.4 (C<sub>q</sub>), 132.2 (C<sub>q</sub>), 130.6 (C<sub>q</sub>), 125.8 (CH), 123.9 (CH), 123.8 (CH), 120.7 (C<sub>q</sub>), 116.7 (CH), 105.6 (CH), 64.1 (CH<sub>2</sub>), 41.9 (C<sub>q</sub>), 30.7 (CH<sub>2</sub>), 28.8 (CH<sub>3</sub>), 19.1 (CH<sub>2</sub>), 18.4 (CH<sub>3</sub>), 13.6 (CH<sub>3</sub>).

**IR** (ATR): 2958, 1705, 1633, 1369, 1285, 1174, 1156, 901, 710 cm<sup>-1</sup>.

**MS** (ESI) *m/z* (relative intensity): 364.2 [M+Na]<sup>+</sup> (100), 342.2 [M+H]<sup>+</sup> (25).

**HR-MS** (ESI): *m/z* calcd for C<sub>21</sub>H<sub>28</sub>NO<sub>3</sub><sup>+</sup> [M+H]<sup>+</sup> 342.2064, found 342.2050.

#### Butyl (*E*)-3-(4-methoxy-1*H*-indol-7-yl)acrylate (**234**)



The general procedure D was followed using 1-(4-methoxy-1*H*-indol-1-yl)-2,2-dimethylpropan-1-one **67c** (116 mg, 0.50 mmol), *n*butyl acrylate **229** (192 mg, 1.50 mmol), [Cp\*RhCl<sub>2</sub>]<sub>2</sub> (15.4 mg, 0.025 mmol, 5.0 mol %), and Na(OAc)<sub>2</sub> (41.0 mg, 1.0 equiv.) in TFE (2.0 mL). Purification by column chromatography on silica gel (*n*hexane/EtOAc: 99/1) yielded **234** (82 mg, 46%) as a yellow liquid.

**<sup>1</sup>H NMR** (400 MHz, CDCl<sub>3</sub>): δ 7.76 (d, *J* = 15.7 Hz, 1H), 7.52 – 7.41 (m, 2H), 6.74 (d, *J* = 3.7 Hz, 1H), 6.70 (d, *J* = 8.3 Hz, 1H), 6.20 (d, *J* = 15.7 Hz, 1H), 4.20 (t, *J* = 6.7 Hz, 2H), 3.95 (s, 3H), 1.83 – 1.62 (m, 2H), 1.55 (s, 9H), 1.52 – 1.36 (m, 2H), 0.96 (t, *J* = 7.4 Hz, 3H).

**<sup>13</sup>C NMR** (101 MHz, CDCl<sub>3</sub>): δ 180.2 (C<sub>q</sub>), 167.8 (C<sub>q</sub>), 154.9 (C<sub>q</sub>), 143.0 (CH), 136.6 (C<sub>q</sub>), 126.0 (CH), 125.4 (CH), 121.7 (C<sub>q</sub>), 116.9 (C<sub>q</sub>), 116.1 (CH), 104.8 (CH), 104.3

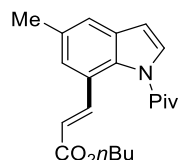
(CH), 64.6 (CH<sub>2</sub>), 56.0 (CH<sub>3</sub>), 42.6 (C<sub>q</sub>), 31.3 (CH<sub>2</sub>), 29.4 (CH<sub>3</sub>), 19.7 (CH<sub>2</sub>), 14.2 (CH<sub>3</sub>).

**IR** (ATR): 2959, 1704, 1602, 1499, 1262, 1173, 1154, 902, 715 cm<sup>-1</sup>.

**MS** (ESI) *m/z* (relative intensity): 380.2 [M+Na]<sup>+</sup> (100), 358.2 [M+H]<sup>+</sup> (30).

**HR-MS** (ESI): *m/z* calcd for C<sub>21</sub>H<sub>28</sub>NO<sub>4</sub><sup>+</sup> [M+H]<sup>+</sup> 358.2013, found 358.2016.

### Butyl (*E*)-3-(5-methyl-1-pivaloyl-1*H*-indol-7-yl)acrylate (**235**)



The general procedure D was followed using 2,2-dimethyl-1-(5-methyl-1*H*-indol-1-yl)propan-1-one **67d** (107.7 mg, 0.50 mmol), *n*butyl acrylate **229** (192 mg, 1.50 mmol), [Cp\**Rh*Cl<sub>2</sub>]<sub>2</sub> (15.4 mg, 0.025 mmol, 5.0 mol %), and Na(OAc)<sub>2</sub> (41.0 mg, 1.0 equiv.) in TFE (2.0 mL). Purification by column chromatography on silica gel (*n*hexane/EtOAc: 97/3) yielded **235** (130 mg, 76%) as a pale-yellow liquid.

**<sup>1</sup>H NMR** (400 MHz, CDCl<sub>3</sub>): δ 7.83 (d, *J* = 15.7 Hz, 1H), 7.56 (d, *J* = 3.7 Hz, 1H), 7.34 (dd, *J* = 30.8, 1.2 Hz, 2H), 6.55 (d, *J* = 3.7 Hz, 1H), 6.28 (d, *J* = 15.7 Hz, 1H), 4.21 (t, *J* = 6.6 Hz, 2H), 2.44 (s, 3H), 1.82 – 1.62 (m, 2H), 1.55 (s, 9H), 1.52 – 1.39 (m, 2H), 0.97 (t, *J* = 7.4 Hz, 3H).

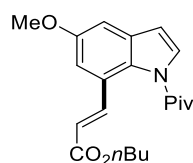
**<sup>13</sup>C NMR** (101 MHz, CDCl<sub>3</sub>): δ 178.9 (C<sub>q</sub>), 166.9 (C<sub>q</sub>), 142.9 (C<sub>q</sub>), 133.0 (C<sub>q</sub>), 132.9 (C<sub>q</sub>), 131.4 (C<sub>q</sub>), 126.5 (CH), 125.2 (CH), 122.8 (C<sub>q</sub>), 122.2 (CH), 117.3 (CH), 107.1 (CH), 64.1 (CH<sub>2</sub>), 41.7 (C<sub>q</sub>), 30.6 (CH<sub>2</sub>), 28.8 (CH<sub>3</sub>), 20.9 (CH<sub>3</sub>), 19.1 (CH<sub>2</sub>), 13.6 (CH<sub>3</sub>).

**IR** (ATR): 2958, 1704, 1634, 1462, 1294, 1160, 1078, 907, 713 cm<sup>-1</sup>.

**MS** (ESI) *m/z* (relative intensity): 364.2 [M+Na]<sup>+</sup> (100), 342.2 [M+H]<sup>+</sup> (50).

**HR-MS** (ESI): *m/z* calcd for C<sub>21</sub>H<sub>28</sub>NO<sub>3</sub><sup>+</sup> [M+H]<sup>+</sup> 342.2064, found 342.2062.

### Butyl (*E*)-3-(5-methoxy-1-pivaloyl-1*H*-indol-7-yl)acrylate (**236**)



The general procedure D was followed using 1-(5-methoxy-1*H*-indol-1-yl)-2,2-

dimethylpropan-1-one **67e** (116 mg, 0.50 mmol), *n*butyl acrylate **229** (192 mg, 1.50 mmol), [Cp\**RhCl*<sub>2</sub>]<sub>2</sub> (15.4 mg, 0.025 mmol, 5.0 mol %), and Na(OAc)<sub>2</sub> (41.0 mg, 1.0 equiv.) in TFE (2.0 mL). Purification by column chromatography on silica gel (*n*hexane/EtOAc: 99/1) yielded **236** (93 mg, 52%) as a yellow liquid.

**<sup>1</sup>H NMR** (400 MHz, CDCl<sub>3</sub>): δ 7.82 (d, *J* = 15.7 Hz, 1H), 7.57 (d, *J* = 3.6 Hz, 1H), 7.10 – 7.03 (m, 2H), 6.54 (d, *J* = 3.6 Hz, 1H), 6.27 (d, *J* = 15.7 Hz, 1H), 4.20 (t, *J* = 6.6 Hz, 2H), 3.85 (s, 3H), 1.69 (m, 2H), 1.53 (s, 9H), 1.45 (m, 2H), 0.96 (t, *J* = 7.4 Hz, 3H).

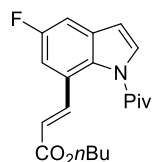
**<sup>13</sup>C NMR** (101 MHz, CDCl<sub>3</sub>): δ 178.9 (C<sub>q</sub>), 167.0 (C<sub>q</sub>), 156.4 (C<sub>q</sub>), 142.9 (CH), 132.40 (C<sub>q</sub>), 129.8 (C<sub>q</sub>), 127.3 (CH), 124.2 (C<sub>q</sub>), 118.0 (CH), 112.3 (CH), 107.6 (CH), 105.2 (CH), 64.3 (CH<sub>2</sub>), 55.8 (CH<sub>3</sub>), 41.9 (C<sub>q</sub>), 30.8 (CH<sub>2</sub>), 29.0 (CH<sub>3</sub>), 19.3 (CH<sub>2</sub>), 13.8 (CH<sub>3</sub>).

**IR** (ATR): 2959, 1705, 1604, 1415, 1270, 1172, 1077, 907, 712 cm<sup>-1</sup>.

**MS** (ESI) *m/z* (relative intensity): 380.2 [M+Na]<sup>+</sup> (100), 358.2 [M+H]<sup>+</sup> (20).

**HR-MS** (ESI): *m/z* calcd for C<sub>21</sub>H<sub>28</sub>NO<sub>4</sub><sup>+</sup> [M+H]<sup>+</sup> 358.2013, found 358.2017.

### Butyl (*E*)-3-(5-fluoro-1*H*-indol-7-yl)acrylate (**237**)



The general procedure D was followed using 1-(5-fluoro-1*H*-indol-1-yl)-2,2-dimethylpropan-1-one **67f** (110 mg, 0.50 mmol), *n*butyl acrylate **229** (192 mg, 1.50 mmol), [Cp\**RhCl*<sub>2</sub>]<sub>2</sub> (15.4 mg, 0.025 mmol, 5.0 mol %), and Na(OAc)<sub>2</sub> (41.0 mg, 1.0 equiv.) in TFE (2.0 mL). Purification by column chromatography on silica gel (*n*hexane/EtOAc: 98/2) yielded **237** (88 mg, 51%) as a colorless liquid.

**<sup>1</sup>H NMR** (400 MHz, CDCl<sub>3</sub>): δ 7.75 (dd, *J* = 15.8, 1.0 Hz, 1H), 7.64 (d, *J* = 3.7 Hz, 1H), 7.26 – 7.15 (m, 2H), 6.60 (d, *J* = 3.7 Hz, 1H), 6.28 (d, *J* = 15.8 Hz, 1H), 4.21 (t, *J* = 6.7 Hz, 2H), 1.69 (m, 2H), 1.55 (s, 9H), 1.50 – 1.41 (m, 2H), 0.96 (t, *J* = 7.4 Hz, 3H).

**<sup>13</sup>C NMR** (101 MHz, CDCl<sub>3</sub>): δ 178.9 (C<sub>q</sub>), 166.5 (C<sub>q</sub>), 160.5 (d, <sup>1</sup>*J*<sub>C-F</sub> = 240.0 Hz, C<sub>q</sub>), 158.1 (C<sub>q</sub>), 141.6 (CH), 132.2 (d, <sup>3</sup>*J*<sub>C-F</sub> = 10.1 Hz, C<sub>q</sub>), 127.9 (CH), 124.4 (d, <sup>4</sup>*J*<sub>C-F</sub> = 8.8 Hz, C<sub>q</sub>), 118.7 (CH), 111.40 (d, <sup>2</sup>*J*<sub>C-F</sub> = 26.7 Hz, CH), 111.1 (CH), 107.6 (d, <sup>2</sup>*J*<sub>C-F</sub> = 23.9 Hz, CH), 64.3 (CH<sub>2</sub>), 41.9 (C<sub>q</sub>), 30.6 (CH<sub>2</sub>), 28.8 (CH<sub>3</sub>), 19.1 (CH<sub>2</sub>), 13.6 (CH<sub>3</sub>).

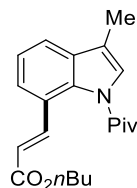
**<sup>19</sup>F NMR** (377 MHz, CDCl<sub>3</sub>) δ -120.1 (s).

**IR** (ATR): 2960, 1713, 1602, 1471, 1412, 1269, 1173, 907, 817, 713 cm<sup>-1</sup>.

**MS** (ESI) *m/z* (relative intensity): 368.2 [M+Na]<sup>+</sup> (100), 346.2 [M+H]<sup>+</sup> (10).

**HR-MS** (ESI): *m/z* calcd for C<sub>20</sub>H<sub>25</sub>NO<sub>3</sub>F<sup>+</sup> [M+Na]<sup>+</sup> 368.1632, found 368.1627.

**Butyl (*E*)-3-(3-methyl-1-pivaloyl-1*H*-indol-7-yl)acrylate (**238**)**



The general procedure D was followed using 2,2-dimethyl-1-(3-methyl-1*H*-indol-1-yl)propan-1-one **67g** (107.7 mg, 0.50 mmol), *n*butyl acrylate **229** (192 mg, 1.50 mmol), [Cp\**Rh*Cl<sub>2</sub>]<sub>2</sub> (15.4 mg, 0.025 mmol, 5.0 mol %), and Na(OAc)<sub>2</sub> (41.0 mg, 1.0 equiv.) in TFE (2.0 mL). Purification by column chromatography on silica gel (*n*hexane/EtOAc: 99/1) yielded **238** (91 mg, 53%) as a colorless liquid.

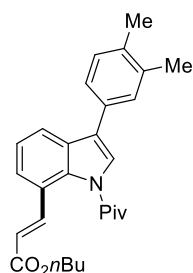
**<sup>1</sup>H NMR** (400 MHz, CDCl<sub>3</sub>): δ 7.81 (d, *J* = 15.8 Hz, 1H), 7.52 (dd, *J* = 7.7, 1.1 Hz, 1H), 7.50 – 7.44 (m, 1H), 7.37 (d, *J* = 1.4 Hz, 1H), 7.29 (t, *J* = 7.7 Hz, 1H), 6.28 (d, *J* = 15.8 Hz, 1H), 4.20 (t, *J* = 6.6 Hz, 2H), 2.29 (d, *J* = 1.2 Hz, 3H), 1.76 – 1.63 (m, 2H), 1.55 (s, 9H), 1.51 – 1.39 (m, 2H), 0.96 (t, *J* = 7.4 Hz, 3H).

**<sup>13</sup>C NMR** (101 MHz, CDCl<sub>3</sub>): δ 179.4 (C<sub>q</sub>), 167.6 (C<sub>q</sub>), 143.6 (CH), 135.8 (C<sub>q</sub>), 132.8 (C<sub>q</sub>), 124.6 (CH), 124.0 (CH), 124.0 (C<sub>q</sub>), 123.8 (CH), 120.7 (CH), 118.0 (CH), 117.0 (C<sub>q</sub>), 64.7 (CH<sub>2</sub>), 42.3 (C<sub>q</sub>), 31.3 (CH<sub>2</sub>), 29.5 (CH<sub>3</sub>), 19.7 (CH<sub>2</sub>), 14.2 (CH<sub>3</sub>), 10.2 (CH<sub>3</sub>).

**IR** (ATR): 2958, 1704, 1635, 1414, 1290, 1252, 1165, 1112, 948, 753 cm<sup>-1</sup>.

**MS** (ESI) *m/z* (relative intensity): 364.2 [M+Na]<sup>+</sup> (100), 342.2 [M+H]<sup>+</sup> (15).

**HR-MS** (ESI): *m/z* calcd for C<sub>21</sub>H<sub>28</sub>NO<sub>3</sub><sup>+</sup> [M+H]<sup>+</sup> 342.2064, found 342.2049.

**Butyl (*E*)-3-[3-(3,4-dimethylphenyl)-1-pivaloyl-1*H*-indol-7-yl]acrylate (**239**)**

The general procedure D was followed using 1-(3-(3,4-dimethylphenyl)-1*H*-indol-1-yl)-2,2-dimethylpropan-1-one **67h** (152.7 mg, 0.50 mmol), *n*butyl acrylate **229** (192 mg, 1.50 mmol), [Cp\**RhCl*<sub>2</sub>]<sub>2</sub> (15.4 mg, 0.025 mmol, 5.0 mol %), and Na(OAc)<sub>2</sub> (41.0 mg, 1.0 equiv.) in TFE (2.0 mL). Purification by column chromatography on silica gel (*n*hexane/EtOAc: 99/1) yielded **239** (120 mg, 56%) as a colourless liquid.

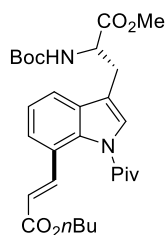
**<sup>1</sup>H NMR** (400 MHz, CDCl<sub>3</sub>): δ 7.89 – 7.77 (m, 2H), 7.61 (s, 1H), 7.52 (d, *J* = 7.5 Hz, 1H), 7.41 – 7.28 (m, 3H), 7.24 (s, 1H), 6.32 (d, *J* = 15.7 Hz, 1H), 4.22 (t, *J* = 6.7 Hz, 2H), 2.35 (d, *J* = 7.3 Hz, 6H), 1.69 (q, *J* = 7.2 Hz, 2H), 1.59 (s, 9H), 1.46 (q, *J* = 7.7 Hz, 2H), 0.97 (t, *J* = 7.4 Hz, 3H).

**<sup>13</sup>C NMR** (101 MHz, CDCl<sub>3</sub>): δ 179.4 (C<sub>q</sub>), 167.1 (C<sub>q</sub>), 142.9 (CH), 137.3 (C<sub>q</sub>), 136.1 (C<sub>q</sub>), 135.7 (C<sub>q</sub>), 130.8 (C<sub>q</sub>), 130.2 (CH), 129.3 (CH), 125.6 (CH), 124.3 (CH), 123.8 (CH), 123.7 (C<sub>q</sub>), 123.1 (CH), 122.7 (C<sub>q</sub>), 121.5 (CH), 117.8 (CH), 64.4 (CH<sub>2</sub>), 42.1 (C<sub>q</sub>), 30.8 (CH<sub>2</sub>), 29.1 (CH<sub>3</sub>), 19.9 (CH<sub>3</sub>), 19.6 (CH<sub>3</sub>), 19.3 (CH<sub>2</sub>), 13.8 (CH<sub>3</sub>).

**IR** (ATR): 2958, 1712, 1637, 1412, 1272, 1170, 1161, 941, 753 cm<sup>-1</sup>.

**MS** (ESI) *m/z* (relative intensity): 454.2 [M+Na]<sup>+</sup> (100).

**HR-MS** (ESI): *m/z* calcd for C<sub>28</sub>H<sub>34</sub>NO<sub>3</sub><sup>+</sup> [M+H]<sup>+</sup> 432.2533, found 432.2529.

**Butyl (*S,E*)-3-(3-(2-[(*tert*-butoxycarbonyl)amino]-3-methoxy-3-oxopropyl)-1-pivaloyl-1*H*-indol-7-yl)acrylate (**240**)**

The general procedure D was followed using methyl N<sup>α</sup>-(*tert*-butoxycarbonyl)-1-

pivaloyltryptophanate **67i** (201 mg, 0.50 mmol), *n*butyl acrylate **229** (192 mg, 1.50 mmol), [Cp\**RhCl*<sub>2</sub>]<sub>2</sub> (15.4 mg, 0.025 mmol, 5.0 mol %), and Na(OAc)<sub>2</sub> (41.0 mg, 1.0 equiv.) in TFE (2.0 mL). Purification by column chromatography on silica gel (*n*hexane/EtOAc: 99/1) yielded **240** (125 mg, 47%) as a pale-yellow oil.

**<sup>1</sup>H NMR** (400 MHz, CDCl<sub>3</sub>): δ 7.78 (d, *J* = 15.8 Hz, 1H), 7.52 (d, *J* = 7.8 Hz, 1H), 7.47 (d, *J* = 7.5 Hz, 1H), 7.43 (s, 1H), 7.28 (t, *J* = 8.0 Hz, 1H), 6.28 (d, *J* = 15.8 Hz, 1H), 5.11 (d, *J* = 8.0 Hz, 1H), 4.71 (d, *J* = 7.5 Hz, 1H), 4.20 (t, *J* = 6.6 Hz, 2H), 3.70 (s, 3H), 3.35 – 3.12 (m, 2H), 1.74 – 1.63 (m, 2H), 1.54 (s, 9H), 1.50 – 1.45 (m, 2H), 1.43 (s, 9H), 0.96 (t, *J* = 7.4 Hz, 3H).

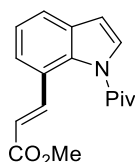
**<sup>13</sup>C NMR** (101 MHz, CDCl<sub>3</sub>): δ 179.1 (C<sub>q</sub>), 172.4 (C<sub>q</sub>), 167.2 (C<sub>q</sub>), 155.2 (C<sub>q</sub>), 143.0 (CH), 135.2 (C<sub>q</sub>), 131.6 (C<sub>q</sub>), 124.8 (CH), 124.5 (CH), 123.7 (C<sub>q</sub>), 123.6 (CH), 120.3 (CH), 117.9 (CH), 115.4 (C<sub>q</sub>), 64.5 (CH<sub>2</sub>), 53.5 (CH), 52.6 (CH<sub>3</sub>), 42.1 (C<sub>q</sub>), 30.9 (CH<sub>2</sub>), 29.1 (CH<sub>3</sub>), 28.5 (CH<sub>3</sub>), 28.0 (CH<sub>2</sub>), 19.4 (CH<sub>2</sub>), 13.9 (CH<sub>3</sub>).

**IR** (ATR): 2958, 1748, 1713, 1413, 1274, 1252, 1170, 1062, 755 cm<sup>-1</sup>.

**MS** (ESI) *m/z* (relative intensity): 551.3 [M+Na]<sup>+</sup> (100).

**HR-MS** (ESI): *m/z* calcd for C<sub>29</sub>H<sub>41</sub>N<sub>2</sub>O<sub>7</sub><sup>+</sup> [M+Na]<sup>+</sup> 551.2728, found 551.2730.

### Methyl (*E*)-3-(1-pivaloyl-1*H*-indol-7-yl)acrylate (**242**)



The general procedure D was followed using 1-(1*H*-indol-1-yl)-2,2-dimethylpropan-1-one **67a** (100.6 mg, 0.50 mmol), methyl acrylate **106a** (129 mg, 1.50 mmol), [Cp\**RhCl*<sub>2</sub>]<sub>2</sub> (15.4 mg, 0.025 mmol, 5.0 mol %), and Na(OAc)<sub>2</sub> (41.0 mg, 1.0 equiv.) in TFE (2.0 mL). Purification by column chromatography on silica gel (*n*hexane/EtOAc: 99/1) yielded **242** (80 mg, 56%) as a white solid.

**M. p.:** 121 °C.

**<sup>1</sup>H NMR** (400 MHz, CDCl<sub>3</sub>): δ 7.83 (d, *J* = 15.7 Hz, 1H), 7.68 – 7.54 (m, 2H), 7.46 (d, *J* = 7.6 Hz, 1H), 7.28 (t, *J* = 7.6 Hz, 1H), 6.64 (d, *J* = 3.8 Hz, 1H), 6.30 (d, *J* = 15.7 Hz, 1H), 3.81 (s, 3H), 1.56 (s, 9H).

**<sup>13</sup>C NMR** (101 MHz, CDCl<sub>3</sub>): δ 179.3 (C<sub>q</sub>), 167.3 (C<sub>q</sub>), 143.2 (CH), 134.7 (C<sub>q</sub>), 131.1 (C<sub>q</sub>), 126.4 (CH), 123.9 (CH), 123.4 (CH), 123.1 (C<sub>q</sub>), 122.2 (CH), 117.0 (CH), 107.3 (CH), 51.4 (CH<sub>3</sub>), 41.9 (C<sub>q</sub>), 28.8 (CH<sub>3</sub>).

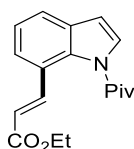
**IR** (ATR): 2977, 1710, 1697, 1639, 1414, 1286, 1163, 1076, 906, 718 cm<sup>-1</sup>.

**MS** (ESI) *m/z* (relative intensity): 308.1 [M+Na]<sup>+</sup> (100), 286.1 [M+H]<sup>+</sup> (25).

**HR-MS** (ESI): *m/z* calcd for C<sub>17</sub>H<sub>20</sub>NO<sub>3</sub><sup>+</sup> [M+H]<sup>+</sup> 286.1438, found 286.1438.

The spectral data were in accordance with those reported in the literature.<sup>[78]</sup>

### Ethyl (*E*)-3-(1-pivaloyl-1*H*-indol-7-yl)acrylate (**243**)



The general procedure D was followed using 1-(1*H*-indol-1-yl)-2,2-dimethylpropan-1-one **67a** (100.6 mg, 0.50 mmol), ethyl acrylate **106b** (150 mg, 1.50 mmol), [Cp<sup>\*</sup>RhCl<sub>2</sub>]<sub>2</sub> (15.4 mg, 0.025 mmol, 5.0 mol %), and Na(OAc)<sub>2</sub> (41.0 mg, 1.0 equiv.) in TFE (2.0 mL). Purification by column chromatography on silica gel (*n*hexane/EtOAc: 98/2) yielded **243** (76 mg, 51%) as a pale-yellow liquid.

**<sup>1</sup>H NMR** (400 MHz, CDCl<sub>3</sub>): δ 7.81 (d, *J* = 15.8 Hz, 1H), 7.64 – 7.55 (m, 2H), 7.47 (dt, *J* = 7.6, 0.8 Hz, 1H), 7.30 (t, *J* = 7.7 Hz, 1H), 6.63 (d, *J* = 3.8 Hz, 1H), 6.30 (d, *J* = 15.8 Hz, 1H), 4.26 (q, *J* = 7.2 Hz, 2H), 1.56 (s, 9H), 1.34 (t, *J* = 7.2 Hz, 3H).

**<sup>13</sup>C NMR** (101 MHz, CDCl<sub>3</sub>): δ 179.3 (C<sub>q</sub>), 166.8 (C<sub>q</sub>), 142.7 (CH), 134.7 (C<sub>q</sub>), 131.1 (C<sub>q</sub>), 126.3 (CH), 123.8 (CH), 123.4 (CH), 123.1 (C<sub>q</sub>), 122.2 (CH), 117.5 (CH), 107.3 (CH), 60.2 (CH<sub>2</sub>), 41.9 (C<sub>q</sub>), 28.8 (CH<sub>3</sub>), 14.2 (CH<sub>3</sub>).

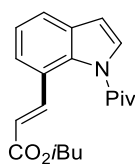
**IR** (ATR): 2970, 1703, 1634, 1414, 1286, 1162, 1036, 907, 715 cm<sup>-1</sup>.

**MS** (ESI) *m/z* (relative intensity): 322.1 [M+Na]<sup>+</sup> (100), 300.2 [M+H]<sup>+</sup> (25).

**HR-MS** (ESI): *m/z* calcd for C<sub>18</sub>H<sub>22</sub>NO<sub>3</sub><sup>+</sup> [M+H]<sup>+</sup> 300.1594, found 300.1594.

The spectral data were in accordance with those reported in the literature.<sup>[151b]</sup>



**Isobutyl (*E*)-3-(1-pivaloyl-1*H*-indol-7-yl)acrylate (244)**

The general procedure D was followed using 1-(1*H*-indol-1-yl)-2,2-dimethylpropan-1-one **67a** (100.6 mg, 0.50 mmol), isobutyl acrylate **106c** (192 mg, 1.50 mmol), [Cp\**RhCl*<sub>2</sub>]<sub>2</sub> (15.4 mg, 0.025 mmol, 5.0 mol %), and Na(OAc)<sub>2</sub> (41.0 mg, 1.0 equiv.) in TFE (2.0 mL). Purification by column chromatography on silica gel (*n*hexane/EtOAc: 99/1) yielded **244** (95 mg, 58%) as a colorless liquid.

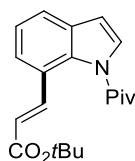
**<sup>1</sup>H NMR** (400 MHz, CDCl<sub>3</sub>): δ 7.85 (d, *J* = 15.8 Hz, 1H), 7.64 – 7.56 (m, 2H), 7.48 (d, *J* = 7.5 Hz, 1H), 7.28 (t, *J* = 7.1 Hz, 1H), 6.65 – 6.62 (m, 1H), 6.32 (dd, *J* = 15.8, 1.5 Hz, 1H), 4.00 (dt, *J* = 6.6, 1.3 Hz, 2H), 2.02 (hept, *J* = 6.6 Hz, 1H), 1.56 (s, 9H), 1.00 (dt, *J* = 6.6, 1.3 Hz, 6H).

**<sup>13</sup>C NMR** (101 MHz, CDCl<sub>3</sub>): δ 179.4 (C<sub>q</sub>), 167.2 (C<sub>q</sub>), 143.1 (CH), 134.9 (C<sub>q</sub>), 131.4 (C<sub>q</sub>), 126.7 (CH), 124.2 (CH), 123.7 (CH), 123.5 (C<sub>q</sub>), 122.5 (CH), 117.9 (CH), 107.6 (CH), 70.7 (CH<sub>2</sub>), 42.1 (C<sub>q</sub>), 29.1 (CH), 28.0 (CH<sub>3</sub>), 19.3 (CH<sub>3</sub>).

**IR** (ATR): 2961, 1704, 1469, 1378, 1287, 1168, 1023, 906, 714 cm<sup>-1</sup>.

**MS** (ESI) *m/z* (relative intensity): 350.2 [M+Na]<sup>+</sup> (100).

**HR-MS** (ESI): *m/z* calcd for C<sub>20</sub>H<sub>25</sub>NO<sub>3</sub>Na<sup>+</sup> [M+Na]<sup>+</sup> 350.1727, found 350.1729.

***Tert*-butyl (*E*)-3-(1-pivaloyl-1*H*-indol-7-yl)acrylate (245)**

The general procedure D was followed using 1-(1*H*-indol-1-yl)-2,2-dimethylpropan-1-one **67a** (100.6 mg, 0.50 mmol), *tert*-butyl acrylate **106d** (192 mg, 1.50 mmol), [Cp\**RhCl*<sub>2</sub>]<sub>2</sub> (15.4 mg, 0.025 mmol, 5.0 mol %), and Na(OAc)<sub>2</sub> (41.0 mg, 1.0 equiv.) in TFE (2.0 mL). Purification by column chromatography on silica gel (*n*hexane/EtOAc: 99/1) yielded **245** (59 mg, 56%) as a colorless liquid.

**<sup>1</sup>H NMR** (400 MHz, CDCl<sub>3</sub>): δ 7.70 (d, *J* = 15.8 Hz, 1H), 7.58 (m, 2H), 7.45 (d, *J* = 7.6

Hz, 1H), 7.31 – 7.23 (m, 1H), 6.63 (d,  $J = 3.8$  Hz, 1H), 6.20 (d,  $J = 15.8$ , 1H), 1.55 (s, 9H), 1.54 (s, 9H).

**$^{13}\text{C}$  NMR** (101 MHz,  $\text{CDCl}_3$ ):  $\delta$  179.1 ( $\text{C}_q$ ), 166.0 ( $\text{C}_q$ ), 141.6 (CH), 134.6 ( $\text{C}_q$ ), 131.0 ( $\text{C}_q$ ), 126.3 (CH), 123.9 (CH), 123.5 (CH), 123.3 ( $\text{C}_q$ ), 121.9 (CH), 119.9 (CH), 107.3 (CH), 80.0 ( $\text{C}_q$ ), 41.9 ( $\text{C}_q$ ), 28.8 ( $\text{CH}_3$ ), 28.1 ( $\text{CH}_3$ ).

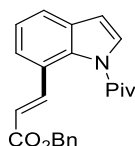
**IR** (ATR): 2975, 1703, 1477, 1413, 1368, 1173, 1152, 905, 729, 651  $\text{cm}^{-1}$ .

**MS** (ESI)  $m/z$  (relative intensity): 350.2  $[\text{M}+\text{Na}]^+$  (100).

**HR-MS** (ESI):  $m/z$  calcd for  $\text{C}_{20}\text{H}_{26}\text{NO}_3^+$   $[\text{M}+\text{H}]^+$  328.1907, found 328.1904.

The spectral data were in accordance with those reported in the literature.<sup>[151b]</sup>

### Benzyl (*E*)-3-(1-pivaloyl-1*H*-indol-7-yl)acrylate (**246**)



The general procedure D was followed using 1-(1*H*-indol-1-yl)-2,2-dimethylpropan-1-one **67a** (100.6 mg, 0.50 mmol), benzyl acrylate **106e** (243 mg, 1.50 mmol),  $[\text{Cp}^*\text{RhCl}_2]_2$  (15.4 mg, 0.025 mmol, 5.0 mol %), and  $\text{Na}(\text{OAc})_2$  (41.0 mg, 1.0 equiv.) in TFE (2.0 mL). Purification by column chromatography on silica gel (*n*hexane/EtOAc: 98/2) yielded **246** (114 mg, 63%) as a colorless liquid.

**$^1\text{H}$  NMR** (400 MHz,  $\text{CDCl}_3$ ):  $\delta$  7.88 (d,  $J = 15.7$  Hz, 1H), 7.62 – 7.60 (m, 1H), 7.59 (d,  $J = 0.9$  Hz, 1H), 7.49 – 7.46 (m, 1H), 7.46 – 7.41 (m, 2H), 7.41 – 7.33 (m, 3H), 7.31 – 7.25 (m, 1H), 6.64 (d,  $J = 3.7$  Hz, 1H), 6.36 (d,  $J = 15.7$  Hz, 1H), 5.26 (s, 2H), 1.52 (s, 9H).

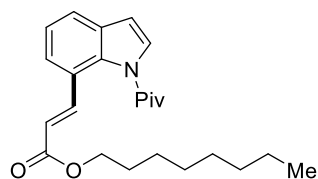
**$^{13}\text{C}$  NMR** (101 MHz,  $\text{CDCl}_3$ ):  $\delta$  179.2 ( $\text{C}_q$ ), 166.6 ( $\text{C}_q$ ), 143.4 (CH), 136.0 ( $\text{C}_q$ ), 134.7 ( $\text{C}_q$ ), 131.1 ( $\text{C}_q$ ), 128.4 (CH), 128.1 (CH), 127.9 (CH), 126.4 (CH), 123.9 (CH), 123.4 (CH), 123.1 ( $\text{C}_q$ ), 122.3 (CH), 117.0 (CH), 107.3 (CH), 66.1 ( $\text{CH}_2$ ), 41.8 ( $\text{C}_q$ ), 28.8 ( $\text{CH}_3$ ).

**IR** (ATR): 1713, 1636, 1414, 1286, 1219, 1155, 1077, 906, 697  $\text{cm}^{-1}$ .

**MS** (ESI)  $m/z$  (relative intensity): 384.2  $[\text{M}+\text{Na}]^+$  (100), 362.2  $[\text{M}+\text{H}]^+$  (25).

**HR-MS** (ESI):  $m/z$  calcd for  $\text{C}_{23}\text{H}_{23}\text{NO}_3\text{K}^+$   $[\text{M}+\text{K}]^+$  400.1310, found 400.1309.

The spectral data were in accordance with those reported in the literature.<sup>[78]</sup>

**Octyl (*E*)-3-(1-pivaloyl-1*H*-indol-7-yl)acrylate (247)**

The general procedure D was followed using 1-(1*H*-indol-1-yl)-2,2-dimethylpropan-1-one **67a** (100.6 mg, 0.50 mmol), *noctyl* acrylate **106f** (276 mg, 1.50 mmol), [Cp\**Rh*Cl<sub>2</sub>]<sub>2</sub> (15.4 mg, 0.025 mmol, 5.0 mol %), and Na(OAc)<sub>2</sub> (41.0 mg, 1.0 equiv.) in TFE (2.0 mL). Purification by column chromatography on silica gel (*n*hexane/EtOAc: 99/1) yielded **247** (111 mg, 58%) as a colorless liquid.

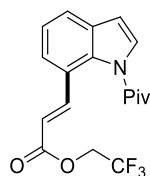
**<sup>1</sup>H NMR** (400 MHz, CDCl<sub>3</sub>): δ 7.81 (d, *J* = 15.8 Hz, 1H), 7.61 – 7.56 (m, 2H), 7.47 (d, *J* = 7.4 Hz, 1H), 7.27 (t, *J* = 7.7 Hz, 1H), 6.64 (d, *J* = 3.7 Hz, 1H), 6.30 (d, *J* = 15.8 Hz, 1H), 4.20 (t, *J* = 6.7 Hz, 2H), 1.81 – 1.64 (m, 2H), 1.56 (s, 9H), 1.44 – 1.37 (m, 2H), 1.35 – 1.23 (m, 8H), 0.95 – 0.81 (m, 3H).

**<sup>13</sup>C NMR** (101 MHz, CDCl<sub>3</sub>): δ 179.4 (C<sub>q</sub>), 167.1 (C<sub>q</sub>), 142.9 (CH), 134.9 (C<sub>q</sub>), 131.3 (C<sub>q</sub>), 126.5 (CH), 124.1 (CH), 123.6 (CH), 123.4 (C<sub>q</sub>), 122.4 (CH), 117.8 (CH), 107.5 (CH), 64.7 (CH<sub>2</sub>), 42.1 (C<sub>q</sub>), 31.8 (CH<sub>2</sub>), 29.3 (CH<sub>2</sub>), 29.2 (CH<sub>2</sub>), 29.0 (CH<sub>3</sub>), 28.8 (CH<sub>2</sub>), 26.1 (CH<sub>2</sub>), 22.7 (CH<sub>2</sub>), 14.1 (CH<sub>3</sub>).

**IR** (ATR): 2928, 2856, 1705, 1414, 1287, 1166, 1076, 907, 799 cm<sup>-1</sup>.

**MS** (ESI) *m/z* (relative intensity): 406.2 [M+Na]<sup>+</sup> (100).

**HR-MS** (ESI): *m/z* calcd for C<sub>24</sub>H<sub>34</sub>NO<sub>3</sub><sup>+</sup> [M+H]<sup>+</sup> 384.2533, found 384.2521.

**2,2,2-Trifluoroethyl (*E*)-3-(1-pivaloyl-1*H*-indol-7-yl)acrylate (248)**

The general procedure D was followed using 1-(1*H*-indol-1-yl)-2,2-dimethylpropan-1-one **67a** (100.6 mg, 0.50 mmol), acrylate **106g** (231 mg, 1.50 mmol), [Cp\**Rh*Cl<sub>2</sub>]<sub>2</sub> (15.4 mg, 0.025 mmol, 5.0 mol %), and Na(OAc)<sub>2</sub> (41.0 mg, 1.0 equiv.) in TFE (2.0 mL). Purification by column chromatography on silica gel (*n*hexane/EtOAc: 99/1) yielded

**248** (112 mg, 63%) as a pale-yellow liquid.

**<sup>1</sup>H NMR** (400 MHz, CDCl<sub>3</sub>): δ 7.94 (d, *J* = 15.8 Hz, 1H), 7.70 – 7.55 (m, 2H), 7.49 (d, *J* = 8.0 Hz, 1H), 7.30 (t, *J* = 7.7 Hz, 1H), 6.65 (d, *J* = 3.7 Hz, 1H), 6.34 (d, *J* = 15.8 Hz, 1H), 4.58 (q, *J* = 8.5 Hz, 2H), 1.56 (s, 9H).

**<sup>13</sup>C NMR** (101 MHz, CDCl<sub>3</sub>): δ 179.4 (C<sub>q</sub>), 165.1 (C<sub>q</sub>), 145.6 (CH), 134.8 (C<sub>q</sub>), 131.3 (C<sub>q</sub>), 126.7 (CH), 124.2 (CH), 123.7 (CH), 123.0 (CH), 122.8 (C<sub>q</sub>), 115.1 (CH), 107.6 (CH), 60.4 (q, <sup>2</sup>*J*<sub>C-F</sub> = 36.5 Hz, CH<sub>2</sub>), 46.2 (C<sub>q</sub>), 42.00 (C<sub>q</sub>), 28.9 (CH<sub>3</sub>).

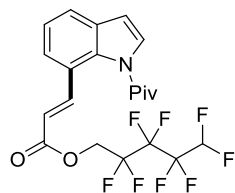
**<sup>19</sup>F NMR** (377 MHz, CDCl<sub>3</sub>): δ -73.6 (t, *J* = 8.5 Hz).

**IR** (ATR): 2972, 1703, 1479, 1414, 1287, 1219, 1168, 1078, 907, 713 cm<sup>-1</sup>.

**MS** (ESI) *m/z* (relative intensity): 376.1 [M+Na]<sup>+</sup> (100), 354.2 [M+H]<sup>+</sup> (5).

**HR-MS** (ESI): *m/z* calcd for C<sub>18</sub>H<sub>19</sub>F<sub>3</sub>NO<sub>3</sub><sup>+</sup> [M+H]<sup>+</sup> 354.1312, found 354.1305.

### 2,2,3,3,4,4,5,5-Octafluoropentyl (*E*)-3-(1-pivaloyl-1*H*-indol-7-yl)acrylate (**249**)



The general procedure D was followed using 1-(1*H*-indol-1-yl)-2,2-dimethylpropan-1-one **67a** (100.6 mg, 0.50 mmol), acrylate **106h** (429 mg, 1.50 mmol), [Cp\**Rh*Cl<sub>2</sub>]<sub>2</sub> (15.4 mg, 0.025 mmol, 5.0 mol %), and Na(OAc)<sub>2</sub> (41.0 mg, 1.0 equiv.) in TFE (2.0 mL). Purification by column chromatography on silica gel (*n*hexane/EtOAc: 99/1) yielded **249** (138 mg, 57%) as a yellow liquid.

**<sup>1</sup>H NMR** (400 MHz, CDCl<sub>3</sub>): δ 7.95 (d, *J* = 15.7 Hz, 1H), 7.66 – 7.60 (m, 2H), 7.49 (d, *J* = 7.5 Hz, 1H), 7.29 (t, *J* = 7.8 Hz, 1H), 6.65 (t, *J* = 2.7 Hz, 1H), 6.34 (d, *J* = 15.7 Hz, 1H), 4.59 (q, *J* = 8.4 Hz, 2H), 1.56 (s, 9H).

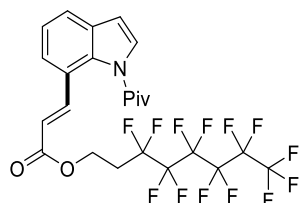
**<sup>13</sup>C NMR** (101 MHz, CDCl<sub>3</sub>): δ 179.2 (C<sub>q</sub>), 165.0 (C<sub>q</sub>), 145.4 (CH), 134.6 (C<sub>q</sub>), 131.2 (C<sub>q</sub>), 126.5 (CH), 124.0 (CH), 123.5 (CH), 122.8 (C<sub>q</sub>), 122.6 (CH), 114.9 (CH), 107.5 (CH), 60.2 (q, <sup>2</sup>*J*<sub>C-F</sub> = 36.6 Hz, CH<sub>2</sub>), 41.8 (C<sub>q</sub>), 28.7 (CH<sub>3</sub>).

**<sup>19</sup>F NMR** (377 MHz, CDCl<sub>3</sub>): δ -73.6 (t, *J* = 8.5 Hz).

**IR** (ATR): 2971, 1702, 1634, 1415, 1287, 1270, 1167, 907, 800 cm<sup>-1</sup>.

**MS** (ESI):  $m/z$  (relative intensity): 510.1  $[M+Na]^+$  (100).

**3,3,4,4,5,5,6,6,7,7,8,8,8-Tridecafluorooctyl (*E*)-3-(1-pivaloyl-1*H*-indol-7-yl)acrylate (250)**



The general procedure D was followed using 1-(1*H*-indol-1-yl)-2,2-dimethylpropan-1-one **67a** (100.6 mg, 0.50 mmol), acrylate **106i** (627 mg, 1.50 mmol),  $[Cp^*RhCl_2]_2$  (15.4 mg, 0.025 mmol, 5.0 mol %), and  $Na(OAc)_2$  (41.0 mg, 1.0 equiv.) in TFE (2.0 mL). Purification by column chromatography on silica gel (*n*hexane/EtOAc: 99/1) yielded **250** (176 mg, 57%) as a yellow liquid.

**$^1H$  NMR** (400 MHz,  $CDCl_3$ ):  $\delta$  7.86 (d,  $J = 15.8$  Hz, 1H), 7.66 – 7.59 (m, 2H), 7.55 – 7.44 (m, 1H), 7.39 – 7.22 (m, 1H), 6.64 (d,  $J = 3.7$  Hz, 1H), 6.29 (d,  $J = 15.8$  Hz, 1H), 4.51 (t,  $J = 6.6$  Hz, 2H), 2.70 – 2.44 (m, 2H), 1.55 (s, 9H).

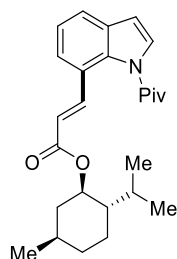
**$^{13}C$  NMR** (101 MHz,  $CDCl_3$ ):  $\delta$  179.3 ( $C_q$ ), 166.4 ( $C_q$ ), 144.3 (CH), 134.8 ( $C_q$ ), 131.3 ( $C_q$ ), 126.6 (CH), 124.2 (CH), 123.6 (CH), 123.1 ( $C_q$ ), 122.6 (CH), 116.4 (CH), 107.6 (CH), 56.3 (t,  $^3J_{C-F} = 4.7$  Hz,  $CH_2$ ), 42.0 ( $C_q$ ), 30.6 (t,  $^2J_{C-F} = 21.6$  Hz,  $CH_2$ ), 28.9 ( $CH_3$ ).

**$^{19}F$  NMR** (377 MHz,  $CDCl_3$ ):  $\delta$  -73.60 (t,  $J = 8.5$  Hz).

**IR** (ATR): 1716, 1415, 1288, 1237, 1202, 1144, 1079, 907, 711  $cm^{-1}$ .

**MS** (ESI):  $m/z$  (relative intensity): 640.1  $[M+Na]^+$  (100), 618.1  $[M+H]^+$  (10).

**HR-MS** (ESI):  $m/z$  calcd for  $C_{24}H_{21}NO_3F_{13}^+$   $[M+H]^+$  618.1308, found 618.1305.

**(1*R*,2*S*,5*R*)-2-isopropyl-5-methylcyclohexyl (*E*)-3-(1-pivaloyl-1*H*-indol-7-yl)acrylate (**251**)**

The general procedure D was followed using 1-(1*H*-indol-1-yl)-2,2-dimethylpropan-1-one **67a** (100.6 mg, 0.50 mmol), acrylate **106j** (315 mg, 1.50 mmol), [Cp\**Rh*Cl<sub>2</sub>]<sub>2</sub> (15.4 mg, 0.025 mmol, 5.0 mol %), and Na(OAc)<sub>2</sub> (41.0 mg, 1.0 equiv.) in TFE (2.0 mL). Purification by column chromatography on silica gel (*n*hexane/EtOAc: 99/1) yielded **251** (109 mg, 53%) as a colorless liquid.

**<sup>1</sup>H NMR** (400 MHz, CDCl<sub>3</sub>): δ 7.79 (d, *J* = 15.8 Hz, 1H), 7.65 – 7.55 (m, 2H), 7.48 (d, *J* = 7.4 Hz, 1H), 7.30 – 7.25 (m, 1H), 6.63 (d, *J* = 3.8 Hz, 1H), 6.28 (d, *J* = 15.8 Hz, 1H), 4.82 (td, *J* = 10.9, 4.4 Hz, 1H), 2.11 (dtd, *J* = 12.2, 4.0, 1.7 Hz, 1H), 1.99 (dq, *J* = 9.8, 7.0, 3.6 Hz, 1H), 1.70 (ddq, *J* = 10.9, 7.7, 4.6, 4.0 Hz, 2H), 1.56 (s, 9H), 1.45 (m, 2H), 1.20 – 0.98 (m, 2H), 0.92 (dd, *J* = 6.9, 3.6 Hz, 6H), 0.89 – 0.87 (m, 1H), 0.80 (d, *J* = 6.9 Hz, 3H).

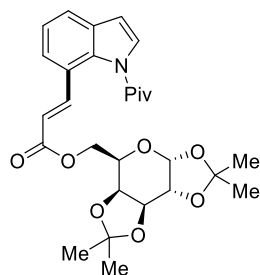
**<sup>13</sup>C NMR** (101 MHz, CDCl<sub>3</sub>): δ 179.5 (C<sub>q</sub>), 166.7 (C<sub>q</sub>), 142.6 (CH), 135.0 (C<sub>q</sub>), 131.4 (C<sub>q</sub>), 126.6 (CH), 124.1 (CH), 123.6 (CH), 123.5 (C<sub>q</sub>), 122.4 (CH), 118.5 (CH), 107.6 (CH), 74.2 (CH), 47.4 (CH), 42.2 (C<sub>q</sub>), 41.2 (CH<sub>2</sub>), 34.5 (CH<sub>2</sub>), 31.6 (CH), 29.1 (CH<sub>3</sub>), 26.3 (CH), 23.6 (CH<sub>2</sub>), 22.2 (CH<sub>3</sub>), 21.0 (CH<sub>3</sub>), 16.5 (CH<sub>3</sub>).

**IR** (ATR): 2957, 1701, 1414, 1287, 1270, 1169, 904, 727, 648 cm<sup>-1</sup>.

**MS** (ESI) *m/z* (relative intensity): 432.3 [M+Na]<sup>+</sup> (100).

**HR-MS** (ESI): *m/z* calcd for C<sub>26</sub>H<sub>35</sub>NO<sub>3</sub>Na<sup>+</sup> [M+Na]<sup>+</sup> 432.2509, found 432.2512.

**((3*aR*,5*R*,5*aS*,8*aS*,8*bR*)-2,2,7,7-Tetramethyltetrahydro-5*H*-bis([1,3]dioxolo)[4,5-*b*:4',5'-*d*]pyran-5-yl)methyl (*E*)-3-(1-pivaloyl-1*H*-indol-7-yl)acrylate (**252**)**



The general procedure D was followed using 1-(1*H*-indol-1-yl)-2,2-dimethylpropan-1-one **67a** (100.6 mg, 0.50 mmol), acrylate **106k** (472 mg, 1.50 mmol), [Cp\**Rh*Cl<sub>2</sub>]<sub>2</sub> (15.4 mg, 0.025 mmol, 5.0 mol %), and Na(OAc)<sub>2</sub> (41.0 mg, 1.0 equiv.) in TFE (2.0 mL). Purification by column chromatography on silica gel (*n*hexane/EtOAc: 99/1) yielded **252** (133 mg, 52%) as a pale-yellow liquid.

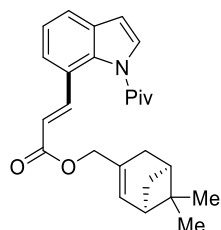
**<sup>1</sup>H NMR** (400 MHz, CDCl<sub>3</sub>): δ 7.84 (d, *J* = 15.8 Hz, 1H), 7.69 – 7.54 (m, 2H), 7.46 (d, *J* = 7.5 Hz, 1H), 7.36 – 7.19 (m, 1H), 6.63 (d, *J* = 3.7 Hz, 1H), 6.35 (d, *J* = 15.8 Hz, 1H), 5.55 (d, *J* = 5.0 Hz, 1H), 4.64 (dd, *J* = 7.9, 2.5 Hz, 1H), 4.42 (dd, *J* = 11.4, 5.4 Hz, 1H), 4.35 – 4.28 (m, 3H), 4.12 (ddd, *J* = 7.3, 5.3, 1.9 Hz, 1H), 1.54 (d, *J* = 6.5 Hz, 9H), 1.47 (s, 6H), 1.34 (d, *J* = 10.0 Hz, 6H).

**<sup>13</sup>C NMR** (101 MHz, CDCl<sub>3</sub>): δ 179.3 (C<sub>q</sub>), 166.8 (C<sub>q</sub>), 143.7 (CH), 134.9 (C<sub>q</sub>), 131.3 (C<sub>q</sub>), 126.6 (CH), 124.2 (CH), 123.6 (CH), 123.3 (C<sub>q</sub>), 122.5 (CH), 117.1 (CH), 109.6 (C<sub>q</sub>), 108.8 (C<sub>q</sub>), 107.5 (CH), 96.4 (CH), 71.1 (CH), 70.7 (CH), 70.6 (CH), 66.0 (CH), 63.3 (CH<sub>2</sub>), 42.0 (C<sub>q</sub>), 29.0 (CH<sub>3</sub>), 26.1 (CH<sub>3</sub>), 26.0 (CH<sub>3</sub>), 25.0 (CH<sub>3</sub>), 24.6 (CH<sub>3</sub>).

**IR** (ATR): 2991, 1704, 1372, 1212, 1164, 1068, 906, 728, 648 cm<sup>-1</sup>.

**MS** (ESI): *m/z* (relative intensity): 536.1 [M+Na]<sup>+</sup> (100), 514.1 [M+H]<sup>+</sup> (90).

**(6,6-Dimethylbicyclo[3.1.1]hept-2-en-3-yl)methyl(*E*)-3-(1-pivaloyl-1*H*-indol-7-yl)acrylate (**253**)**



The general procedure D was followed using 1-(1*H*-indol-1-yl)-2,2-dimethylpropan-1-one **67a** (100.6 mg, 0.50 mmol), acrylate **106l** (309 mg, 1.50 mmol), [Cp\*RhCl<sub>2</sub>]<sub>2</sub> (15.4 mg, 0.025 mmol, 5.0 mol %), and Na(OAc)<sub>2</sub> (41.0 mg, 1.0 equiv.) in TFE (2.0 mL). Purification by column chromatography on silica gel (*n*hexane/EtOAc: 99/1) yielded **253** (114 mg, 56%) as a colorless liquid.

**<sup>1</sup>H NMR** (400 MHz, CDCl<sub>3</sub>): δ 7.84 (d, *J* = 15.7 Hz, 1H), 7.65 – 7.57 (m, 2H), 7.50 – 7.44 (m, 1H), 7.32 – 7.23 (m, 1H), 6.64 (d, *J* = 3.8 Hz, 1H), 6.29 (d, *J* = 15.7 Hz, 1H), 5.63 (dp, *J* = 3.0, 1.5 Hz, 1H), 4.71 – 4.50 (m, 2H), 2.43 (dt, *J* = 8.7, 5.6 Hz, 1H), 2.39 – 2.23 (m, 2H), 2.20 (td, *J* = 5.6, 1.5 Hz, 1H), 2.12 (m, 1H), 1.56 (s, 9H), 1.31 (s, 3H), 1.23 (d, *J* = 8.7 Hz, 1H), 0.87 (s, 3H).

**<sup>13</sup>C NMR** (101 MHz, CDCl<sub>3</sub>): δ 179.0 (C<sub>q</sub>), 166.7 (C<sub>q</sub>), 143.0 (CH), 143.0 (C<sub>q</sub>), 134.6 (C<sub>q</sub>), 131.1 (C<sub>q</sub>), 126.4 (CH), 124.0 (CH), 123.4 (CH), 123.3 (C<sub>q</sub>), 122.2 (CH), 121.0 (CH), 117.5 (CH), 107.3 (CH), 66.8 (C<sub>q</sub>), 43.4 (CH), 41.8 (CH<sub>2</sub>), 40.6 (CH), 37.9 (C<sub>q</sub>), 31.3 (CH<sub>2</sub>), 31.1 (CH<sub>2</sub>), 28.8 (CH<sub>3</sub>), 26.0 (CH<sub>3</sub>), 20.9 (CH<sub>3</sub>).

**IR** (ATR): 2914, 1705, 1636, 1414, 1287, 1167, 1077, 907, 799 cm<sup>-1</sup>.

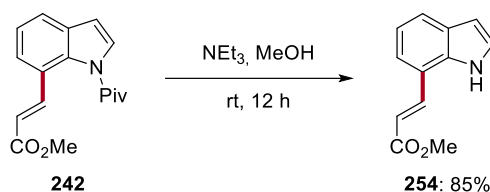
**MS** (ESI): *m/z* (relative intensity): 428.2 [M+Na]<sup>+</sup> (100).

**HR-MS** (ESI): *m/z* calcd for C<sub>26</sub>H<sub>31</sub>NO<sub>3</sub>Na<sup>+</sup> [M+Na]<sup>+</sup> 428.2196, found 428.2192.



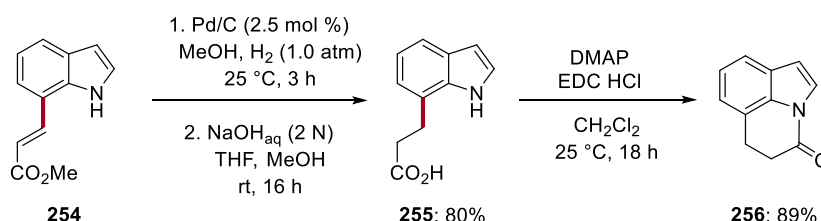
Diversification of Product **242**

## Procedure for the Traceless Removal of Pivaloyl Group



**Figure 5-9.** Traceless removal of pivaloyl directing group.

A suspension of methyl (*E*)-3-(1-pivaloyl-1*H*-indol-7-yl)acrylate **242** (1.4 mmol) in NEt<sub>3</sub> (2.8 mL, 14.5 equiv.) and MeOH (2.8 mL) was stirred at room temperature for 12 h.<sup>[164]</sup> The mixture was concentrated *in vacuo*. Purification by column chromatography on silica gel afforded the desired product **254** as a white solid in 85% yield (240 mg).

Synthesis of 5,6-dihydro-4*H*-pyrrolo[3,2,1-*ij*]quinolin-4-one

**Figure 5-10.** Synthesis of **256**.

A flame-dried round bottom flask equipped with a stir bar was charged with methyl (*E*)-3-(1*H*-indol-7-yl)acrylate **254** (200 mg, 1.0 mmol, 1.00 equiv.) and Pd/C (5% Pd loading, 50% wetted, 0.025 mmol, 0.025 equiv.) and evacuated/backfilled with N<sub>2</sub> three times. Methanol (20.0 mL, reagent grade) was then added, and the reaction was stirred under balloon-pressure of H<sub>2</sub> for 3 h at room temperature. The mixture was filtered over a pad of celite and concentrated. The product was used in the next step without further purification.

A round bottom flask equipped with a stir bar was charged with methyl 3-(1*H*-indol-7-yl)propanoate (150 mg, 0.740 mmol, 1.00 equiv.), methanol (3.7 mL, reagent grade), and NaOH (2.00 N aq., 3.7 mL, 7.4 mmol, 10.0 equiv.). The reaction was stirred at

room temperature under air until completion. Afterwards, the reaction was cooled to room temperature and then 1 M HCl (48 mL) was added, and the mixture was concentrated *in vacuo*. The crude material was re-dissolved in THF (30 mL), and gravity filtered. After concentrating *in vacuo* the desired 3-(1*H*-indol-7-yl)propanoic acid **255** was obtained as a white solid in 94% yield (132 mg).

A flame-dried round bottom flask equipped with a stir bar was charged with 3-(1*H*-indol-7-yl)propanoic acid (132 mg, 0.70 mmol, 1.00 equiv.). After being evacuated/backfilled with N<sub>2</sub> three times, DCM (7.5 mL) was added, followed by DMAP (147.5 mg, 1.2 mmol, 1.70 equiv.) in one portion by quick removal of the septum. The reaction was stirred for 10 minutes at room temperature, then EDC HCl (145 mg, 0.75 mmol) was added in one portion and the reaction was stirred at room temperature under N<sub>2</sub> for 18 h. The reaction was extracted with H<sub>2</sub>O (1 X 10 mL), 1 M HCl (1 X 10 mL), sat. aq. NaHCO<sub>3</sub> (1 X 10 mL), and brine (1 X 10 mL). The organic layer was dried over MgSO<sub>4</sub> and concentrated *in vacuo*. Purification by silica gel column chromatography (10% ethyl acetate in *n*hexane) yielded 5,6-dihydro-4*H*-pyrrolo[3,2,1-*ij*]quinolin-4-one **256** as a white solid in 89% yield (107 mg).

**M. p.:** 62–64 °C.

**<sup>1</sup>H NMR** (400 MHz, CDCl<sub>3</sub>): δ 7.69 (d, *J* = 3.6 Hz, 1H), 7.46 (dd, *J* = 7.8, 0.9 Hz, 1H), 7.21 (t, *J* = 7.5 Hz, 1H), 7.13 (dd, *J* = 7.2, 1.0 Hz, 1H), 6.70 (d, *J* = 3.6 Hz, 1H), 3.27 (t, *J* = 7.7 Hz, 2H), 3.00 (t, *J* = 7.4 Hz, 2H).

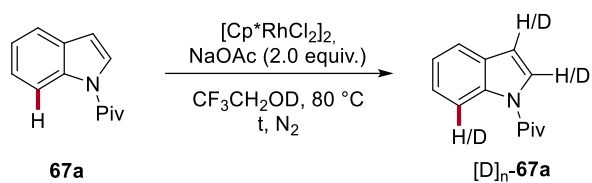
**<sup>13</sup>C NMR** (101 MHz, CDCl<sub>3</sub>): δ 166.6 (C<sub>q</sub>), 135.3 (C<sub>q</sub>), 128.2 (C<sub>q</sub>), 123.7 (CH), 121.7 (CH), 121.4 (CH), 120.3 (C<sub>q</sub>), 119.0 (CH), 110.0 (CH), 32.6 (CH<sub>2</sub>), 24.3 (CH<sub>2</sub>).

**IR** (ATR): 3133, 2915, 2847, 1690, 1478, 1435, 1295, 958, 725 cm<sup>-1</sup>.

**HR-MS** (ESI): *m/z* calcd for C<sub>11</sub>H<sub>11</sub>NO<sup>+</sup> [M+H]<sup>+</sup> 172.0757, found 172.0757.

The spectral data were in accordance with those reported in the literature.<sup>[157, 165]</sup>

## Deuterium Exchange Experiment



Time (h)	C2-H	C3-H	C7-H
0	1.00	0.99	1.00
2	0.95	0.96	0.64
4	0.84	0.93	0.29
15	0.52	0.82	0.06

**Figure 5-11.** H/D exchange experiment.

A J. Youngs tap NMR tube was loaded with  $[\text{Cp}^*\text{RhCl}_2]_2$  (10.0 mg, 0.0162 mmol), indole **67a** (6.5 mg, 0.032 mmol), NaOAc (5.3 mg, 0.065 mmol), and TFE-D (0.5 mL). The mixture was sonicated for 30 min at room temperature, forming a refined suspension, and then the  $^1\text{H}$  NMR spectrum was recorded ( $t = 0$  s). Subsequently, the mixture was kept at 80 °C with occasional agitation, with the  $^1\text{H}$  NMR spectrum recorded at 2, 4, and 15 hours of reaction.

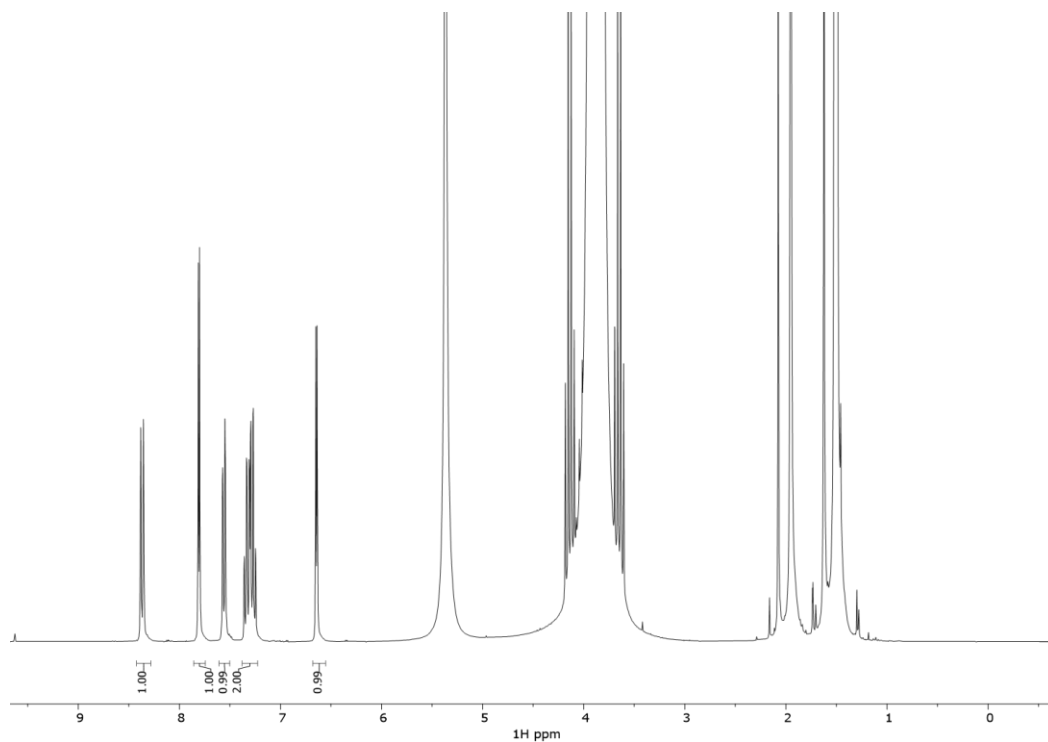


Figure 5-12. <sup>1</sup>H NMR spectra recorded at t = 0 s.

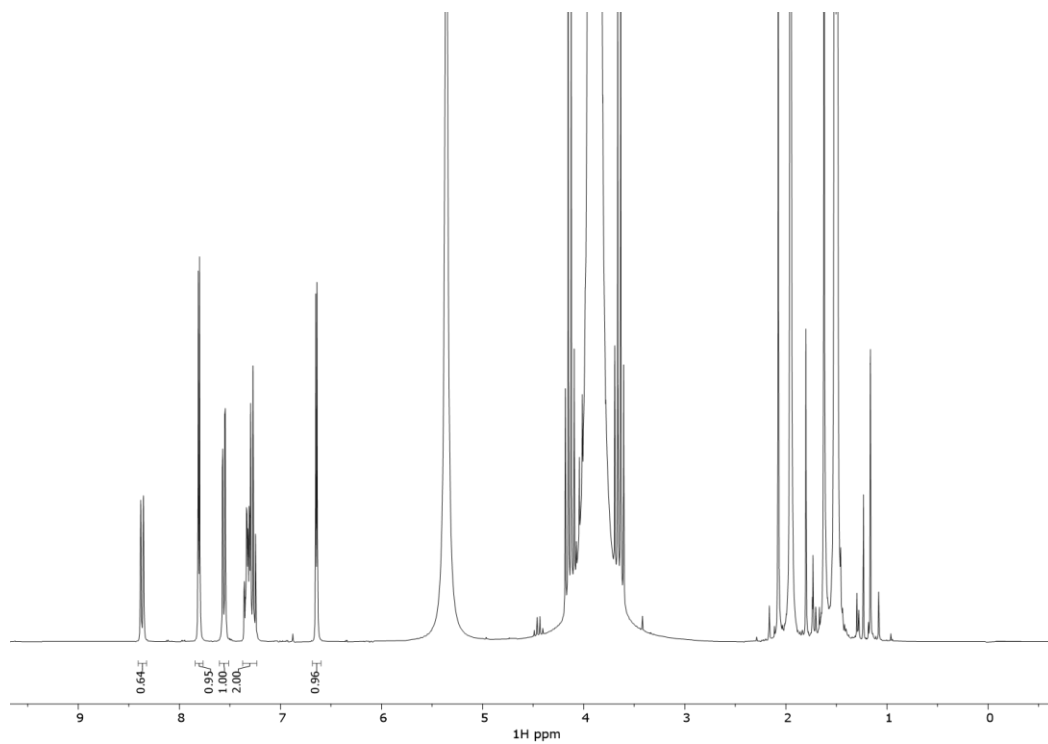


Figure 5-13. <sup>1</sup>H NMR spectra recorded after t = 2 h.

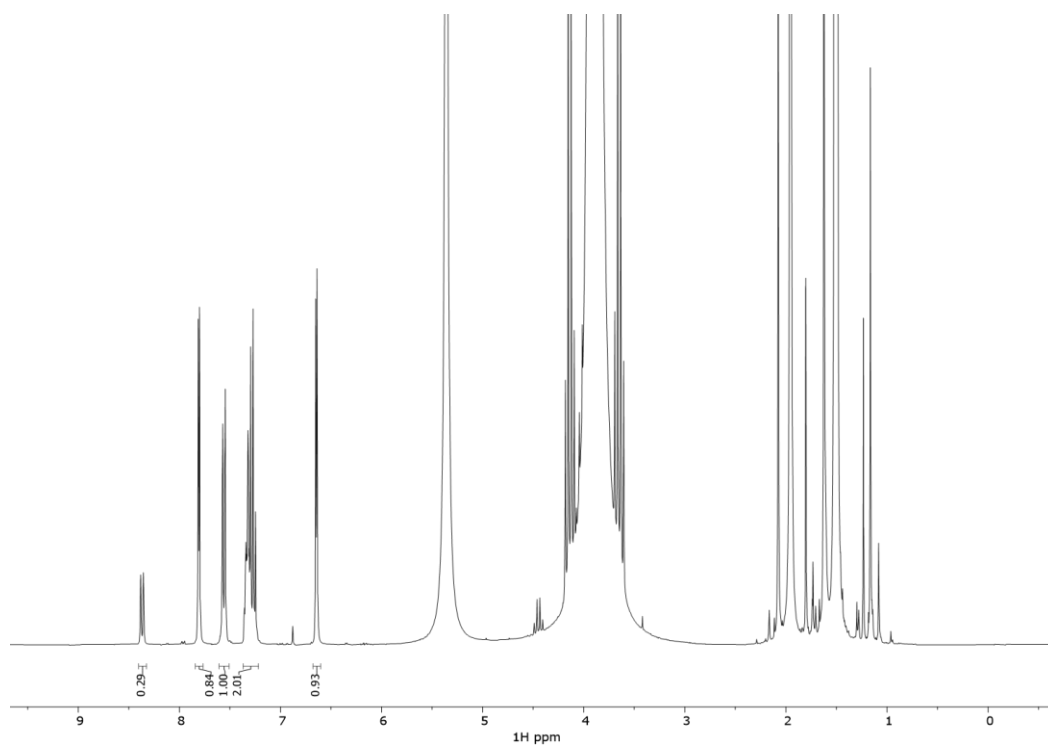


Figure 5-14. <sup>1</sup>H NMR spectra recorded after t = 4 h.

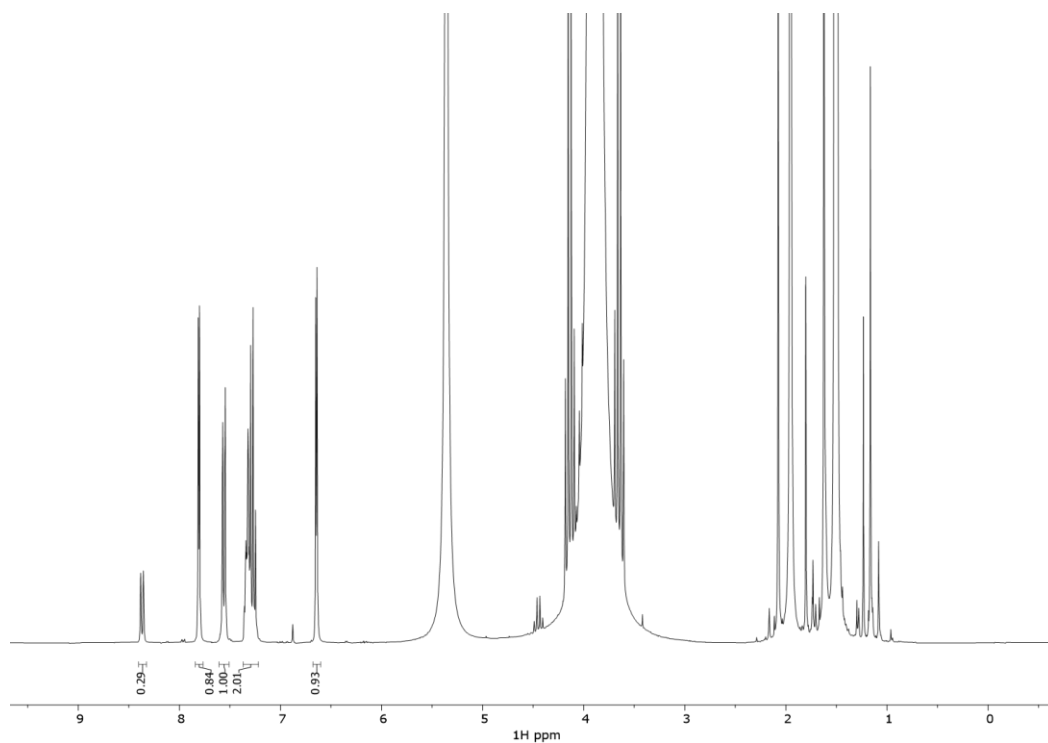
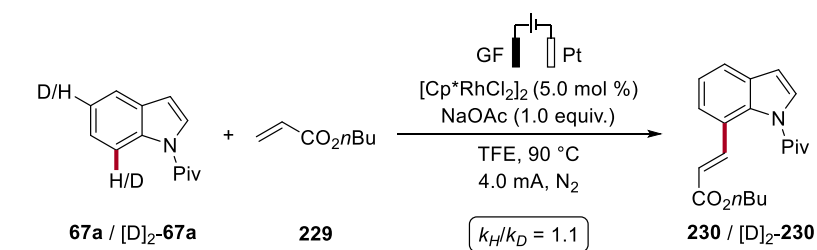


Figure 5-13. <sup>1</sup>H NMR spectra recorded after t = 15 h.

## KIE Studies

Two independent reactions using substrate **67a** and  $[D]_2$ -**67a** were performed to determine the KIE by comparison of the initial rates. The reaction was analyzed *via*  $^1H$  NMR spectroscopy using 1,3,5-trimethoxybenzene as the internal standard.



time (min) \ yield (%)	60	70	80	90	100
<b>230</b>	9.7	11.7	12.9	13.8	15.2
$[D]_2$ - <b>230</b>	5.4	6.3	7.6	9.1	10.0

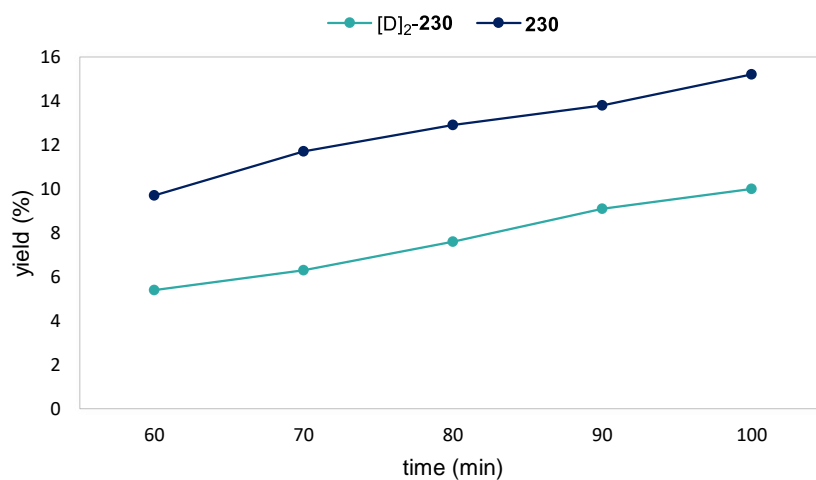
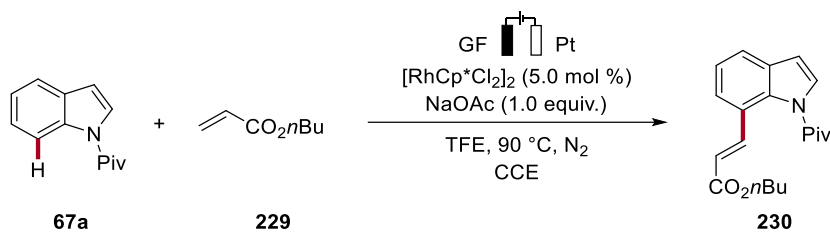


Figure 5-14. KIE studies.

## Current Dependence of the Reaction Rate



**Figure 5-15.** Current dependence analysis.

The general procedure was followed for five independent reactions using substrate **67a** (0.50 mmol), *n*-butyl acrylate **229** (3.0 equiv.) under three different currents (2.0 mA, 4.0 mA, 6.0 mA) for specified reaction time (60 min, 120 min, 240 min, and 360 min). The crude mixture was dried *in vacuo* and analyzed *via* <sup>1</sup>H NMR using 1,3,5-trimethoxybenzene as the internal standard.

## 6 References

- [1] N. Gaiand, A. Abbott, A. Witze, E. Gibney, J. Tollefson, A. Irwin, R. Van Noorden, *Nature* **2022**, *607*, 440-443.
- [2] B. M. Trost, *Angew. Chem. Int. Ed.* **1995**, *34*, 259-281.
- [3] B. M. Trost, *Science* **1983**, *219*, 245-250.
- [4] a) P. T. Anastas, J. C. Warner, *Green chemistry : theory and practice*, Oxford University Press, Oxford [England], **1998**; b) P. T. Anastas, J. J. Breen, *J. Clean. Prod.* **1997**, *5*, 97-102.
- [5] Y. Chen, C. Rosenkranz, S. Hirte, J. Kirchmair, *Nat. Prod. Rep.* **2022**, *39*, 1544-1556.
- [6] K. C. Nicolaou, P. G. Bulger, D. Sarlah, *Angew. Chem. Int. Ed.* **2005**, *44*, 4442-4489.
- [7] a) A. Casitas, X. Ribas, in *Copper - Mediated Cross - Coupling Reactions*, **2013**, pp. 253-279; b) F. Monnier, M. Taillefer, *Angew. Chem. Int. Ed.* **2009**, *48*, 6954-6971; c) G. Evano, N. Blanchard, M. Toumi, *Chem. Rev.* **2008**, *108*, 3054-3131; d) W. R. H. Hurtley, *J. Chem. Soc.* **1929**, 1870-1873; e) I. Goldberg, *Ber. Dtsch. Chem. Ges.* **1906**, *39*, 1691-1692; f) F. Ullmann, P. Sponagel, *Ber. Dtsch. Chem. Ges.* **1905**, *38*, 2211-2212; g) F. Ullmann, J. Bielecki, *Ber. Dtsch. Chem. Ges.* **1901**, *34*, 2174-2185.
- [8] a) R. F. Heck, *Synlett* **2006**, *2006*, 2855-2860; b) R. F. Heck, *Acc. Chem. Res.* **1979**, *12*, 146-151; c) R. F. Heck, J. P. Nolley, *J. Org. Chem.* **1972**, *37*, 2320-2322; d) T. Mizoroki, K. Mori, A. Ozaki, *Bull. Chem. Soc. Jap.* **1971**, *44*, 581-581.
- [9] a) K. Tamao, K. Sumitani, M. Kumada, *J. Am. Chem. Soc.* **1972**, *94*, 4374-4376; b) R. J. P. Corriu, J. P. Masse, *J. Chem. Soc., Chem. Commun.* **1972**, 144a-144a.
- [10] a) K. Sonogashira, *J. Organomet. Chem.* **2002**, *653*, 46-49; b) K. Sonogashira, Y. Tohda, N. Hagihara, *Tetrahedron Lett.* **1975**, *16*, 4467-4470.
- [11] a) E. Negishi, *Acc. Chem. Res.* **1982**, *15*, 340-348; b) E. Negishi, A. O. King,



- N. Okukado, *J. Org. Chem.* **1977**, *42*, 1821-1823; c) S. Baba, E. Negishi, *J. Am. Chem. Soc.* **1976**, *98*, 6729-6731.
- [12] a) J. K. Stille, *Angew. Chem. Int. Ed.* **1986**, *25*, 508-524; b) D. Milstein, J. K. Stille, *J. Am. Chem. Soc.* **1978**, *100*, 3636-3638; c) M. Kosugi, Y. Shimizu, T. Migita, *Chem. Lett.* **1977**, *6*, 1423-1424.
- [13] a) N. Miyaura, A. Suzuki, *Chem. Rev.* **1995**, *95*, 2457-2483; b) N. Miyaura, K. Yamada, A. Suzuki, *Tetrahedron Lett.* **1979**, *20*, 3437-3440.
- [14] a) M. Fujita, T. Hiyama, *J. Org. Chem.* **1988**, *53*, 5415-5421; b) T. Hiyama, M. Obayashi, I. Mori, H. Nozaki, *J. Org. Chem.* **1983**, *48*, 912-914.
- [15] a) J. F. Hartwig, *Nature* **2008**, *455*, 314-322; b) A. R. Muci, S. L. Buchwald, in *Cross-Coupling Reactions: A Practical Guide* (Ed.: N. Miyaura), Springer Berlin Heidelberg, Berlin, Heidelberg, **2002**, pp. 131-209; c) J. F. Hartwig, *Angew. Chem. Int. Ed.* **1998**, *37*, 2046-2067.
- [16] a) J. X. Qiao, P. Y. S. Lam, *Synthesis* **2011**, *2011*, 829-856; b) J. X. Qiao, P. Y. S. Lam, in *Boronic Acids*, **2011**, pp. 315-361; c) P. Y. S. Lam, G. Vincent, D. Bonne, C. G. Clark, *Tetrahedron Lett.* **2003**, *44*, 4927-4931; d) D. M. T. Chan, K. L. Monaco, R. Li, D. Bonne, C. G. Clark, P. Y. S. Lam, *Tetrahedron Lett.* **2003**, *44*, 3863-3865; e) P. Y. S. Lam, C. G. Clark, S. Saubern, J. Adams, M. P. Winters, D. M. T. Chan, A. Combs, *Tetrahedron Lett.* **1998**, *39*, 2941-2944.
- [17] The Nobel Prize in Chemistry 2010, <https://www.nobelprize.org/prizes/chemistry/2010/summary/>, **Accessed on June 11th, 2021**.
- [18] L. Ackermann, in *Modern Arylation Methods* (Ed.: L. Ackermann), Wiley-VCH, Weinheim, **2009**.
- [19] a) P. A. Wender, B. L. Miller, *Nature* **2009**, *460*, 197-201; b) P. A. Wender, M. P. Croatt, B. Witulski, *Tetrahedron* **2006**, *62*, 7505-7511; c) B. M. Trost, *Science* **1991**, *254*, 1471-1477.
- [20] a) F. Colobert, J. Wencel-Delord, *C-H Activation for Asymmetric Synthesis*, Wiley-VCH, Weinheim, **2019**; b) L. Ackermann, T. B. Gunnoe, L. G. Habgood, *Catalytic hydroarylation of carbon-carbon multiple bonds*, Wiley-VCH,

- Weinheim, **2018**; c) P. H. Dixneuf, H. Doucel, *C–H Bond Activation and Catalytic Functionalization I*, Springer International Publishing, Switzerland, **2016**; d) P. H. Dixneuf, H. Doucel, *C–H Bond Activation and Catalytic Functionalization II*, Springer International Publishing, Switzerland, **2016**; e) J. J. Li, *C-H bond activation in organic synthesis*, CRC Press, Boca Raton, **2015**;
- f) X. Ribas, Royal Society of Chemistry, Thomas Graham House, Cambridge, **2013**; g) J.-Q. Yu, Z. Shi, *C–H Activation*, Springer-Verlag Berlin, Heidelberg, **2010**.
- [21] a) R. C. Samanta, T. H. Meyer, I. Siewert, L. Ackermann, *Chem. Sci.* **2020**, *11*, 8657-8670; b) P. Gandeepan, L. H. Finger, T. H. Meyer, L. Ackermann, *Chem. Soc. Rev.* **2020**, *49*, 4254-4272; c) L. Ackermann, S.-L. You, M. Oestreich, S. Meng, D. MacFarlane, Y. Yin, *Trends Chem.* **2020**, *2*, 275-277; d) T. H. Meyer, L. H. Finger, P. Gandeepan, L. Ackermann, *Trends Chem.* **2019**, *1*, 63-76.
- [22] a) J. Wencel-Delord, T. Dröge, F. Liu, F. Glorius, *Chem. Soc. Rev.* **2011**, *40*, 4740-4761; b) H. Lu, X. P. Zhang, *Chem. Soc. Rev.* **2011**, *40*, 1899-1909; c) L. Ackermann, *Chem. Rev.* **2011**, *111*, 1315-1345; d) D. Balcells, E. Clot, O. Eisenstein, *Chem. Rev.* **2010**, *110*, 749-823; e) H. M. L. Davies, J. R. Manning, *Nature* **2008**, *451*, 417-424; f) L. Ackermann, in *Directed Metallation* (Ed.: N. Chatani), Springer Berlin Heidelberg, Berlin, Heidelberg, **2007**, pp. 35-60.
- [23] a) S. A. Girard, T. Knauber, C.-J. Li, *Angew. Chem. Int. Ed.* **2014**, *53*, 74-100; b) C. S. Yeung, V. M. Dong, *Chem. Rev.* **2011**, *111*, 1215-1292; c) C. J. Scheuermann, *Chem. Asian J.* **2010**, *5*, 436-451; d) C.-J. Li, Z. Li, *Pure Appl. Chem.* **2006**, *78*, 935-945.
- [24] a) S. Rej, Y. Ano, N. Chatani, *Chem. Rev.* **2020**, *120*, 1788-1887; b) H. Yi, G. Zhang, H. Wang, Z. Huang, J. Wang, A. K. Singh, A. Lei, *Chem. Rev.* **2017**, *117*, 9016-9085.
- [25] J. R. Webb, S. A. Burgess, T. R. Cundari, T. B. Gunnoe, *Dalton Trans.* **2013**, *42*, 16646-16665.
- [26] J. Kua, X. Xu, R. A. Periana, W. A. Goddard, *Organometallics* **2002**, *21*, 511-525.

- [27] Z. Lin, *Coord. Chem. Rev.* **2007**, *251*, 2280-2291.
- [28] a) T. R. Cundari, T. R. Klinckman, P. T. Wolczanski, *J. Am. Chem. Soc.* **2002**, *124*, 1481-1487; b) J. L. Bennett, P. T. Wolczanski, *J. Am. Chem. Soc.* **1997**, *119*, 10696-10719.
- [29] a) J. C. Gaunt, B. L. Shaw, *J. Organomet. Chem.* **1975**, *102*, 511-516; b) J. M. Duff, B. E. Mann, B. L. Shaw, B. Turtle, *J. Chem. Soc., Dalton Trans.* **1974**, 139-145; c) J. M. Duff, B. L. Shaw, *J. Chem. Soc., Dalton Trans.* **1972**, 2219-2225.
- [30] a) D. L. Davies, S. A. Macgregor, C. L. McMullin, *Chem. Rev.* **2017**, *117*, 8649-8709; b) L. Ackermann, *Acc. Chem. Res.* **2014**, *47*, 281-295.
- [31] a) L. Wang, L. Ackermann, *Org. Lett.* **2013**, *15*, 176-179; b) W. Ma, K. Graczyk, L. Ackermann, *Org. Lett.* **2012**, *14*, 6318-6321; c) B. Li, H. Feng, N. Wang, J. Ma, H. Song, S. Xu, B. Wang, *Chem. Eur. J.* **2012**, *18*, 12873-12879; d) L. Ackermann, L. Wang, A. V. Lygin, *Chem. Sci.* **2012**, *3*, 177-180; e) L. Ackermann, A. V. Lygin, *Org. Lett.* **2012**, *14*, 764-767; f) L. Ackermann, A. V. Lygin, N. Hofmann, *Angew. Chem. Int. Ed.* **2011**, *50*, 6379-6382; g) L. Ackermann, A. V. Lygin, N. Hofmann, *Org. Lett.* **2011**, *13*, 3278-3281; h) L. Ackermann, R. Vicente, A. Althammer, *Org. Lett.* **2008**, *10*, 2299-2302.
- [32] S. I. Gorelsky, D. Lapointe, K. Fagnou, *J. Am. Chem. Soc.* **2008**, *130*, 10848-10849.
- [33] a) Y. Boutadla, D. L. Davies, S. A. Macgregor, A. I. Poblador-Bahamonde, *Dalton Trans.* **2009**, 5887-5893; b) D. L. Davies, S. M. A. Donald, S. A. Macgregor, *J. Am. Chem. Soc.* **2005**, *127*, 13754-13755.
- [34] a) D. Zell, M. Bursch, V. Müller, S. Grimme, L. Ackermann, *Angew. Chem. Int. Ed.* **2017**, *56*, 10378-10382; b) W. Ma, R. Mei, G. Tenti, L. Ackermann, *Chem. Eur. J.* **2014**, *20*, 15248-15251.
- [35] a) D. J. Abrams, P. A. Provencher, E. J. Sorensen, *Chem. Soc. Rev.* **2018**, *47*, 8925-8967; b) W. R. Gutekunst, P. S. Baran, *Chem. Soc. Rev.* **2011**, *40*, 1976-1991.
- [36] a) J. Wang, G. Dong, *Chem. Rev.* **2019**, *119*, 7478-7528; b) B. Niu, K. Yang, B.

- Lawrence, H. Ge, *ChemSusChem* **2019**, *12*, 2955-2969; c) C. Sambigioglio, D. Schönbauer, R. Blicek, T. Dao-Huy, G. Pototschnig, P. Schaaf, T. Wiesinger, M. F. Zia, J. Wencel-Delord, T. Besset, B. U. W. Maes, M. Schnürch, *Chem. Soc. Rev.* **2018**, *47*, 6603-6743; d) M. Ghosh, S. De Sarkar, *Asian J. Org. Chem.* **2018**, *7*, 1236-1255; e) P. Gandeepan, L. Ackermann, *Chem* **2018**, *4*, 199-222; f) X.-S. Xue, P. Ji, B. Zhou, J.-P. Cheng, *Chem. Rev.* **2017**, *117*, 8622-8648; g) J. A. Leitch, C. G. Frost, *Chem. Soc. Rev.* **2017**, *46*, 7145-7153; h) M. Font, J. M. Quibell, G. J. P. Perry, I. Larrosa, *Chem. Commun.* **2017**, *53*, 5584-5597; i) Z. Chen, B. Wang, J. Zhang, W. Yu, Z. Liu, Y. Zhang, *Org. Chem. Front.* **2015**, *2*, 1107-1295.
- [37] K. Shen, Y. Fu, J.-N. Li, L. Liu, Q.-X. Guo, *Tetrahedron* **2007**, *63*, 1568-1576.
- [38] T. P. Pabst, P. J. Chirik, *Organometallics* **2021**, *40*, 813-831.
- [39] a) J. Li, S. De Sarkar, L. Ackermann, in *C-H Bond Activation and Catalytic Functionalization I* (Eds.: P. H. Dixneuf, H. Doucet), Springer International Publishing, Cham, **2016**, pp. 217-257; b) G. Cera, L. Ackermann, *Top. Curr. Chem.* **2016**, *374*, 57; c) L. Ackermann, J. Li, *Nat. Chem.* **2015**, *7*, 686-687; d) L. Ackermann, R. Vicente, in *C-H Activation* (Eds.: J.-Q. Yu, Z. Shi), Springer Berlin Heidelberg, Berlin, Heidelberg, **2010**, pp. 211-229; e) L. Ackermann, R. Vicente, A. R. Kapdi, *Angew. Chem. Int. Ed.* **2009**, *48*, 9792-9826.
- [40] a) P. Y. Choy, S. M. Wong, A. Kapdi, F. Y. Kwong, *Org. Chem. Front.* **2018**, *5*, 288-321; b) O. Baudoin, *Acc. Chem. Res.* **2017**, *50*, 1114-1123; c) F. Kakiuchi, T. Kochi, *Isr. J. Chem.* **2017**, *57*, 953-963; d) N. Della Ca', M. Fontana, E. Motti, M. Catellani, *Acc. Chem. Res.* **2016**, *49*, 1389-1400; e) J. Ye, M. Lautens, *Nat. Chem.* **2015**, *7*, 863-870; f) C.-L. Sun, B.-J. Li, Z.-J. Shi, *Chem. Comm.* **2010**, *46*, 677-685; g) X. Chen, K. M. Engle, D. H. Wang, J. Q. Yu, *Angew. Chem. Int. Ed.* **2009**, *48*, 5094-5115; h) M. Catellani, E. Motti, N. Della Ca', *Acc. Chem. Res.* **2008**, *41*, 1512-1522.
- [41] a) Y. K. Xing, X. R. Chen, Q. L. Yang, S. Q. Zhang, H. M. Guo, X. Hong, T. S. Mei, *Nat. Commun.* **2021**, *12*, 930; b) P. H. Dixneuf, H. Doucet, L. Ackermann, *C-H Bond Activation and Catalytic Functionalization I, Vol. 55*, **2016**; c) S.-S. Li,

- L. Qin, L. Dong, *Org. Biomol. Chem.* **2016**, *14*, 4554-4570; d) B. Ye, N. Cramer, *Acc. Chem. Res.* **2015**, *48*, 1308-1318; e) D. A. Colby, A. S. Tsai, R. G. Bergman, J. A. Ellman, *Acc. Chem. Res.* **2012**, *45*, 814-825; f) G. Song, F. Wang, X. Li, *Chem. Soc. Rev.* **2012**, *41*, 3651-3678; g) J. D. Bois, *Org. Process Res. Dev.* **2011**, *15*, 758-762; h) D. A. Colby, R. G. Bergman, J. A. Ellman, *Chem. Rev.* **2010**, *110*, 624-655.
- [42] a) O. M. Ogba, N. C. Warner, D. J. O'Leary, R. H. Grubbs, *Chem. Soc. Rev.* **2018**, *47*, 4510-4544; b) B. M. Trost, F. D. Toste, A. B. Pinkerton, *Chem. Rev.* **2001**, *101*, 2067-2096.
- [43] a) C. Haldar, M. Emdadul Hoque, R. Bisht, B. Chattopadhyay, *Tetrahedron Lett.* **2018**, *59*, 1269-1277; b) J. Kim, S. Chang, *Angew. Chem. Int. Ed.* **2014**, *53*, 2203-2207; c) S. Pan, T. Shibata, *ACS Catal.* **2013**, *3*, 704-712.
- [44] J. Chatt, J. Davidson, *J. Chem. Soc.* **1965**, 843-855.
- [45] L. N. Lewis, J. F. Smith, *J. A. Chem. Soc.* **1986**, *108*, 2728-2735.
- [46] a) J. I. Higham, J. A. Bull, *Org. Biomol. Chem.* **2020**, *18*, 7291-7315; b) M. I. Lapuh, S. Mazeh, T. Besset, *ACS Catal.* **2020**, *10*, 12898-12919; c) H. Sun, N. Guimond, Y. Huang, *Org. Biomol. Chem.* **2016**, *14*, 8389-8397.
- [47] S. Murai, F. Kakiuchi, S. Sekine, Y. Tanaka, A. Kamatani, M. Sonoda, N. Chatani, *Nature* **1993**, *366*, 529-531.
- [48] a) S. Oi, Y. Ogino, S. Fukita, Y. Inoue, *Org. Lett.* **2002**, *4*, 1783-1785; b) S. Oi, S. Fukita, N. Hirata, N. Watanuki, S. Miyano, Y. Inoue, *Org. Lett.* **2001**, *3*, 2579-2581.
- [49] a) L. Ackermann, A. Althammer, R. Born, *Angew. Chem. Int. Ed.* **2006**, *45*, 2619-2622; b) L. Ackermann, *Org. Lett.* **2005**, *7*, 3123-3125.
- [50] I. Özdemir, S. Demir, B. Çetinkaya, C. Gourlaouen, F. Maseras, C. Bruneau, P. H. Dixneuf, *J. A. Chem. Soc.* **2008**, *130*, 1156-1157.
- [51] a) L. Ackermann, *Org. Process Res. Dev.* **2015**, *19*, 260-269; b) J. Li, L. Ackermann, *Org. Chem. Front.* **2015**, *2*, 1035-1039; c) M. Schinkel, I. Marek, L. Ackermann, *Angew. Chem. Int. Ed.* **2013**, *52*, 3977-3980; d) L. Ackermann, E. Diers, A. Manvar, *Org. Lett.* **2012**, *14*, 1154-1157; e) L. Ackermann, N.

- Hofmann, R. Vicente, *Org. Lett.* **2011**, *13*, 1875-1877; f) L. David, F. Keith, *Chem. Lett.* **2010**, *39*, 1118-1126; g) S. I. Gorelsky, D. Lapointe, K. Fagnou, *J. A. Chem. Soc.* **2008**, *130*, 10848-10849; h) M. Lafrance, K. Fagnou, *J. A. Chem. Soc.* **2006**, *128*, 16496-16497.
- [52] S. Oi, R. Funayama, T. Hattori, Y. Inoue, *Tetrahedron* **2008**, *64*, 6051-6059.
- [53] S. Oi, E. Aizawa, Y. Ogino, Y. Inoue, *J. Org. Chem.* **2005**, *70*, 3113-3119.
- [54] S. G. Ouellet, A. Roy, C. Molinaro, R. m. Angelaud, J.-F. Marcoux, P. D. O'Shea, I. W. Davies, *J. Org. Chem.* **2011**, *76*, 1436-1439.
- [55] L. Ackermann, A. Althammer, R. Born, *Synlett* **2007**, *2007*, 2833-2836.
- [56] L. Ackermann, R. Vicente, A. Althammer, *Org. Lett.* **2008**, *10*, 2299-2302.
- [57] L. Ackermann, R. Vicente, H. K. Potukuchi, V. Pirovano, *Org. Lett.* **2010**, *12*, 5032-5035.
- [58] S. G. Ouellet, A. Roy, C. Molinaro, R. Angelaud, J.-F. Marcoux, P. D. O'Shea, I. W. Davies, *J. Org. Chem.* **2011**, *76*, 1436-1439.
- [59] M. Simonetti, G. J. P. Perry, X. C. Cambeiro, F. Juliá-Hernández, J. N. Arokianathar, I. Larrosa, *J. Am. Chem. Soc.* **2016**, *138*, 3596-3606.
- [60] M. Simonetti, D. M. Cannas, X. Just-Baringo, I. J. Vitorica-Yrezabal, I. Larrosa, *Nat. Chem.* **2018**, *10*, 724-731.
- [61] S. Oi, Y. Tanaka, Y. Inoue, *Organometallics* **2006**, *25*, 4773-4778.
- [62] R. Manikandan, P. Madasamy, M. Jeganmohan, *Chemistry—A European Journal* **2015**, *21*, 13934-13938.
- [63] X.-Q. Hu, Z. Hu, A. S. Trita, G. Zhang, L. J. Gooßen, *Chemical Science* **2018**, *9*, 5289-5294.
- [64] D. Singh, G. S. Kumar, M. Kapur, *The Journal of Organic Chemistry* **2019**, *84*, 12881-12892.
- [65] a) J. A. Osborn, F. H. Jardine, J. F. Young, G. Wilkinson, *J. Chem. Soc. A* **1966**, 1711-1732; b) J. Young, J. Osborn, F. Jardine, G. Wilkinson, *Chem. Comm. (London)* **1965**, 131-132.
- [66] a) G. Song, F. Wang, X. Li, *Chem. Soc. Rev.* **2012**, *41*, 3651-3678; b) T. Satoh, M. Miura, *Chem. Eur. J.* **2010**, *16*, 11212-11222.

- [67] a) D. A. Colby, R. G. Bergman, J. A. Ellman, *Chem. Rev.* **2010**, *110*, 624-655; b) B. de Bruin, P. H. Budzelaar, A. W. Gal, *Angew. Chem.* **2004**, *116*, 4236-4251.
- [68] a) D. K. Leahy, P. A. Evans, *Modern Rhodium - Catalyzed Organic Reactions* **2005**, 191-214; b) A. Fazlur-Rahman, J.-C. Tsai, K. M. Nicholas, *J. Chem. Soc., Chem. Comm.* **1992**, 1334-1335; c) H. Mimoun, *Angew. Chem. Int. Ed.* **1982**, *21*, 734-750; d) H. Mimoun, M. M. Perez Machirant, I. Sere de Roch, *J. A. Chem. Soc.* **1978**, *100*, 5437-5444.
- [69] Y.-G. Lim, Y. H. Kim, J.-B. Kang, *J. Chem. Soc., Chem. Commun.* **1994**, 2267-2268.
- [70] a) T. Matsumoto, R. A. Periana, D. J. Taube, H. Yoshida, *J. Catal.* **2002**, *206*, 272-280; b) M. Takaya, Y. Hajime, *Chem. Lett.* **2000**, *29*, 1064-1065.
- [71] a) S. Mochida, K. Hirano, T. Satoh, M. Miura, *J. Org. Chem.* **2011**, *76*, 3024-3033; b) N. Umeda, K. Hirano, T. Satoh, M. Miura, *J. Org. Chem.* **2009**, *74*, 7094-7099.
- [72] a) F. W. Patureau, T. Besset, F. Glorius, *Angew. Chem. Int. Ed.* **2011**, *50*, 1064-1067; b) F. W. Patureau, F. Glorius, *J. Am. Chem. Soc.* **2010**, *132*, 9982-9983.
- [73] P. Zhao, R. Niu, F. Wang, K. Han, X. Li, *Org. Lett.* **2012**, *14*, 4166-4169.
- [74] F. W. Patureau, C. Nimphius, F. Glorius, *Org. Lett.* **2011**, *13*, 6346-6349.
- [75] B. Li, J. Ma, W. Xie, H. Song, S. Xu, B. Wang, *Chem. Eur. J.* **2013**, *19*, 11863-11868.
- [76] a) M. Wu, S. Wang, Y. Wang, H. Gao, W. Yi, Z. Zhou, *Eur. J. Org. Chem.* **2021**, *2021*, 5507-5517; b) M. Chaitanya, P. Anbarasan, *J. Org. Chem.* **2015**, *80*, 3695-3700; c) S. Sharma, S. Han, M. Kim, N. K. Mishra, J. Park, Y. Shin, J. Ha, J. H. Kwak, Y. H. Jung, I. S. Kim, *Org. Biomol. Chem.* **2014**, *12*, 1703-1706; d) S. Sharma, S. Han, Y. Shin, N. K. Mishra, H. Oh, J. Park, J. H. Kwak, B. S. Shin, Y. H. Jung, I. S. Kim, *Tetrahedron Lett.* **2014**, *55*, 3104-3107; e) J. Shi, G. Zhao, X. Wang, H. E. Xu, W. Yi, *Org. Biomol. Chem.* **2014**, *12*, 6831-6836; f) M. Kim, J. Park, S. Sharma, S. Han, S. H. Han, J. H. Kwak, Y. H. Jung, I. S. Kim, *Org. Biomol. Chem.* **2013**, *11*, 7427-7434; g) L. Joucla, L. Djakovitch, *Adv. Synth.*

- Catal.* **2009**, *351*, 673-714.
- [77] a) S. Devkota, S. Kim, S. Y. Yoo, S. Mohandoss, M.-H. Baik, Y. R. Lee, *Chem. Sci.* **2021**, *12*, 11427-11437; b) K. Urbina, D. Tresp, K. Sipps, M. Szostak, *Adv. Synth. Catal.* **2021**, *363*, 2723-2739; c) J. Wen, Z. Shi, *Acc. Chem. Res.* **2021**, *54*, 1723-1736; d) Q. Wu, P. Gao, Y. Yuan, *Asian J. Org. Chem.* **2021**, *10*, 749-752; e) J.-B. Chen, Y.-X. Jia, *Org. Biomol. Chem.* **2017**, *15*, 3550-3567; f) J. A. Leitch, Y. Bhonoah, C. G. Frost, *ACS Catal.* **2017**, *7*, 5618-5627.
- [78] L. Xu, C. Zhang, Y. He, L. Tan, D. Ma, *Angew. Chem. Int. Ed.* **2016**, *55*, 321-325.
- [79] L. Xu, L. Tan, D. Ma, *Synlett* **2017**, *28*, 2839-2844.
- [80] X. Qiu, P. Wang, D. Wang, M. Wang, Y. Yuan, Z. Shi, *Angew. Chem. Int. Ed.* **2019**, *58*, 1504-1508.
- [81] C. N. Kona, Y. Nishii, M. Miura, *Org. Lett.* **2021**, *23*, 6252-6256.
- [82] a) B. Hong, T. Luo, X. Lei, *ACS Cent. Sci.* **2020**, *6*, 622-635; b) K. Korvorapun, R. Kuniyil, L. Ackermann, *ACS Catal.* **2020**, *10*, 435-440; c) W. Wang, M. M. Lorion, J. Shah, A. R. Kapdi, L. Ackermann, *Angew. Chem. Int. Ed.* **2018**, *57*, 14700-14717; d) J. Wencel-Delord, F. Glorius, *Nature Chem.* **2013**, *5*, 369-375; e) H.-X. Dai, A. F. Stepan, M. S. Plummer, Y.-H. Zhang, J.-Q. Yu, *J. Am. Chem. Soc.* **2011**, *133*, 7222-7228.
- [83] a) T. Dalton, T. Faber, F. Glorius, *ACS Cent. Sci.* **2021**, *7*, 245-261; b) N. V. Tzouras, I. K. Stamatopoulos, A. T. Papastavrou, A. A. Liori, G. C. Vougioukalakis, *Coord. Chem. Rev.* **2017**, *343*, 25-138.
- [84] a) L. Guillemard, J. Wencel-Delord, *Beilstein J. Org. Chem.* **2020**, *16*, 1754-1804; b) L. Marzo, S. K. Pagire, O. Reiser, B. König, *Angew. Chem. Int. Ed.* **2018**, *57*, 10034-10072; c) M. D. Kärkäs, J. A. Porco, Jr., C. R. J. Stephenson, *Chem. Rev.* **2016**, *116*, 9683-9747; d) K. L. Skubi, T. R. Blum, T. P. Yoon, *Chem. Rev.* **2016**, *116*, 10035-10074; e) R. Brimiouille, D. Lenhart, M. M. Maturi, T. Bach, *Angew. Chem. Int. Ed.* **2015**, *54*, 3872-3890; f) C. K. Prier, D. A. Rankic, D. W. C. MacMillan, *Chem. Rev.* **2013**, *113*, 5322-5363.
- [85] a) T. H. Meyer, I. Choi, C. Tian, L. Ackermann, *Chem* **2020**, *6*, 2484-2496; b) D.



- Pollok, S. R. Waldvogel, *Chem. Sci.* **2020**, *11*, 12386-12400; c) Y. Kawamata, P. S. Baran, *Joule* **2020**, *4*, 701-704.
- [86] a) S. Santoro, F. Ferlin, L. Ackermann, L. Vaccaro, *Chem. Soc. Rev.* **2019**, *48*, 2767-2782; b) D. Pletcher, R. A. Green, R. C. D. Brown, *Chem. Rev.* **2018**, *118*, 4573-4591; c) A. A. Folgueiras-Amador, T. Wirth, *J. Flow Chem.* **2017**, *7*, 94-95; d) M. B. Plutschack, B. Pieber, K. Gilmore, P. H. Seeberger, *Chem. Rev.* **2017**, *117*, 11796-11893; e) H. P. L. Gemoets, Y. Su, M. Shang, V. Hessel, R. Luque, T. Noël, *Chem. Soc. Rev.* **2016**, *45*, 83-117; f) J. C. Pastre, D. L. Browne, S. V. Ley, *Chem. Soc. Rev.* **2013**, *42*, 8849-8869; g) T. Noël, S. L. Buchwald, *Chem. Soc. Rev.* **2011**, *40*, 5010-5029; h) S. Saaby, K. R. Knudsen, M. Ladlow, S. V. Ley, *Chem. Commun.* **2005**, 2909-2911.
- [87] D. Kalyani, K. B. McMurtrey, S. R. Neufeldt, M. S. Sanford, *J. Am. Chem. Soc.* **2011**, *133*, 18566-18569.
- [88] D. Kalyani, N. R. Deprez, L. V. Desai, M. S. Sanford, *J. Am. Chem. Soc.* **2005**, *127*, 7330-7331.
- [89] N. Hofmann, L. Ackermann, *J. Am. Chem. Soc.* **2013**, *135*, 5877-5884.
- [90] J. Li, S. Warratz, D. Zell, S. De Sarkar, E. E. Ishikawa, L. Ackermann, *J. Am. Chem. Soc.* **2015**, *137*, 13894-13901.
- [91] A. J. Paterson, S. St John-Campbell, M. F. Mahon, N. J. Press, C. G. Frost, *Chem. Commun.* **2015**, *51*, 12807-12810.
- [92] P. Gandeepan, J. Koeller, K. Korvorapun, J. Mohr, L. Ackermann, *Angew. Chem. Int. Ed.* **2019**, *58*, 9820-9825.
- [93] A. Sagadevan, M. F. Greaney, *Angew. Chem. Int. Ed.* **2019**, *58*, 9826-9830.
- [94] A. Sagadevan, A. Charitou, F. Wang, M. Ivanova, M. Vuagnat, M. F. Greaney, *Chem. Sci.* **2020**, *11*, 4439-4443.
- [95] A. Volta, *Philos. Trans. R. Soc. London* **1800**, *90*, 403-431.
- [96] M. Faraday, *Ann. Phys.* **1834**, *109*, 481-520.
- [97] a) M. C. Leech, K. Lam, *Acc. Chem. Res.* **2020**, *53*, 121-134; b) H.-J. Schäfer, Springer Berlin Heidelberg, Berlin, Heidelberg, **1990**, pp. 91-151; c) L. Becking, H. J. Schäfer, *Tetrahedron Lett.* **1988**, *29*, 2797-2800; d) H. Kolbe, *Liebigs Ann.*

- Chem.* **1849**, 69, 257-294; e) H. Kolbe, *J. Prakt. Chem.* **1847**, 41, 137-139; f) H. Kolbe, *Liebigs Ann. Chem.* **1845**, 54, 145-188.
- [98] a) C. Tian, T. H. Meyer, M. Stangier, U. Dhawa, K. Rauch, L. H. Finger, L. Ackermann, *Nat. Protoc.* **2020**, 15, 1760-1774; b) M. Yan, Y. Kawamata, P. S. Baran, *Angew. Chem. Int. Ed.* **2018**, 57, 4149-4155.
- [99] a) R. D. Little, *J. Org. Chem.* **2020**, 85, 13375-13390; b) C. Kingston, M. D. Palkowitz, Y. Takahira, J. C. Vantourout, B. K. Peters, Y. Kawamata, P. S. Baran, *Acc. Chem. Res.* **2020**, 53, 72-83; c) S. R. Waldvogel, S. Lips, M. Selt, B. Riehl, C. J. Kampf, *Chem. Rev.* **2018**, 118, 6706-6765; d) M. Yan, Y. Kawamata, P. S. Baran, *Chem. Rev.* **2017**, 117, 13230-13319; e) J. B. Sperry, D. L. Wright, *Chem. Soc. Rev.* **2006**, 35, 605-621.
- [100] J. H. Simons, *J. Electrochem. Soc.* **1949**, 95, 47-67.
- [101] a) M. M. Baizer, *Tetrahedron* **1984**, 40, 935-969; b) M. M. Baizer, *J. Electrochem. Soc.* **1964**, 111, 215.
- [102] a) M. C. Leech, A. D. Garcia, A. Petti, A. P. Dobbs, K. Lam, *React. Chem. Eng.* **2020**, 5, 977-990; b) D. S. P. Cardoso, B. Šljukić, D. M. F. Santos, C. A. C. Sequeira, *Org. Process Res. Dev.* **2017**, 21, 1213-1226.
- [103] a) H. J. Schäfer, *C. R. Chim.* **2011**, 14, 745-765; b) H. J. Schäfer, *Angew. Chem. Int. Ed. Engl.* **1981**, 20, 911-934.
- [104] a) C. Lefrou, P. Fabry, J.-C. Poignet, C. Amatore, *Electrochemistry : the basics, with examples*, Springer, Heidelberg, **2012**; b) C. Amatore, C. Cammoun, A. Jutand, *Eur. J. Org. Chem.* **2008**, 2008, 4567-4570; c) A. J. L. Pombeiro, C. Amatore, *Trends in molecular electrochemistry*, Marcel Dekker [and] Fontis Media ; [Taylor & Francis], New York; [London], **2004**.
- [105] a) A. Jutand, *Chem. Rev.* **2008**, 108, 2300-2347; b) C. Amatore, E. Carre, A. Jutand, A. M'Barki, G. Meyer, Springer Japan, Tokyo, **1998**, pp. 379-382.
- [106] a) R. Francke, R. D. Little, *Chem. Soc. Rev.* **2014**, 43, 2492-2521; b) R. D. Little, M. K. Schwaebe, in *Electrochemistry VI Electroorganic Synthesis: Bond Formation at Anode and Cathode* (Ed.: E. Steckhan), Springer Berlin Heidelberg, Berlin, Heidelberg, **1997**, pp. 1-48; c) C. Gregory Sowell, R. L.

- Wolin, R. Daniel Little, *Tetrahedron Lett.* **1990**, *31*, 485-488; d) R. D. Little, D. P. Fox, L. Van Hijfte, R. Dannecker, G. Sowell, R. L. Wolin, L. Moens, M. M. Baizer, *J. Org. Chem.* **1988**, *53*, 2287-2294.
- [107] a) J.-i. Yoshida, K. Kataoka, R. Horcajada, A. Nagaki, *Chem. Rev.* **2008**, *108*, 2265-2299; b) J.-i. Yoshida, S. Suga, S. Suzuki, N. Kinomura, A. Yamamoto, K. Fujiwara, *J. Am. Chem. Soc.* **1999**, *121*, 9546-9549.
- [108] a) P. E. Iversen, H. Lund, *Tetrahedron Lett.* **1969**, *10*, 3523-3524; b) H. Lund, P. Lunde, *Acta Chem. Scand.* **1967**, *21*, 1067-1080.
- [109] a) T. Gieshoff, A. Kehl, D. Schollmeyer, K. D. Moeller, S. R. Waldvogel, *J. Am. Chem. Soc.* **2017**, *139*, 12317-12324; b) H.-C. Xu, J. M. Campbell, K. D. Moeller, *J. Org. Chem.* **2014**, *79*, 379-391; c) K. D. Moeller, *Tetrahedron* **2000**, *56*, 9527-9554.
- [110] a) J. E. Erchinger, M. van Gemmeren, *Asian J. Org. Chem.* **2021**, *10*, 50-60; b) H. Wu, Q. An, C. He, X. Fan, W. Guo, M. Zuo, C. Xu, R. Guo, W. Chu, Z. Sun, *Adv. Synth. Catal.* **2020**, *362*, 2459-2465; c) U. Dhawa, C. Tian, T. Wdowik, J. C. A. Oliveira, J. Hao, L. Ackermann, *Angew. Chem. Int. Ed.* **2020**, *59*, 13451-13457; d) A. Shrestha, M. Lee, A. L. Dunn, M. S. Sanford, *Org. Lett.* **2018**, *20*, 204-207; e) K. Sano, N. Kimura, T. Kochi, F. Kakiuchi, *Asian J. Org. Chem.* **2018**, *7*, 1311-1314; f) M. Konishi, K. Tsuchida, K. Sano, T. Kochi, F. Kakiuchi, *J. Org. Chem.* **2017**, *82*, 8716-8724; g) F. Saito, H. Aiso, T. Kochi, F. Kakiuchi, *Organometallics* **2014**, *33*, 6704-6707; h) H. Aiso, T. Kochi, H. Mutsutani, T. Tanabe, S. Nishiyama, F. Kakiuchi, *J. Org. Chem.* **2012**, *77*, 7718-7724; i) D. Kalyani, A. R. Dick, W. Q. Anani, M. S. Sanford, *Org. Lett.* **2006**, *8*, 2523-2526.
- [111] C. Amatore, C. Cammoun, A. Jutand, *Adv. Synth. Catal.* **2007**, *349*, 292-296.
- [112] a) C. Jia, T. Kitamura, Y. Fujiwara, *Acc. Chem. Res.* **2001**, *34*, 633-639; b) Y. Fujiwara, I. Moritani, S. Danno, R. Asano, S. Teranishi, *J. Am. Chem. Soc.* **1969**, *91*, 7166-7169; c) I. Moritani, Y. Fujiwara, *Tetrahedron Lett.* **1967**, *8*, 1119-1122.
- [113] F. Kakiuchi, T. Kochi, H. Mutsutani, N. Kobayashi, S. Urano, M. Sato, S. Nishiyama, T. Tanabe, *J. Am. Chem. Soc.* **2009**, *131*, 11310-11311.
- [114] H. Aiso, T. Kochi, H. Mutsutani, T. Tanabe, S. Nishiyama, F. Kakiuchi, *J. Org.*

- Chem.* **2012**, *77*, 7718-7724.
- [115] Q.-L. Yang, X.-Y. Wang, T.-L. Wang, X. Yang, D. Liu, X. Tong, X.-Y. Wu, T.-S. Mei, *Org. Lett.* **2019**, *21*, 2645-2649.
- [116] Y. B. Dudkina, D. Y. Mikhaylov, T. V. Gryaznova, A. I. Tufatullin, O. N. Kataeva, D. A. Vicic, Y. H. Budnikova, *Organometallics* **2013**, *32*, 4785-4792.
- [117] Q.-L. Yang, Y.-Q. Li, C. Ma, P. Fang, X.-J. Zhang, T.-S. Mei, *J. Am. Chem. Soc.* **2017**, *139*, 3293-3298.
- [118] Y. Qiu, W.-J. Kong, J. Struwe, N. Sauermann, T. Rogge, A. Scheremetjew, L. Ackermann, *Angew. Chem. Int. Ed.* **2018**, *57*, 5828-5832.
- [119] a) Y. Qiu, C. Zhu, M. Stangier, J. Struwe, L. Ackermann, *CCS Chem.* **2021**, *3*, 1529-1552; b) S.-K. Zhang, R. C. Samanta, A. Del Vecchio, L. Ackermann, *Chem. Eur. J.* **2020**, *26*, 10936-10947; c) R. Mei, U. Dhawa, R. C. Samanta, W. Ma, J. Wencel-Delord, L. Ackermann, *ChemSusChem* **2020**, *13*, 3306-3356; d) L. Ackermann, *Acc. Chem. Res.* **2020**, *53*, 84-104; e) Y. Qiu, J. Struwe, L. Ackermann, *Synlett* **2019**, *30*, 1164-1173; f) N. Sauermann, T. H. Meyer, Y. Qiu, L. Ackermann, *ACS Catal.* **2018**, *8*, 7086-7103; g) N. Sauermann, T. H. Meyer, L. Ackermann, *Chem. Eur. J.* **2018**, *24*, 16209-16217.
- [120] a) P. Wang, X. Gao, P. Huang, A. Lei, *ChemCatChem* **2020**, *12*, 27-40; b) Y. Yuan, A. Lei, *Acc. Chem. Res.* **2019**, *52*, 3309-3324; c) H. Wang, X. Gao, Z. Lv, T. Abdelilah, A. Lei, *Chem. Rev.* **2019**, *119*, 6769-6787; d) S. Tang, L. Zeng, A. Lei, *J. Am. Chem. Soc.* **2018**, *140*, 13128-13135.
- [121] a) Z.-J. Wu, F. Su, W. Lin, J. Song, T.-B. Wen, H.-J. Zhang, H.-C. Xu, *Angew. Chem. Int. Ed.* **2019**, *58*, 16770-16774; b) F. Xu, Y.-J. Li, C. Huang, H.-C. Xu, *ACS Catal.* **2018**, *8*, 3820-3824.
- [122] a) K.-J. Jiao, Y.-K. Xing, Q.-L. Yang, H. Qiu, T.-S. Mei, *Acc. Chem. Res.* **2020**, *53*, 300-310; b) Q.-L. Yang, P. Fang, T.-S. Mei, *Chin. J. Chem.* **2018**, *36*, 338-352; c) C. Ma, P. Fang, T.-S. Mei, *ACS Catal.* **2018**, *8*, 7179-7189; d) K.-J. Jiao, C.-Q. Zhao, P. Fang, T.-S. Mei, *Tetrahedron Lett.* **2017**, *58*, 797-802.
- [123] a) Y. H. Budnikova, *Chem. Rec.* **2021**, *21*, DOI: [10.1002/tcr.202100009](https://doi.org/10.1002/tcr.202100009); b) X. Ye, C. Wang, S. Zhang, J. Wei, C. Shan, L. Wojtas, Y. Xie, X. Shi, *ACS Catal.*

- 2020**, *10*, 11693-11699; c) Z.-Q. Wang, C. Hou, Y.-F. Zhong, Y.-X. Lu, Z.-Y. Mo, Y.-M. Pan, H.-T. Tang, *Org. Lett.* **2019**, *21*, 9841-9845; d) M.-J. Luo, T.-T. Zhang, F.-J. Cai, J.-H. Li, D.-L. He, *Chem. Commun.* **2019**, *55*, 7251-7254; e) M.-J. Luo, M. Hu, R.-J. Song, D.-L. He, J.-H. Li, *Chem. Commun.* **2019**, *55*, 1124-1127; f) S. Kathiravan, S. Suriyanarayanan, I. A. Nicholls, *Org. Lett.* **2019**, *21*, 1968-1972.
- [124] a) L. Zhang, T. Ritter, *J. Am. Chem. Soc.* **2022**, *144*, 2399-2414; b) J. Börgel, T. Ritter, *Chem* **2020**, *6*, 1877-1887; c) F. Berger, M. B. Plutschack, J. Riegger, W. Yu, S. Speicher, M. Ho, N. Frank, T. Ritter, *Nature* **2019**, *567*, 223-228.
- [125] a) S. D. Friis, M. J. Johansson, L. Ackermann, *Nat. Chem.* **2020**, *12*, 511-519; b) J. R. Clark, K. Feng, A. Sookezian, M. C. White, *Nat. Chem.* **2018**, *10*, 583-591; c) T. Nanjo, E. C. de Lucca Jr, M. C. White, *J. Am. Chem. Soc.* **2017**, *139*, 14586-14591; d) M. A. Larsen, J. F. Hartwig, *J. Am. Chem. Soc.* **2014**, *136*, 4287-4299; e) J. Wencel-Delord, F. Glorius, *Nat. Chem.* **2013**, *5*, 369-375.
- [126] H. J. Shine, J. J. Silber, *J. Org. Chem.* **1971**, *36*, 2923-2926.
- [127] K. Hartke, D. Teuber, H.-D. Gerber, *Tetrahedron* **1988**, *44*, 3261-3270.
- [128] K. Kafuta, A. Korzun, M. Böhm, C. Golz, M. Alcarazo, *Angew. Chem. Int. Ed.* **2020**, *59*, 1950-1955.
- [129] M. H. Aukland, M. Šiaučiulis, A. West, G. J. Perry, D. J. Procter, *Nature Catal.* **2020**, *3*, 163-169.
- [130] N. Kaplaneris, A. Puet, F. Kallert, J. Pöhlmann, L. Ackermann, *Angew. Chem. Int. Ed.* **2023**, *62*, e202216661.
- [131] a) C. Zhu, N. W. J. Ang, T. H. Meyer, Y. Qiu, L. Ackermann, *ACS Cent. Sci.* **2021**, *7*, 415-431; b) A. Dey, T. B. Gunnoe, V. R. Stamenkovic, *ACS Catal.* **2020**, *10*, 13156-13158; c) R. Francke, R. D. Little, *ChemElectroChem* **2019**, *6*, 4373-4382.
- [132] a) J. Li, S. De Sarkar, L. Ackermann, *Top. Organomet. Chem.* **2016**, *55*, 217-257; b) L. Ackermann, *Chem. Rev.* **2011**, *111*, 1315-1345; c) L. Ackermann, R. Vicente, *Top. Curr. Chem.* **2010**, *292*, 211-229; d) L. Ackermann, *Synlett* **2007**, *2007*, 0507-0526.

- [133] a) M. H. Aukland, F. J. Talbot, J. A. Fernández - Salas, M. Ball, A. P. Pulis, D. J. Procter, *Angew. Chem.* **2018**, *130*, 9933-9937; b) S.-M. Wang, H.-X. Song, X.-Y. Wang, N. Liu, H.-L. Qin, C.-P. Zhang, *Chem. Commun.* **2016**, *52*, 11893-11896.
- [134] a) N. M. Grob, R. Schibli, M. Behe, I. E. Valverde, T. L. Mindt, *ACS Med. Chem. Lett.* **2021**, *12*, 585-592; b) S. Kumari, A. V. Carmona, A. K. Tiwari, P. C. Trippier, *J. Med. Chem.* **2020**, *63*, 12290-12358; c) P. Prasher, M. Sharma, *Med. Chem. Commun.* **2019**, *10*, 1302-1328; d) I. Mohammed, I. R. Kummetha, G. Singh, N. Sharova, G. Lichinchi, J. Dang, M. Stevenson, T. M. Rana, *J. Med. Chem.* **2016**, *59*, 7677-7682; e) V. Subramanian, J. S. Knight, S. Parelkar, L. Anguish, S. A. Coonrod, M. J. Kaplan, P. R. Thompson, *J. Med. Chem.* **2015**, *58*, 1337-1344; f) C. Ballatore, D. M. Huryn, A. B. Smith III, *ChemMedChem* **2013**, *8*, 385-395; g) R. J. Herr, *Bioorg. Med. Chem.* **2002**, *10*, 3379-3393.
- [135] P. B. Arockiam, C. Bruneau, P. H. Dixneuf, *Chem. Rev.* **2012**, *112*, 5879-5918.
- [136] a) S. De Sarkar, W. Liu, S. I. Kozhushkov, L. Ackermann, *Adv. Synth. Catal.* **2014**, *356*, 1461-1479; b) P. B. Arockiam, C. Bruneau, P. H. Dixneuf, *Chem. Rev.* **2012**, *112*, 5879-5918.
- [137] a) P. V. Thanikachalam, R. K. Maurya, V. Garg, V. Monga, *Eur. J. Med. Chem.* **2019**, *180*, 562-612; b) N. Chadha, O. Silakari, *Eur. J. Med. Chem.* **2017**, *134*, 159-184; c) R. D. Taylor, M. MacCoss, A. D. Lawson, *J. Med. Chem.* **2014**, *57*, 5845-5859; d) A. J. Kochanowska-Karamyan, M. T. Hamann, *Chem. Rev.* **2010**, *110*, 4489-4497; e) F. R. de Sa Alves, E. J. Barreiro, C. A. Manssour Fraga, *Mini-Rev. Med. Chem.* **2009**, *9*, 782-793; f) C. V. Galliford, K. A. Scheidt, *Angew. Chem. Int. Ed.* **2007**, *46*, 8748-8758; g) G. W. Gribble, *J. Chem. Soc. Perkin Trans. 1* **2000**, 1045-1075; h) A. Andreani, M. Rambaldi, *J. Heterocycl. Chem.* **1988**, *25*, 1519-1523.
- [138] F. Mao, W. Ni, X. Xu, H. Wang, J. Wang, M. Ji, J. Li, *Molecules* **2016**, *21*, 75.
- [139] a) N. Siddiqui, A. Husain, L. Chaudhry, M. S. Alam, M. Mitra, P. S. Bhasin, *J. Appl. Pharm. Sci.* **2011**, 12-19; b) D. A. Sica, T. W. Gehr, S. Ghosh, *Clin. Pharmacokinet.* **2005**, *44*, 797-814.

- [140] L. Ackermann, A. Althammer, R. Born, *Tetrahedron* **2008**, *64*, 6115-6124.
- [141] a) S. Dutta, T. Bhattacharya, D. B. Werz, D. Maiti, *Chem* **2021**, *7*, 555-605; b) R. M. Magid, *Tetrahedron* **1980**, *36*, 1901-1930.
- [142] a) Y. Tao, B. Wang, J. Zhao, Y. Song, L. Qu, J. Qu, *J. Org. Chem.* **2012**, *77*, 2942-2946; b) J. D. Weaver, A. Recio, III, A. J. Grenning, J. A. Tunge, *Chem. Rev.* **2011**, *111*, 1846-1913; c) S. Lu, Z. Xu, M. Bao, Y. Yamamoto, *Angew. Chem. Int. Ed.* **2008**, *47*, 4366-4369; d) M. Bao, H. Nakamura, Y. Yamamoto, *J. Am. Chem. Soc.* **2001**, *123*, 759-760; e) J. A. Marshall, *Chem. Rev.* **2000**, *100*, 3163-3186.
- [143] N. K. Mishra, S. Sharma, J. Park, S. Han, I. S. Kim, *ACS Catal.* **2017**, *7*, 2821-2847.
- [144] a) C.-S. Wang, P. H. Dixneuf, J.-F. o. Soulé, *Chem. Rev.* **2018**, *118*, 7532-7585; b) J. Twilton, C. Le, P. Zhang, M. H. Shaw, R. W. Evans, D. W. MacMillan, *Nat. Rev. Chem.* **2017**, *1*, 0052; c) D. C. Fabry, M. Rueping, *Acc. Chem. Res.* **2016**, *49*, 1969-1979; d) J. M. Narayanam, C. R. Stephenson, *Chem. Soc. Rev.* **2011**, *40*, 102-113.
- [145] a) X. Zhang, D. W. MacMillan, *J. Am. Chem. Soc.* **2017**, *139*, 11353-11356; b) D. R. Heitz, J. C. Tellis, G. A. Molander, *J. Am. Chem. Soc.* **2016**, *138*, 12715-12718; c) M. H. Shaw, V. W. Shurtleff, J. A. Terrett, J. D. Cuthbertson, D. W. MacMillan, *Science* **2016**, *352*, 1304-1308; d) J. D. Cuthbertson, D. W. MacMillan, *Nature* **2015**, *519*, 74-77.
- [146] a) P. Natarajan, N. Kumar, M. Sharma, *Org. Chem. Front.* **2016**, *3*, 1265-1270; b) M. Osawa, H. Nagai, M. Akita, *Dalton Trans.* **2007**, 827-829.
- [147] J. Struwe, K. Korvorapun, A. Zangarelli, L. Ackermann, *Chem. Eur. J.* **2021**, *27*, 16237-16241.
- [148] K. Korvorapun, J. Struwe, R. Kuniyil, A. Zangarelli, A. Casnati, M. Waeterschoot, L. Ackermann, *Angew. Chem. Int. Ed.* **2020**, *59*, 18103-18109.
- [149] a) V. Garg, R. K. Maurya, P. V. Thanikachalam, G. Bansal, V. Monga, *Eur. J. Med. Chem.* **2019**, *180*, 562-612; b) R. D. Taylor, M. MacCoss, A. D. G. Lawson, *J. Med. Chem.* **2014**, *57*, 5845-5859; c) A. Srivastava, S. Pandeya, *Int. J. Curr.*

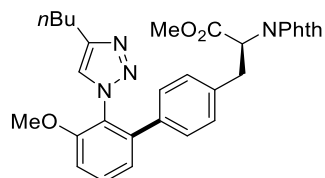
- Pharm. Rev. Res* **2011**, *4*, 5-8; d) C. V. Galliford, K. A. Scheidt, *Angew. Chem. Int. Ed.* **2007**, *46*, 8748-8758; e) Y. Wang, J. B. Gloer, J. A. Scott, D. Malloch, *J. Nat. Prod.* **1995**, *58*, 93-99.
- [150] a) T. A. Shah, P. B. De, S. Pradhan, T. Punniyamurthy, *Chem. Commun.* **2019**, *55*, 572-587; b) Y. Yang, Z. Shi, *Chem. Commun.* **2018**, *54*, 1676-1685.
- [151] a) D. Wang, X. Chen, J. J. Wong, L. Jin, M. Li, Y. Zhao, K. N. Houk, Z. Shi, *Nat. Commun.* **2021**, *12*, 524; b) I. Choi, A. M. Messinis, L. Ackermann, *Angew. Chem. Int. Ed.* **2020**, *59*, 12534-12540; c) B. Dong, J. Qian, M. Li, Z.-J. Wang, M. Wang, D. Wang, C. Yuan, Y. Han, Y. Zhao, Z. Shi, *Science Advances* **2020**, *6*, eabd1378; d) W. Wang, J. Wu, R. Kuniyil, A. Kopp, R. N. Lima, L. Ackermann, *Chem* **2020**, *6*, 3428-3439; e) A. J. Borah, Z. Shi, *J. Am. Chem. Soc.* **2018**, *140*, 6062-6066; f) Y. Kim, Y. Park, S. Chang, *ACS Cent. Sci.* **2018**, *4*, 768-775.
- [152] T. Fukuda, R. Maeda, M. Iwao, *Tetrahedron* **1999**, *55*, 9151-9162.
- [153] Y. Yang, X. Qiu, Y. Zhao, Y. Mu, Z. Shi, *J. Am. Chem. Soc.* **2016**, *138*, 495-498.
- [154] a) S. C. Fosu, C. M. Hambira, A. D. Chen, J. R. Fuchs, D. A. Nagib, *Chem* **2019**, *5*, 417-428; b) T. Brandhofer, O. García Mancheño, *Eur. J. Org. Chem.* **2018**, *2018*, 6050-6067; c) K. Hirano, M. Miura, *Chem. Sci.* **2018**, *9*, 22-32; d) K. Liao, Y.-F. Yang, Y. Li, J. N. Sanders, K. N. Houk, D. G. Musaev, H. M. L. Davies, *Nat. Chem.* **2018**, *10*, 1048-1055; e) W. Ma, P. Gandeepan, J. Li, L. Ackermann, *Org. Chem. Front.* **2017**, *4*, 1435-1467; f) W. Song, S. I. Kozhushkov, L. Ackermann, *Angew. Chem. Int. Ed.* **2013**, *52*, 6576-6578; g) S. R. Neufeldt, M. S. Sanford, *Acc. Chem. Res.* **2012**, *45*, 936-946; h) H. M. L. Davies, D. Morton, *Chem. Soc. Rev.* **2011**, *40*, 1857-1869; i) R. J. Phipps, N. P. Grimster, M. J. Gaunt, *J. Am. Chem. Soc.* **2008**, *130*, 8172-8174.
- [155] a) J. Kalepu, L. T. Pilarski, *Molecules* **2019**, *24*, 830; b) K. M. Engle, T.-S. Mei, M. Wasa, J.-Q. Yu, *Acc. Chem. Res.* **2012**, *45*, 788-802.
- [156] A. Zangarelli, B. Yuan, L. Ackermann, *Isr. J. Chem.*, *n/a*, e202300103.
- [157] G. L. Trammel, R. Kuniyil, P. F. Crook, P. Liu, M. K. Brown, *J. Am. Chem. Soc.* **2021**, *143*, 16502-16511.
- [158] L. Ackermann, H. K. Potukuchi, D. Landsberg, R. Vicente, *Org. Lett.* **2008**, *10*, 170



- 3081-3084.
- [159] M. Seki, M. Nagahama, *J. Org. Chem.* **2011**, *76*, 10198-10206.
- [160] Z.-Y. Tian, C.-P. Zhang, *Org. Chem. Front.* **2022**, *9*, 2220-2227.
- [161] V. P. Böhm, T. Weskamp, C. W. Gstöttmayr, W. A. Herrmann, *Angew. Chem. Int. Ed.* **2000**, *39*, 1602-1604.
- [162] a) A. Bechtoldt, M. E. Baumert, L. Vaccaro, L. Ackermann, *Green Chem.* **2018**, *20*, 398-402; b) L. Xu, C. Zhang, Y. He, L. Tan, D. Ma, *Angew. Chem. Int. Ed.* **2016**, *55*, 321-325.
- [163] S. R. Yetra, T. Rogge, S. Warratz, J. Struwe, W. Peng, P. Vana, L. Ackermann, *Angew. Chem. Int. Ed.* **2019**, *58*, 7490-7494.
- [164] Y. Kim, J. Park, S. Chang, *Org. Lett.* **2016**, *18*, 1892-1895.
- [165] R. A. Bunce, B. Nammalwar, *J. Heterocycl. Chem.* **2009**, *46*, 172-177.

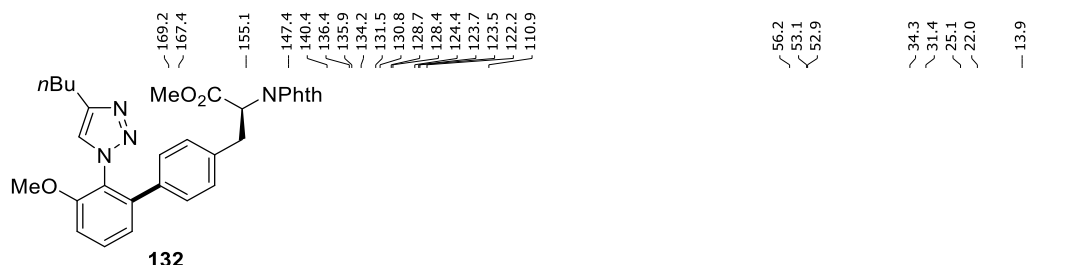
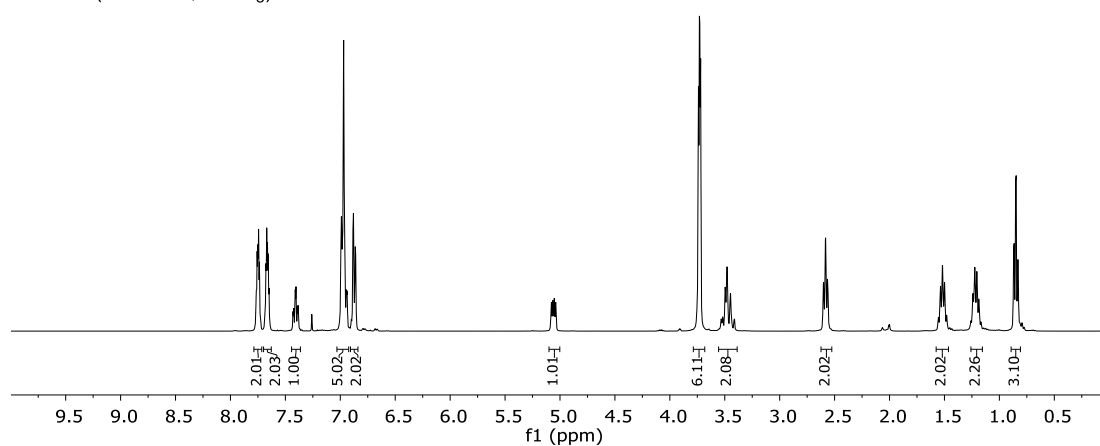
## 7 NMR Spectra

### 7.1 Ruthenium-Catalyzed C–H Arylation with Sulfonium Salts



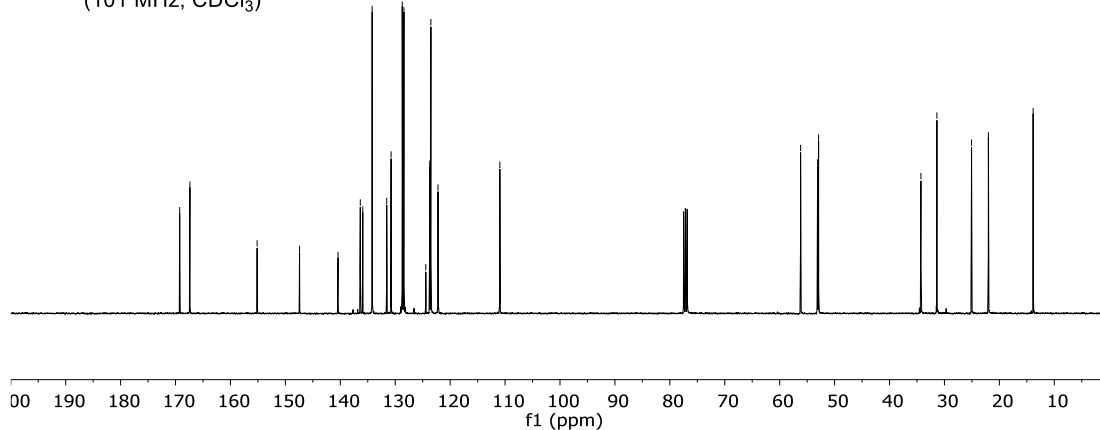
**132**

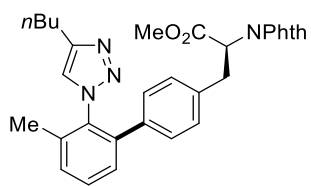
<sup>1</sup>H-NMR  
(400 MHz, CDCl<sub>3</sub>)



**132**

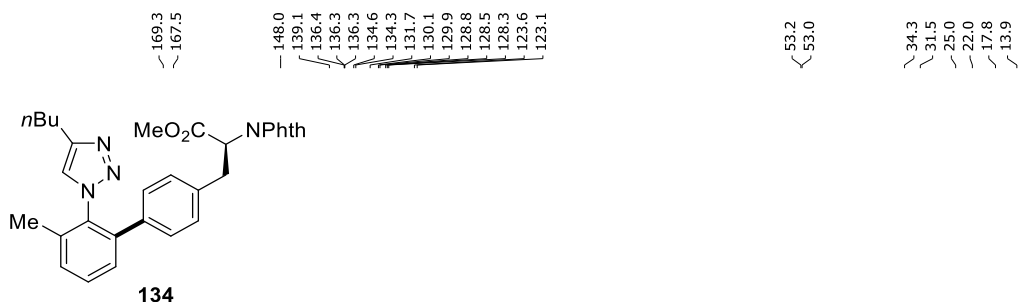
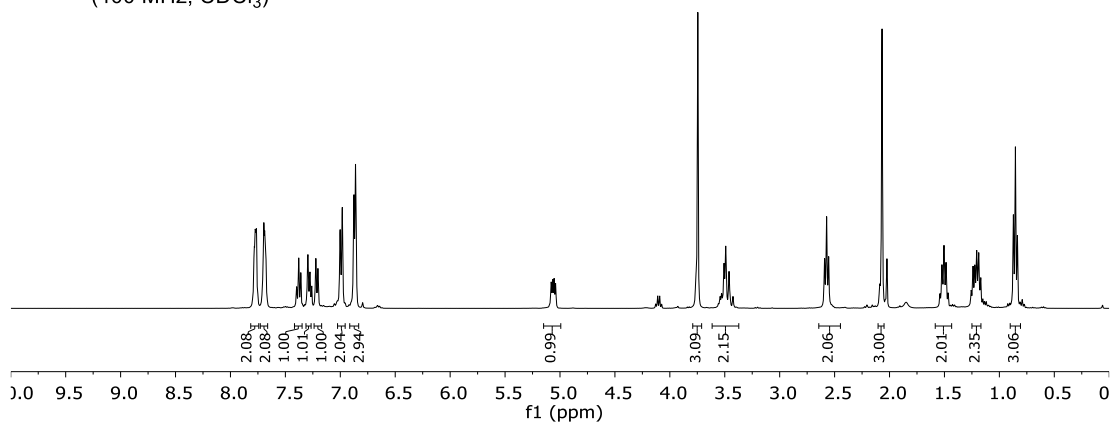
<sup>13</sup>C-NMR  
(101 MHz, CDCl<sub>3</sub>)





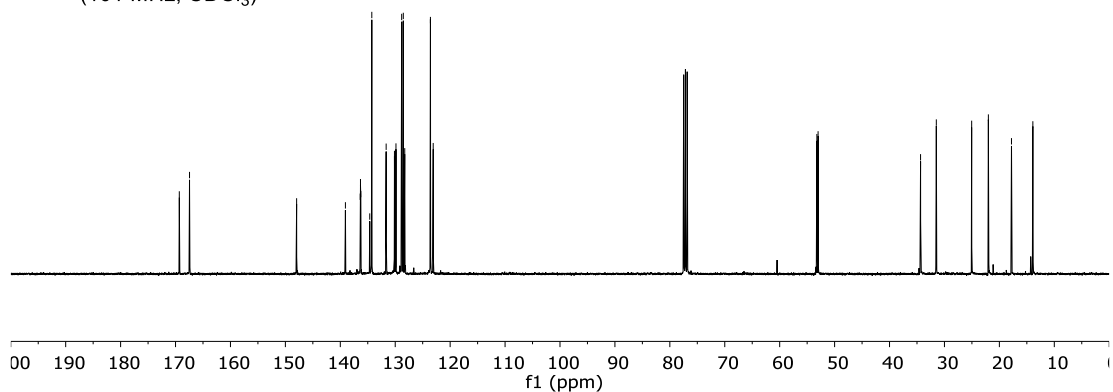
**134**

<sup>1</sup>H-NMR  
(400 MHz, CDCl<sub>3</sub>)

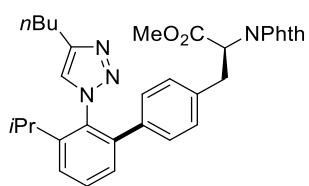


**134**

<sup>13</sup>C-NMR  
(101 MHz, CDCl<sub>3</sub>)

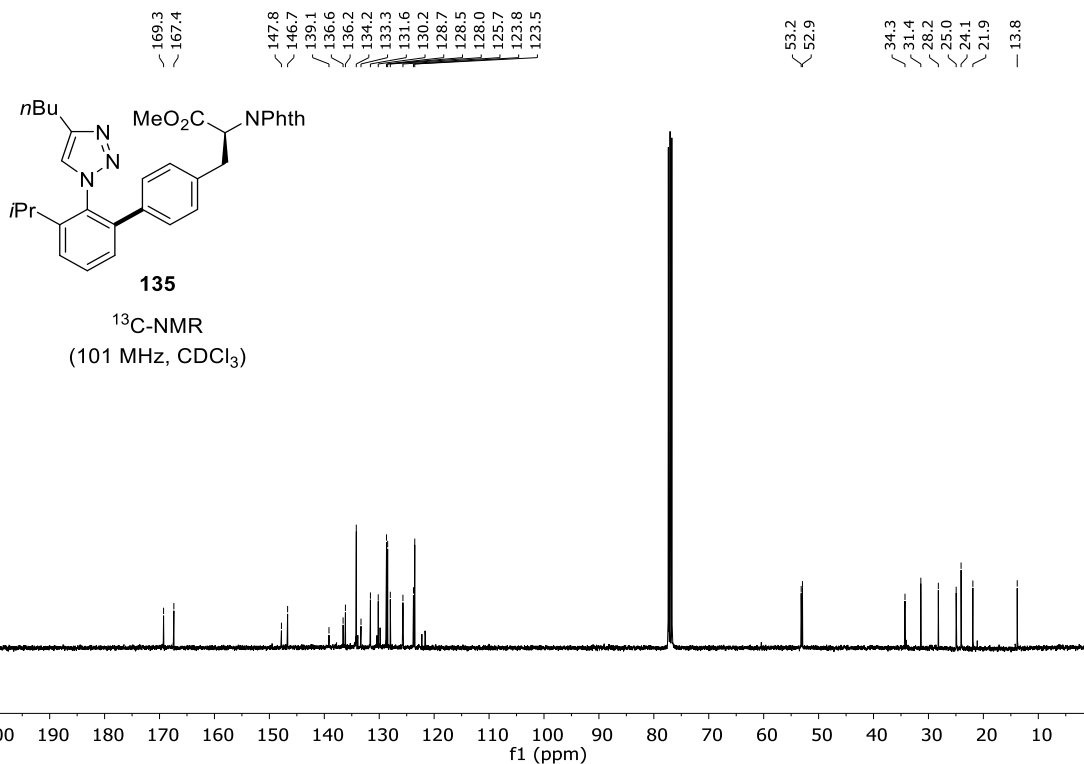
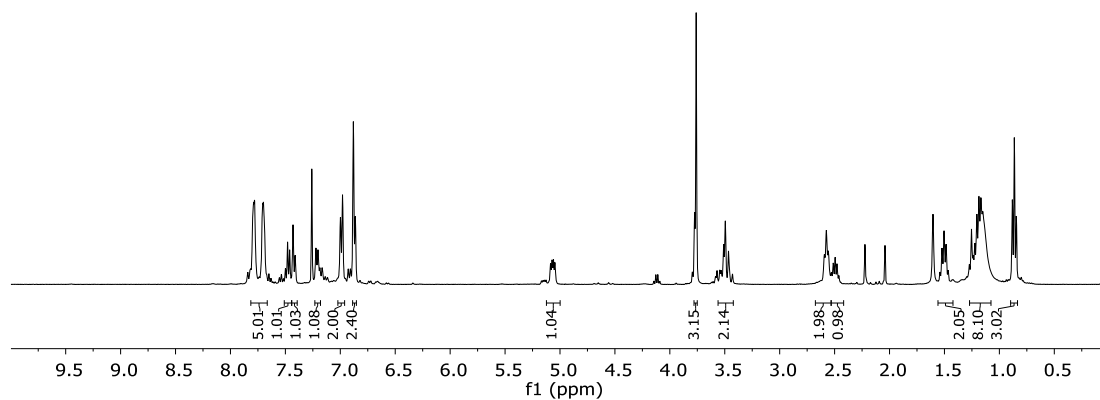


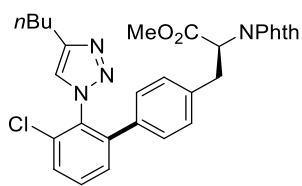
# NMR Spectra



**135**

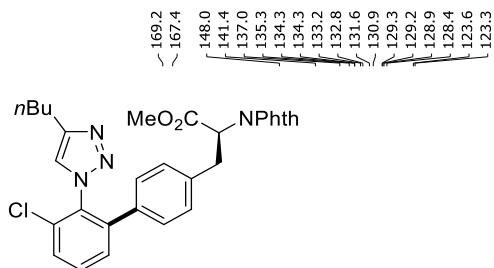
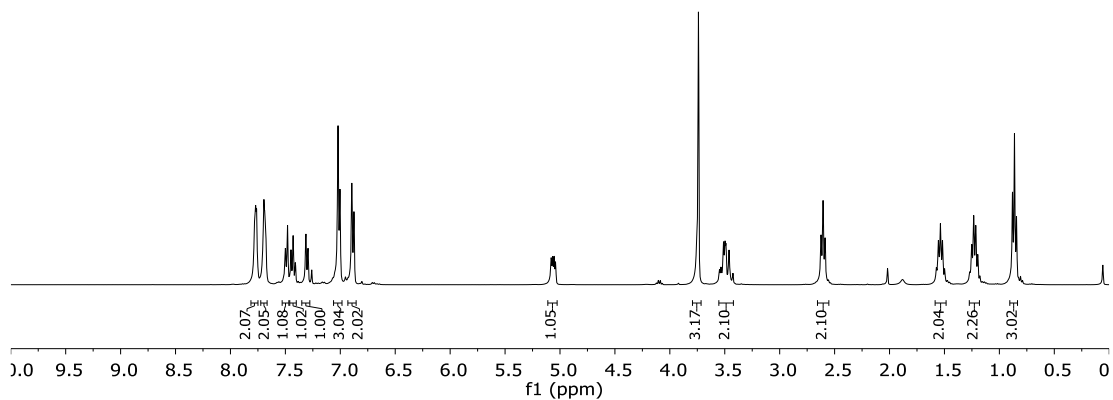
<sup>1</sup>H-NMR  
(400 MHz, CDCl<sub>3</sub>)





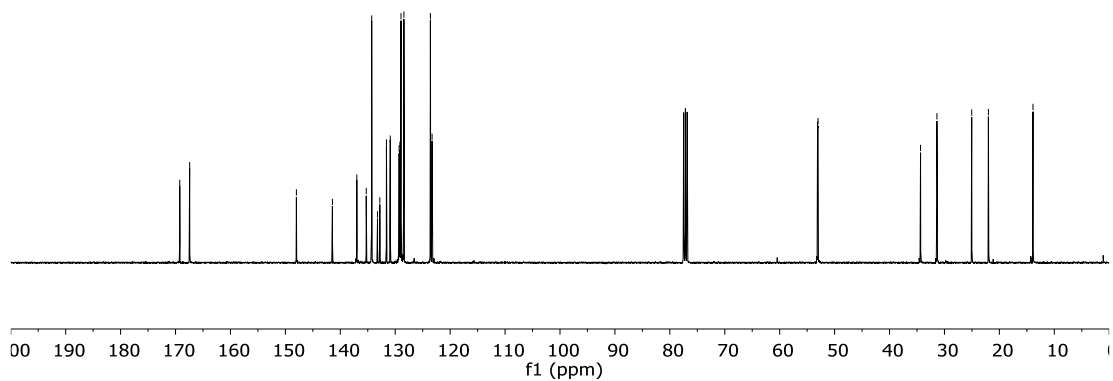
**136**

<sup>1</sup>H-NMR  
(400 MHz, CDCl<sub>3</sub>)

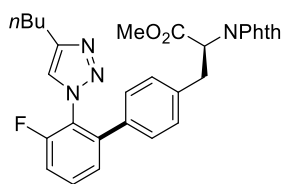


**136**

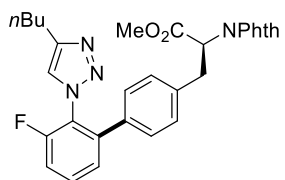
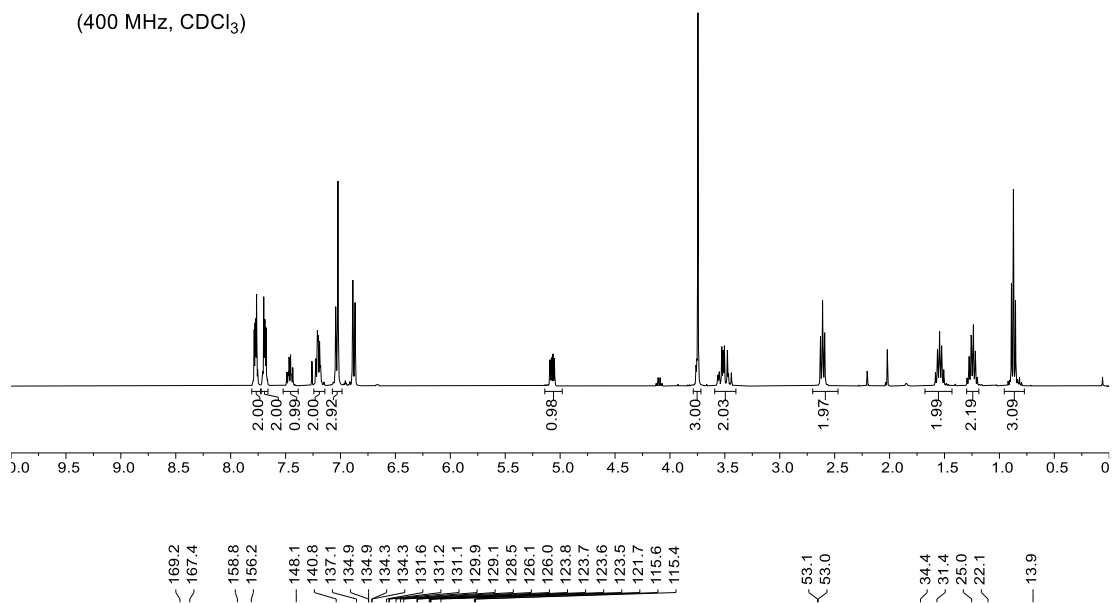
<sup>13</sup>C-NMR  
(101 MHz, CDCl<sub>3</sub>)



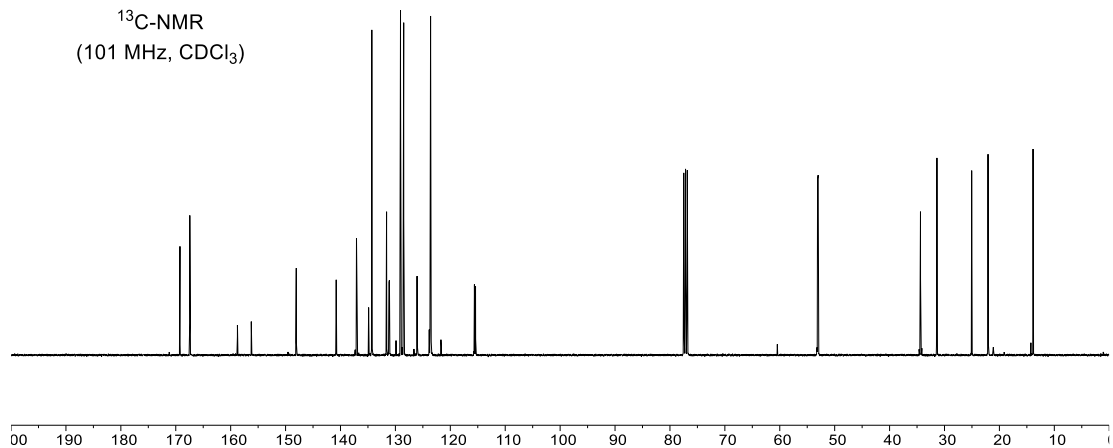
# NMR Spectra

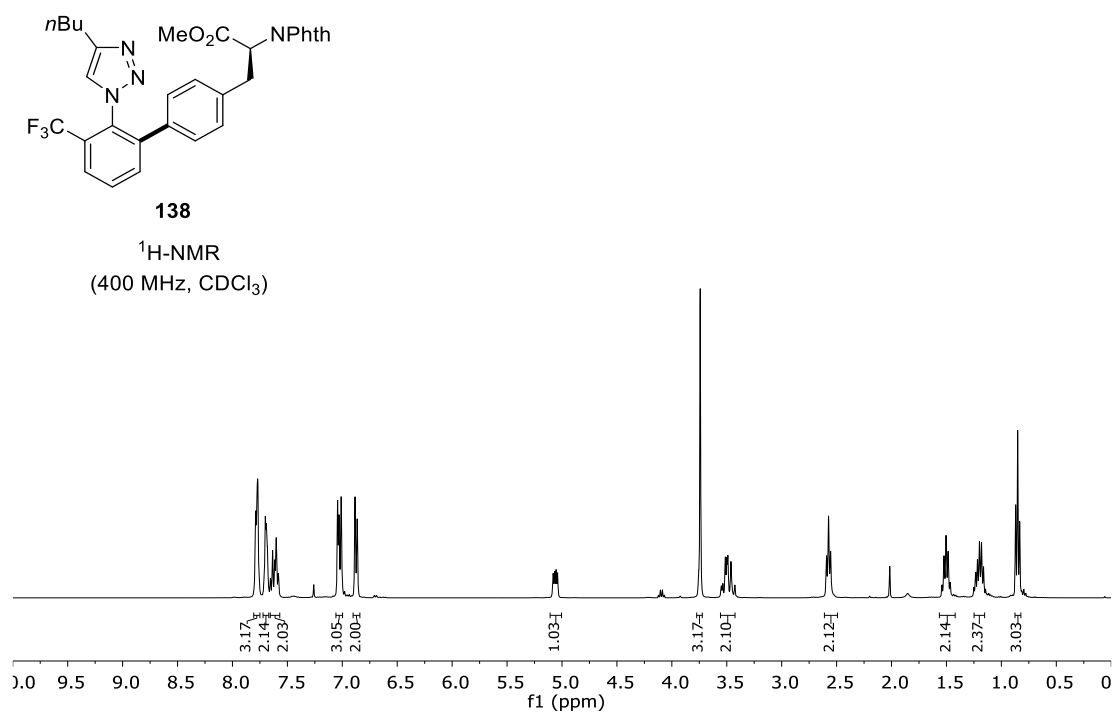
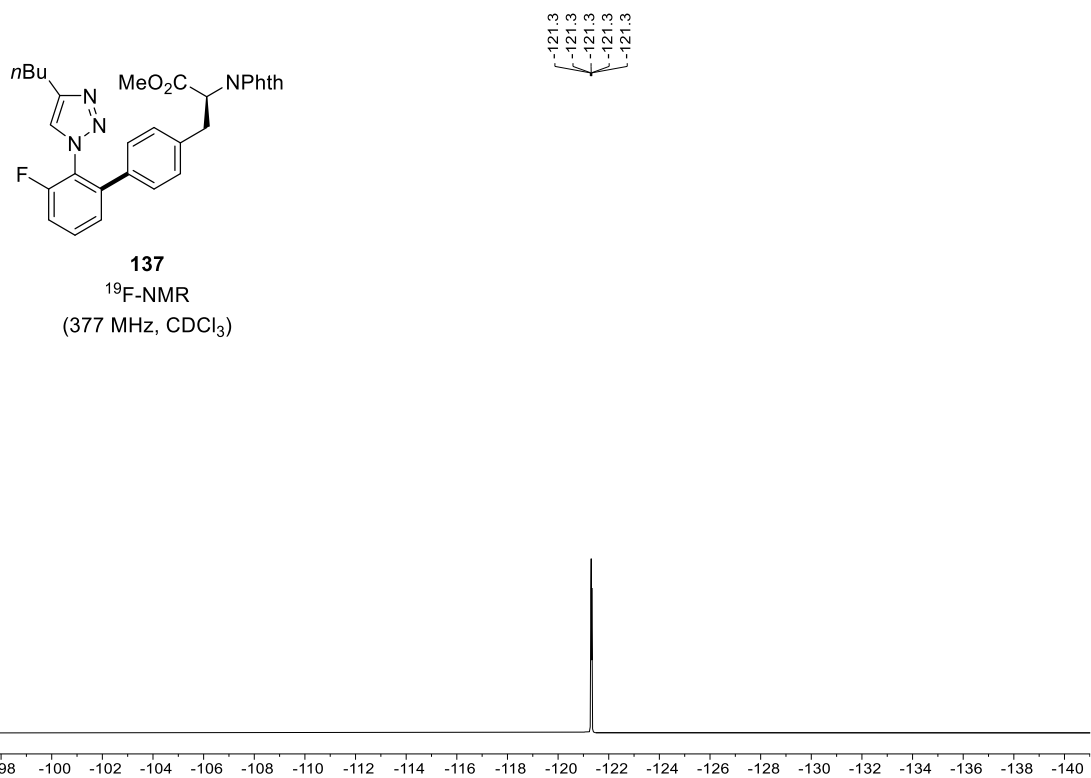


**137**  
<sup>1</sup>H-NMR  
 (400 MHz, CDCl<sub>3</sub>)

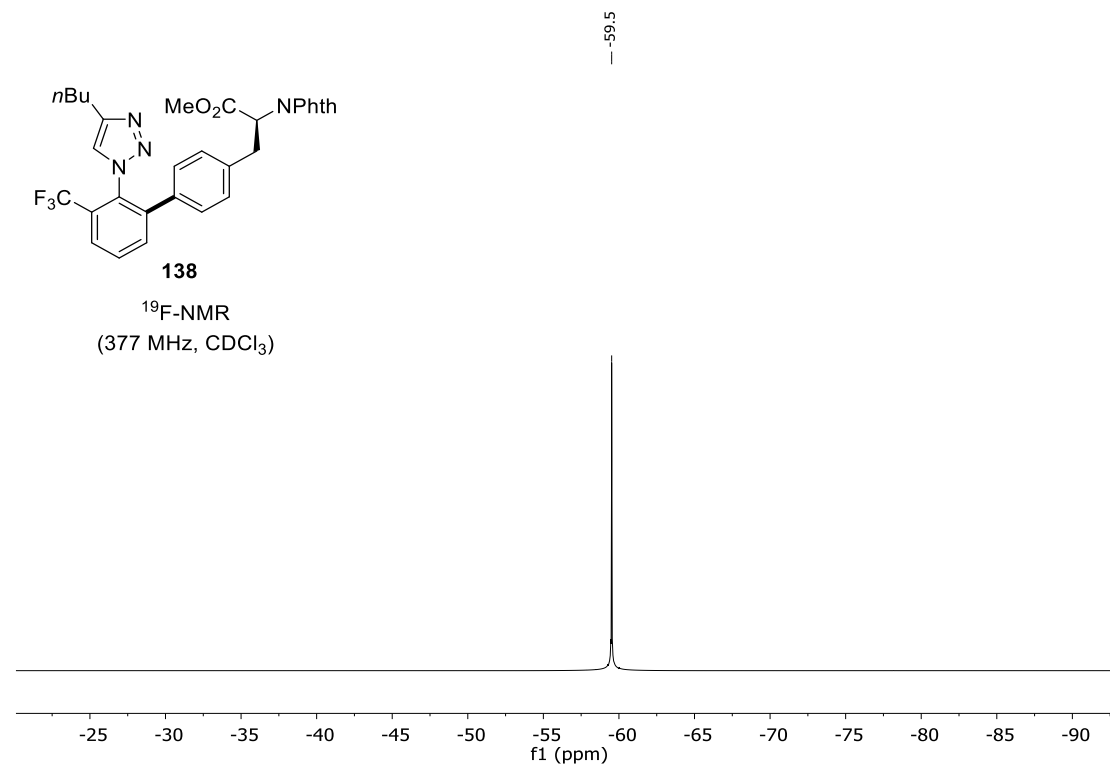
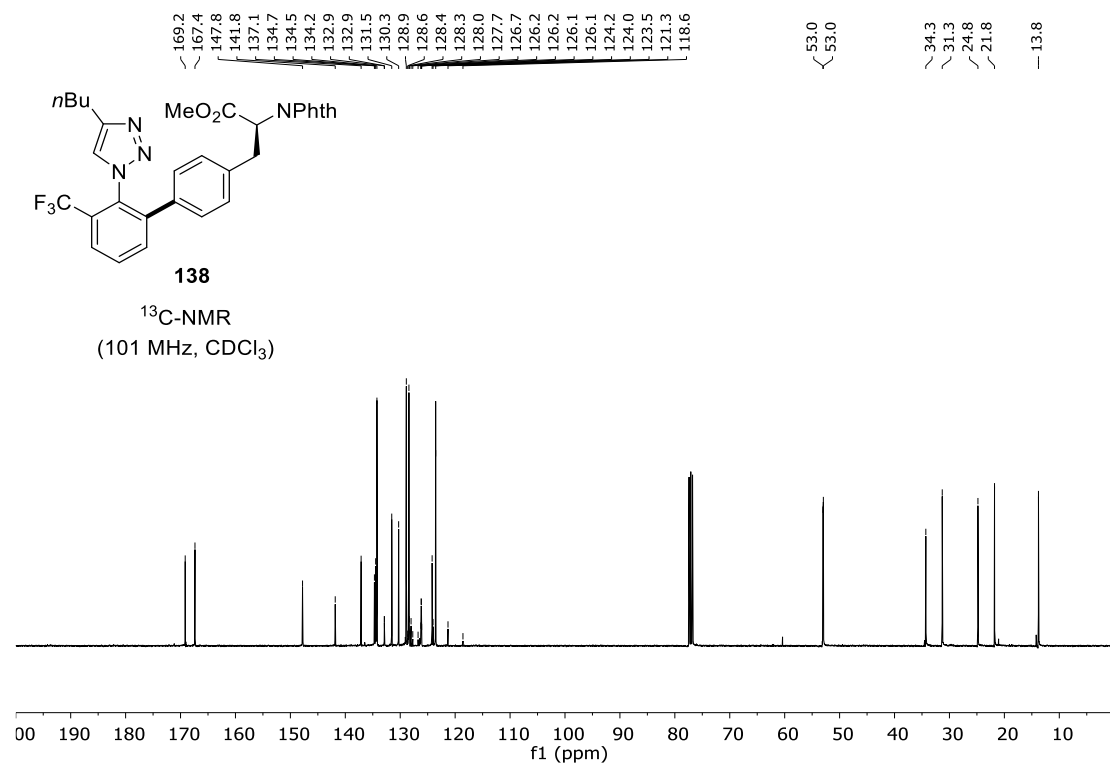


**137**  
<sup>13</sup>C-NMR  
 (101 MHz, CDCl<sub>3</sub>)

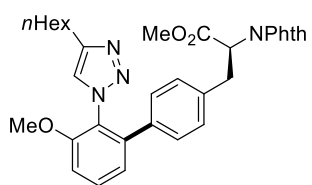




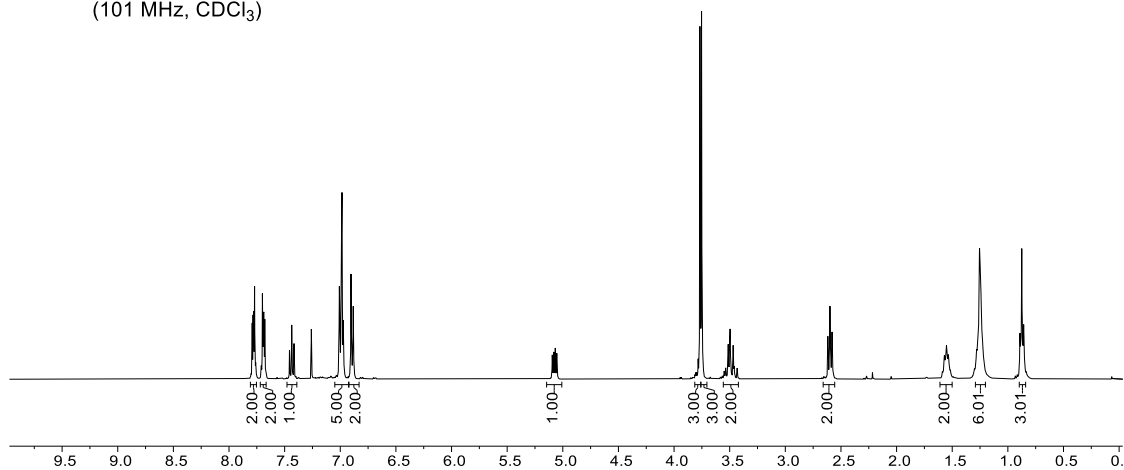
# NMR Spectra



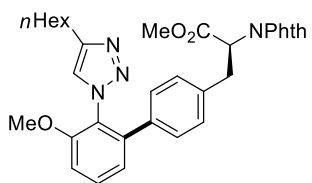




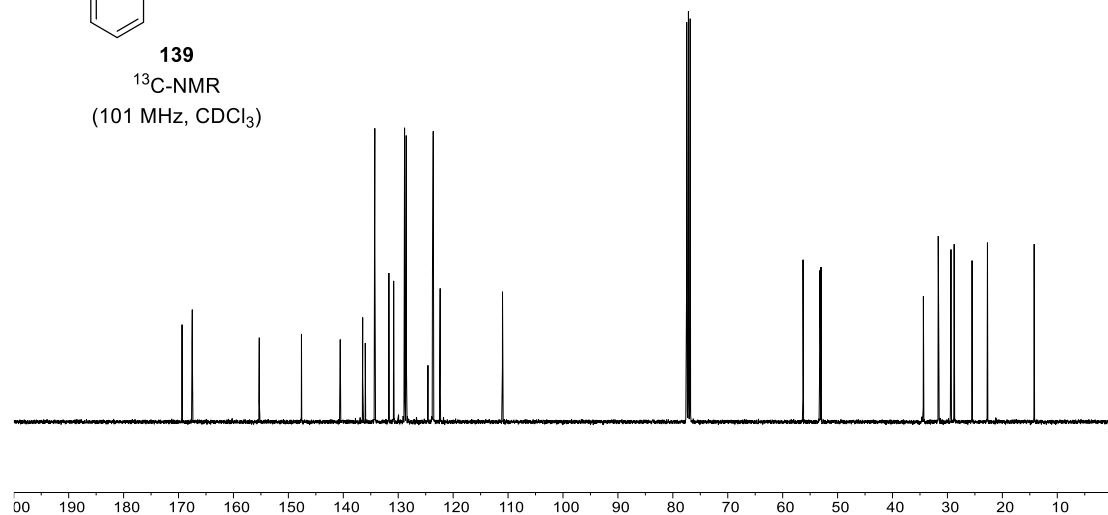
**139**  
<sup>13</sup>C-NMR  
 (101 MHz, CDCl<sub>3</sub>)



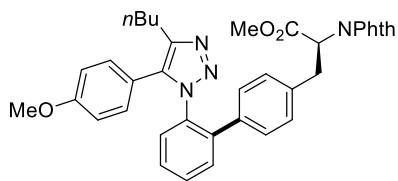
- |       |       |       |       |       |       |       |       |       |       |       |       |       |       |       |       |       |      |      |      |      |      |      |      |      |      |      |
|-------|-------|-------|-------|-------|-------|-------|-------|-------|-------|-------|-------|-------|-------|-------|-------|-------|------|------|------|------|------|------|------|------|------|------|
| 169.4 | 167.5 | 155.3 | 147.6 | 140.6 | 136.5 | 136.0 | 134.3 | 131.7 | 130.8 | 128.8 | 128.5 | 124.6 | 123.8 | 123.6 | 122.4 | 111.0 | 56.3 | 53.2 | 53.0 | 34.4 | 31.7 | 29.4 | 28.8 | 25.5 | 22.7 | 14.2 |
|-------|-------|-------|-------|-------|-------|-------|-------|-------|-------|-------|-------|-------|-------|-------|-------|-------|------|------|------|------|------|------|------|------|------|------|



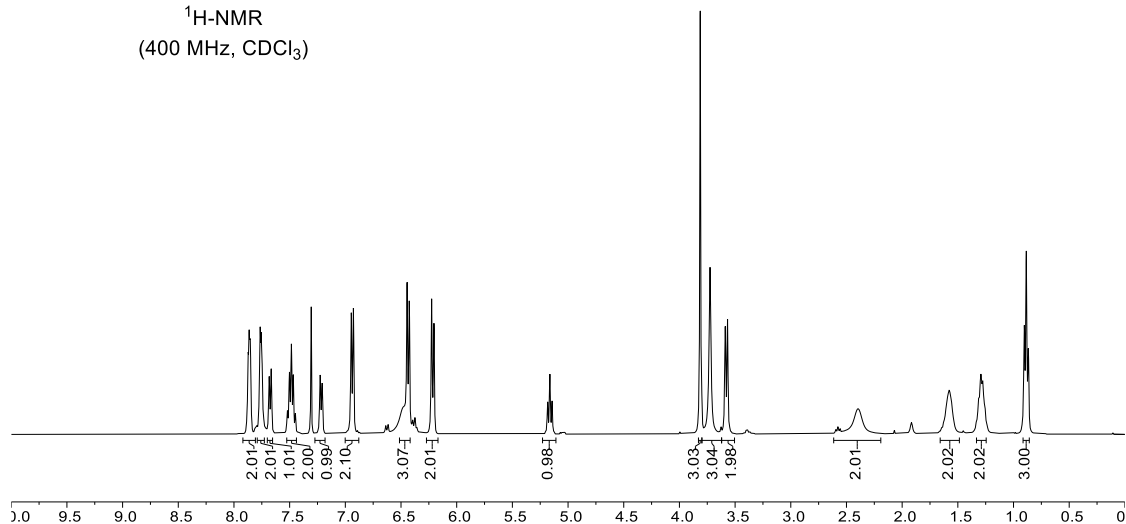
**139**  
<sup>13</sup>C-NMR  
 (101 MHz, CDCl<sub>3</sub>)



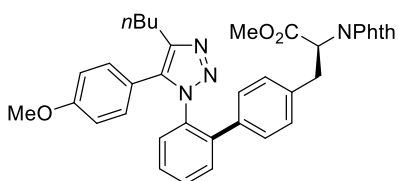
# NMR Spectra



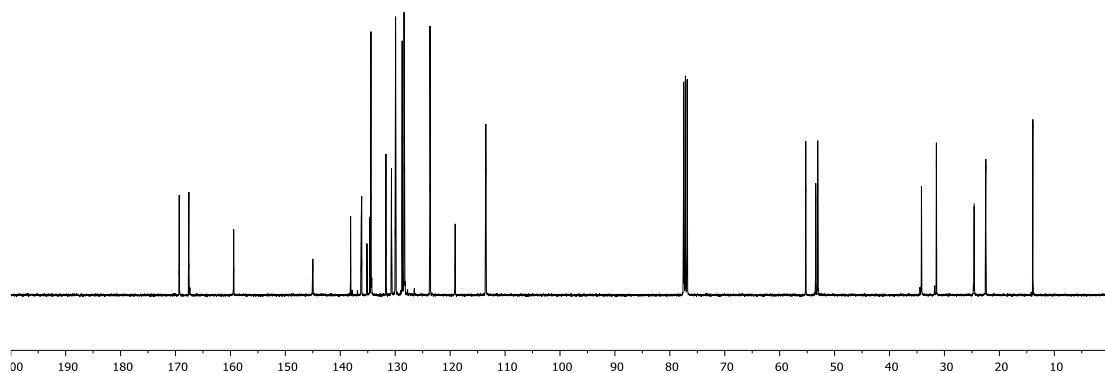
**140**  
<sup>1</sup>H-NMR  
 (400 MHz, CDCl<sub>3</sub>)

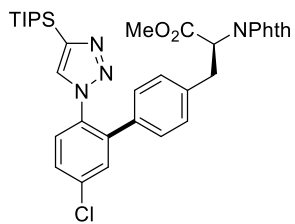


169.3  
 167.6  
 159.4  
 145.0  
 138.1  
 136.2  
 136.1  
 135.1  
 134.6  
 134.5  
 131.7  
 130.7  
 130.0  
 129.5  
 128.7  
 128.4  
 128.4  
 128.3  
 123.7  
 119.1  
 113.5  
 55.3  
 53.4  
 53.1  
 34.2  
 31.5  
 24.6  
 22.5  
 13.9



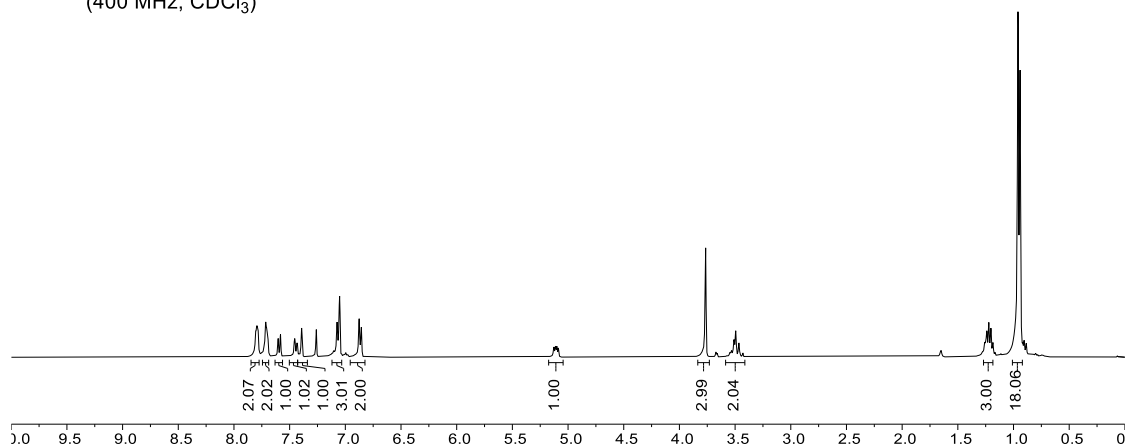
**140**  
<sup>13</sup>C-NMR  
 (101 MHz, CDCl<sub>3</sub>)



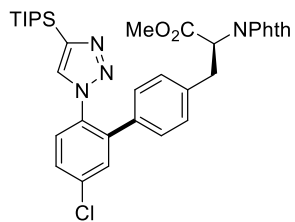


**141**

<sup>1</sup>H-NMR  
(400 MHz, CDCl<sub>3</sub>)

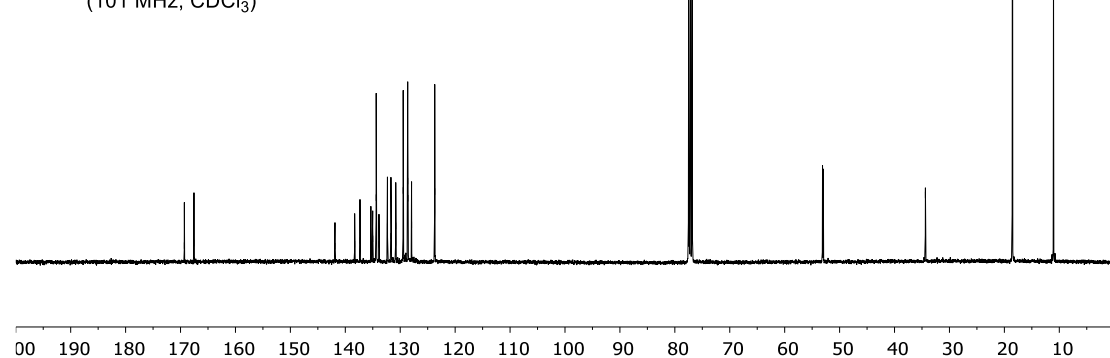


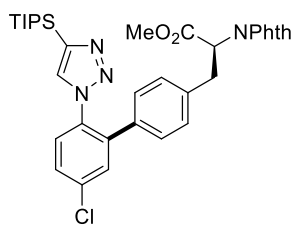
169.3  
167.6  
141.6  
138.3  
137.3  
137.3  
135.3  
135.3  
134.4  
133.5  
132.3  
131.7  
130.6  
129.5  
128.6  
128.6  
127.5  
123.7  
53.1  
53.0  
34.4  
18.5  
11.1



**141**

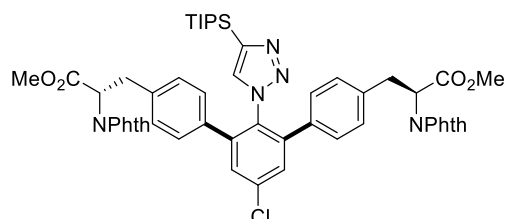
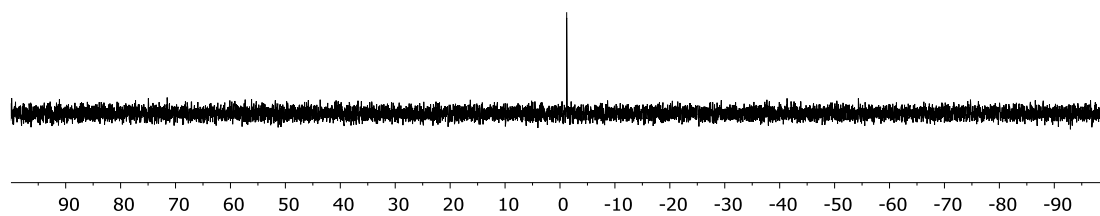
<sup>13</sup>C-NMR  
(101 MHz, CDCl<sub>3</sub>)





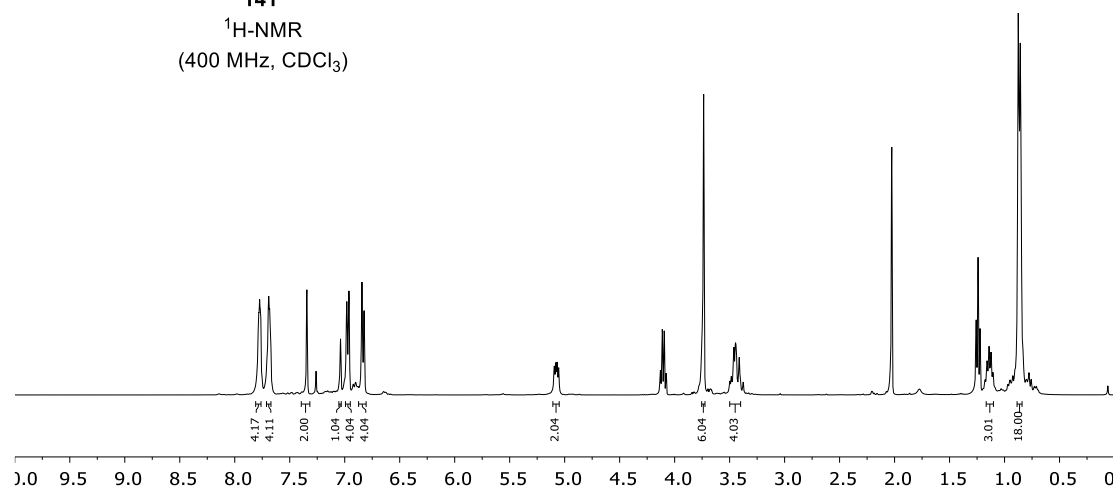
**141**

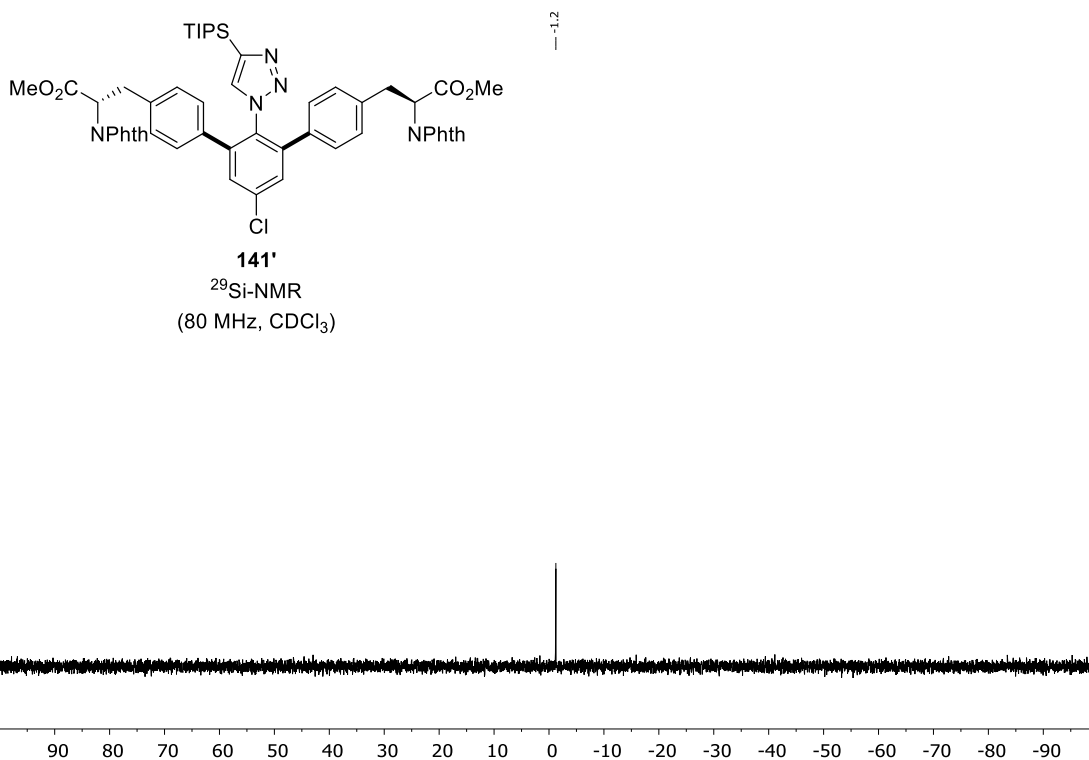
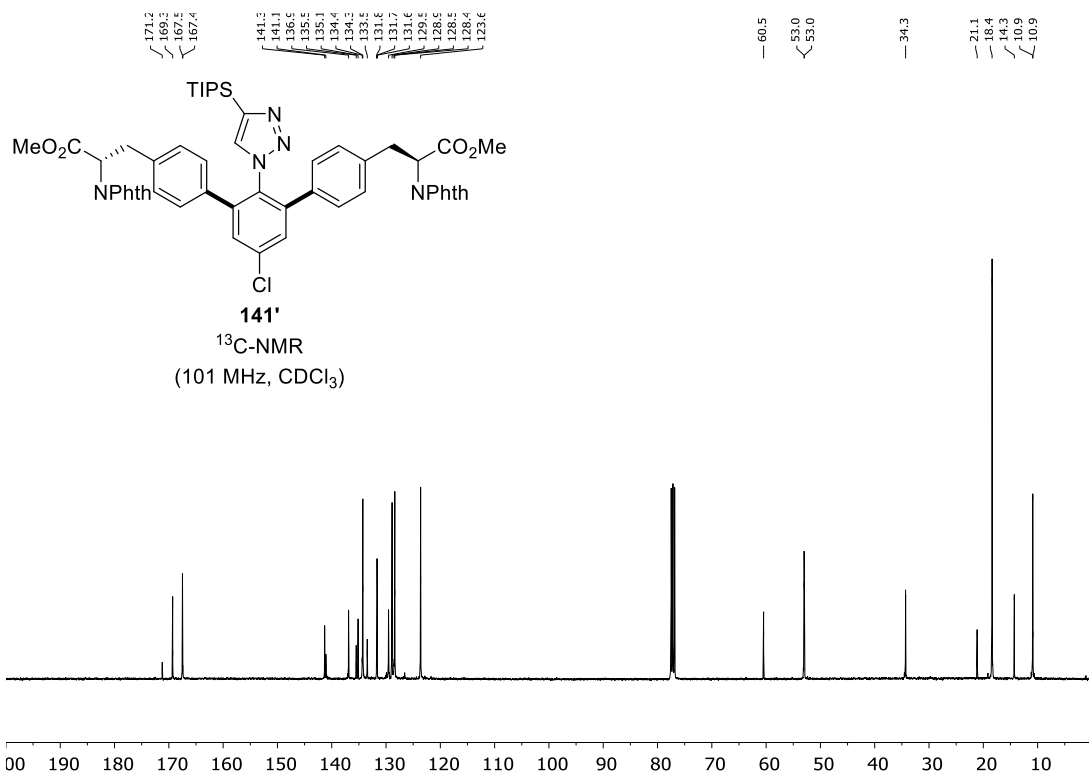
$^{29}\text{Si-NMR}$   
(80 MHz,  $\text{CDCl}_3$ )



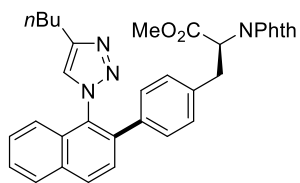
**141'**

$^1\text{H-NMR}$   
(400 MHz,  $\text{CDCl}_3$ )

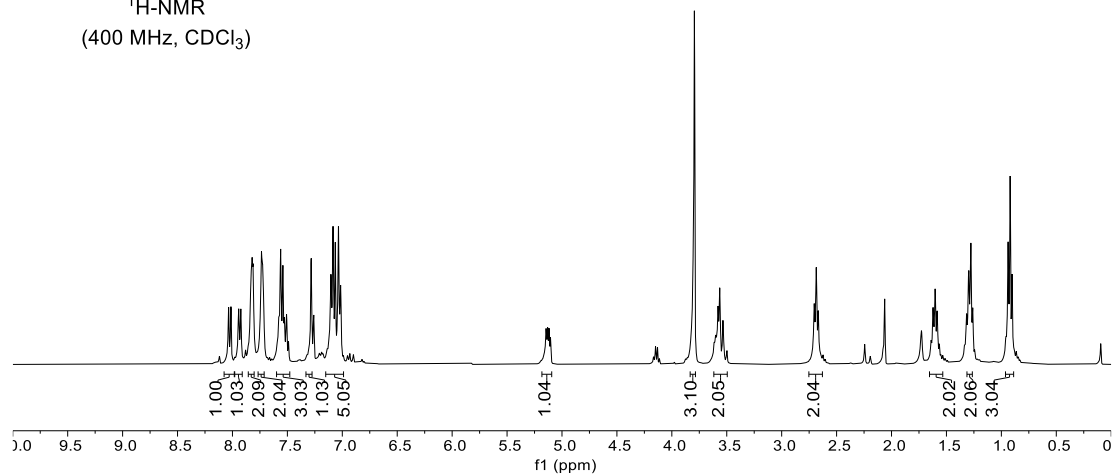




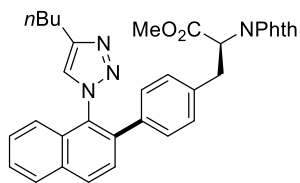
# NMR Spectra



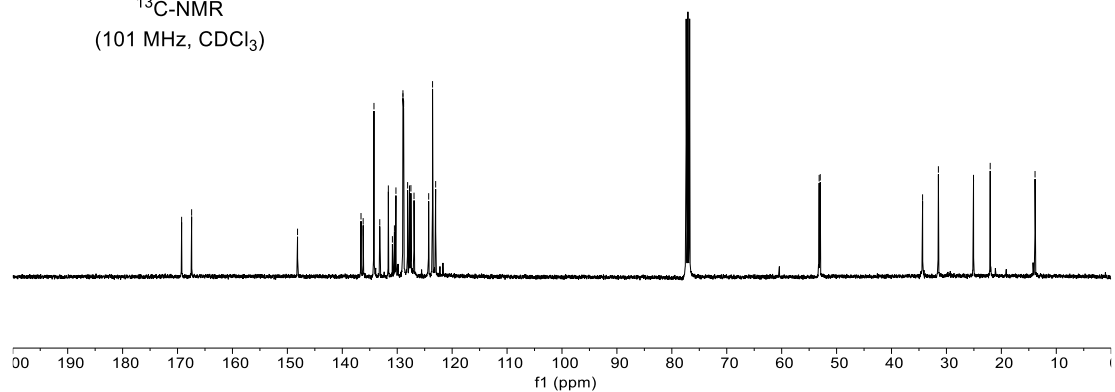
**142**  
<sup>1</sup>H-NMR  
 (400 MHz, CDCl<sub>3</sub>)

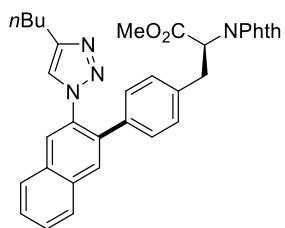


169.3  
 167.4  
 148.1  
 136.6  
 136.2  
 136.2  
 134.2  
 133.2  
 131.6  
 130.9  
 130.5  
 130.2  
 129.0  
 128.8  
 128.1  
 127.8  
 127.5  
 126.9  
 124.3  
 123.6  
 123.0  
 53.2  
 53.0  
 34.3  
 31.5  
 25.1  
 22.0  
 13.9

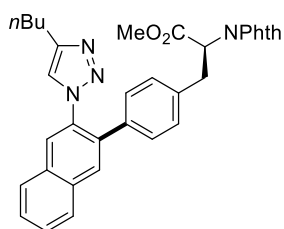
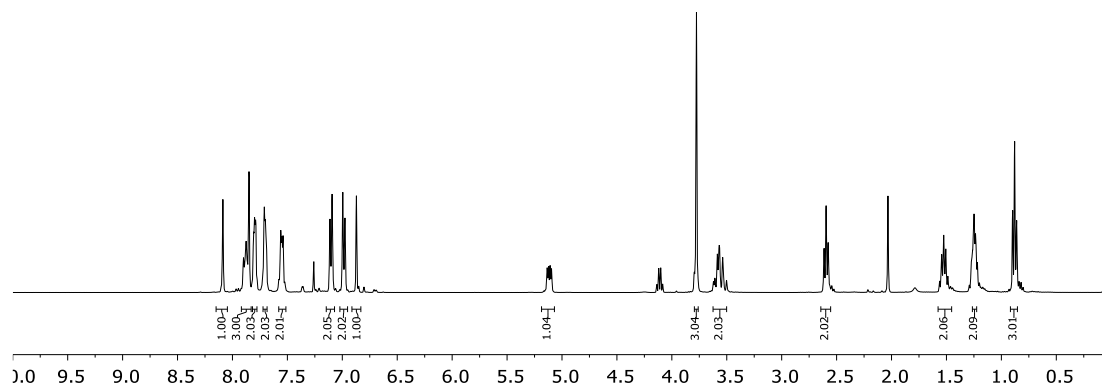


**142**  
<sup>13</sup>C-NMR  
 (101 MHz, CDCl<sub>3</sub>)

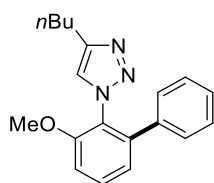
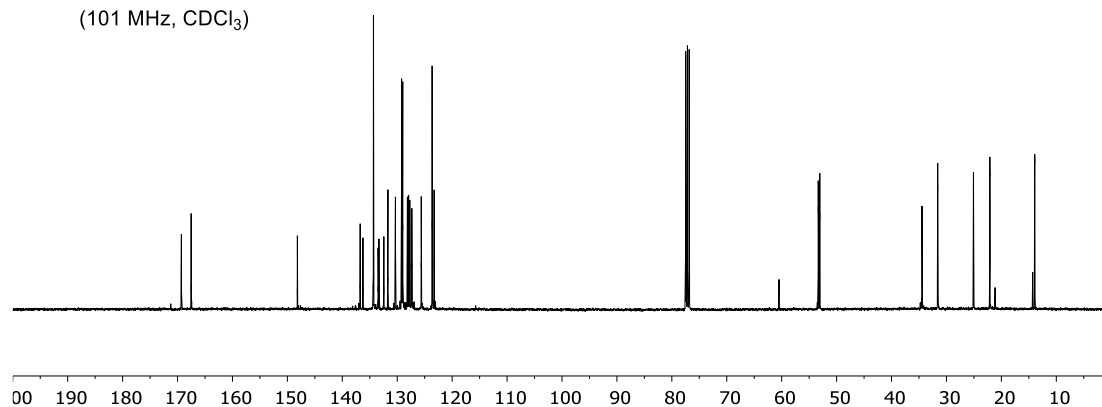




**143**  
<sup>1</sup>H-NMR  
 (400 MHz, CDCl<sub>3</sub>)

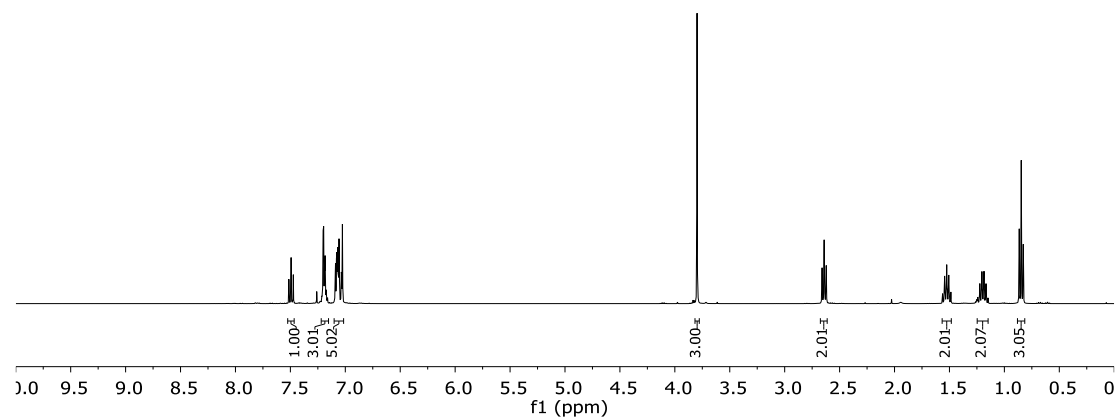


**143**  
<sup>13</sup>C-NMR  
 (101 MHz, CDCl<sub>3</sub>)



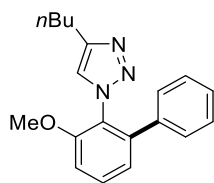
**145**  
<sup>1</sup>H-NMR  
 (400 MHz, CDCl<sub>3</sub>)

# NMR Spectra



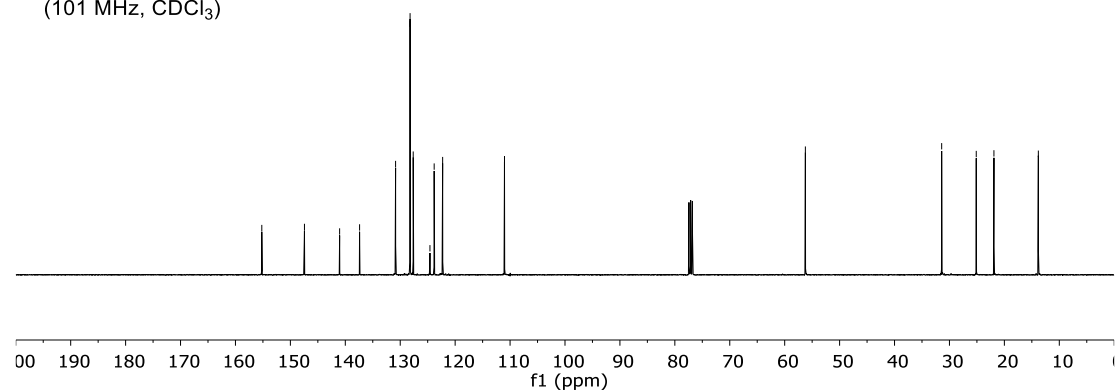
$^{13}\text{C}$  NMR chemical shifts (ppm):

- 155.2
- 147.4
- 141.0
- 137.4
- 130.8
- 128.2
- 128.2
- 127.6
- 124.6
- 123.8
- 122.3
- 111.0
- 56.2
- 31.4
- 25.1
- 21.9
- 13.8

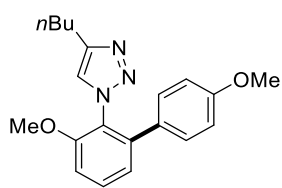


**145**

$^{13}\text{C}$ -NMR  
(101 MHz,  $\text{CDCl}_3$ )

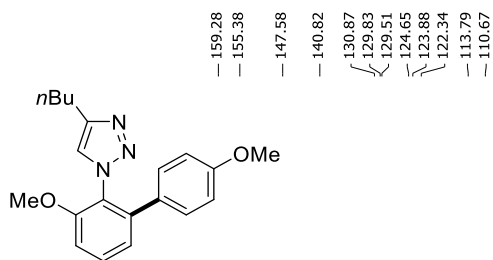
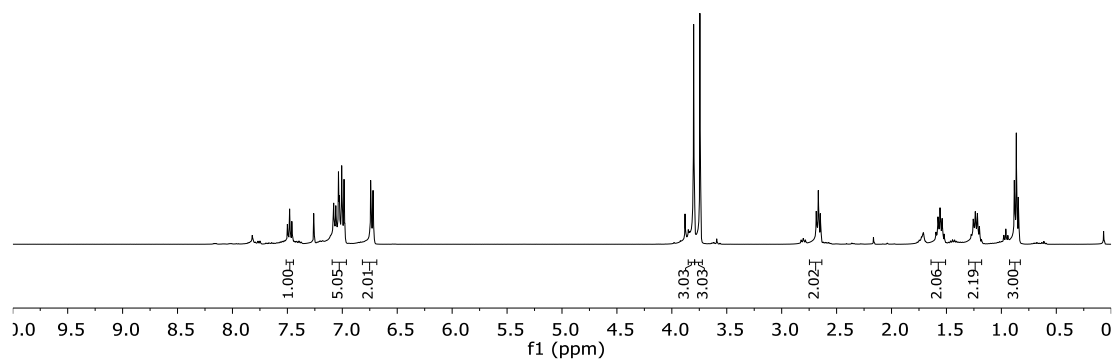






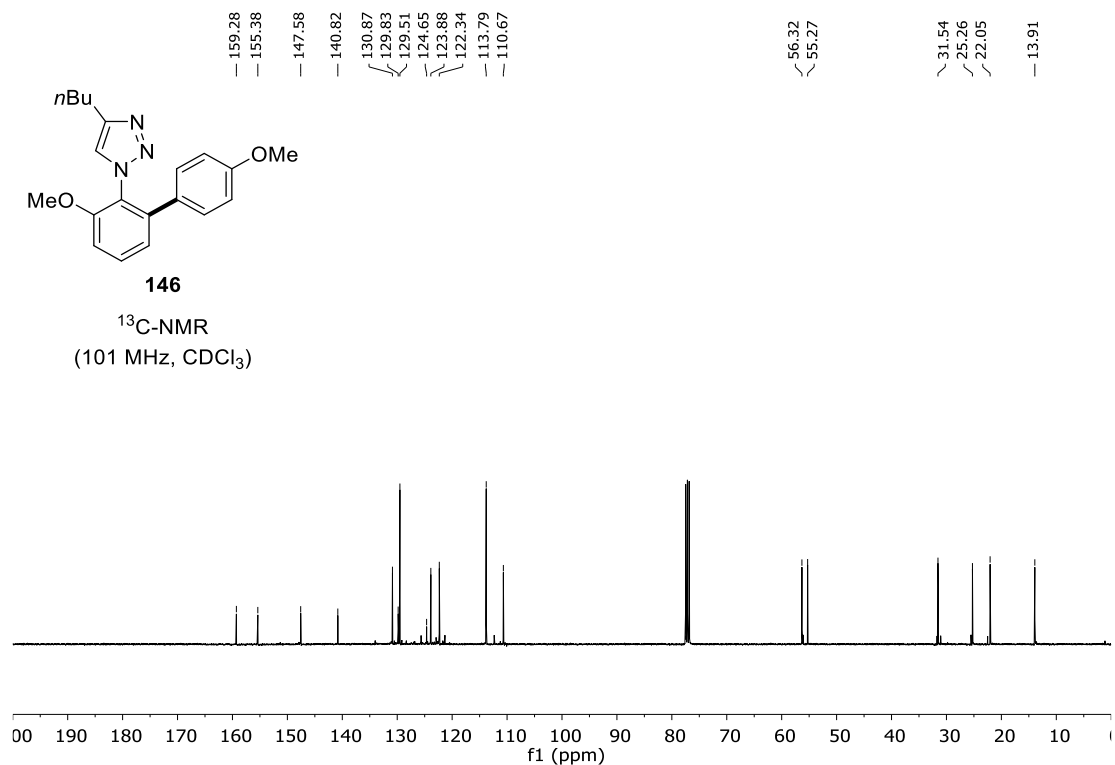
**146**

<sup>1</sup>H-NMR  
(400 MHz, CDCl<sub>3</sub>)

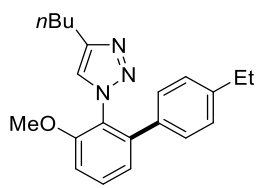


**146**

<sup>13</sup>C-NMR  
(101 MHz, CDCl<sub>3</sub>)

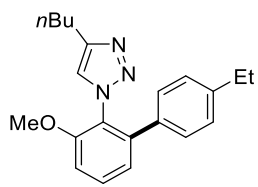
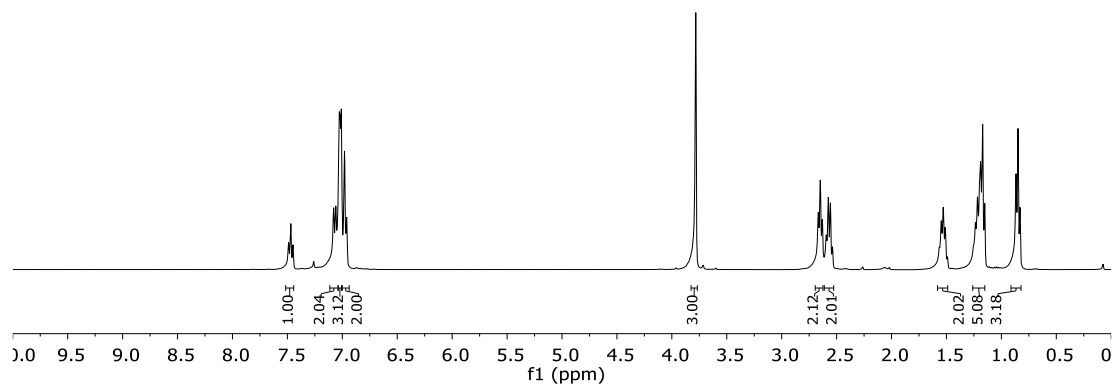


# NMR Spectra



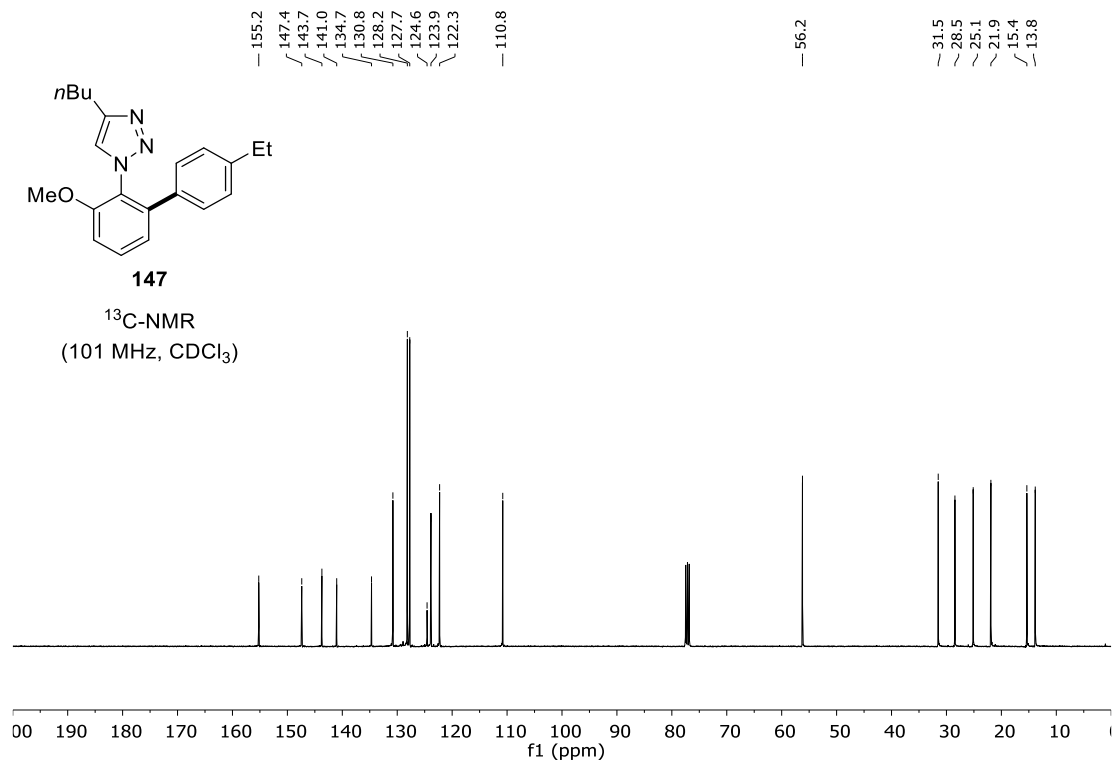
**147**

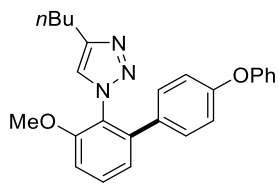
<sup>1</sup>H-NMR  
(400 MHz, CDCl<sub>3</sub>)



**147**

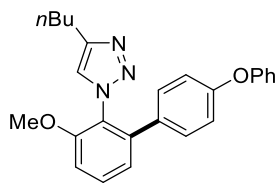
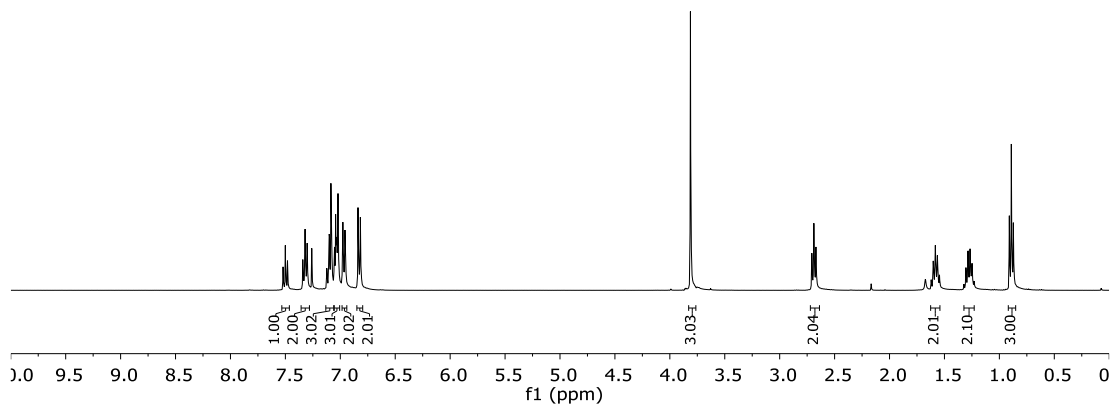
<sup>13</sup>C-NMR  
(101 MHz, CDCl<sub>3</sub>)





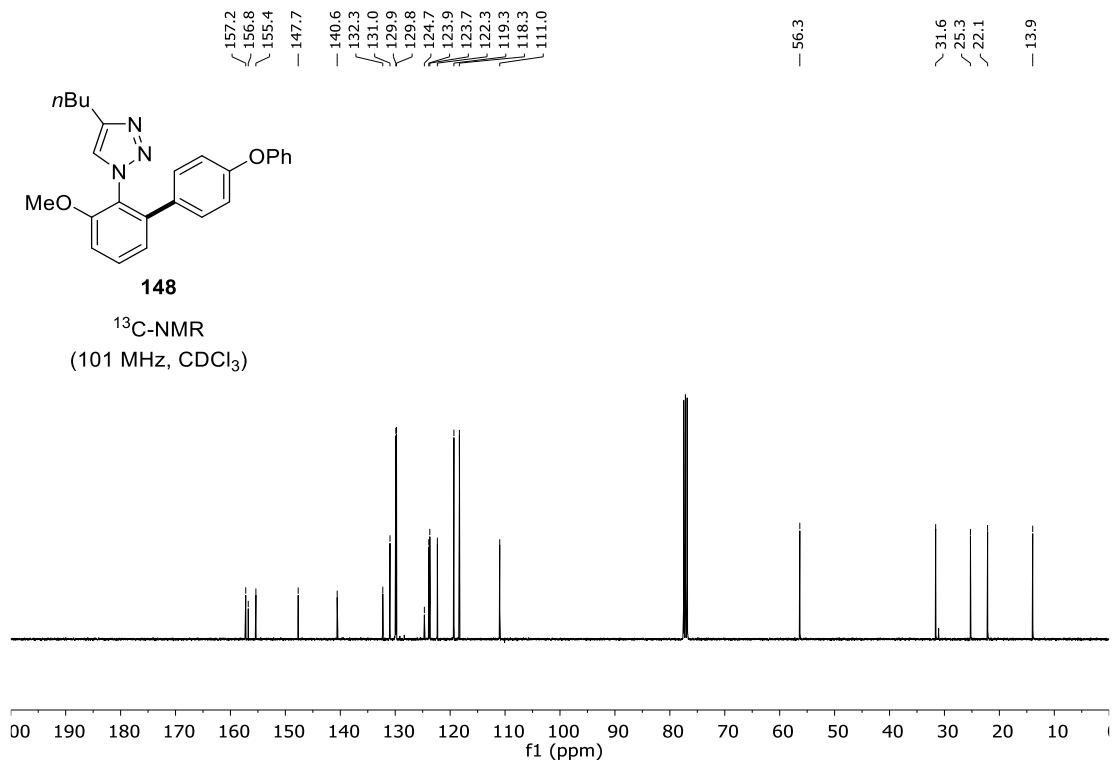
**148**

<sup>1</sup>H-NMR  
(400 MHz, CDCl<sub>3</sub>)

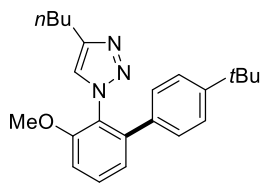


**148**

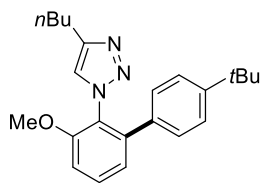
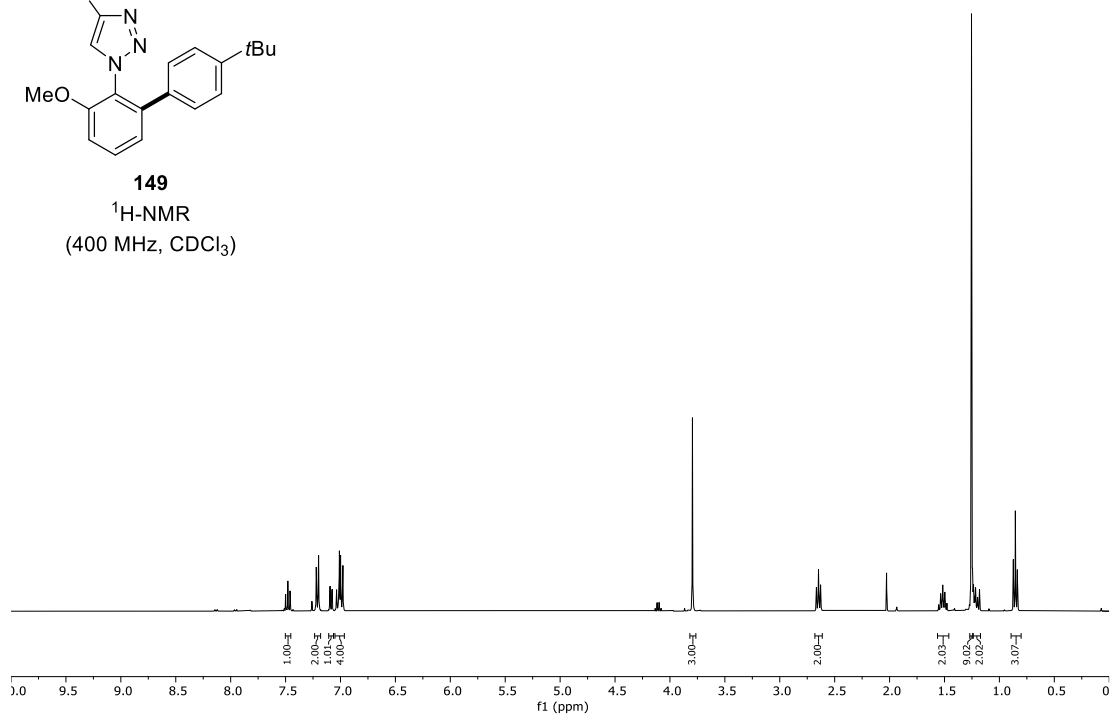
<sup>13</sup>C-NMR  
(101 MHz, CDCl<sub>3</sub>)



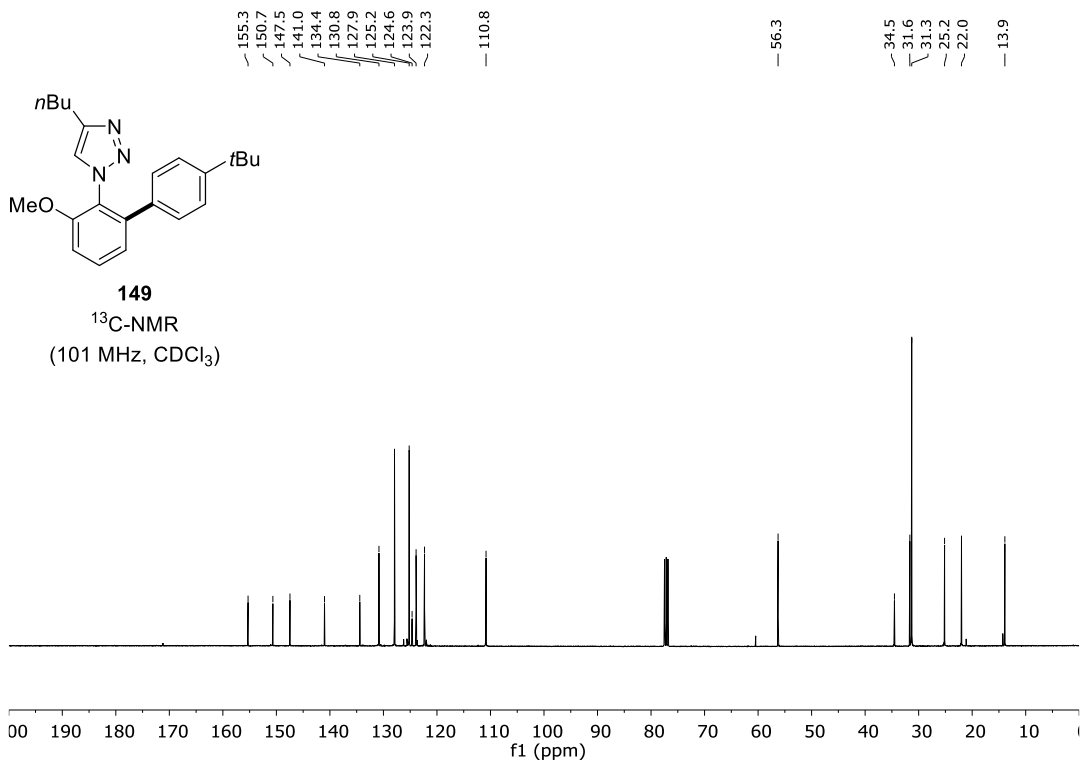
# NMR Spectra

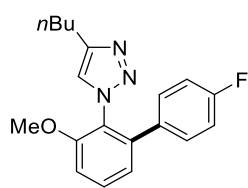


**149**  
<sup>1</sup>H-NMR  
 (400 MHz, CDCl<sub>3</sub>)



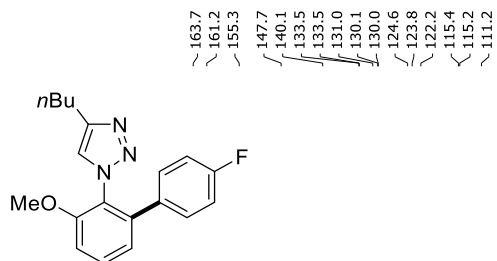
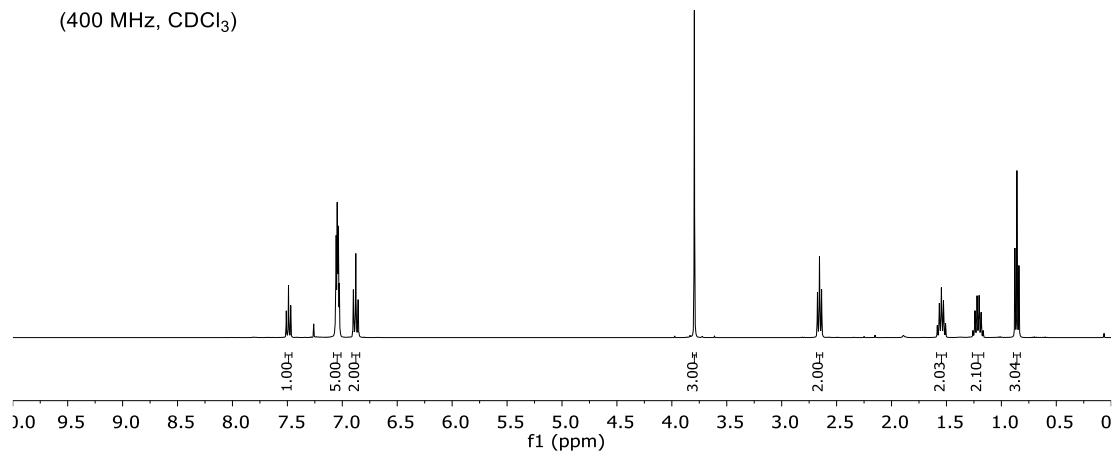
**149**  
<sup>13</sup>C-NMR  
 (101 MHz, CDCl<sub>3</sub>)





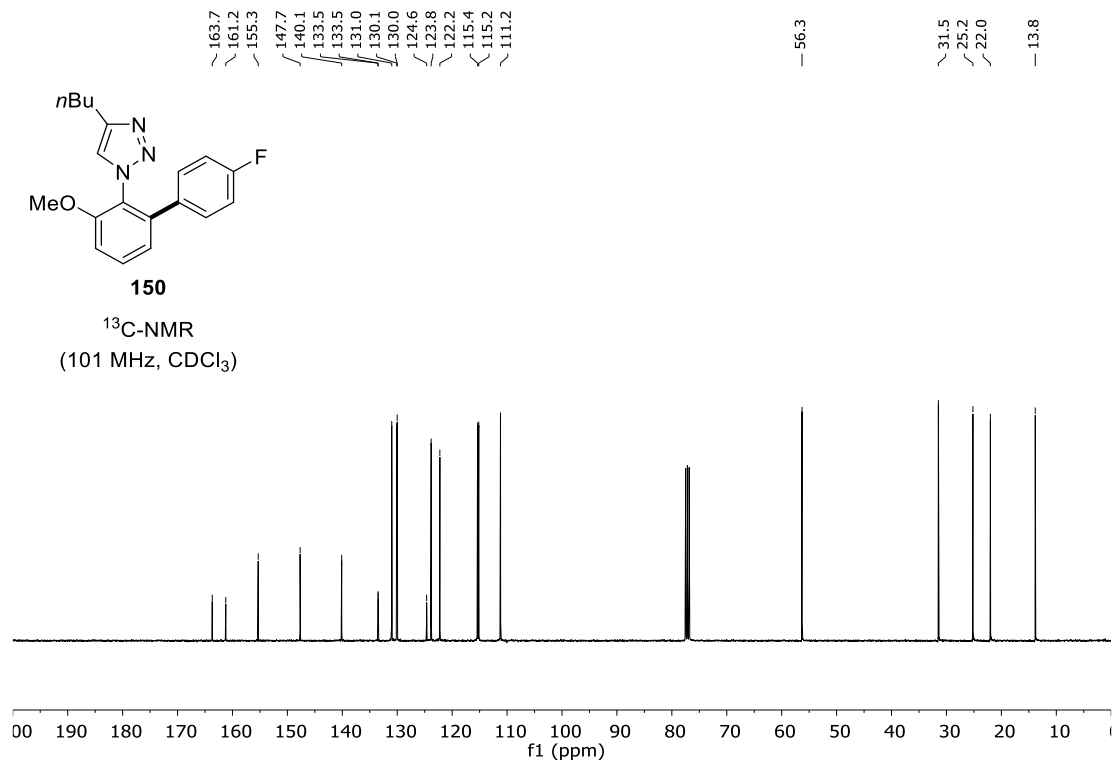
**150**

<sup>1</sup>H-NMR  
(400 MHz, CDCl<sub>3</sub>)

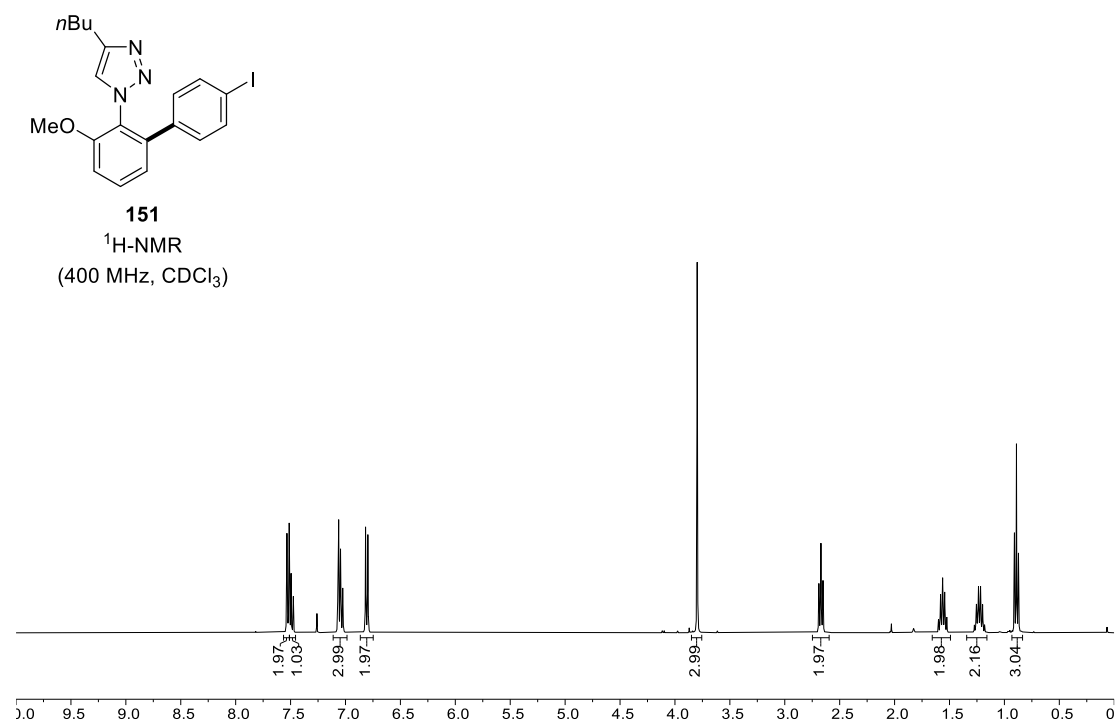
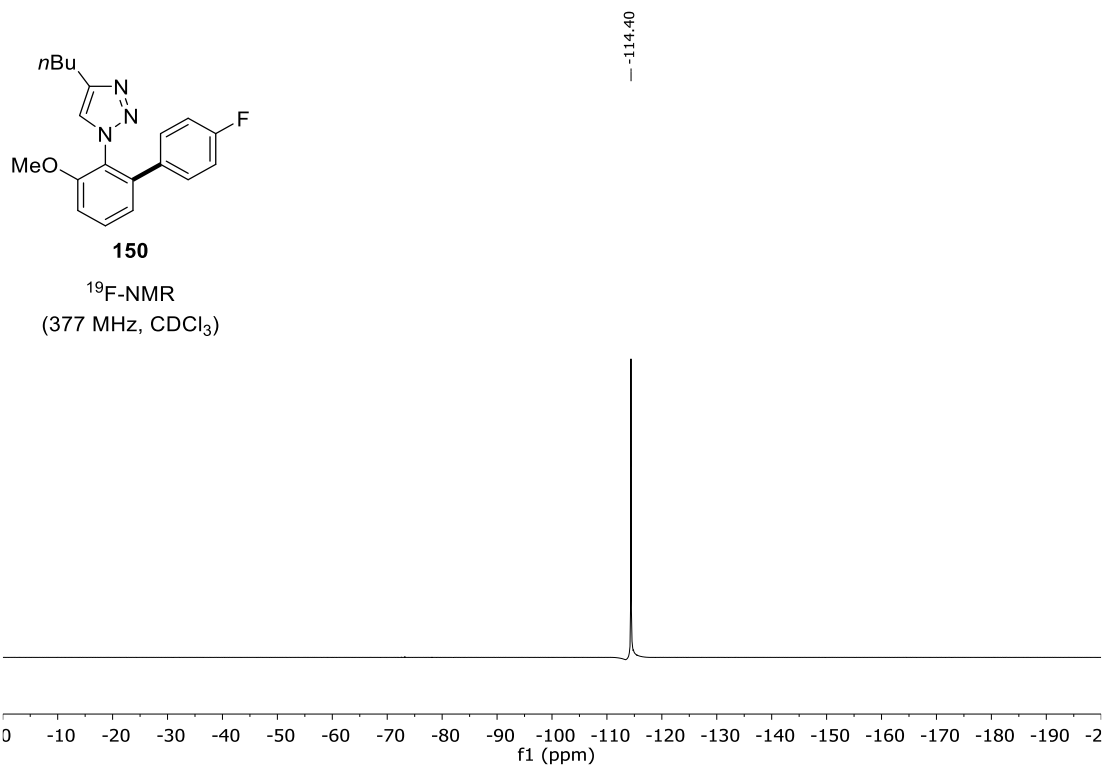


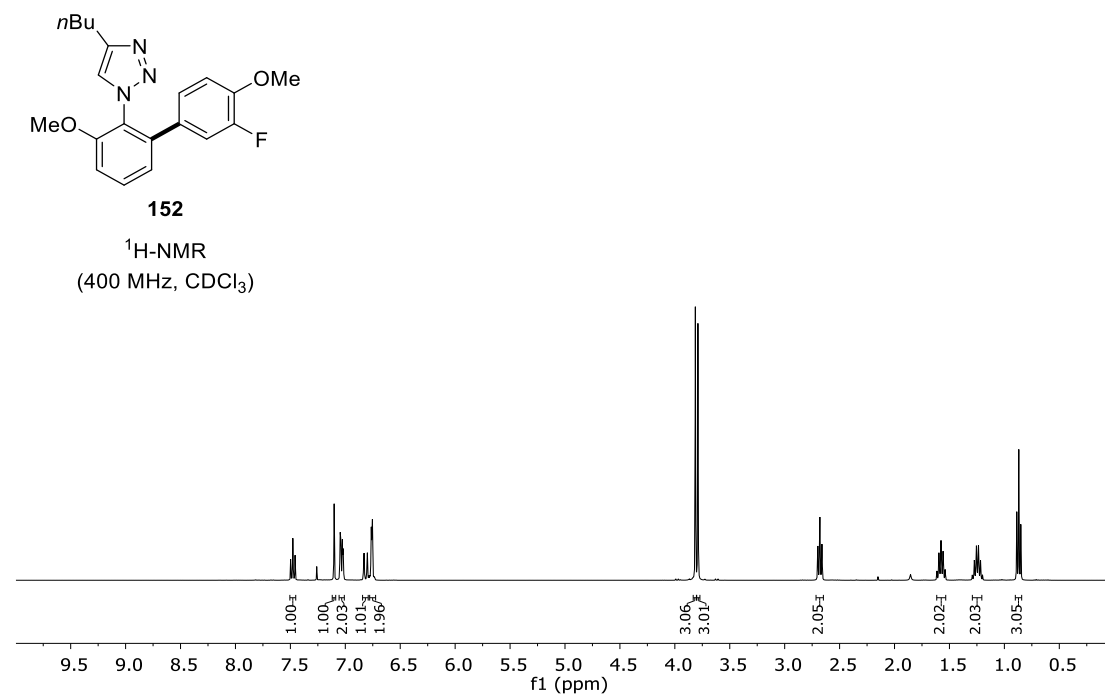
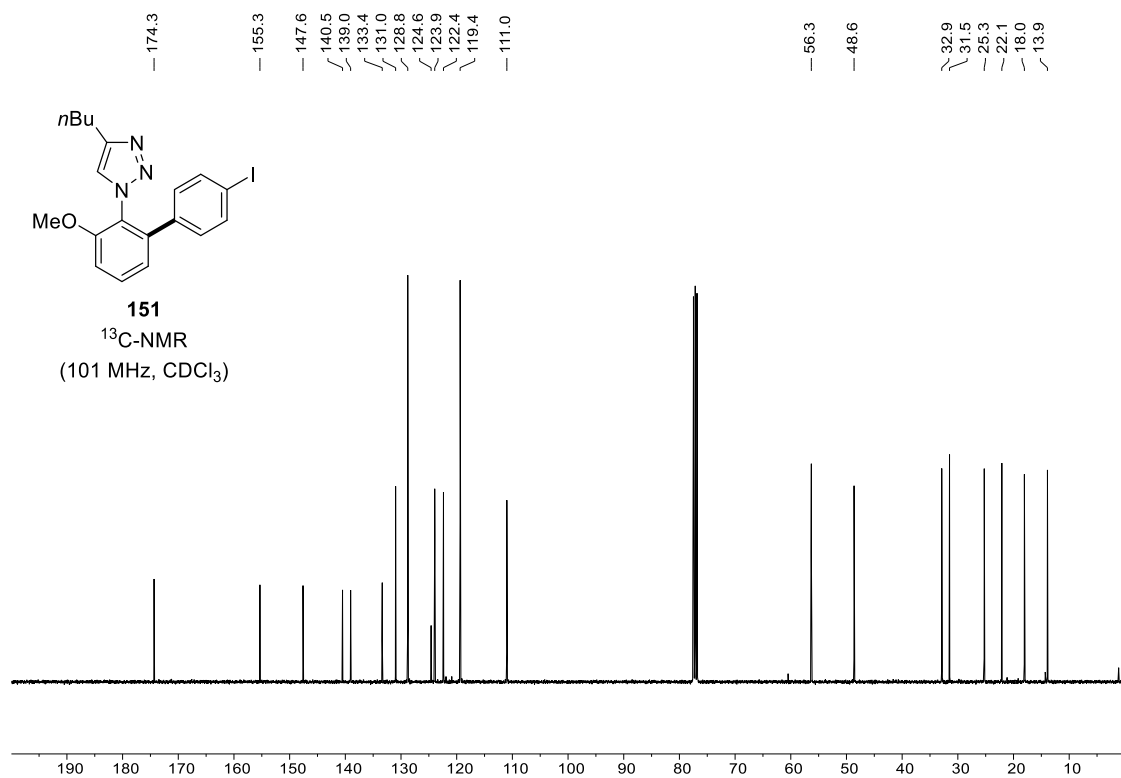
**150**

<sup>13</sup>C-NMR  
(101 MHz, CDCl<sub>3</sub>)

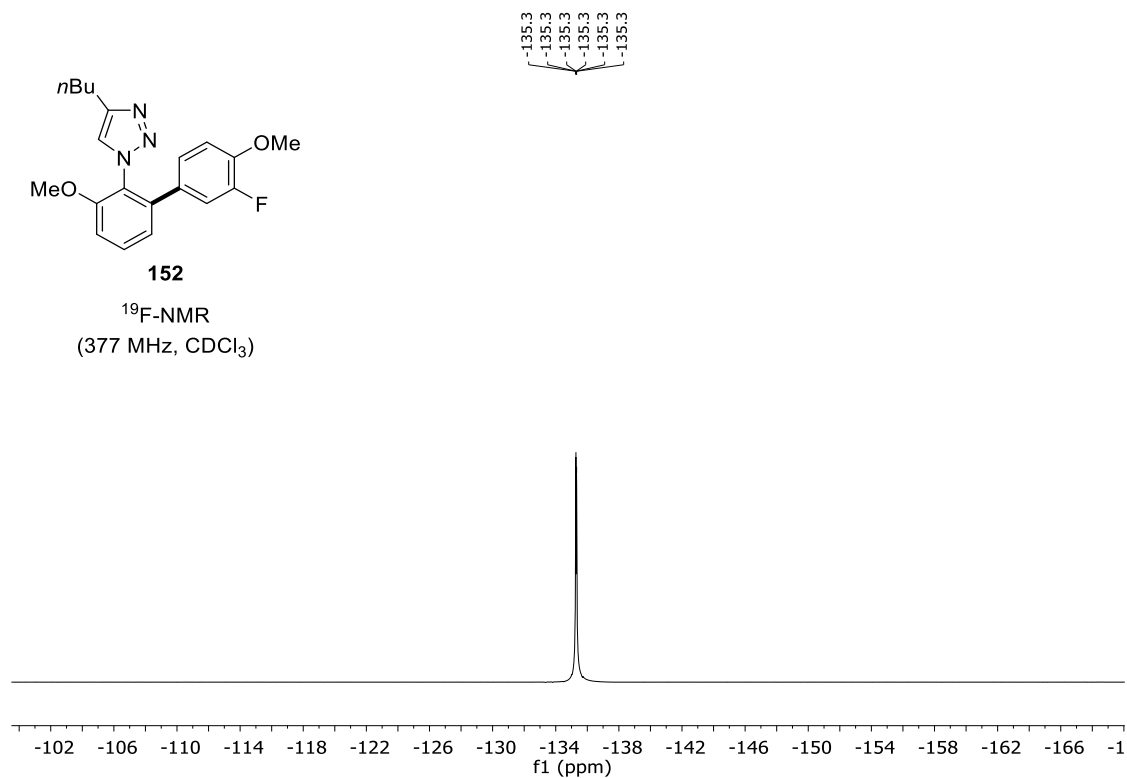
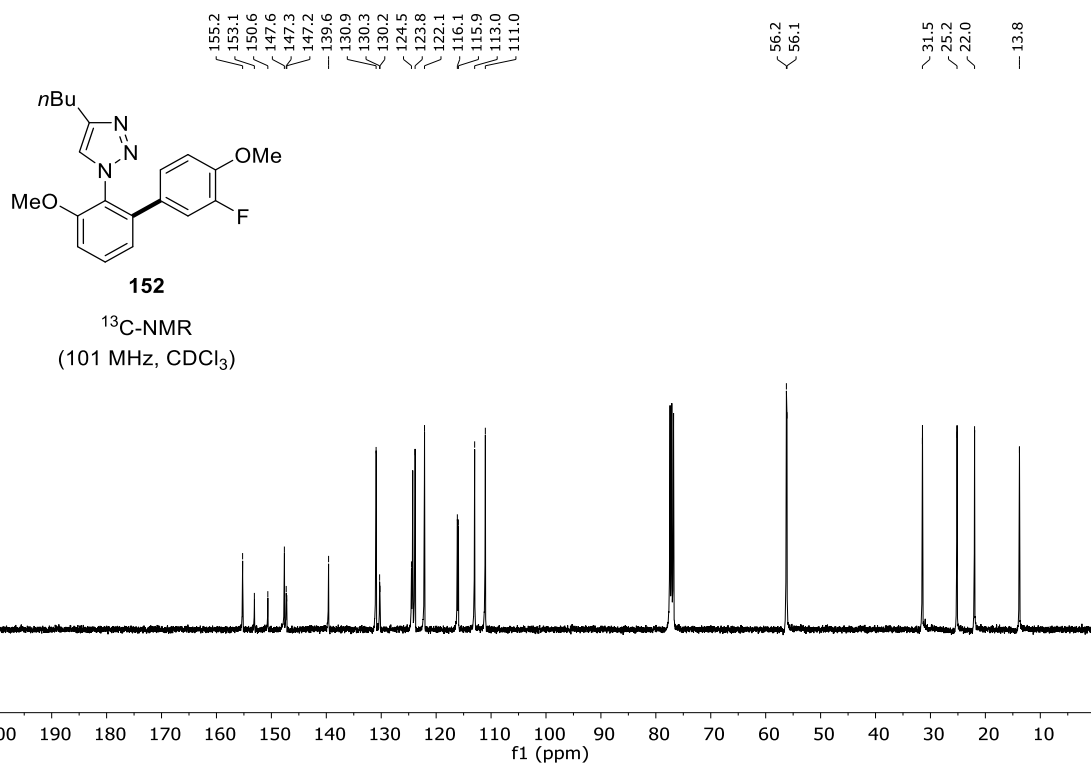


# NMR Spectra

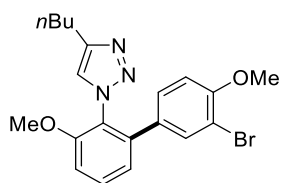




# NMR Spectra

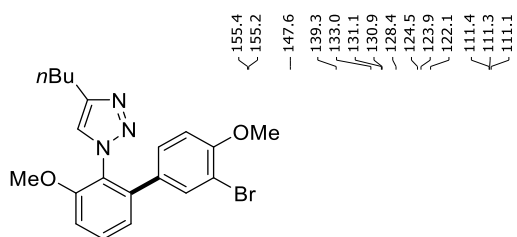
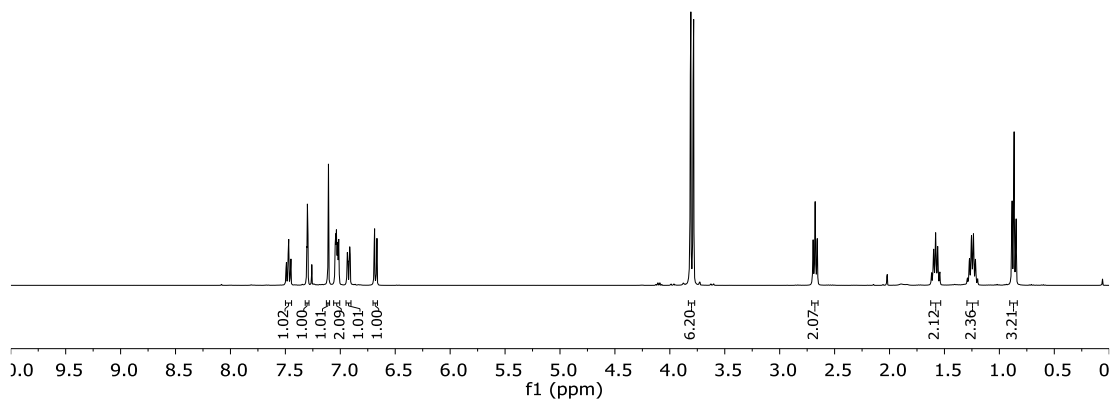






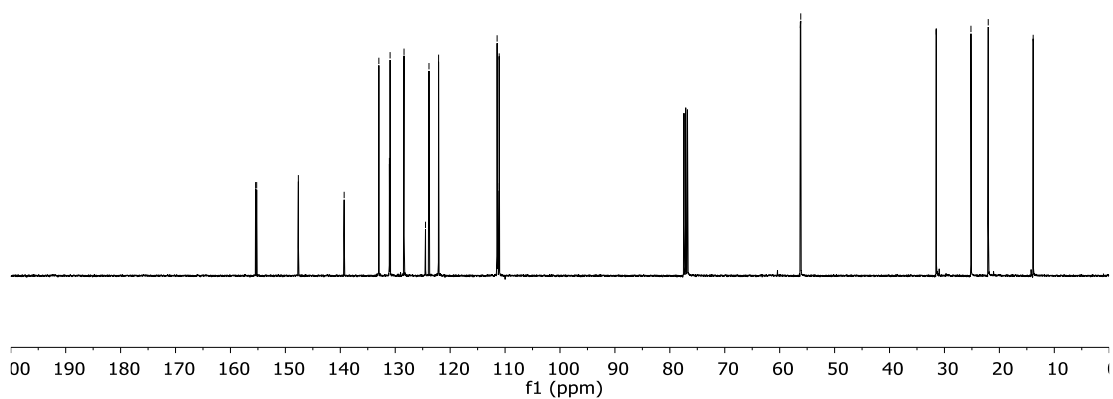
**153**

<sup>1</sup>H-NMR  
(400 MHz, CDCl<sub>3</sub>)

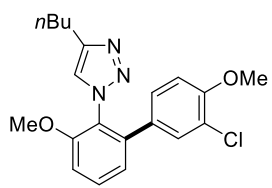


**153**

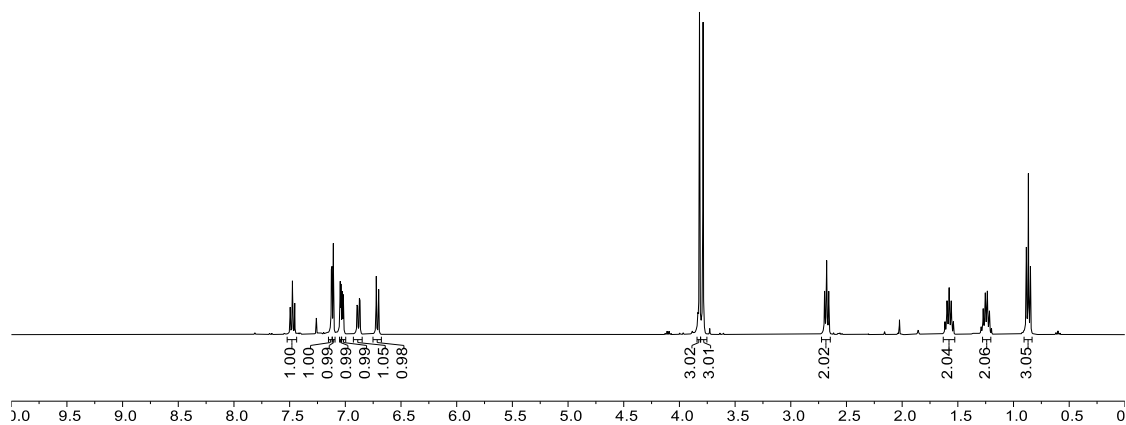
<sup>13</sup>C-NMR  
(101 MHz, CDCl<sub>3</sub>)



# NMR Spectra



**154**  
<sup>1</sup>H-NMR  
 (400 MHz, CDCl<sub>3</sub>)

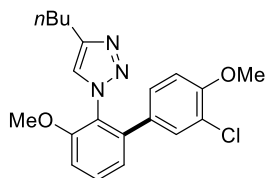


155.3  
 154.6  
 147.7  
 139.5  
 131.0  
 130.7  
 130.0  
 127.7  
 124.6  
 123.9  
 122.3  
 122.2  
 111.7  
 111.1

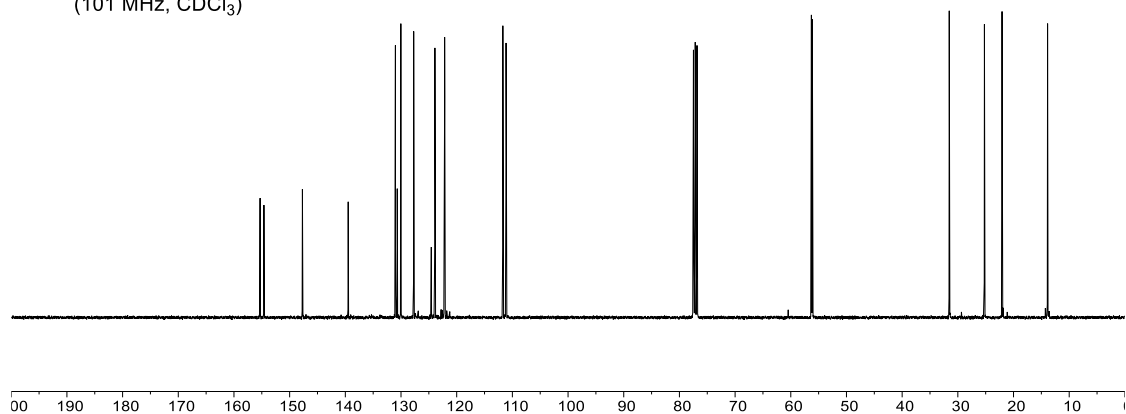
56.3  
 56.1

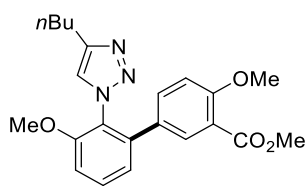
31.5  
 25.2  
 22.1

13.9



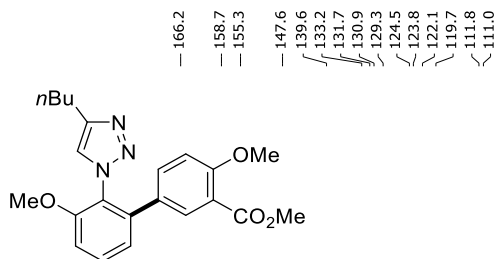
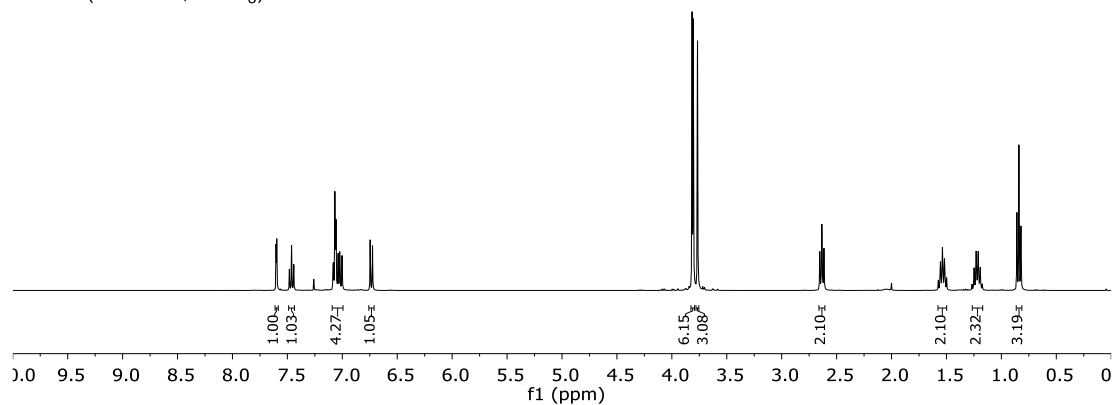
**154**  
<sup>13</sup>C-NMR  
 (101 MHz, CDCl<sub>3</sub>)





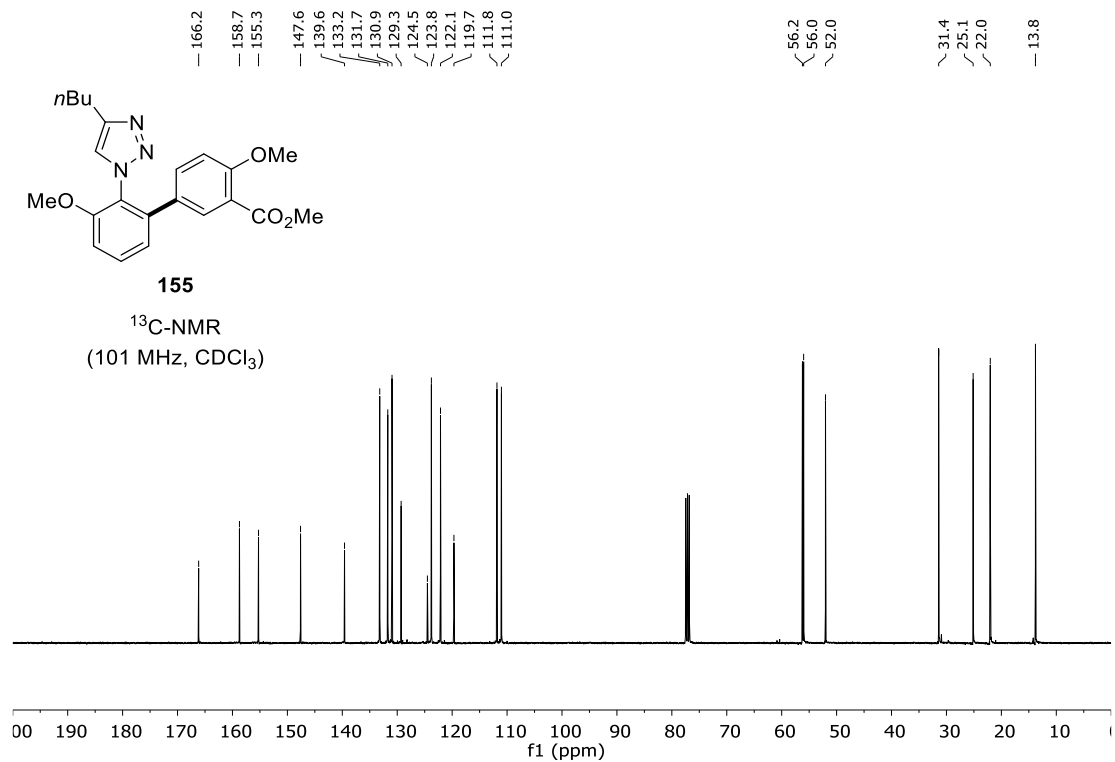
**155**

<sup>1</sup>H-NMR  
(400 MHz, CDCl<sub>3</sub>)

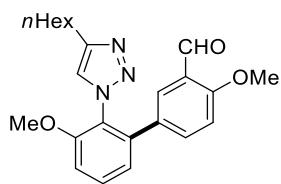


**155**

<sup>13</sup>C-NMR  
(101 MHz, CDCl<sub>3</sub>)

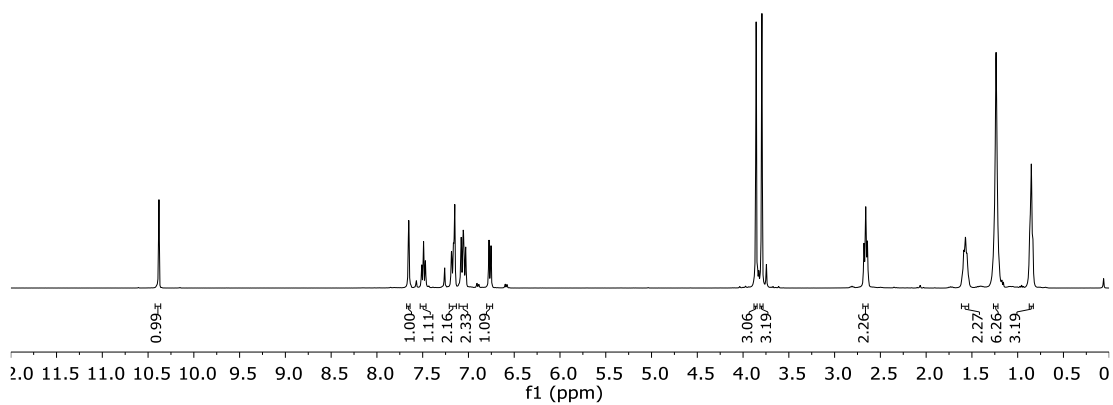


# NMR Spectra

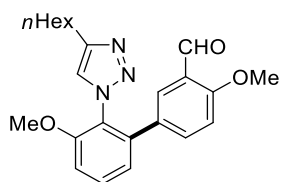


**156**

<sup>1</sup>H-NMR  
(400 MHz, CDCl<sub>3</sub>)

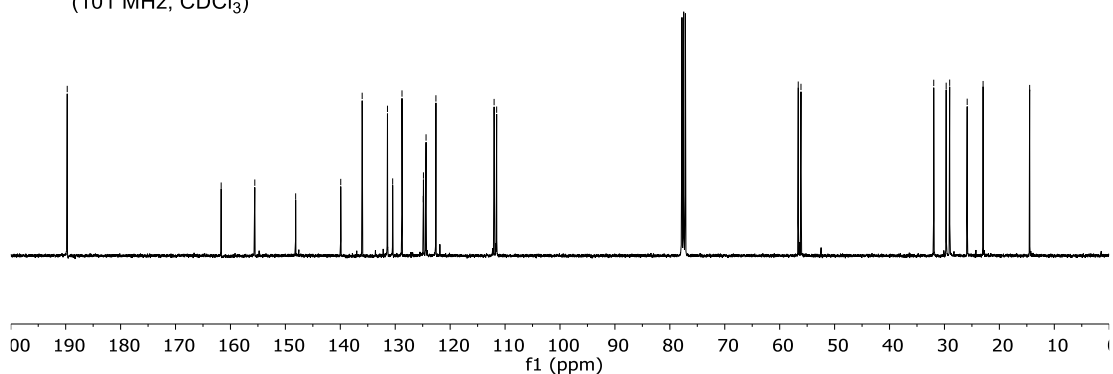


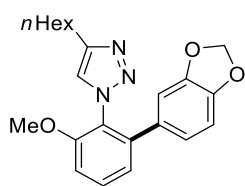
-189.7  
 -161.7  
 -155.6  
 -148.1  
 -139.9  
 -136.0  
 -131.4  
 -130.5  
 -128.8  
 -124.9  
 -124.9  
 -124.4  
 -122.6  
 -112.0  
 -111.5  
 56.6  
 56.1  
 32.0  
 29.7  
 29.0  
 25.9  
 23.0  
 -14.5



**156**

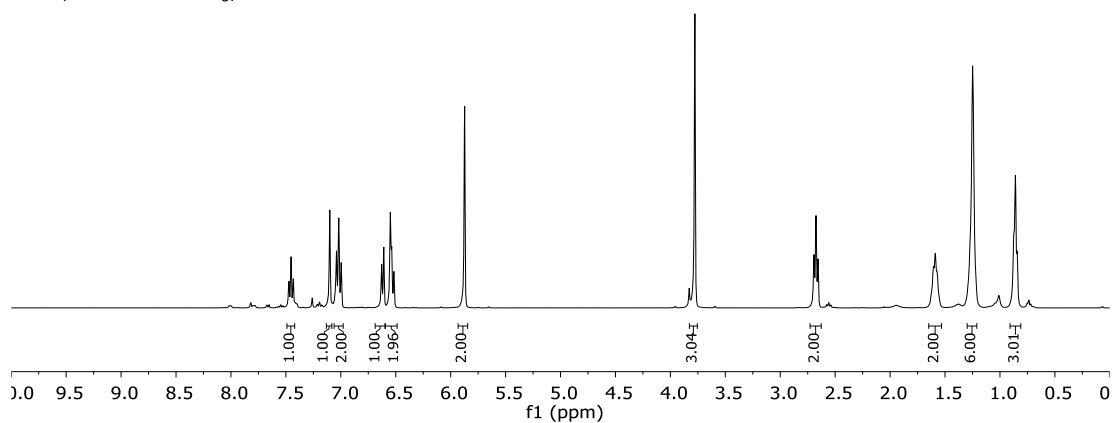
<sup>13</sup>C-NMR  
(101 MHz, CDCl<sub>3</sub>)



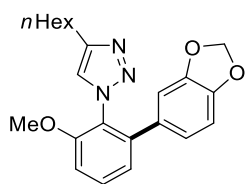


**157**

<sup>1</sup>H-NMR  
(400 MHz, CDCl<sub>3</sub>)

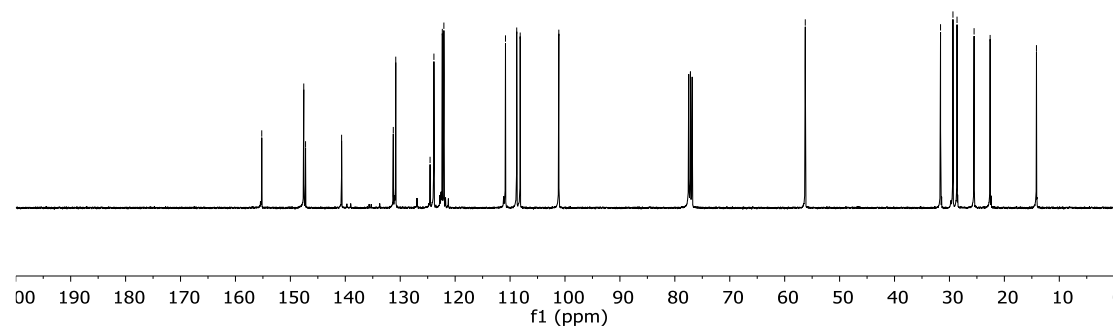


-155.2  
 147.6  
 147.2  
 -140.7  
 131.3  
 130.8  
 124.6  
 123.9  
 122.3  
 122.1  
 110.8  
 108.8  
 108.2  
 -101.1  
 -56.2  
 31.6  
 29.4  
 28.6  
 25.5  
 22.6  
 -14.2

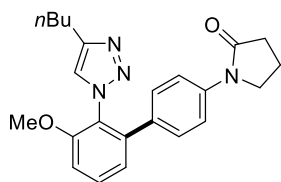


**157**

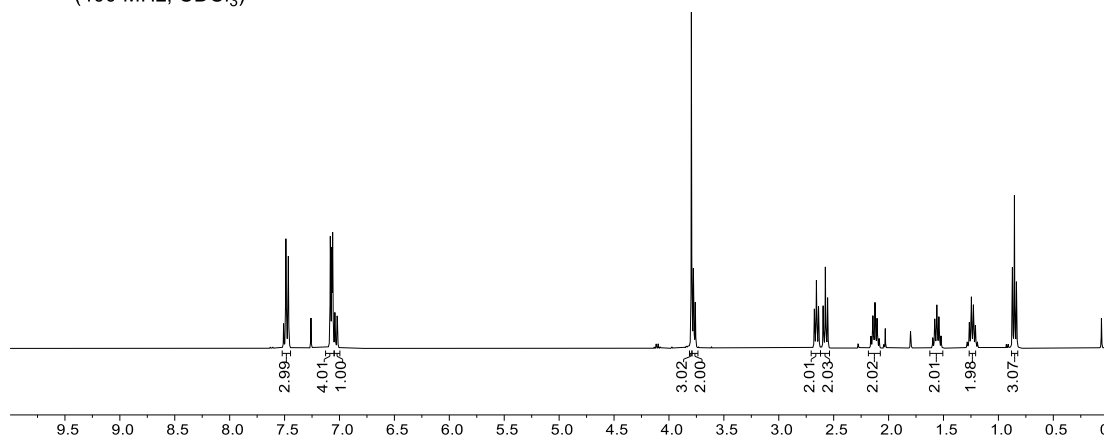
<sup>13</sup>C-NMR  
(101 MHz, CDCl<sub>3</sub>)



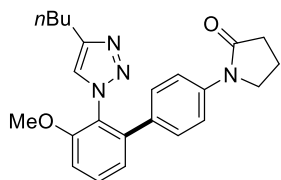
# NMR Spectra



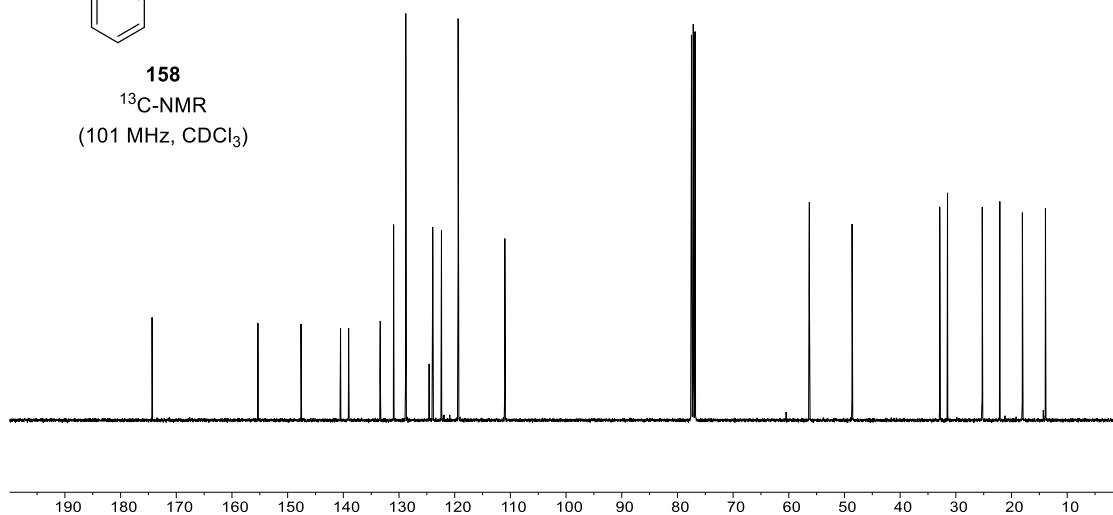
**158**  
<sup>1</sup>H-NMR  
 (400 MHz, CDCl<sub>3</sub>)

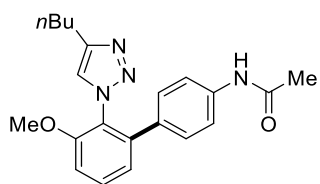


— 174.3 — 155.3 — 147.6 — 140.5 — 139.0 — 133.4 — 131.0 — 128.8 — 124.6 — 123.9 — 122.4 — 119.4 — 111.0 — 56.3 — 48.6 — 32.9 — 31.5 — 25.3 — 22.1 — 18.0 — 13.9



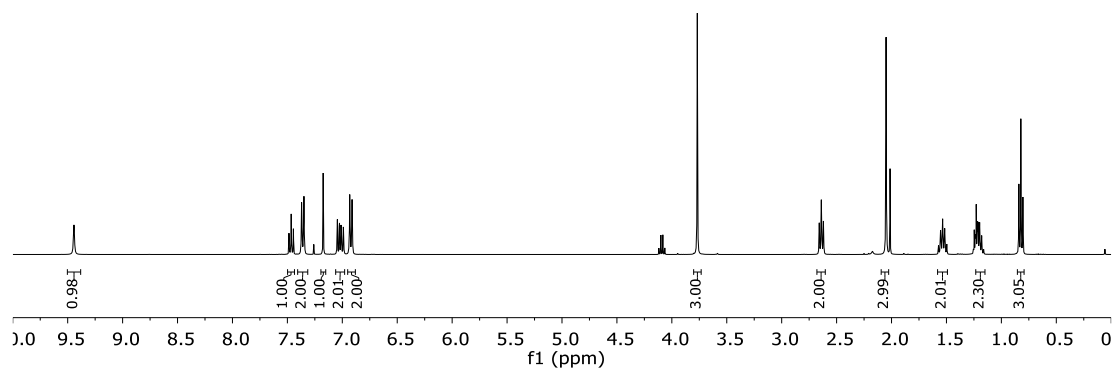
**158**  
<sup>13</sup>C-NMR  
 (101 MHz, CDCl<sub>3</sub>)





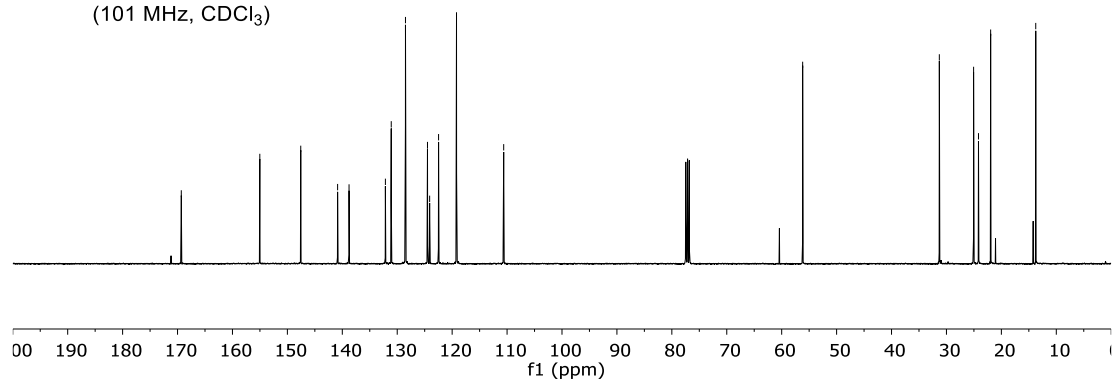
**159**

<sup>1</sup>H-NMR  
(400 MHz, CDCl<sub>3</sub>)

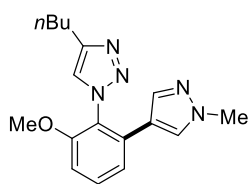


**159**

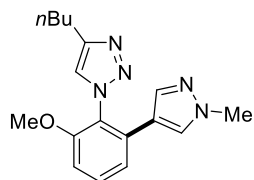
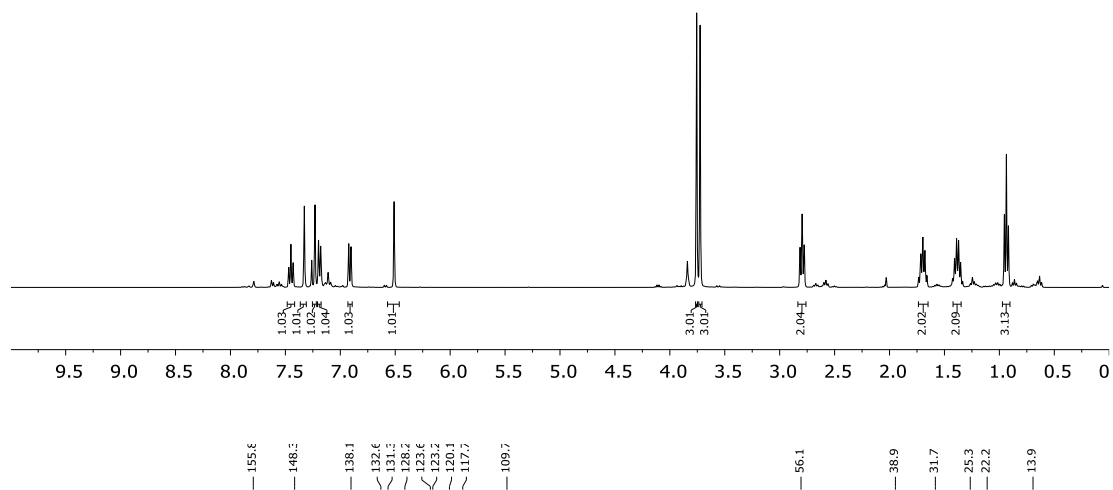
<sup>13</sup>C-NMR  
(101 MHz, CDCl<sub>3</sub>)



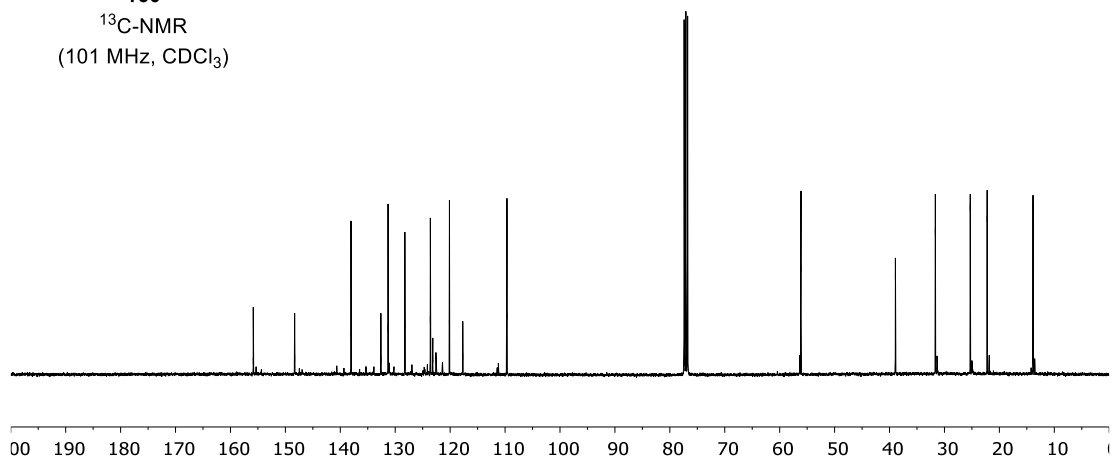
# NMR Spectra



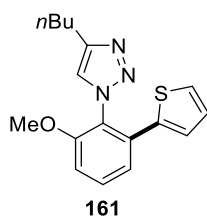
**160**  
<sup>1</sup>H-NMR  
 (400 MHz, CDCl<sub>3</sub>)



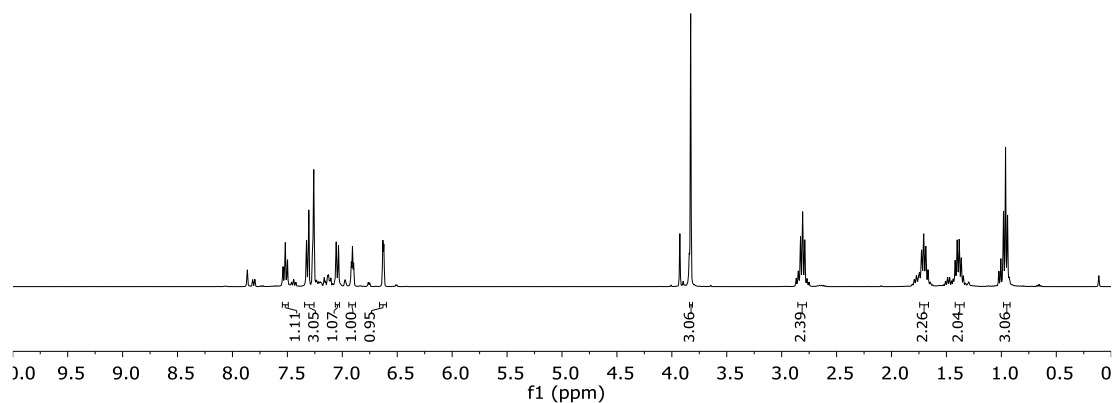
**160**  
<sup>13</sup>C-NMR  
 (101 MHz, CDCl<sub>3</sub>)



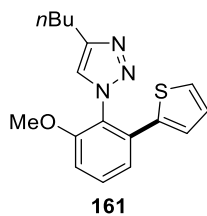




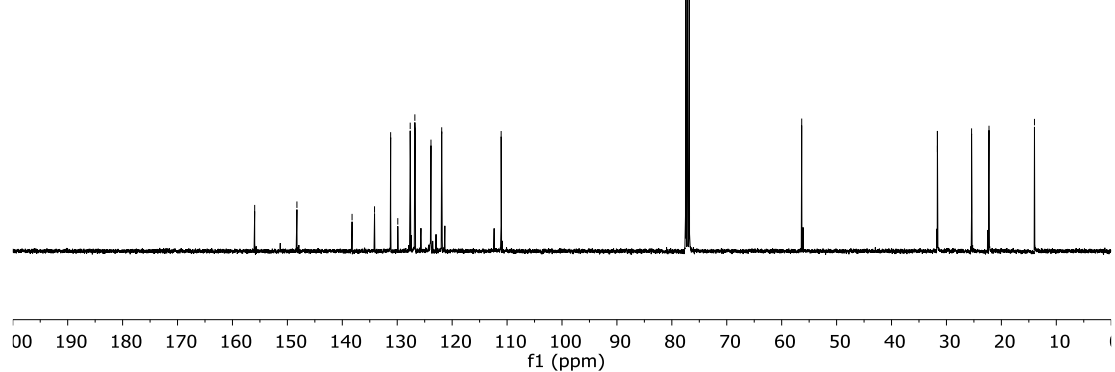
<sup>1</sup>H-NMR  
(400 MHz, CDCl<sub>3</sub>)



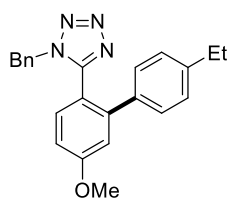
156.0  
148.3  
138.2  
134.1  
131.2  
129.9  
127.6  
126.8  
126.7  
123.9  
121.9  
111.1  
56.4  
31.6  
25.4  
22.3  
14.0



<sup>13</sup>C-NMR  
(101 MHz, CDCl<sub>3</sub>)

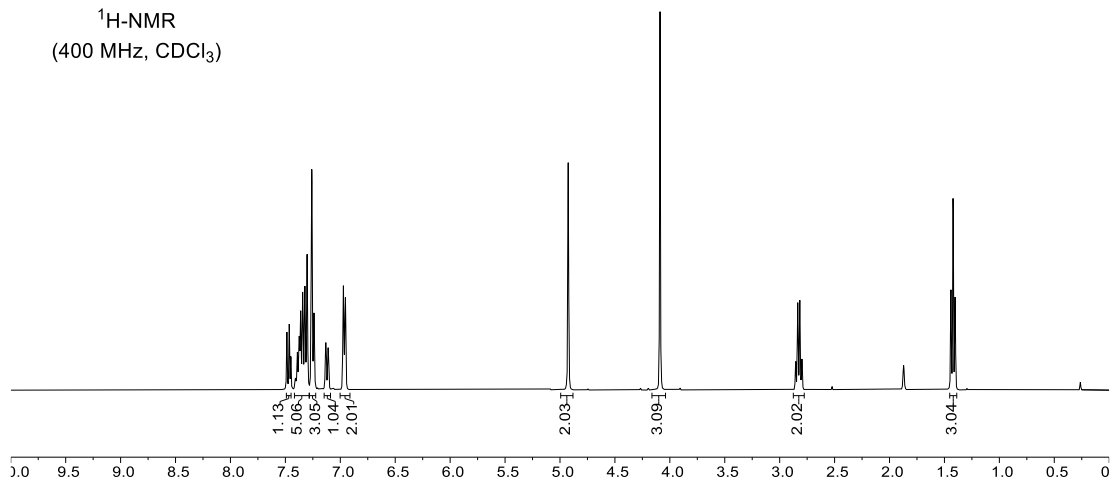


# NMR Spectra

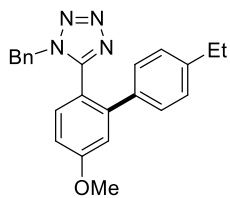


**164**

<sup>1</sup>H-NMR  
(400 MHz, CDCl<sub>3</sub>)

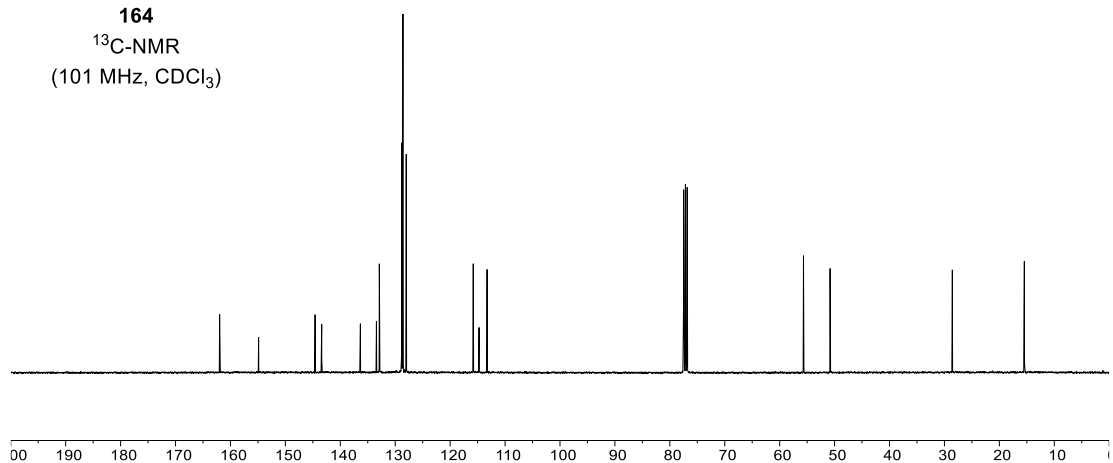


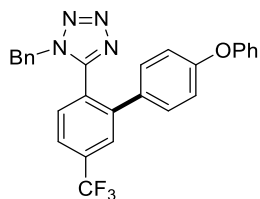
162.0  
154.9  
144.6  
143.4  
136.3  
133.4  
132.9  
128.8  
128.6  
128.6  
128.5  
128.0  
128.0  
115.8  
114.7  
113.3  
55.7  
50.8  
28.6  
15.5



**164**

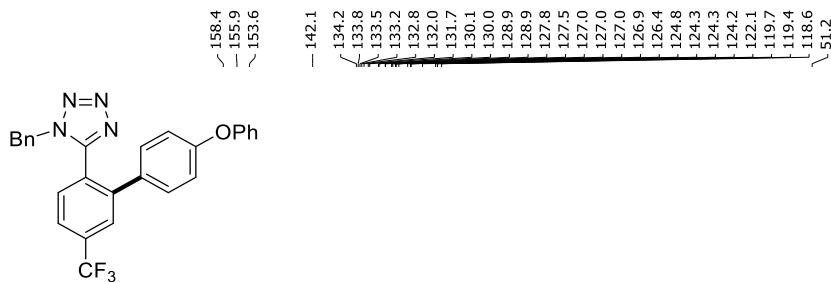
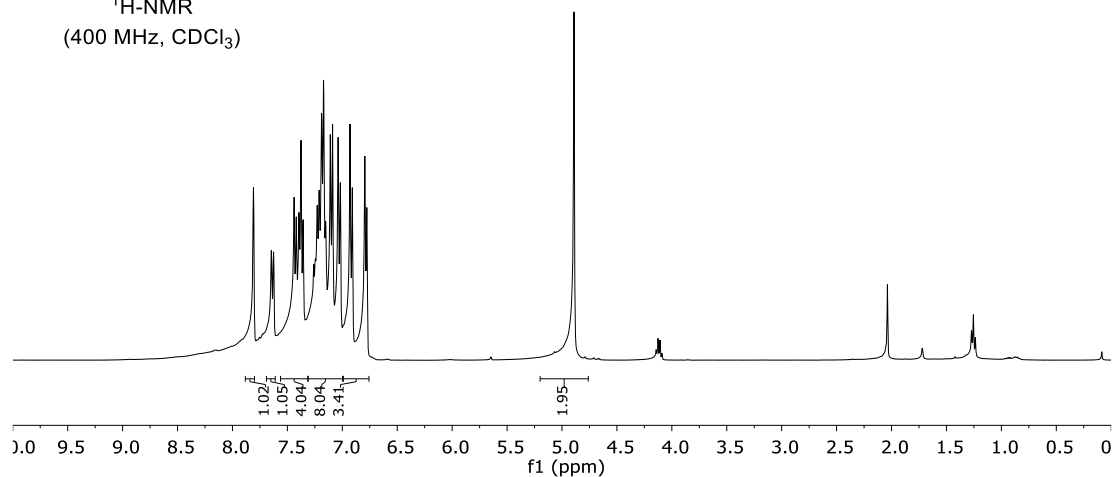
<sup>13</sup>C-NMR  
(101 MHz, CDCl<sub>3</sub>)





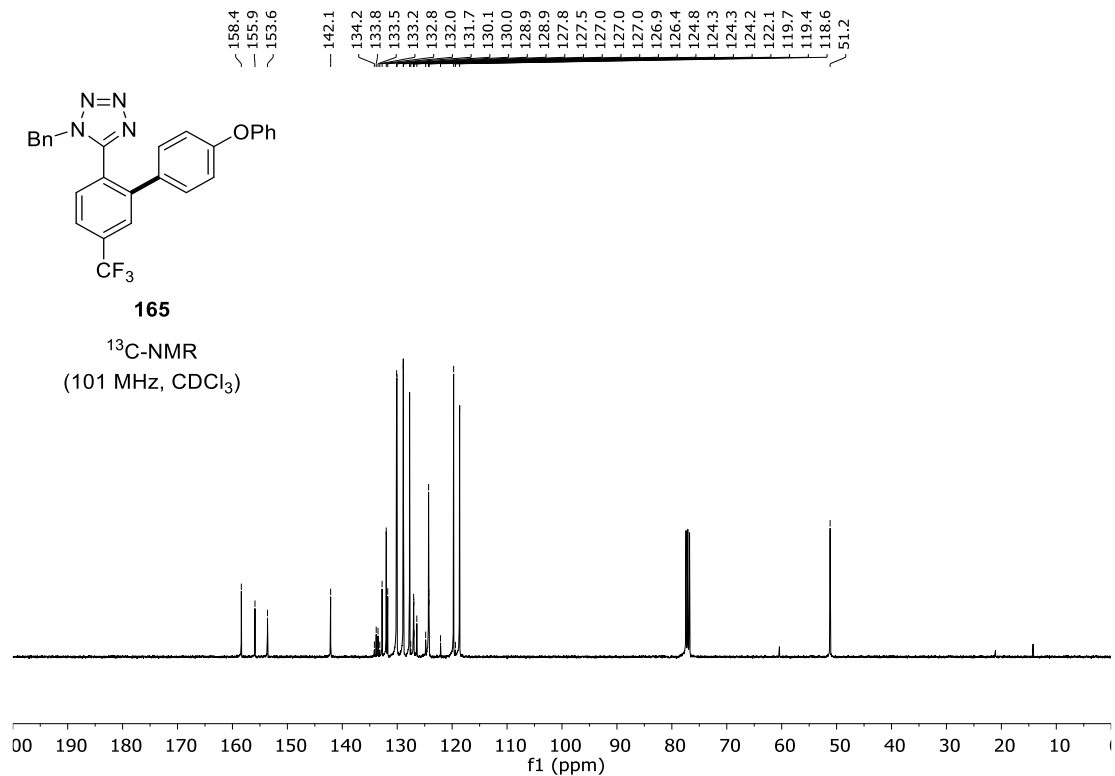
**165**

<sup>1</sup>H-NMR  
(400 MHz, CDCl<sub>3</sub>)

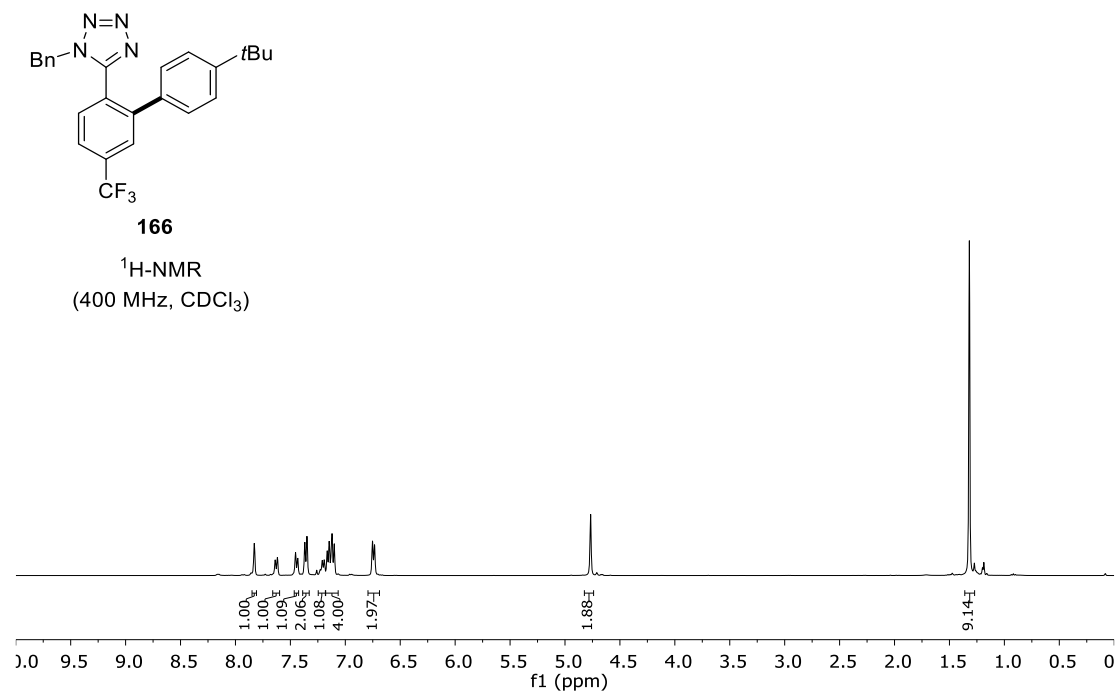
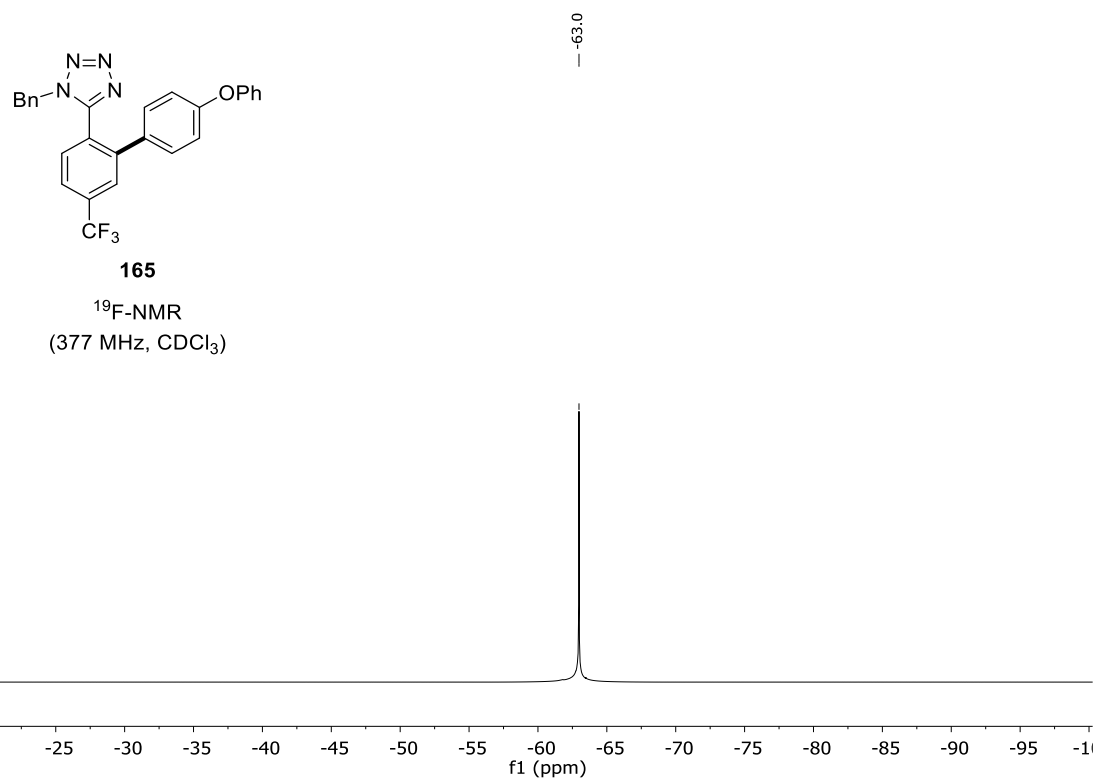


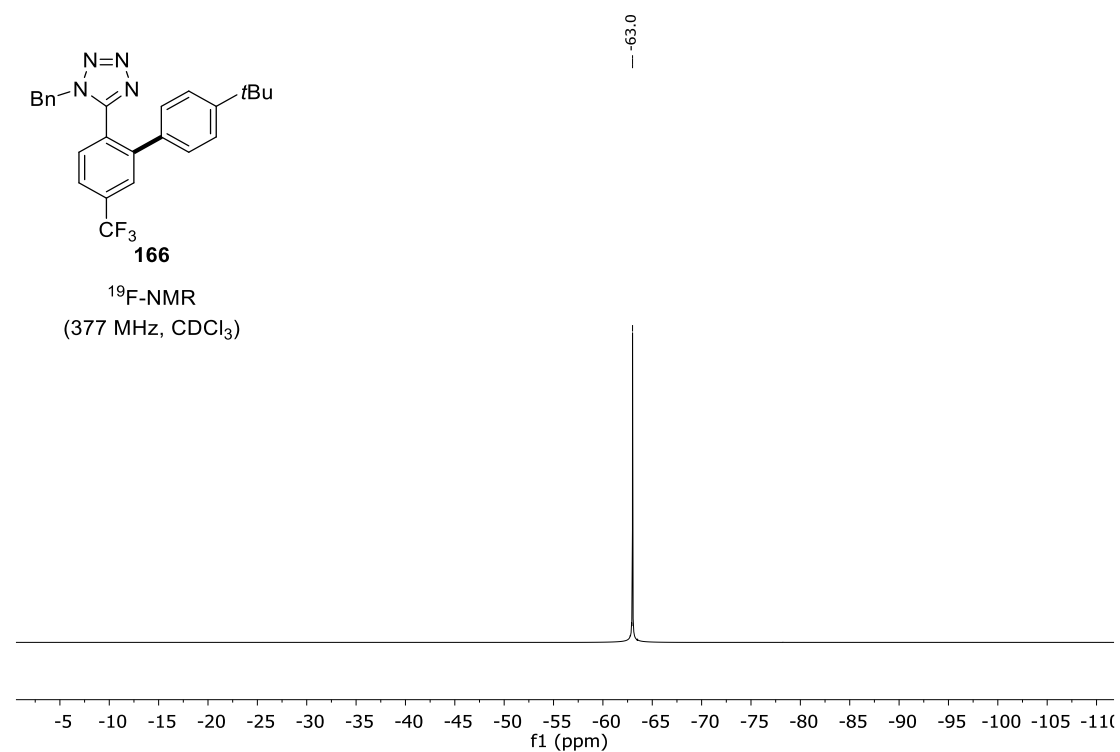
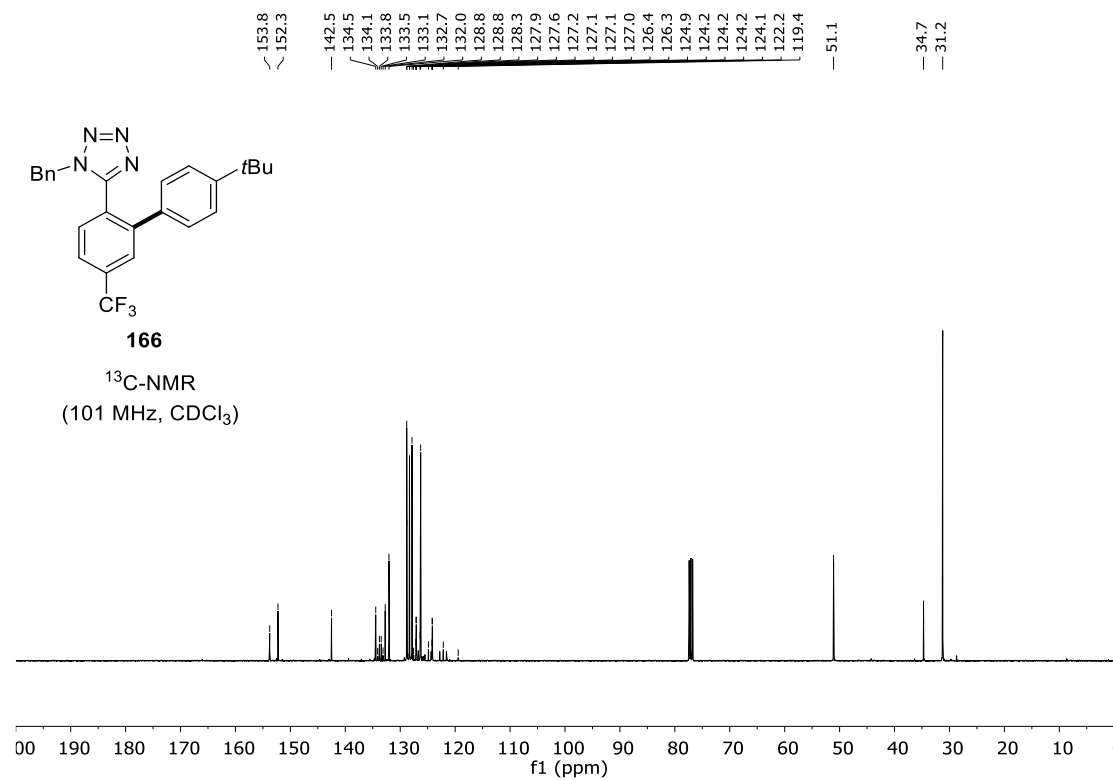
**165**

<sup>13</sup>C-NMR  
(101 MHz, CDCl<sub>3</sub>)

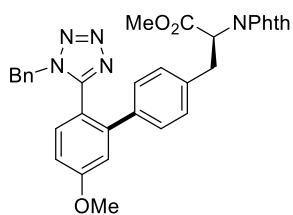


# NMR Spectra



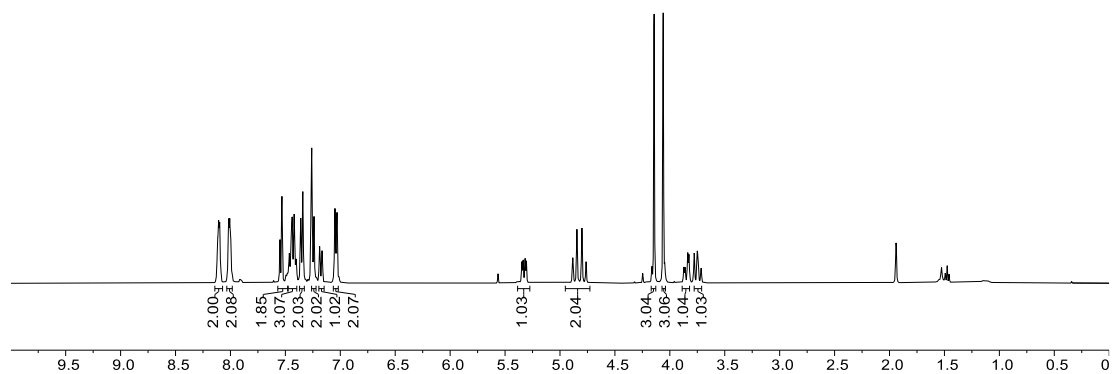


# NMR Spectra

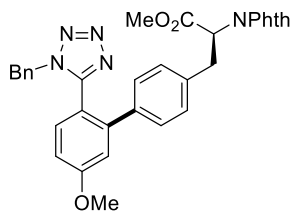


**167**

<sup>1</sup>H-NMR  
(400 MHz, CDCl<sub>3</sub>)

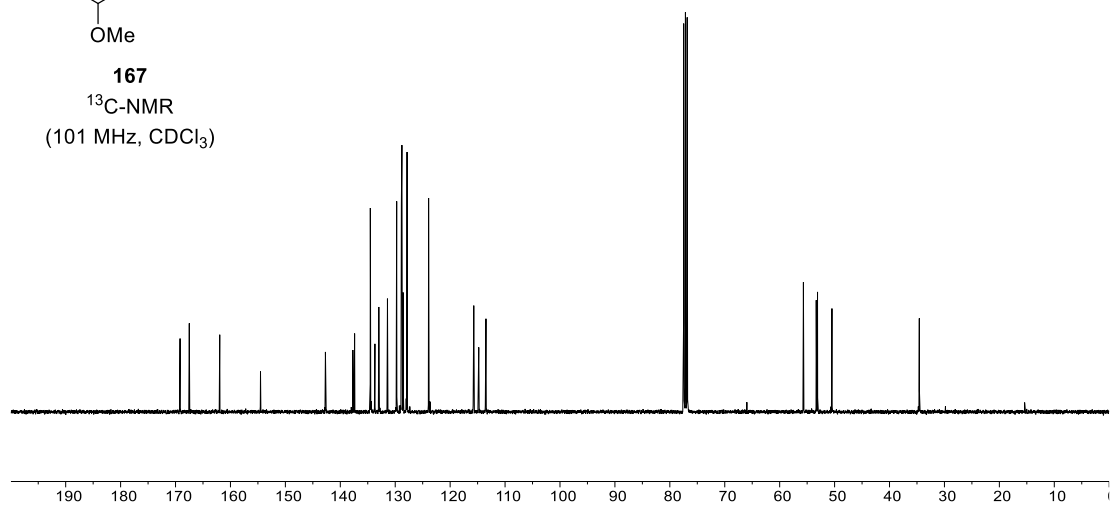


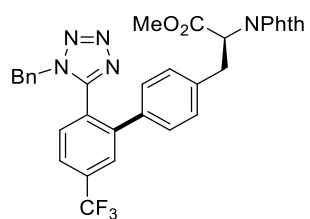
169.2  
167.5  
161.9  
154.5  
142.7  
137.7  
137.4  
134.5  
133.7  
133.0  
131.4  
129.7  
128.9  
128.8  
128.5  
127.8  
123.9  
115.7  
114.8  
113.5  
55.7  
53.3  
53.1  
50.5  
34.6



**167**

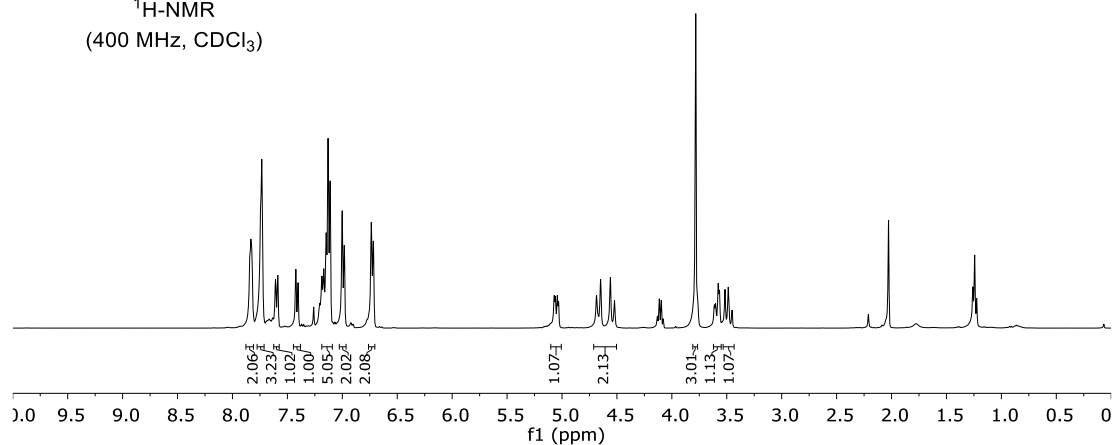
<sup>13</sup>C-NMR  
(101 MHz, CDCl<sub>3</sub>)



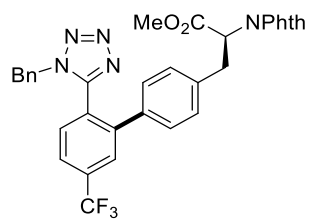


**168**

<sup>1</sup>H-NMR  
(400 MHz, CDCl<sub>3</sub>)

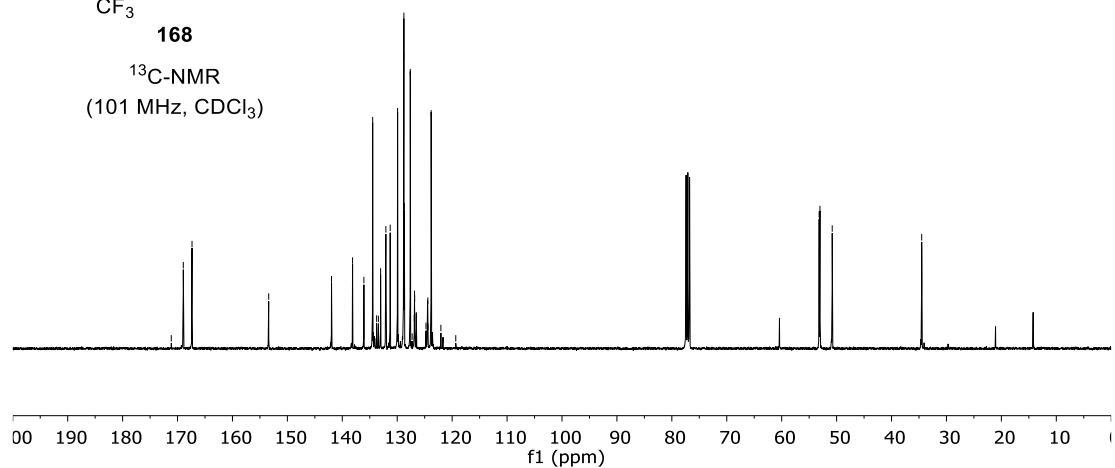


171.1  
168.9  
167.4  
153.4  
142.0  
138.1  
136.1  
134.5  
133.8  
133.4  
133.0  
132.1  
131.3  
129.9  
128.8  
128.7  
127.6  
127.3  
126.9  
126.8  
124.8  
124.5  
124.4  
124.4  
123.8  
122.1  
119.3  
53.2  
53.0  
50.8  
34.5

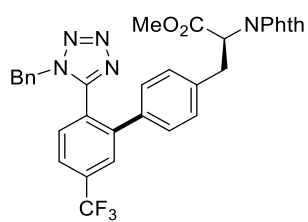


**168**

<sup>13</sup>C-NMR  
(101 MHz, CDCl<sub>3</sub>)

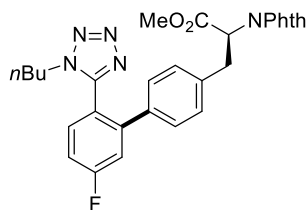
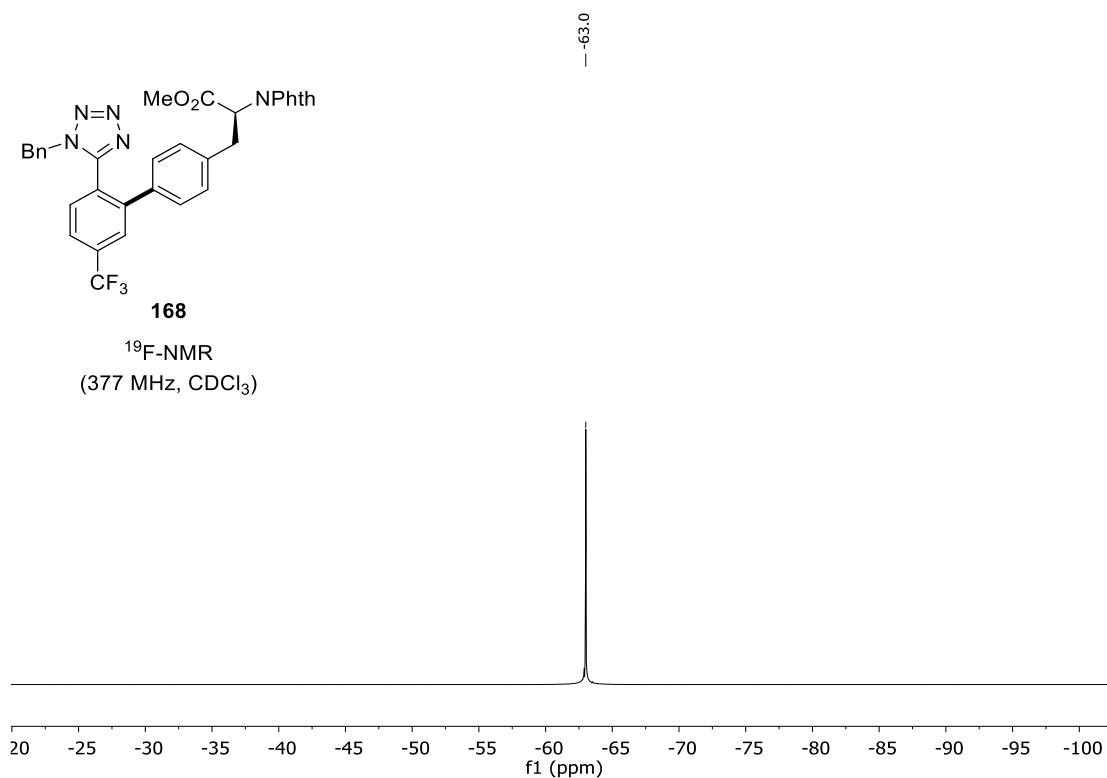


# NMR Spectra



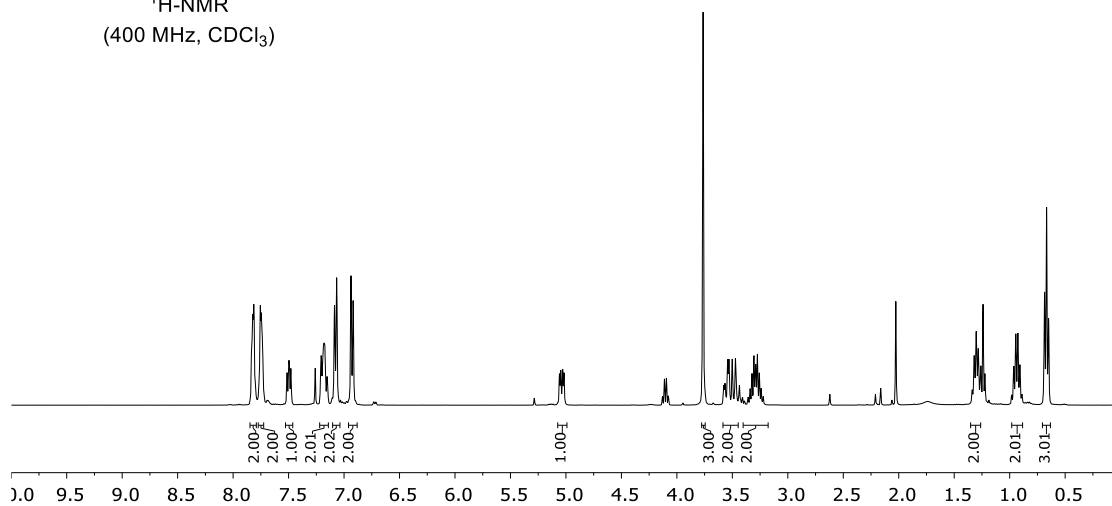
**168**

<sup>19</sup>F-NMR  
(377 MHz, CDCl<sub>3</sub>)

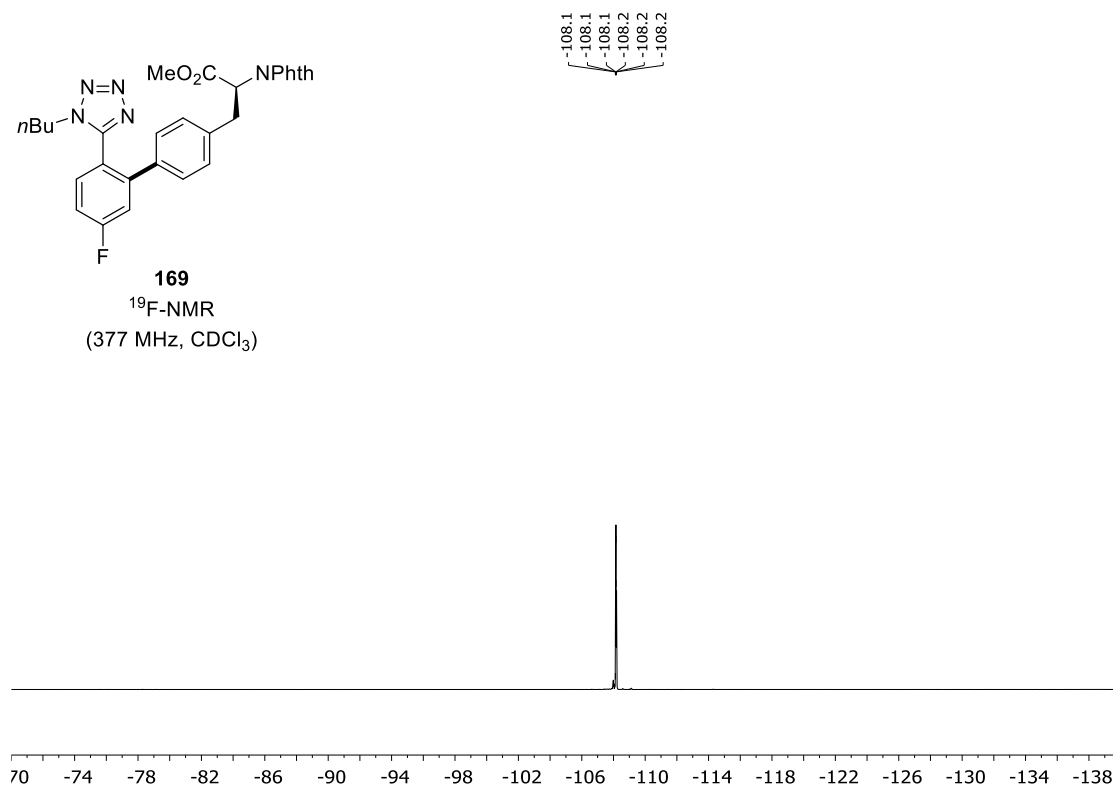
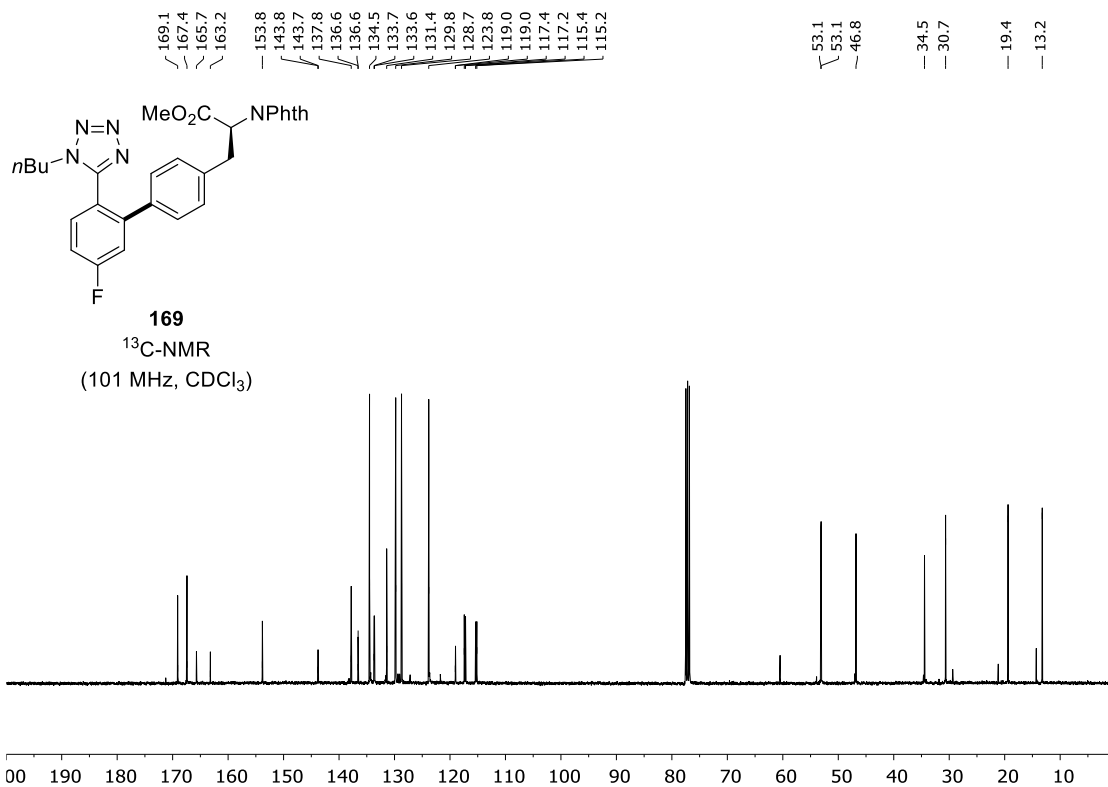


**169**

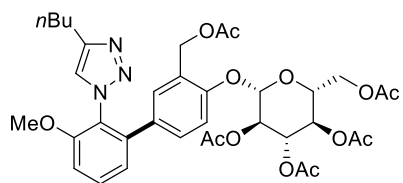
<sup>1</sup>H-NMR  
(400 MHz, CDCl<sub>3</sub>)



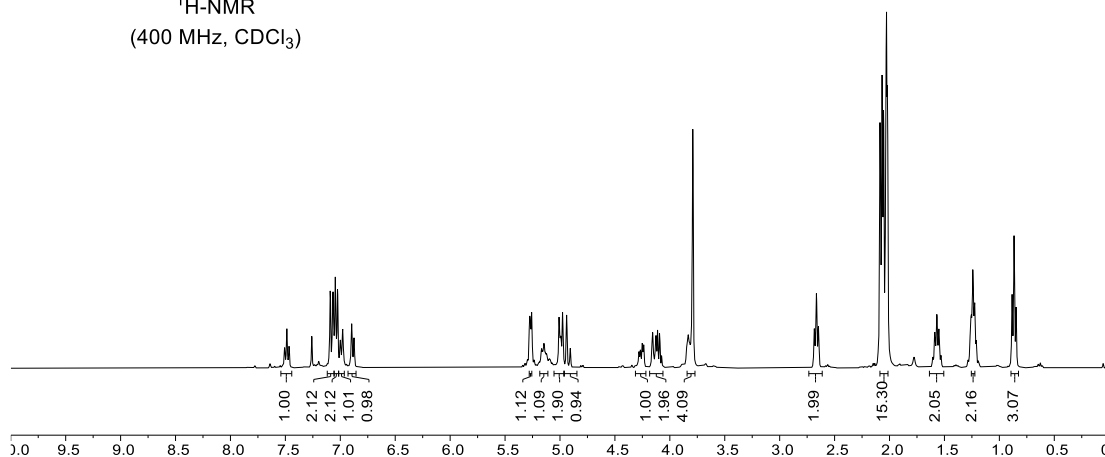




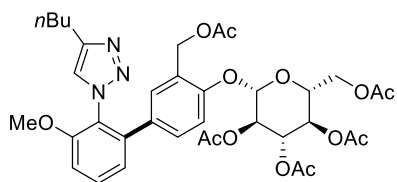
# NMR Spectra



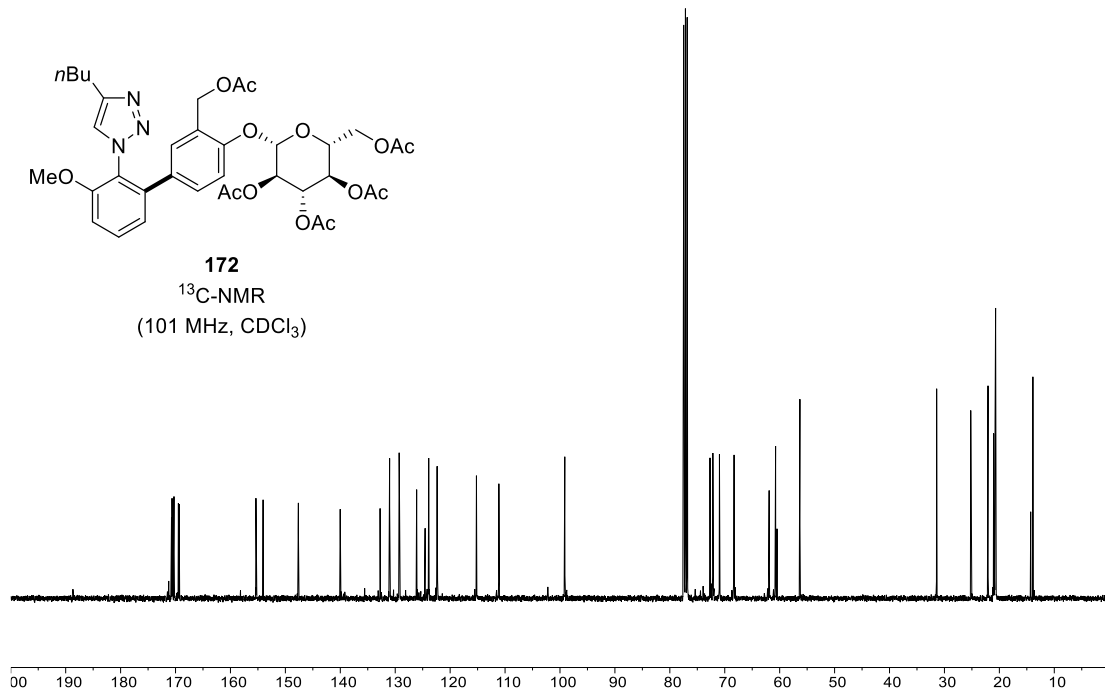
**172**  
<sup>1</sup>H-NMR  
 (400 MHz, CDCl<sub>3</sub>)

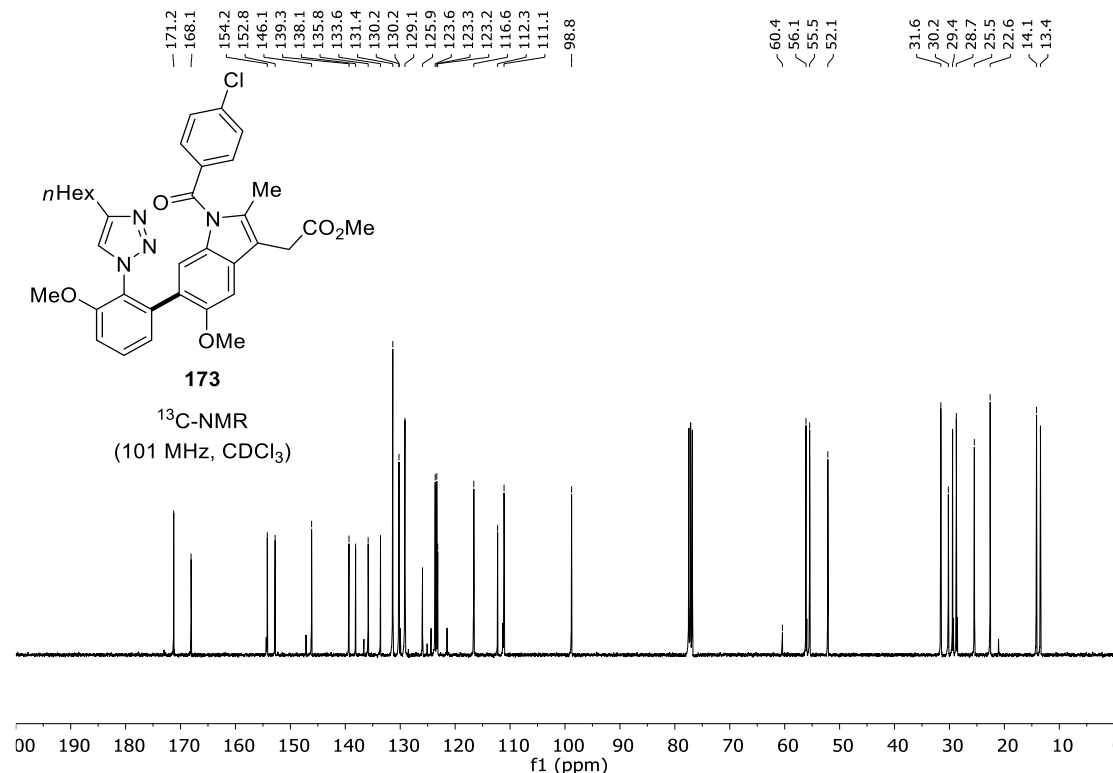
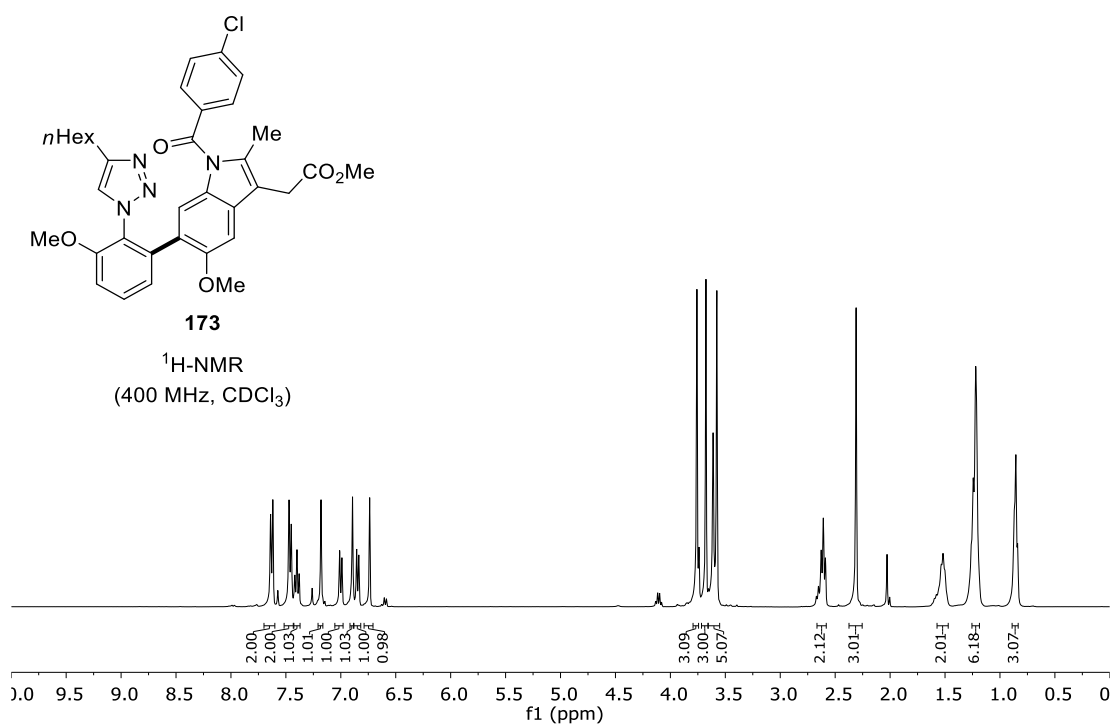


170.7  
 170.6  
 170.3  
 169.5  
 169.3  
 155.4  
 154.1  
 147.6  
 140.0  
 132.8  
 131.0  
 129.3  
 129.2  
 126.1  
 124.6  
 123.9  
 122.4  
 115.2  
 111.1  
 99.1  
 72.7  
 72.2  
 71.0  
 68.3  
 61.9  
 60.7  
 60.5  
 56.3  
 31.4  
 25.2  
 22.1  
 21.0  
 20.8  
 20.7  
 20.7  
 13.9

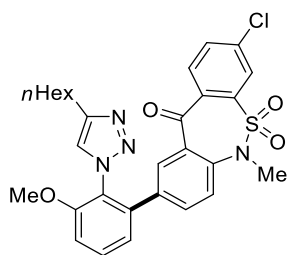


**172**  
<sup>13</sup>C-NMR  
 (101 MHz, CDCl<sub>3</sub>)



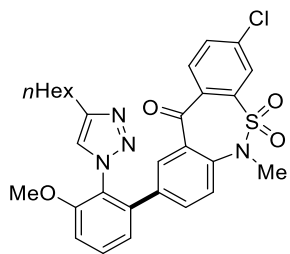
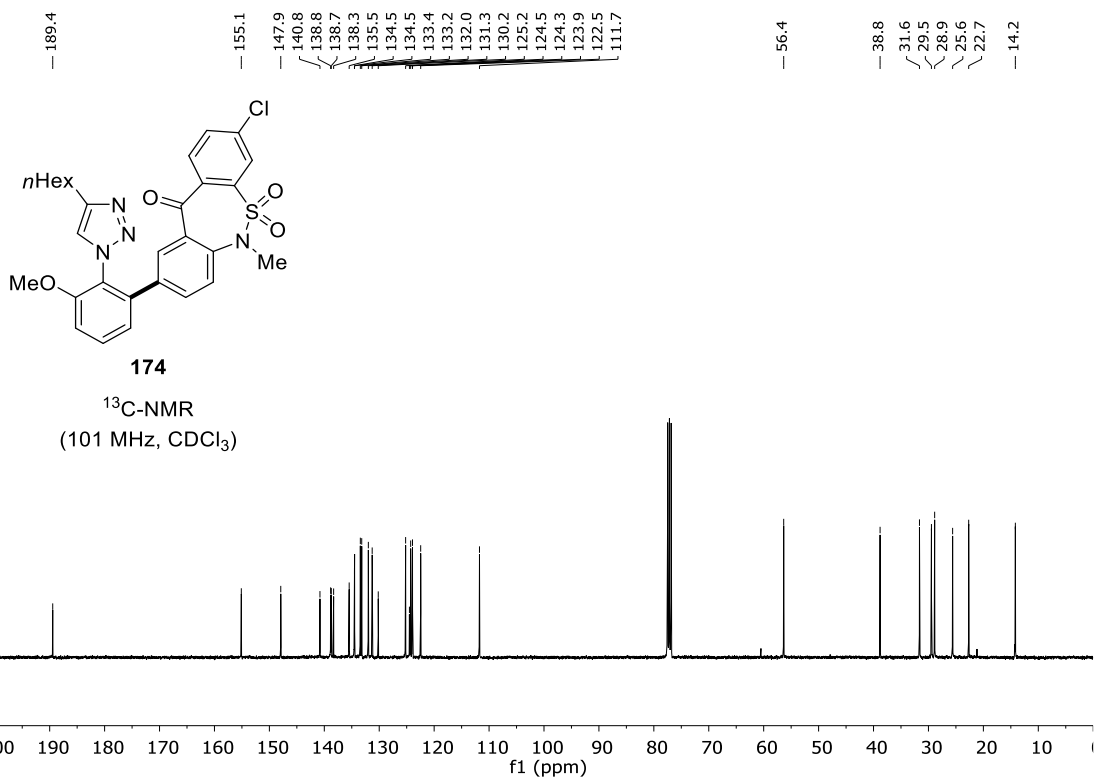
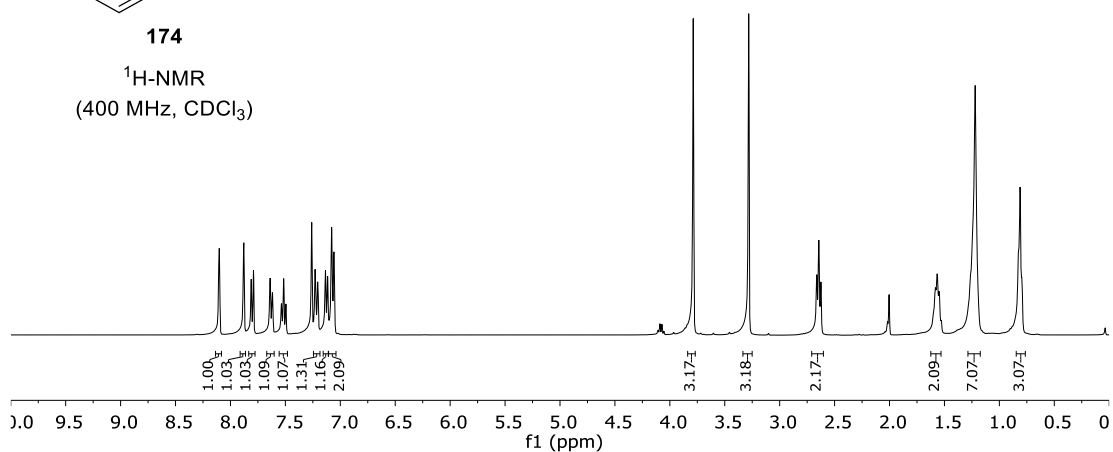


# NMR Spectra



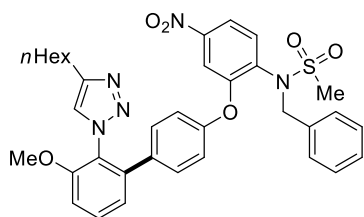
**174**

<sup>1</sup>H-NMR  
(400 MHz, CDCl<sub>3</sub>)

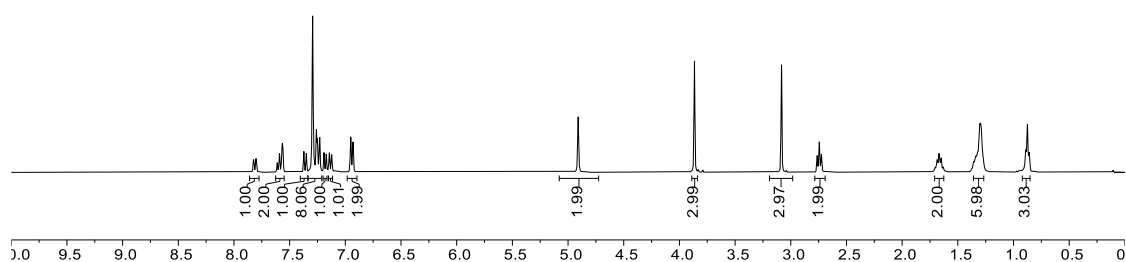


**174**

<sup>13</sup>C-NMR  
(101 MHz, CDCl<sub>3</sub>)



**175**  
<sup>1</sup>H-NMR  
 (400 MHz, CDCl<sub>3</sub>)



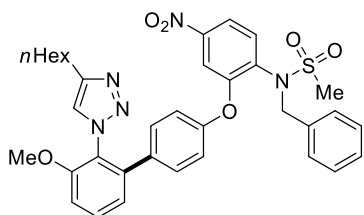
155.3  
 155.2  
 153.9  
 148.0  
 147.9  
 139.7  
 135.4  
 135.3  
 134.6  
 134.4  
 131.2  
 130.8  
 128.8  
 128.4  
 124.6  
 123.9  
 122.4  
 119.7  
 118.0  
 112.4  
 111.5

56.4  
 54.0

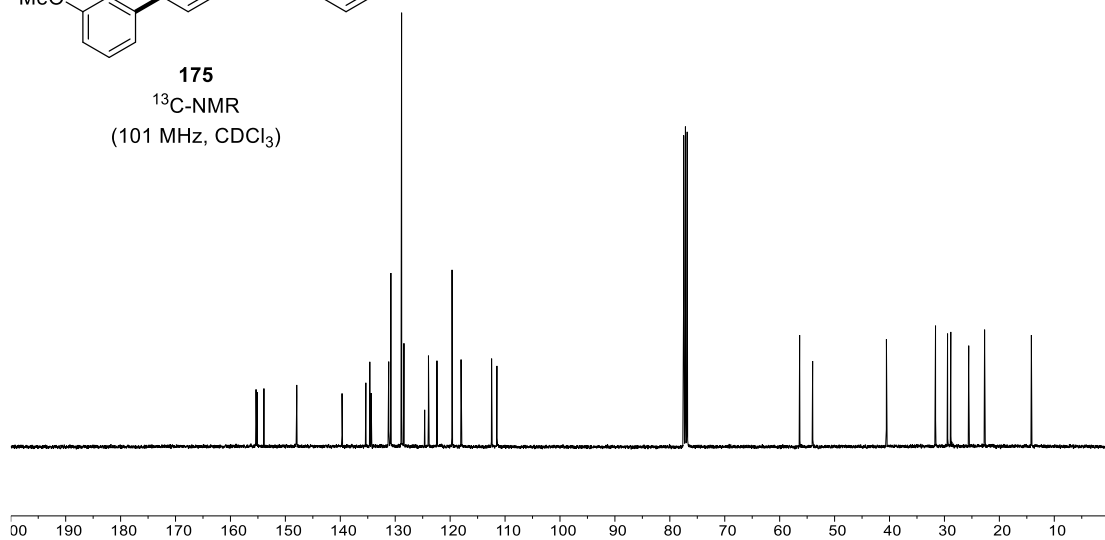
40.6

31.6  
 29.4  
 28.8  
 25.6  
 22.7

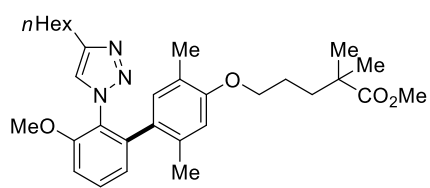
14.2



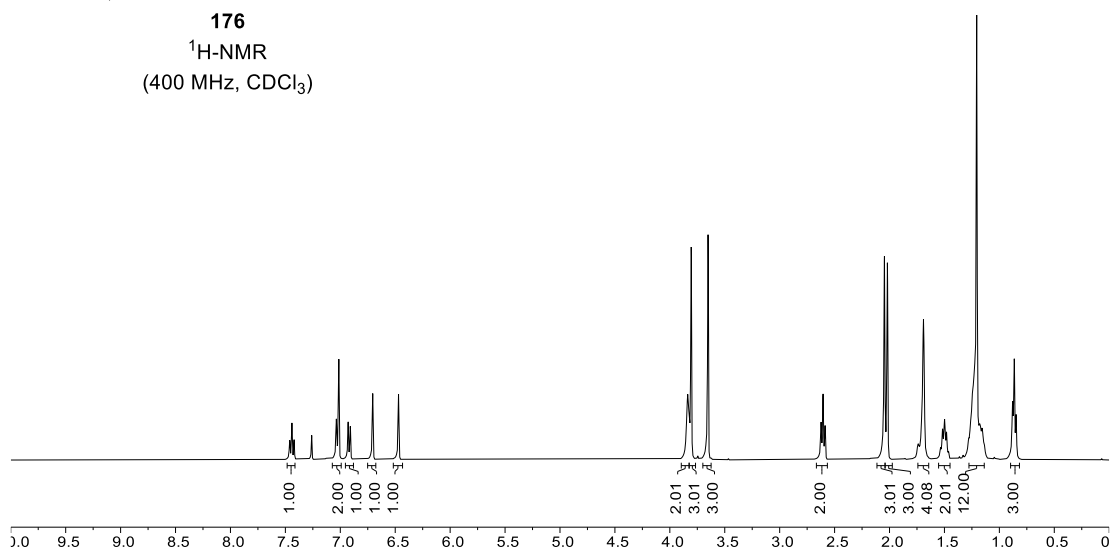
**175**  
<sup>13</sup>C-NMR  
 (101 MHz, CDCl<sub>3</sub>)



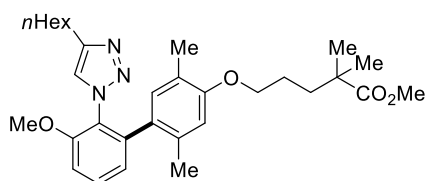
# NMR Spectra



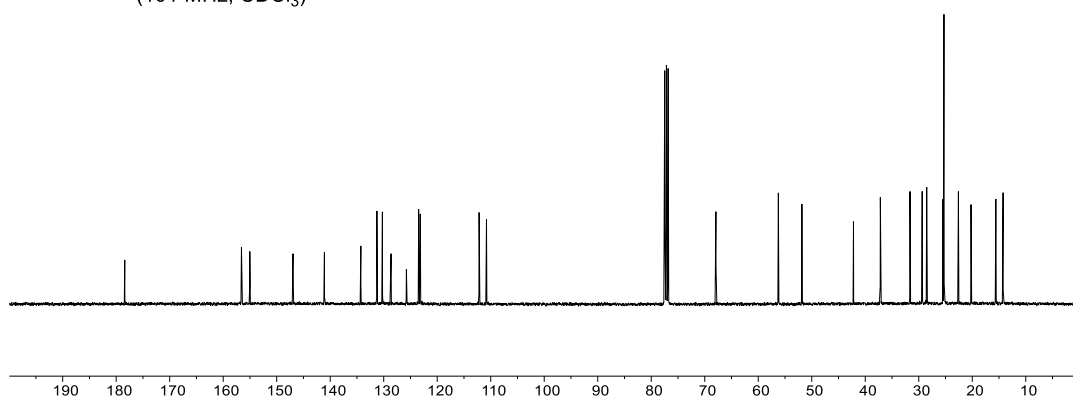
**176**  
<sup>1</sup>H-NMR  
 (400 MHz, CDCl<sub>3</sub>)

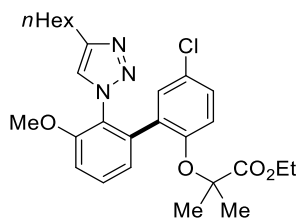


— 178.4  
 — 156.6  
 — 155.0  
 — 147.0  
 — 141.1  
 — 134.3  
 — 131.3  
 — 130.2  
 — 128.6  
 — 125.8  
 — 123.5  
 — 123.4  
 — 123.2  
 — 112.2  
 — 110.8  
 — 67.9  
 — 56.2  
 — 51.8  
 — 42.2  
 — 37.2  
 — 31.6  
 — 29.4  
 — 28.5  
 — 25.5  
 — 25.3  
 — 25.3  
 — 22.6  
 — 20.2  
 — 15.6  
 — 14.2



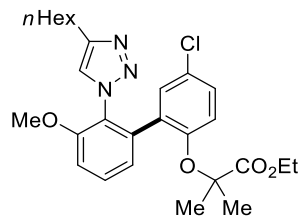
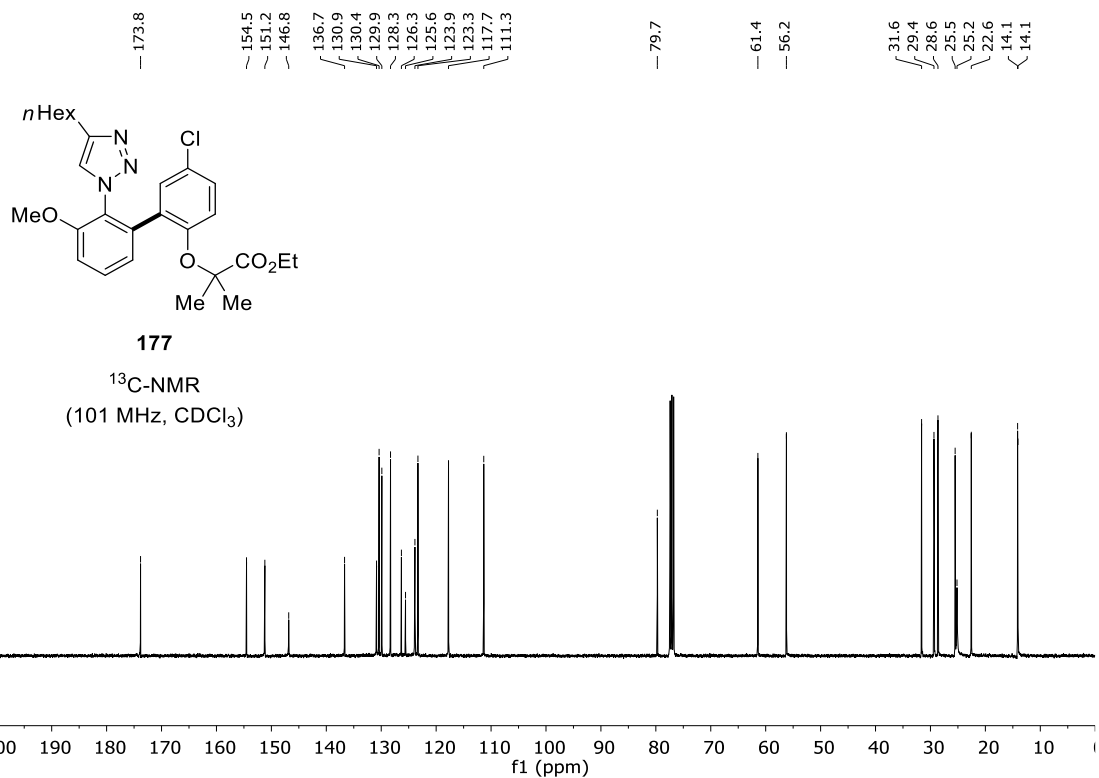
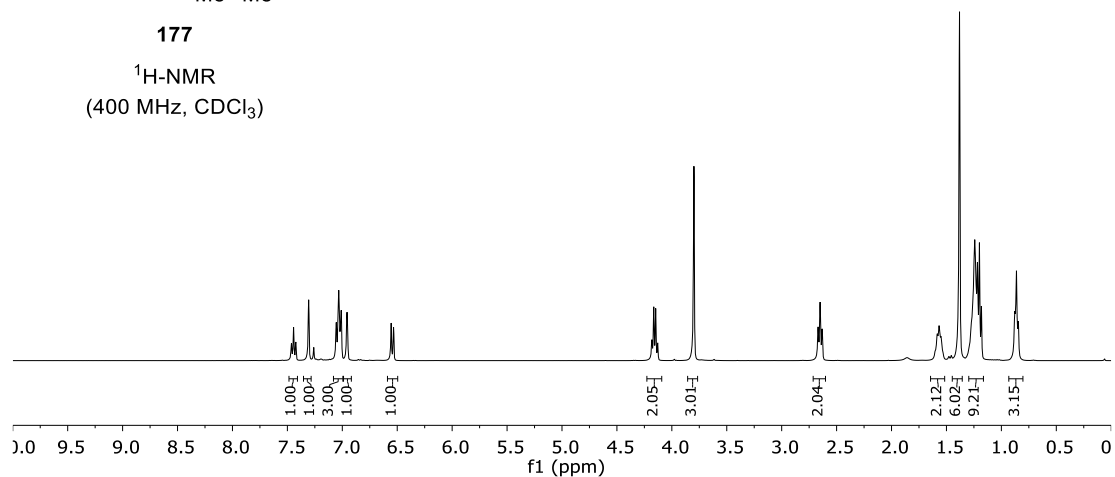
**176**  
<sup>13</sup>C-NMR  
 (101 MHz, CDCl<sub>3</sub>)





177

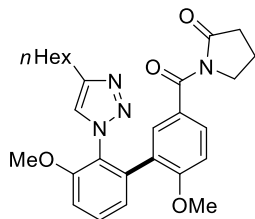
<sup>1</sup>H-NMR  
(400 MHz, CDCl<sub>3</sub>)



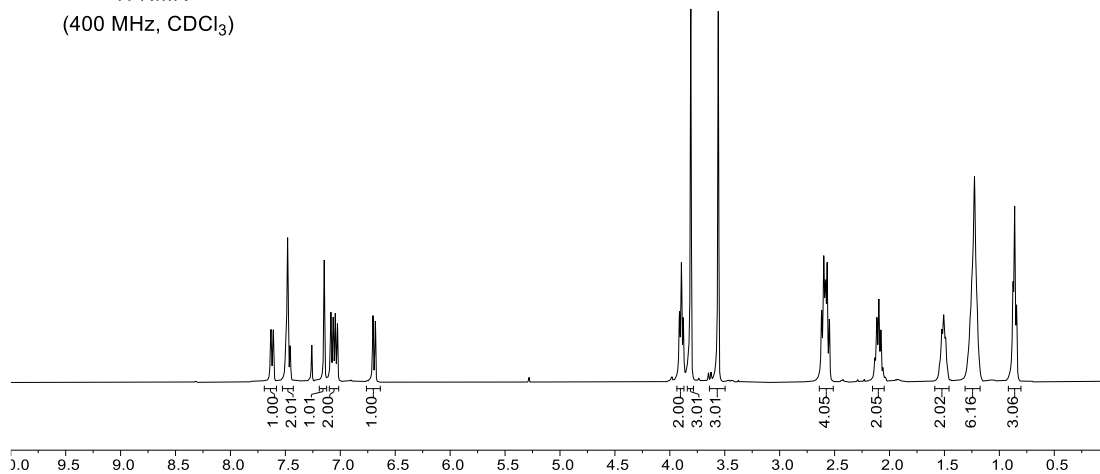
177

<sup>13</sup>C-NMR  
(101 MHz, CDCl<sub>3</sub>)

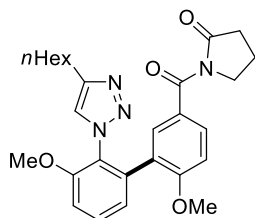
# NMR Spectra



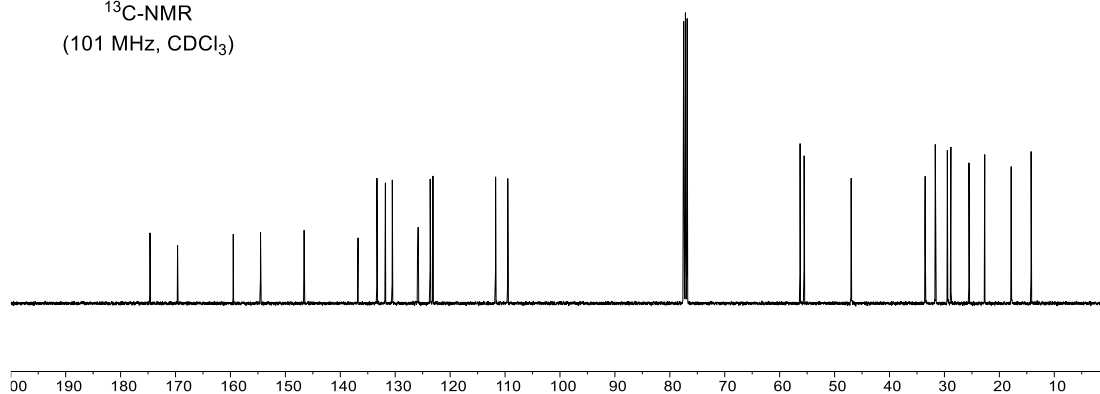
**178**  
<sup>1</sup>H-NMR  
 (400 MHz, CDCl<sub>3</sub>)



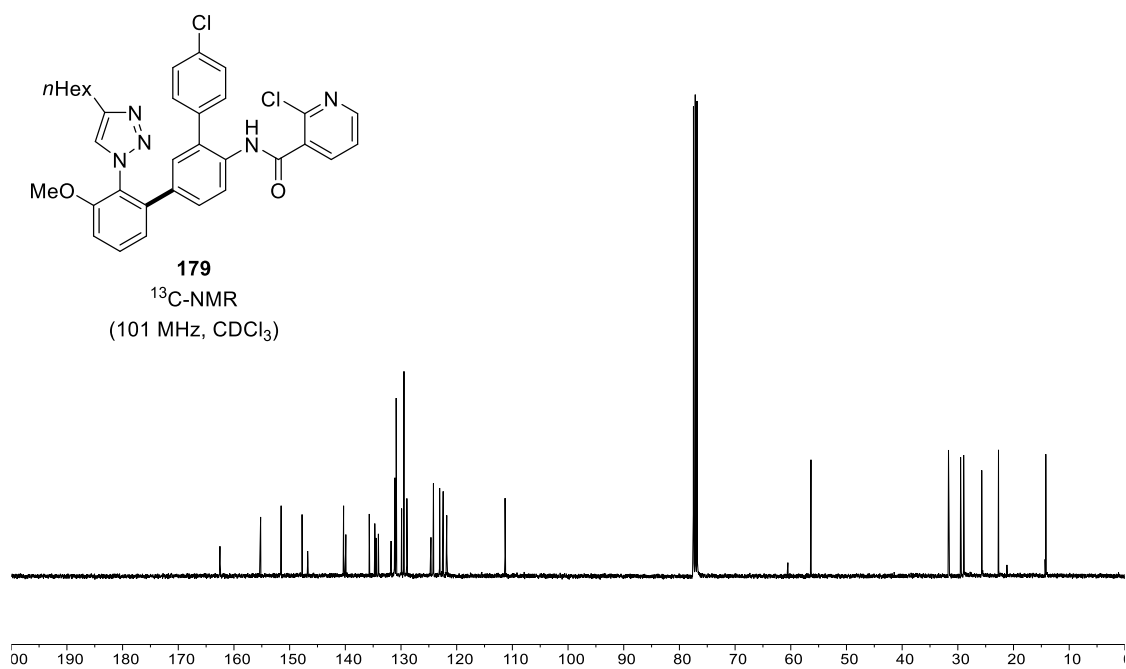
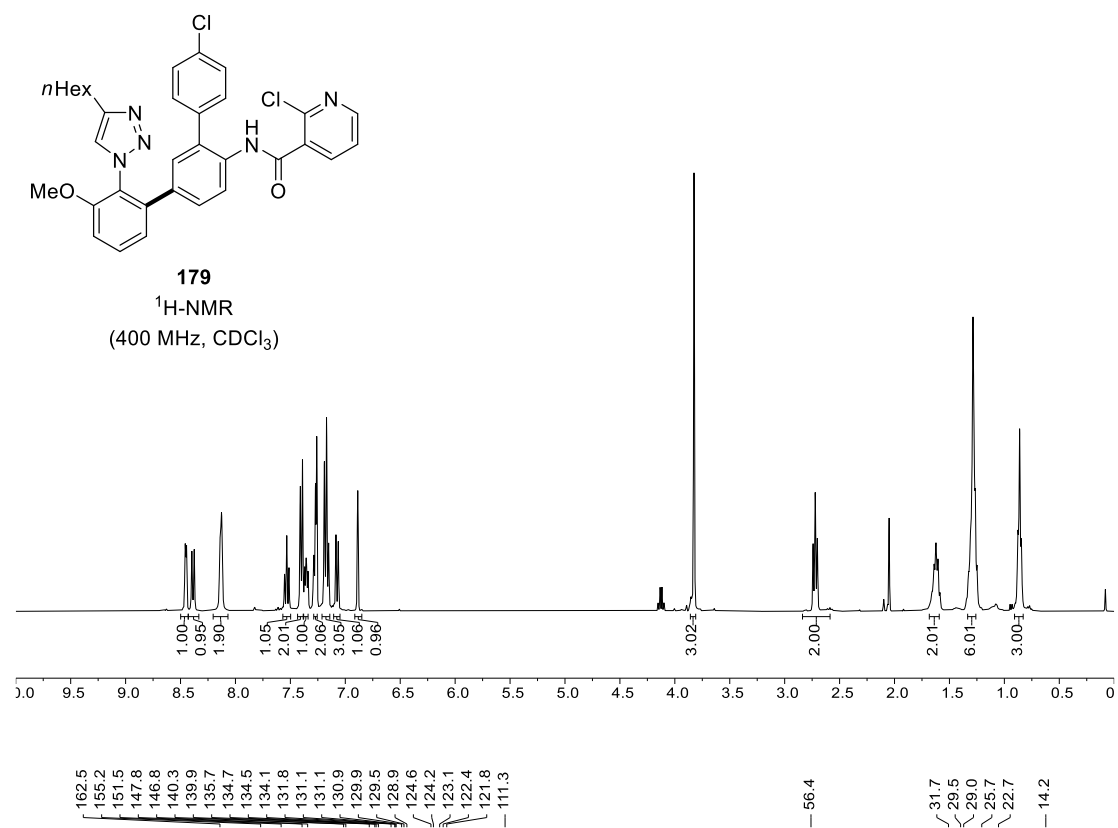
- 174.6
- 169.6
- 159.5
- 154.5
- 146.6
- 136.8
- 133.3
- 131.8
- 130.5
- 125.9
- 125.8
- 123.6
- 123.1
- 111.7
- 109.5
- 56.3
- 55.5
- 47.0
- 33.5
- 31.7
- 29.5
- 28.8
- 25.5
- 22.7
- 17.8
- 14.2



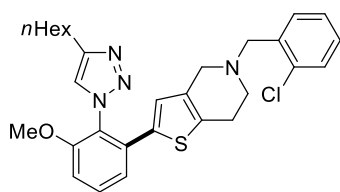
**178**  
<sup>13</sup>C-NMR  
 (101 MHz, CDCl<sub>3</sub>)



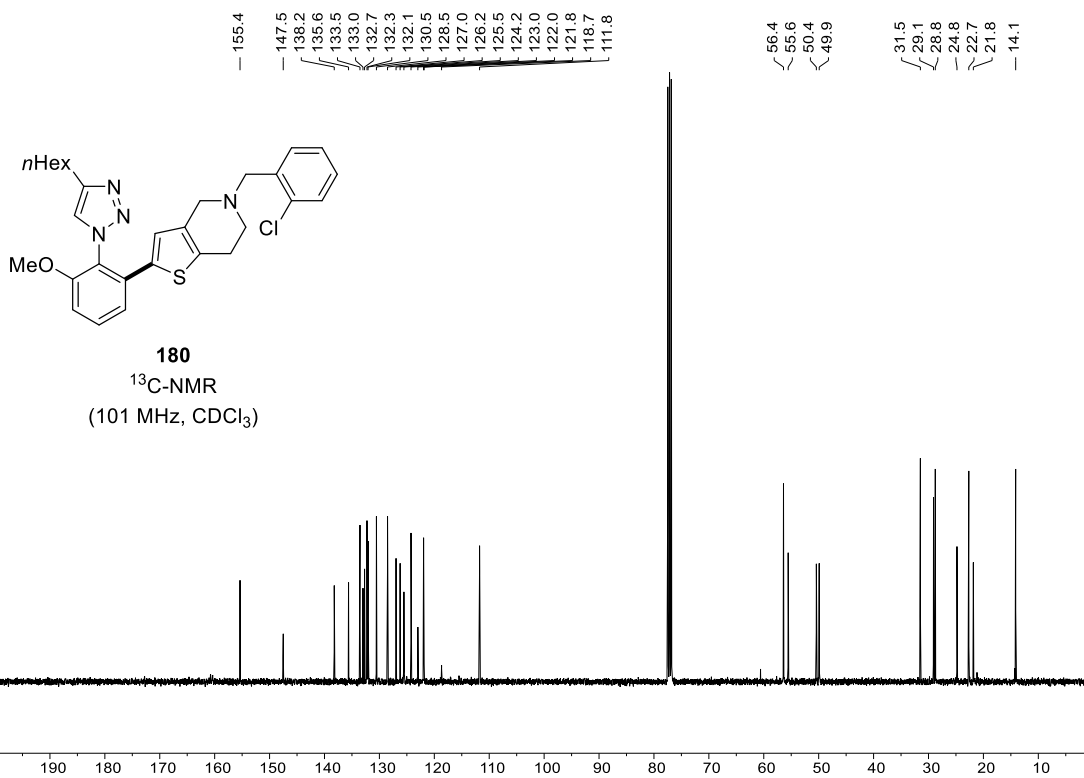
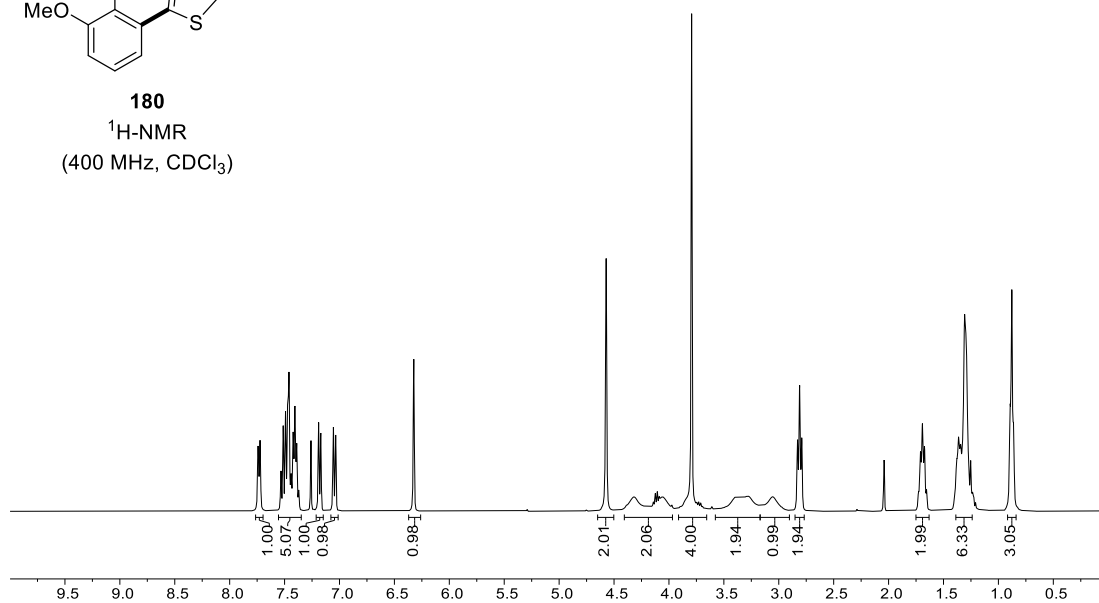


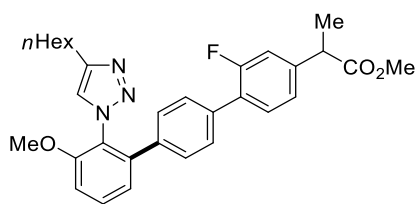


# NMR Spectra



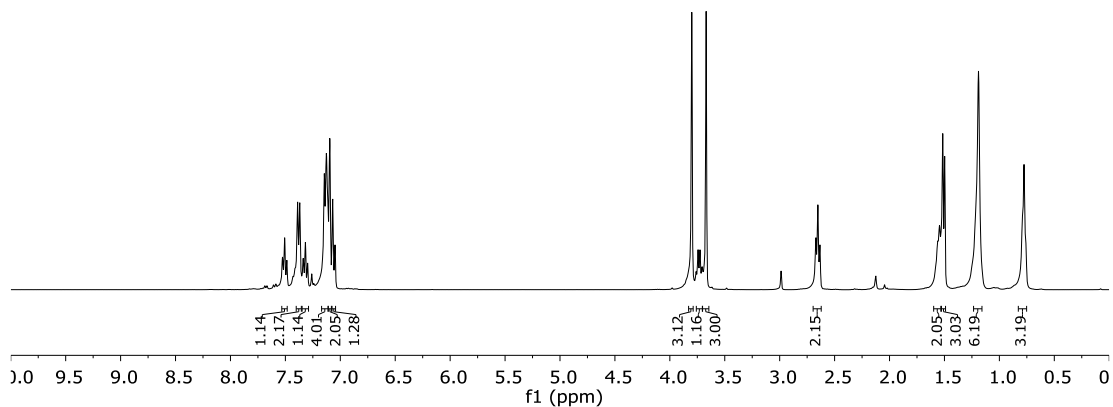
**180**  
<sup>1</sup>H-NMR  
 (400 MHz, CDCl<sub>3</sub>)





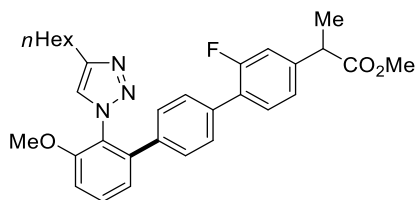
**181**

<sup>1</sup>H-NMR  
(400 MHz, CDCl<sub>3</sub>)



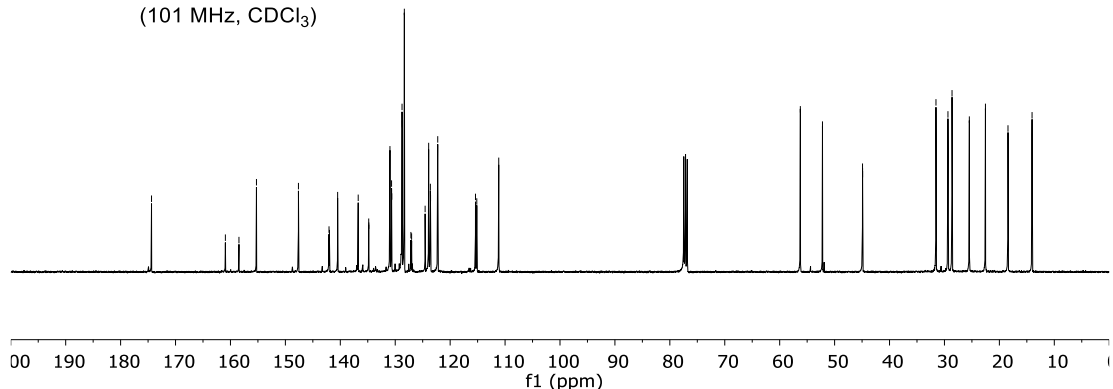
Chemical shift values (ppm) for <sup>13</sup>C-NMR spectrum:

- 174.4
- 160.9
- 158.5
- 155.3
- 147.6
- 142.1
- 142.0
- 140.5
- 136.7
- 134.8
- 131.0
- 130.7
- 130.6
- 128.8
- 128.7
- 128.3
- 127.1
- 127.0
- 124.6
- 123.9
- 123.6
- 123.6
- 122.3
- 115.4
- 115.1
- 111.2
- 56.2
- 52.2
- 44.9
- 44.9
- 31.5
- 29.4
- 28.6
- 25.5
- 22.5
- 18.4
- 14.0

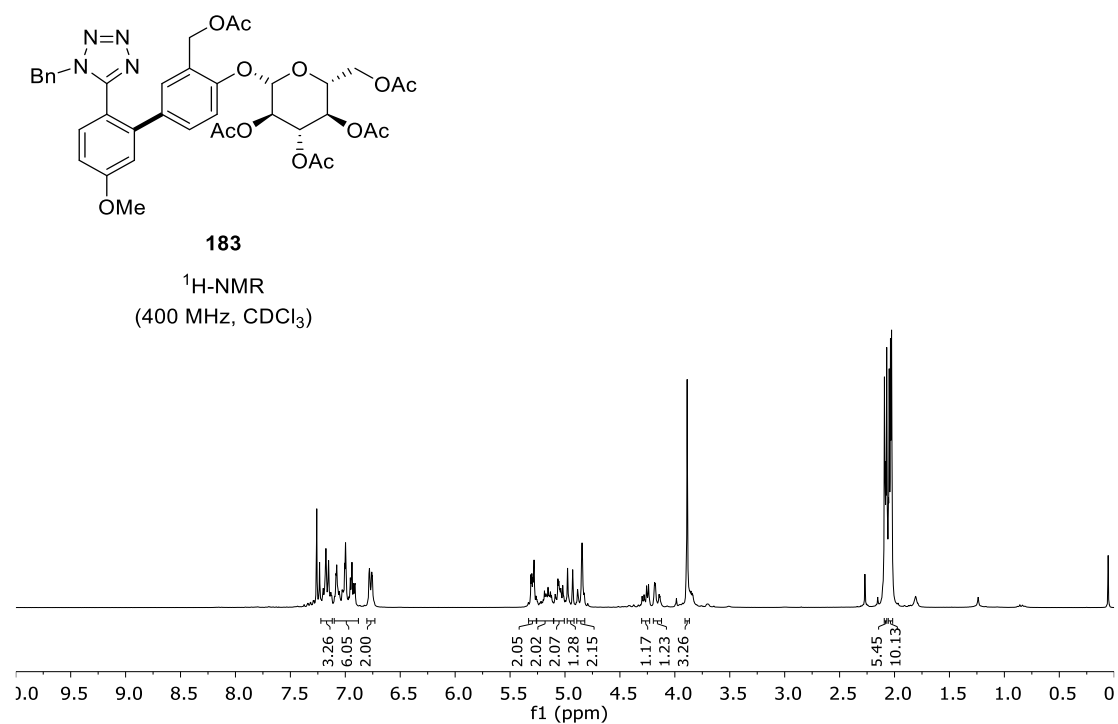
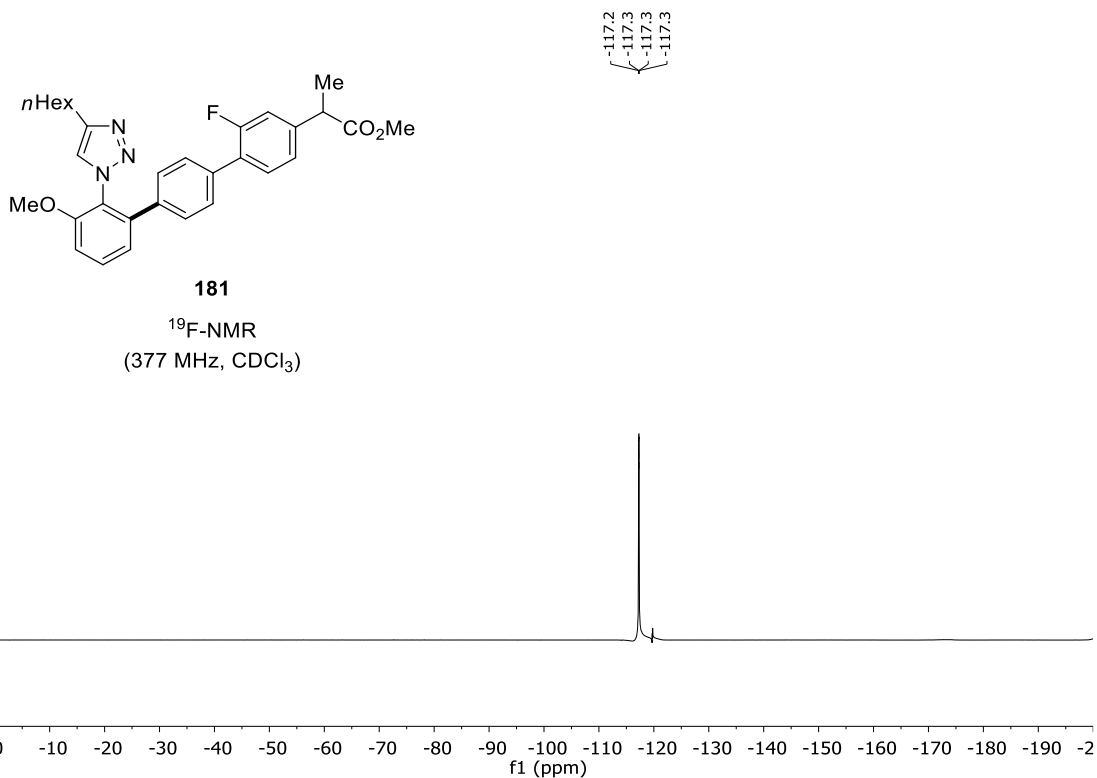


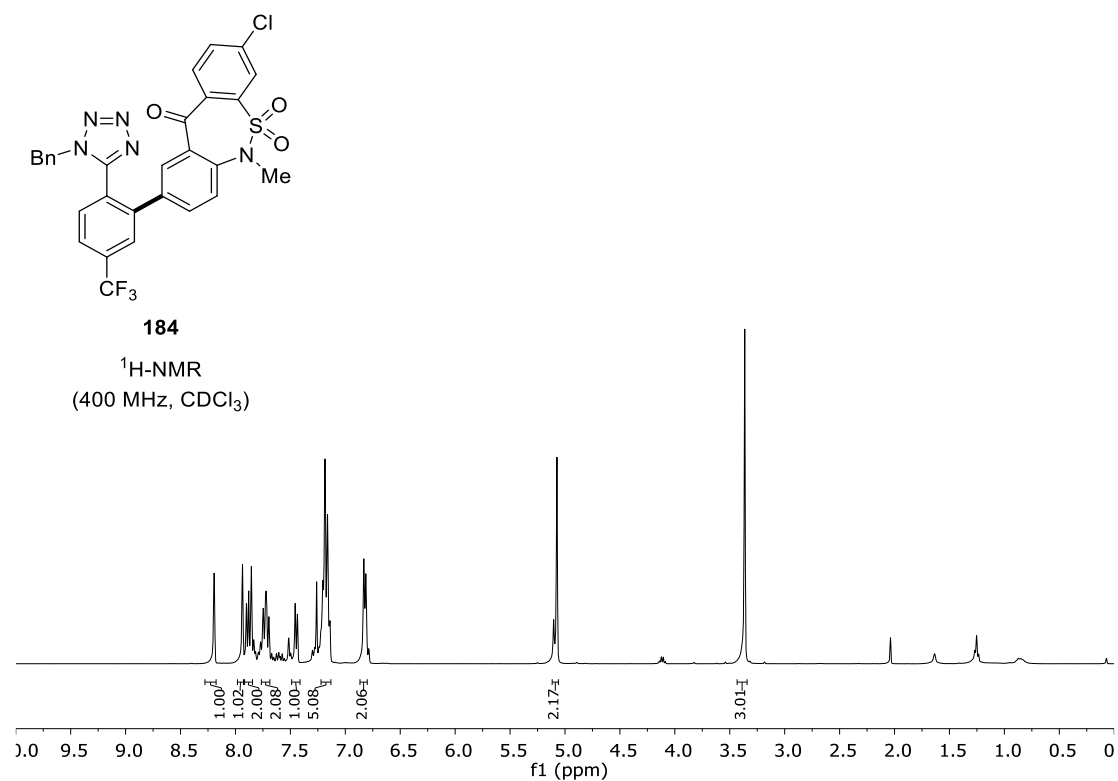
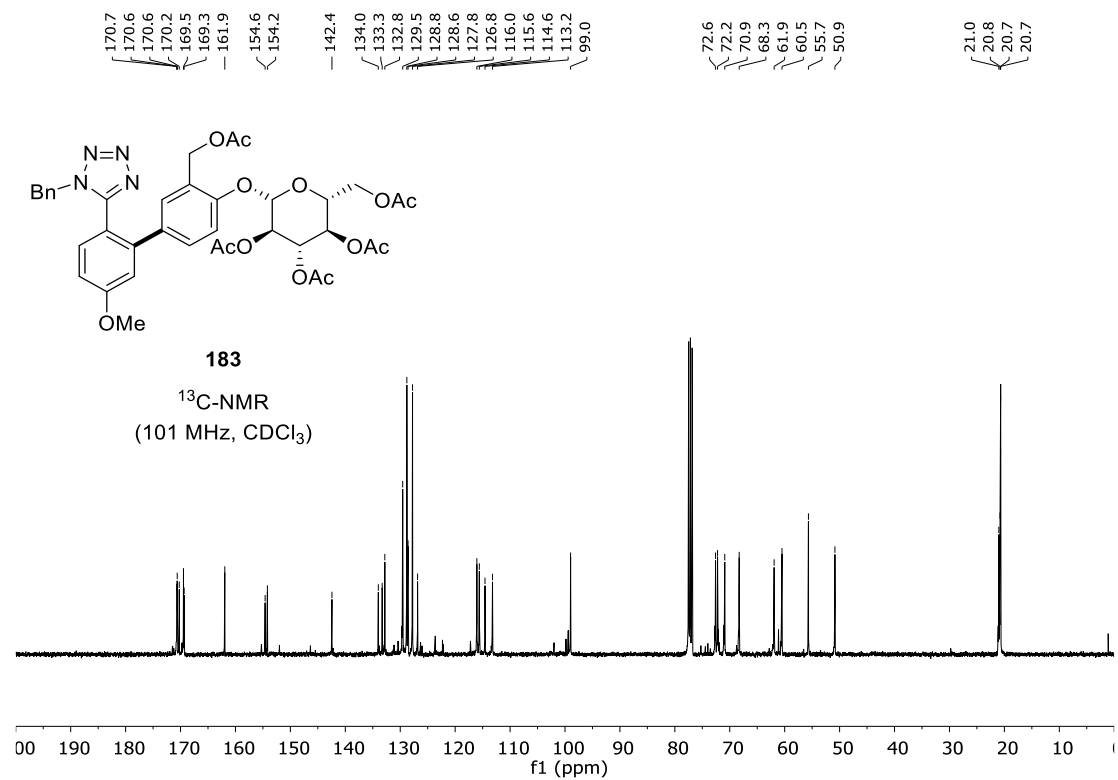
**181**

<sup>13</sup>C-NMR  
(101 MHz, CDCl<sub>3</sub>)

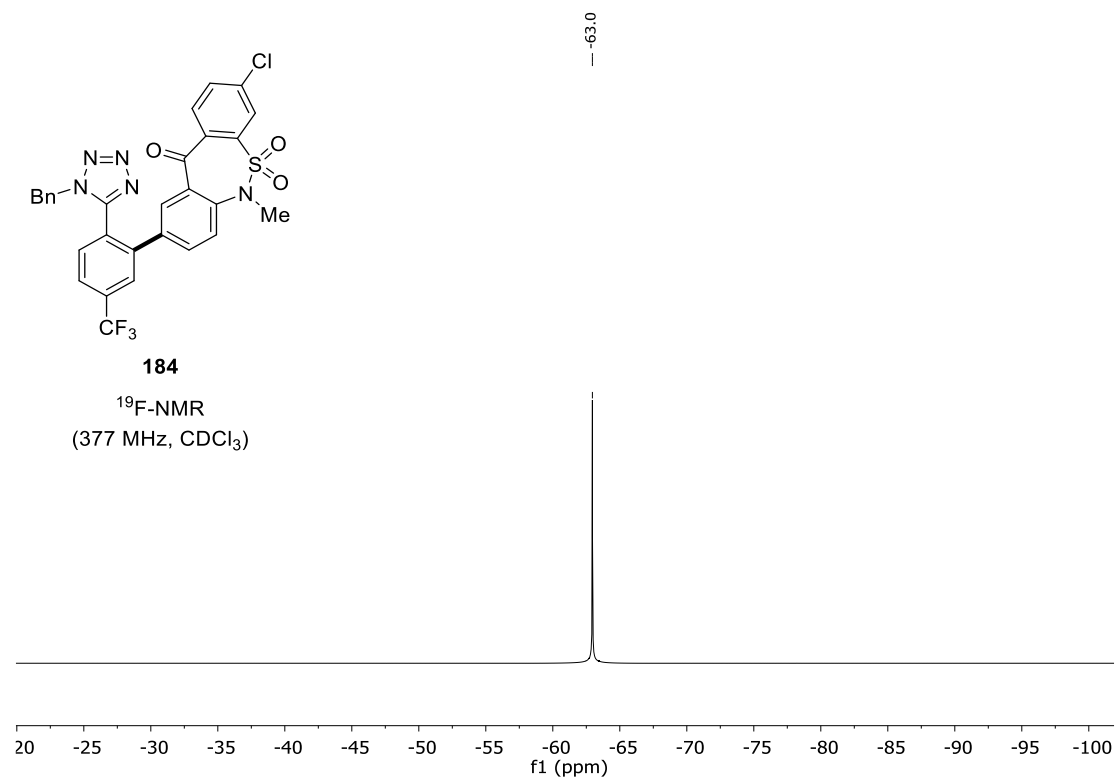
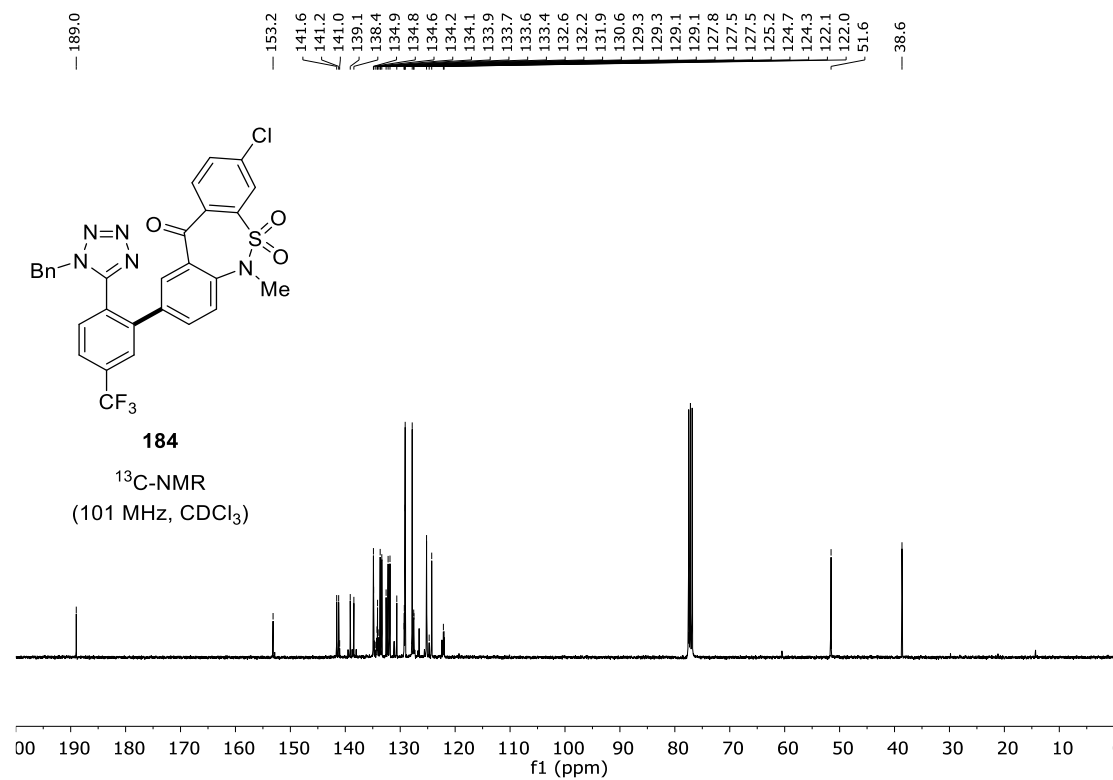


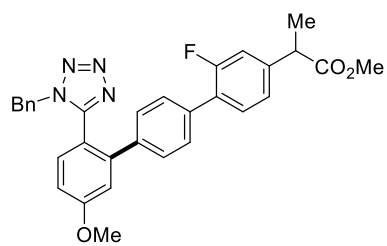
# NMR Spectra



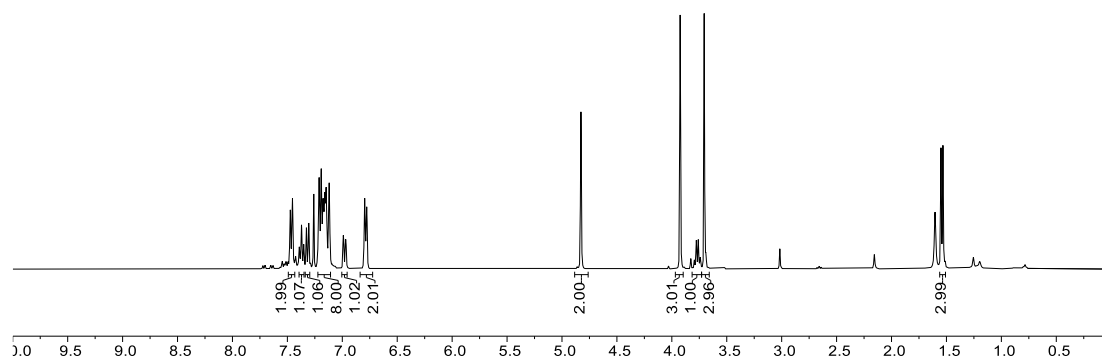


# NMR Spectra

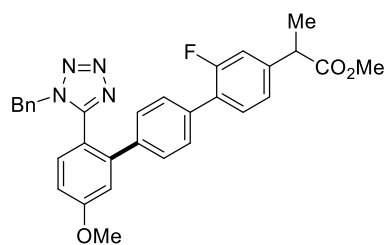




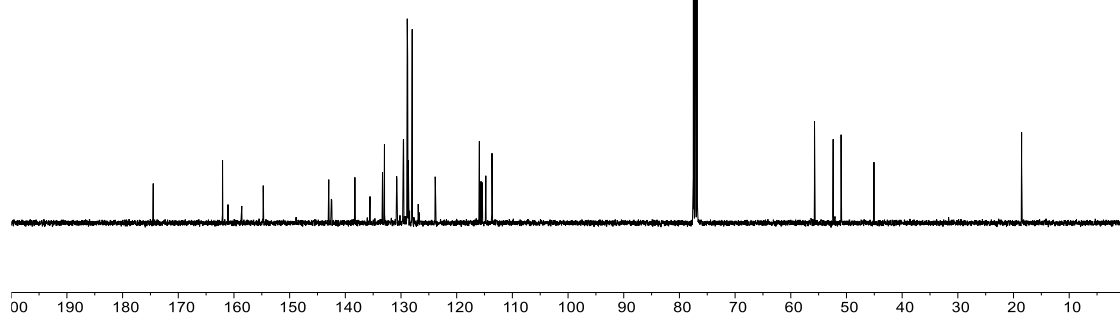
**185**  
<sup>1</sup>H-NMR  
(400 MHz, CDCl<sub>3</sub>)



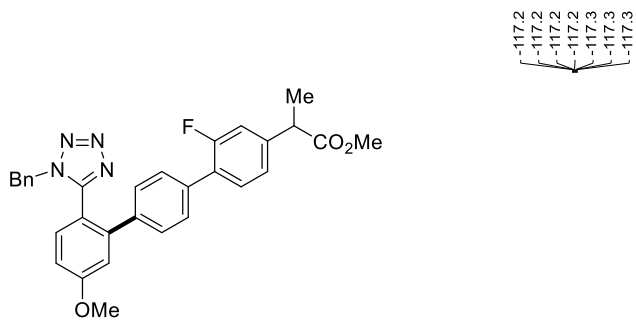
174.5  
162.1  
161.1  
158.6  
154.7  
143.0  
142.5  
142.4  
138.3  
136.6  
133.3  
133.0  
130.8  
130.7  
129.6  
129.5  
128.9  
128.9  
128.8  
128.7  
128.5  
128.0  
128.0  
126.9  
126.8  
123.9  
123.8  
115.9  
115.6  
115.4  
114.8  
113.7  
55.7  
52.4  
51.0  
45.1  
18.5



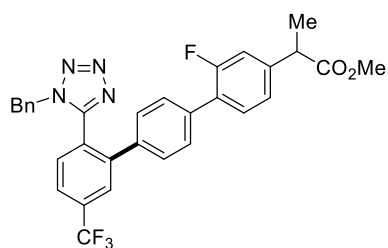
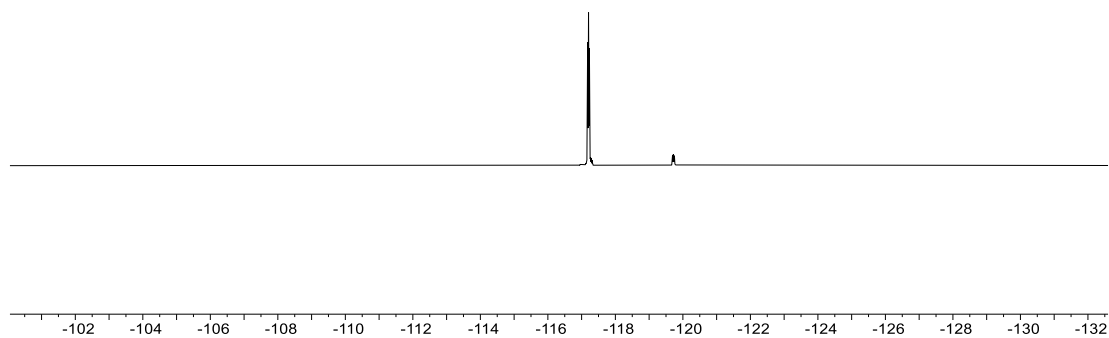
**185**  
<sup>13</sup>C-NMR  
(101 MHz, CDCl<sub>3</sub>)



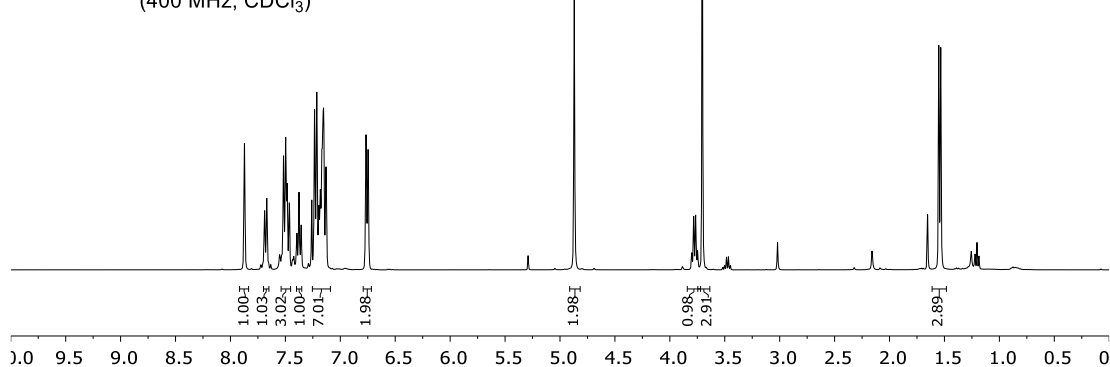
# NMR Spectra



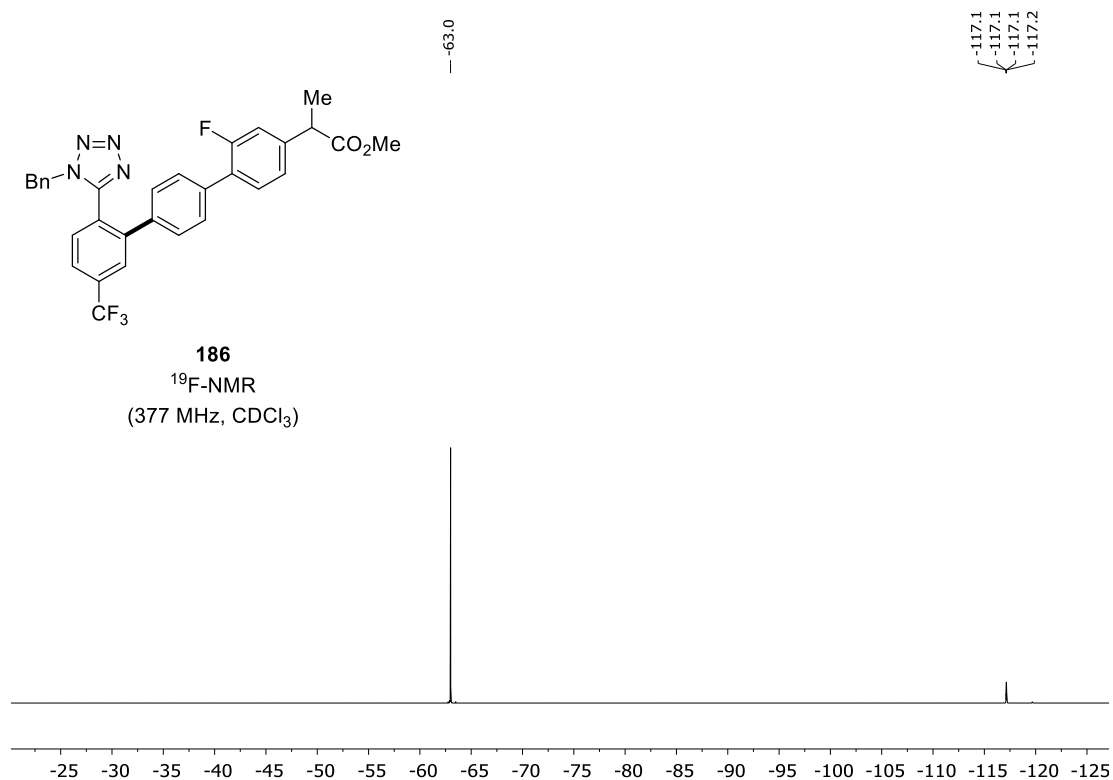
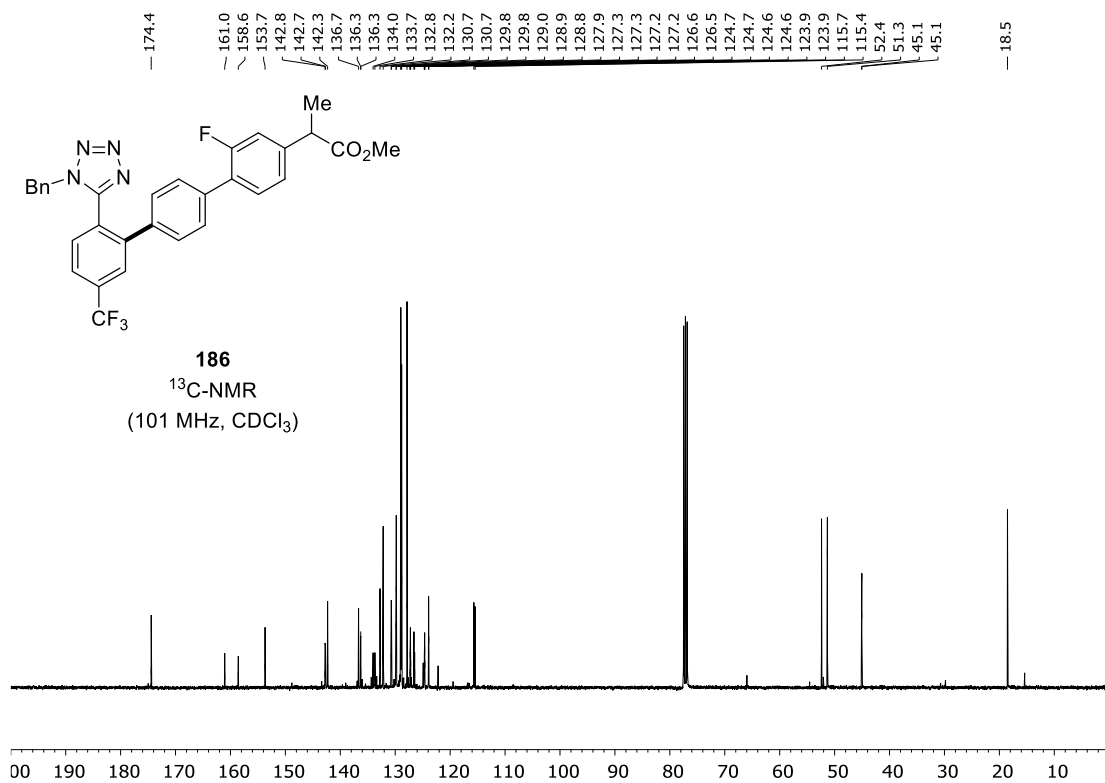
**185**  
<sup>19</sup>F-NMR  
 (377 MHz, CDCl<sub>3</sub>)



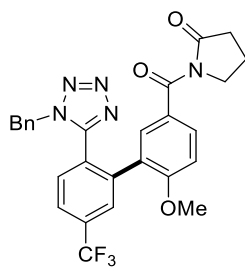
**186**  
<sup>1</sup>H-NMR  
 (400 MHz, CDCl<sub>3</sub>)





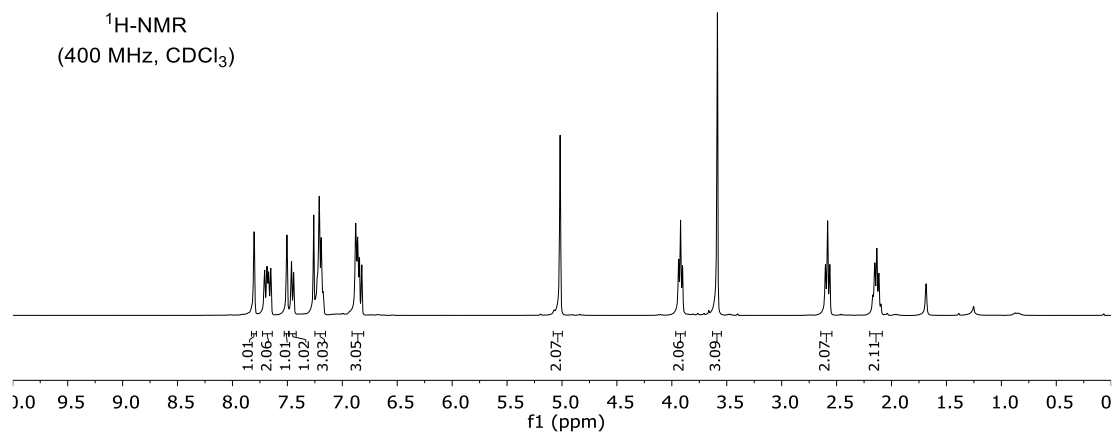


# NMR Spectra

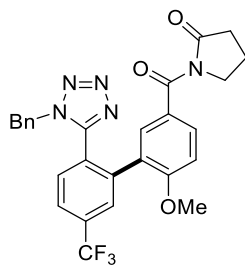


**187**

<sup>1</sup>H-NMR  
(400 MHz, CDCl<sub>3</sub>)

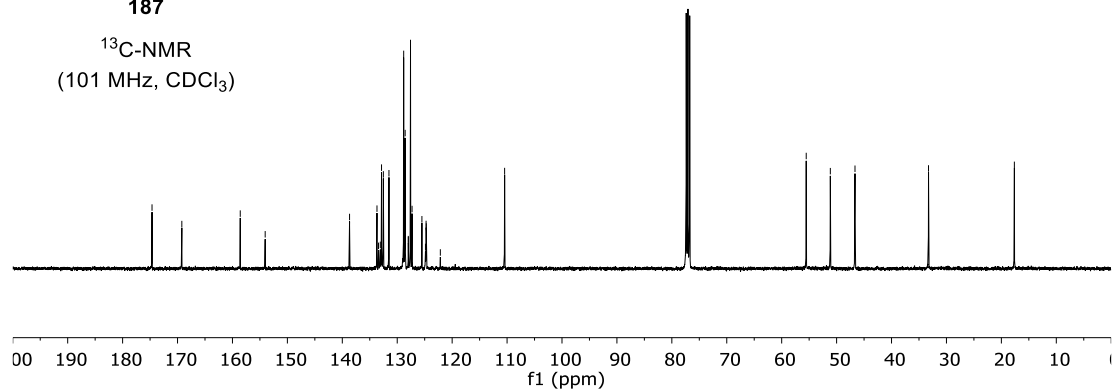


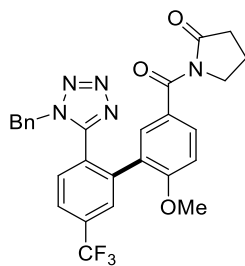
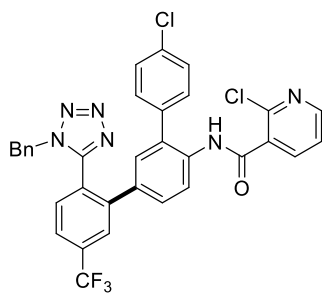
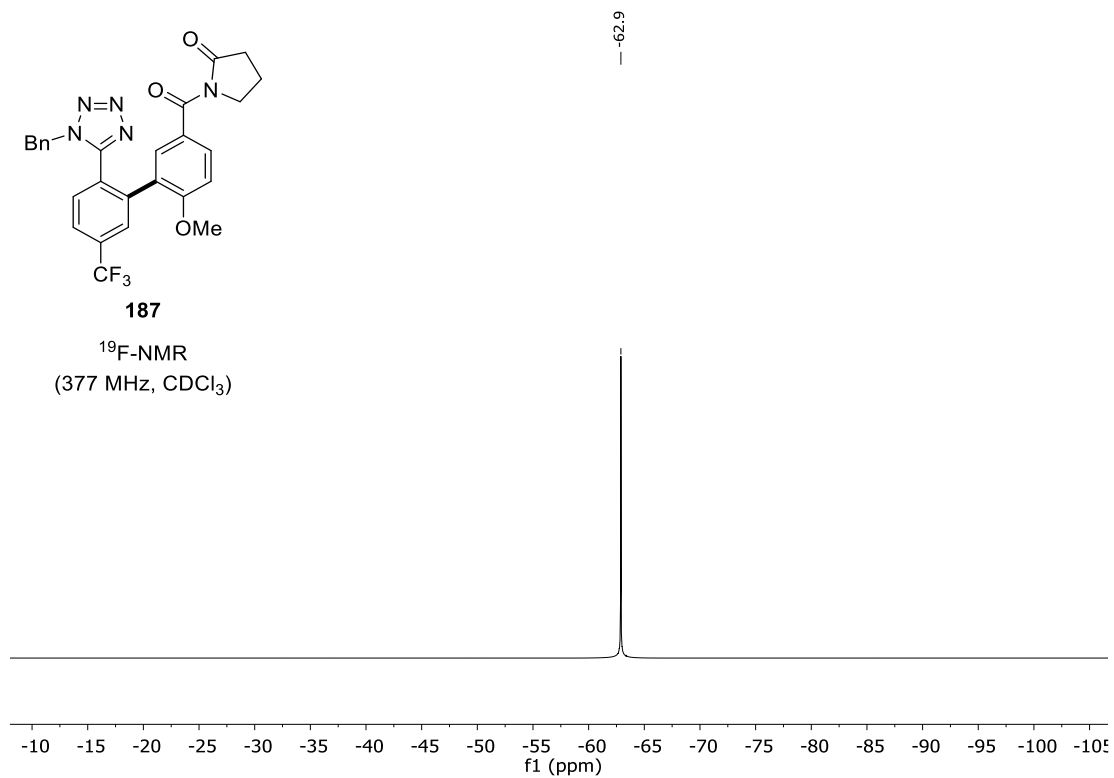
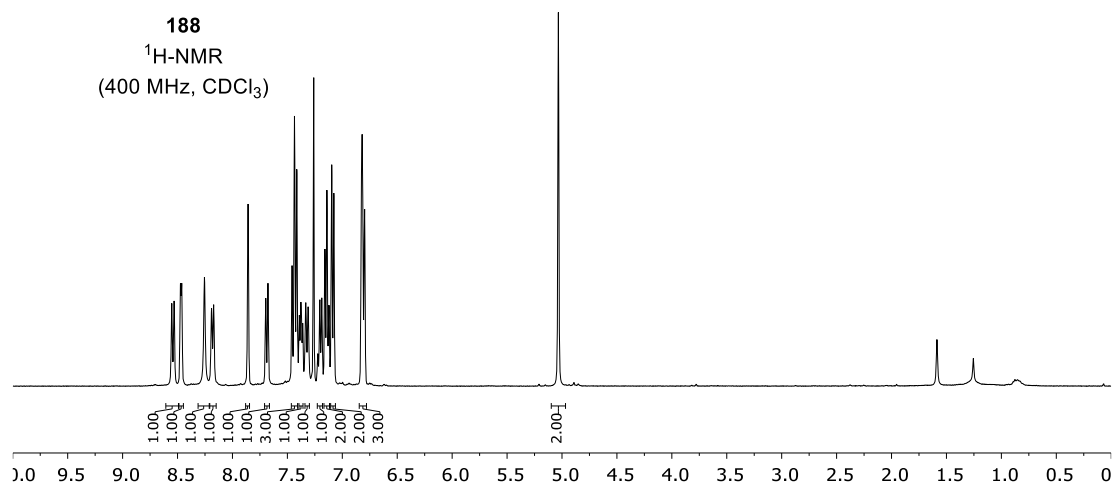
174.6  
169.2  
158.6  
154.0  
138.7  
133.7  
133.4  
133.1  
132.9  
132.5  
131.5  
128.8  
128.6  
128.6  
128.0  
128.0  
127.6  
127.3  
125.5  
124.9  
124.7  
124.7  
122.1  
110.4  
55.5  
51.1  
46.7  
33.3  
17.6



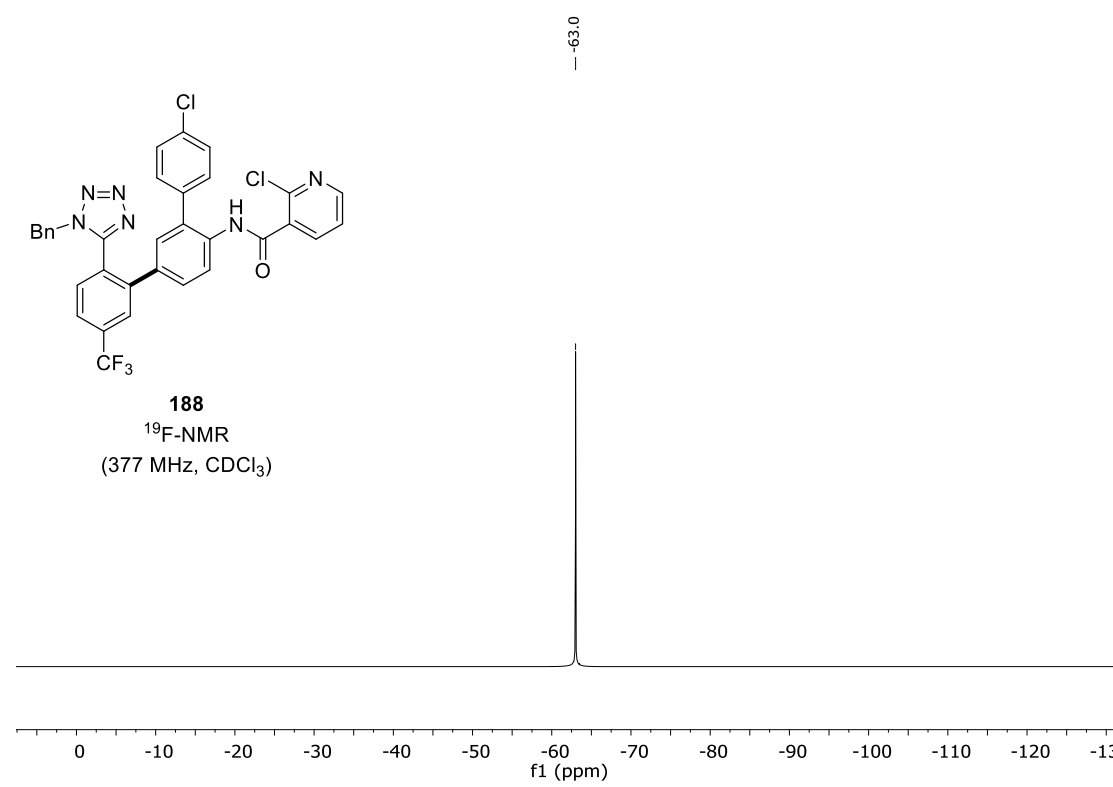
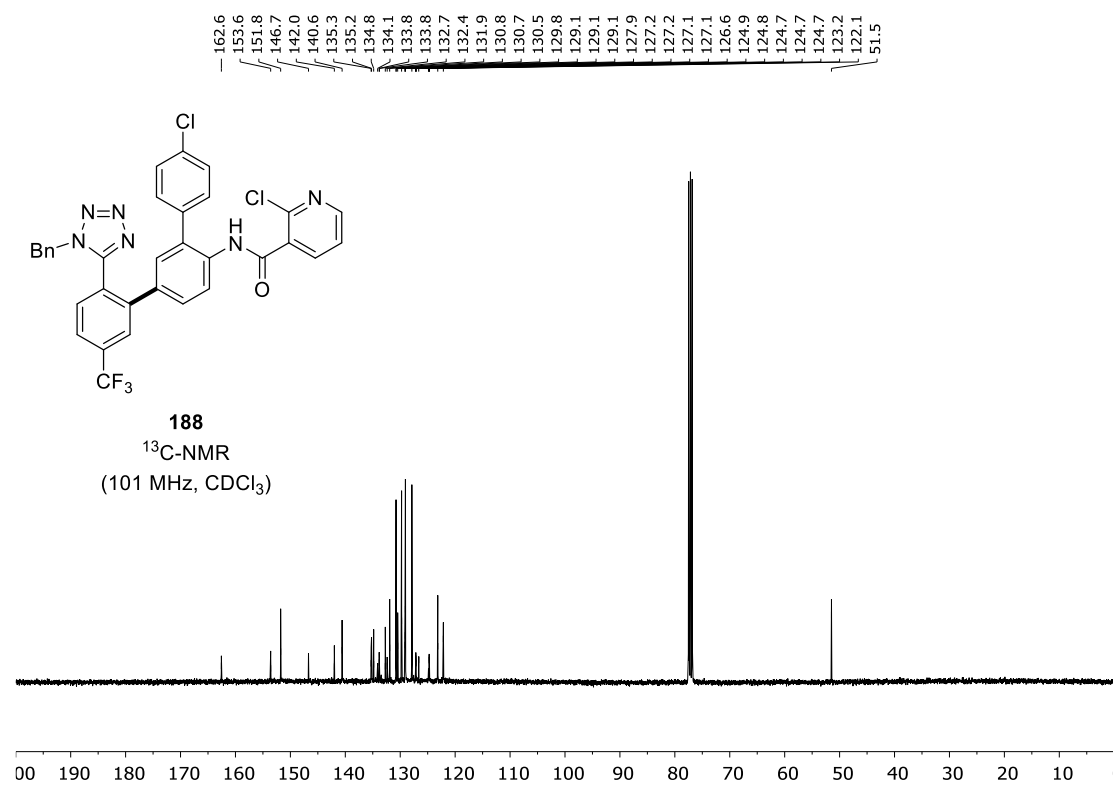
**187**

<sup>13</sup>C-NMR  
(101 MHz, CDCl<sub>3</sub>)

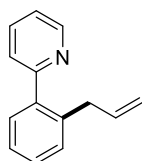


**187**<sup>19</sup>F-NMR  
(377 MHz, CDCl<sub>3</sub>)**188**<sup>1</sup>H-NMR  
(400 MHz, CDCl<sub>3</sub>)

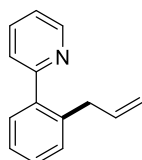
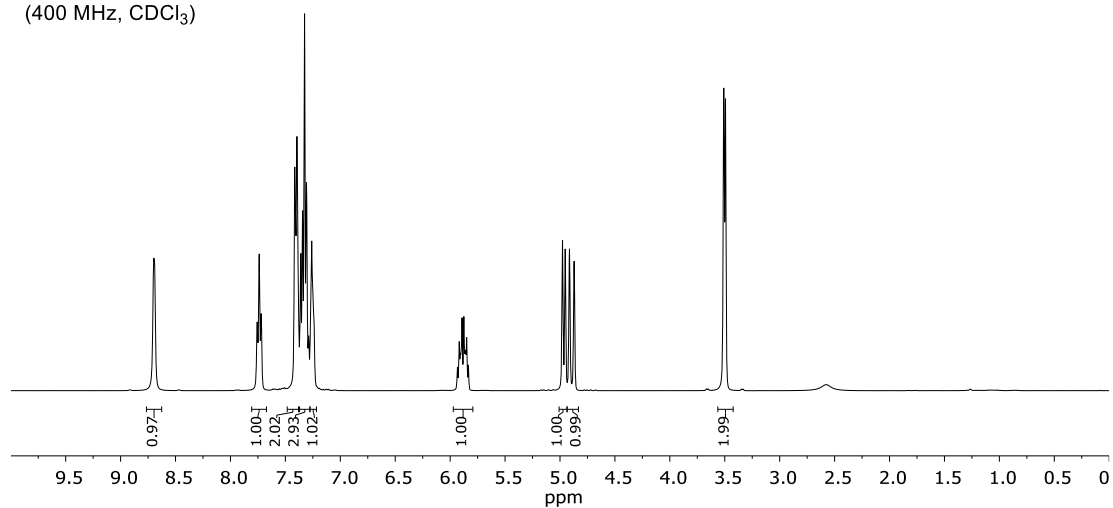
# NMR Spectra



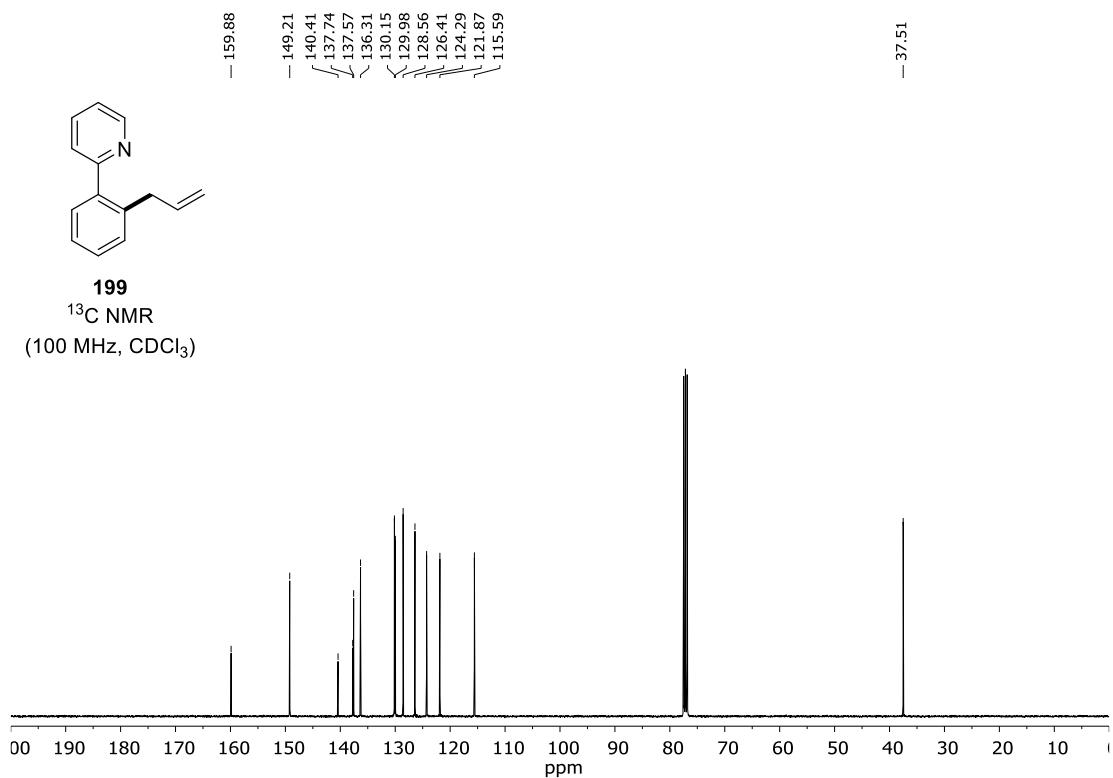
## 7.2 Photo-Induced Ruthenium-Catalyzed C–H Alkylation



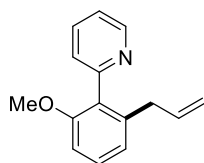
**199**  
 $^1\text{H}$  NMR  
(400 MHz,  $\text{CDCl}_3$ )



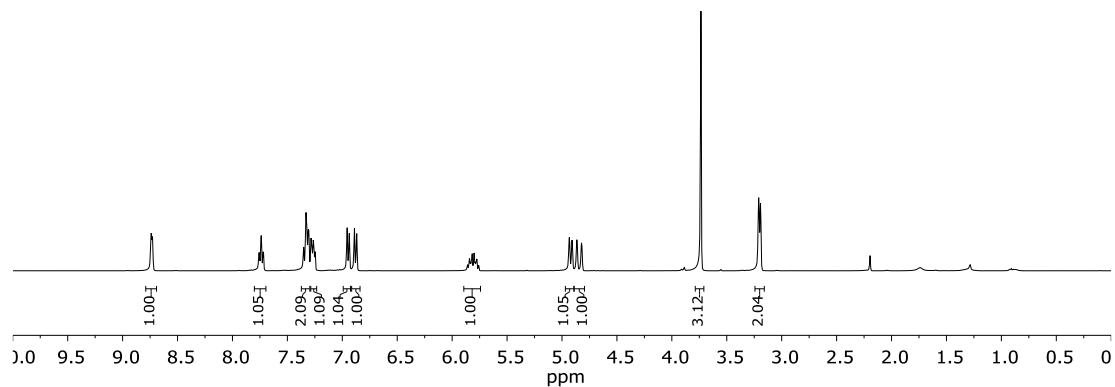
**199**  
 $^{13}\text{C}$  NMR  
(100 MHz,  $\text{CDCl}_3$ )



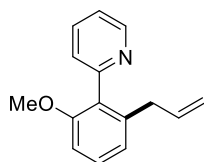
# NMR Spectra



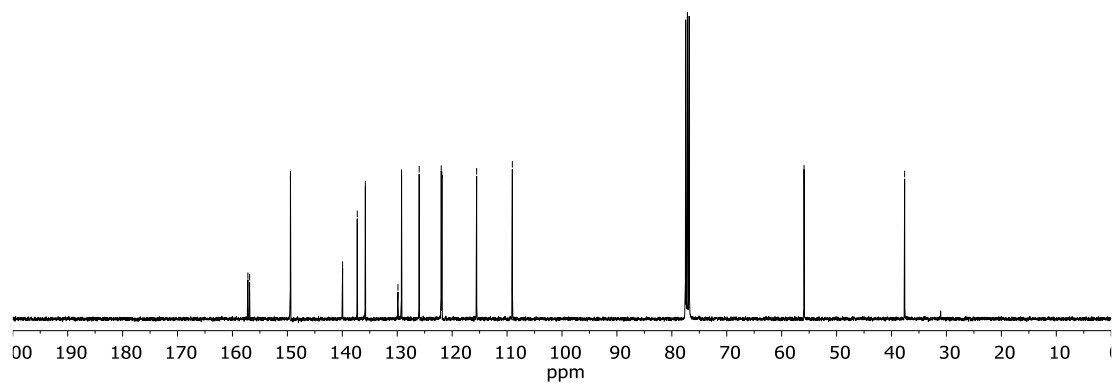
**203**  
<sup>1</sup>H NMR  
 (400 MHz, CDCl<sub>3</sub>)

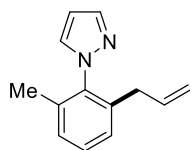


157.19  
 156.88  
 149.44  
 139.94  
 137.28  
 135.80  
 129.87  
 129.21  
 126.00  
 121.99  
 121.87  
 115.54  
 109.04  
 55.93  
 37.61

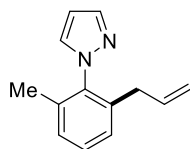
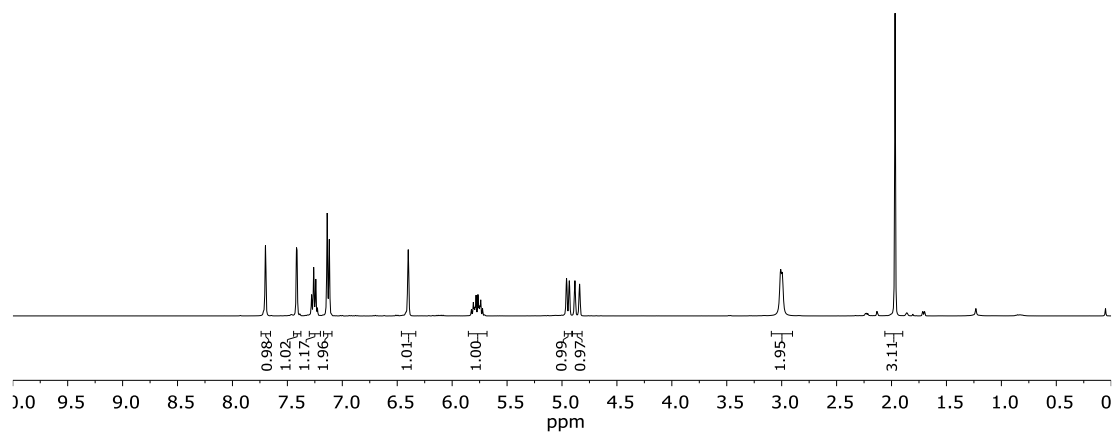


**203**  
<sup>13</sup>C NMR  
 (100 MHz, CDCl<sub>3</sub>)

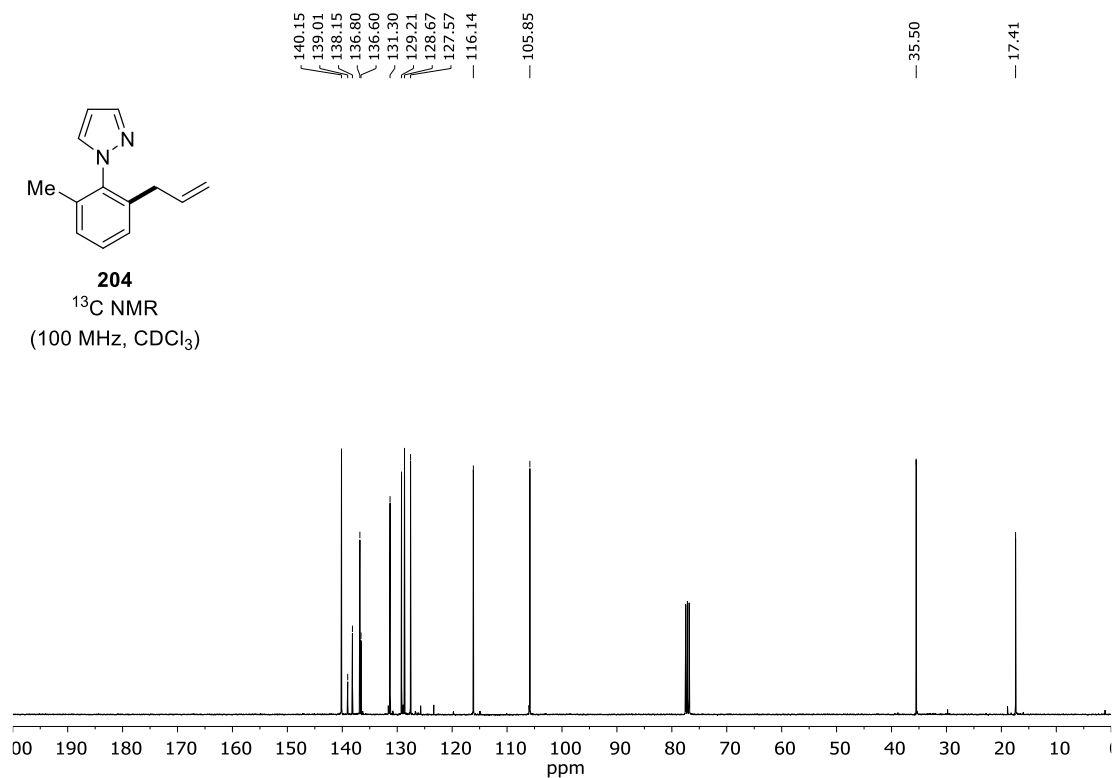




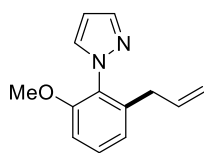
**204**  
<sup>1</sup>H NMR  
 (400 MHz, CDCl<sub>3</sub>)



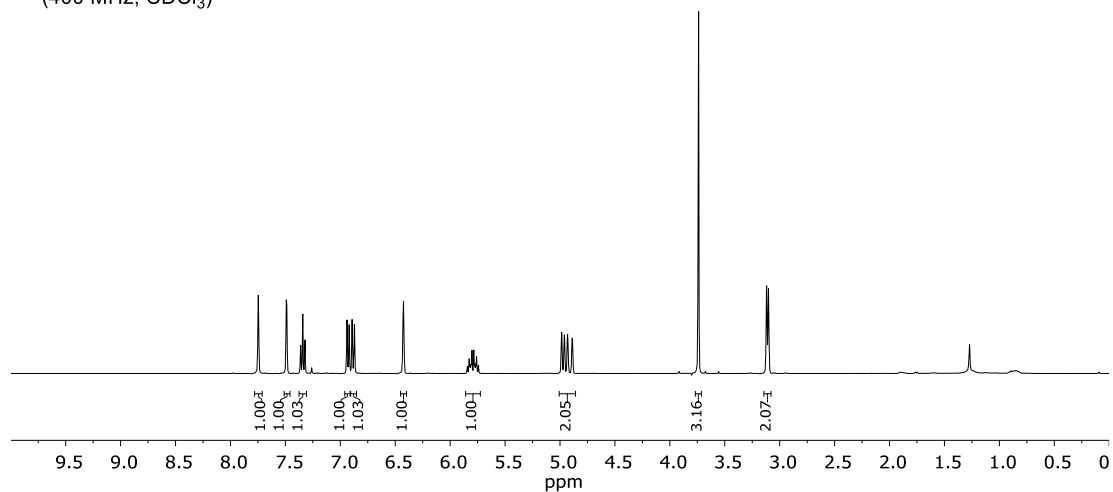
**204**  
<sup>13</sup>C NMR  
 (100 MHz, CDCl<sub>3</sub>)



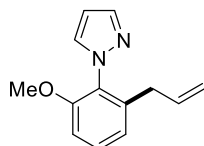
# NMR Spectra



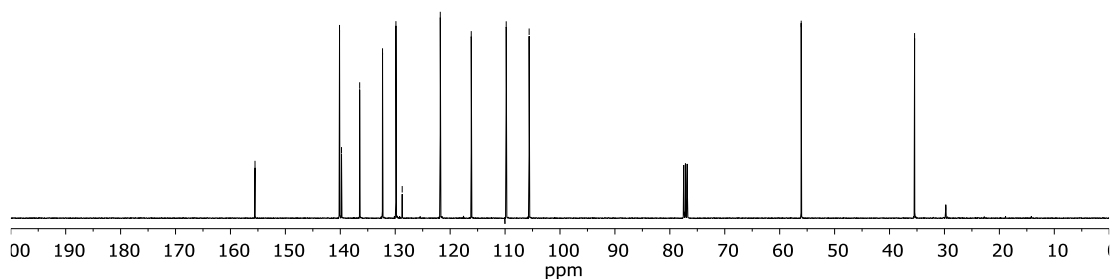
**205**  
<sup>1</sup>H NMR  
(400 MHz, CDCl<sub>3</sub>)



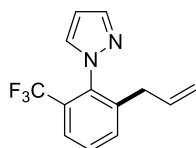
155.53  
140.14  
139.78  
136.47  
132.31  
129.87  
128.73  
121.80  
116.16  
109.79  
105.62  
56.08  
35.44



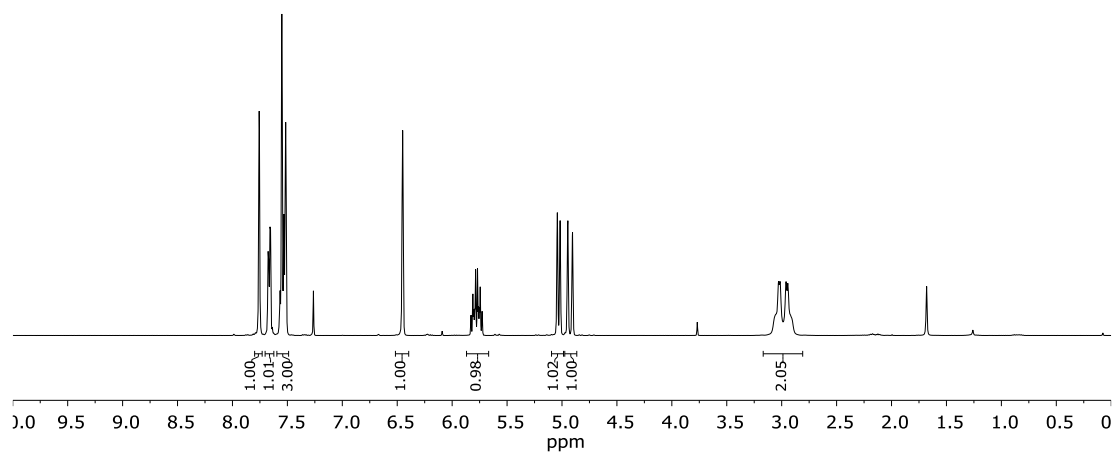
**205**  
<sup>13</sup>C NMR  
(100 MHz, CDCl<sub>3</sub>)





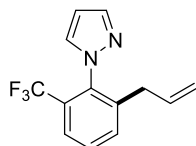


**206**  
 $^1\text{H}$  NMR  
(400 MHz,  $\text{CDCl}_3$ )

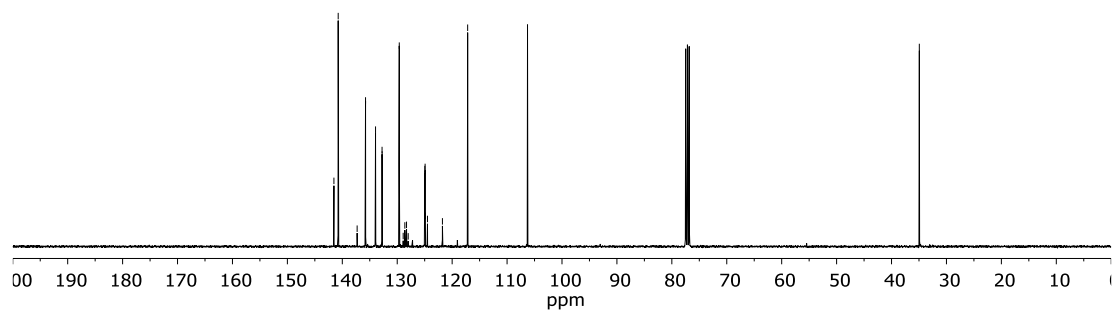


141.53  
140.75  
137.30  
135.77  
133.95  
132.76  
132.75  
129.63  
128.92  
128.61  
128.31  
128.00  
125.02  
124.97  
124.92  
124.87  
124.49  
121.77  
117.18  
106.28

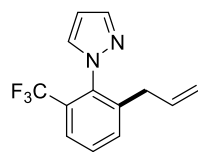
34.94



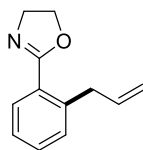
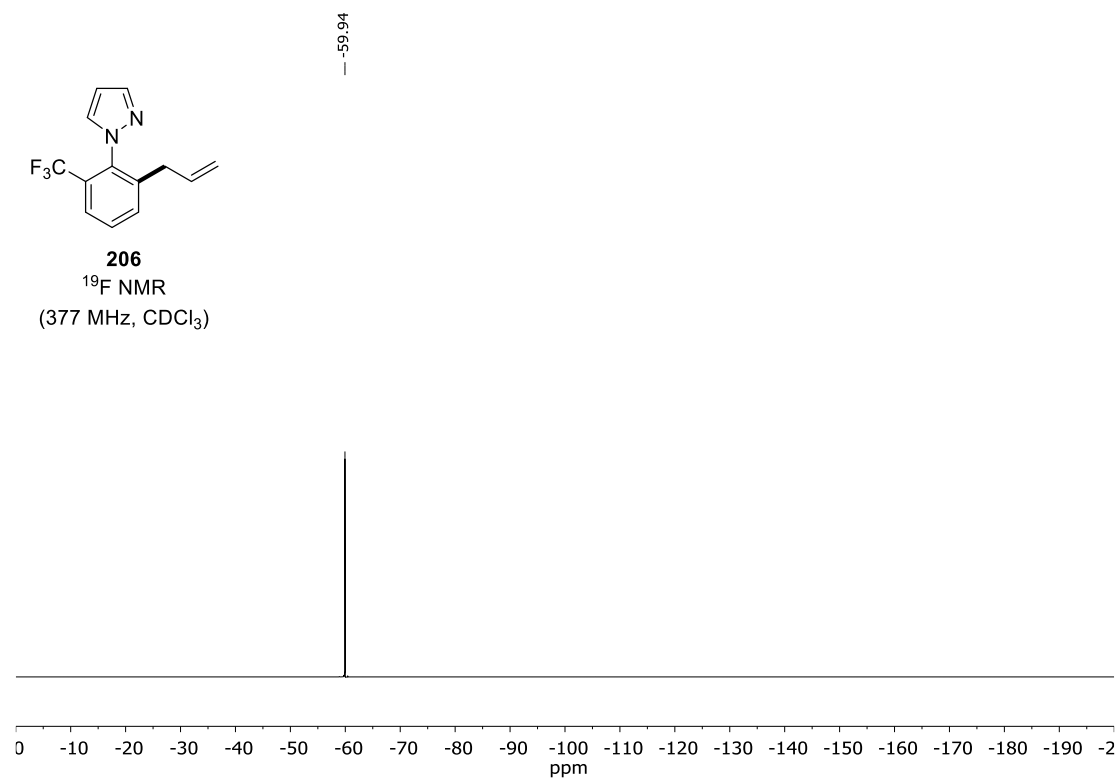
**206**  
 $^{13}\text{C}$  NMR  
(100 MHz,  $\text{CDCl}_3$ )



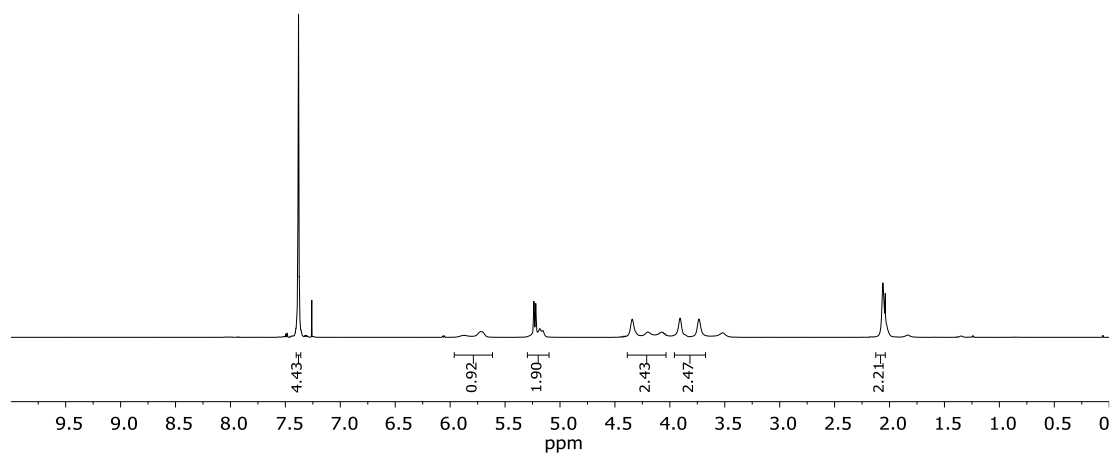
# NMR Spectra

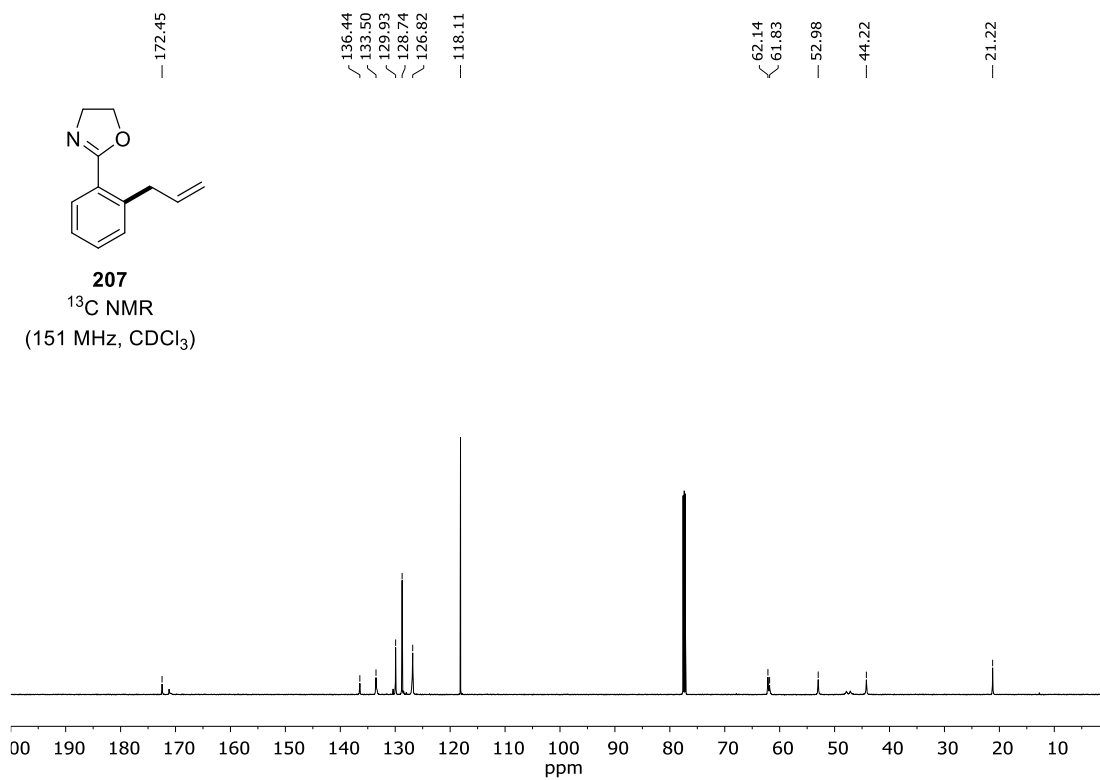


**206**  
<sup>19</sup>F NMR  
(377 MHz, CDCl<sub>3</sub>)



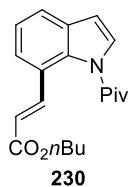
**207**  
<sup>1</sup>H NMR  
(600 MHz, CDCl<sub>3</sub>)



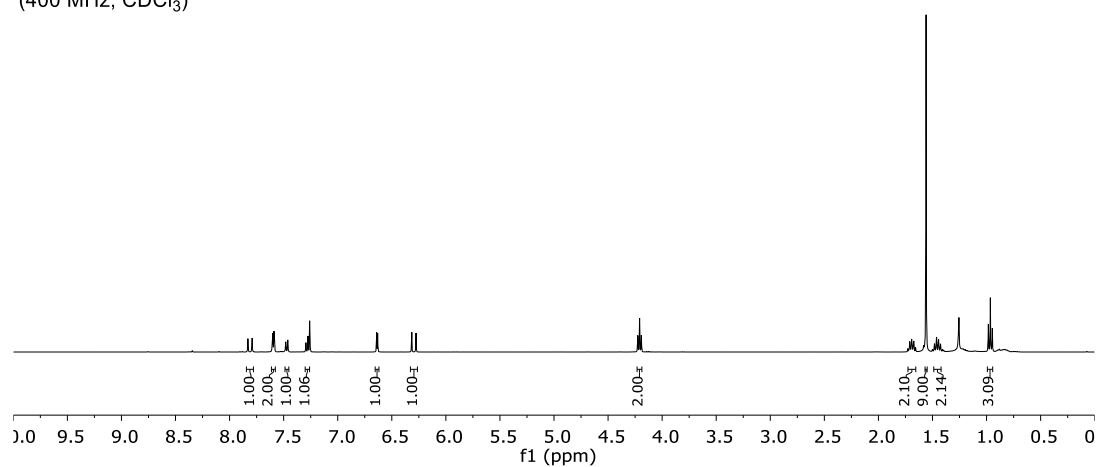


## 7.3 Electrochemical C7-Indole Alkenylation *via* Rhodium Catalysis

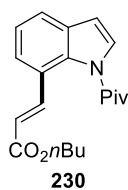
### Catalysis



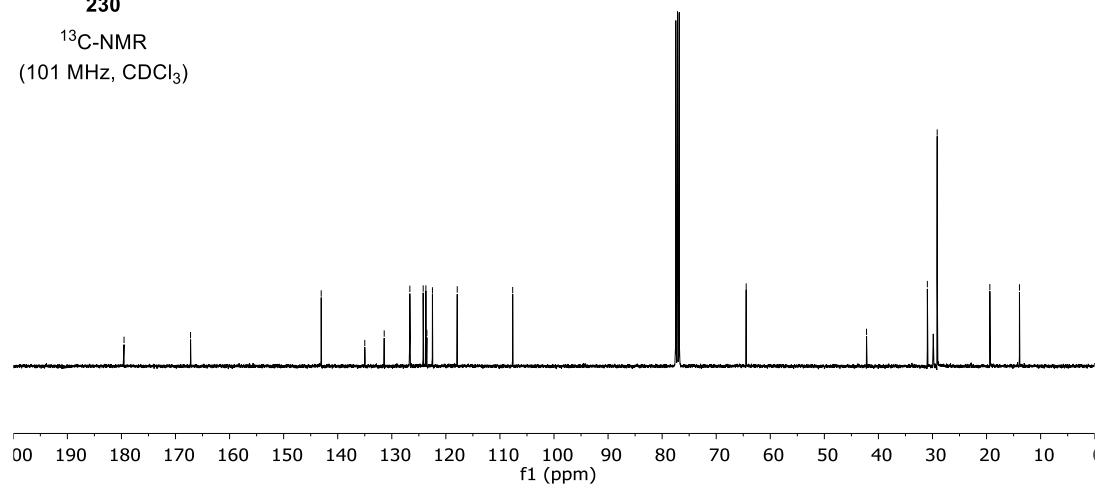
$^1\text{H-NMR}$   
(400 MHz,  $\text{CDCl}_3$ )

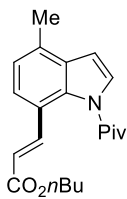


— 179.5 — 167.2 — 143.1 — 135.0 — 131.4 — 126.7 — 124.2 — 123.7 — 123.5 — 122.5 — 117.9 — 107.6 — 64.5 — 42.2 — 30.9 — 29.1 — 19.4 — 13.9



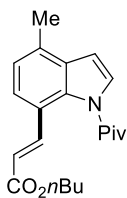
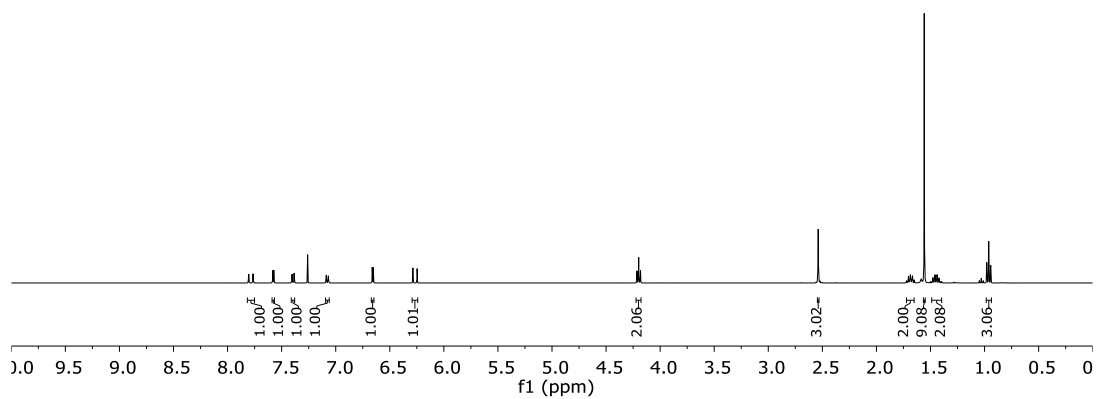
$^{13}\text{C-NMR}$   
(101 MHz,  $\text{CDCl}_3$ )





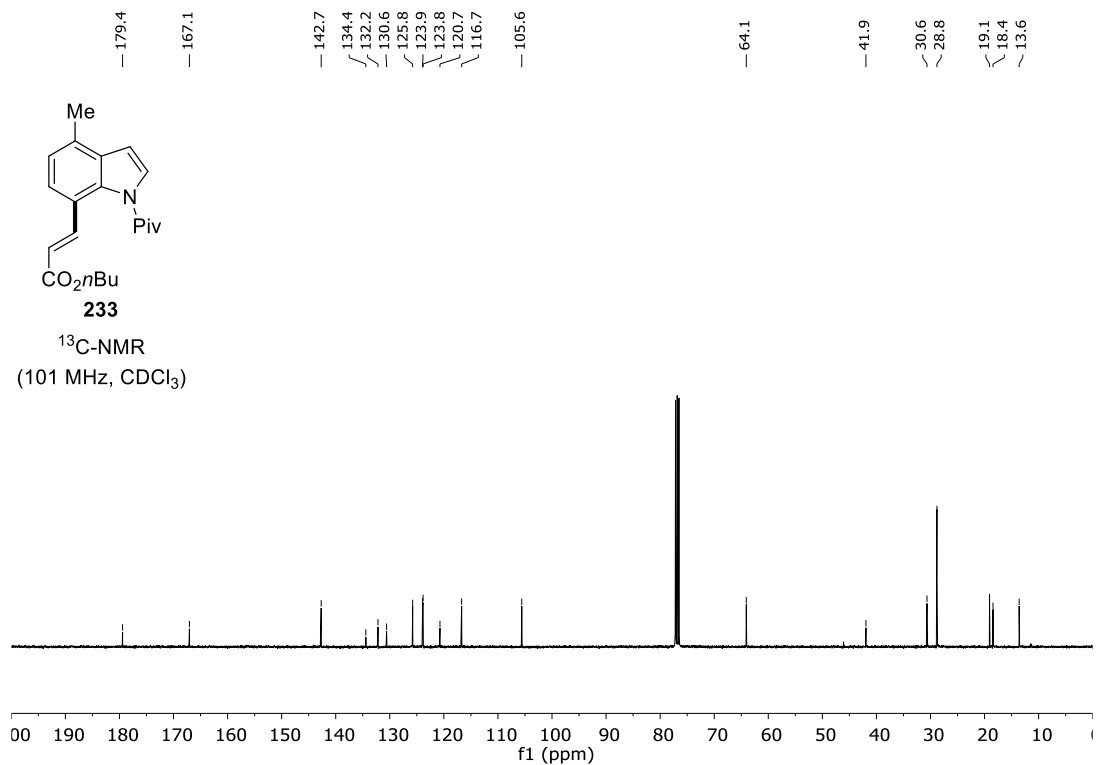
**233**

<sup>1</sup>H-NMR  
(400 MHz, CDCl<sub>3</sub>)

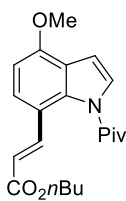


**233**

<sup>13</sup>C-NMR  
(101 MHz, CDCl<sub>3</sub>)

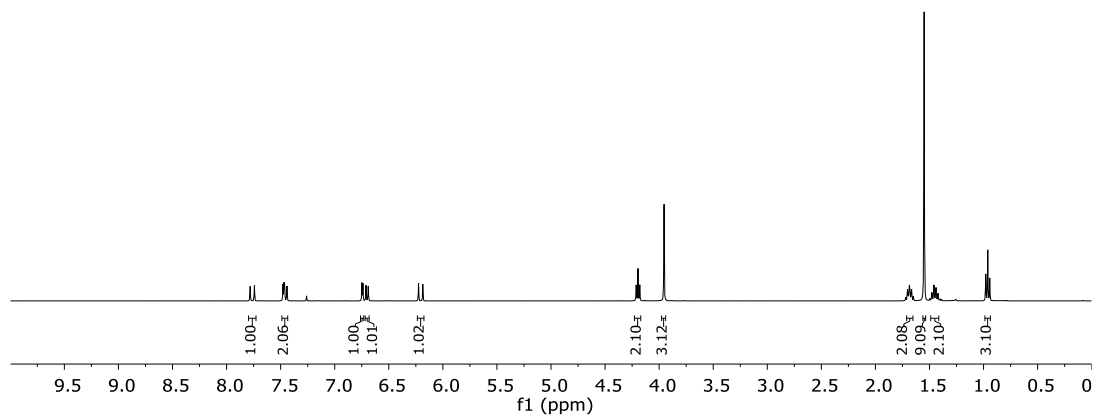


# NMR Spectra

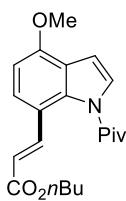


**234**

<sup>1</sup>H-NMR  
(400 MHz, CDCl<sub>3</sub>)

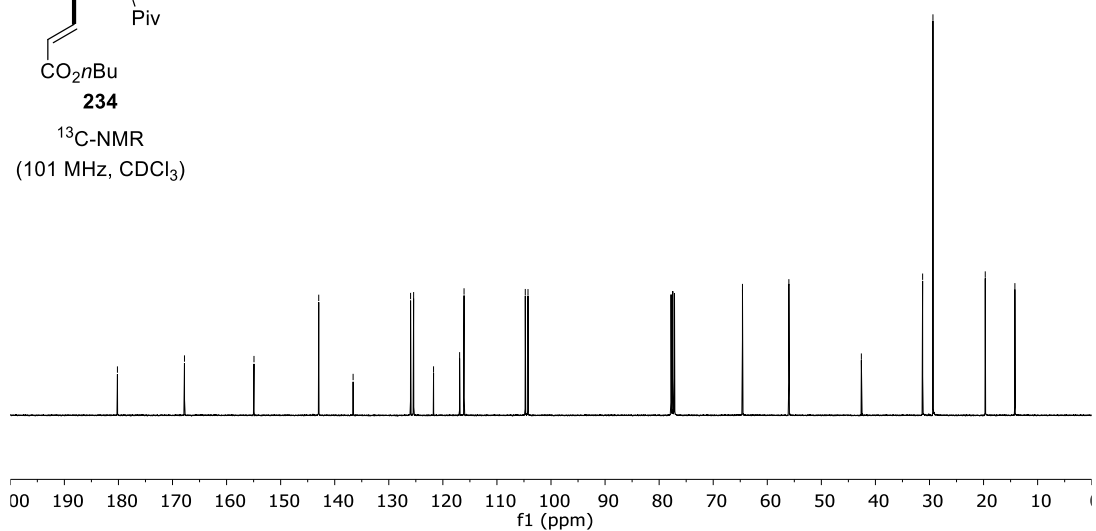


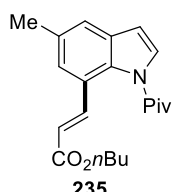
— 180.2  
— 167.8  
— 154.9  
— 143.0  
— 136.6  
~ 126.0  
~ 125.4  
~ 121.7  
~ 116.9  
~ 116.1  
~ 104.8  
~ 104.3  
  
— 64.6  
— 56.0  
— 42.6  
~ 31.3  
~ 29.4  
— 19.7  
— 14.2



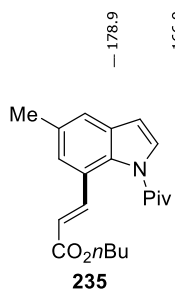
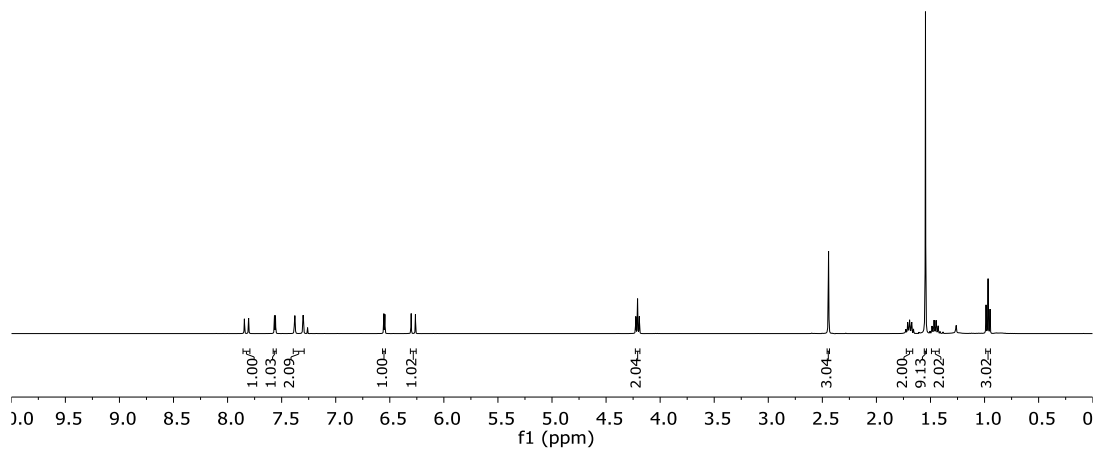
**234**

<sup>13</sup>C-NMR  
(101 MHz, CDCl<sub>3</sub>)

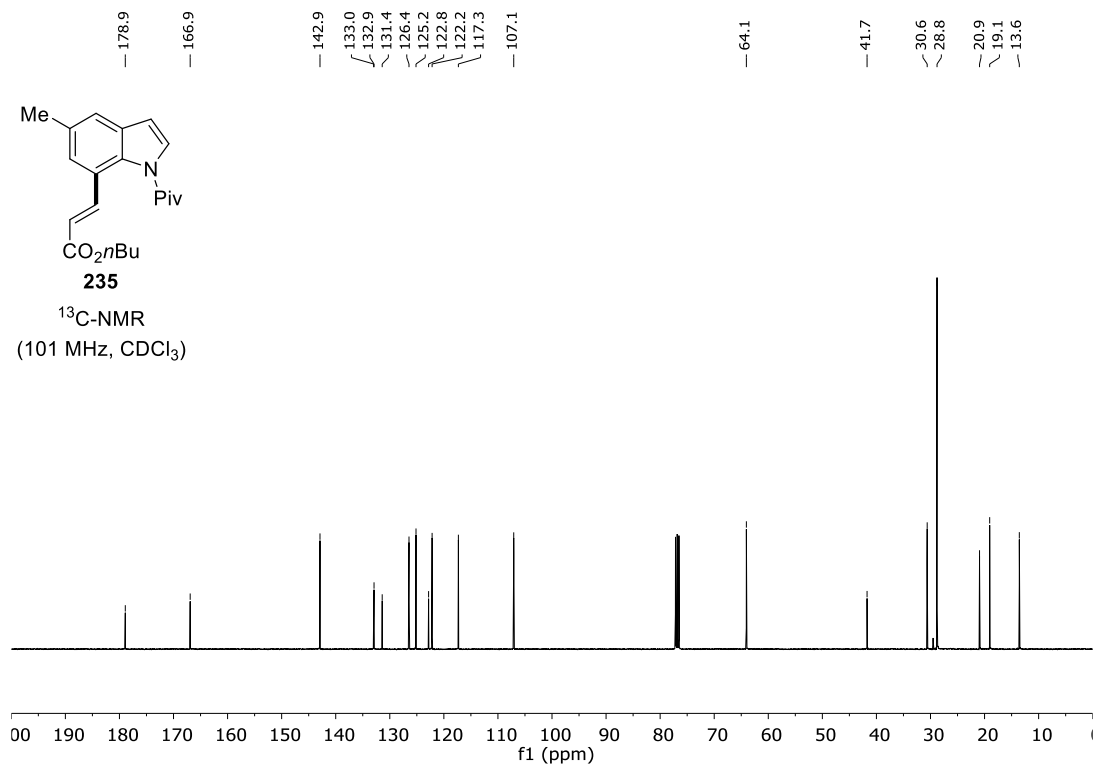




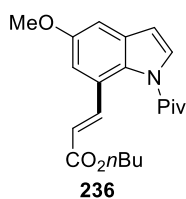
<sup>1</sup>H-NMR  
(400 MHz, CDCl<sub>3</sub>)



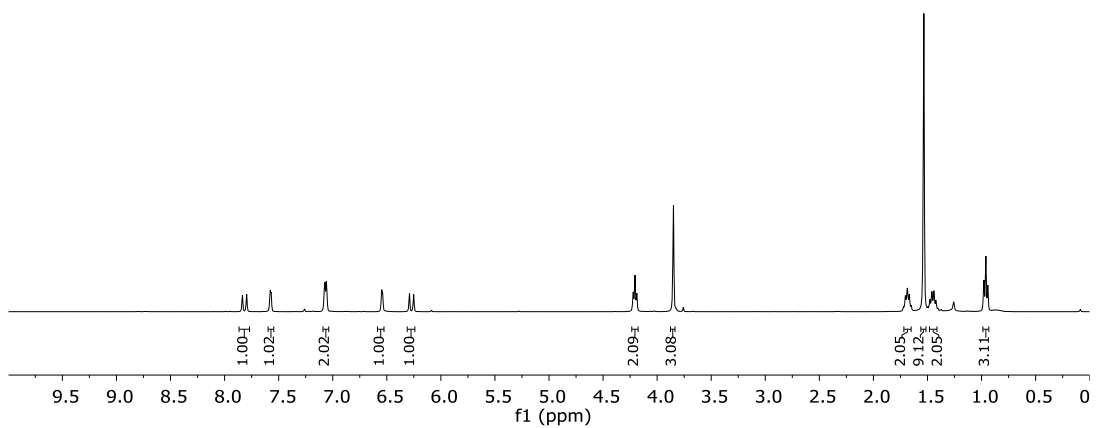
<sup>13</sup>C-NMR  
(101 MHz, CDCl<sub>3</sub>)



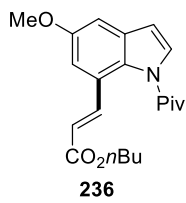
# NMR Spectra



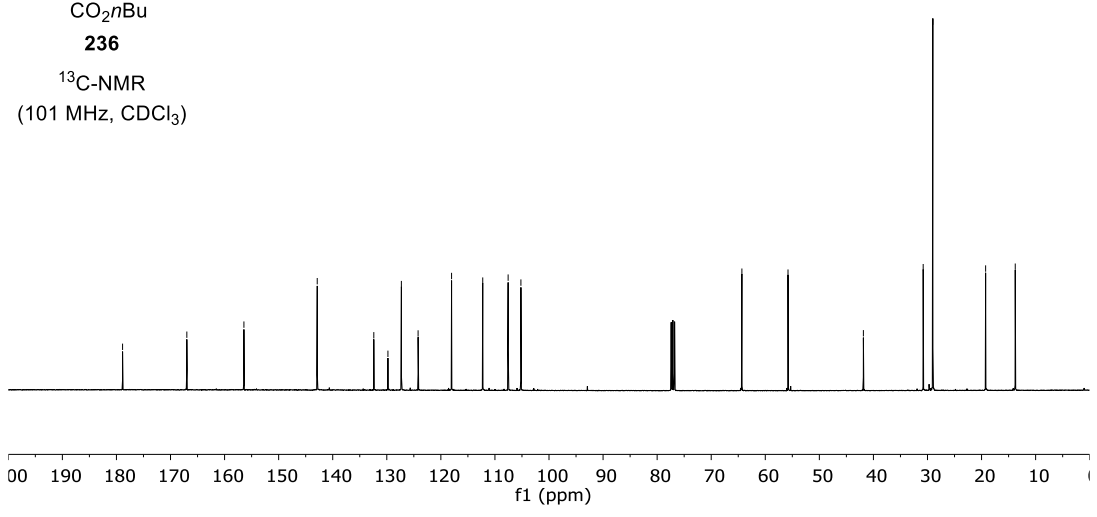
<sup>1</sup>H-NMR  
(400 MHz, CDCl<sub>3</sub>)



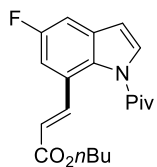
- 178.9
- 167.0
- 156.4
- 142.9
- 132.4
- 129.8
- 127.3
- 124.2
- 118.0
- 112.3
- 107.6
- 105.2
- 64.3
- 55.8
- 41.9
- 30.8
- 29.0
- 19.2
- 13.8



<sup>13</sup>C-NMR  
(101 MHz, CDCl<sub>3</sub>)

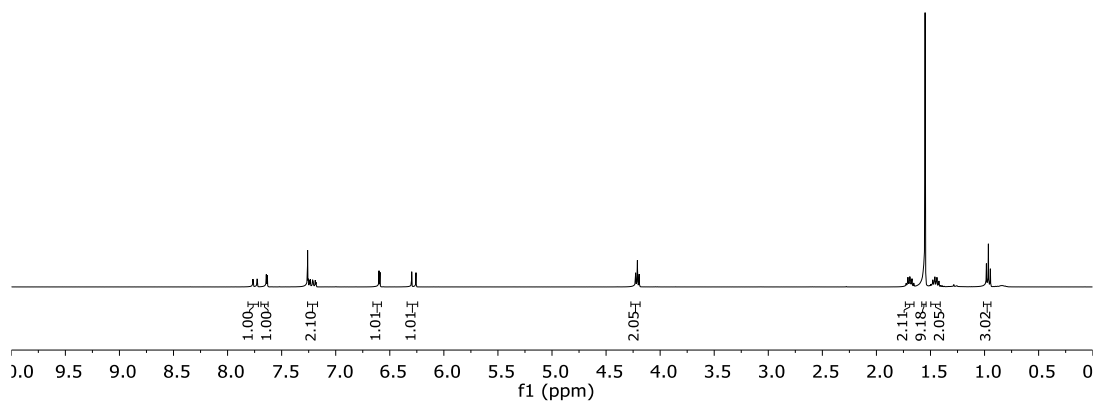




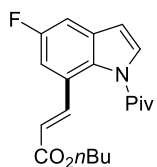


**237**

<sup>1</sup>H-NMR  
(400 MHz, CDCl<sub>3</sub>)

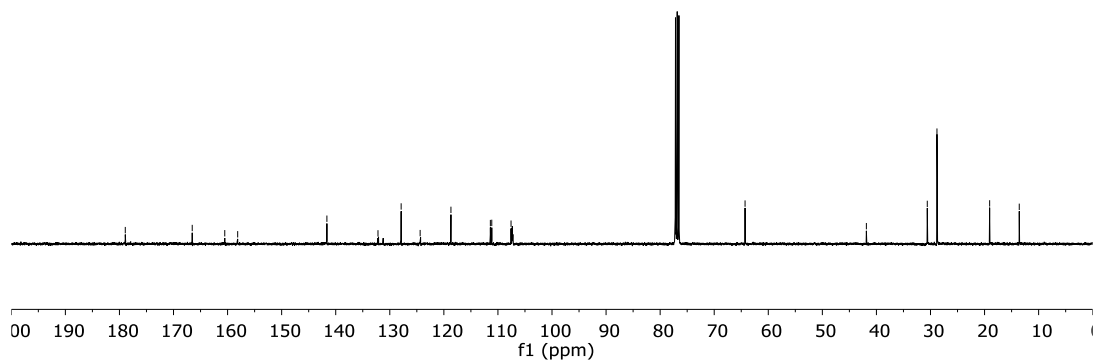


— 178.9  
 ~ 166.5  
 ~ 160.5  
 ~ 158.1  
 — 141.6  
 ~ 132.2  
 ~ 127.9  
 ~ 124.4  
 ~ 118.7  
 ~ 111.4  
 ~ 111.1  
 ~ 107.6  
 — 64.3  
 — 41.9  
 ~ 30.6  
 ~ 28.8  
 — 19.1  
 — 13.6

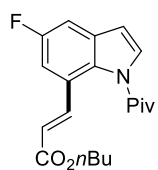


**237**

<sup>13</sup>C-NMR  
(101 MHz, CDCl<sub>3</sub>)

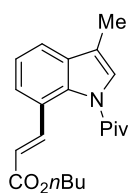
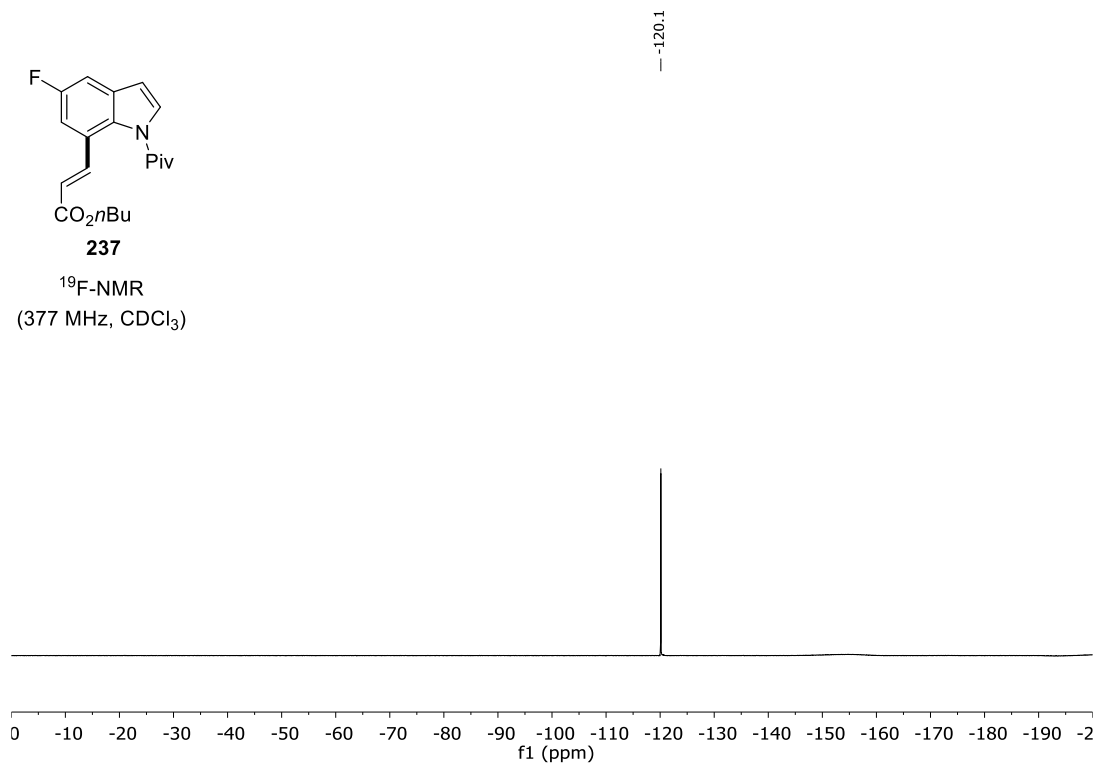


# NMR Spectra



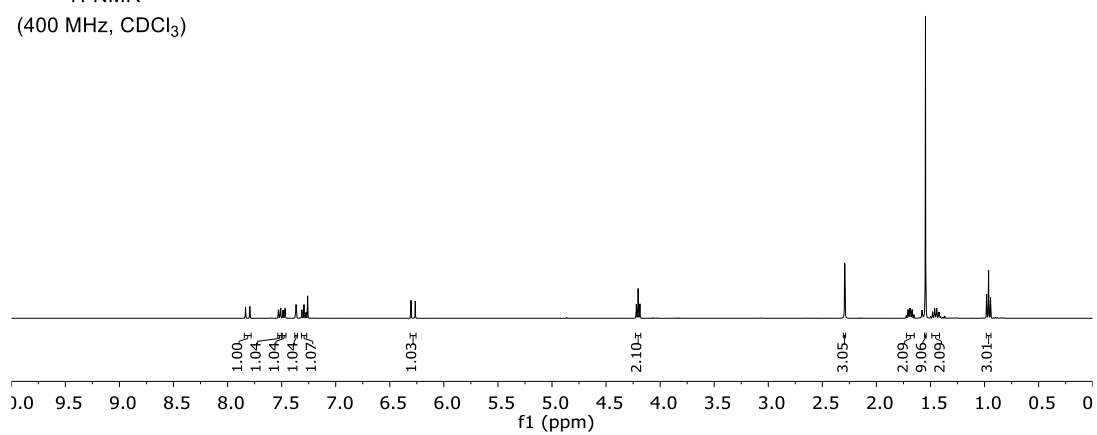
**237**

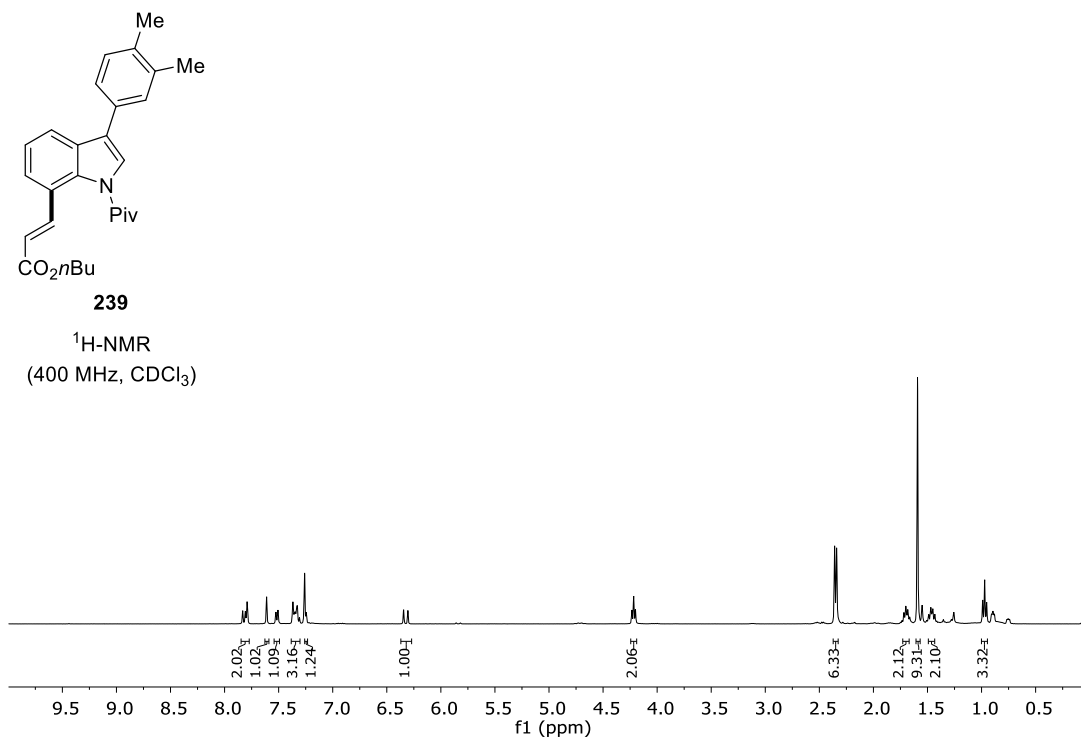
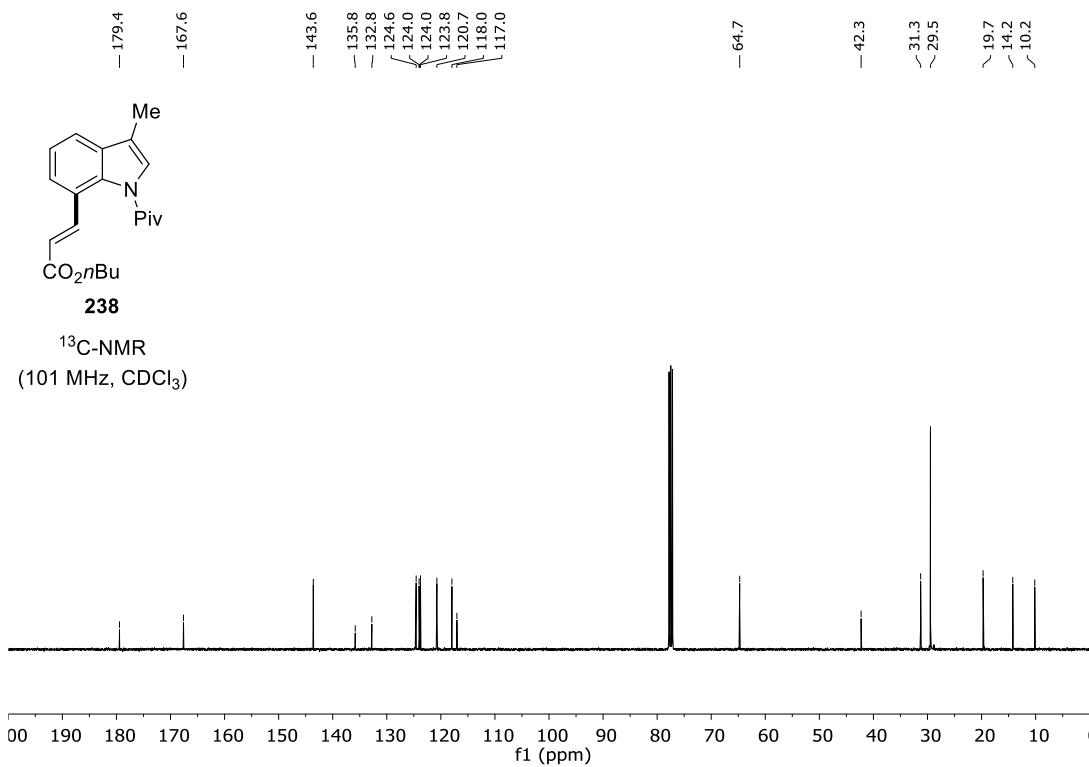
<sup>19</sup>F-NMR  
(377 MHz, CDCl<sub>3</sub>)



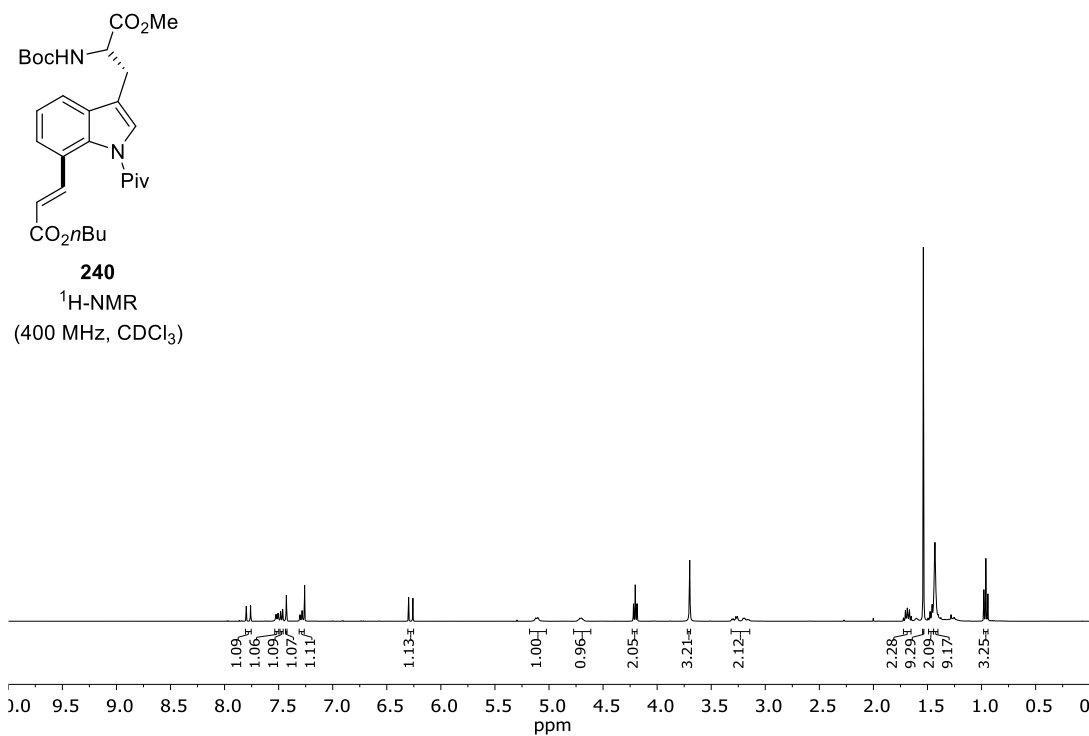
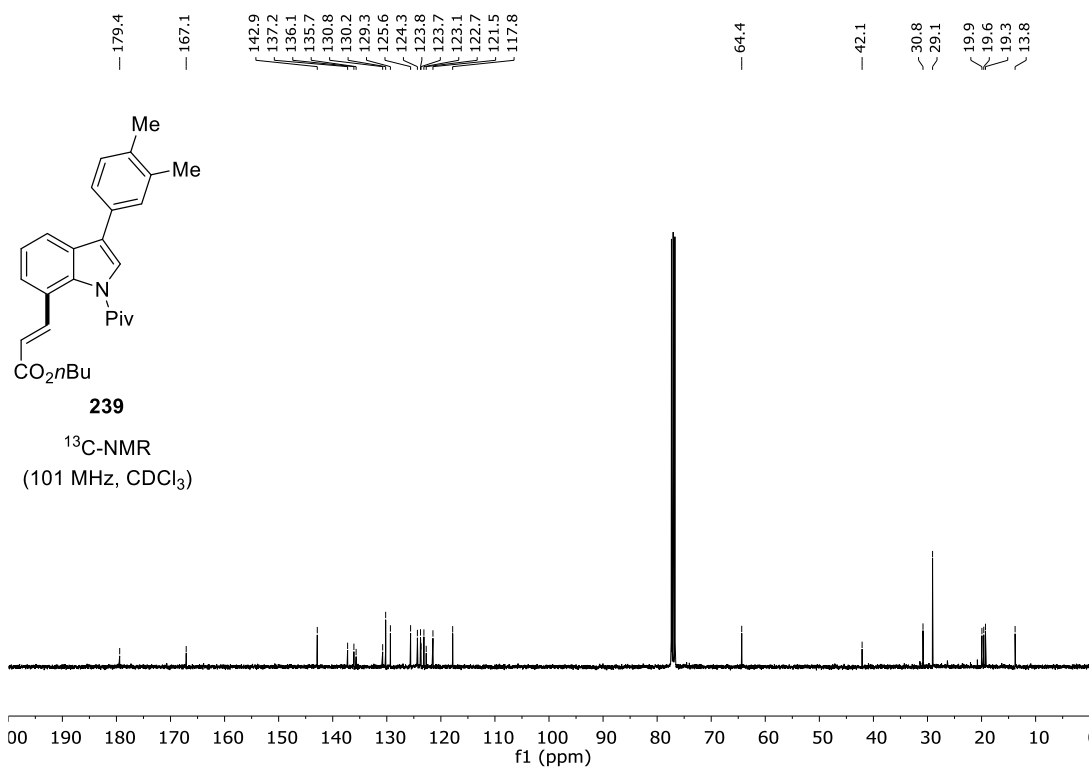
**238**

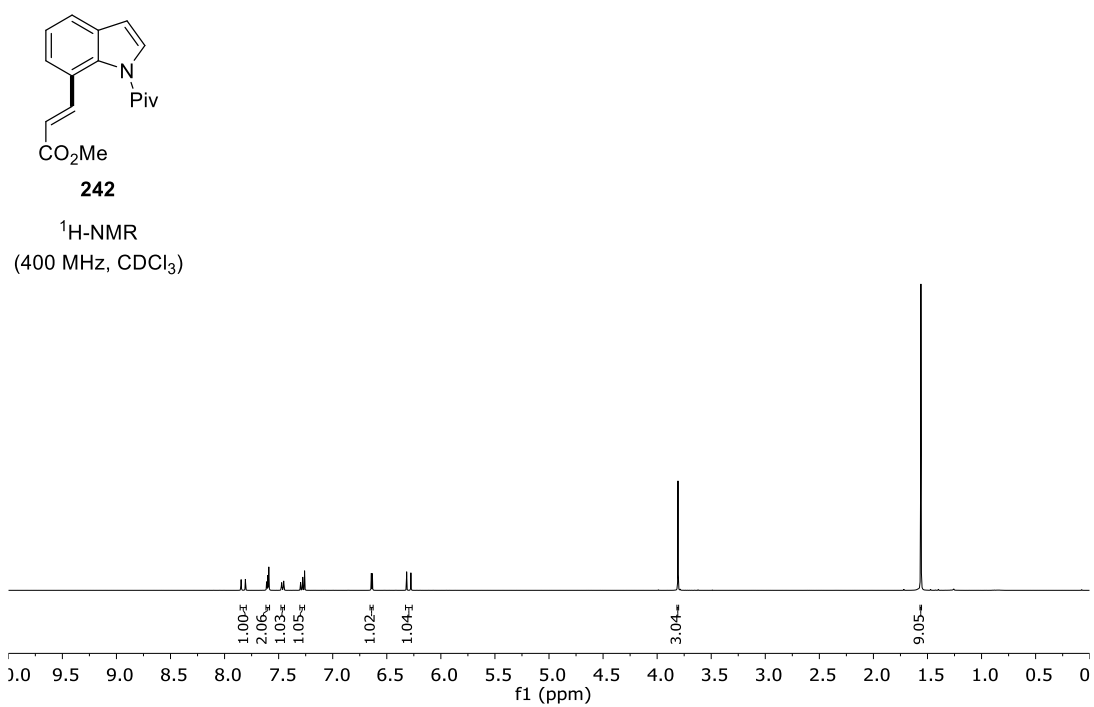
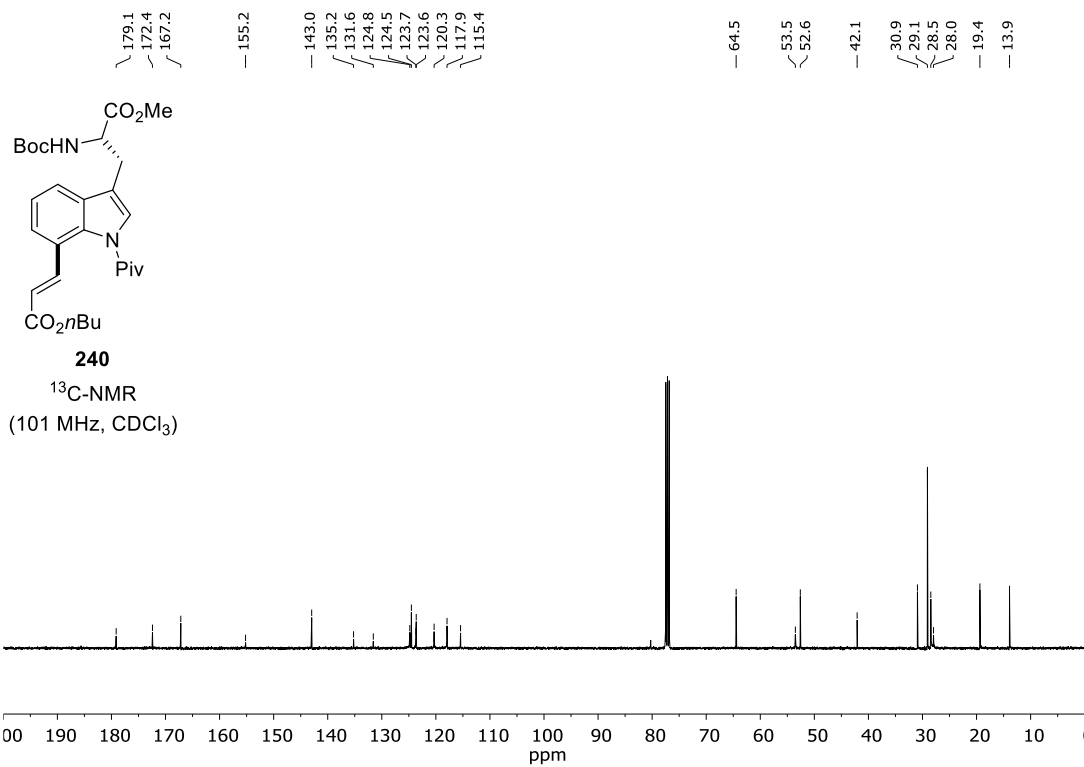
<sup>1</sup>H-NMR  
(400 MHz, CDCl<sub>3</sub>)



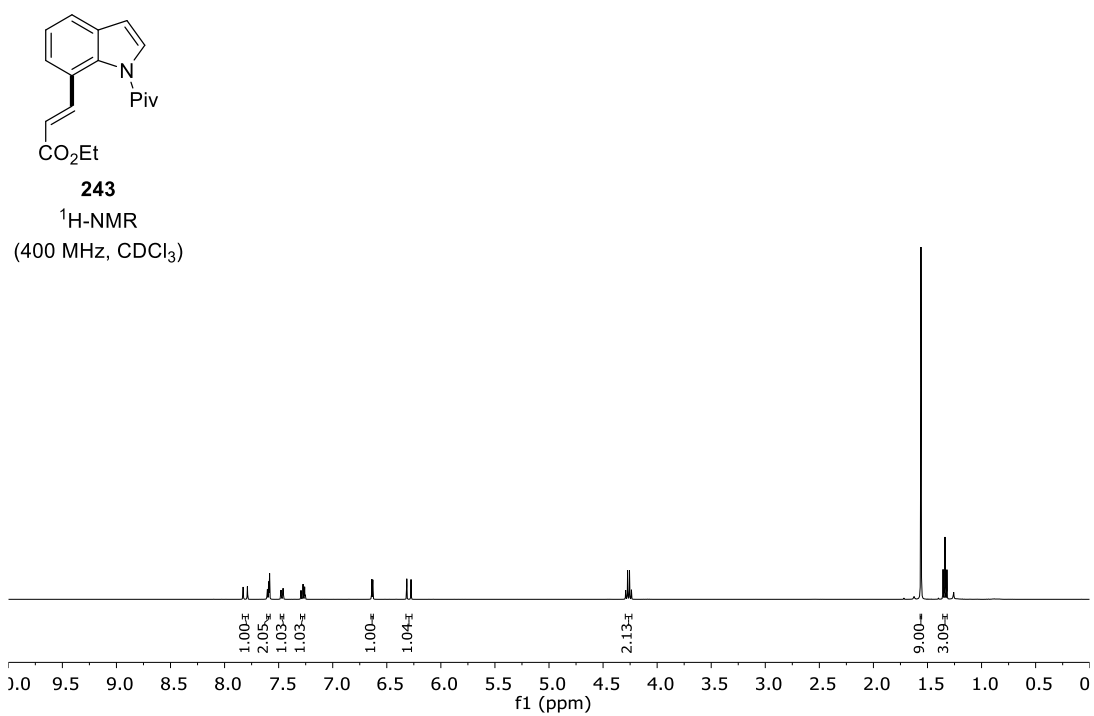
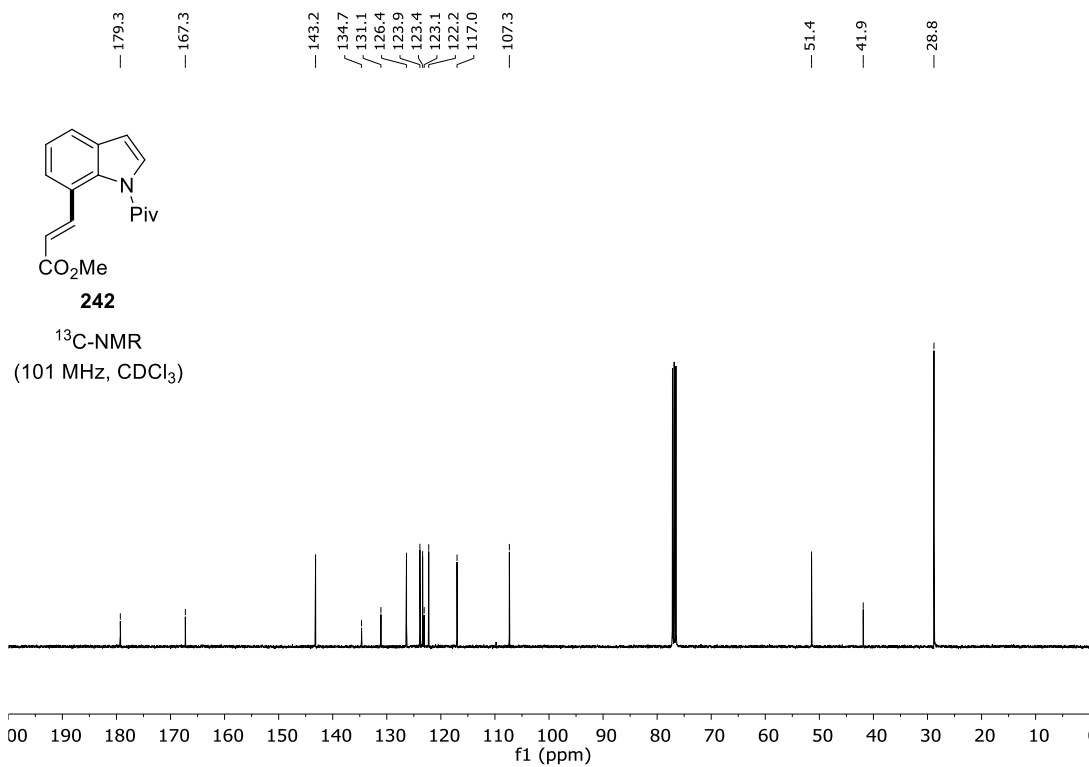


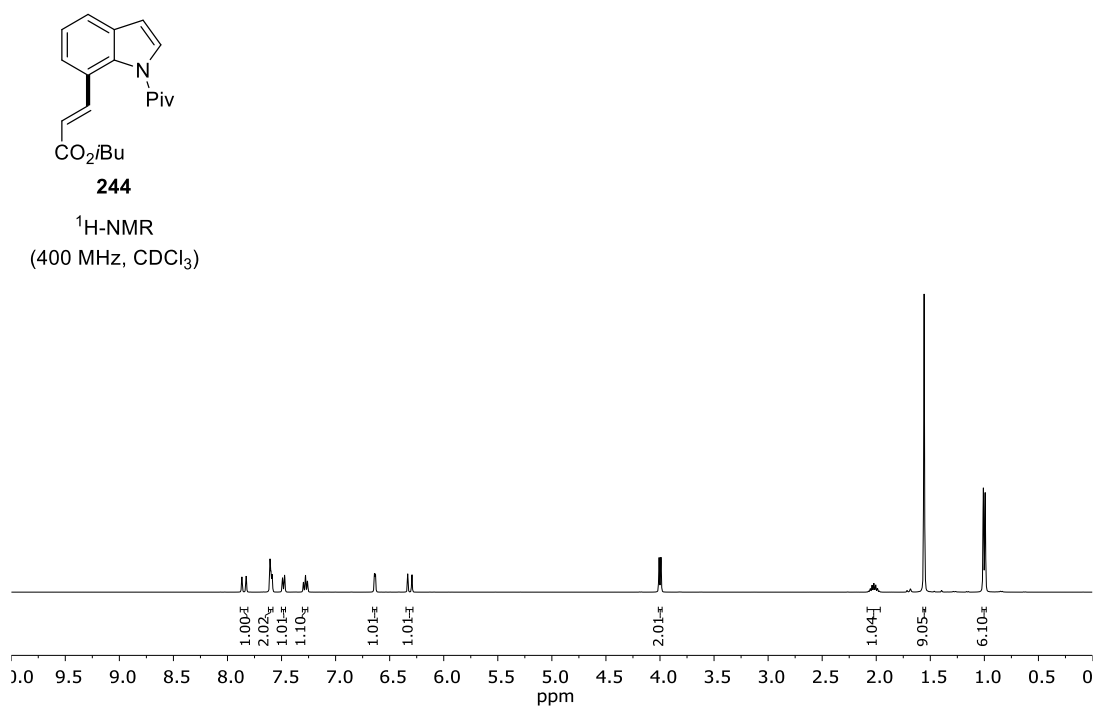
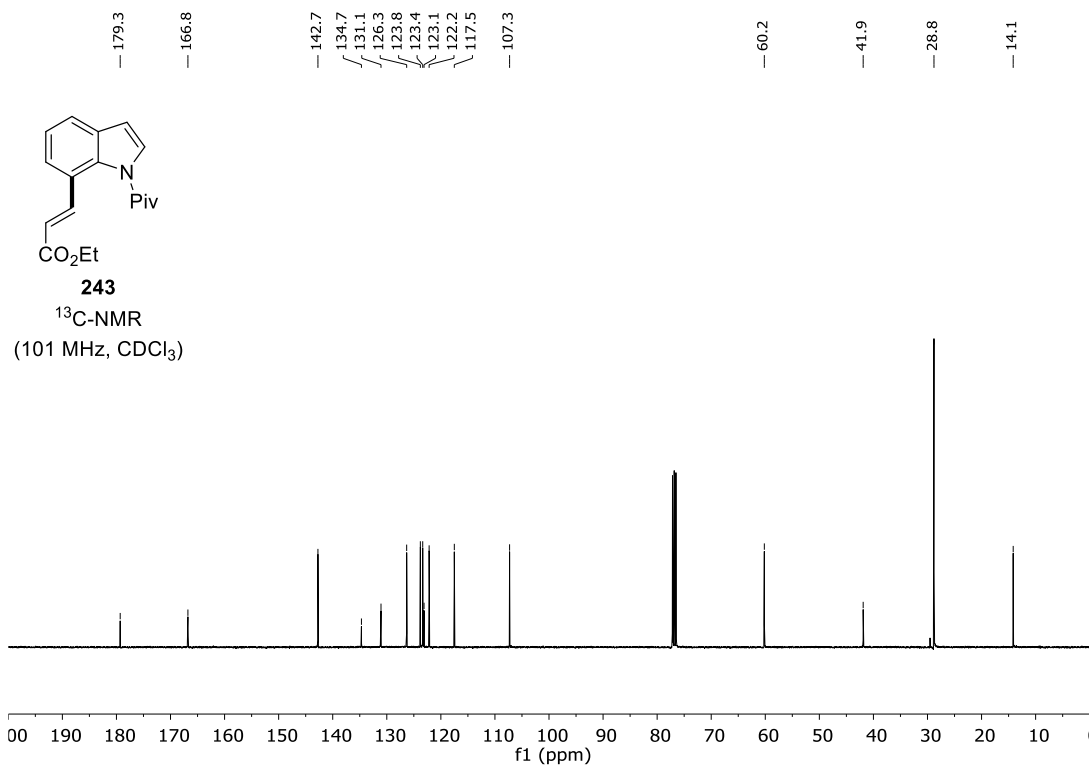
# NMR Spectra



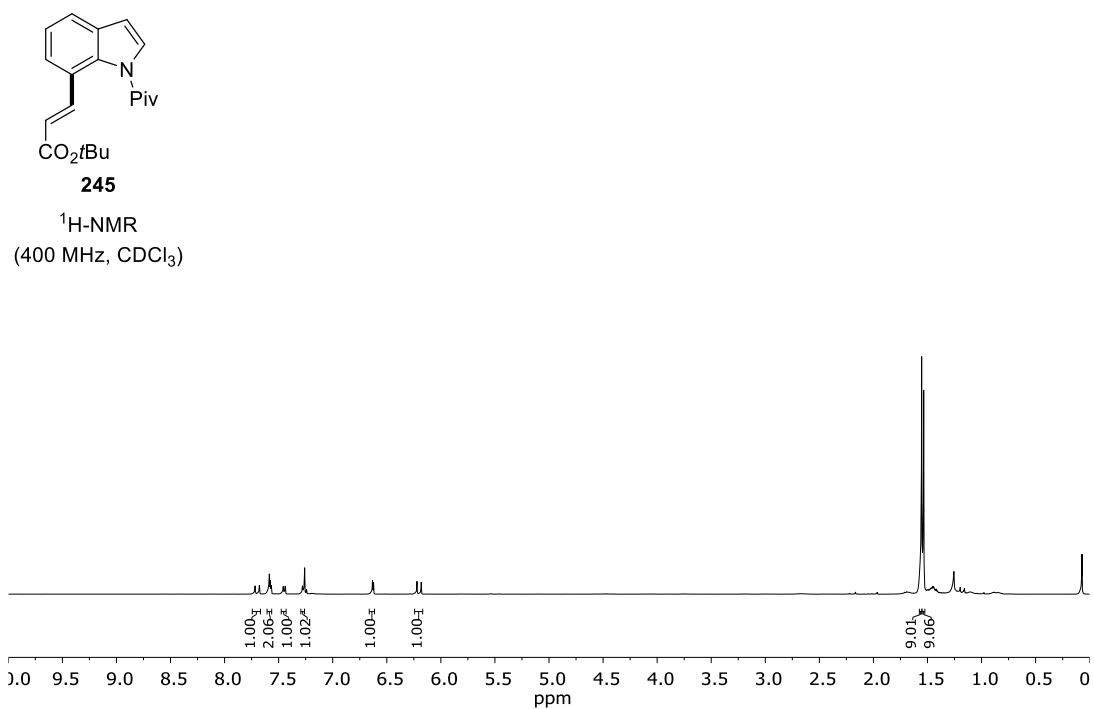
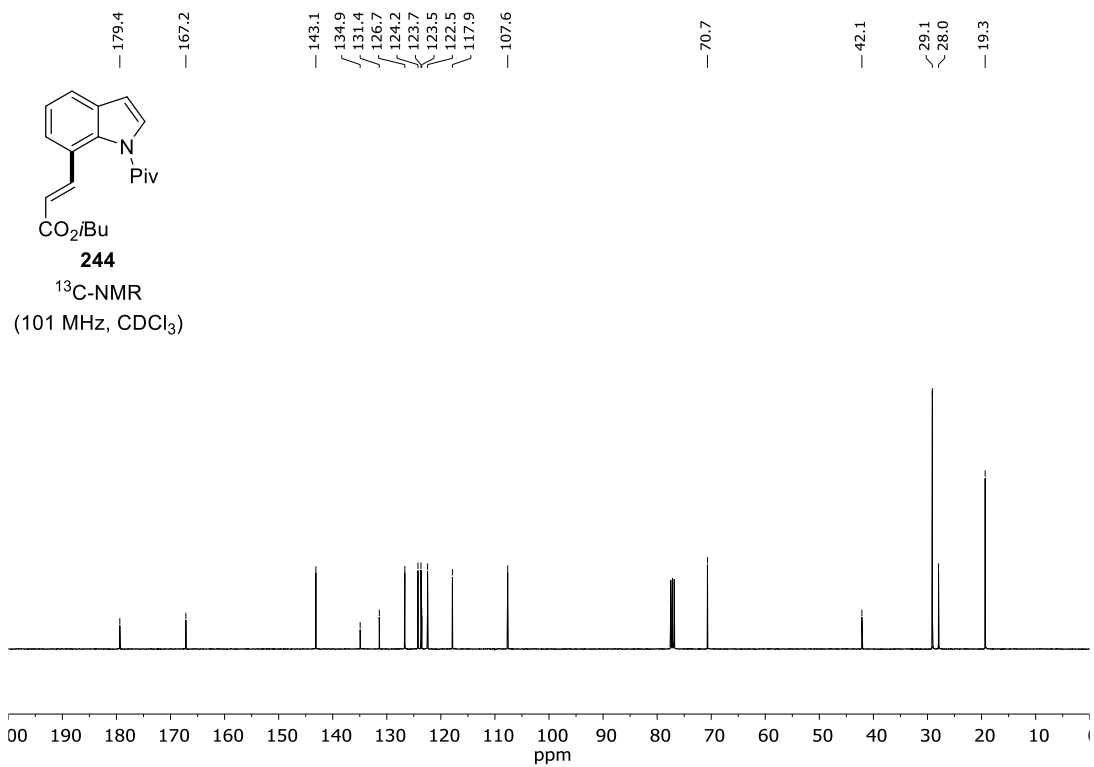


# NMR Spectra

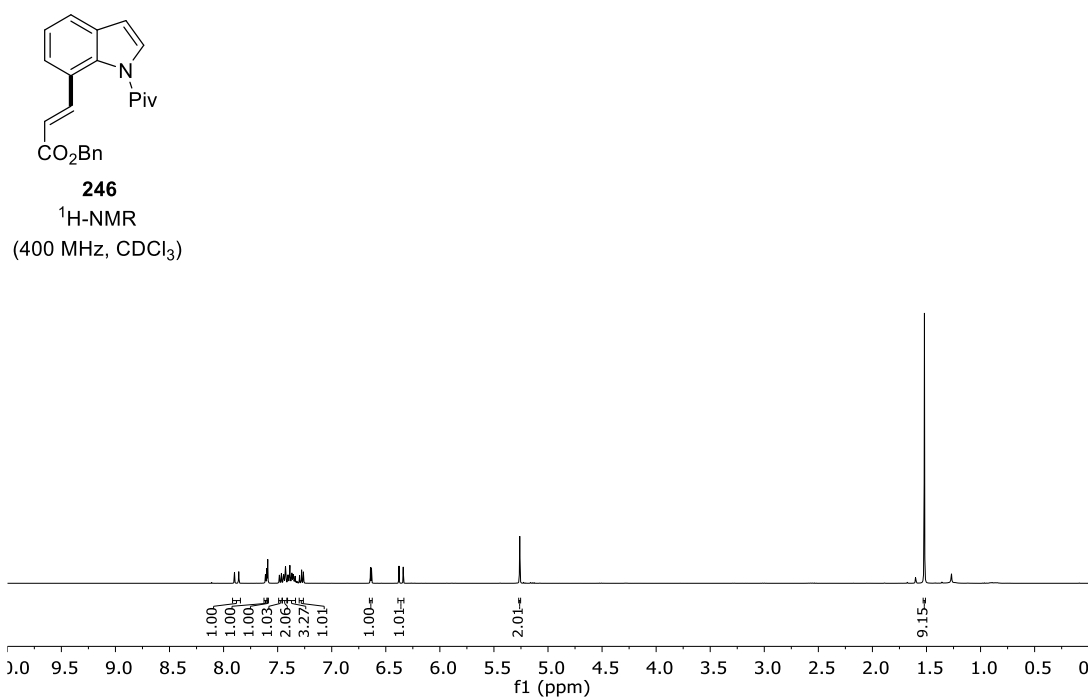
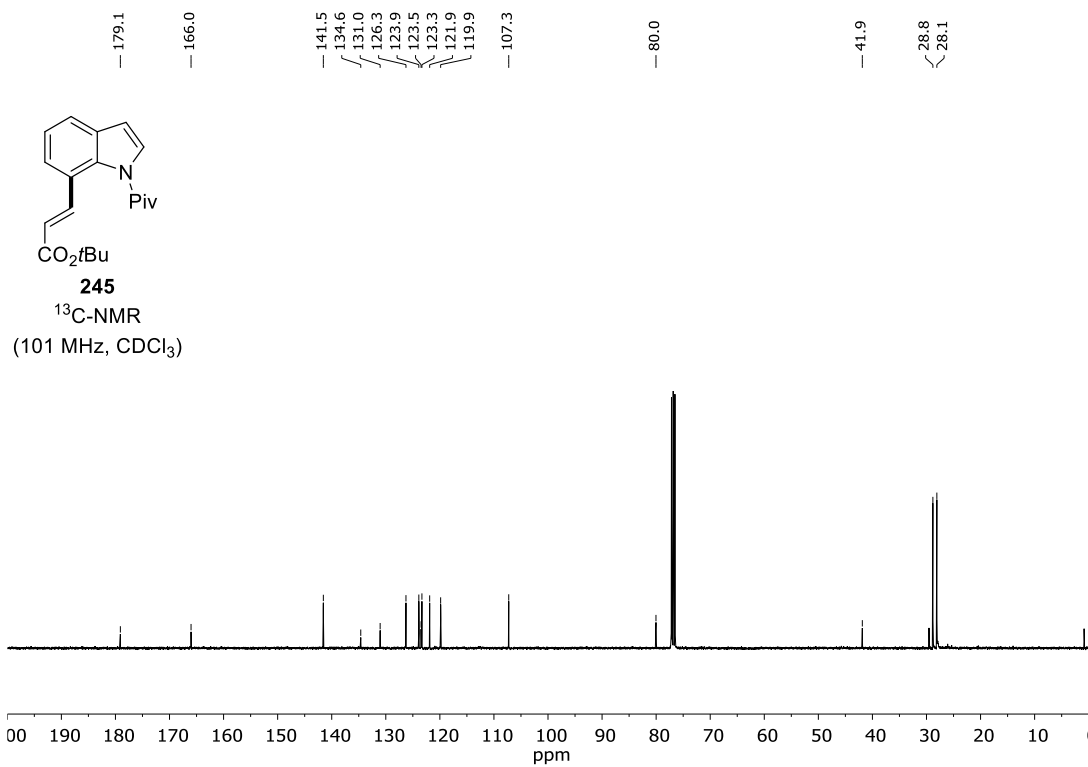




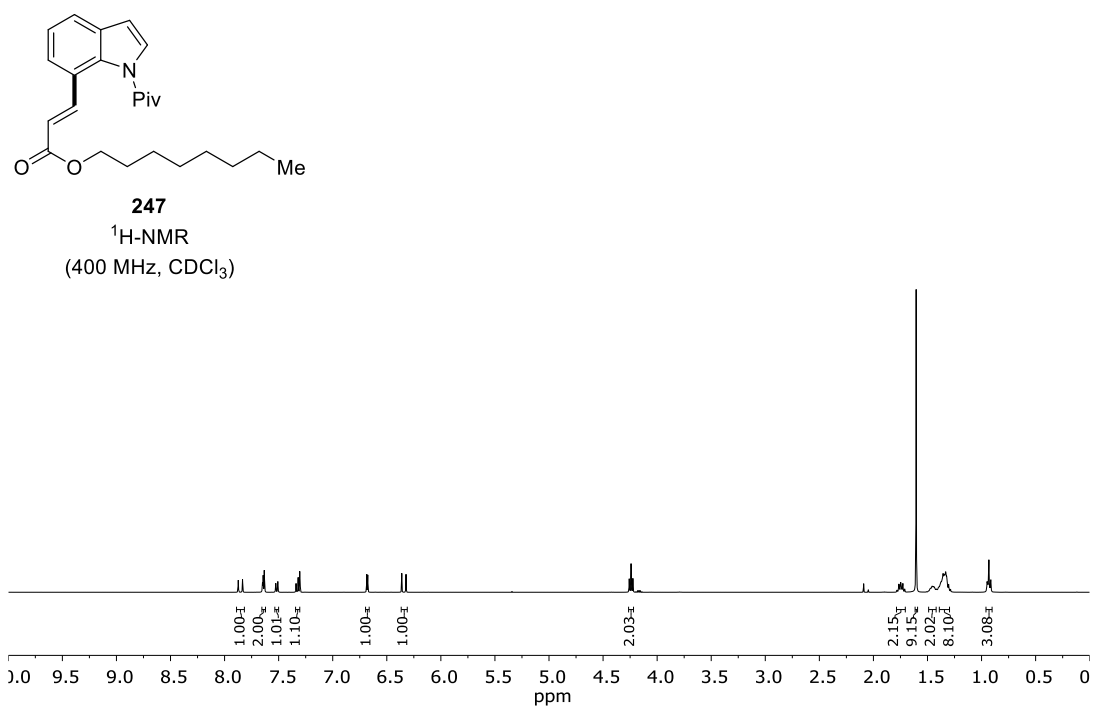
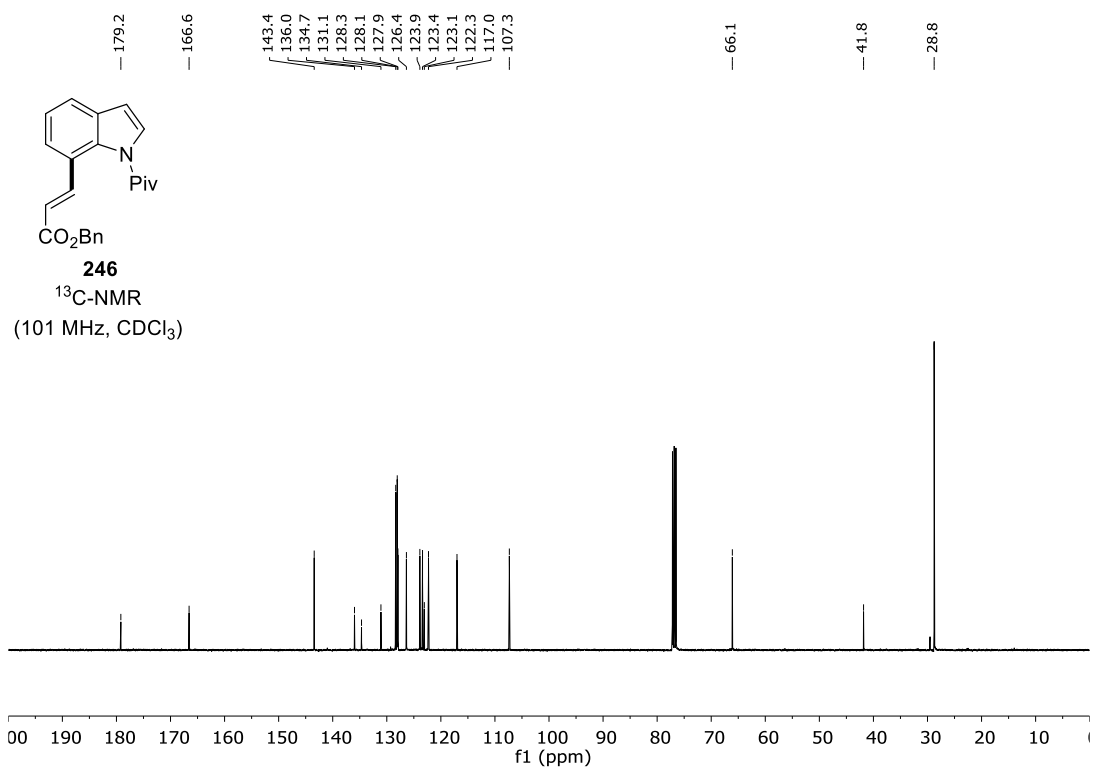
# NMR Spectra

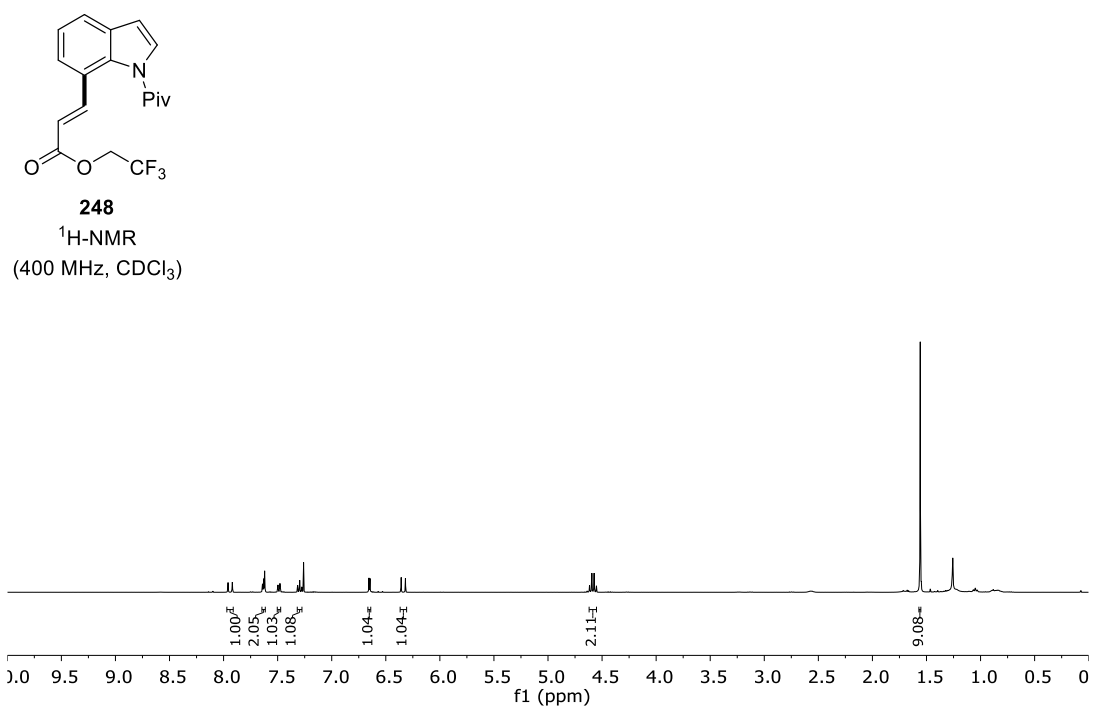
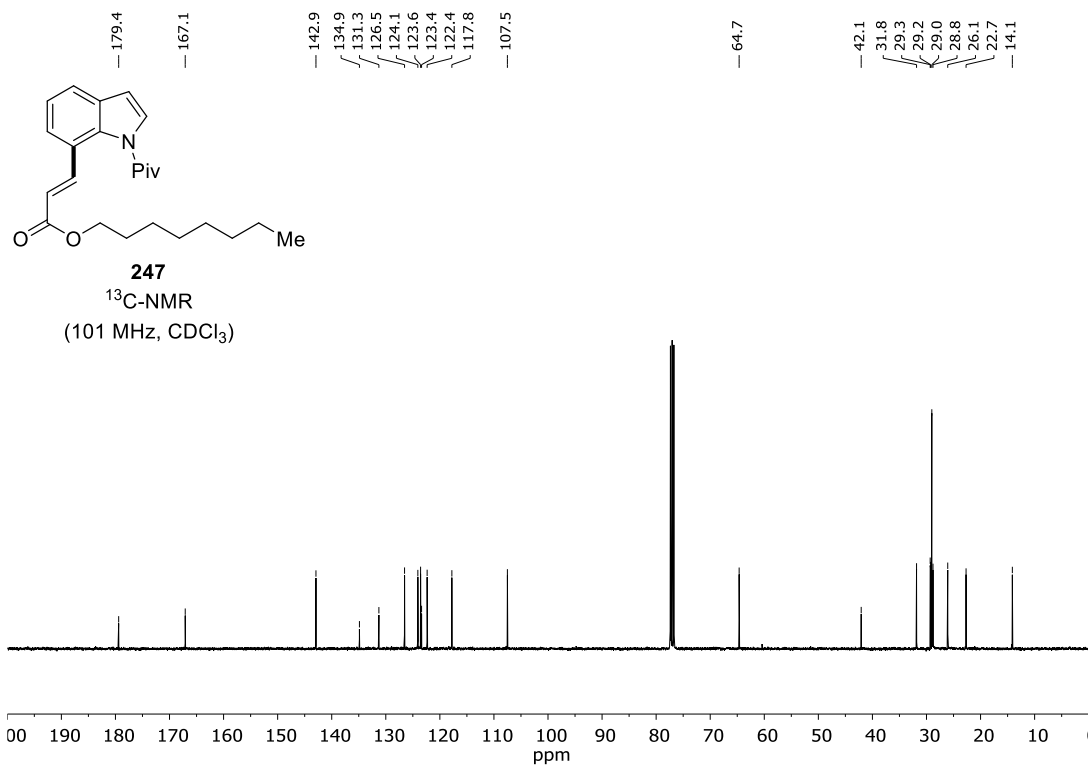




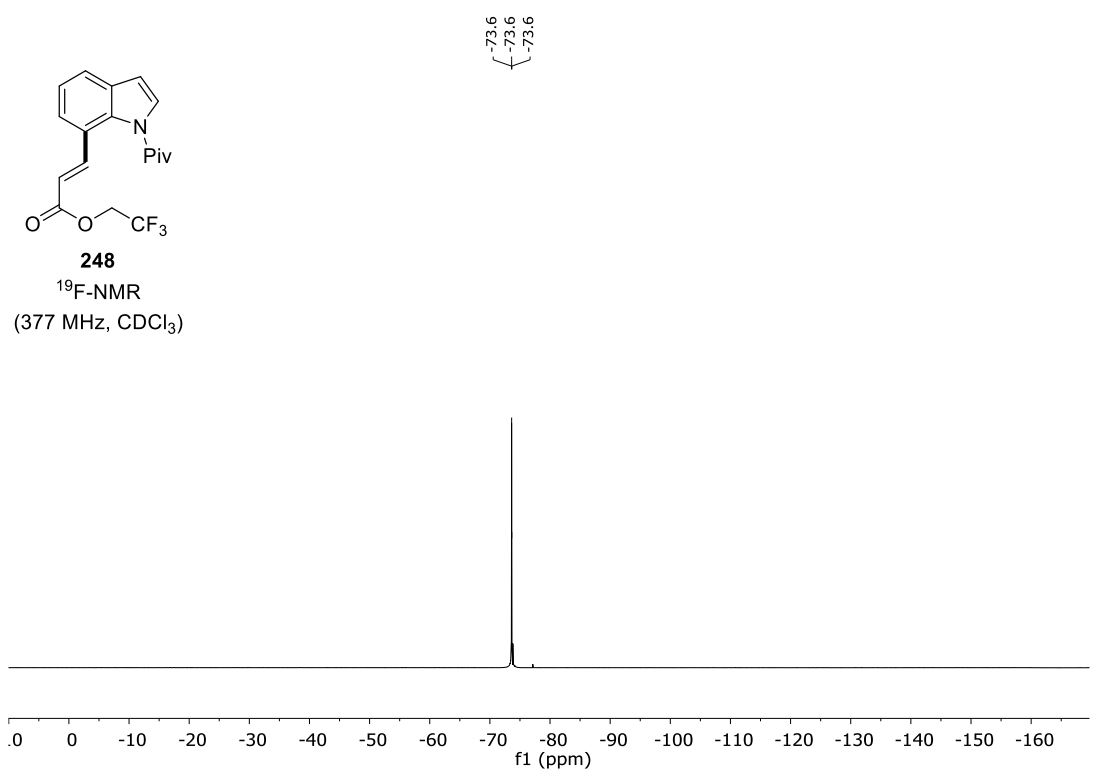
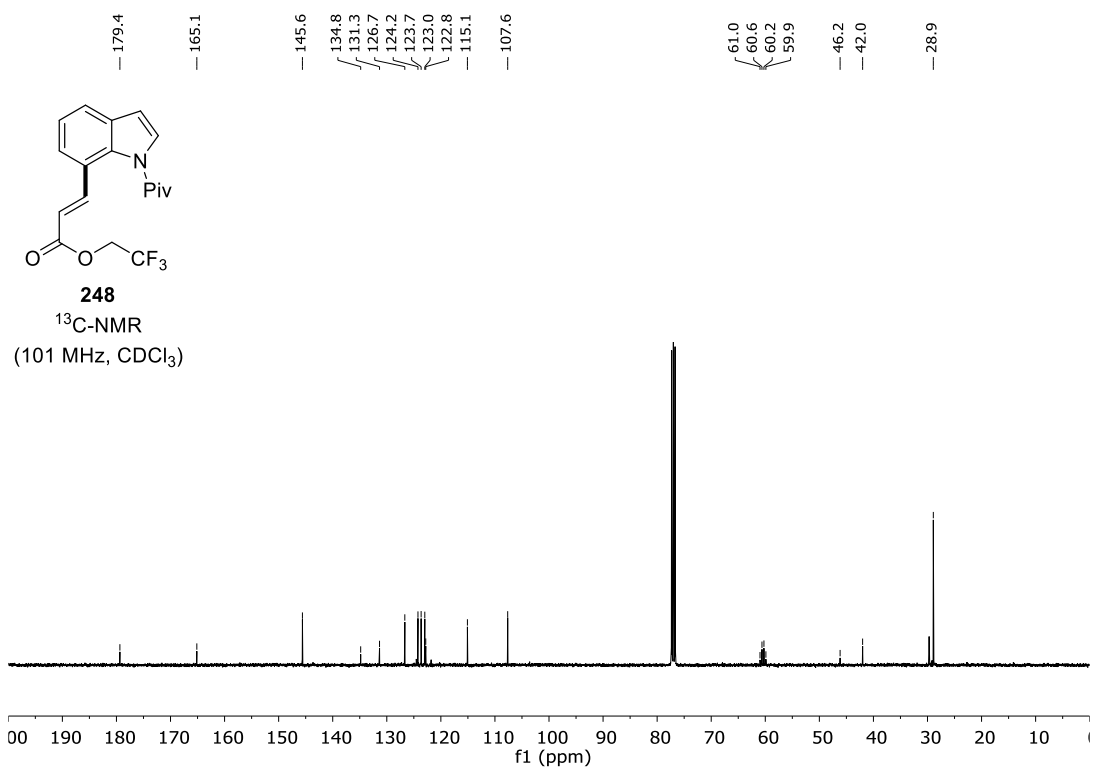


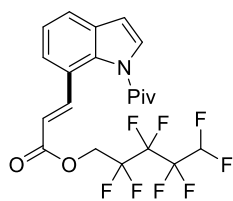
# NMR Spectra



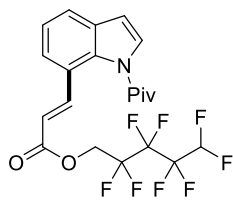
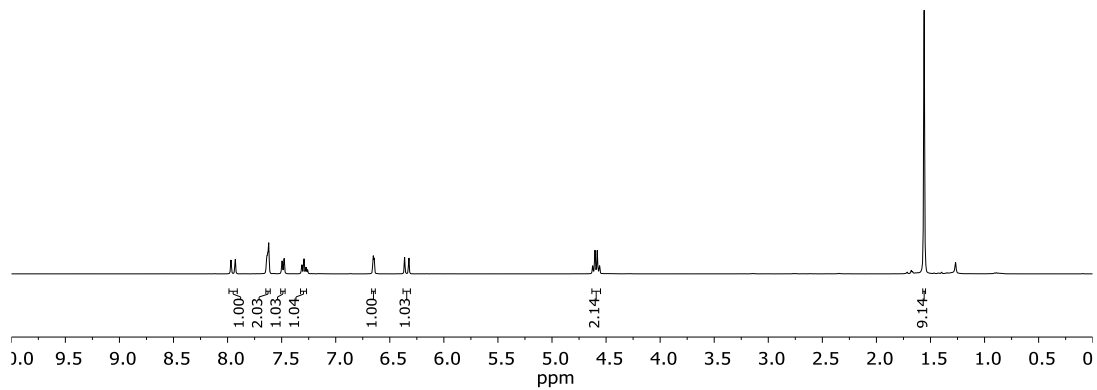


# NMR Spectra

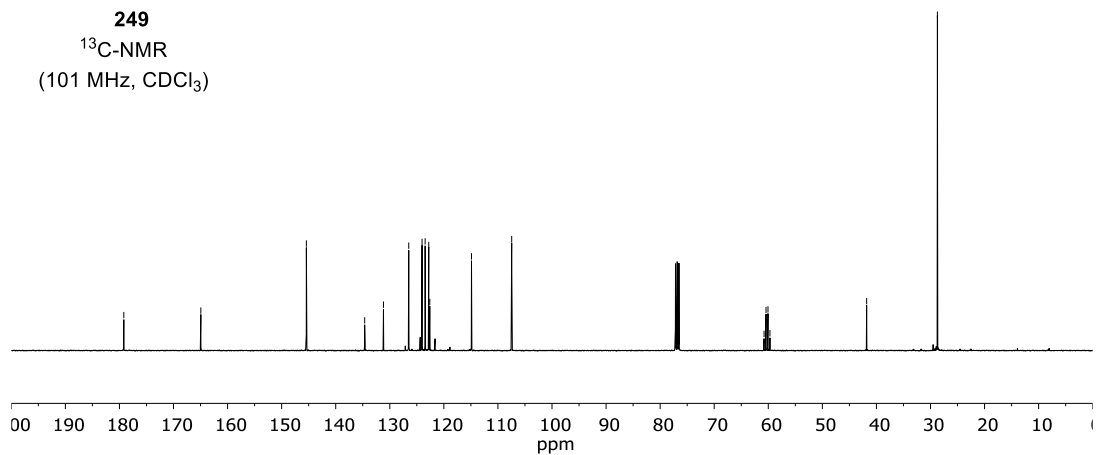




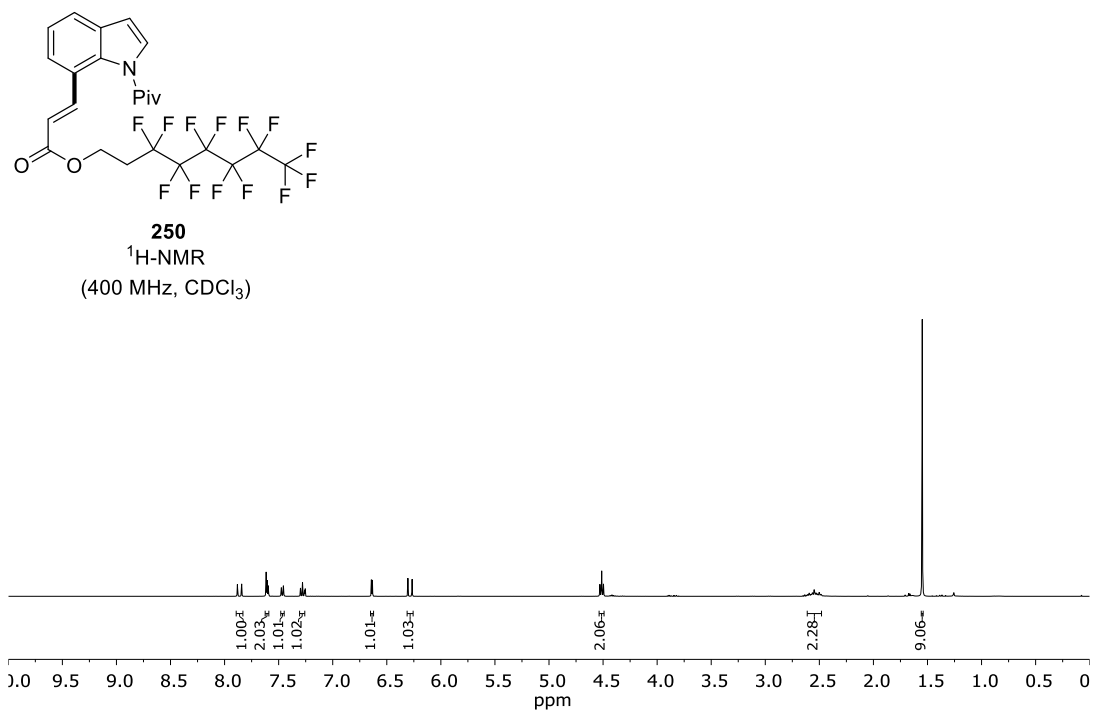
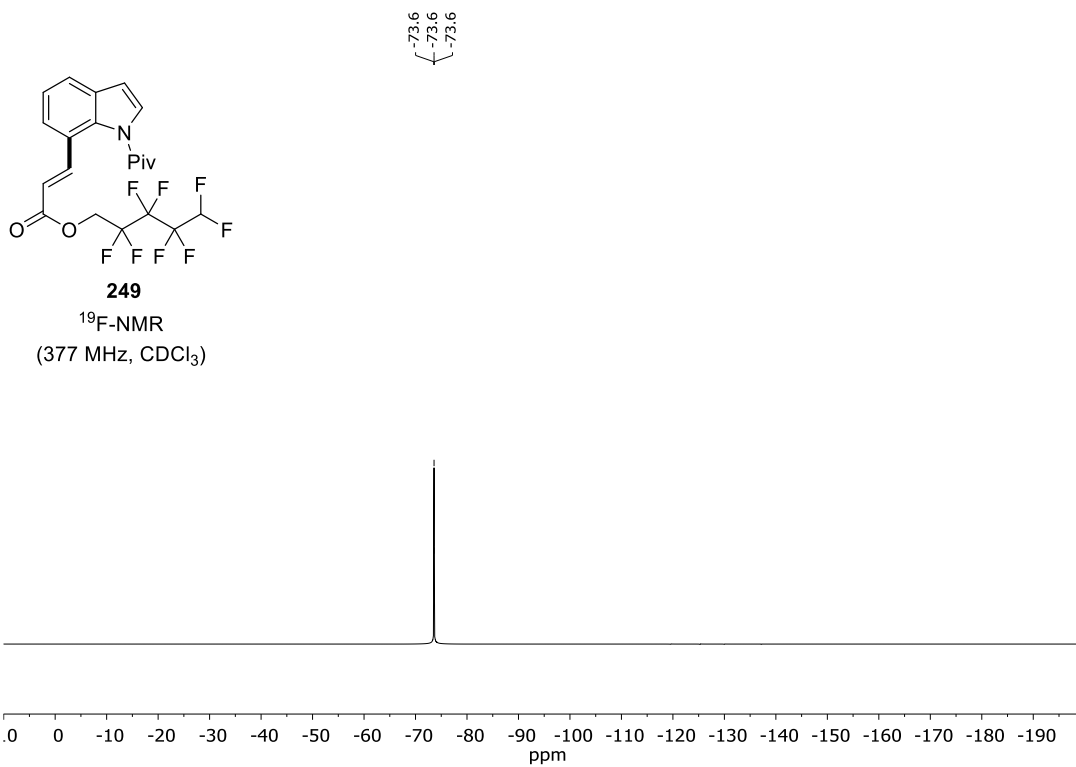
**249**  
<sup>1</sup>H-NMR  
 (400 MHz, CDCl<sub>3</sub>)

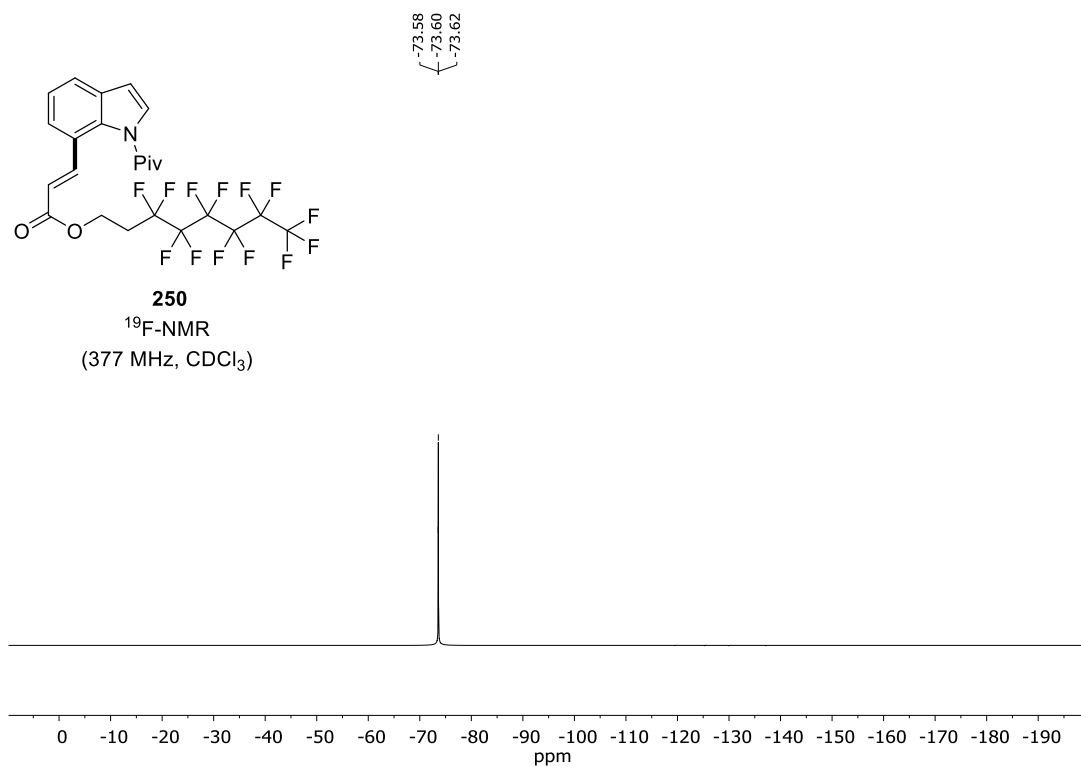
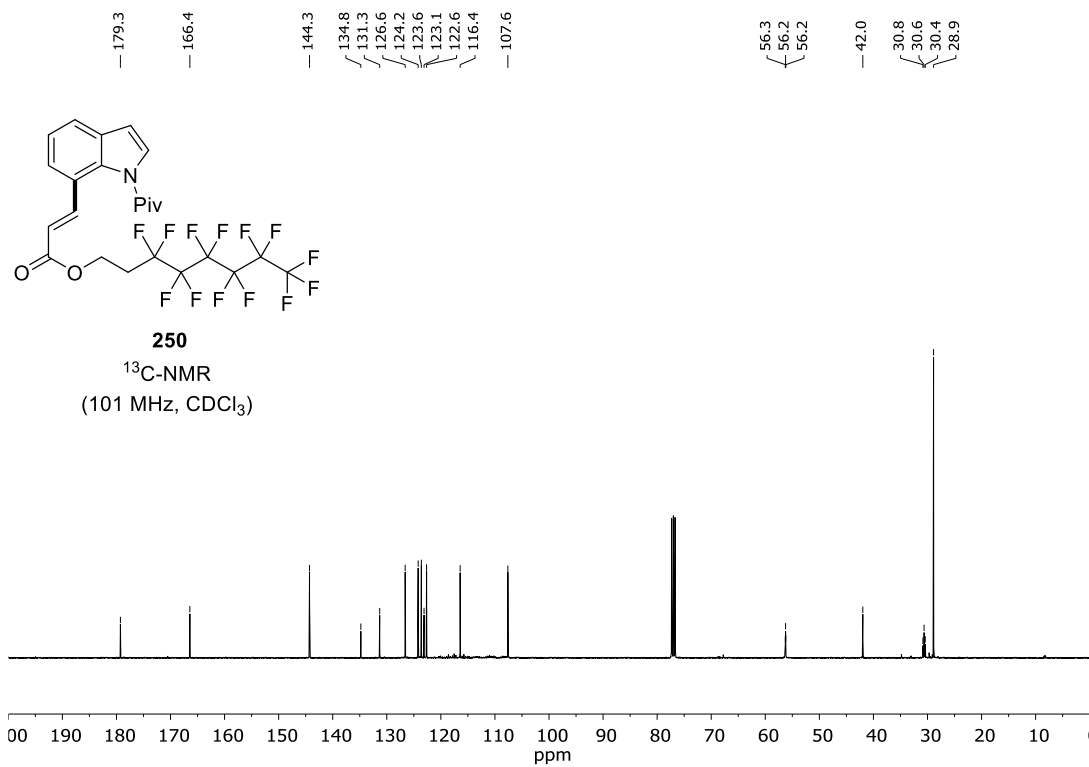


**249**  
<sup>13</sup>C-NMR  
 (101 MHz, CDCl<sub>3</sub>)

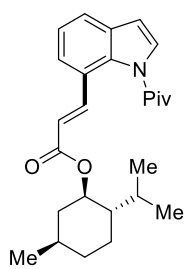


# NMR Spectra

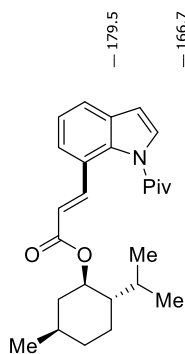
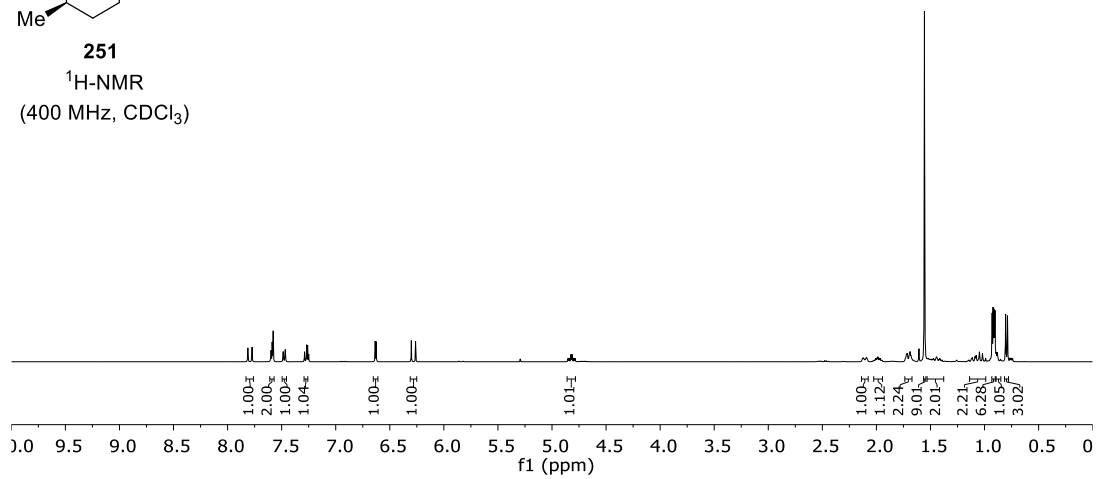




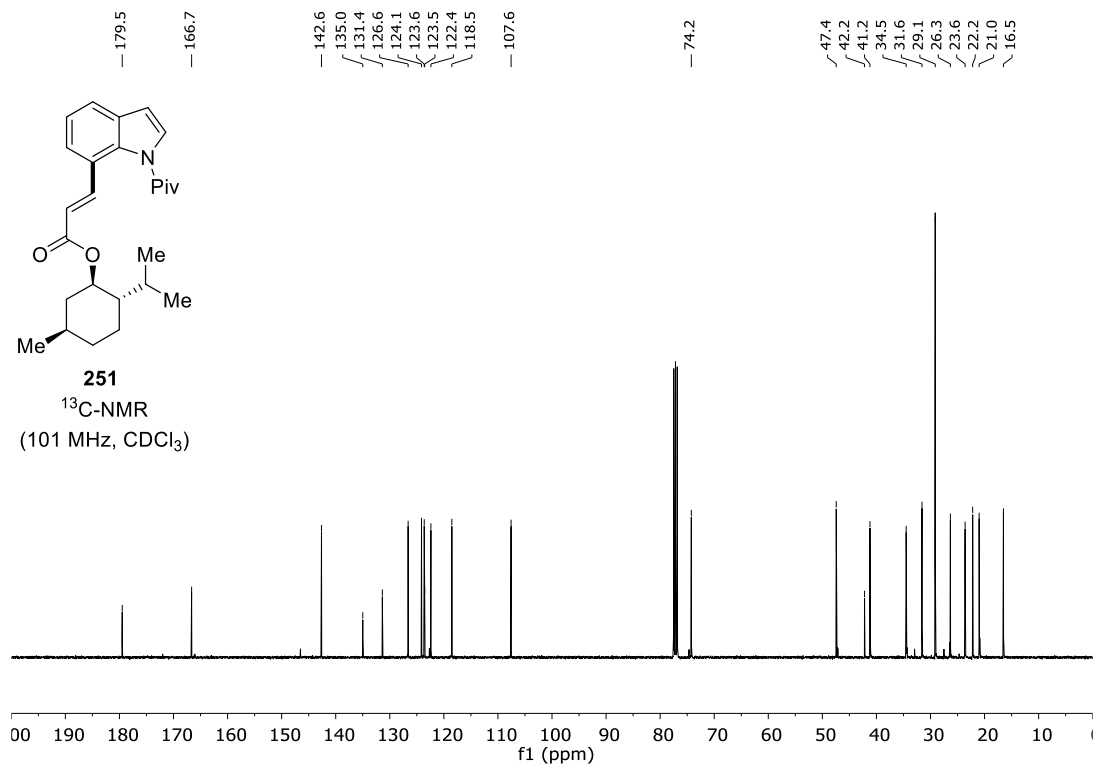
# NMR Spectra



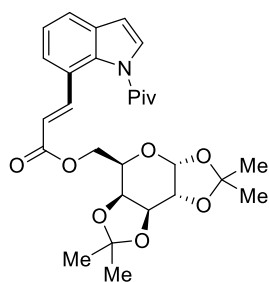
**251**  
<sup>1</sup>H-NMR  
 (400 MHz, CDCl<sub>3</sub>)



**251**  
<sup>13</sup>C-NMR  
 (101 MHz, CDCl<sub>3</sub>)

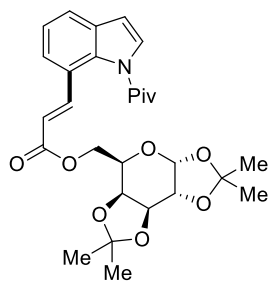
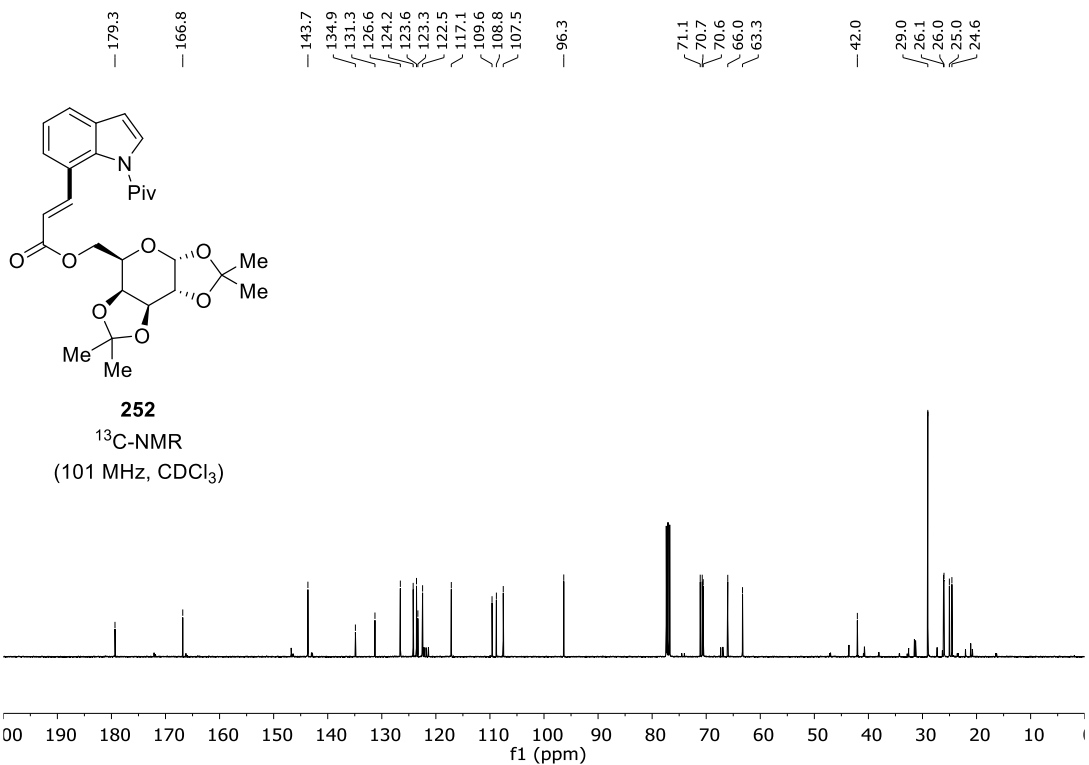
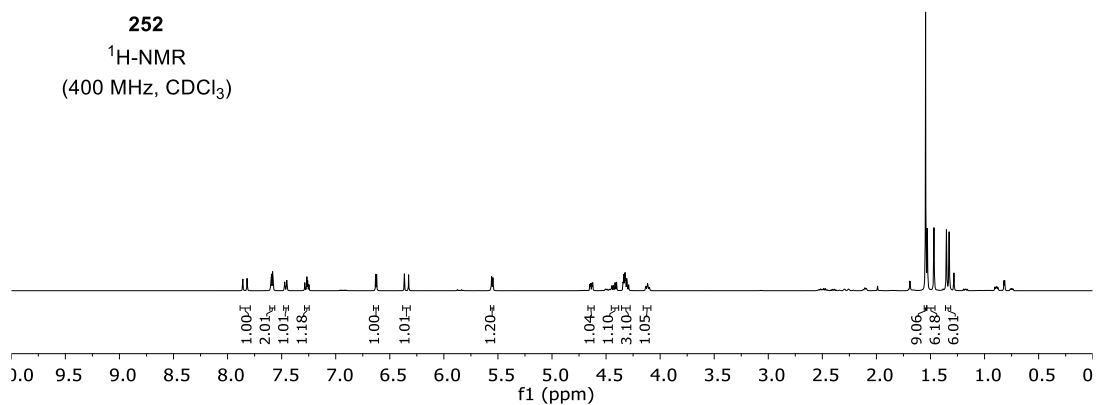






**252**

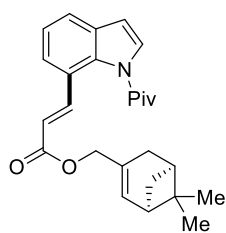
<sup>1</sup>H-NMR  
(400 MHz, CDCl<sub>3</sub>)



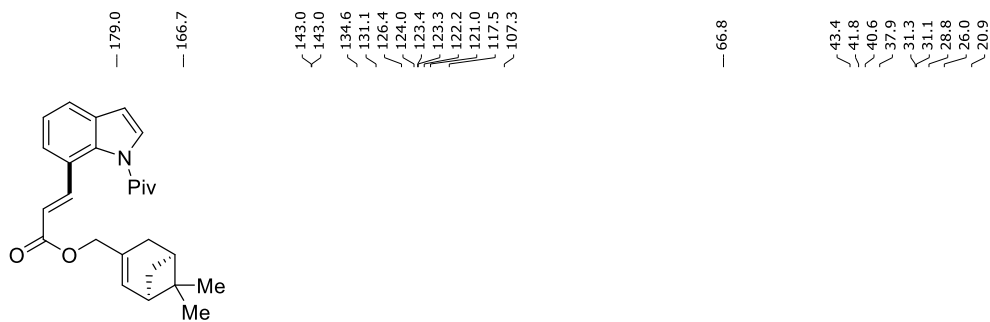
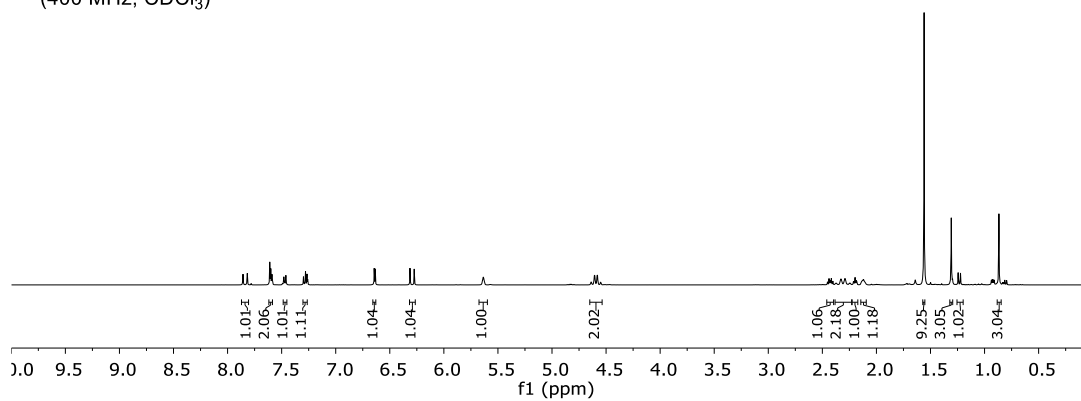
**252**

<sup>13</sup>C-NMR  
(101 MHz, CDCl<sub>3</sub>)

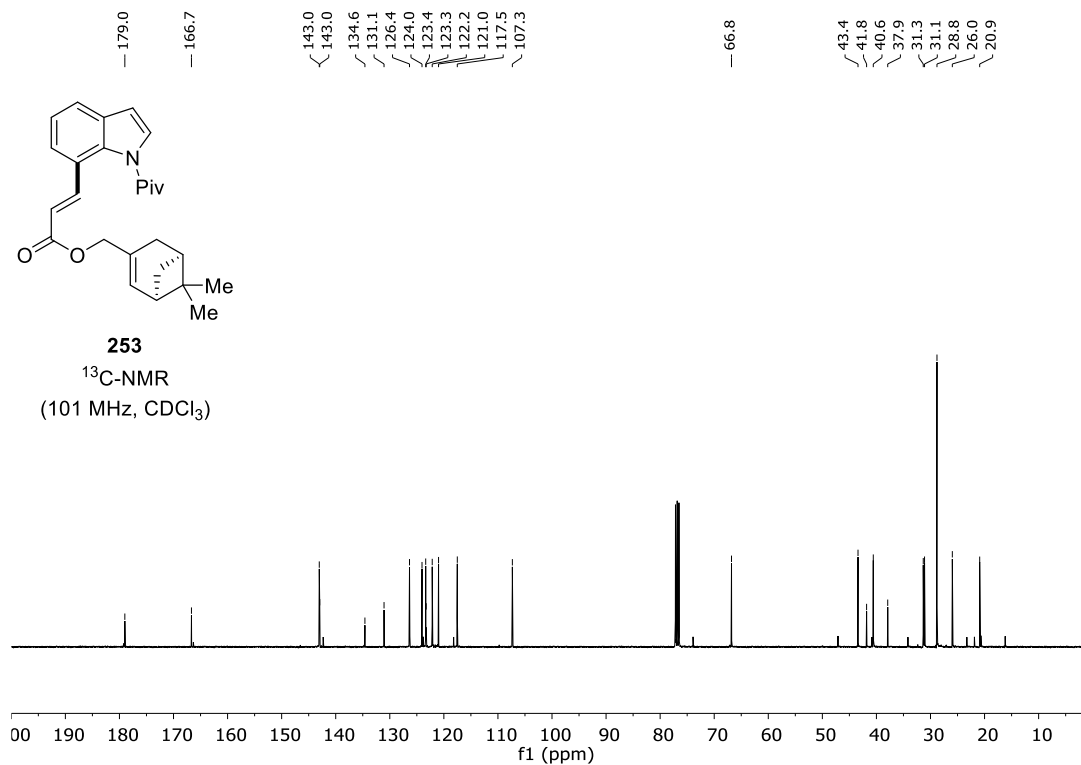
# NMR Spectra

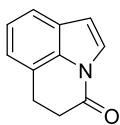


**253**  
<sup>1</sup>H-NMR  
 (400 MHz, CDCl<sub>3</sub>)

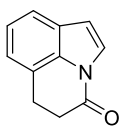
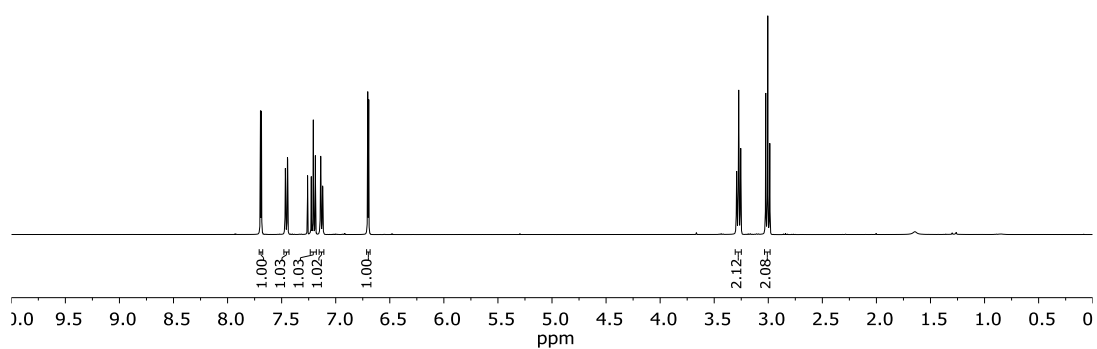


**253**  
<sup>13</sup>C-NMR  
 (101 MHz, CDCl<sub>3</sub>)

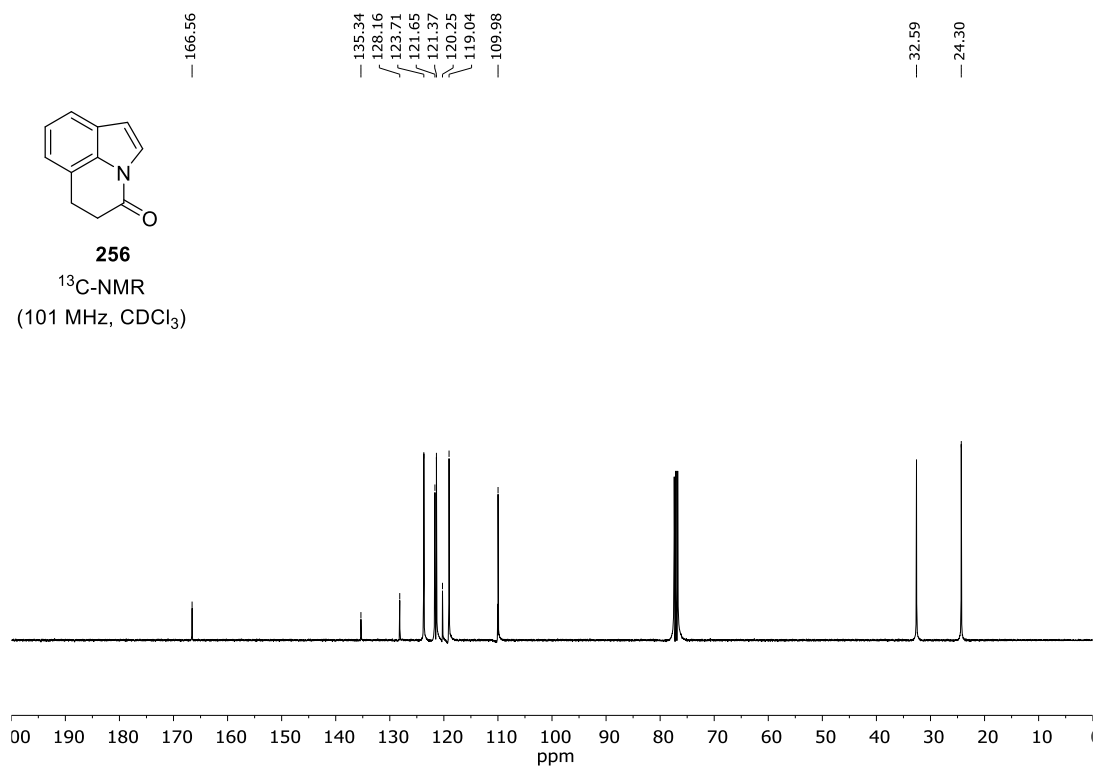




**256**  
<sup>1</sup>H-NMR  
(400 MHz, CDCl<sub>3</sub>)



**256**  
<sup>13</sup>C-NMR  
(101 MHz, CDCl<sub>3</sub>)



## Acknowledgement

It has been a very rewarding journey here in the Ackermann group, which would have not been possible without the assistance of Prof. Dr. Lutz Ackermann. Hence, first and foremost, I would like to thank him for trusting me and for giving me this opportunity. It was truly an empowering experience for one's knowledge in chemical research.

Second, I am thankful to my second and third supervisors Prof. Dr. Konrad Koszinowski and Prof. Dr. Franc Meyer. Their help and advice were indeed encouraging. I am also grateful to the other members of my thesis committee, Prof. Dr. Dr. h.c.mult. Lutz F. Tietze, Dr. Daniel Janßen-Müller, and Dr. Holm Frauendorf.

Third, I would like to share my appreciation to a few of my co-workers whom I have either worked with or have had great discussions for ideas and thoughtful comments: Hendrik Simon, Dr. Nate W. J. Ang, Dr. João C. A. Oliveira, Tristan von Münchow, Philipp Boos, Hasret Can Gülen, Wen Wei, Dr. Alexej Scheremetjew, Xiaoyan Hou, Zhipeng Lin, Binbin Yuan, Dr. Nikolaos Kaplaneris, Dr. Antonis Messinis, Dr. Isaac Choi, Dr. Korkit Korvorapun, Dr. Leonardo Massignan, Dr. Julia Struwe, Dr. Maximilian Stangier, and Dr. Yulei Wang.

Fourth, the thesis would not have been completed without the great help of many, namely: Hendrik Simon, Philipp Boos, Max Surke, Isaac Maksso, Simon Homölle, Dr. Alexej Scheremetjew and Dr. Nate W. J. Ang.

Fifth, I am very much grateful to the permanent working staffs that have made the journey much smoother than it would have been. Without their help, the working laboratory runs short of fuel: Dr. Svenja Warratz, Stefan Beußhausen, Karsten Rauch, Sabine Schacht, and Vanessa Bergmann.

Sixth, to all the friends I have made during these four years in Germany. To Cinzia, who gave me not only a place to stay when I was struggling with finding a flat in Göttingen, but also a solid friendship. To Nancy and Matteo, who share with me the love for cats. To Valentia, my confident and dearest supporter, the person you can always count on. To Hendrik and his loving family, thank you for embracing me wholeheartedly.

Seventh, a very warm thank you goes to my best friend Giovanna for being my rock and constant source of joy. Your friendship brightens my days and enriches my journey.

Eighth, thanks to Mila, my feline companion, for supervising me during the thesis writing. Your presence brought warmth into my life.

Finally, endless gratitude to my family for their boundless love, guidance, and understanding. You are my foundation, and every goal achieved is amplified with you. This voyage was made only plausible by you. Being away from home has been a challenge, but thanks to you I have always felt supported.

## Curriculum Vitae

### Personal Information

---

**Name:** Agnese Zangarelli

**Date of birth:** January 14<sup>th</sup>, 1995

**Place of birth:** Città di Castello

**Nationality:** Italian

**Address:** Tammannstrasse 2, 37077, Göttingen, Germany

**Email:** [agnese.zangarelli@unigoettingen.de](mailto:agnese.zangarelli@unigoettingen.de) or [agnese.zangarelli95@gmail.com](mailto:agnese.zangarelli95@gmail.com)

### Academic Education

---

**10.2019–present Ph.D. Candidate in Organic Chemistry**

Georg-August-Universität Göttingen

Supervisor: Prof. Dr. Lutz Ackermann

**Thesis:** Sustainable Transformations for the C–H Activation of Small Molecules

**10.2017–07.2019 Joined Double M.Sc. in Chemical Sciences**

University of Perugia and Hebrew University of Jerusalem

Supervisor: Prof. Dr. Luigi Vaccaro

**Thesis:** C–H Functionalization of Quinoline *N*-Oxide Iron-Catalyzed

**08.2018–09.2018 Training Course in Modern Physicochemical Methods in Chemistry and Pharmacy**

Peoples' Friendship University of Russia

**10.2014–09.2017 B.Sc. in Chemistry**

University of Perugia

Supervisor: Prof. Dr. Fausto Ortica

**Thesis:** Study of the Photochromic Behavior of Benzopyrans Bearing a *N*-Phenyl-Carbazole Moiety

## Attended Symposia

---

6<sup>th</sup> International Symposium on C–H Activation. Georg-August-Universität Göttingen, Germany, June 19-22, 2022.

C–H•Air Virtual Summer School 2021 on C–H Activation. Georg-August-Universität Göttingen, Germany, June 22-24, 2021.

5<sup>th</sup> International Symposium on C–H Activation. Georg-August-Universität Göttingen, Germany, July 27-30, 2020.

## Publications

---

1. **A. Zangarelli**, B. Yuan, and L. Ackermann\*. "Electrochemical C7-Indole Alkenylation *via* Rhodium Catalysis", *Isr. J. Chem.* **2023**, *63*, e202300103.
2. Y. Wang, S. Chen, X. Chen, **A. Zangarelli**, and L. Ackermann\*. "Photo-Induced Ruthenium-Catalyzed Double Remote C(sp<sup>2</sup>)-H/ C(sp<sup>3</sup>)-H Functionalizations by Radical Relay", *Angew. Chem. Int. Ed.* **2022**, *61*, e202205562.
3. J. Struwe, K. Korvorapun, **A. Zangarelli**, and L. Ackermann\*. "Photo-Induced Ruthenium-Catalyzed C–H Benzylations and Allylations at Room Temperature", *Chem. Eur. J.* **2021**, *27*, 16237–16241.
4. W. Wei, H. Yu, **A. Zangarelli**, and L. Ackermann\*. "Deaminative meta-C–H Alkylation by Ruthenium(II) Catalysis", *Chem. Sci.* **2021**, *12*, 8073–8078.
5. K. Korvorapun, J. Struwe, R. Kuniyil, **A. Zangarelli**, A. Casnati, M. Waeterschoot, and L. Ackermann\*. "Photo-Induced Ruthenium-Catalyzed C–H Arylation at Ambient Temperature", *Angew. Chem. Int. Ed.* **2020**, *59*, 18103–18109.
6. F. Ferlin, **A. Zangarelli**, S. Lilli, S. Santoro, and L. Vaccaro\*. "Waste-Minimized Synthesis of C2 Functionalized Quinolines Exploiting Iron-Catalyzed C–H Activation", *Green Chem.* **2021**, *23*, 490–495.
7. M. Frigoli, T. Jousselein-Oba, M. Mamada, J. Marrot, **A. Zangarelli**, D. Pannacci, C. Adachi, and F. Ortica\*. "Synthesis and photochromic behavior of a series of benzopyrans bearing an *N*-phenyl-carbazole moiety: photochromism control by the steric effect", *Photochem. Photobiol. Sci.* **2020**, *19*, 1344–1355.